Advances in Mathematical Physics

Application of Fuzzy Set and its Extensions in Engineering and Sciences: Theory, Models, and Simulations

Lead Guest Editor: S. E. Najafi
Guest Editors: Ranjan Kumar and Shangkun Deng

Application of Fuzzy Set and its Extensions in Engineering and Sciences: Theory, Models, and Simulations

Advances in Mathematical Physics

Application of Fuzzy Set and its Extensions in Engineering and Sciences: Theory, Models, and Simulations

Lead Guest Editor: S. E. Najafi
Guest Editors: Ranjan Kumar and Shangkun Deng

Contents

Hindawi
Advances in Mathematical Physics
Volume 2023, Article ID 4469908, 6 pages
https://doi.org/10.1155/2023/4469908

Research Article

An Efficient Technique for Algebraic System of Linear Equations Based on Neutrosophic Structured Element

Wenbo Xu,[1] Qunli Xia,[1] Hitesh Mohapatra,[2] and Sangay Chedup[3]

[1]*School of Astronautics, Beijing Institute of Technology, Beijing 100081, China*
[2]*School of Computer Engineering, KIIT Deemed to be University, Bhubaneswar 751024, Odisha, India*
[3]*Jigme Namgyel Engineering College, Deothang, Bhutan*

Correspondence should be addressed to Sangay Chedup; sangaychedup.jnec@rub.edu.bt

Received 26 August 2022; Revised 8 June 2023; Accepted 16 July 2023; Published 5 August 2023

Academic Editor: Zine El Abiddine Fellah

Neutrosophic logic is frequently applied to the engineering technology, scientific administration, and financial matters, among other fields. In addition, neutrosophic linear systems can be used to illustrate various practical problems. Due to the complexity of neutrosophic operators, however, solving linear neutrosophic systems is challenging. This work proposes a new straightforward method for solving the neutrosophic system of linear equations based on the neutrosophic structured element (NSE). Here unknown and right-hand side vectors are considered as triangular neutrosophic numbers. Based on the NSE, analytical expressions of the solution to this equation and its degrees are also provided. Finally, several examples of the methodology are provided.

1. Introduction

In modeling various physical phenomena, we are confronted with two types of uncertainty and indeterminacy: the first category is due to the inability of human knowledge and tools to comprehend the intricacies of an event. For instance, to determine the temperature of a city, thermometers are placed at various locations and the average is then calculated. Obviously, the calculated temperature differs from the actual temperature of that city, for two reasons: first, just a few points of that city were used in the calculations and second, the inaccuracy of the measuring person and the devices generates uncertainty in the reported temperature. The second category relates to a lack of clarity and transparency regarding a certain phenomenon or characteristic. A phenomenon may be fundamentally ambiguous and subjectively determined. For instance, there is no universal definition of what constitutes hot weather, so that one person may regard 30° to be hot while another believes 40° to be hot. Therefore, to obtain a realistic model, we must consider certainty and uncertainty in the model.

It is commonly recognized that in recent years, when less, incomplete, ambiguous, or imprecise information about variables or parameters has been available, fuzzy set (FS) and its extensions are particularly valuable modeling tools for these types of data [1–5]. Consequently, many physical or real-world issues involving uncertainty and indeterminacy frequently include the systems of linear equations in their solution methods. Numerous industries, including advertising, logistics, finance, optimization, and more, can benefit from this type of systems.

A number of scholars have also put forth models for linear systems in a fuzzy setting. Fuzzy linear systems (FLSs) did not develop until at least 1980 [6]. However, Friedman et al. [7] introduced an embedding approach to solve a FLS with a definite matrix coefficient and an arbitrarily fuzzy number vector on the right-hand side. This model was later modified by further researchers. Allahviranloo [8, 9] studied iterative algorithms for FLS with convergence theorems, including Jacobi, Gauss Seidel, and SOR approaches. Dehghan et al. [10] provided certain ways to solve FLS that are equivalent to well-known methods as

Gaussian elimination, Cramer's rule, Doolittle algorithm, and its simplification.

Muzzioli and Reynaerts [11] examined a dual type of FLS and highlighted the connection between interval linear systems (ILS) and FLS. Wang and Zheng [12] explored an inconsistent FLS and derived the fuzzy and weak fuzzy least squares solutions by applying the generalized inverses of the coefficient matrix. Tian et al. [13] investigated the perturbation analysis of FLS and determined the relative error limitations for FLS solutions. Otadi et al. [14] presented a hybrid method based on fuzzy neural network for approximate solution of FLS. Behera and Chakraverty [15] examined the solution technique for both real and complicated fuzzy systems. Saberi Najafi and Edalatpanah [16] analyzed various existing iterative methods employing the embedding method for finding the solution FLS and devised a numerical method for enhancing these algorithms. They demonstrated that their technique outperforms all previously mentioned numerical iterative algorithms. Lodwick and Dubois [17] argued that ILS is an essential process in the solution of FLS and emphasized four unique definitions of systems of linear equations in which coefficients are substituted by intervals.

Akram et al. [18] defined some concepts, including a bipolar fuzzy number in parametric form and propose a method for the bipolar FLS solution procedure. Fully FLS with trapezoidal and hexagonal fuzzy numbers have been studied by Ziqan et al. [19]. Abbasi and Allahviranloo [20] also investigated and the reported a new concept based on transmission-average-based operations for solving fully FLS. Recently, numerous scholars investigated the system of linear equations for the various types of fuzzy numbers such as horizontal fuzzy numbers [21], LR-bipolar fuzzy numbers [22], thick fuzzy number [23], and fuzzy complex numbers [24]. Although the solution of a system of linear equation with FS) is intriguing, FS only considers the truth membership function of each element. Atanassov [25] proposed intuitionistic fuzzy sets (IFSs), which accounted for both the falsity and truth membership functions, to address this issue.

However, in real-life decision-making problems, both FS and IFS are unable to deal with indeterminacy. In actual decision-making difficulties, both FS and IFS are incapable of handling indeterminacy that in the context of actual decision-making it is highly crucial. In terms of independent truth, falsity, and indeterminacy membership functions, Smarandache [26] created neutrosophic sets (NS) in 1998. Subsequently, several new extensions to NSs have emerged, including NSs [27, 28] defined over a specific interval, bipolar NSs [29] characterized by their dual nature, single-valued NSs [30] consisting of single values, quadripartitioned single valued NSs [31] divided into four partitions, n-refined NSs [32] refined through additional considerations, simplified NSs [33], and pentapartitioned NS [34] introduced for ease of comprehension. These contexts are used in a variety of ways in research and engineering, such as transportation problem [35], statistical analysis [36], management evaluation [37], bioenergy production technologies [38], centrifugal pump [39], waste management [40], etc.

To the best of our knowledge, there have only been a limited number of studies on the system of neutrosophic linear equations [41, 42], despite the fact that there are numerous methods for addressing various issues under NSs. These methods [41, 42] used the (α, β, γ)-cut technique. Some neutrosophic modeling approaches carefully handle the original neutrosophic data, which can easily result in information loss and potentially lead to biased results. These techniques have not strayed too far from the mainstream decision-making domain. Moreover, the calculating procedure is occasionally disrupted by parameter ergodicity issues. For example, the (α, β, γ)-cut technique requires the parameter to be set to [0, 1], which is unrealistic. The neutrosophic structured element (NSE) is among the substantial extensions of NS. Edalatpanah [43] was the founder of the NSE theory, which expresses NS as a linear structure.

NSs can be analyzed and sorted based on the relationship between the truth, indeterminacy, and falsity membership functions, however the formulae are complicated and certain procedures do not satisfy the rational hypothesis of economic phenomenon. However, modeling with NSE can remove these shortcomings. However, simulation with NSE can eliminate these deficiencies. NSE is based on the homeomorphism between a closed NS and a group of restricted functions on $[-1, 1]$. To avoid the ergodicity of the extension idea, the NSE was utilized to represent NSs and their operations. In addition, the NSs transmission of the calculation process and the analytic expression of computed values can be implemented. Therefore, this work proposes a new approach for solving neutrosophic linear systems (NLS) of the form $Ax = b$, where A is a crisp matrix and b is the triangular single-valued neutrosophic number (TSVNN) vector.

The structure of this work is as follows: Section 1 covers the concepts of TSVNN and NSE; Section 2, various notations and definitions are provided; Section 3, both the NLS and the proposed approach have been introduced; Section 4, numerical examples are then solved; Section 5 concludes with the conclusions.

2. Preliminaries

Here are provided various notations and definitions pertinent to the presented study [43].

Definition 1. Consider $\Lambda = <(\delta_1, \delta_2, \delta_3), (\iota_1, \iota_2, \iota_3), (\xi_1, \xi_2, \xi_3)>$ as the TSVNN. Then the truth $(T_\Lambda(x))$, indeterminacy $(\Gamma_\Lambda(x))$, and falsity $(\Psi_\Lambda(x))$ membership functionsare described as follows:

$$\mathrm{T}_{\Lambda}(x)=\begin{cases}\dfrac{(x-\delta_1)}{(\delta_2-\delta_1)} & \delta_1\le x<\delta_2,\\ 1 & x=\delta_2,\\ \dfrac{(\delta_3-x)}{(\delta_3-\delta_2)} & \delta_2<x\le\delta_3,\\ 0 & \text{otherwise.}\end{cases}\quad \Gamma_{\Lambda}(x)=\begin{cases}\dfrac{(\iota_2-x)}{(\iota_2-\iota_1)} & \iota_1\le x<\iota_2,\\ 0 & x=\iota_2,\\ \dfrac{(x-\iota_2)}{(\iota_3-\iota_2)} & \iota_2<x\le\iota_3,\\ 1 & \text{otherwise.}\end{cases}\quad \Psi_{\Lambda}(x)=\begin{cases}\dfrac{(\xi_2-x)}{(\xi_2-\xi_1)} & \xi_1\le x<\xi_2,\\ 0 & x=\xi_2,\\ \dfrac{(x-\xi_2)}{(\xi_3-\iota_2)} & \xi_2<x\le\xi_3,\\ 1 & \text{otherwise.}\end{cases} \tag{1}$$

where $0\le \mathrm{T}_{\Lambda}(x)+\Gamma_{\Lambda}(x)+\Psi_{\Lambda}(x)\le 3, x\in\Lambda$.

Definition 2. For TSVNN $\Lambda=<(\delta_1,\delta_2,\delta_3),(\iota_1,\iota_2,\iota_3),(\xi_1,\xi_2,\xi_3)>$, there are $p,q,r:[-1,1]\to[0,1]$ such that $\mathrm{T}_{\Lambda}(x)=p_{\Lambda}(x), \Gamma_{\Lambda}(x)=q_{\Lambda}(x),$ and $\Psi_{\Lambda}(x)=r_{\Lambda}(x)$, where:

$$p_{\Lambda}(x)=\begin{cases}(\delta_2-\delta_1)x+\delta_2, & -1\le x\le 0,\\ (\delta_3-\delta_2)x+\delta_2, & 0\le x\le 1,\\ 0, & \text{others,}\end{cases} \tag{2}$$

$$q_{\Lambda}(E)=\begin{cases}(\iota_2-\iota_1)x+\iota_2, & -1\le x\le 0,\\ (\iota_3-\iota_2)x+\iota_2, & 0\le x\le 1,\\ 0, & \text{others,}\end{cases} \tag{3}$$

$$r_{\Lambda}(x)=\begin{cases}(\xi_2-\xi_1)x+\xi_2, & -1\le x\le 0,\\ (\xi_3-\xi_2)x+\xi_2, & 0\le x\le 1,\\ 0, & \text{others,}\end{cases} \tag{4}$$

where $\Lambda=<p_{\Lambda}(x),q_{\Lambda}(x),r_{\Lambda}(x)>$, is called NSE number (NSEN).

Definition 3. For $M=<p_M(x),q_M(x),r_M(x)>$, and $N=<s_N(x),t_N(x),u_N(x)>$, we have:

(i) $M\oplus N=<(p_M+s_N)(x),(q_M+t_N)(x),(r_M+u_N)(x)>$,
(ii) $M-N=<(p_M(x)+s'_N(x)),(q_M(x)+t'_N(x)),(r_M(x)+u'_N(x))>$,
(iii) $\lambda N=\lambda<(s'_N(x)),(t'_N(x)),(u'_N(x))>$,

where

$$s'_N(x)=-s_N(-x),\ t'_N(x)=-t_N(-x),\ u'_N(x)=-u_N(-x). \tag{5}$$

3. NLS and the Proposed Method

Let us consider a $n\times n$ NLS

$$[A]\{\widetilde{X}\}=\{\widetilde{b}\}. \tag{6}$$

Here $[A]=(a_{kj})$ for $1\le k\le n$ and $1\le j\le n$ is a $n\times n$ crisp real matrix, $\{\tilde{b}\}=\{\tilde{b}_k\}$ is a column vector of TSVNN and $\{\tilde{X}\}=\{\tilde{x}_j\}$ is the vector of neutrosophic unknown.

Equation (6) can be represented by the following expressions:

$$\sum_{j=1}^{n}a_{kj}\tilde{x}_j=\tilde{b}_k,\ \text{for } k=1,\ldots,n. \tag{7}$$

In [43], Edalatpanah studied the solution of $n\times n$ NLS with embedding method, and gave the necessary and sufficient conditions for a unique neutrosophic solution. In this section, instead of using two monotonic functions to represent the neutrosophic numbers in [43], we will use the NSE methodology to study the problem of NLS. Suppose that the solution of the NLS of Equation (6) be $\tilde{x}$ and its NSE form be $\tilde{\Psi}(x)=<p_{\Psi}(x),q_{\Psi}(x),r_{\Psi}(x)>$. Also, let the NSE form of $\{\tilde{b}\}$ be $\tilde{b}(x)=<s_{\tilde{b}}(x),t_{\tilde{b}}(x),u_{\tilde{b}}(x)>$. Then, in the special case if for each row $a_{kj}\ge 0$ we have:

$$\sum_{j=1}^{n}a_{kj}\Psi_j(x)=\tilde{b}_k(x),\ \text{for } k=1,\ldots,n, \tag{8}$$

$$\sum_{j=1}^{n}a_{kj}\Psi_j(-x)=\tilde{b}_k(-x),\ \text{for } k=1,\ldots,n, \tag{9}$$

which are two common NLSs and can be solved easily.

Now to solve Equation (7), define:

$$Y=(\Psi_1(x),\ \Psi_2(x),\ldots,\Psi_n(x),\Psi_1(-x),\ \Psi_2(-x),\ldots,\Psi_n(-x))^t, \tag{10}$$

$$B=(\tilde{b}_1(x),\tilde{b}_2(x),\ldots,\tilde{b}_n(x),\tilde{b}_1(-x),\tilde{b}_2(-x),\ldots,\tilde{b}_n(-x))^t. \tag{11}$$

Then Equation (7) can equivalently be written as follows:

$$HY=B, \tag{12}$$

where $H=(h_{ij})_{2n\times 2n}$ is as follows:

$$\begin{cases}a_{ij}\ge 0\to h_{ij}=a_{ij}, & h_{i+n,j+n}=a_{ij},\\ a_{ij}<0\to h_{i,j+n}=h_{ij}, & d_{i+n,j}=h_{ij}\end{cases}. \tag{13}$$

Furthermore, to specify the truth, indeterminacy, and falsity parts of solution we define:

$$Y = <P_Y(x),\ Q_Y(x),\ R_Y(x)>, \tag{14}$$

$$B = <S_B(x),\ T_B(x),\ U_B(x)>, \tag{15}$$

where

$$P_Y(x) = (p_1(x),\ p_2(x),\ \ldots,\ p_n(x),\ p_1(-x),\ p_2(-x),\ \ldots,\ p_n(-x))^t, \tag{16}$$

$$Q_Y(x) = (q_1(x),\ q_2(x),\ \ldots,\ q_n(x),\ q_1(-x),\ q_2(-x),\ \ldots,\ q_n(-x))^t, \tag{17}$$

$$R_Y(x) = (r_1(x),\ r_2(x),\ \ldots,\ r_n(x),\ r_1(-x),\ r_2(-x),\ \ldots,\ r_n(-x))^t, \tag{18}$$

$$S_B(x) = (s_1(x),\ s_2(x),\ \ldots,\ s_n(x),\ s_1(-x),\ s_2(-x),\ \ldots,\ s_n(-x))^t, \tag{19}$$

$$Q_B(x) = (q_1(x),\ q_2(x),\ \ldots,\ q_n(x),\ q_1(-x),\ q_2(-x),\ \ldots,\ q_n(-x))^t, \tag{20}$$

$$U_B(x) = (u_1(x),\ u_2(x),\ \ldots,\ u_n(x),\ u_1(-x),\ u_2(-x),\ \ldots,\ u_n(-x))^t. \tag{21}$$

Therefore, the three parts of solution of NLS can be obtained by computing the following formulas:

$$P_Y(x) = H^{-1}S_B(x), \tag{22}$$

$$Q_Y(x) = H^{-1}T_B(x), \tag{23}$$

$$R_Y(x) = H^{-1}U_B(x). \tag{24}$$

In the next section sometests have been solved using the proposed method and also compared with existing results for the validation.

4. Numerical Examples

Example 1. Let us consider a 2×2 TSVNN system of linear equations as follows:

$$\begin{cases} 4\tilde{x}_1 - \tilde{x}_2 = <(2,\ 3,\ 7),\ (3,\ 5,\ 6),\ (0,\ 1,\ 3)> = \tilde{b}_1(x), \\ \tilde{x}_1 + 3\tilde{x}_2 = <(4,\ 5,\ 6),\ (5,\ 7,\ 9),\ (1,\ 2,\ 4)> = \tilde{b}_2(x). \end{cases} \tag{25}$$

Next using our approach, we have:

$$H = \begin{bmatrix} 4 & 0 & 0 & -1 \\ 1 & 3 & 0 & 0 \\ 0 & -1 & 4 & 0 \\ 0 & 0 & 1 & 3 \end{bmatrix}, \tag{26}$$

$$b_1(x) = \left\langle \begin{cases} x+3, & -1\le x\le 0, \\ 4x+3, & 0\le x\le 1, \end{cases}, \begin{cases} 2x+5, & -1\le x\le 0, \\ x+5, & 0\le x\le 1, \end{cases}, \begin{cases} x+1, & -1\le x\le 0, \\ 2x+1, & 0\le x\le 1, \end{cases} \right\rangle, \tag{27}$$

$$b_1(-x) = \left\langle \begin{cases} -4x+3, & -1\le x\le 0, \\ -x+3, & 0\le x\le 1, \end{cases}, \begin{cases} -x+5, & -1\le x\le 0, \\ -2x+5, & 0\le x\le 1, \end{cases}, \begin{cases} -2x+1, & -1\le x\le 0, \\ -x+1, & 0\le x\le 1, \end{cases} \right\rangle, \tag{28}$$

$$b_2(x) = \left\langle \begin{cases} x+5, & -1\le x\le 0, \\ x+5, & 0\le x\le 1, \end{cases}, \begin{cases} 2x+7, & -1\le x\le 0, \\ 2x+7, & 0\le x\le 1, \end{cases}, \begin{cases} x+2, & -1\le x\le 0, \\ 2x+2, & 0\le x\le 1, \end{cases} \right\rangle, \tag{29}$$

$$b_2(-x) = \left\langle \begin{cases} -x+5, & -1\le x\le 0, \\ -x+5, & 0\le x\le 1, \end{cases}, \begin{cases} -2x+7, & -1\le x\le 0, \\ -2x+7, & 0\le x\le 1, \end{cases}, \begin{cases} -2x+2, & -1\le x\le 0, \\ -x+2, & 0\le x\le 1, \end{cases} \right\rangle. \tag{30}$$

$$\widetilde{b}(x) = <s_{\widetilde{b}}(x),\ t_{\widetilde{b}}(x),\ u_{\widetilde{b}}(x)>. \tag{31}$$

So, using Equations (22)–(24), for $-1 \le x \le 0$:

$$P_Y(x) = \begin{bmatrix} p_1(x) \\ p_2(x) \\ p_1(-x) \\ p_2(-x) \end{bmatrix} = H^{-1} \begin{bmatrix} x+3 \\ x+5 \\ -4x+3 \\ -x+5 \end{bmatrix} = \begin{bmatrix} \frac{35}{143}x + \frac{14}{13} \\ \frac{36}{143}x + \frac{17}{13} \\ -\frac{134}{143}x + \frac{14}{13} \\ -\frac{3}{143}x + \frac{17}{13} \end{bmatrix}. \tag{32}$$

And for $0 \le x \le 1$:

$$P_Y(x) = \begin{bmatrix} p_1(x) \\ p_2(x) \\ p_1(-x) \\ p_2(-x) \end{bmatrix} = H^{-1} \begin{bmatrix} 4x+3 \\ x+5 \\ -x+3 \\ -x+5 \end{bmatrix} = \begin{bmatrix} \frac{134}{143}x + \frac{14}{13} \\ \frac{3}{143}x + \frac{17}{13} \\ -\frac{35}{143}x + \frac{14}{13} \\ -\frac{36}{143}x + \frac{17}{13} \end{bmatrix}. \tag{33}$$

So by setting $x = -1, 0$ in Equation (32) and also set $x = 1$ in Equation (33), we can get the triangular truth part of solution as follows:

$$x_{\text{true}} = \begin{bmatrix} <\frac{119}{143}, \frac{14}{13}, \frac{288}{143}> \\ <\frac{151}{143}, \frac{17}{13}, \frac{190}{143}> \end{bmatrix}. \tag{34}$$

In similar way, we can obtain the indeterminacy, and falsity parts of solution as follows:

$$\begin{aligned} x_{\text{in deter}} &= \begin{bmatrix} <\frac{193}{143}, \frac{22}{13}, \frac{258}{143}> \\ <\frac{174}{143}, \frac{23}{13}, \frac{343}{143}> \end{bmatrix}, \\ x_{\text{fals}} &= \begin{bmatrix} <\frac{38}{143}, \frac{5}{13}, \frac{116}{143}> \\ <\frac{35}{143}, \frac{7}{13}, \frac{152}{143}> \end{bmatrix}. \end{aligned} \tag{35}$$

Therefore, the final solution for NLS (25) is as follows:

$$\widetilde{x} = \left\langle \begin{bmatrix} \left(\frac{119}{143}, \frac{14}{13}, \frac{288}{143}\right) \\ \left(\frac{151}{143}, \frac{17}{13}, \frac{190}{143}\right) \end{bmatrix}, \begin{bmatrix} \left(\frac{193}{143}, \frac{22}{13}, \frac{258}{143}\right) \\ \left(\frac{174}{143}, \frac{23}{13}, \frac{343}{143}\right) \end{bmatrix}, \begin{bmatrix} \left(\frac{38}{143}, \frac{5}{13}, \frac{116}{143}\right) \\ \left(\frac{35}{143}, \frac{7}{13}, \frac{152}{143}\right) \end{bmatrix} \right\rangle. \tag{36}$$

5. Conclusions

In this paper, we introduced the NLS with a single-valued triangular neutrosophic number and developed a model based on neutrosophic structural elements for its solution. Using the monotone function on $[-1, 1]$, the $n \times n$ NLS is changed in this manner into $2n \times 2n$ crisp systems. The results demonstrate that the model is effective, straightforward, and involves far less work than the alternatives.

Data Availability

Data supporting this research article are available from the corresponding author on reasonable request.

Conflicts of Interest

The authors declare that they have no conflicts of interest.

References

[1] D. J. Dubois, *Fuzzy Sets and Systems: Theory and Applications*, vol. 144, Academic press, 1980.

[2] J. Wu, M. Brackstone, and M. McDonald, "Fuzzy sets and systems for a motorway microscopic simulation model," *Fuzzy Sets and Systems*, vol. 116, no. 1, pp. 65–76, 2000.

[3] T. Javanbakht and S. Chakravorty, "Prediction of human behavior with TOPSIS," *Journal of Fuzzy Extension and Applications*, vol. 3, no. 2, pp. 109–125, 2022.

[4] L. de Souza Oliveira, A. Argou, R. Dilli, A. Yamin, R. Reiser, and B. Bedregal, "Exploring fuzzy set consensus analysis in IoT resource ranking," *Engineering Applications of Artificial Intelligence*, vol. 109, Article ID 104617, 2022.

[5] C.-N. Wang, N.-A.-T. Nguyen, and T.-T. Dang, "Offshore wind power station (OWPS) site selection using a two-stage MCDM-based spherical fuzzy set approach," *Scientific Reports*, vol. 12, Article ID 4260, 2022.

[6] D. Dubois and H. Prade, "Systems of linear fuzzy constraints," *Fuzzy Sets and Systems*, vol. 3, pp. 37–48, 1980.

[7] M. Friedman, M. Ming, and A. Kandel, "Fuzzy linear systems," *Fuzzy Sets and Systems*, vol. 96, no. 2, pp. 201–209, 1998.

[8] T. Allahviranloo, "Numerical methods for fuzzy system of linear equations," *Applied Mathematics and Computation*, vol. 155, no. 2, pp. 493–502, 2004.

[9] T. Allahviranloo, "Successive over relaxation iterative method for fuzzy system of linear equations," *Applied Mathematics and Computation*, vol. 162, no. 1, pp. 189–196, 2005.

[10] M. Dehghan, B. Hashemi, and M. Ghatee, "Computational methods for solving fully fuzzy linear systems," *Applied Mathematics and Computation*, vol. 179, no. 1, pp. 328–343, 2006.

[11] S. Muzzioli and H. Reynaerts, "Fuzzy linear systems of the form $A_1x+ b_1 = A_2x+ b_2$," *Fuzzy Sets and Systems*, vol. 157, no. 7, pp. 939–951, 2006.

[12] K. Wang and B. Zheng, "Inconsistent fuzzy linear systems," *Applied Mathematics and Computation*, vol. 181, no. 2, pp. 973–981, 2006.

[13] Z. Tian, L. Hu, and D. Greenhalgh, "Perturbation analysis of fuzzy linear systems," *Information Sciences*, vol. 180, no. 23, pp. 4706–4713, 2010.

[14] M. Otadi, M. Mosleh, and S. Abbasbandy, "Numerical solution of fully fuzzy linear systems by fuzzy neural network," *Soft Computing*, vol. 15, pp. 1513–1522, 2011.

[15] D. Behera and S. Chakraverty, "A new method for solving real and complex fuzzy systems of linear equations," *Computational Mathematics and Modeling*, vol. 23, pp. 507–518, 2012.

[16] H. Saberi Najafi and S. A. Edalatpanah, "An improved model for iterative algorithms in fuzzy linear systems," *Computational Mathematics and Modeling*, vol. 24, pp. 443–451, 2013.

[17] W. A. Lodwick and D. Dubois, "Interval linear systems as a necessary step in fuzzy linear systems," *Fuzzy Sets and Systems*, vol. 281, pp. 227–251, 2015.

[18] M. Akram, G. Muhammad, and T. Allahviranloo, "Bipolar fuzzy linear system of equations," *Computational and Applied Mathematics*, vol. 38, Article ID 69, 2019.

[19] A. Ziqan, S. Ibrahim, M. Marabeh, and A. Qarariyah, "Fully fuzzy linear systems with trapezoidal and hexagonal fuzzy numbers," *Granular Computing*, vol. 7, pp. 229–238, 2022.

[20] F. Abbasi and T. Allahviranloo, "Solving fully fuzzy linear system: a new solution concept," *Information Sciences*, vol. 589, pp. 608–635, 2022.

[21] M. Landowski, "Method with horizontal fuzzy numbers for solving real fuzzy linear systems," *Soft Computing*, vol. 23, pp. 3921–3933, 2019.

[22] M. Akram, T. Allahviranloo, W. Pedrycz, and M. Ali, "Methods for solving *LR*-bipolar fuzzy linear systems," *Soft Computing*, vol. 25, pp. 85–108, 2021.

[23] R. Boukezzoula, L. Jaulin, and D. Coquin, "A new methodology for solving fuzzy systems of equations: thick fuzzy sets based approach," *Fuzzy Sets and Systems*, vol. 435, pp. 107–128, 2022.

[24] Z. Xiao and Z. Gong, "The fuzzy complex linear systems based on a new representation of fuzzy complex numbers," *Mathematics*, vol. 10, no. 15, Article ID 2822, 2022.

[25] K. T. Atanassov, "Intuitionistic fuzzy sets," *Fuzzy Sets and Systems*, vol. 20, no. 1, pp. 87–96, 1986.

[26] F. Smarandache, "Neutrosophic set—a generalization of the intuitionistic fuzzy set," in *2006 IEEE International Conference on Granular Computing*, vol. 24, pp. 38–42, IEEE, Atlanta, GA, USA, 2006.

[27] J. Wang, H. Gao, and M. Lu, "Approaches to strategic supplier selection under interval neutrosophic environment," *Journal of Intelligent & Fuzzy Systems*, vol. 37, no. 2, pp. 1707–1730, 2019.

[28] D. Zhang, Y. Su, M. Zhao, and X. Chen, "CPT-TODIM method for interval neutrosophic MAGDM and its application to third-party logistics service providers selection," *Technological and Economic Development of Economy*, vol. 28, no. 1, pp. 201–219, 2022.

[29] A. Chakraborty, S. P. Mondal, S. Alam, and A. Dey, "Classification of trapezoidal bipolar neutrosophic number, de-bipolarization technique and its execution in cloud service-based MCGDM problem," *Complex & Intelligent Systems*, vol. 7, pp. 145–162, 2021.

[30] H. Garg, "SVNMPR: a new single-valued neutrosophic multiplicative preference relation and their application to decision-making process," *International Journal of Intelligent Systems*, vol. 37, no. 3, pp. 2089–2130, 2022.

[31] R. Radha and A. Stanis Arul Mary, "Quadripartitioned neutrosophic pythagorean lie subalgebra," *Journal of Fuzzy Extension and Applications*, vol. 2, no. 3, pp. 283–296, 2021.

[32] M. Abobala, "A study of maximal and minimal ideals of n-refined neutrosophic rings," *Journal of Fuzzy Extension and Applications*, vol. 2, no. 1, pp. 16–22, 2021.

[33] J. Ye, "Improved cosine similarity measures of simplified neutrosophic sets for medical diagnoses," *Artificial Intelligence in Medicine*, vol. 63, no. 3, pp. 171–179, 2015.

[34] R. Mallick and S. Pramanik, "Pentapartitioned neutrosophic set and its properties," *Neutrosophic Sets and Systems*, vol. 36, 2020.

[35] N. Qiuping, T. Yuanxiang, S. Broumi, and V. Uluçay, "A parametric neutrosophic model for the solid transportation problem," *Management Decision*, vol. 61, no. 2, pp. 421–442, 2022.

[36] S. Debnath, "Neutrosophication of statistical data in a study to assess the knowledge, attitude and symptoms on reproductive tract infection among women," *Journal of Fuzzy Extension and Applications*, vol. 2, no. 1, pp. 33–40, 2021.

[37] K. Zhang, Y. Xie, S. A. Noorkhah, M. Imeni, and S. K. Das, "Neutrosophic management evaluation of insurance companies by a hybrid TODIM-BSC method: a case study in private insurance companies," *Management Decision*, vol. 61, no. 2, pp. 363–381, 2022.

[38] I. M. Hezam, A. R. Mishra, P. Rani, A. Saha, F. Smarandache, and D. Pamucar, "An integrated decision support framework using single-valued neutrosophic-MASWIP-COPRAS for sustainability assessment of bioenergy production technologies," *Expert Systems with Applications*, vol. 211, Article ID 118674, 2023.

[39] G. Vashishtha, S. Chauhan, N. Yadav, A. Kumar, and R. Kumar, "A two-level adaptive chirp mode decomposition and tangent entropy in estimation of single-valued neutrosophic cross-entropy for detecting impeller defects in centrifugal pump," *Applied Acoustics*, vol. 197, Article ID 108905, 2022.

[40] A. E. Torkayesh, M. Tavana, and F. J. Santos-Arteaga, "A multi-distance interval-valued neutrosophic approach for social failure detection in sustainable municipal waste management," *Journal of Cleaner Production*, vol. 336, Article ID 130409, 2022.

[41] S. A. Edalatpanah, "Systems of neutrosophic linear equations," *Neutrosophic Sets and Systems*, vol. 33, pp. 92–104, 2020.

[42] S. A. Edalatpanah, "General non-square systems of linear equations in neutrosophic environment," in *Neutrosophic Theories in Communication*, F. Smarandache and S. Broumi, Eds., pp. 42–49, Nova Science Publishers, Inc, 2020.

[43] S. A. Edalatpanah, "Neutrosophic structured element," *Expert Systems*, vol. 37, no. 5, Article ID e12542, 2020.

Hindawi
Advances in Mathematical Physics
Volume 2023, Article ID 4430103, 10 pages
https://doi.org/10.1155/2023/4430103

Research Article

On the Characterization of Antineutrosophic Subgroup

Sudipta Gayen,[1] **S. A. Edalatpanah**,[2] **Sripati Jha**,[3] **and Ranjan Kumar**[4]

[1]*Centre for Data Science, Faculty of Engineering & Technology, Siksha 'O' Anusandhan (Deemed to be University), Odisha, India*
[2]*Department of Applied Mathematics, Ayandegan Institute of Higher Education, Tonekabon, Iran*
[3]*Department of Mathematics, National Institute of Technology Jamshedpur, Jharkhand, India*
[4]*School of Advanced Sciences, VIT-AP University, Amaravati AP, India*

Correspondence should be addressed to Ranjan Kumar; ranjank.nit52@gmail.com

Received 11 July 2022; Revised 28 December 2022; Accepted 10 April 2023; Published 17 May 2023

Academic Editor: Mohammad Mirzazadeh

This article gives some essential scopes to study the characterizations of the antineutrosophic subgroup and antineutrosophic normal subgroup. Again, several theories and properties have been mentioned which are essential for analyzing their mathematical framework. Moreover, their homomorphic properties have been discussed.

1. Introduction

Fuzzy set (FS) [1] theory was introduced to handle uncertain situations more precisely than crisp sets. But there may exist some complex uncertain situations for which even FS theory is insufficient. As a result, intuitionistic fuzzy set (IFS) [2] and neutrosophic set (NS) [3] theories evolved, where the latter is more capable of dealing with uncertainties. Apart from these, there exist several byproducts of these set theories, like interval-valued versions [4–6]; type-I, type-II, and type-III versions; and soft [7–9] and hard versions. Presently, these theories have been adopted by several researchers in different applied fields. Also, in several pure mathematical fields, these notions are being utilized. In abstract algebra, Rosenfeld [10] was the pioneer to do so. He defined and studied the characteristics of a fuzzy subgroup (FSG). Thereafter, Das [11] presented the concept of the level subgroup of a FSG and showed several beautiful relationships between them. Afterward, Anthony and Sherwood [12, 13] redefined FSG by applying general T-norms and defined function generated FSG and subgroup generated FSG. In 1984, Mukherjee and Bhattacharya [14] introduced normal versions of FSG and cosets. Furthermore, Biswas [15] established the concept of intuitionistic fuzzy subgroup (IFSG). Similarly, Çetkin and Aygün [16] developed the neutrosophic subgroup (NSG) and studied its homomorphic properties. They have also established some connections between an NSG and its level subgroup.

The concept of the antifuzzy subgroup (AFSG) [17] is a kind of dual to FSG. It was defined and characterized by Biswas in 1990. He has mentioned some relationships between FSG and AFSG and studied several other properties. Similarly, there is notion of the intuitionistic antifuzzy subgroup (IAFSG) [18], which was developed by Li et al. in 2009. They have also studied its homomorphic properties and established some connections with its intuitionistic fuzzy counterpart. Table 1 contains some contributions of various researchers involving different antialgebraic notions under uncertainty.

Hence, it is obvious that antiversions of FSG, IFSG, etc. have been adopted by different researchers for the anticipation of unique and impactful results. In neutrosophic group theory, so far, authors have discussed NSGs and some of their algebraic structures. But still, the antineutrosophic subgroup (ANSG) is undefined. Also, the relationship between NSG and ANSG are still unexplored. Hence, this can be a fruitful area which can generate some scope of future research. Based on the aforementioned gaps, the objectives of this paper are as follows:

(i) to introduce ANSG and investigate its algebraic features

(ii) to define the antineutrosophic normal subgroup (ANNSG) and explore its algebraic characteristics

Table 1: Desk research of different antialgebraic notions.

Author & references	Year	Contributions in various fields
Kim et al. [19]	2005	Introduced the concept of antifuzzy ideals of near-rings and investigated some of its properties.
Feng & Yao [20]	2012	Introduced (λ, μ)-antifuzzy subgroups and studied its properties.
Kausar [21]	2019	Introduced intuitionistic fuzzy normal subrings and intuitionistic anti fuzzy normal subrings over a nonassociative ring and studied their properties.
Ejegwa et al. [22]	2021	Studied antifuzzy multigroup and its characteristics.
Hoskova-Mayerova & Al Tahan [23]	2021	Introduced different operations on fuzzy multi-ideals of near-rings and defined antifuzzy multisubnear-rings of near-rings and study their properties.
Ahmad et al. [24]	2021	Defined kernel subgroup of a FSG and AFSG and presented several results involving them.
Kalaiarasi et al. [25]	2022	Studied the properties of γ-antifuzzy normal subgroup and γ-fuzzy normal subgroup and presented their application in gene mutation.
Hemabala & Kumar [26]	2022	Introduced and analyzed anti neutrosophic multifuzzy ideals of γ near-ring and studied their product.

(iii) to figure out the relationships between NSG and ANSG

(iv) to study several homomorphic attributes of ANSG and ANNSG

This article has been structured in the following manner. In Section 2, desk research of FSG, IFSG, and NSG and their normal versions are given. Also, antiversions of FSG and IFSG are discussed. In Section 3, the notions of ANSG and ANNSG are introduced along with some other essential definitions and theories are given. Finally, in Section 4, conclusion is given by mentioning some scopes of further research.

2. Preliminaries

Here, some elementary set theories under uncertainties are discussed which are required for our current study.

Definition 1 (see [1]). A FS λ of a crisp set V is defined as $\lambda : V \longrightarrow [0, 1]$.

Definition 2 (see [2]). An IFS γ of a crisp set V is defined as $\gamma = \{(r, t_\gamma(r), f_\gamma(r)) : r \in V\}$, where t_γ and f_γ are, respectively, known as the membership and nonmembership degrees.

Definition 3 (see [3]). A NS η of a crisp set V is defined as $\eta = \{(r, t_\eta(r), i_\eta(r), f_\eta(r)) : r \in V\}$, where $t_\eta, i_\eta,$ and f_η are, respectively, known as the truth, indeterminacy, and falsity degrees.

Definition 4 (see [1]). Let ψ be a FS of V. Then, the set $\psi_t = \{r \in V : \psi(r) \geq t\} \forall t \in [0, 1]$ is denoted as a level subset of ψ.

Definition 5 (see [17]). Let φ be a FS of V. Then, the set $\bar{\varphi}_t = \{r \in V : \varphi(r) \leq t\} \forall t \in [0, 1]$ is denoted as a lower level subset of φ.

Next, the notions of FSG, IFSG, NSG, and a few of their essential properties are addressed.

2.1. Fuzzy, Intuitionistic Fuzzy, and Neutrosophic Subgroup

Definition 6 (see [10]). For a classical group V, a FS ψ is denoted as a FSG iff $\forall m, r \in V$, the subsequent conditions are fulfilled:

(i) $\psi(m \cdot r) \geq \min \{\psi(m), \psi(r)\}$

(ii) $\psi(r^{-1}) \geq \psi(r)$

Theorem 7 (see [10]). *ψ is a FSG of V iff $\forall m, r \in V$ $\psi(mr^{-1}) \leq \min \{\psi(m), \psi(r)\}$.*

Proposition 8 (see [10]). *Homomorphic image and preimage of a FSG is a FSG.*

Theorem 9 (see [11]). *Let V be a classical group and $\psi \in FSG(V)$, then $\forall t \in [0, 1]$ with $\psi(e) \geq t$, ψ_t are classical subgroups of V.*

Theorem 10 (see [11]). *Let V be a classical group and $\forall t \in [0, 1]$ with $\psi(e) \geq t$, ψ_t are classical subgroups of V, then $\psi \in FSG(V)$.*

Definition 11 (see [11]). Let ψ be a FSG of a classical group V. Then, $\forall t \in [0, 1]$ and $\psi(e) \geq t$ the subgroups ψ_t are termed as level subgroups of ψ.

Definition 12 (see [15]). For a classical group V, an IFS $\gamma = \{(r, t_\gamma(r), f_\gamma(r)) : r \in V\}$ is denoted an IFSG iff $\forall m, r \in V$,

(i) $t_\gamma(m \cdot r) \geq \min \{t_\gamma(m), t_\gamma(r)\}$

(ii) $t_\gamma(r^{-1}) \geq t_\gamma(r)$

(iii) $f_\gamma(m \cdot r) \leq \max \{f_\gamma(m), f_\gamma(r)\}$

(iv) $f_\gamma(r^{-1}) \leq f_\gamma(r)$

Proposition 13 (see [15]). *For a classical group V, an IFS $\gamma = \{(m, t_\gamma(m), f_\gamma(m)): m \in V\}$ is an IFSG iff $\forall m, r \in V$*

(i) $t_\gamma(mr^{-1}) \geq \min\{t_\gamma(m), t_\gamma(r)\}$

(ii) $f_\gamma(mr^{-1}) \leq \max\{f_\gamma(m), f_\gamma(r)\}$

Theorem 14 (see [27]). *Let V and R be two classical groups and $l: V \longrightarrow R$ be a homomorphism. Also, let $\gamma \in IFSG(V)$ and $\gamma' \in IFSG(R)$. Then,*

(i) If γ has the supremum property, then $l(\gamma) \in IFSG(R)$

(ii) $l^{-1}(\gamma') \in IFSG(V)$

Definition 15 (see [27]). Let γ be an IFS of V and let $s_1, s_2 \in [0, 1]$ with $s_1 + s_2 \leq 1$. Then, the set $\gamma_{(s_1,s_2)} = \{m \in V : t_\gamma(m) \geq s_1 \& f_\gamma(m) \leq s_2\}$ is known as (s_1, s_2)-level set of γ.

Theorem 16 (see [27]). *Let V be a classical group and $\gamma \in IFSG(V)$. Then, $\forall s_1, s_2 \in [0, 1]$ with $t_\gamma(e) \geq s_1$ and $f_\gamma(e) \leq s_2$, $\gamma_{(s_1,s_2)}$ are classical subgroups of V.*

Theorem 17 (see [27]). *Let V be a classical group and $\forall s_1, s_2 \in [0, 1]$ with $t_\gamma(e) \geq s_1$ and $f_\gamma(e) \leq s_2$, $\gamma_{(s_1,s_2)}$ are classical subgroups of V. Then, $\gamma \in IFSG(V)$.*

Definition 18 (see [16]). For a classical group V, a NS δ is defined as an NSG of V iff the subsequent terms are fulfilled:

(i) $\delta(m \cdot r) \geq \min\{\delta(m), \delta(r)\}$, i.e., $t_\delta(m \cdot r) \geq \min\{t_\delta(m), t_\delta(r)\}$, $i_\delta(m \cdot r) \geq \min\{i_\delta(m), i_\delta(r)\}$ and $f_\delta(m \cdot r) \leq \max\{f_\delta(m), f_\delta(r)\}$

(ii) $\delta(m^{-1}) \geq \delta(m)$, i.e., $t_\delta(m^{-1}) \geq t_\delta(r)$, $i_\delta(m^{-1}) \geq i_\delta(r)$, and $f_\delta(m^{-1}) \leq f_\delta(r)$

A set of all the NSGs will be signified as $\mathrm{NSG}(V)$. Here, note that t_δ and i_δ are following Definition 6, i.e., they are FSGs of V whereas, f_δ is following Definition 24, i.e., it is an AFS of V.

Theorem 19 (see [16]). *For a classical group $V\delta \in NSG(V)$ iff $\forall m, r \in V$*

$$\delta\left(m \cdot r^{-1}\right) \geq \min\{\delta(m), \delta(r)\}, \tag{1}$$

i.e., $t_\delta(m \cdot r^{-1}) \geq \min\{t_\delta(m), t_\delta(r)\}$, $i_\delta(m \cdot r^{-1}) \geq \min\{i_\delta(m), i_\delta(r)\}$, *and* $f_\delta(m \cdot r^{-1}) \leq \max\{f_\delta(m), f_\delta(r)\}$.

Theorem 20 (see [16]). *$\delta \in NSG(V)$ iff the p-level sets $(t_\delta)_p$, $(i_\delta)_p$, and p-lower level set $(\bar{f}_\delta)_p$ are classical subgroups of $V\forall p \in [0, 1]$.*

Theorem 21 (see [16]). *Homomorphic image and preimage of any NSG is a NSG.*

Definition 22 (see [16]). For a classical group V, a neutrosophic δ is called an NNSG of V iff $\forall m, r \in V$

$$\delta\left(m \cdot r \cdot m^{-1}\right) \leq \delta(r), \tag{2}$$

i.e., $t_\delta(m \cdot r \cdot m^{-1}) \leq t_\delta(r)$, $i_\delta(m \cdot r \cdot m^{-1}) \leq i_\delta(r)$, and $f_\delta(m \cdot r \cdot m^{-1}) \geq f_\delta(r)$.

The set of all NNSG of V will be signified as $\mathrm{NNSG}(V)$. Also, notice that $\eta \in \mathrm{NNSG}(V)$ implies that t_δ and i_δ are fuzzy normal subgroups (FNSG) of V and f_δ is the antifuzzy normal subgroup (AFNSG) of V.

Theorem 23 (see [16]). *Homomorphic image and preimage of any NNSG is a NNSG.*

In the next segment, the notions of AFSG and IAFSG are discussed.

2.2. Antifuzzy Subgroup and Intuitionistic Antifuzzy Subgroup

Definition 24 (see [17]). For a classical group V, a FS φ is denoted as an AFSG of V if $\forall m, r \in V$, the subsequent terms are fulfilled:

(i) $\varphi(m \cdot r) \leq \max\{\varphi(m), \varphi(r)\}$

(ii) $\varphi(r^{-1}) \leq \varphi(r)$

Theorem 25 (see [17]). *φ is an AFSG of V iff $\forall m, r \in V$ $\varphi(mr^{-1}) \leq \max\{\varphi(m), \varphi(r)\}$.*

Proposition 26 (see [17]). *φ is a FSG of the group V iff its complement φ^c is an AFSG of V.*

Definition 27 (see [17]). Let φ be an AFSG of a group V. Then, $\forall t \in [0, 1]$ and $\varphi(e) \leq t$, the subgroups $\bar{\varphi}_t$ are called lower-level subgroups of φ.

Proposition 28 (see [17]). *Let φ be an AFSG of V. Then, $\forall t \in [0, 1]$ such that $t \geq \mu(e)$, $\overline{\varphi_t}$ are classical subgroups of V.*

Proposition 29 (see [17]). *Let φ be a FS of a classical group V such that $\bar{\varphi}_t$ is a classical subgroup of $V\forall t \in [0, 1]$ with $t \geq \mu(e)$. Then, μ is an AFSG of V.*

Definition 30 (see [28]). For a classical group V, an IFS $\gamma = \{(m, t_\gamma(m), f_\gamma(m)): m \in V\}$ is called an IAFSG of V iff $\forall m, r \in V$

(i) $t_\gamma(mr^{-1}) \leq \max\{t_\gamma(m), t_\gamma(r)\}$

(ii) $f_\gamma(mr^{-1}) \geq \min\{f_\gamma(m), f_\gamma(r)\}$

Proposition 31 (see [28]). *γ is a IFSG of the group V iff its complement γ^c is an IAFSG of V.*

Theorem 32 (see [28]). *$\gamma \in IFSG(V)$ iff $\forall s_1, s_2 \in [0, 1]$ with $t_\gamma(e) \geq s_1$ and $f_\gamma(e) \leq s_2$, (s_1, s_2)-level set of γ, i.e., $\gamma_{(s_1,s_2)}$ are classical subgroups of V.*

Theorem 33 (see [18]). *Homomorphic image and preimage of any IAFSG is a IAFSG.*

In the following section, the notions of ANSG and ANNSG have been introduced and some of their fundamental properties are discussed.

3. Antineutrosophic Subgroup

Definition 34. For a classical group V, a neutrosophic set η is called an ANSG of V iff the following terms are fulfilled:

(i) $\eta(m \cdot r) \leq \max\{\eta(m), \eta(r)\}$, i.e., $t_\eta(m \cdot r) \leq \max\{t_\eta(m), t_\eta(r)\}$, $i_\eta(m \cdot r) \leq \max\{i_\eta(m), i_\eta(r)\}$, and $f_\eta(m \cdot r) \geq \min\{f_\eta(m), f_\eta(r)\}$

(ii) $\eta(r^{-1}) \leq \eta(r)$, i.e., $t_\eta(r^{-1}) \leq t_\eta(r)$, $i_\eta(r^{-1}) \leq i_\eta(r)$, and $f_\eta(r^{-1}) \geq f_\eta(r)$

The set of all ANSGs will be signified as $\mathrm{ANSG}(V)$

Proposition 35. *$\eta \in ANSG(V)$ iff t_η and i_η are AFSGs of V and f_η is FSG of V.*

Proof. Let $\eta \in \mathrm{ANSG}(V)$ then from Definition 34, it is evident that t_η and i_η are following Definition 24, i.e., they are AFSGs of V. Whereas f_η is following Definition 6, i.e., it is a FSG of V. Again, if t_η and i_η are AFSGs of V and f_η is a FSG of V then $\eta \in \mathrm{ANSG}(V)$. □

Example 36. Let $V = \{1, i, -1, -i\}$ be a classical group of order 4 and η be a neutrosophic set of V, where the memberships of truth (t_η), indeterminacy (i_η), and falsity (f_η) of elements in η are given in Figure 1.
Notice that t_η and i_η are following Definition 24, i.e., are AFSGs of V. Again, f_η is following Definition 6, i.e., is a FSG of V. Hence, η is an ANSG of V.

Example 37. Let $V = \{a, e\}$ be a classical group of order 2 and η be a NS of V, where considering $\theta \in [\pi/4, \pi/2]$, let $\eta = \{(a, \sin\theta/2, \sin\theta/4, (\sin\theta + \cos\theta)/2), (e, \cos\theta/2, \cos\theta/4, (\sin\theta + \cos\theta)/2)\}$. In Figures 2 and 3, memberships of a and e have been described graphically.

Here, η is following Definition 34 and hence it is an ANSG.

Theorem 38. *Let $\eta \in ANSG(V)$ where V is a classical group. Then, $\forall r \in V$*

(i) $\eta(r^{-1}) = \eta(r)$

(ii) $\eta(e) \leq \eta(r)$, where e is the neutral element of V

Proof.

(i) Here, f_η is a FSG and both t_η and i_η are AFSGs of V, by Definition 6. So, $f_\eta(r) = f_\eta((r^{-1})^{-1}) \geq f_\eta(r^{-1})$ and hence $f_\eta(r^{-1}) = f_\eta(r)$. Again, from Definition 24, $t_\eta(r^{-1}) \leq t_\eta(r)$. So, $t_\eta(r) = t_\eta((r^{-1})^{-1}) \leq t_\eta(r^{-1})$ and hence $t_\eta(r^{-1}) = t_\eta(r)$. Similarly, using Definition 24, we can prove $i_\eta(r^{-1}) = i_\eta(r)$. So, $\eta(r^{-1}) = \eta(r)$

(ii) Using Definition 6, we have $f_\eta(e) = f_\eta(r \cdot r^{-1}) \geq \min\{f_\eta(r), f_\eta(r^{-1})\} = f_\eta(r)$. Again, using Definition 24,

$$t_\eta(e) = t_\eta\left(r \cdot r^{-1}\right) \leq \max\left\{t_\eta(r), t_\eta\left(r^{-1}\right)\right\} = t_\eta(r).$$

Similarly, using Definition 24, we have

$$i_\eta(e) = i_\eta\left(r \cdot r^{-1}\right) \leq \max\left\{i_\eta(r), i_\eta\left(r^{-1}\right)\right\} = i_\eta(r).$$

Hence, $\eta(e) \leq \eta(r)$

□

Theorem 39. *$\eta \in ANSG(V)$ iff $\forall m, r \in V$ $\eta(m \cdot r^{-1}) \leq \max\{\eta(m), \eta(r)\}$.*

Proof. Let $\eta \in \mathrm{ANSG}(V)$. Then, by Definition 34, we have $\eta(m \cdot r^{-1}) \leq \max\{\eta(m), \eta(r^{-1})\}$. Again, by Definition 34, $\eta(r^{-1}) = \eta(r)$ and hence

$$\eta\left(m \cdot r^{-1}\right) \leq \max\left\{\eta(m), \eta\left(r^{-1}\right)\right\} = \max\{\eta(m), \eta(r)\}. \quad (3)$$

Conversely, let $\eta(m \cdot r^{-1}) \leq \max\{\eta(m), \eta(r)\}$. So,

$$\begin{aligned} t_\eta\left(m \cdot r^{-1}\right) &\leq \max\left\{t_\eta(m), t_\eta(r)\right\}, \\ i_\eta\left(m \cdot r^{-1}\right) &\leq \max\left\{i_\eta(m), i_\eta(r)\right\}, \\ f_\eta\left(m \cdot r^{-1}\right) &\geq \min\left\{f_\eta(m), f_\eta(r)\right\}. \end{aligned} \quad (4)$$

Notice that,

$$\begin{aligned} t_\eta\left(r^{-1}\right) = t_\eta\left(e \cdot r^{-1}\right) &\leq \max\left\{t_\eta(e), t_\eta(r)\right\} = \max\left\{t_\eta\left(r \cdot r^{-1}\right), t_\eta(r)\right\} \\ &\leq \max\left\{t_\eta(r), t_\eta(r), t_\eta(r)\right\} = t_\eta(r). \end{aligned} \quad (5)$$

Similarly, $i_\eta(r^{-1}) \leq i_\eta(r)$ and $f_\eta(r^{-1}) \geq f_\eta(r)$.
Again,

$$\begin{aligned} t_\eta(m \cdot r) = t_\eta\left(m \cdot \left(r^{-1}\right)^{-1}\right) &\leq \max\left\{i_\eta(m), i_\eta\left(r^{-1}\right)\right\} \\ &\leq \max\left\{i_\eta(m), i_\eta(r)\right\}. \end{aligned} \quad (6)$$

Similarly, $i_\eta(m \cdot r) \leq \max\{i_\eta(m), i_\eta(r)\}$ and $f_\eta(m \cdot r) \geq$

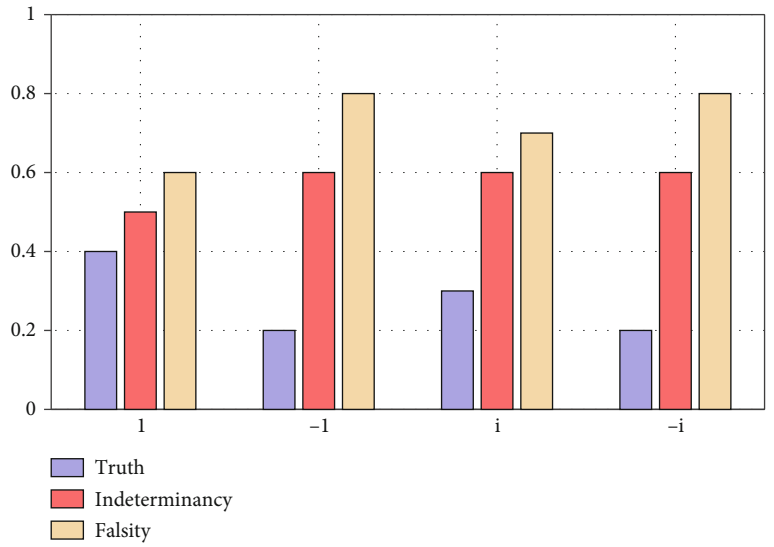

Figure 1: Memberships of elements in η.

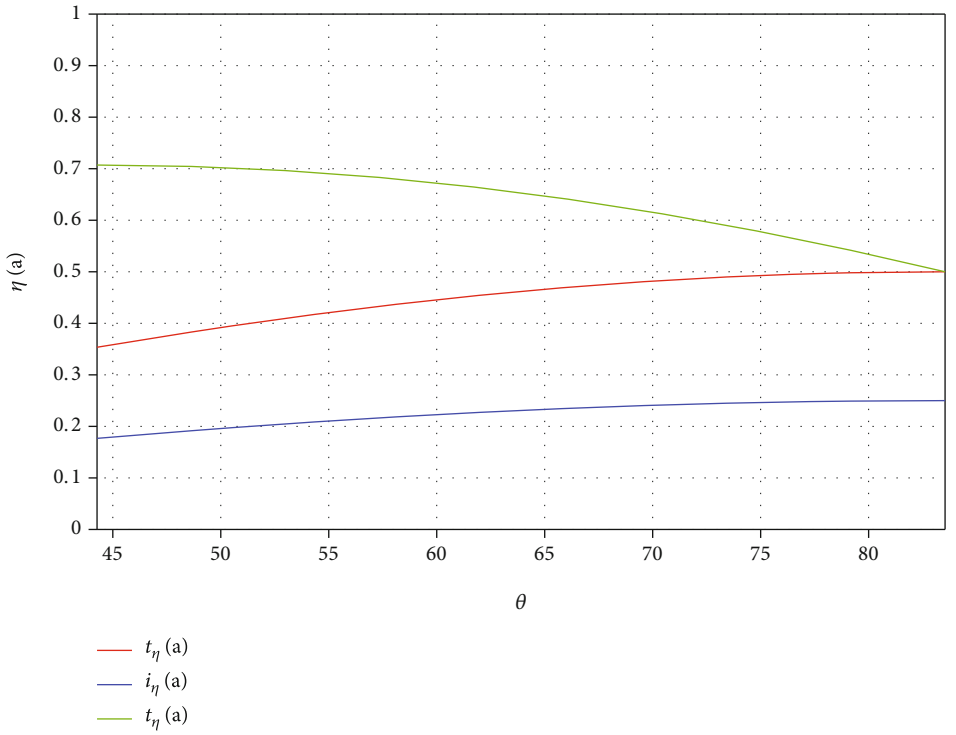

Figure 2: Memberships of elements in a.

min $\{f_\eta(m), f_\eta(r)\}$ can be proved. Hence, η satisfies Definition 34, i.e., $\eta \in \mathrm{ANSG}(V)$. □

Theorem 40. *$\eta \in ANSG(V)$ iff $\eta^c \in NSG(V)$.*

Proof. If we take the complement of η, i.e., η^c then corresponding degree of truth and degree of falsity will interchange their positions in η^c. Also, the degree of indeterminacy will have its complement, i.e., $i_\eta^c = 1 - i_\eta$. In other words, if

$$\begin{aligned}\eta &= \left\{\left(r, t_\eta(r), i_\eta(r), f_\eta(r)\right): r \in V\right\} \text{ then } \eta^c \\ &= \left\{\left(r, f_\eta(r), i_\eta^c(r), t_\eta(r)\right): r \in V\right\}.\end{aligned} \tag{7}$$

Let $\eta \in \mathrm{ANSG}(V)$ then by Proposition 35 t_η and i_η are AFSGs of V and f_η is FSG of V. So, in case of η^c, f_η and i_η^c

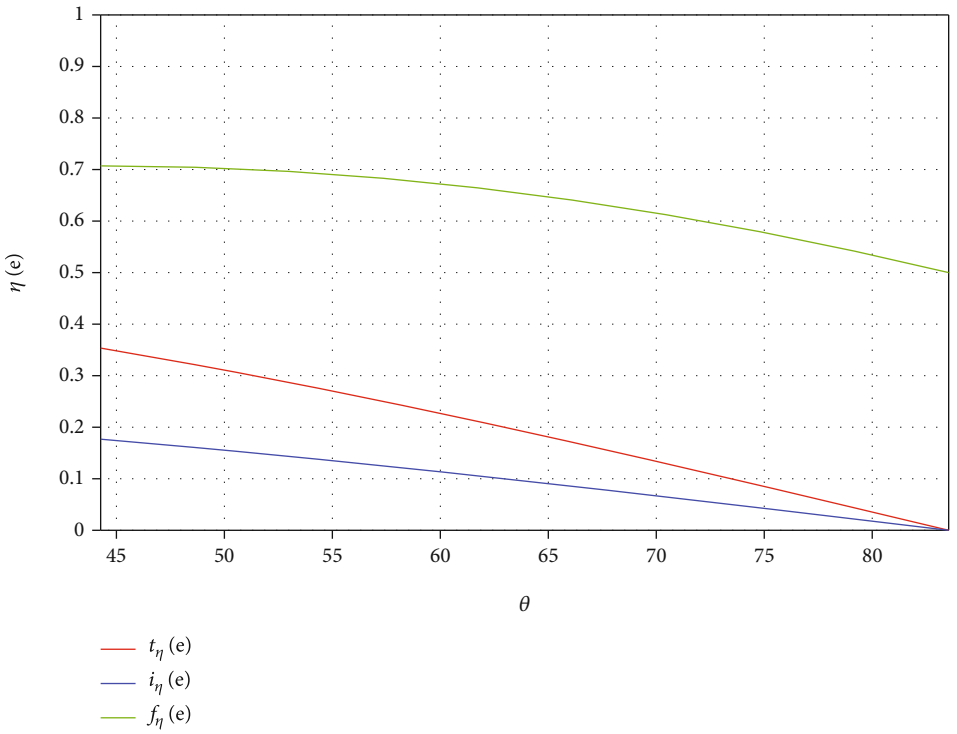

Figure 3: Memberships of elements in e.

will become FSGs and t_η will become AFS of V. Hence, they will follow Definition 18, i.e., $\eta^c \in \mathrm{NSG}(V)$. Similarly, the converse part can also be proved. □

Example 41. Let $(\mathbb{Z}_4, +)$ be the group of integers modulo 4 with usual addition and $\eta = \{(r, t_\eta(r), i_\eta(r), f_\eta(r)) : r \in \mathbb{Z}_4\}$ is a NS of $\mathbb{Z}_4$, where t_η, i_η and f_η are mentioned in Table 2.

According to Definition 34, η is an ANSG of $\mathbb{Z}_4$.

Now $\eta^c = \{(r, t_{\eta^c}(r), i_{\eta^c}(r), f_{\eta^c}(r)) : r \in \mathbb{Z}_4\}$, where t_{η^c}, i_{η^c}, and f_{η^c} are mentioned in Table 3.

Here, according to Definition 18, η^c is a NSG of $\mathbb{Z}_4$.

Theorem 42. *$\eta \in ANSG(V)$ iff the p-lower level sets $(\bar{t}_\eta)_p$, $(\bar{i}_\eta)_p$, and p-level set $(f_\eta)_p$ are classical subgroups of V $\forall p \in [0, 1]$.*

Proof. Let $\eta \in \mathrm{ANSG}(V)$, $p \in [0, 1]$ and $m, r \in (\bar{t}_\eta)_p$. Then, $t_\eta(m) \le p$ and $t_\eta(r) \le p$. Since $\eta \in \mathrm{ANSG}(V)$, we have $t_\eta(m \cdot r^{-1}) \le \max\{t_\eta(m), t_\eta(r)\} \le p$ and hence $m \cdot r^{-1} \in (\bar{t}_\eta)_p$. Similarly, it can be shown that $m \cdot r^{-1} \in (\bar{i}_\eta)_p$ and $m \cdot r^{-1} \in (f_\eta)_p$. So, $(\bar{t}_\eta)_p$, $(\bar{i}_\eta)_p$, and $(f_\eta)_p$ are classical subgroups of V.

Conversely, let $\forall p \in [0, 1] (\bar{t}_\eta)_p$ is a classical subgroup of V. Let $m, r \in V$ such that $t_\eta(m) = p_1$ and $t_\eta(r) = p_2$ for some $p_1, p_2 \in [0, 1]$. Then, $m \in (\bar{t}_\eta)_{p_1}$ and $r \in (\bar{t}_\eta)_{p_2}$.

Table 2: Membership values of elements belonging to η.

η	t_η	i_η	f_η
$\bar{0}$	0.66	0.31	0.78
$\bar{1}$	0.85	0.35	0.59
$\bar{2}$	0.72	0.32	0.67
$\bar{3}$	0.85	0.35	0.59

Table 3: Membership values of elements belonging to η^c.

η^c	t_{η^c}	i_{η^c}	f_{η^c}
$\bar{0}$	0.78	0.69	0.66
$\bar{1}$	0.59	0.65	0.85
$\bar{2}$	0.67	0.68	0.72
$\bar{3}$	0.59	0.65	0.85

Let $p_1 \le p_2$. Then, $m, r \in (\bar{t}_\eta)_{p_2}$ and hence $mu^{-1} \in (\bar{t}_\eta)_{p_2}$. So, $t_\eta(mr^{-1}) \le p_2 \le \max\{t_\eta(m), t_\eta(r)\}$, i.e., t_η is an AFSG of V. Similarly, it can be proved that i_η is an AFSG and f_η is a FSG of V. So, $\eta \in \mathrm{ANSG}(V)$. □

Theorem 43. *Intersection of any two ANSG of any group is an ANSG.*

Proof. Let $\eta_1, \eta_2 \in \mathrm{ANSG}(V)$. To prove this, using Theorem 39, we can show that

$$\begin{aligned}
&(\eta_1 \cap \eta_2)\left(m \cdot r^{-1}\right) \le \max\{(\eta_1 \cap \eta_2)(m), (\eta_1 \cap \eta_2)(r)\}, \text{i.e.,}\\
&t_{(\eta_1\cap\eta_2)}\left(m \cdot r^{-1}\right) \le \max\left\{t_{(\eta_1\cap\eta_2)}(m), t_{(\eta_1\cap\eta_2)}(r)\right\},\\
&i_{(\eta_1\cap\eta_2)}\left(m \cdot r^{-1}\right) \le \max\left\{i_{(\eta_1\cap\eta_2)}(m), i_{(\eta_1\cap\eta_2)}(r)\right\},\\
&f_{(\eta_1\cap\eta_2)}\left(m \cdot r^{-1}\right) \ge \min\left\{f_{(\eta_1\cap\eta_2)}(m), f_{(\eta_1\cap\eta_2)}(r)\right\}.
\end{aligned} \tag{8}$$

Here,

$$\begin{aligned}
t_{(\eta_1\cap\eta_2)}\left(m \cdot r^{-1}\right) &= \max\left\{t_{\eta_1}\left(m \cdot r^{-1}\right), t_{\eta_2}\left(m \cdot r^{-1}\right)\right\}\\
&\le \max\left\{\max\left\{t_{\eta_1}(m), t_{\eta_1}(r)\right\}, \max\left\{t_{\eta_2}(m), t_{\eta_2}(r)\right\}\right\}\\
&= \max\left\{\max\left\{t_{\eta_1}(m), t_{\eta_2}(m)\right\}, \max\left\{t_{\eta_1}(r), t_{\eta_2}(r)\right\}\right\}\\
&= \max\left\{t_{(\eta_1\cap\eta_2)}(m), t_{(\eta_1\cap\eta_2)}(r)\right\}.
\end{aligned} \tag{9}$$

Similarly, we can show that

$$i_{(\eta_1\cap\eta_2)}\left(m \cdot r^{-1}\right) \le \max\left\{i_{(\eta_1\cap\eta_2)}(m), i_{(\eta_1\cap\eta_2)}(r)\right\}. \tag{10}$$

Again,

$$\begin{aligned}
f_{(\eta_1\cap\eta_2)}\left(m \cdot r^{-1}\right) &= \min\left\{f_{\eta_1}\left(m \cdot r^{-1}\right), f_{\eta_2}\left(m \cdot r^{-1}\right)\right\}\\
&\ge \min\left\{\min\left\{f_{\eta_1}(m), f_{\eta_1}(r)\right\}, \min\left\{f_{\eta_2}(m), f_{\eta_2}(r)\right\}\right\}\\
&= \min\left\{\min\left\{f_{\eta_1}(m), f_{\eta_2}(m)\right\}, \min\left\{f_{\eta_1}(r), f_{\eta_2}(r)\right\}\right\}\\
&= \min\left\{f_{(\eta_1\cap\eta_2)}(m), f_{(\eta_1\cap\eta_2)}(r)\right\}.
\end{aligned} \tag{11}$$

Hence, $\eta_1 \cap \eta_2 \in \mathrm{ANSG}(V)$. □

Theorem 44. *Homomorphic image of any ANSG is an ANSG.*

Proof. Let U_1 and U_2be two classical groups and $s : U_1 \longrightarrow U_2$ be a homomorphism. Let $\eta \in \mathrm{ANSG}(U_1)$. Then, $\forall\, m_1, m_2 \in U_1$, we have

$$\begin{aligned}
t_\eta\left(m_1 \cdot {m_2}^{-1}\right) &\le \max\left\{t_\eta(m_1), t_\eta(m_2)\right\},\\
i_\eta\left(m_1 \cdot {m_2}^{-1}\right) &\le \max\left\{i_\eta(m_1), i_\eta(m_2)\right\},\\
f_\eta\left(m_1 \cdot {m_2}^{-1}\right) &\ge \min\left\{f_\eta(m_1), f_\eta(m_2)\right\}.
\end{aligned} \tag{12}$$

Here, we have to show that $s(\eta)$ is an ANSG of U_2.

Let $\exists n_1, n_2 \in U_2$ such that $n_1 = s(m_1)$ and $n_2 = s(m_2)$. Now, as s is a group homomorphism, we have

$$\begin{aligned}
s\left(t_\eta\right)\left(n_1 \cdot n_2^{-1}\right) &= \min_{m \in s^{-1}\left(n_1 \cdot n_2^{-1}\right)} t_\eta(m) \le t_\eta\left(m_1 \cdot m_2^{-1}\right)\\
&\le \max\left\{t_\eta(m_1), t_\eta(m_2)\right\}.
\end{aligned} \tag{13}$$

Again, $s(t_\eta)(n_1) = \min_{m \in s^{-1}(n_1)} t_\eta(m) \le t_\eta(m_1)$. Where-from $\max s(t_\eta)(n_1) = t_\eta(m_1)$ and hence,

$$\begin{aligned}
s\left(t_\eta\right)\left(n_1 \cdot n_2^{-1}\right) &\le \max\left\{t_\eta(m_1), t_\eta(m_2)\right\}\\
&= \max\left\{\max s\left(t_\eta\right)(n_1), \max s\left(t_\eta\right)(n_2)\right\}\\
&= \max\left\{s\left(t_\eta\right)(n_1), s\left(t_\eta\right)(n_2)\right\}.
\end{aligned} \tag{14}$$

Similarly, it can be shown that $s(i_\eta)(n_1 \cdot n_2^{-1}) \le \max\{s(i_\eta)(n_1), s(i_\eta)(n_2)\}$.

Also,

$$\begin{aligned}
s\left(f_\eta\right)\left(n_1 \cdot n_2^{-1}\right) &= \max_{m \in s^{-1}\left(n_1 \cdot n_2^{-1}\right)} f_\eta(m) \ge f_\eta\left(m_1 \cdot m_2^{-1}\right)\\
&\ge \min\left\{f_\eta(m_1), f_\eta(m_2)\right\}.
\end{aligned} \tag{15}$$

Again $s(f_\eta)(n_1) = \max_{m \in s^{-1}(n_1)} f_\eta(m) \ge t_\eta(m_1)$. Where-from $\min s(f_\eta)(n_1) = f_\eta(m_1)$ and hence

$$\begin{aligned}
s\left(f_\eta\right)\left(n_1 \cdot n_2^{-1}\right) &\ge \min\left\{f_\eta(m_1), f_\eta(m_2)\right\}\\
&= \min\left\{\min s\left(f_\eta\right)(n_1), \min s\left(f_\eta\right)(n_2)\right\}\\
&= \min\left\{s\left(f_\eta\right)(n_1), s\left(f_\eta\right)(n_2)\right\}.
\end{aligned} \tag{16}$$

So, $s(\eta)$ is an ANSG of U_2. □

Theorem 45. *Homomorphic preimage of any ANSG is an ANSG.*

Proof. Let U_1 and U_2 be two classical groups and $s : U_1 \longrightarrow U_2$ be a homomorphism. Let $\delta \in \mathrm{ANSG}(U_2)$. Then, $\forall\, n_1, n_2 \in U_2$, we have

$$\begin{aligned}
t_\delta\left(n_1 \cdot {n_2}^{-1}\right) &\le \max\left\{t_\delta(n_1), t_\delta(n_2)\right\},\\
i_\delta\left(n_1 \cdot {n_2}^{-1}\right) &\le \max\left\{i_\delta(n_1), i_\delta(n_2)\right\},\\
f_\delta\left(n_1 \cdot {n_2}^{-1}\right) &\ge \min\left\{f_\delta(n_1), f_\delta(n_2)\right\}.
\end{aligned} \tag{17}$$

Here, we have to show that $s^{-1}(\delta)$ is an ANSG of U_1.

Let $m_1, m_2 \in U_1$. Since s is a group homomorphism,

$$\begin{aligned} s^{-1}(t_\delta)\left(m_1 \cdot m_2^{-1}\right) &= t_\delta\left(s\left(m_1 \cdot m_2^{-1}\right)\right) = t_\delta\left(s(m_1) \cdot s\left(m_2^{-1}\right)\right) \\ &= t_\delta\left(s(m_1) \cdot s(m_2)^{-1}\right) \le \max\left\{t_\delta(s(m_1)), t_\delta(s(m_2))\right\} \\ &= \max\left\{s^{-1}(t_\delta(m_1)), s^{-1}(t_\delta(m_2))\right\}. \end{aligned} \tag{18}$$

Similarly, we can show that

$$\begin{aligned} s^{-1}(i_\delta)\left(m_1 \cdot m_2^{-1}\right) &\le \max\left\{s^{-1}(i_\delta(m_1)), s^{-1}(i_\delta(m_2))\right\}, \\ s^{-1}(f_\delta)\left(m_1 \cdot m_2^{-1}\right) &\ge \min\left\{s^{-1}(f_\delta(m_1)), s^{-1}(f_\delta(m_2))\right\}. \end{aligned} \tag{19}$$

Hence, $s^{-1}(\delta)$ is an ANSG of U_1. □

Theorem 46. *Let $\eta \in ANSG(V)$ and l be a homomorphism on V. Let $\eta^{-1} : V \longrightarrow [0,1] \times [0,1] \times [0,1]$ is defined as $\eta^{-1}(r) = \eta(r^{-1})$ for any $r \in V$ then $\eta^{-1} \in ANSG(V)$ and $(l(\eta))^{-1} = l(\eta^{-1})$.*

Proof. Here,

$$\begin{aligned} \eta^{-1}\left(m \cdot r^{-1}\right) &= \eta\left(m \cdot r^{-1}\right)^{-1} = \eta\left(\left(r^{-1}\right)^{-1} \cdot m^{-1}\right) \\ &= \eta\left(r \cdot m^{-1}\right) \le \max\left\{\eta(r), \eta\left(m^{-1}\right)\right\} \\ &= \max\left\{\eta\left(r^{-1}\right), \eta\left(m^{-1}\right)\right\} [\text{as } \eta \text{ is an ANSG}] \\ &= \max\left\{\eta^{-1}(m), \eta^{-1}(r)\right\}. \end{aligned} \tag{20}$$

Hence, by Theorem 39, $\eta^{-1} \in \text{ANSG}(V)$.

Again, notice that,

$$\begin{aligned} l\left(t_\eta\right)^{-1}(q) &= l\left(t_\eta\right)\left(q^{-1}\right) = l\left(t_\eta\right)(q) \left[\text{as } l\left(t_\eta\right) \text{ is an ANSG}\right] \\ &= \min_{m \in l^{-1}(q)} t_\eta(m) = \min_{m \in l^{-1}(q)} t_\eta\left(m^{-1}\right) = \min_{m \in l^{-1}(q)} t_{\eta^{-1}}(m) \\ &= l\left(t_{\eta^{-1}}\right)(q). \end{aligned} \tag{21}$$

Similarly, it can be shown that $l(i_\eta)^{-1} = l(i_{\eta^{-1}})$ and $l(f_\eta)^{-1} = l(f_{\eta^{-1}})$.

Hence, $(l(\eta))^{-1} = l(\eta^{-1})$ □

Theorem 47. *Let $\eta \in ANSG(V)$ and l be an isomorphism on V, then $l^{-1}(l(\eta)) = \eta$.*

Proof. Here

$$l^{-1}\left(l\left(t_\eta\right)\right)(p) = l\left(t_\eta\right)(l(p)) = \min_{m \in l^{-1}(l(p))} t_\eta(m) = t_\eta(p). \tag{22}$$

Similarly, it can be shown that $l^{-1}(l(i_\eta)) = i_\eta$ and $l^{-1}(l(f_\eta)) = f_\eta$.

Hence, $l^{-1}(l(\eta)) = \eta$. □

In the next segment, ANNSG has been introduced. Also, its homomorphic characteristics are mentioned.

3.1. Antineutrosophic Normal Subgroup

Definition 48. For a classical group V, a neutrosophic set η is called an ANNSG of V iff $\forall m, r \in V \eta(m \cdot r \cdot m^{-1}) \le \eta(r)$, i.e., $t_\eta(m \cdot r \cdot m^{-1}) \le t_\eta(r)$, $i_\eta(m \cdot r \cdot m^{-1}) \le i_\eta(r)$, and $f_\eta(m \cdot r \cdot m^{-1}) \ge f_\eta(r)$.

The set of all ANNSGs of V will be signified as ANNSG(V).

Example 49. Let $V = \{e, m, r, mr\}$ be the Klien's 4-group and $\eta = \{(r, t_\eta(r), i_\eta(r), f_\eta(r)) : r \in V\}$ is a NS of V, where t_η, i_η, and f_η are mentioned in Table 4.

Here, η follows Definition 48, i.e., it is an ANNSG.

Proposition 50. *$\eta \in ANNSG(V)$ iff t_η and i_η are AFNSs of V and f_η is FNS of V.*

Proof. Using Definition 48, this can be observed. □

Theorem 51. *Intersection of any two ANNSG of any group is an ANNSG.*

Proof. Using Theorem 43, this can be proved. □

Theorem 52. *Let $\eta \in ANNSG(V)$. Then, the subsequent conditions are equivalent:*

(i) $\eta \in ANNS(U)$

(ii) $\eta(m \cdot r \cdot m^{-1}) = \eta(r)$, $\forall m, r \in V$

(iii) $\eta(m \cdot r) = \eta(V \cdot m)$, $\forall m, r \in V$

Proof. Let (i) be true. Then, by Definition 48, we have $\eta(m \cdot r \cdot m^{-1}) \le \eta(r)$, i.e., $t_\eta(m \cdot r \cdot m^{-1}) \le t_\eta(r)$, $i_\eta(m \cdot r \cdot m^{-1}) \le i_\eta(r)$, and $f_\eta(m \cdot r \cdot m^{-1}) \ge f_\eta(r)$.

To prove (ii), we need to show

$$\begin{aligned} t_\eta\left(m \cdot r \cdot m^{-1}\right) &\ge t_\eta(r), \\ i_\eta\left(m \cdot r \cdot m^{-1}\right) &\ge i_\eta(r), \\ f_\eta\left(m \cdot r \cdot m^{-1}\right) &\le f_\eta(r). \end{aligned} \tag{23}$$

In other words, we need to prove

$$\begin{aligned} t_\eta\left(m \cdot r \cdot m^{-1}\right) &= t_\eta(r), \\ i_\eta\left(m \cdot r \cdot m^{-1}\right) &= i_\eta(r), \\ f_\eta\left(m \cdot r \cdot m^{-1}\right) &= f_\eta(r). \end{aligned} \tag{24}$$

Table 4: Membership values of elements belonging to η.

η	t_η	i_η	f_η
e	0.1	0.5	0.9
a	0.3	0.6	0.7
b	0.4	0.5	0.6
ab	0.4	0.3	0.6

Notice that

$$t_\eta\left(m^{-1}\cdot r\cdot m\right)=t_\eta\left(m^{-1}\cdot r\cdot\left(m^{-1}\right)^{-1}\right)\le t_\eta(r). \tag{25}$$

Again,

$$t_\eta(r)=t_\eta\left(m^{-1}\cdot\left(m\cdot r\cdot m^{-1}\right)\cdot m\right)\le t_\eta\left(m\cdot r\cdot m^{-1}\right). \tag{26}$$

Hence, $t_\eta(m\cdot r\cdot m^{-1})=t_\eta(r)$.

Similarly, it can be shown that $i_\eta(m\cdot r\cdot m^{-1})=i_\eta(r)$ and $f_\eta(m\cdot r\cdot m^{-1})=f_\eta(r)$. Hence (i)⇒(ii).

Let condition (ii) be true. In (ii), substituting r in place of $r\cdot m^{-1}$ (iii) can easily be proved. So, (ii)⇒(iii).

Let condition (iii) be true. Applying $\eta(m\cdot r)=\eta(r\cdot m)$ in $t_\eta(m\cdot r\cdot m^{-1})$, we have

$$t_\eta\left(m\cdot r\cdot m^{-1}\right)=t_\eta\left(r\cdot m^{-1}\cdot m\right)=t_\eta(r)\le t_\eta(r). \tag{27}$$

So, (iii) ⇒ (i). □

Theorem 53. *$\eta\in ANNSG(V)$ iff the p-lower level sets $(\bar{t}_\eta)_p$, $(\bar{i}_\eta)_p$, and p-level set $(f_\eta)_p$ are classical normal subgroups of $V\forall p\in[0,1]$.*

Proof. Using Theorem 42, this can be proved. □

Theorem 54. *Let $\eta\in ANNSG(V)$. The set $U_\eta=\{m\in V:\eta(m)=\eta(e)\}$ is a classical normal subgroup of V, where e is the identity element of V.*

Proof. Since $\eta\in\mathrm{ANNSG}(V)$, we have $\eta\in\mathrm{ANSG}(V)$. Let $m, r\in U_\eta$ then by Theorem 39

$$\eta\left(m\cdot r^{-1}\right)\le\max\{\eta(m),\eta(r)\}=\max\{\eta(e),\eta(e)\}=\eta(e). \tag{28}$$

Again, by Theorem 38, we have $\eta(m\cdot r^{-1})\ge\eta(e)$ and hence $\eta(m\cdot r^{-1})=\eta(e)$, i.e., $m\cdot r^{-1}\in U_\eta$. Since $\eta\in\mathrm{ANNSG}(V)$, we have

$$\eta\left(m\cdot r\cdot m^{-1}\right)=\eta\left(r\cdot m\cdot m^{-1}\right)=\eta(r)=\eta(e), \tag{29}$$

i.e., $m\cdot r\cdot m^{-1}\in U_\eta$ or U_η is a normal subgroup of V. □

Theorem 55. *Let $\eta\in ANNSG(V)$ and l be a homomorphism on V. Then, the homomorphic pre-image of η, i.e., $l^{-1}(\eta)\in ANNSG(V)$.*

Proof. Using Theorem 44, we have $l^{-1}(\eta)\in\mathrm{ANSG}(V)$. Then, by Proposition 50, we can easily prove normality of $l^{-1}(\eta)$. Hence, $l^{-1}(\eta)\in\mathrm{ANNSG}(V)$. □

Theorem 56. *Let $\eta\in ANNSG(V)$ and l be a surjective homomorphism on V. Then the homomorphic image of η, i.e., $l(\eta)\in ANNSG(V)$.*

Proof. Using Theorem 44, we have $l(\eta)\in\mathrm{ANSG}(V)$. Again, by Proposition 50, the normality condition can easily be proved. So, $l(\eta)\in\mathrm{ANNSG}(V)$. □

4. Conclusion

The studies of ANSG and its normal version might open some new directions of research. Here, homomorphism has been introduced in ANSG and ANNSG to understand their algebraic characteristics. Moreover, connections with their nonantiversions are provided. For these, numerous examples, theories, and propositions are given. In the future, these studies can be further extended by introducing various notions like the antineutrosophic ideal, antineutrosophic ring, antineutrosophic field, and antineutrosophic topological space. Furthermore, their interval-valued versions can be introduced and studied.

Data Availability

This work is a contribution towards the theoretical development of fuzzy algebra and its generalizations. The data that support the findings of this study are not publicly available due to the fact that they were created specifically for this study. We have not used any additional data set for drafting this manuscript.

Conflicts of Interest

The authors declare that they have no conflicts of interest.

References

[1] L. A. Zadeh, "Fuzzy sets," *Information and Control*, vol. 8, no. 3, pp. 338–353, 1965.

[2] K. T. Atanassov, "Intuitionistic fuzzy sets," *Fuzzy Sets and Systems*, vol. 20, no. 1, pp. 87–96, 1986.

[3] F. Smarandache, "Neutrosophic set - a generalization of the intuitionistic fuzzy set," *International Journal of Pure and Applied Mathematics*, vol. 24, no. 3, pp. 287–297, 2005.

[4] L. A. Zadeh, "The concept of a linguistic variable and its application to approximate reasoning–I," *Information Sciences*, vol. 8, no. 3, pp. 199–249, 1975.

[5] K. T. Atanassov, "Interval valued intuitionistic fuzzy sets," in *Intuitionistic Fuzzy Sets: Theory and Applications*, pp. 139–177, Springer, 1999.

[6] H. Wang, F. Smarandache, Y. Q. Zhang, and R. Sunderraman, *Interval Neutrosophic Sets and Logic: Theory and Applications in Computing*, vol. 5, Infinite Study, 2005.

[7] P. Majumdar and S. K. Samanta, "Generalised fuzzy soft sets," *Computers & Mathematics with Applications*, vol. 59, no. 4, pp. 1425–1432, 2010.

[8] P. K. Maji, "More on intuitionistic fuzzy soft sets," in *International Workshop on Rough Sets, Fuzzy Sets, Data Mining, and Granular-Soft Computing*, Springer, 2009.

[9] P. K. Maji, "Neutrosophic Soft Set," *Annals of Fuzzy Mathematics and Informatics*, vol. 5, no. 1, pp. 157–168, 2013.

[10] A. Rosenfeld, "Fuzzy groups," *Journal of Mathematical Analysis and Applications*, vol. 35, no. 3, pp. 512–517, 1971.

[11] P. S. Das, "Fuzzy groups and level subgroups," *Journal of Mathematical Analysis and Applications*, vol. 84, no. 1, pp. 264–269, 1981.

[12] J. M. Anthony and H. Sherwood, "Fuzzy groups redefined," *Journal of Mathematical Analysis and Applications*, vol. 69, no. 1, pp. 124–130, 1979.

[13] J. M. Anthony and H. Sherwood, "A characterization of fuzzy subgroups," *Fuzzy Sets and Systems*, vol. 7, no. 3, pp. 297–305, 1982.

[14] N. P. Mukherjee and P. Bhattacharya, "Fuzzy normal subgroups and fuzzy cosets," *Information Sciences*, vol. 34, no. 3, pp. 225–239, 1984.

[15] R. Biswas, "Intuitionistic fuzzy subgroups," *Notes on IFS*, vol. 3, no. 2, pp. 53–60, 1997.

[16] V. Çetkin and H. Aygün, "An approach to neutrosophic subgroup and its fundamental properties," *Journal of Intelligent & Fuzzy Systems*, vol. 29, no. 5, pp. 1941–1947, 2015.

[17] R. Biswas, "Fuzzy subgroups and anti fuzzy subgroups," *Fuzzy Sets and Systems*, vol. 35, no. 1, pp. 121–124, 1990.

[18] D. Li, C. Zhang, and S. Ma, "The intuitionistic anti-fuzzy subgroup in group G," in *Fuzzy Information and Engineering*, pp. 145–151, Springer, 2009.

[19] K. H. Kim, Y. B. Jun, and Y. H. Yon, "On anti fuzzy ideals in near-rings," *Iranian Journal of Fuzzy Systems*, vol. 2, no. 2, pp. 71–80, 2005.

[20] Y. Feng and B. Yao, "On (λ, μ)-anti-fuzzy subgroups," *Journal of Inequalities and Applications*, vol. 2012, Article ID 78, 2012.

[21] N. Kausar, "Direct product of finite intuitionistic anti fuzzy normal subrings over non-associative rings," *European Journal of Pure and Applied Mathematics*, vol. 12, no. 2, pp. 622–648, 2019.

[22] P. A. Ejegwa, J. A. Awolola, J. M. Agbetayo, and I. M. Adamu, "On the characterisation of anti-fuzzy multigroups," *Annals of Fuzzy Mathematics and Informatics*, vol. 21, pp. 307–318, 2021.

[23] S. Hoskova-Mayerova and M. Al Tahan, "Anti-fuzzy multi-ideals of near ring," *Mathematics*, vol. 9, no. 5, p. 494, 2021.

[24] K. Ahmad, M. Bal, and M. Aswad, "The kernel of fuzzy and anti-fuzzy groups," *Journal of Neutrosophic and Fuzzy Systems*, vol. 1, no. 1, pp. 48–54, 2021.

[25] K. Kalaiarasi, P. Sudha, N. Kausar, S. Kousar, D. Pamucar, and N. A. D. Ide, "The characterization of substructures of γ-anti fuzzy subgroups with application in genetics," *Discrete Dynamics in Nature and Society*, vol. 2022, Article ID 1252885, 8 pages, 2022.

[26] K. Hemabala and B. S. Kumar, "Anti neutrosophic multi fuzzy ideals of near ring," *Neutrosophic Sets and Systems*, vol. 48, pp. 66–85, 2022.

[27] K. Hur, H. W. Kang, and H. K. Song, "Intuitionistic fuzzy subgroups and subrings," *Honam Mathematical Journal*, vol. 25, pp. 19–41, 2003.

[28] P. K. Sharma, "On intuitionistic anti-fuzzy subgroup of a group," *International Journal of Mathematics and Applied Statistics*, vol. 3, pp. 147–153, 2012.

Hindawi
Advances in Mathematical Physics
Volume 2023, Article ID 1296165, 8 pages
https://doi.org/10.1155/2023/1296165

Research Article

Research on Model Construction of Electric Energy Metering System Based on Intelligent Sensor Data

Hang Li,[1] Luwei Bai,[2] Jia Yu,[2] Yongmei Mao,[2] and Zhenzhen Hui[2]

[1]*Inner Mongolia Power (Group) Co., Ltd., Inner Mongolia Power Research Institute Branch, Hohhot, 010020 Inner Mongolia, China*
[2]*Electric Energy Measurement Supervision Center, Inner Mongolia Power (Group) Co., Ltd., Inner Mongolia Power Research Institute Branch, Hohhot, 010020 Inner Mongolia, China*

Correspondence should be addressed to Luwei Bai; b20160901216@stu.ccsu.edu.cn

Received 23 September 2022; Revised 31 October 2022; Accepted 20 March 2023; Published 3 May 2023

Academic Editor: S. E. Najafi

The informatization construction of the power grid is becoming increasingly popular, business application systems are constantly emerging, and power-related data is rapidly expanding. These discrete power data are scattered in various application systems, and it is not easy to directly provide advanced enterprise applications. The establishment of intelligent power statistical model is an urgent need for constructing power grid informatization. This paper proposes a model of an electric energy metering system based on intelligent sensor data and introduces the existing digital metering system. This model is the integration and promotion of business integration based on the digital metering system. It is the first time to apply new metering equipment, such as measurement and control devices with integrated metering functions, and new metering technologies, such as IEC 61850 electricity meter reading applications. It is hoped that this paper can lay a foundation for further research.

1. Introduction

Science and technology have developed rapidly, and the intelligence and informatization are becoming increasingly popular in the industrial field. The digital energy meter calibrator can accept the output signal of the standard power, and, after AD conversion, use the internal digital energy meter to calculate the electric energy and output the electric energy pulse to the higher precision electric energy metering equipment to carry out the calibration to achieve the quantity value transmission. Although the accuracy of digital metering equipment has been significantly improved, there are still many problems in actual operation, such as frequent communication failures and abnormally large measurement errors under the condition of good equipment performance, resulting in the inability to upload measurements and inaccurate upload data [1, 2]. The virtual load verification function controls the output of the standard power source by editing the verification scheme of the electric energy meter, verifies the digital electric energy meter in detail, and automatically generates a report. The actual load verification function can verify the inspected digital electric energy meter at the substation site without affecting the use of the inspected digital electric energy meter. Various problems, such as power imbalance, seriously hinder the engineering application process of digital metering technology. According to relevant data statistics, in 2020, among the 10 kV lines of Wuhan Power Supply Company, the ratio of users with a line loss rate of more than 5% was 12.6%, the percentage of users with a line loss rate of more than 10% was 7.1%, and the percentage of users with a line loss rate of more than 8% covered by unique transformer customers was 5.3%. During 2018-2021, more than 20000 defaulters and power thieves were found, saving more than 80 million yuan of economic losses. Currently, the annual loss due to electric energy theft in China is up to 20 billion yuan, and the value is increasing yearly. Taking the yearly electricity sales of 70 billion kWh in a province as an example, if the line loss caused by artificial electricity theft increases by one percentage point, the power loss will be up to more than 700 million

kWh, equivalent to nearly 400 million yuan [3]. Inductive equipment must absorb active and reactive power from the power system during operation. Therefore, after installing shunt capacitor reactive power compensation equipment in the power grid, it will be able to provide reactive power consumed by compensating inductive load, reducing the reactive power supplied by the power grid side inductive load and transmitted by the line. To effectively grasp the existing issues in the actual operation of the digital electric energy metering system and to clarify the aspects and contents of the practical work of digital metering in the next step, the State Grid Jiangsu Electric Power Company selected Wuxi as the research object to investigate the operation of all digital electric energy meters under the jurisdiction of its urban area. Statistics were carried out, a field investigation was conducted on the application status of the digital electric energy metering system in Xijing intelligent substation, and valuable first-hand information was obtained [4].

The main work done in the paper can be described as follows: (1) introduces the statistics of operating faults of Wuxi digital electric energy meters and analyzes the possible causes of various spots; (2) taking the digital power measurement on the high-voltage side of the main transformer in Xijing No.1 substation as an example, combined with digital measurement; the basic structure of the system points out its shortcomings in practical applications; (3) this paper summarizes the current practical problems faced by the power metering system based on intelligent sensor data in engineering applications and proposes corresponding solutions to provide a reference for the next step in the development of intelligent power systems.

2. Theoretical Analysis on Electric Energy Metering

Electric energy measurement has two main functions: on the one hand, it is used for internal assessment and settlement of power grid enterprises, and on the other hand, it is used as the basis for trade settlement between power generation, power supply, and electricity consumption [5]. To ensure that the electric energy metering device can accurately measure the electric energy, first of all, the category of electric energy metering device should be correctly selected. Secondly, choose the electric energy meter and instrument transformer with excellent performance and quality, as well as the secondary circuit wire section, and install and maintain them as required to ensure the safe, accurate, and reliable operation of the electric energy metering device. Electric energy measurement accuracy directly affects the internal assessment and analysis results of power grid companies or the fairness of trade settlements. Therefore, the electric energy measurement system must be accurate and reliable. The role of electric energy measurement standards in energy conservation and consumption reduction includes that scientific and advanced electric energy measurement tools provide accurate data for energy-saving transformation, and the analysis of electric energy measurement data provides the scientific basis for energy-saving change.

In traditional substations, the energy metering system consists of transformers and electronic energy meters. The transformers convert high voltage/large current into small voltage/current signals of 100/57.7 V or 1/5 A and then input them to the electronic energy meter [6]. The structure of an electronic watt-hour meter is similar to that of an induction watt-hour meter, composed of two parts: a measuring mechanism and auxiliary components. The measuring instrument is mainly written as an electronic circuit. Its measuring elements are composed of a UI multiplier, U/f converter, and counter. The auxiliary components are the same as those of the inductive watt-hour meter. To complete the accumulation of electrical energy. In the intelligent substation, the electric energy metering system has two forms: the first is to use electronic transformers, digital input merging units, and digital electric energy meters. The electronic transformers directly output digital quantities, and the subsequent data transmissions all use optical fibers. The second is to use traditional electromagnetic transformers still. The analog input merging unit digitizes the voltage and current signals output by the conventional transformers on the spot. This measurement system structure is adopted because the technology of electronic transformers is immature [7]. The configuration principle of the electric energy metering device includes that the secondary circuit of the voltage transformer in the electric energy metering device for trade settlement above 35 kV shall not be equipped with the auxiliary contact of disconnector. The electric energy metering device for trade settlement is installed at the user's place, and the user supplying power at 10 kV and below should be equipped with a national unified standard electric energy metering cabinet or electric energy metering box. To improve the accuracy of low load metering, electric energy meters with the overload of 4 times or more shall be selected. Figure 1 shows the structural comparison of these three metering systems.

$$W = U \times I \times t, \tag{1}$$

or

$$\begin{aligned} W &= P \times t, \\ W_n &= W_1 + W_2 + W_3 + \cdots W_n. \end{aligned} \tag{2}$$

In the above formula, W represents electric energy, U represents the actual voltage value, I represents the actual current value, P stands for electrical power, and t represents the electricity consumption time.

3. Research and Analysis

3.1. Statistical Analysis on Operation of Wuxi Digital Electric Energy Meter. Wuxi, Jiangsu, has several smart substations. The city with the most extensive range of digital power metering systems in Jiangsu Province is Wuxi Power Supply Company. The technical advantages of intelligent substations include the following: the smart substation can achieve an excellent low-carbon environmental protection effect, and the intelligent substation has good interaction and reliability characteristics.

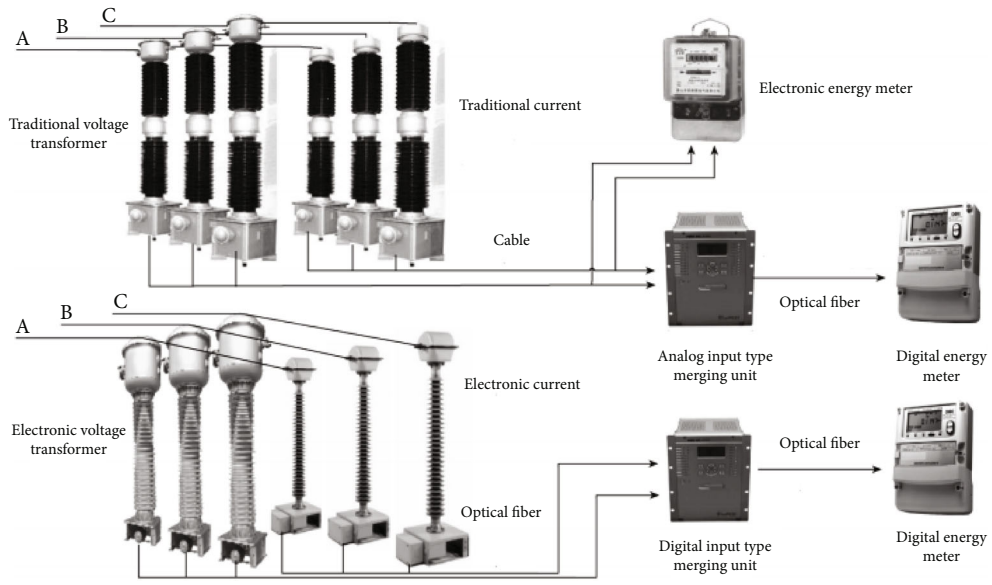

Figure 1: Structure comparison of three metering systems.

Up to now, the total number of digital meters under the jurisdiction of Wuxi city is 251, involving 43 substations of 3 voltage levels. Among them are three 500 kV substations involving 32 photoelectric meters, 17 220 kV substations involving 91 photoelectric meters, and 23 110 kV substations involving 128 photoelectric meters. The intelligent substation uses reliable, economic, integrated, low-carbon, and environment-friendly equipment and design, which can support the real-time online analysis and control decision-making of the power grid, with the basic requirements of the whole station information digitization, communication platform networking, information sharing standardization, system function integration, structural design compactness, high-voltage equipment intelligence, and operation status visualization.

This paper mainly conducts statistics on the operation of digital meters in operation under the jurisdiction of the Wuxi urban area. The failure rate of digital electric energy meters is generally 16%, which is higher than the failure rate of traditional electronic energy meters. To further analyze the operation of the digital electric energy meter, Table 1 is by voltage level, Table 2 is by fault type, and Table 3 is the classification statistics of manufacturers.

From the above data, we can preliminarily summarize the following conclusions (Figure 2). It can be seen from Table 1 that as the voltage level decreases, the failure rate gets higher and higher. Many faults include failure to upload power and power error. The primary responsibility is that the administration cannot be uploaded due to communication failure; different manufacturers' digital electric energy meters significantly differ in failure rate. The communication failures of digital watt-hour meters mainly include frame loss, communication delay, and channel abnormality (Figure 3).

Through exchanges and discussions with relevant technical personnel of the operation and maintenance unit and on-site inspection, the possible causes of various failures were further analyzed. A communication failure causes the inability to upload the electricity. The judgment is based on the standard measurement of the electric energy meter, but the centralized meter reading center cannot read the electric energy. The power error should be the wrong configuration of the parameters of the electric energy meter. The

Table 1: Statistics by voltage level.

Voltage level (kV)	Total number of digital tables	Number of failure tables	Failure rate (%)
500	32	1	3.1
220	91	5	5.5
110	128	39	30.5

Table 2: Statistics by fault type.

Fault type	Number of fault tables	Percentage of failure table (%)
Battery cannot be uploaded	21	46.7
Battery error	9	20.0
Other faults	15	33.3

Table 3: Statistics by manufacturer.

Manufacturer	The number of digital meters supplied by the manufacturer	Number of fault tables	Percentage of failure table (%)
1	90	2	2.2
2	74	19	25.7
3	36	2	0.56
4	17	2	11.8
5	9	7	77.8
6	5	3	60.0

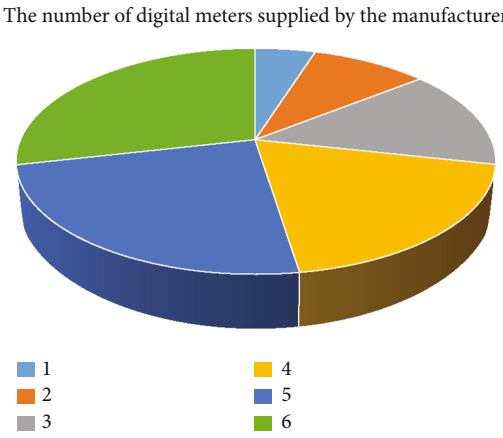

Figure 2: The digital meter number supplied by the manufacturer.

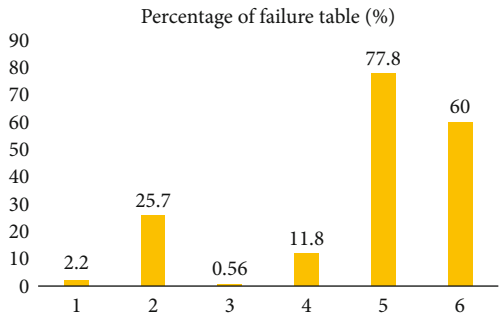

Figure 3: Percentage of failure table.

basis for the judgment is that the current protection and metering data sources in the intelligent substation are the same. If the data source is incorrect, the protection device should respond first. Other faults mainly refer to the crash of the electric energy meter, black screen, no indicator light, etc. The cause of such failures is defective software or hardware of the electric energy meter itself.

3.2. Investigation of the Fault Situation of Digital Electric Energy Metering in Xijing Substation. Xijing Substation is the first batch of pilot projects for intelligent substations of the State Grid Corporation of China. Construction started in July 2010 and was put into operation in December of the same year. The station is an intelligent substation in a complete sense. The operational characteristics and responsibilities of intelligent substations make them have good interactivity. It is responsible for the data statistics of power grid operation, which requires it to feed back safe, reliable, accurate, and detailed information to the power grid. After the intelligent substation realizes the function of information collection and analysis, it can not only share the data internally but also interact well with more complex and advanced systems in the network. It adopts the design of "three layers and two networks." The SV, GOOSE, and IEEE 1588 networks share the transmission network, and the dual network is redundant [8]. The voltage and current measurement equipment all uses electronic transformers. The current transformer is based on the optical principle, and the voltage transformer is based on the capacitive voltage divider principle [9]. The idea of single server sharing is to use one PC as the server to provide network-sharing services to other PCs. There are mainly two schemes to realize this method: (1) proxy server scheme and (2) URL conversion scheme.

Since Xijing Substation was put into operation, there have been relatively few problems in the digital metering system, but there are still faults, and on-site fault investigation is required.

Taking the digital power metering of the high-voltage side of the main transformer of Xijing Substation No. 1 as an example, the schematic diagram of the system structure is shown in Figure 4.

As shown in Figure 4, the digital energy metering system is very different from the traditional system in structure, mainly because the energy meter is no longer directly connected to the transformer, and there are more remote modules, photoelectric units, and merging units in the middle. The design principles of the electric energy metering system include that the electric energy metering system should be designed as an independent and complete system. Electric energy acquisition has low requirements for real time but high requirements for simultaneity, increased requirements for electric energy acquisition accuracy, the principle of uniqueness of data source, and the high reliability of software. The transmission signal has also become a digital quantity, switches, and other equipment. From the perspective of on-site operation and maintenance of metering, although the wiring is less, the remote modules, voltage-combining units, current-combining units, switches, and other equipment are widely distributed and partially overlap with the automation system in the substation. The secondary wiring of the metering system becomes less clear, making the whole system more complex. As electric energy is a cumulative value, even small errors will reach an incredible degree after accumulation. For both the seller and the user of electricity, this cumulative value is an economic loss. Therefore, the selection principle of measurement accuracy should be that the greater the capacity, the higher the accuracy. It is better to use energy meters with an accuracy of 0.2 level and above for large-capacity power plants and transmission lines.

During the on-site investigation of the digital power metering fault on the high-voltage side of the main substation of Xijing Substation No. 1, it was difficult for traditional substation operation and maintenance personnel to locate and analyze the fault. In contrast, professional technicians familiar with digital power metering could infer the fault point and cause. Substation operation and maintenance experiences are also difficult to verify and figure out. In addition, because the digital power metering system and the automation system in the substation have some overlapping equipment, such as merging units and switches, the equipment focal point is not clear, which makes troubleshooting very difficult. The problem-solving efficiency is low, so the coordination and cooperation of multiple departments are required to complete the work [10]. The electric energy acquisition device is the communication center of electric energy data. On the one hand, it collects and stores the electric energy data output by the digital electric energy meter in

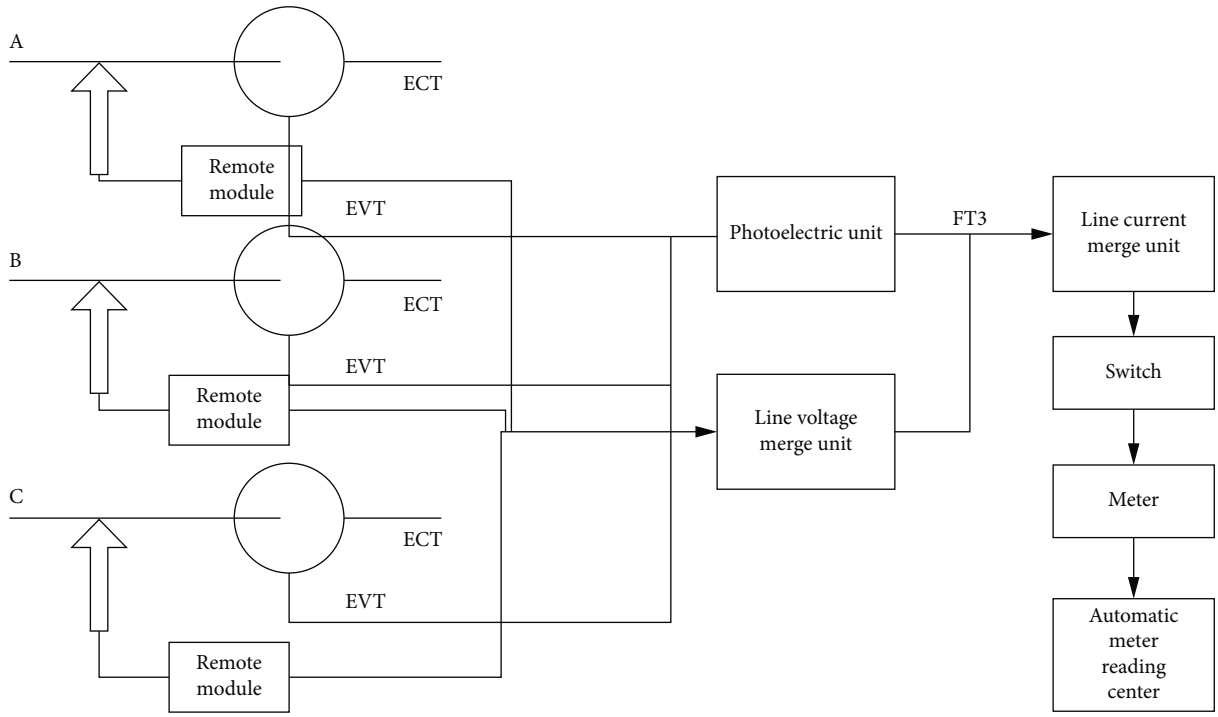

Figure 4: Xijing Substation No. 1 main transformer high-voltage side digital electric energy metering.

the form of serial communication. On the other hand, the collected electric energy data is transmitted to the master station of the electric energy billing automation system through the uplink channel.

4. Problems Faced by Digital Energy Metering

Through the research on the application of digital energy metering in Wuxi, Jiangsu Province, and combined with the actual situation of digital metering technology, the problems that still exist in trade settlement are divided into three aspects;

4.1. Normative. The meaning of normative includes the normativeness of the metering system structure and the normativeness of metering equipment management. The intelligent electricity meter can realize accurate and real-time cost settlement information processing, simplifying the complex process of past account processing. In the power market environment, dispatchers can switch energy retailers more timely and conveniently and even realize fully automatic switching in the future. At the same time, users can also obtain more accurate and timely energy consumption and accounting information.

(1) Structural normative

Electric energy metering not only requires correct functions, especially the electric energy metering system used for trade settlement, but also conforms to national mandatory requirements.

In the process of intelligent substation design, the design unit mainly focuses on the stability and reliability of the relay protection and measurement and control automation system. The method of the electric energy metering system is only at the functional level [11]. For example, in terms of synchronization time synchronization, some use IRIG-B code time synchronization, and some use IEEE 1588 time synchronization, while the "direct sampling and direct hopping" protection does not depend on time synchronization. Some sampling devices do not even access the time synchronization signal, relying entirely on interpolation synchronization, and the data source of the energy meter comes from the switch. In this extreme case, even if the errors of the various components of the power calculation system are acceptable, the overall measurement error will exceed the tolerance.

While for the Department of Metrology, due to the limitation of majors and responsibilities, most universities and scientific research institutions mainly focus on the research of measurement accuracy and traceability technology.

The normative aspect of statistical structure has not been paid enough attention to, so the design of the current digital measurement system is not unified, which affects the accuracy of measurement and the reliability of measurement data.

(2) Management normative

There should be a unified management specification to ensure that the digital energy metering system is accurate, stable, and reliable. Traditional energy metering systems, according to DL/T 448-2000 "Technical Management Regulations for Electric Energy Metering Devices" and SD 109-1983 "Inspection Regulations for Electric Energy Metering Devices," strictly stipulate the classification of metering points, metering device configuration, procurement,

installation, weekly inspection, and other links, so traditional electric energy metering system can measure electric energy accurately, stably, and reliably. However, no mandatory or recommended standard documents for managing digital energy metering systems exist. After the digital metering system is put into operation from the infrastructure, there is almost no management department, and its acceptance is also completed by the automation professional. In addition, the follow-up operation and maintenance of the digital energy metering system are also tricky. The data on water, gas, and heat consumption collected by smart meters can be used for load analysis and prediction. The total energy consumption and peak demand can be estimated and predicted by comprehensively analyzing the above information, load characteristics, time changes, etc. This information will provide convenience for users, energy retailers, and distribution network dispatchers; promote rational power use, energy conservation, and consumption reduction; and optimize grid planning and dispatching. (1) Up to now, there is neither detection equipment nor detection basis and means for judging the failure of digital electric energy metering equipment; (2) there are no relevant technical normative documents on how to deal with the disappointment after the occurrence of the fault; and (3) the digital power metering system and the substation automation system have some overlapping equipment, and it is necessary to coordinate multiple departments to carry out the daily operation and maintenance of the metering system. By feeding back the energy consumption information provided by smart meters to users, users can be encouraged to reduce energy consumption or convert energy utilization methods. For households equipped with distributed generation equipment, it can also provide users with reasonable power generation and electricity use schemes to maximize the interests of users.

Under the current situation of the lack mentioned above of normative management, it is impossible for the digital electric energy metering system to operate as accurately, stably, and reliably as the traditional electric energy metering system. In response to this problem, the design, operation and maintenance, marketing, and other relevant departments should be coordinated to formulate a multiparty recognized smart substation digital energy metering system design and operation and maintenance plan, including system wiring, equipment management, and equipment inspection, to form technical normative documents be enforced.

4.2. Detection Capability. In terms of laboratory testing, several testing standards, including electronic transformers, merging units, and digital energy meters, have been formulated concerning traditional electric energy metering equipment, and corresponding testing platforms have been developed or established. Although imperfect, it can guarantee the stable and reliable operation of the digital electric energy metering system under reasonable operating conditions. However, there are still deficiencies in an on-site inspection. It has also been mentioned that there is a lack of detection equipment and related technical specification documents for the current on-site fault detection of digital electric energy metering systems. For example, when there is a fault that cannot be transmitted back to the electricity, the cause of the defect cannot be determined, and the fault point cannot be located. The most common fault in the survey is the failure to send power back. Due to the numerous causes of such marks and the enormous scope involved, it is challenging to locate the spot. In response to this problem, related testing equipment should be developed. In Jiangsu, the electric energy accumulated by the user's intelligent meters is collected by the local collection terminal. Then, the electric energy is read by the remote server. Therefore, the equipment that detects the power that cannot be returned on-site should have the following functions:

(1) Simulate the local acquisition terminal to check whether the communication function of the electric energy meter is in good condition

(2) Simulate the remote server to check whether the function of the acquisition terminal is in good condition

(3) The simulated negative control center sends a meter reading instruction to check whether the remote server can be accessed commonly

4.3. Quantitative Traceability. For a digital energy metering system to be used for trade settlement, value traceability is one of the problems that must be solved. The value traceability research related to digital energy metering includes three aspects:

(1) High-precision digital energy metering algorithm

(2) A high-accuracy digital power source generation method

(3) Traceability of digital quantities to analog quantities. There have been many studies on the first two problems, and there is no recognized perfect solution for the third

5. Electric Energy Metering System with Intelligent Sensor Data

5.1. Electric Energy Metering System Model of Intelligent Sensor Data. At present, there is no research on electric energy metering system models based on intelligent sensor data at home and abroad. For the sake of realizing the metering data's standardization and ensuring the interoperability and interchangeability of various devices in the metering system, the following extensions are made on the premise of analyzing the research function of the model about power metering, demand calculating, freezing, incident report, time-sharing, and segmented metering which can be clearly shown in Figure 5.

(1) The extended model logic node MMTR is used for forward and reverse active energy and four-quadrant reactive energy and demand measurement (MMTR for three-phase electric energy meters, MMTN for single-phase electric energy meters).

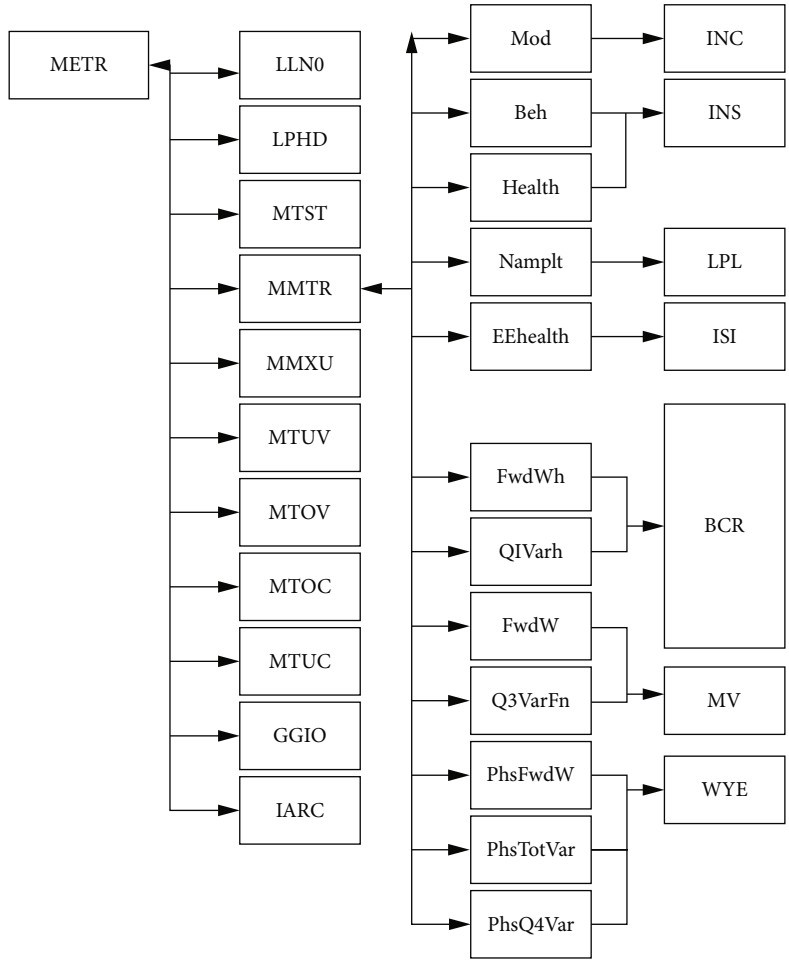

Figure 5: Smart energy metering model.

Under different conditions, such as electricity metering MMTR1 and demand metering MMTR2, they are distinguished by Arabic numerals suffixes

(2) The original MMXU logic node is used for remote measurement of voltage and current (MMXU for three-phase watt-hour meter and MMXN for single-phase watt-hour meter)

(3) Since metering has different limits for voltage loss, phase loss, and current loss and protection measurement and control alarm limits, new MTUV, MTOV, MTUC, and MTOC are created to complete the monitoring and alarm functions. Different alarms of the same type of event alarms are designed with other instances, respectively, such as undervoltage MTUV1 and undervoltage MTUV2; different models are distinguished by Arabic numeral suffixes

(4) Using the original logic node GGIO, there is no need to set customized alarm events such as sampling abnormality, watt-hour meter failure, power failure, and voltage reverse phase sequence

(5) Using the original IARC recording, the programming events, for example, the time zone timetable programming, the demand cycle programming, the energy meter clearing, the demand clearing, the event clearing, the opening of the meter cover, and opening the button box

(6) Create a new MTST logical node to save and record the time zone period table

(7) Take rated voltage and current, active or reactive combined status word, energetic energy pulse constant, reactive energy pulse steady, and other energy meter asset information as the extended data object of the symbolic logical node LLN0

5.2. Characteristics of Electric Energy Metering System Based on Intelligent Sensor Data

(1) With the design inspiration of simplifying the communication network in the station, we adopt a technical solution that combines all-digital computing systems and computing services with other specialties. The private communication network in the measurement system station is merged into the public communication network based on IEC 61850. The measurement service shares data sources and

hardware resources with other majors which simplifies the secondary system in the station and lays a foundation for improving the intelligence level of the measurement system

(2) According to the measurement business needs, the measurement is subdivided into three categories: assessment, settlement, and measurement points that may be converted into settlement points. Different metering points design various implementation schemes and propose other technical conditions

(3) The IEC 61850 node and service model are established for the new generation of intelligent substation metering and metering management. The IEC 61850 file service is used to realize the real-time recording of a large number of frozen data and the convenient transfer afterward and use of the IEC 61850 report. The service recognizes the real-time operational reporting of abnormal events

6. Conclusion

According to the research in this paper, we can see that the research and development of the digital electric energy metering system should be based on the actual application, supplemented by the feeling of use, and comprehensively consider the system operation efficiency and business needs, while meeting the subsequent expansion of the system. Therefore, with the development of science and technology, the following design principles should be followed in the design process of the system in the future:

(1) Reliability. When the environment changes or external virus attacks occur, the system needs to ensure the stable output of its functions. Therefore, in the design process, we should focus on the rigorous testing of the underlying database and various functional modules of the system. Automatic backup of internal data is realized during operation to ensure the safe and reliable operation of the system database and the realization of required functions

(2) Expandability. Thoroughly consider the development of computer hardware technology, new testing projects, and new electric energy metering devices, so the system should have good scalability and compatibility. It not only maximizes the utilization of existing software and hardware equipment and network resources but also can meet the construction needs of future development

(3) Ease of use. To meet the user needs of the system business as the central axis, the design of each functional module should be people-oriented, show the required content output concisely, and conform to the user's operating habits. The action and response process of the system, the typesetting sequence of information, the minimum eye movement distance, and the simple user interface all need to be designed from the user's perspective

(4) Standardization. For the content of the digital simulation module architecture, it is required to comply with the standards issued by the relevant national departments, applicable international regulations, corresponding industry requirements, and the provisions of pertinent power organizations to ensure the accuracy and standardization of the system simulation data. Distinguish the characteristics of metering devices in different cities and counties. Conduct digital simulation modeling of electric energy metering devices based on the principle of "unified standard, unified platform, and unified implementation"

Data Availability

The data underlying the results presented in the study are available within the manuscript.

Conflicts of Interest

The authors declare that they have no conflicts of interest.

References

[1] T. Yi, J. Bo, L. Hongbin, and C. Xianshun, "Review of verification methods for digital energy metering systems," *Journal of Electrotechnical Technology*, vol. S2, pp. 372–377, 2019.

[2] Z. Qiuyan, C. Hanmiao, L. Hongbin, and W. Wei, "Error multi-parameter degradation evaluation model and method of digital power metering system," *Power Grid Technology*, vol. 39, no. 11, pp. 3202–3207, 2020.

[3] D. Zhigang and S. Tengfei, "Development status and application prospect of electronic current transformer," *Instrument Technology*, vol. 2019, no. 5, pp. 37–40, 2019.

[4] H. Shu, Z. Yunlu, and G. Chuan, "Inter-bay measurement and test system for smart substations," *Power Equipment Management*, vol. 9, pp. 95–97, 2019.

[5] L. Yue, Q. Hua, and S. Chunjun, "Design of secondary system of 220 kV Xijing intelligent substation," *East China Electric Power*, vol. 39, no. 5, pp. 0732–0736, 2019.

[6] L. Yue and Q. Hua, "Research on secondary system design technology of 220k Xijing intelligent substation," *Electric Power Survey and Design*, vol. 39, no. 5, pp. 60–64, 2019.

[7] H. Shu, Z. Yunlu, and G. Chuan, "Research on error factors of inter-bay metering system in smart substations," *Standardization in China*, vol. 20, pp. 182-183, 2019.

[8] L. Zhongchen and Z. Ruimin, "New digital substation electric energy metering error detection scheme and design," *Electrical Technology*, vol. 17, no. 10, pp. 135–138, 2016.

[9] W. Wei, *Research on measurement performance of digital electric energy meter and its detection method and detection technology*, Huazhong University of Science and Technology, 2016.

[10] S. Weishan, *Software design and development of multi-functional test platform for digital electric energy metering device*, Huazhong University of Science and Technology, 2019.

[11] W. Xiaobing, "Design and implementation of a network packet capture system," *Information Communication*, vol. 2, pp. 96–98, 2018.

Hindawi
Advances in Mathematical Physics
Volume 2023, Article ID 4009056, 8 pages
https://doi.org/10.1155/2023/4009056

Research Article

Analysis of Fuzzy Differential Equation with Fractional Derivative in Caputo Sense

Qura Tul Ain,[1] **Muhammad Nadeem**,[2] **Devendra Kumar**,[3] **and Mohd Asif Shah**[4]

[1]*School of Mathematics, Guizhou University, 550025 Guiyang, China*
[2]*School of Mathematics and Statistics, Qujing Normal University, 655011 Qujing, China*
[3]*Department of Mathematics, University of Rajasthan, Jaipur, 302004 Rajasthan, India*
[4]*Kebri Dehar University, PO Box 250, Ethiopia*

Correspondence should be addressed to Mohd Asif Shah; drmohdasifshah@kdu.edu.et

Received 11 June 2022; Revised 8 July 2022; Accepted 20 March 2023; Published 20 April 2023

Academic Editor: S. E. Najafi

In this article, the dynamics of the fuzzy fractional order enzyme Michaelis Menten model are investigated. To study problems with uncertainty, fuzzy fractional technique is applied. Using fuzzy theory, the sequential iterations of the model are calculated by applying fractional calculus theory and the homotopy perturbation method. A comparison is given for fractional and fuzzy results, and the numerical findings validate the fuzzy fractional case. Using MATLAB software, the results are simulated for various fractional orders, corresponding to the provided data. The simulations demonstrate the model's appropriateness.

1. Introduction

When doing an unusual experiment, such as putting a fraction into the sequence of differentiation, it is critical to remain intrigued about the results, as this is how many unique scientific studies are conducted. When venturing into unknown territory, however, one should be prepared to fore-go much of what is currently known and is taken normal and obvious. The fractional integral and derivative is not the only different-integral operators available; there is still a vast universe of generalizing differentiation and integration with which we are both comfortable and secure, such as chain and product laws. Another important attribute of fractional derivatives is nonlocality [1–3]. If the result of calculating the value of an integer-order derivative at a point is dependent on that point, we call this property as locality. With the fractional derivative, things are a little different. When studying physical systems, the case where $\alpha = 0$ is common because the dependent variable is always time. The fractional derivative is determined by the state of the system, which includes all moments after the experiment begins at $t = 0$. This nonlocality is one of the primary drivers of interest in fractional calculus in applications. Memory effects refer to a group of remarkable physical phenomena in which the state is influenced not only by time and place, but also by prior states. For example, consider a section of an electric circuit whose resistance is based on the total amount of charge that has gone through it over a set period of time. Memory effects can be difficult to represent and analyze using conventional differential equations, but nonlocality provides a built-in capacity for fractional derivatives to integrate memory effects. As a result, fractional calculus could be a valuable tool for analyzing this type of system.

In mathematical modeling, memory is used to explain the present by emphasizing what happened in the past. Previous experiences, for example, may indicate that, depending on the type of disease, social distance or additional hygiene practices are protective behaviors in the case of an infectious disease being transmitted to people. Because the vaccination has a long-lasting effect, it may also have a long-term memory effect. Fractional calculus is an excellent tool for understanding real-life phenomena involving the memory effect. For example, we assume $g(t, x_0)$ as the solution of an autonomous ODE of first order, provided x_0 at $t = 0$; hence, the property $g(t + s, x_0) = g(t, g(s, x_0))$ is assured, which implies that the results are unchanged by taking $g(s, x_0)$ as the initial

condition as $g(t, x_0)$ belongs to results. As a result, for any domain point, the solution is uniquely specified given an initial value. This statement is not true for fractional differential equations in general. Adjusting the order of a classical model's derivative such that it becomes noninteger is one approach for a mathematical model to integrate the memory effect.

Conventional mathematical optimization approaches for reactive biological systems include equations containing empirical or semiempirical expressions rather than the traditional mass-action law. By applying the memory effect, the kinetics of such reactive systems can be accurately represented using fractional calculus, providing forms similar to those given by the law of mass action. As a result, a great mechanism for explaining the dynamical behavior of many chemical and biological systems has been developed. Several research papers have been published on the use of FDEs in biological and chemical reactions. As a result, fractional derivative focused models have a greater potential for description accuracy. Theoretical advancements are also being made in order to expand the application of this technology in research and engineering. Hans-Jürgen [4] shows the validity and possibilities of fractional calculus as a tool for modeling dynamic systems in the field of process systems engineering. They developed a fractional calculus-based model for the fermentation problem and used experimental data to demonstrate the model's validity in biological reactions.

For examining the approximate solution of the Michaelis Menten enzymatic reaction equation, Manal and Saad [5] suggested an extension of the spectral homotopy analysis method. They compared the accuracy and efficiency of Runge-Kutta methods. He and Li [6] used the Laplace transformation and Adomian decomposition approach to analyze the semianalytical results of fractional time enzyme kinetics.

Further developments in the related areas can be seen in [7–13].

2. Motivation

Many academics have given numerical, approximate approaches and applications to handle this problem in general, due to the difficulty that many researchers encounter in obtaining accurate solutions to fractional differential equations [14–17]. The authors of [5] looked into spectrum approaches in the context of fractal fractional differentiation. However, it only included research that used the Mittag-Leffler kernel. The significance of our research resides in the fact that we give a fuzzy solution to the uncertainty challenge. One of the major benefits of the Caputo fractional derivative is that it makes it possible to formulate the problem with conventional initial and boundary conditions. Its derivative for a constant is also zero. We take the Michaelis Menten differential equation system as

$$D_t R_1(t) = -\alpha R_1 R_2 + \beta R_3, \tag{1}$$

$$D_t R_2(t) = -\alpha R_1 R_2 + (\beta + \gamma) R_3, \tag{2}$$

$$D_t R_3(t) = \alpha R_1 R_2 (\beta + \gamma) R_3, \tag{3}$$

$$D_t R_4(t) = \gamma R_3. \tag{4}$$

The description of the model is given in Table 1.

$$R_1(\mathrm{t}) + R_2(t)(\mathrm{t}) \rightleftharpoons R_3(\mathrm{t}) \longrightarrow R_2(\mathrm{t}) + R_4(t). \tag{5}$$

According to this illustration, a complex R_3 is the result of a process involving a substrate R_1 and an enzyme R_2. Finally, the enzyme R_2 converts a complex R_3 into a product R_4.

3. Contribution

For more than a century, the Michaelis Menten equation has been used to predict the rate of product generation in enzymatic reactions. It specifically indicates that when substrate concentration increases, the rate of an enzymatic reaction increases, but greater unbinding of enzyme-substrate complexes decreases the reaction rate. This is the first investigation of the fractional Michaelis Menten enzymatic process using fuzzy approach. The fractional Michaelis Menten differential equation system can be written as

$$D_t^{\zeta} R_1(t) = -\alpha R_1 R_2 + \beta R_3, \tag{6}$$

$$D_t^{\zeta} R_2(t) = -\alpha R_1 R_2 + (\beta + \gamma) R_3, \tag{7}$$

$$D_t^{\zeta} R_3(t) = \alpha R_1 R_2 - (\beta + \gamma) R_3, \tag{8}$$

$$D_t^{\zeta} R_4(t) = \gamma R_3. \tag{9}$$

Introducing the fuzzy fractional parameters, the system can be written as

$$D_t^{\zeta}(F_{1k}) = -\tilde{\alpha} F_{1k} F_{2k} + \tilde{\beta} F_{3k}, \tag{10}$$

$$D_t^{\zeta}(F_{2k}) = -\tilde{\alpha} F_{1k} F_{2k} + \left(\tilde{\beta} + \tilde{\gamma}\right) F_{3k}, \tag{11}$$

$$D_t^{\zeta}(F_{3k}) = \tilde{\alpha} F_{1k} F_{2k} - \left(\tilde{\beta} + \tilde{\gamma}\right) F_{3k}, \tag{12}$$

$$D_t^{\zeta}(F_{4k}) = \tilde{\gamma} F_{3k}, \tag{13}$$

with fuzzy initial conditions given by

$$F_1^{\check{}}(0, p) = \left(\underline{F_1}(0, p), \overline{F_1}(0.p)\right), \tag{14}$$

$$F_2^{\check{}}(0, p) = \left(\underline{F_2}(0, p), \overline{F_2}(0.p)\right), \tag{15}$$

$$F_3^{\check{}}(0, p) = \left(\underline{F_3}(0, p), \overline{F_3}(0.p)\right), \tag{16}$$

$$F_4^{\check{}}(0, p) = \left(\underline{F_4}(0, p), \overline{F_4}(0.p)\right). \tag{17}$$

The following is an overview of the article's structure. The definitions of the fractional calculus and fuzzy operators are discussed in Section 2. In Section 3, we use the homotopy perturbation approach with fuzzy initial conditions to generate successive iterations of the fractional Michaelis Menten enzymatic reaction. The numerical results are presented in Section 4. Finally, in Sections 5 and 6, we explain and

Table 1: Parameters' values.

Parameters	Interpretation
$R_1(t)$	Concentration of substrate
$R_2(t)$	Concentration of enzyme
$R_3(t)$	Concentration of the resulting complex
$R_4(t)$	Concentration of resulting product
α, β, γ	Rate of reaction

examine the numerical results as well as make some final observations.

4. Preliminaries

In this section, we provide the definitions which will be used in the solution of the system [4, 18–20].

Definition 1. Let $\eta : \mathbb{R} \longrightarrow [0, 1]$ be a fuzzy set. η is said to be a fuzzy number if it satisfies the following properties:

(1) η is normal, i.e., $\eta(c_0) = 1$ for any $c_0 \in \mathbb{R}$

(2) η is semicontinuous on $\mathbb{R}$, i.e., for all $\varepsilon > 0$, there exists a $\delta > 0$ such that $|\eta(c) - \eta(c_0)| < \varepsilon$ for $|c - c_0| < \delta$

(3) η is convex

(4) $d1\{c \in \mathbb{R}\,; \eta(c) > 0\}$ is compact

Definition 2. If η is a fuzzy number, for $n \in (0, 1]$ and $c \in \mathbb{R}$, the n-th level set defined on η is given by

$$[\eta]n = \{c \in \mathbb{R} : \eta(a) \geq n\}. \tag{18}$$

Definition 3. Let $[\underline{\eta(\theta)}, \overline{\eta(\theta)}]$ for $0 \leq \theta \leq 1$ be the parametric form of a fuzzy number η, satisfying the following properties:

(1) $\underline{\eta(\theta)}$,is left continuous, bounded, and increasing over (0,1], and right continuous at 0

(2) $\overline{\eta(\theta)}$ is right continuous, bounded, and decreasing over [0,1], and right continuous at 0

(3) $\underline{\eta(\theta)} \leq \overline{\eta(\theta)}$

Also, if $\underline{\eta(\theta)} = \overline{\eta(\theta)}$; then, θ is called a crisp number.

Definition 4. Let ξ be the continuous fuzzy function on $[0, B] \subseteq R$, further if $\xi \in C^f[0, B] \cap L^f[0, B]$, where $C^f[0, B]$ is a fuzzy continuous space and $L^f[0, B]$ is a fuzzy Lebesgue integrable function such that $\xi = [\underline{\xi n(t)}, \overline{\xi n(t)}]$ for $0 \leq n \leq 1$ and $t \in (0, B)$; then, the fuzzy fractional derivative is defined as

$$[D^\kappa \xi(t_0)]n = \left[D^\kappa \underline{\xi_n}(t_0), D^\kappa \overline{\xi_n}(t_0)\right], \tag{19}$$

$$D^\kappa \underline{\xi_n}(t_0) = \left[\frac{1}{\Gamma(i-\kappa)}\right]\left[\int_0^t (t-\varsigma)^{i-\kappa-1}\left(\frac{d^i}{d\varsigma i}\right)\underline{\xi_n}(\varsigma)d\varsigma\right]_{t=t0}, \tag{20}$$

$$D^\kappa \overline{\xi_n}(t_0) = \left[\frac{1}{\Gamma(i-\kappa)}\right]\left[\int_0^t (t-\varsigma)^{i-\kappa-1}\left(\frac{d^i}{d\varsigma i}\right)\overline{\xi_n}(\varsigma)d\varsigma\right]_{t=t0}. \tag{21}$$

Definition 5. Let ξ be the continuous fuzzy function on $[0, B] \subseteq R$, further if $\xi \in C^f[0, B] \cap L^f[0, B]$, the Laplace transform of fuzzy fractional model derivative in Caputo sense is given as

$$L\left[D^\kappa \xi(t)_n\right] = s^k L[\xi(t)] - s^{k-1}[\xi(0)]. \tag{22}$$

Definition 6. We can construct a homotopy $v(r, P)$: $\Omega \times [0, 1] \longrightarrow R$

$$H(v, P) = (1 - P)[L(v) - L(v0)] + q[L(v) + N(v) - f(r)] = 0, \tag{23}$$

where L is the linear part, N is the nonlinear part, and $r \in \Omega$ and $P \in [0, 1]$ are the embedding parameter.

4.1. HPM for Fuzzy Fractional Model.

$$(1 - P)\left[D_t^\theta L\tilde{U} - D_t^\theta L\tilde{U}_0\right] + P\left[D_t^\theta L\tilde{U} + D_t^\theta N\tilde{U} + \widetilde{f}(r)\right] = 0, \tag{24}$$

Here, we will apply the HPM to the considered model

$$(1 - P)\left[D_t^\theta R_1(t) - D_t^\theta R_{10}(t)\right] + P\left[D_t^\theta R_1(t) + \tilde{\alpha}R_1R_2 + \tilde{\beta}R_3\right] = 0, \tag{25}$$

$$(1 - P)\left[D_t^\theta R_2(t) - D_t^\theta R_{20}(t)\right] + P\left[D_t^\theta R_2(t) + \tilde{\alpha}R_1R_2 + \left(\tilde{\beta} + \tilde{\gamma}\right)R_3\right] = 0, \tag{26}$$

$$(1 - P)\left[D_t^\theta R_3(t) - D_t^\theta R_{30}(t)\right] + P\left[D_t^\theta R_3(t) - \tilde{\alpha}R_1R_2 - \left(\tilde{\beta} + \tilde{\gamma}\right)R_3\right] = 0, \tag{27}$$

$$(1 - P)\left[D_t^\theta R_4(t) - D_t^\theta R_{40}(t)\right] + P\left[D_t^\theta R_4(t) - \widetilde{\gamma}R_3\right] = 0. \tag{28}$$

If $P = 0$, we get

$$D_t^\theta R_1(t) - D_t^\theta R_{10}(t) = 0, \tag{29}$$

$$D_t^\theta R_2(t) - D_t^\theta R_{20}(t) = 0, \tag{30}$$

$$D_t^\theta R_3(t) - D_t^\theta R_{30}(t) = 0, \tag{31}$$

$$D_t^\theta R_4(t) - D_t^\theta R_{40}(t) = 0. \tag{32}$$

We define following sums,

$$\tilde{R}_1(t) = \sum_{n=0}^{\infty} P^n \tilde{R}_{1_n}, \tag{33}$$

$$\tilde{R}_2(t) = \sum_{n=0}^{\infty} P^n \tilde{R}_{2_n}(t), \tag{34}$$

$$\tilde{R}_3(t) = \sum_{n=0}^{\infty} P^n \tilde{R}_{3_n}(t), \tag{35}$$

$$\tilde{R}_4(t) = \sum_{n=0}^{\infty} P^n \tilde{R}_{4_n}(t). \tag{36}$$

Similarly,

$$\underline{R_{10}}(t) = \underline{R_1}(0,\vartheta), \bar{R_{10}}(t) = \bar{R_1}(0,\vartheta), \tag{37}$$

$$\underline{R_{20}}(t) = \underline{R_2}(0,\vartheta), \bar{R_{20}}(t) = \bar{R_2}(0,\vartheta), \tag{38}$$

$$\underline{R_{30}}(t) = \underline{R_3}(0,\vartheta), \bar{R_{30}}(t) = \bar{R_3}(0,\vartheta), \tag{39}$$

$$\underline{R_{40}}(t) = \underline{R_4}(0,\vartheta), \bar{R_{40}}(t) = \bar{R_4}(0,\vartheta). \tag{40}$$

Eventually, we get the following calculations

$$\underline{R}_{1_n}(t) = \underline{R_{10}}(t) + \underline{R_{11}}(t) + \underline{R_{12}}(t) + \cdots, \tag{41}$$

$$\bar{R}_{1n}(t) = \bar{R_{10}}(t) + \bar{R_{11}}(t) = \bar{R_{12}}(t) + \cdots, \tag{42}$$

$$\underline{R}_{2_n}(t) = \underline{R_{20}}(t) + \underline{R_{21}}(t) + \underline{R_{22}}(t) + \cdots, \tag{43}$$

$$\bar{R}_{2n}(t) = \bar{R_{20}}(t) + \bar{R_{21}}(t) = \bar{R_{22}}(t) + \cdots, \tag{44}$$

$$\underline{R}_{3_n}(t) = \underline{R_{30}}(t) + \underline{R_{31}}(t) + \underline{R_{32}}(t) + \cdots, \tag{45}$$

$$\bar{R}_{3n}(t) = \bar{R_{30}}(t) + \bar{R_{31}}(t) = \bar{R_{32}}(t) + \cdots, \tag{46}$$

$$\underline{R}_{4_n}(t) = \underline{R_{40}}(t) + \underline{R_{41}}(t) + \underline{R_{42}}(t) + \cdots, \tag{47}$$

$$\bar{R}_{4n}(t) = \bar{R_{40}}(t) + \bar{R_{41}}(t) = \bar{R_{42}}(t) + \cdots, \tag{48}$$

with following conditions,

$$\tilde{R}_1(0,\vartheta) = (2\vartheta - 1, 1 - 2\vartheta), \tag{49}$$

$$\tilde{R}_2(0,\vartheta) = (2\vartheta - 1, 1 - 2\vartheta), \tag{50}$$

$$\tilde{R}_3(0,\vartheta) = (2\vartheta - 1, 1 - 2\vartheta), \tag{51}$$

$$\tilde{R}_4(0,\vartheta) = (2\vartheta - 1, 1 - 2\vartheta). \tag{52}$$

Followed by iterations calculated as

$$\underline{R_{10}}(t,\vartheta) = (2\vartheta - 1), \bar{R_{10}}(t,\vartheta) = (1 - 2\vartheta), \tag{53}$$

$$\underline{R_{20}}(t,\vartheta) = (2\vartheta - 1), \bar{R_{20}}(t,\vartheta) = (1 - 2\vartheta), \tag{54}$$

$$\underline{R_{30}}(t,\vartheta) = (2\vartheta - 1), \bar{R_{30}}(t,\vartheta) = (1 - 2\vartheta), \tag{55}$$

$$\underline{R_{40}}(t,\vartheta) = (2\vartheta - 1), \bar{R_{40}}(t,\vartheta) = (1 - 2\vartheta). \tag{56}$$

Second term of solution is calculated as

$$\underline{R_{11}}(t,\vartheta) = -\tilde{\alpha}\left\{(2\vartheta - 1)^2 + (2\vartheta - 1)\right\}\frac{t^\theta}{\Gamma(\theta + 1)}, \tag{57}$$

$$\bar{R}_{11}(t,\vartheta) = -\tilde{\alpha}\left\{(1 - 2\vartheta)^2 + (1 - 2\vartheta)\right\}\frac{t^\theta}{\Gamma(\theta + 1)}, \tag{58}$$

$$\underline{R_{21}}(t,\vartheta) = \tilde{\alpha}\left\{(2\vartheta - 1)^2 - \tilde{\beta}(2\vartheta - 1)\right\}\frac{t^\theta}{\Gamma(\theta + 1)}, \tag{59}$$

$$\bar{R}_{21}(t,\vartheta) = \tilde{\alpha}\left\{(1 - 2\vartheta)^2 - \tilde{\beta}(1 - 2\vartheta)\right\}\frac{t^\theta}{\Gamma(\theta + 1)}, \tag{60}$$

$$\underline{R_{31}}(t,\vartheta) = \tilde{\alpha}\left\{(2\vartheta - 1)^2 - \left(\tilde{\beta} + \tilde{\gamma}\right)(2\vartheta - 1)\right\}\frac{t^\theta}{\Gamma(\theta + 1)}, \tag{61}$$

$$\bar{R}_{31}(t,\vartheta) = \tilde{\alpha}\left\{(1 - 2\vartheta)^2 - \left(\tilde{\beta} + \tilde{\gamma}\right)(1 - 2\vartheta)\right\}\frac{t^\theta}{\Gamma(\theta + 1)}, \tag{62}$$

$$\underline{R_{41}}(t,\vartheta) = \tilde{\gamma}(2\vartheta - 1), \tag{63}$$

$$\bar{R}_{41}(t,\vartheta) = \tilde{\gamma}(1 - 2\vartheta). \tag{64}$$

Applying the same process, we can find the higher terms as follows

$$\begin{aligned}\underline{R_{12}}(t,\vartheta) = \Bigg(&\left[\left\{-\tilde{\alpha}(2\vartheta - 1)^2 + (2\vartheta - 1)\right\}2\vartheta - 1\right] \\ &- \left[\left\{\tilde{\alpha}(2\vartheta - 1)^2 + \tilde{\beta}(2\vartheta - 1)\right\}(2\vartheta - 1)\right] \\ &+ \left[\left\{-\tilde{\alpha}(2\vartheta - 1)^2 + \left(\tilde{\beta} + \tilde{\gamma}\right)(2\vartheta - 1)\right\}(2\vartheta - 1)\right]\Bigg)\frac{t^{2\theta}}{\Gamma(2\theta + 1)},\end{aligned} \tag{65}$$

$$\begin{aligned}\bar{R}_{21}(t,\vartheta) = \Bigg(&\left[\left\{-\tilde{\alpha}(1 - 2\vartheta)^2 + (1 - 2\vartheta)\right\}(1 - 2\vartheta)\right] \\ &- \left[\left\{\tilde{\alpha}(1 - 2\vartheta)^2 + \tilde{\beta}(c)\right\}(1 - 2\vartheta)\right] \\ &+ \left[\left\{-\tilde{\alpha}(1 - 2\vartheta)^2 + \left(\tilde{\beta} + \tilde{\gamma}\right)(1 - 2\vartheta)\right\}(1 - 2\vartheta)\right]\Bigg)\frac{t^{2\theta}}{\Gamma(2\theta + 1)},\end{aligned} \tag{66}$$

$$\begin{aligned}\underline{R_{22}}(t,\vartheta) = \Bigg(&\Bigg[-\Bigg\{\tilde{\alpha}\Bigg\{\tilde{\alpha}(2\vartheta - 1)^3 + \tilde{\alpha}\left[(2\vartheta - 1)^3 - \tilde{\beta}(2\vartheta - 1)^2\right] \\ &- \tilde{\beta}(2\vartheta - 1)\Bigg\} + \tilde{\beta}\left[\tilde{\alpha}(2\vartheta - 1)^2 - \tilde{\beta} + \tilde{\gamma}(2\vartheta - 1)\right]\Bigg\}\Bigg]\Bigg)\frac{t^{2\theta}}{\Gamma(2\theta + 1)},\end{aligned} \tag{67}$$

$$\begin{aligned}\bar{R}_{22}(t,\vartheta) = \Bigg(&\Bigg[-\Bigg\{\tilde{\alpha}\Bigg\{\tilde{\alpha}(1 - 2\vartheta)^3 + \tilde{\alpha}\left[(1 - 2\vartheta)^3 - \tilde{\beta}(1 - 2\vartheta)^2\right] \\ &- \tilde{\beta}(1 - 2\vartheta)\Bigg\} + \tilde{\beta}\left[\tilde{\alpha}(1 - 2\vartheta)^2 - \tilde{\beta} + \tilde{\gamma}(1 - 2\vartheta)\right]\Bigg\}\Bigg]\Bigg)\frac{t^{2\theta}}{\Gamma(2\theta + 1)},\end{aligned} \tag{68}$$

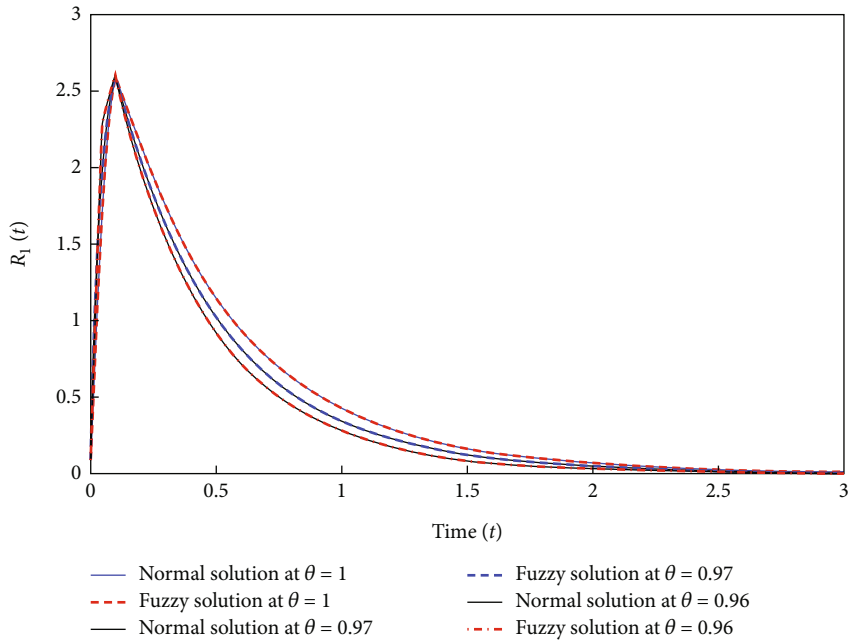

Figure 1: Fractional dynamics of reactants R_1 in the enzymatic reaction.

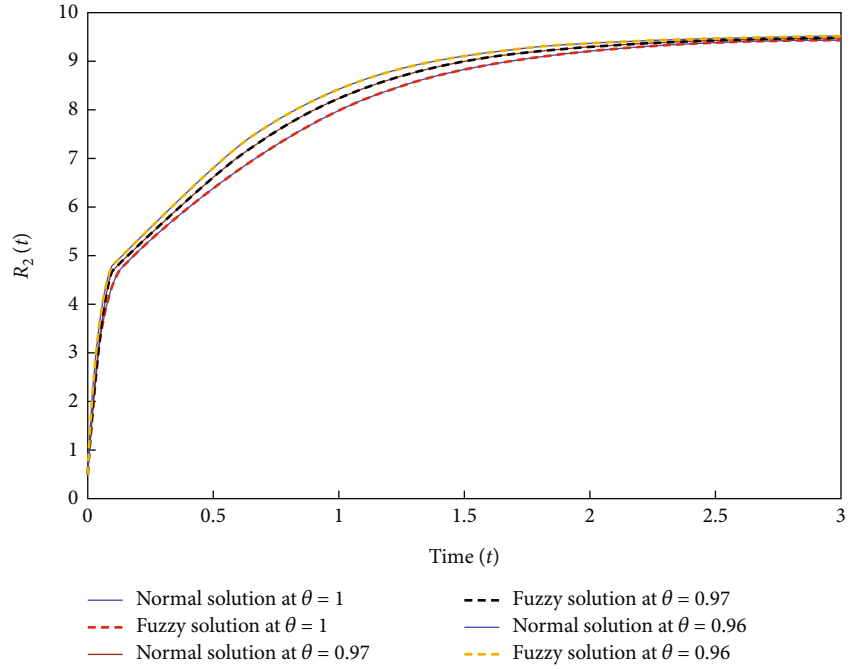

Figure 2: Fractional dynamics of reactants R_2 in the enzymatic reaction.

$$\underline{R_{32}}(t,\vartheta) = \left(\left[\left\{\tilde{\alpha}\left\{\tilde{\alpha}(2\vartheta-1)^3 + \tilde{\alpha}\left[(2\vartheta-1)^3 - \tilde{\beta}(2\vartheta-1)^2\right] - \tilde{\beta}(2\vartheta-1)\right\}\right.\right.\right.$$
$$\left.\left.\left. + \tilde{\beta}\left[\tilde{\alpha}(2\vartheta-1)^2 - \tilde{\beta} + \tilde{\gamma}(2\vartheta-1)\right]\right\}\right]\right)\frac{t^{2\theta}}{\Gamma(2\theta+1)}, \tag{69}$$

$$\bar{R_{32}}(t,\vartheta) = \left(\left[\left\{\tilde{\alpha}\left\{\tilde{\alpha}(1-2\vartheta)^3 + \tilde{\alpha}\left[(1-2\vartheta)^3 - \tilde{\beta}(1-2\vartheta)^2\right] - \tilde{\beta}(1-2\vartheta)\right\}\right.\right.\right.$$
$$\left.\left.\left. + \tilde{\beta}\left[\tilde{\alpha}(1-2\vartheta)^2 - \tilde{\beta} + \tilde{\gamma}(1-2\vartheta)\right]\right\}\right]\right)\frac{t^{2\theta}}{\Gamma(2\theta+1)}, \tag{70}$$

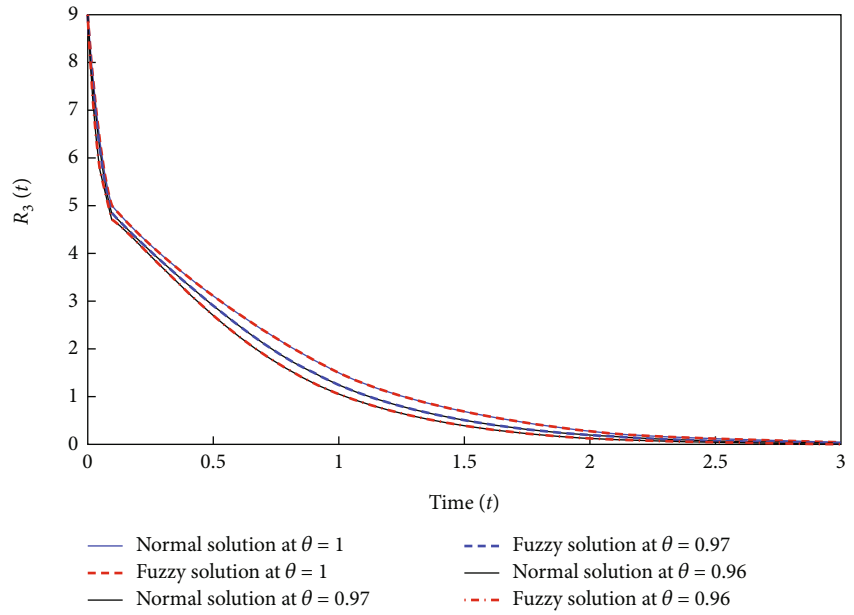

Figure 3: Fractional dynamics of reactants R_3 in the enzymatic reaction.

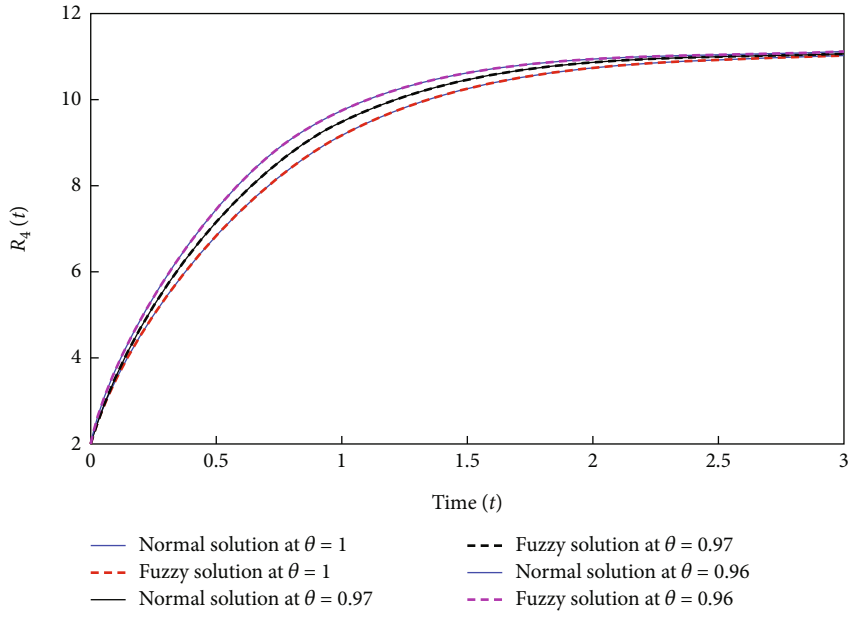

Figure 4: Fractional dynamics of reactants R_4 in the enzymatic reaction.

$$\underline{R_{42}}(t,\vartheta) = \tilde{\beta}\left[\tilde{\alpha}\left\{(2\vartheta-1)^2 - \tilde{\beta} + \tilde{\gamma}(2\vartheta-1)\right\}\right]\frac{t^{2\theta}}{\Gamma(2\theta+1)}, \tag{71}$$

$$\overline{R_{42}}(t,\vartheta) = \tilde{\beta}\left[\tilde{\alpha}\left\{(1-2\vartheta)^2 - \tilde{\beta} + \tilde{\gamma}(1-2\vartheta)\right\}\right]\frac{t^{2\theta}}{\Gamma(2\theta+1)}. \tag{72}$$

5. Numerical Results

Now we analyze the dynamics of a substrate's concentration, the enzyme's concentration, the concentration of the resulting complex, and the concentration of the resulting product in terms of fractional operators using the Homotopy perturbation method solution of fractional order. In Figures 1–4, we evaluated by comparing fuzzy and normal approximate solutions for the problem under discussion at various fractional orders against the observed uncertainty. The figures show that fuzzy logic, when combined with fractional calculus, provides global dynamics to nonlinear problems with uncertain data. Given that stochastic and random parameters are far more harder to resolve, and that uncertainty may lead to increases in estimation costs, modeling such physical problems using fuzzy notions is the right approach.

The values of R_1 first increases and then decreases drastically with a decrease in the fractional parameter θ.

The values of R_2 first increases at a slower rate and then increases exponentially with an increase in the fractional parameter θ.

The values of R_3 first decrease at a slower rate and then decrease exponentially with an increase in the fractional parameter θ.

The values of R_4 increase exponentially with a decrease in the fractional parameter θ.

6. Conclusion

Many academics have given numerical, approximate approaches and applications to handle Michaelis Menten enzymatic reaction model in general, due to the difficulty that appeared in obtaining accurate solutions to fractional differential equations. For examining the approximate solution of the Michaelis Menten enzymatic reaction equation, extension of the spectral homotopy analysis method, Runge-Kutta method, Laplace transformation, and Adomian decomposition approach has been used by researchers. We have developed a proper strategy for obtaining an approximate solution for the suggested model using the fuzzy theory and Homotopy perturbation method. To demonstrate the effectiveness of this strategy, we compared fuzzy and normal solutions up to three iterations. We discovered that fuzzy theory combined with fractional calculus technique yielded outstanding dynamics of Michaelis Menten enzymatic reaction model in instances where data uncertainty exists. By substituting classical differential derivatives with fractional derivatives based on fuzzy theory, we have suggested the new approach to Michaelis Menten enzymatic reaction model. The sequential iterations were built using fractional calculus theory and homotopy perturbation method in fuzzy sense. The numerical findings validated the fuzzy fractional case when compared to fractional order results.

7. Future Recommendations

As a result, developing various approaches known in the sense of fuzzy fractional differentials remains a future aim for us and many other scholars [21–25]. Finally, using the homotopy perturbation approach, the impacts of a wide range of fuzzy theory values and fractional order on the dynamics of fractional enzymatic reactions were examined. We propose that in future work, we concentrate on expanding this study with the help of other special functions and the use of two-scale fractal dimension. In addition, we can get additional results by using the modified homotopy perturbation method and He's fractal derivative.

Data Availability

All the data are available within the article.

Conflicts of Interest

The authors declare that they have no conflicts of interest.

References

[1] J. H. He, "A short review on analytical methods for a fully fourth-order nonlinear integral boundary value problem with fractal derivatives," *International Journal of Numerical Methods for Heat and Fluid Flow*, vol. 30, no. 11, pp. 4933–4943, 2020.

[2] J. H. He, "Lagrange crisis and generalized variational principle for 3D unsteady flow," *International Journal of Numerical Methods for Heat and Fluid Flow*, vol. 30, no. 3, pp. 1189–1196, 2019.

[3] J. H. He, "A short remark on fractional variational iteration method," *Physics Letters A*, vol. 375, no. 38, pp. 3362–3364, 2011.

[4] Z. Hans-Jürgen, *Fuzzy Set Theory—And Its Applications*, Springer Science and Business Media, 2011.

[5] A. Manal and K. M. Saad, "Fractal fractional Michaelis Menten enzymatic reaction model via different kernels," *Fractal and Fractional*, vol. 6, no. 1, p. 13, 2022.

[6] J. H. He and Z. B. Li, "Converting fractional differential equations into partial differential equations," *Thermal Science*, vol. 16, no. 2, pp. 331–334, 2012.

[7] J. H. He, "Homotopy perturbation method for bifurcation of nonlinear problems," *International Journal of Nonlinear Sciences and Numerical Simulation*, vol. 6, no. 2, pp. 207-208, 2005.

[8] S. Salahshour, A. Ahmadian, M. Salimi, M. Ferrara, and D. Baleanu, "Asymptotic solutions of fractional interval differential equations with nonsingular kernel derivative," *Chaos: An Interdisciplinary Journal of Nonlinear Science*, vol. 29, no. 8, article 083110, 2019.

[9] S. Salahshour, A. Ahmadian, B. A. Pansera, and M. Ferrara, "Uncertain inverse problem for fractional dynamical systems using perturbed collage theorem," *Communications in Nonlinear Science and Numerical Simulation*, vol. 94, article 105553, 2021.

[10] K. L. Wang, "Fractal solitary wave solutions for fractal nonlinear dispersive Boussinesq-like models," *Fractals*, vol. 30, no. 4, pp. 1–8, 2022.

[11] K. L. Wang and H. Wang, "Fractal variational principles for two different types of fractal plasma models with variable coefficients," *Fractals*, vol. 30, no. 3, pp. 2250043–2250381, 2022.

[12] K. L. Wang, "Exact travelling wave solutions for the local fractional Kadomtsov-Petviashvili-Benjamin-Bona-Mahony model by variational perspective," *Fractals*, vol. 30, no. 6, article 2250101, 2022.

[13] K. L. Wang, "A novel perspective to the local fractional bidirectional wave model on cantor sets," *Fractals*, vol. 30, no. 6, article 2250107, 2022.

[14] Z. A. Khan, A. Khan, T. Abdeljawad, and H. Khan, "Computational analysis of fractional order imperfect testing infection disease model," *Fractals*, vol. 30, no. 5, 2022.

[15] A. Khan, Z. A. Khan, T. Abdeljawad, and H. Khan, "Analytical analysis of fractional-order sequential hybrid system with numerical application," *Advances in Continuous and Discrete Models*, vol. 2022, no. 1, article 12, pp. 1–19, 2022.

[16] A. Din and Y. Li, "Stochastic optimal analysis for the hepatitis B epidemic model with Markovian switching," *Mathematical Methods in the Applied Sciences*, 2022.

[17] A. Din, Y. Li, A. Yusuf, and A. I. Ali, "Caputo type fractional operator applied to hepatitis B system," *Fractals*, vol. 30, no. 1, article 2240023, 2022.

[18] Z. Lotfi Asker, "Fuzzy sets as a basis for a theory of possibility," *Fuzzy Sets and Systems*, vol. 1, no. 1, pp. 3–28, 1978.

[19] S. Salahshour, T. Allahviranloo, and S. Abbasbandy, "Solving fuzzy fractional differential equations by fuzzy Laplace transforms," *Communications in Nonlinear Science and Numerical Simulation*, vol. 17, no. 3, pp. 1372–1381, 2012.

[20] S. K. Miller and B. Ross, *An Introduction to the Fractional Calculus and Fractional Differential Equations*, Wiley, 1993.

[21] Q. T. Ain and J. H. He, "On two-scale dimension and its applications," *Thermal Science*, vol. 23, no. 3 Part B, pp. 1707–1712, 2019.

[22] Q. T. Ain, N. Anjum, A. Din, A. Zeb, S. Djilali, and Z. A. Khan, "On the analysis of Caputo fractional order dynamics of Middle East lungs coronavirus (MERS-CoV) model," *Alexandria Engineering Journal*, vol. 61, no. 7, pp. 5123–5131, 2022.

[23] Q. T. Ain, N. Anjum, and C. H. He, "An analysis of time-fractional heat transfer problem using two-scale approach," *GEM-International Journal on Geomathematics*, vol. 12, no. 1, pp. 1–10, 2021.

[24] Q. T. Ain, M. Ali, M. Yousif, and Bilqees, "A study of pseudo spectral Galerkin method for solving differential equations," *Engineering Heritage Journal (GWK)*, vol. 2, pp. 31–33, 2020.

[25] Q. T. Ain, G. Rehman, and M. Zaheer, "An analysis of water flow in subsurface environment by using Adomian decomposition method," *Water Conservation and Management*, vol. 3, no. 1, pp. 27–29, 2019.

Hindawi
Advances in Mathematical Physics
Volume 2023, Article ID 5822589, 10 pages
https://doi.org/10.1155/2023/5822589

Research Article

Application of Engineering Science Model Based on Fuzzy Sets in Enterprise Financial Evaluation Index

Yue Wang

School of Economics and Management, Xi'an Aeronautical Institute, Xi'an, Shaanxi, China

Correspondence should be addressed to Yue Wang; 201407012@xaau.edu.cn

Received 8 October 2022; Revised 3 February 2023; Accepted 20 March 2023; Published 1 April 2023

Academic Editor: S. E. Najafi

With the continuous development of society and the increasingly fierce competition among enterprises, it is necessary to analyze the production and operation conditions of enterprises in a timely and effective manner. In the context of the development of information technology, many companies analyze financial data, and corporate financial analysis indicators are the analysis of various report data of the company's operations, which can effectively reflect the company's debt repayment, operation, profit, and development capabilities. Enterprises can judge the operation status of the enterprise and make strategic changes in time according to the indicators of enterprise financial analysis. However, due to the large amount of operational data of enterprises and different relationships among different types of data, the analysis of enterprise financial data is not accurate enough when using traditional enterprise financial analysis indicators for analysis. This paper established an engineering scientific model through fuzzy sets and improved the data analysis ability of enterprise financial analysis indicators in enterprises by means of fuzzy analysis. By comparing the enterprise financial analysis indicators of the engineering science model based on fuzzy sets and the traditional enterprise financial analysis indicators, the experimental results showed that the average financial information analysis accuracy of the enterprise financial analysis index based on the engineering science model based on fuzzy sets and the traditional enterprise financial analysis index are 84% and 74%, respectively. Therefore, applying the engineering science model based on fuzzy sets to the corporate financial analysis indicators can effectively improve the accuracy of financial information analysis.

1. Introduction

The financial status of an enterprise is an important part of enterprise management. During the normal operation of the enterprise, a large amount of enterprise operation data would be generated, which records the operation status and economic situation of the enterprise. However, enterprises do not fully apply these operational data, and most of the data are abandoned and eventually disappear. With the continuous development of information technology, people use information data more and more frequently, and various information analysis techniques are applied in various fields. By establishing a data warehouse for enterprise operation data and realizing data transformation, it can obtain analytical indicators for evaluating enterprise finance. Enterprise financial analysis indicators directly reflect the operating status of the enterprise and evaluate the financial status, operating status, and profitability of the enterprise by analyzing the data in the financial statements of the enterprise. The enterprise financial analysis index is a common and effective enterprise evaluation method, which can adjust the operating status of the enterprise in time through the analyzed data to maximize the economic benefits of the enterprise. However, the traditional enterprise financial analysis index analysis is not accurate enough, and the comprehensive analysis ability of various types of data is not good enough. How to improve the accuracy of the analysis of enterprise financial indicators is very important. However, enterprise financial indicators have fuzzy attributes, so it is necessary to build an engineering scientific model through fuzzy sets for analysis. The use of fuzzy sets to build an engineering scientific model can improve the analysis accuracy of enterprise financial analysis indicators, hereby improving the accuracy

of the enterprise's grasp of business data. Therefore, this paper has research significance.

The operation status of the enterprise is hidden in the various report data of the enterprise, and many people have studied the financial analysis indicators of the enterprise. Among them, Abutaber et al. effectively analyzed the annual operation status of the enterprise through data analysis of the annual financial statements of enterprise transactions [1]. Law and Yuen used enterprise financial analysis indicators to study the profitability indicators, financial liabilities, and operating performance of the enterprise to adjust the economic weight of the enterprise in time, so that the capital operation of the enterprise is more timely and effective and enterprises can make correct decisions according to financial information data, thus effectively improving the business performance of enterprises [2]. The research of Muhmad showed that the use of enterprise financial analysis indicators can effectively analyze the financial status and operating results of the enterprise and can effectively find the weak links in the production and operation of the enterprise [3]. Prasetya et al. conducted a detailed analysis of the corporate financial information of Polish companies and made the company clear about its own development status by analyzing its profitability, corporate reputation, and corporate development scale [4]. The analysis of enterprise financial analysis indicators can enable enterprises to fully understand their own operating conditions, but the analysis of data by enterprise financial analysis indicators is not accurate enough.

Fuzzy sets have excellent data analysis capabilities, and many researchers have applied engineering science models based on fuzzy sets to corporate financial analysis indicators. Among them, Sun used fuzzy mathematics to comprehensively analyze the financial data of the enterprise, which improved the analysis of the solvency of the enterprise [5]. Docekalova et al. built an engineering scientific model through fuzzy sets to analyze the financial statement data of the enterprise, which effectively improved the management ability of the enterprise [6]. Ruzakova proposed a fuzzy set modeling method to analyze the financial status of enterprises, which improved the ability to analyze the financial data of enterprises [7]. The research of Muhacheva indicated that the financial status of an enterprise can be effectively analyzed by establishing an engineering mathematical model of fuzzy sets, and the operational capability of an enterprise can be accurately judged through the financial analysis indicators of the enterprise [8]. The engineering mathematical model based on fuzzy sets can be applied to the financial analysis indicators of enterprises to accurately analyze the financial status and operating results of enterprises, but it lacks the comparison with traditional financial analysis indicators of enterprises.

Fuzzy sets are often used to solve multidata analysis problems. They are used to construct engineering scientific models and systematically analyze the financial data of enterprises [9, 10]. The innovation of this paper is as follows: the engineering mathematical model of fuzzy sets is used to study the financial analysis indexes of enterprises, and the analytic hierarchy process (AHP) is used to analyze the factors that affect the financial analysis results of enterprises. Comparing and analyzing the enterprise financial analysis indexes of the engineering science model based on fuzzy sets and traditional enterprise financial analysis indexes, the enterprise financial analysis indexes based on the engineering science model of fuzzy sets can effectively improve the management ability of enterprises.

2. Methods of Business Financial Evaluation

As the main participants in market economic activities and the direct undertaker of social production and circulation, enterprises maintain sustainable operations. The purpose of sustainable management of enterprises is to keep the profit growth of enterprises for a long time, adapt to the changes of the time environment, and make them prosperous for a long time. In the process of production and development, enterprises must generate a series of added values. The development of the entire market economy is closely related to the production and operation of enterprises [11, 12]. For example, enterprises create jobs, pay taxes, invest in public welfare projects, etc. Therefore, in order to assess the comprehensive management level of an enterprise, discover the weak links in its production and operation activities, analyze its causes, and then propose effective improvement measures, it becomes necessary to establish a complete set of comprehensive financial indicators system.

Enterprises would generate a large amount of data in the production process. These data describing the operation status of the enterprise play a key role in the management and decision-making of the enterprise. Corporate financial analysis is to describe the data generated by corporate finance and provides visual financial information for corporate managers. The process of corporate financial analysis is shown in Figure 1.

In Figure 1, the process of enterprise financial analysis is described. Through enterprise financial analysis, enterprise managers can analyze the financial information of the enterprise intuitively, effectively analyze the operating conditions of the enterprise, and make reasonable enterprise management decisions.

2.1. Corporate Financial Evaluation Indicators. The enterprise financial analysis index is the evaluation of the analysis of various financial information of the enterprise. The enterprise financial index is comprehensive, and the enterprise manager can accurately know the business operation status of the enterprise through the enterprise financial analysis index [13, 14]. Corporate financial analysis indicators are generally divided into four parts, namely, corporate debt repayment indicators, corporate operation indicators, corporate profit indicators, and corporate development indicators. The structural model of corporate financial analysis indicators is shown in Figure 2.

In Figure 2, the importance of corporate financial analysis indicators and the main manifestations of corporate financial analysis indicators are described. Enterprise managers can improve the efficiency of enterprise production and development through the analysis of various indicators.

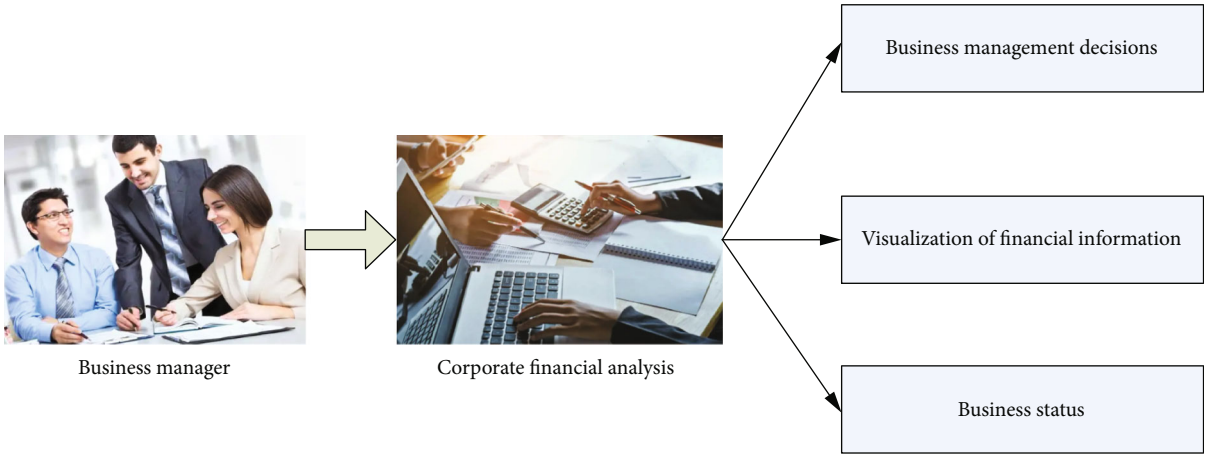

Figure 1: Process diagram of enterprise financial analysis.

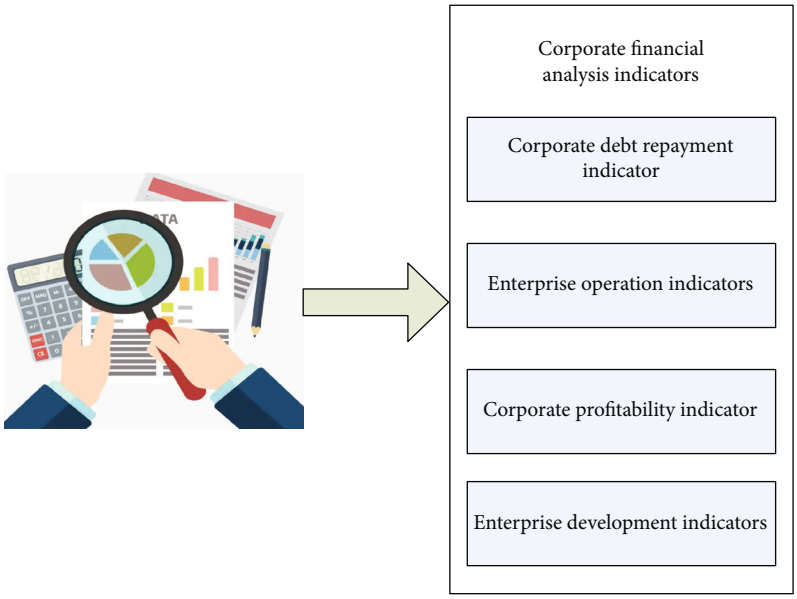

Figure 2: Structure model diagram of corporate financial analysis indicators.

Corporate debt repayment index: corporate debt repayment index analyzes and evaluates a company's solvency. It also provides information on corporate debt levels, the impact of debt management, and the efficiency of long-term and short-term debt [15].

Business operation indicators: business operation indicators show the effectiveness and efficiency of asset use and production. The profitability of a company depends to a large extent on the efficiency of its asset operation, which is also the main guarantee that it can repay its debts on time. The modification of the company's asset structure and the decision-making of creditors benefit from the analysis of this indicator.

Corporate profitability metrics: corporate profitability metrics measure a company's ability to generate profits and realize capital gains. Because it is a relative measure, the profitability of a business cannot be determined solely by its profit margin. Therefore, the profit margin indicator is mainly used to analyze the profitability of a business.

Enterprise development indicators: enterprise development indicators assess the ability of enterprises to transform resources and enhance overall value while pursuing self-sufficiency and sustainable development [16].

Through the accounting and analysis of the financial statement data of the enterprise, the development direction and strategic investment of the enterprise can be comprehensively evaluated, and the operation mode of the enterprise can be adjusted in time through the enterprise financial analysis to maximize the economic benefit of the enterprise.

The company's statement data is incomplete, and the accounting statement data mainly reflects the historical cost of asset acquisition, but cannot reflect the current cost or realizable value, and has no significant reference value for the company's future decision-making. These are the limitations of corporate financial analysis indicators.

Enterprise financial analysis indicators play an important role in analyzing the operating conditions of enterprises.

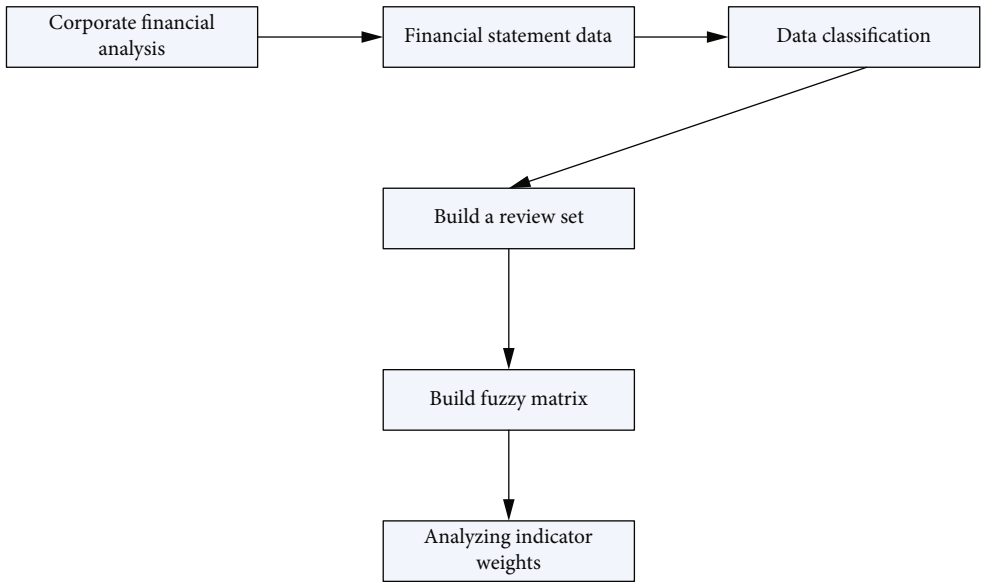

Figure 3: Flow chart of engineering science model based on fuzzy set.

Enterprise managers need to strengthen the use of enterprise financial analysis indicators in order to improve business performance [17].

2.2. Engineering Science Model Based on Fuzzy Sets. Fuzzy set is a collection used to express and analyze fuzzy concepts. The attributes of things are divided into two types. One is concrete and the other is vague [18, 19]. In corporate finance, many financial attributes are ambiguous, and no unilateral attributes can be expressed. For example, corporate operating risks include many aspects.

Engineering science models based on fuzzy sets can effectively analyze model problems and are widely used in financial analysis, scientific computing, and multivariate problems and can effectively and accurately analyze corporate financial analysis indicators [20].

Enterprise financial analysis is affected by many factors. Fuzzy set-based engineering science model realizes quantitative analysis of enterprise financial analysis indicators through fuzzy mathematics. The process of enterprise financial analysis based on the engineering science model of a fuzzy set is shown in Figure 3.

In Figure 3, the process of enterprise financial analysis based on the engineering science model of fuzzy sets is described, including the collection and classification of financial statement data, building a comment set, the construction of a fuzzy matrix, and the weight of analysis indicators. Among them, the data sources of enterprise financial analysis and various financial statements of enterprises are classified into assets, liabilities, cash flows, and other data, and a comment set is constructed to analyze the indicators that affect enterprise financial analysis.

The comment set is a set of judgments on the results of the financial analysis of the enterprise. If there are n comments in the comment set, it can be expressed as

$$A = \{a_1, a_2, \cdots, a_n\}. \tag{1}$$

In Formula (1), a_n represents the nth comment in the comment set.

Assuming that there are m financial analysis indicators of the enterprise, then the financial analysis indicators of the enterprise can be expressed as

$$B = \{b_1, b_2, \cdots, b_m\}. \tag{2}$$

The membership relationship between the enterprise financial analysis indicators and the comments is constructed, and the membership degree of the jth index to the ith comment is k_{ij}, and then the membership relationship of the ith index in the index set to all comments is expressed as

$$k_j = \left(k_{j1}, k_{j2}, \cdots, k_{\mathrm{jn}}\right). \tag{3}$$

Constructing a fuzzy matrix for all indicators, the result is

$$K = \begin{bmatrix} k_1 \\ k_2 \\ \cdots \\ k_m \end{bmatrix} = \begin{bmatrix} k_{11} & k_{12} & \cdots & k_{1n} \\ k_{21} & k_{22} & \cdots & k_{2n} \\ \cdots & \cdots & \cdots & \cdots \\ k_{m1} & k_{m2} & \cdots & k_{mn} \end{bmatrix}. \tag{4}$$

Assuming that the weight of the corporate financial analysis indicator is W, then the weight is expressed as

$$W = \{w_1, w_2, \cdots, w_m\}. \tag{5}$$

The weights of corporate financial analysis indicators should have the following relationships:

$$w_1 + w_2 + \cdots + w_m = 1. \tag{6}$$

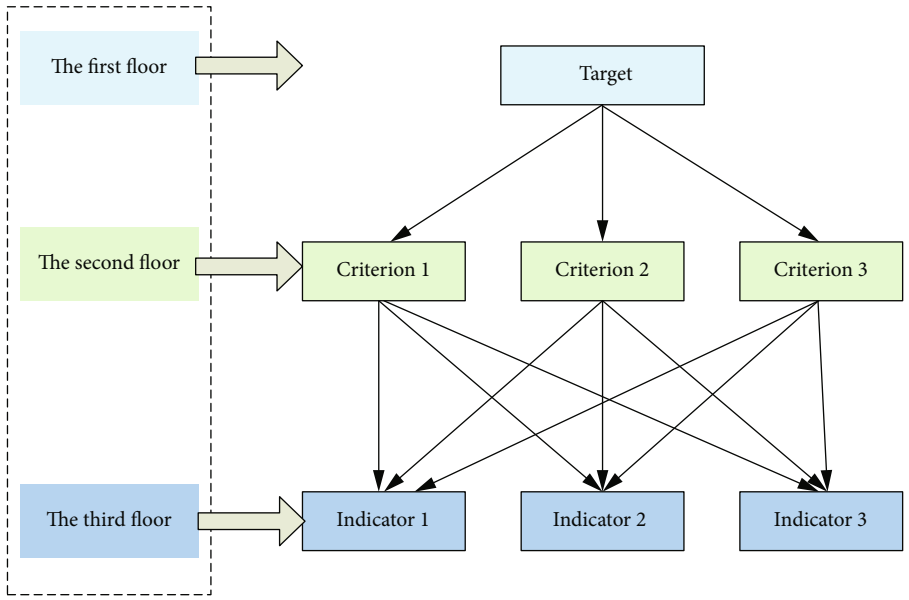

Figure 4: AHP structure diagram.

Using the weights and fuzzy matrix of corporate financial analysis indicators, the impact of each indicator on corporate finance can be analyzed.

$$Y = W \bullet K = (y_1, y_2, \cdots, y_m). \tag{7}$$

In Formula (6), y_m represents the enterprise financial analysis result of the mth index.

Therefore, as long as the weights of the corporate financial analysis indicators are analyzed, the corporate financial analysis results of each indicator can be calculated through the engineering scientific model based on fuzzy sets [21, 22]. In this paper, the analytic hierarchy process is used to analyze the weights of the enterprise financial analysis indicators.

2.3. Analytic Hierarchy Process. The analytic hierarchy process (AHP) is a combination of qualitative and quantitative analysis methods, which can effectively determine the weight of corporate financial analysis indicators. It divides the problem of enterprise financial analysis into three layers for analysis [23]. The structure of AHP is shown in Figure 4.

In Figure 4, the structure of the AHP is described. From top to bottom are the target layer, the criterion layer, and the indicator layer, focusing on the analysis of the weights between the financial analysis indicators of each enterprise.

From the engineering science model based on fuzzy sets, it is concluded that the enterprise financial analysis index is $B = \{b_1, b_2, \cdots, b_m\}$, and the impact of the enterprise financial analysis index on the enterprise financial analysis is $C = \{c_1, c_2, \cdots, c_m\}$. Assuming that the influence of any two indicators is c_r, c_t, of which $r, t \in \{1, 2, \cdots, m\}$, the ratio of the impact of any two indicators on the financial analysis of the enterprise can be expressed as

$$C_{\mathrm{rt}} = \frac{C_r}{C_t}. \tag{8}$$

In Formula (8), C_{rt} represents the ratio of the influence of the rth index to the tth index on the financial analysis of the enterprise.

Conversely, the ratio of the tth index to the rth index's impact on the financial analysis of the enterprise can be expressed as

$$C_{\mathrm{tr}} = \frac{C_t}{C_r}. \tag{9}$$

All the indicators in $B = \{b_1, b_2, \cdots, b_m\}$ are compared to the impact of enterprise financial analysis, and the results of the comparison are formed into a judgment matrix.

$$C = \begin{bmatrix} 1 & c_{12} & \cdots & c_{1m} \\ c_{21} & 1 & \cdots & c_{2m} \\ \vdots & \vdots & \ddots & \vdots \\ c_{m1} & c_{\mathrm{m2}} & \cdots & 1 \end{bmatrix}. \tag{10}$$

In Formula (10), each column of the judgment matrix represents the relative influence of each indicator.

The column vector of the judgment matrix is normalized to obtain

$$\bar{c}_{\mathrm{rt}} = \frac{c_{\mathrm{rt}}}{\sum_{k=1}^{m} c_{\mathrm{kt}}}. \tag{11}$$

The normalized results of the column vectors are added to obtain

$$\bar{E}_r = \sum_{t=1}^{m} \bar{c}_{\mathrm{rt}}. \tag{12}$$

$\bar{E} = [\bar{e}_1, \bar{e}_2, \bar{e}_3, \cdots, \bar{e}_m]^T$ is normalized to get

$$E_r = \frac{\bar{E}}{\sum_{t=1}^{m} \bar{E}_t} \tag{13}$$

By normalizing the judgment matrix, the maximum eigenvalue of the judgment matrix is calculated.

$$s_{\max} = \sum_{r=1}^{m} \frac{(CE)_r}{mE_r}. \tag{14}$$

In Formula (14), $s_{\max}$ represents the largest eigenvalue of the judgment matrix C.

The consistency index of the judgment matrix is obtained.

$$Q = \frac{S_{\max} - m}{m - 1}. \tag{15}$$

Then, the consistency ratio is expressed as

$$U = \frac{Q}{G}. \tag{16}$$

In Formula (16), U is the consistency ratio, and G represents the high-order average consistency index.

When $U < 0.1$, it indicates that the judgment matrix can be used to analyze the index weight, and when $U > 0.1$, it indicates that the judgment matrix is not standard and needs to be modified [24].

Using the judgment matrix, the weight of each indicator is calculated, which is expressed as

$$w_r = \frac{C_{1r} + C_{2r} + \cdots + C_{\mathrm{mr}}}{m}. \tag{17}$$

In Formula (17), M represents the number of financial analysis indicators of the enterprise.

3. Experiments in Corporate Financial Evaluation

3.1. Enterprise Financial Evaluation Indicator Data. The enterprise financial analysis index reflects the operation status of the enterprise. In order to effectively analyze the comprehensive enterprise financial analysis index, this paper would conduct a questionnaire survey on 200 enterprise managers and 300 enterprise financial personnel. It mainly investigates the corporate financial analysis indicators considered by those who are in close contact with corporate financial analysis. The results of the questionnaire survey on corporate financial analysis indicators are shown in Table 1.

In Table 1, a total of 6 types of corporate financial analysis indicators are counted, of which the corporate management capability index accounts for the highest proportion, accounting for 19%, and the company's core competitiveness index accounts for the least proportion of 14%. Since the proportion of the number of people occupied by the abovementioned six indicators is not much different, it is necessary to further analyze the weight of the impact of each indicator on the financial analysis of enterprises.

Table 1: Questionnaire survey result table.

Index	Number of people (person)	Proportion
Corporate solvency	80	16%
Corporate profitability	90	18%
Enterprise management ability	95	19%
Financial information analysis accuracy	80	16%
Enterprise development ability	85	17%
Enterprise's core competitiveness	70	14%

The hierarchical structure is constructed by the analytic hierarchy process, and the weights of the indicators of the second layer are analyzed. The hierarchical structure constructed by the enterprise financial analysis is shown in Table 2.

In Table 2, the hierarchical structure that affects the effect of enterprise financial analysis is analyzed, and the criterion layer is divided into three categories, namely, enterprise operation, enterprise competition, and financial information analysis. Among them, the maximum weight of the standard layer occupied by enterprise operation is 75%, while the weight of the standard layer occupied by enterprise competition is at least 3%.

The judgment matrix is used to analyze the weights of the index layers in Table 2, and the weight analysis results of each index are shown in Table 3.

In Table 3, using the judgment matrix to count the weight results of the six indicators, the weight of the enterprise management ability index is the highest at 26%, followed by the enterprise profitability index, the accuracy index of financial analysis accounts for 22%. Because the weights of the enterprise development capability index and the enterprise's core competitiveness index are too small compared with other indicators, and they are 6% and 3%, respectively, the experiment would not analyze the enterprise development capability index and the enterprise's core competitiveness index.

3.2. Experiment Design of Corporate Financial Evaluation Indicators. In order to analyze the application of the engineering science model based on fuzzy sets in the corporate financial analysis indicators, this paper compares the enterprise financial analysis index based on the engineering science model of fuzzy sets with the traditional enterprise financial analysis index and observes the impact of the two methods of enterprise financial analysis on the operation effect of the enterprise.

Among them, the traditional enterprise financial analysis indicators are still obtained by analyzing various report data, while the enterprise financial analysis index based on the engineering science model of fuzzy set conducts fuzzy

Table 2: Hierarchical structure table of enterprise financial analysis.

Target layer	Criterion layer	Criterion layer weights	Indicator layer
Corporate financial analysis	Business operation	75%	Corporate solvency
			Corporate profitability
			Enterprise management ability
			Enterprise development ability
	Business competition	3%	Enterprise's core competitiveness
	Financial information analysis	22%	Financial information analysis accuracy

Table 3: Weight analysis results of each indicator.

Serial number	Indicator layer	Weights
1	Corporate solvency	20%
2	Corporate profitability	23%
3	Enterprise management ability	26%
4	Enterprise development ability	6%
5	Enterprise's core competitiveness	3%
6	Financial information analysis accuracy	22%

analysis on different types of report data through fuzzy mathematics and other methods and obtains a comprehensive enterprise financial analysis index. In order to make the comparison of the financial analysis indicators of the two companies more obvious, the experiment would be set for 5 months, and the data of the financial analysis indicators of the two companies would be counted once every month. Due to differences in financial analysis indicator data for companies of different sizes, small and large companies would be analyzed separately.

4. Results of Business Financial Evaluation

4.1. Corporate Solvency. Enterprise debt repayment is the periodical repayment of debt. To analyze the influence of two types of enterprise financial indicators on enterprise debt repayment ability, the experiment selected 20 large enterprises and 20 small enterprises as the research objects. Among them, half use traditional enterprise financial analysis indicators to analyze enterprises, and the other half use enterprise financial analysis indicators based on fuzzy sets of engineering science models to analyze enterprises. Figure 5 shows the impact of two corporate financial indicators on corporate solvency.

In Figure 5(a), the impact of two corporate financial indicators on the solvency of small enterprises is described. Among them, the solvency of enterprises under the traditional corporate financial indicators is gradually improving, from 62% in the first month to 68% in the third month. The solvency of the enterprise under the enterprise financial analysis index based on the engineering science model of fuzzy sets is also constantly improving, and the overall solvency of the enterprise is better than that under the traditional enterprise financial index. In Figure 5(b), the impact of two corporate financial indicators on the solvency of large companies is described. The corporate solvency under traditional corporate financial indicators reaches a minimum of 66% in the first month and reaches a maximum of 72% in the third month. The solvency of the enterprise under the enterprise financial analysis index based on the engineering science model of fuzzy sets reaches a minimum of 76% in the first month and a maximum of 84% in the fifth month. Therefore, applying the engineering science model based on fuzzy sets to the financial analysis indicators of enterprises can effectively improve the solvency of enterprises.

4.2. Enterprise Profitability. The profitability of an enterprise is also an important criterion for measuring the operating effect of an enterprise. All the behaviors of an enterprise are aimed at making profits. Comparing the enterprise financial analysis indicators based on the engineering science model of fuzzy sets and traditional enterprise financial analysis indicators, the comparison results of enterprise profitability under the two enterprise financial analysis indicators are shown in Figure 6.

In Figure 6(a), the impact of two corporate financial analysis indicators on the profitability of small enterprises is described, in which the corporate profitability under the traditional corporate financial indicators first decreased and then increased, reaching a minimum of 48% in the fourth month. However, the profitability of the enterprise under the enterprise financial analysis index based on the engineering science model of fuzzy sets is constantly improving, reaching a maximum of 72% in the fifth month. In Figure 6(b), it describes the impact of two corporate financial analysis indicators on the profitability of large enterprises. Among them, the corporate profitability under the traditional corporate financial indicators reached a minimum of 62% in the fourth month and an average of 65.6%. The profitability of the enterprise under the enterprise financial analysis index based on the engineering science model of fuzzy sets is constantly improving, from 70% in the first month to 78% in the fifth month. Therefore, the analysis of enterprise finance through the engineering science model based on fuzzy sets can effectively improve the profitability of the enterprise.

4.3. Enterprise Management Ability. The management capability of an enterprise reflects the relationship between the investment of the enterprise and the production of economic benefits. Through the enterprise financial analysis index based on the engineering science model of fuzzy sets and

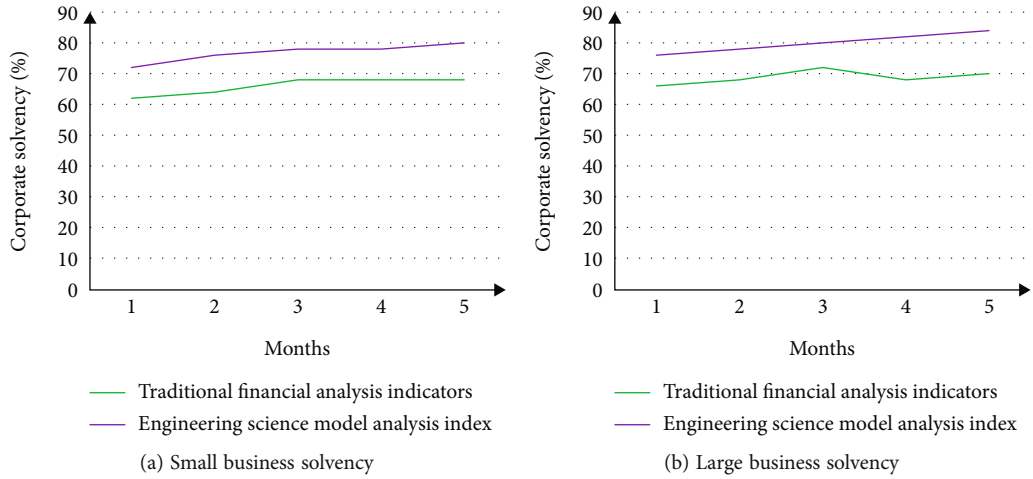

Figure 5: Comparison results of corporate solvency.

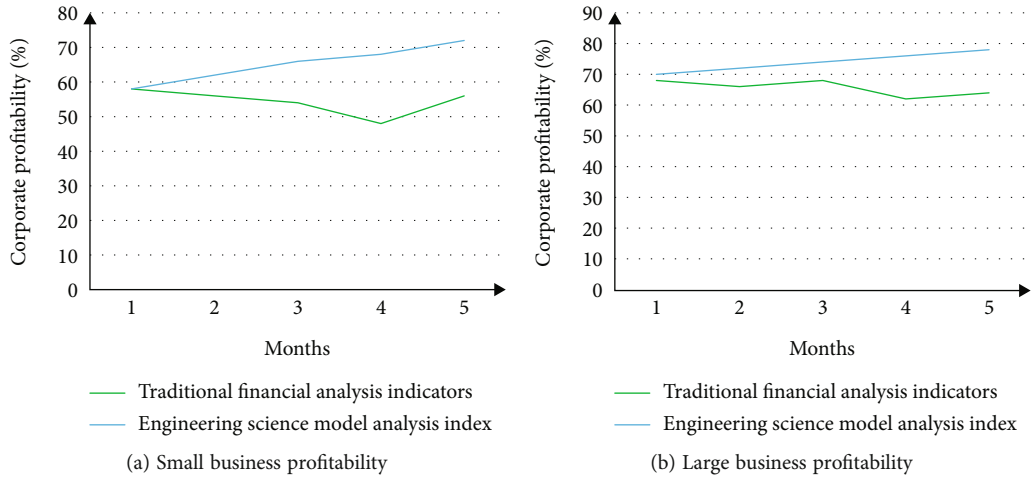

Figure 6: Comparison results of corporate profitability.

the traditional enterprise financial index, the enterprise management ability is compared. Because the enterprise's management ability cannot be reflected in a short time, the comparison period of the two kinds of enterprise financial indicators is set to 5 months. The enterprise management ability under the two enterprise financial analysis indicators is shown in Figure 7.

In Figure 7(a), the impact of the two corporate financial analysis indicators on the management capabilities of small enterprises is described. The corporate management capabilities under the traditional corporate financial analysis indicators reached a maximum of 72% in the fourth month, and the average enterprise management capabilities were 67.6%. The enterprise management ability under the enterprise financial analysis index based on the engineering science model of fuzzy sets was constantly improving, reaching 78% in the fifth month, and the average enterprise management ability was 75.6%. In Figure 7(b), the impact of two corporate financial analysis indicators on the management capacity of large enterprises was described, in which the average enterprise management capacity of traditional enterprise financial analysis indicators was 71.2%, while the average enterprise management capability under the enterprise financial analysis index based on the engineering science model of fuzzy sets was 81.8%. Therefore, the application of the engineering science model based on fuzzy sets in the enterprise financial analysis index can improve the management ability of the enterprise.

4.4. Accuracy of Financial Information Evaluation. Enterprise financial analysis index is to analyze the data of various financial statements of the enterprise and to judge the operation status of the enterprise by analyzing the financial information. Then, the accuracy of the financial information analysis of the enterprise is very important. The accuracy of financial information analysis is compared between the enterprise financial analysis index based on the engineering science model of fuzzy sets and the traditional enterprise financial analysis index. The comparison results of the accuracy of financial information analysis under the two corporate financial analysis indicators are shown in Figure 8.

In Figure 8, the comparison of the accuracy of financial information analysis by two corporate financial analysis indicators is described. The accuracy of financial

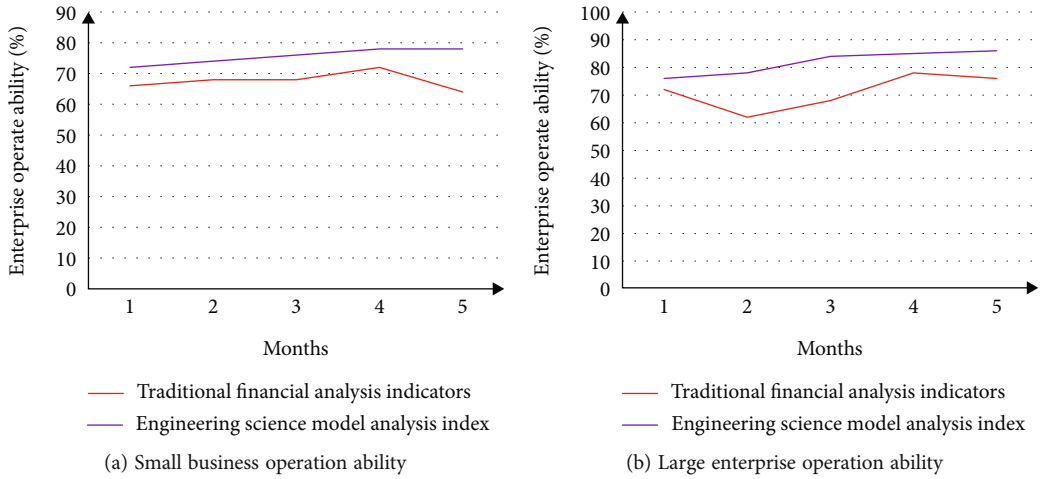

Figure 7: Comparison results of enterprise management capabilities.

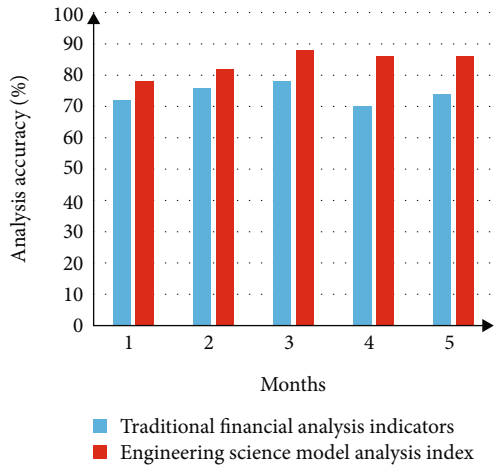

Figure 8: The comparison result of the accuracy of financial information analysis.

information analysis under the traditional corporate financial analysis indicators reached a minimum of 72% in the first month and reached a maximum of 78% in the 3rd month, and the average financial information analysis accuracy was 74%. The accuracy of financial information analysis under the enterprise financial analysis index based on the engineering science model of fuzzy sets reached a maximum of 88% in the third month, and the average financial information analysis accuracy was 84%. Therefore, the enterprise financial analysis index based on the engineering science model of fuzzy sets can more accurately analyze the financial information.

5. Conclusions

The living environment of enterprises is getting worse and worse, and enterprises must develop according to the correct strategy so as not to be eliminated. However, financial analysis is to provide enterprises with data-based guidance programs to reflect the operation and development capabilities of enterprises. This paper used the AHP to analyze the main influencing factors that affect the financial analysis effect of enterprises, which are the solvency of the enterprise, the profitability of the enterprise, the management ability of the enterprise, and the accuracy of financial information analysis. The engineering science model based on fuzzy sets was used to effectively analyze various financial data and apply it to the enterprise financial analysis index and compare it with the traditional enterprise financial analysis index. The results showed that the application of the engineering scientific model with fuzzy nature to the financial analysis index of the enterprise can effectively improve the debt repayment, profitability, and management ability of the enterprise. Analyzing the financial status of an enterprise is very important to the development of the enterprise. The operation status of the enterprise was evaluated through the financial analysis indicators of the enterprise, and a strategic policy was provided for the development of the enterprise. However, when comparing the enterprise financial analysis index based on the engineering science model based on fuzzy sets and the traditional enterprise financial analysis index, this paper only analyzed the two types of objects: small enterprises and large enterprises, and did not compare and analyze medium-sized enterprises. The proportion of medium-sized enterprises is very large, and small and medium-sized enterprises occupy a large economic market, so it is very important to analyze the financial analysis indicators of medium-sized enterprises. Therefore, it would be the direction of future research to expand the comparison of two kinds of enterprise financial analysis indicators in medium-sized enterprises.

Data Availability

The data can be obtained by contacting the author within reasonable requirements.

Conflicts of Interest

This paper has no potential competing interests.

References

[1] T. A. Abutaber, A. Bzur, M. H. Odeh, M. Alathamneh, and M. Kamal, "The effect of corporate governance indicators on enhancing the financial performance of industrial listed companies on the Amman stock exchange," *Accounting*, vol. 7, no. 2, pp. 415–422, 2021.

[2] P. Law and D. Yuen, "Financial analysis and corporate governance of AA: a case study," *Corporate Ownership and Control*, vol. 16, no. 2, pp. 19–24, 2019.

[3] S. N. Muhmad, "The influence of the financial indicators towards the changes of the corporate tax avoidance," *Journal of Advanced Research in Dynamical and Control Systems*, vol. 12, no. 1, pp. 167–171, 2020.

[4] H. D. Prasetya, E. Saraswati, and A. Ghofar, "Corporate social responsibility disclosure and corporate financial performance: a meta-analysis," *Russian Journal of Agricultural and Socio-Economic Sciences*, vol. 68, no. 8, pp. 3–11, 2017.

[5] G. Sun, "Quantitative analysis of enterprise chain risk based on SVM algorithm and mathematical fuzzy set," *Journal of Intelligent Fuzzy Systems*, vol. 39, no. 4, pp. 5773–5783, 2020.

[6] M. P. Docekalova, K. Doubravsky, M. Dohnal, and A. Kocmanova, "Evaluations of corporate sustainability indicators based on fuzzy similarity graphs," *Ecological Indicators*, vol. 78, pp. 108–114, 2017.

[7] O. Ruzakova, "Fuzzy-sets modeling of the financial condition of the enterprise," *Economy, Finances, Management*, vol. 4, no. 4 (44), pp. 67–76, 2019.

[8] A. Muhacheva, "Financial analysis of an industrial enterprise," *Bulletin of Kemerovo State University Series Political Sociological and Economic Sciences*, vol. 2019, no. 4, pp. 415–424, 2019.

[9] H. Parsian, H. Kazemi, and J. Rezazadeh, "Identification of voluntary disclosure indicators and corporate governance: the gap between current and expected situations," *Applied Research in Financial Reporting*, vol. 8, no. 1, pp. 67–95, 2019.

[10] C. Freire, F. Carrera, P. Auquilla, and G. Hurtado, "Independence of corporate governance and its relation to financial performance," *Problems and Perspectives in Management*, vol. 18, no. 3, pp. 150–159, 2020.

[11] C. Dura, A. P. Pun, and R. I. Moraru, "Empirical analysis on the relationship between corporate health and safety performance and the financial outcome within socially responsible companies," *Quality - Access to Success*, vol. 19, no. 162, pp. 155–160, 2018.

[12] E. Najimi and N. Shorkar, "Understanding the relationship between corporate social responsibility and financial performance," *International Journal of Advanced Research*, vol. 7, no. 10, pp. 528–536, 2019.

[13] S. Li, D. Gao, and X. Hui, "Corporate governance, agency costs, and corporate sustainable development: a mediating effect analysis," *Discrete Dynamics in Nature and Society*, vol. 2021, Article ID 5558175, 15 pages, 2021.

[14] S. Balagobei, "Corporate governance and financing choices in firms: a panel data analysis of Sri Lankan companies," *Asia Pacific Management Review*, vol. 15, no. 1, pp. 97–113, 2020.

[15] E. A. Demyanova, "Criteria for assessing corporate development risks arising with introduction of financial technologies," *Finance Theory and Practice*, vol. 21, no. 4, pp. 182–190, 2017.

[16] A. Shrivastava, N. Kumar, and P. Kumar, "Bayesian analysis of working capital management on corporate profitability: evidence from India," *Journal of Economic Studies*, vol. 44, no. 4, pp. 568–584, 2017.

[17] G. Ernius and L. Birkyt, "Financial information and management decisions: impact of accounting policy on financial indicators of the firm," *Verslas Teorija ir Praktika*, vol. 21, no. 1, pp. 48–57, 2020.

[18] X. Zhu, Y. Zhang, Y. Hou, and M. Jiang, "Evaluation and analysis of land input-output comprehensive benefit based on fuzzy mathematics and analytic hierarchy process," *Adv. Math. Phys.*, vol. 2022, article 1113693, pp. 1–10, 2022.

[19] J. Li, Y. Wang, and B. Yang, "Research on fuzzy decision-making method of task allocation for ship multiagent collaborative design," *Adv. Math. Phys.*, vol. 2022, article 6368110, pp. 1–20, 2022.

[20] O. G. Tretyakova and T. I. Chinaeva, "Statistical analysis of the financial state of the banking sector," *Statistics and Economics*, vol. 15, no. 2, pp. 20–29, 2018.

[21] P. Peykani, M. Nouri, and F. Eshghi, "A novel mathematical approach for fuzzy multi-period multi-objective portfolio optimization problem under uncertain environment and practical constraints," *Journal of Fuzzy Extension and Applications*, vol. 2, no. 3, pp. 191–203, 2021.

[22] M. Imeni, "Fuzzy logic in accounting and auditing," *Journal of Fuzzy Extension and Applications*, vol. 1, no. 1, pp. 69–75, 2020.

[23] R. Kountur and L. Aprilia, "A factor analysis of corporate financial performance: prospect for new dimension," *ACRN Journal of Finance and Risk Perspectives*, vol. 9, no. 1, pp. 113–119, 2020.

[24] L. Alfaro, G. Asis, A. Chari, and U. Panizza, "Corporate debt, firm size and financial fragility in emerging markets," *Journal of International Economics*, vol. 118, pp. 1–19, 2019.

Hindawi
Advances in Mathematical Physics
Volume 2022, Article ID 7622906, 10 pages
https://doi.org/10.1155/2022/7622906

Research Article

Financial Futures Prediction Using Fuzzy Rough Set and Synthetic Minority Oversampling Technique

Shangkun Deng, Yingke Zhu, Ruijie Liu, and Wanyu Xu

College of Economics and Management, China Three Gorges University, Yichang 443002, China

Correspondence should be addressed to Yingke Zhu; 202012530021115@ctgu.edu.cn

Received 30 June 2022; Revised 15 September 2022; Accepted 8 October 2022; Published 16 November 2022

Academic Editor: Khalid K. Ali

In this research, a novel approach called SMOTE-FRS is proposed for movement prediction and trading simulation of the Chinese Stock Index 300 (CSI300) futures, which is the most crucial financial futures in the Chinese A-share market. First, the SMOTE- (Synthetic Minority Oversampling Technique-) based method is employed to address the sample unbalance problem by oversampling the minority class and undersampling the majority class of the futures price change. Then, the FRS- (fuzzy rough set-) based method, as an efficient tool for analyzing complex and nonlinear information with high noise and uncertainty of financial time series, is adopted for the price change multiclassification of the CSI300 futures. Next, based on the multiclassification results of the futures price movement, a trading strategy is developed to execute a one-year simulated trading for an out-of-sample test of the trained model. From the experimental results, it is found that the proposed method averagely yielded an accumulated return of 6.36%, a F1-measure of 65.94%, and a hit ratio of 62.39% in the four testing periods, indicating that the proposed method is more accurate and more profitable than the benchmarks. Therefore, the proposed method could be applied by the market participants as an alternative prediction and trading system to forecast and trade in the Chinese financial futures market.

1. Introduction

As a crucial part of the world financial markets, the Chinese financial futures market could have a significant impact on the global economy [1, 2]. Stock index futures, which are efficient financial derivatives for hedging trading risk, have become more and more popular among market participants, and numerous scholars have conducted research on their price predictions [3–7]. With the fast development of communication technology, the ability of investors to capture opportunities in the shorter term gradually increases [8]. Subsequently, there is an increasing number of individual and institutional investors participating in High-Frequency Trading (HFT), and many researchers have focused on the studies of high-frequency price forecasting [9, 10]. However, some scholars found that the traditional methods are difficult to achieve a satisfactory performance due to the nonlinear and uncertain character of financial time series [11, 12].

In the last few decades, with the rapid development of artificial intelligence (AI) technologies, machine learning-based approaches have been widely applied to the analysis of massive and nonlinear data in various applications, which include the finance field [13–15]. Among them, the fuzzy set and rough set are efficient tools for analyzing complex and nonlinear information with high noise and uncertainty. Thus, some researchers combined fuzzy set- and rough set-based theories to solve relevant problems. For instance, Dubois and Prade designed the fuzzy rough set-based method by combining two theories [16, 17], and it has been widely applied by many researchers. The complex and nonlinear concept is approximated by the fuzzy rough lower and upper approximation, and it allows the elements to be recognizable from each other to some extent, rather than being either discernible or not.

With the rapid development of technology, an increasing number of investors prefer high-frequency trading [9, 10].

However, the performance of a trading decision support model will be affected by significant differences in the base price of various stocks [18]. Therefore, their trading decision support systems tend to forecast price movements as a trading signal for the trading strategies. Additionally, for solving the multiclassification problem of financial price movement prediction, the training samples of each class are usually unbalanced, which could lead to biased prediction results and unsatisfactory accuracy [19, 20]. Therefore, it is also necessary to balance the sample labels of price direction and magnitude for the CSI300 futures.

In this research, by integrating the SMOTE-based oversampling method and fuzzy rough set (FRS), we propose a high-frequency price trend multiclassification and simulation trading method for the CSI300 futures, which is the most crucial financial futures in the Chinese A-share market. The SMOTE-based method is adopted to balance the label ratios, and the FRS is employed as the base classifier for price movement prediction. Based on the multiclassification prediction results, we also design a trading strategy for simulation trading. The main contributions of this study could be summed up as follows: (1) by integration of SMOTE and FRS-based methods, a novel price movement multiclassification and simulation trading approach is developed for the CSI300 futures; (2) the SMOTE-based method is applied in this study to deal with the unbalanced samples, which effectively avoided biased prediction results and improved the prediction accuracy; and (3) a trading strategy based on the multiclassification results is designed for enhancing the trading performance of the proposed method.

The rest of this article is arranged as follows: Section 2 introduces the related works of this study. The background of relevant methods is described in Section 3. In Section 4, we provide an explanation of the proposed method in detail. The experimental results are reported and discussed in Section 5. In Section 6, we conclude this study and provide several research directions.

2. Related Work

In the last two decades, machine learning-based methods have been widely used as an efficient and remarkable classification and regression tool in the financial fields. For instance, Lin et al. constructed a novel ensemble machine learning method with six commonly used machine learning algorithms including SVM (Support Vector Machine), RF (Random Forest), and KNN (K-Nearest Neighbor) to predict the daily price movements of stocks in the Chinese stock market. The experimental results show that the accuracy and profitability of their proposed method outperformed the traditional methods [21]. Kamalov proposed a Neural Network- (NN-) based method for significant change prediction in stock price, and the experimental results show that the proposed method obtained the best accuracy [22]. Yu and Yan developed a stock price prediction model based on a deep learning- (DL-) based algorithm, and they concluded that their proposed method produced a larger prediction accuracy than traditional models [23]. However, those methods not only require a large amount of complete data but also need preprocessing prior to the model training.

The fuzzy set and rough set, as efficient tools in machine learning algorithms for analyzing complex and nonlinear information with high noise and uncertainty, have been widely applied in the financial fields. For instance, Sun et al. proposed a price prediction model for the stock index in the Chinese stock market by combining the traditional fuzzy time series model and rough set method [24]. Kumar et al. proposed a stock price forecasting method based on the fuzzy set, and they tested it in the Indian stock market. Experimental results showed that the proposed method outperformed the benchmark methods [25]. In addition to these applications of fuzzy sets and rough sets to build classifiers for forecasting stock prices, it is also widely used for reducing data dimensionality [26, 27]. Jensen et al. proposed a novel hybrid fuzzy rough rule induction approach, which combines the process of rule induction and attribute reduction. They improved the greedy hill-climbing strategy, which made it perform better than the benchmark methods [28, 29]. Thus, in this article, the CSI 300 index futures prediction is selected as the research object, and the approach proposed by Jensen et al. [28, 29] is employed to generate rules for its price change prediction.

Additionally, for solving the multiclassification problem of financial price movement prediction, the training samples of each class are usually unbalanced, which leads to biased classification results and low accuracy [30, 31]. The Synthetic Minority Oversampling Technique (SMOTE), which was proposed by Chawla et al. [32], is an efficient method for solving unbalanced samples by oversampling the minority [33], and it has been successfully and widely applied in many fields [33–36]. Therefore, following the research of Chawla et al. [32], the SMOTE-based approach is employed and integrated into the proposed method to balance the model training samples of different classes before the model training of fuzzy rough set (FRS).

3. Background

The fuzzy set approach can be used to handle fuzzy data, while rough sets can deal with incomplete information. By expanding equivalence relations in rough sets to fuzzy equivalence relations, it results in an integration of rough set and fuzzy set theories [37–39]. For variables x, y, z in U $(\forall x, y, z \in U)$, the fuzzy equivalence relation R should satisfy the following three properties: (1) reflexivity: $\mu_R(x, x) = 1$; (2) symmetry: $\mu_R(x, y) = \mu_R(y, x)$; and (3) transitivity: $\mu_R(x, z) \geq \mu_R(x, y) \wedge \mu_R(y, z)$. The partition of U, generated by the associated equivalence relation R_P of nonempty finite set P of attributes, $U/P = \{F_1, \cdots, F_m\}$, which can be calculated by using the conjunction of constituent fuzzy equivalence classes F_i $(1 \leq i \leq m)$. For any fuzzy concept X in the universe of discourse to be approximated $(\forall X \in U)$, the fuzzy lower and upper approximations are redefined as

$$\mu_{\underline{P}X}(x) = \sup_{F \in U/P} \min \left(\mu_F(x), \inf_{y \in U} \max \{1 - \mu_F(y), \mu_X(y)\} \right),$$
$$\mu_{\bar{P}X}(x) = \sup_{F \in U/P} \min \left(\mu_F(x), \sup_{y \in U} \min \{\mu_F(y), \mu_X(y)\} \right), \tag{1}$$

where the tuple $\langle \bar{P}X, \underline{P}X \rangle$ that generated from the fuzzy lower and upper approximations is the fuzzy rough set. The fuzzy positive region can be defined as

$$\mu_{\mathrm{POS}_P(Q)}(x) = \sup_{X \in U/Q} \mu_{\underline{P}X}(x). \tag{2}$$

In addition, the fuzzy rough dependency function could be defined as follows:

$$\gamma'_P(Q) = \frac{\sum_{x \in U} \mu_{\mathrm{pos}_P(Q)}(x)}{|U|}. \tag{3}$$

The dependency of Q on P is equal to the proportion of identifiable objects in the entire dataset, which corresponds to determining the fuzzy cardinality of positive region $\mu_{\mathrm{POS}_P(Q)}(x)$ divided by the total number of objects in the universe U. R is the approximation of the set C for all conditional properties when $\gamma'_{R-|a|}(D) \neq \gamma'_C(D)(\forall a \in R)$ and $\gamma'_R(D) = \gamma'_C(D)$.

For the fuzzy rough rule induction and feature selection approach proposed by Jensen et al., it merges the processes of rule induction and feature selection, and it improves the hill-climbing strategy of the original algorithm, which can generate a rule on the fly that completely covers the training samples [28, 29]. Equation (4) is used to assess the quality of approximation of all conditional attributes. The core features are identified through the dependency change of the full set of the conditional features when the individual attributes are removed:

$$\mathrm{Core}(C) = \left\{ a \in C | \gamma'_{C-\{a\}}(Q) < \gamma'_C(Q) \right\}. \tag{4}$$

A subset of the attribute set that maintains invariance with the fuzzy rough positive region is then defined as the relative reduction, and each rule generated from the fuzzy rough set will contain a more compact subset [29, 37].

4. Proposed Method

In this study, a novel approach SMOTE-FRS is proposed for the price movement multiclassification of the CSI300 futures. The main structure of the proposed method is presented in Figure 1. There are mainly four parts of the proposed method: (1) Data preprocessing part. In this part, the 1 min frequency trading data of the CSI300 futures are collected and transformed into the 1-hour frequency data and features. Then, the datasets containing the normalized data of features are divided into several training and testing datasets. (2) Training sample reconstruction part. The SMOTE-based approach is employed for minority class oversampling and majority class undersampling in the training dataset to generate a balanced group of training samples. (3) Signal generation part. The training datasets are used for model training to generate trading signals based on the fuzzy rough rule (see more details in Section 5.2). (4) Simulated trading and result evaluation part. In this part, a predesigned trading strategy is applied, and simulated trading is carried out for one year of out-of-sample testing. Finally, three evaluation indicators are employed to judge the prediction performance and profit-making ability of the proposed method.

5. Experimental Design

5.1. Data Preprocessing. In the data preprocessing part, first, the 1 min frequency trading data of the CSI300 futures that range from January 2020 and December 2021 is derived from the Choice Database (the formal website of the Choice Database is http://choice.eastmoney.com/). The trading data for experiments consists of the open and close prices, trading volume, and open interest in the 1 min timeframe. The original data are used to calculate the hourly return (Return), volume change rate (VCR), and the open interest change rate (OICR). The calculation ways of those indicators are shown as Equation (5). The indicators within the ten hours prior to the prediction points are then standardized to provide the prediction features for the initial input datasets, as listed in Table 1, in which the Return, VCR, and OICR are denoted by R, V, and H, respectively. For instance, R_4 represents the Return four hours before the forecasting point. Then, the entire dataset is separated into training and testing datasets with a ratio of about 4 : 1. Next, the SMOTE-based approach is used to address the sample unbalanced problem by oversampling the minority class and undersampling the majority class of samples. Details about the unbalanced sample processing are reported in Table 2, in which label = 1, 2, 3, 4 are multiclassification classes that represent the small rise, large rise, small fall, and large fall in price, respectively. Label = 0 represents the minor changes in price that do not meet the transaction conditions. Additionally, the experiment dataset window will be slid forward one period (three months) by the sliding window technique after one round of model training and testing, and the entire testing period lasts for one year in total. Details of the experiment data design are provided in Table 3:

$$\mathrm{Return}_t = \frac{\mathrm{Close}_t - \mathrm{Open}_{t-9}}{\mathrm{Open}_{t-9}},$$
$$\mathrm{VCR}_t = \frac{\mathrm{Volume}_t - \mathrm{Volume}_{t-9}}{\mathrm{Volume}_{t-9}}, \tag{5}$$
$$\mathrm{OICR}_t = \frac{\mathrm{OI}_t - \mathrm{OI}_{t-9}}{\mathrm{OI}_{t-9}},$$

where Close_t, Open_t, Volume_t, and OI_t, respectively, represent the closing price, opening price, trading volume, and open interest at the t hour.

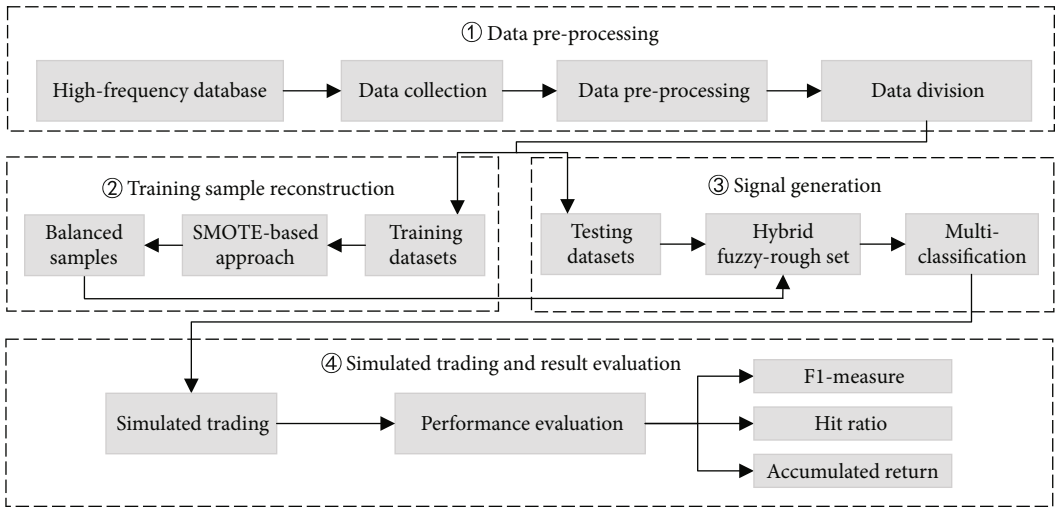

Figure 1: The main structure and working procedures of the proposed method SMOTE-FRS.

Table 1: The list of input features for multiclassification.

Indicator	Input features
Hourly return (Return)	$R_{10}, R_9, R_8, R_7, R_6, R_5, R_4, R_3, R_2, R_1$
Volume change rate (VCR)	$V_{10}, V_9, V_8, V_7, V_6, V_5, V_4, V_3, V_2, V_1$
Open interest change rate (OICR)	$H_{10}, H_9, H_8, H_7, H_6, H_5, H_4, H_3, H_2, H_1$

Table 2: The data preprocessing results of the SMOTE-based approach. Note that the class imbalance ratio = majority class/minority class.

Multiclassification	Label = 0	Label = 1	Label = 2	Label = 3	Label = 4
Class	Majority class	Minority class	Minority class	Minority class	Minority class
The unbalanced samples before processing					
Training period 1	717	99	18	92	21
Class imbalance ratio	\	7.24	39.83	7.79	34.14
Training period 2	770	93	12	80	17
Class imbalance ratio	\	8.28	64.17	9.63	45.29
Training period 3	756	104	11	87	18
Class imbalance ratio	\	7.27	68.73	8.69	42.00
Training period 4	772	90	8	87	11
Class imbalance ratio	\	8.58	96.50	8.87	70.18
The sample numbers after processing by SMOTE					
Training period 1	396	297	54	276	63
Class imbalance ratio	\	1.33	7.33	1.43	6.29
Training period 2	372	279	36	240	51
Class imbalance ratio	\	1.33	10.33	1.55	7.29
Training period 3	416	312	33	261	54
Class imbalance ratio	\	1.33	12.61	1.59	7.70
Training period 4	360	270	24	261	33
Class imbalance ratio	\	1.33	15.00	1.38	10.91

5.2. Trading Strategy Design. The training datasets are used to generate rules based on a fuzzy rough set for multiclassification of the CSI300 futures direction change, which results in labels representing the price changes (expressed as the FR, Forecasting Return) one hour after the prediction. Additionally, a predesigned trading strategy is employed to validate

Table 3: The four subdatasets for model training and model testing.

Subdataset	Model training period	Model testing period
Dataset 1	2020/Jan.–2020/Dec. (1 year)	2021/Jan.–2021/Mar. (3 months)
Dataset 2	2020/Apr.–2021/Mar. (1 year)	2021/Apr.–2021/June (3 months)
Dataset 3	2020/Jul.–2021/June (1 year)	2021/Jul.–2021/Sept. (3 months)
Dataset 4	2020/Oct.–2021/Sept. (1 year)	2021/Oct.–2021/Dec. (3 months)

the prediction accuracy and profitability of the proposed method in trading simulation based on the classification results. An example of multiclassification and trading simulation of the proposed method is plotted in Figure 2. As shown in Figure 2, the hourly return (Return), volume change rate (VCR), and open interest change rate (OICR) within the ten hours prior to the prediction points are employed as the input features, and the FRS is used as the base classifier to forecast the price changes one hour after the forecast points with the output of the price change label (label). If the Forecasting Return (FR) is greater than T_4, the classification label is 2; if FR is larger than T_3 and less than or equal to T_4, the classification label is 1; when FR is greater than or equal to T_2 and less than or equal to T_3, the classification label is 0; if FR is larger than or equal to T_1 and less than T_2, the classification label is 3; if FR is smaller than T_1, the classification label is 4. As reported in Table 4, the multiclassification results are then also used as trading signals to design a trading strategy, which is set out as follows: if the classification label is 2, a long transaction with a leverage of 2 is applied; if the classification label is 1, a long transaction with small leverage of 1 will be used; when the classification label is 0, no transaction will be executed; if the classification label is 3, a short-selling transaction with small leverage of 1 is executed; if the classification label is 4, the proposed method will execute a short-selling transaction with large leverage of 2. Note that the abovementioned T_1, T_2, T_3, and T_4 are the level thresholds, in which T_1 is set to -0.02, T_2 is set to -0.01, T_3 is set to 0.01, and T_4 is set to 0.02. Additionally, the value of small leverage is set to 1, and the large leverage value is set to 2. The trading commission is set to 0.1% per transaction. Finally, the position holding period length for each transaction is set to five hours.

5.3. Benchmark Design. For judging the performance of the proposed method SMOTE-FRS, several popular machine learning methods are adopted to design the benchmarks. In the benchmark methods, the SVM, ANN, RF, XGBoost, and the deep learning method multilayer perceptron (MLP) are adopted as the basic classifier for multiclassification of the CSI300 futures movement. Note that for each benchmark method, the SMOTE-based approach is also used by them to produce balanced samples for model training. In addition, the FRS-based method without using SMOTE (FRS-no-SMOTE) is designed as one of the benchmarks, and it is used for testing the functions of the SMOTE method in the proposed method. Furthermore, two classic passive trading strategies, Buy-and-Hold (BAH) and Short-and-Hold (SAH), are employed as benchmark methods to evaluate the performance of the proposed method.

5.4. Performance Evaluation Measures

5.4.1. F1-Measure. In order to evaluate the performance of the proposed model in price change prediction of the CSI300 futures, the F1-measure (see Equation (6)) is employed as the accuracy evaluator based on the results of the confusion matrix (see Table 5):

$$\text{F1-measure} = \frac{2^{*}\text{TPR}^{*}\text{PPV}}{\text{TPR} + \text{PPV}}, \tag{6}$$

$$\text{TPR} = \frac{\text{TP}}{\text{TP} + \text{FN}}, \tag{7}$$

$$\text{PPV} = \frac{\text{TP}}{\text{TP} + \text{FP}}. \tag{8}$$

In Table 5, TP represents the correct times of positive predictions (including small and large rises for the price change, label = 1 or label = 2); TN represents the correct times of negative predictions (both small and large declines for the price change, label = 3 or label = 4); FN indicates the times of positive price changes that are incorrectly predicted as negative changes, and FP denotes the times of negative changes that are incorrectly predicted as positive changes. TPR and PPV stands for true positive rate and positive predictive value, respectively.

5.4.2. Hit Ratio (HR). The HR is a measure of the price direction forecasting accuracy, which can be calculated from

$$\text{HR} = \frac{\text{PF} + \text{NF}}{N}, \tag{9}$$

where PF denotes the times of correct positive forecasting, NF is the times of correct negative forecasting, and N means the total times of direction forecasting.

5.4.3. Accumulated Return (AR). Accumulated return (AR) is an indicator that measures the profitability of the trading system with the formulas shown in

$$\text{AR} = \sum_{n=1}^{N} (P_n * l_n - C), \tag{10}$$

$$P_n = \frac{\text{Close}_{n+1} - \text{Open}_n}{\text{Open}_n}, \tag{11}$$

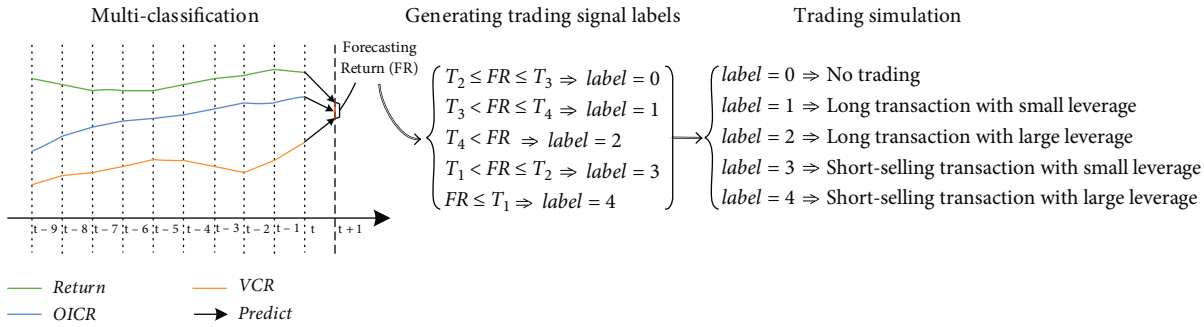

Figure 2: The design of multiclassification and trading simulation of the proposed method.

Table 4: The design of label, threshold, trading signal, and leverage of the trading strategy for the proposed method.

Label	Level threshold	Trading signal	Leverage
0	$[T_2, T_3]$	No trading	N/A
1	$(T_3, T_4]$	Long	1
2	$>T_4$	Long	2
3	$[T_1, T_2)$	Short-selling	1
4	$<T_1$	Short-selling	2

Table 5: The confusion matrix for price movement prediction of the CSI300 futures.

	Positive change	Negative change
Positive prediction	True positive (TP)	False positive (FP)
Negative prediction	False negative (FN)	True negative (TN)

where P_n denotes the return yielded by the nth transaction, which can be calculated from Equation (11), and l_n indicates the leverage chosen for the nth transaction; C denotes the trading cost for each transaction. Note that the trading cost C is zero for the current trading if the current trading signal is the same as the former one, because there is no need to close the position if the current trading signal is identical to the former one. Otherwise, the value of the trading cost C is 0.1% per round trip. N means the total transaction times.

6. Experimental Results

6.1. Multiclassification Results. In this study, the FRS is used as the rule-based classifier for price change multiclassification of CSI300 futures, resulting in the price change labels. The decision rules extracted based on the FRS are in the form of IF-THEN, and some examples of the rules are shown as follows.

Rule 1. IF R6 is around 0.0089 and H3 is around 0.1015 and R1 is around 0.0038 and R5 is around 0.0064 and R8 is around 0.0036 and V8 is around 0.1866 THEN label is 4.

Rule 2. IF R4 is around −0.0113 and H3 is around 0.0918 and R1 is around −0.0012 and R5 is around −0.0082 and R8 is around −0.0005 and V8 is around 0.1072 THEN label is 0.

Rule 3. IF R7 is around −0.0018 and H3 is around 0.1235 and R1 is around 0.0025 and R5 is around 0.0004 and R8 is around 0.0018 and V8 is around 0.0648 THEN label is 3.

Rule 4. IF R10 is around 0.0152 and H3 is around 0.1098 and R1 is around −0.0034 and R5 is around −0.0035 and R8 is around 0.0012 and V8 is around 0.0726 THEN label is 1.

Rule 5. IF R9 is around −0.0010 and H3 is around 0.1130 and R1 is around −0.0003 and R5 is around 0.0002 and R8 is around 0.0025 and V8 is around 0.1536 THEN label is 1.

Based on the decision rules extracted from the training datasets with the FRS, a predesigned trading strategy is applied for transaction simulation with the multiclassification results out-of-sample. The confusion matrix results of the proposed method over the four testing periods are presented in Figure 3, where the horizontal blocks in each subplot indicate the predicted classes and actual classes on the vertical blocks. The darker the color of the blocks, the greater the number of classes.

Based on the confusion matrix results, the F1-measure results of the proposed method and benchmark methods for the testing periods are reported in Table 6. First, as shown in Table 6, the average result of the F1-measure over the four testing periods for the proposed method (SMOTE-FRS) is 65.94%, which is larger than the results of SMOTE-SVM (60.63%), SMOTE-ANN (60.66%), SMOTE-RF (61.59%), and SMOTE-XGBoost (62.02%). Moreover, the results of all benchmark methods experienced at least one F1-measure lower than 60% within the testing periods. It indicates that compared to these traditional machine learning algorithms, the proposed method produced a more accurate and robust performance in price change multiclassification of the CSI300 futures. Although the SMOTE-MLP-based method produced the excellent F1-measure result in the fourth quarter (72.41%), the results within the second and third quarters are less than 65%, while the proposed method consistently yielded F1-measure results

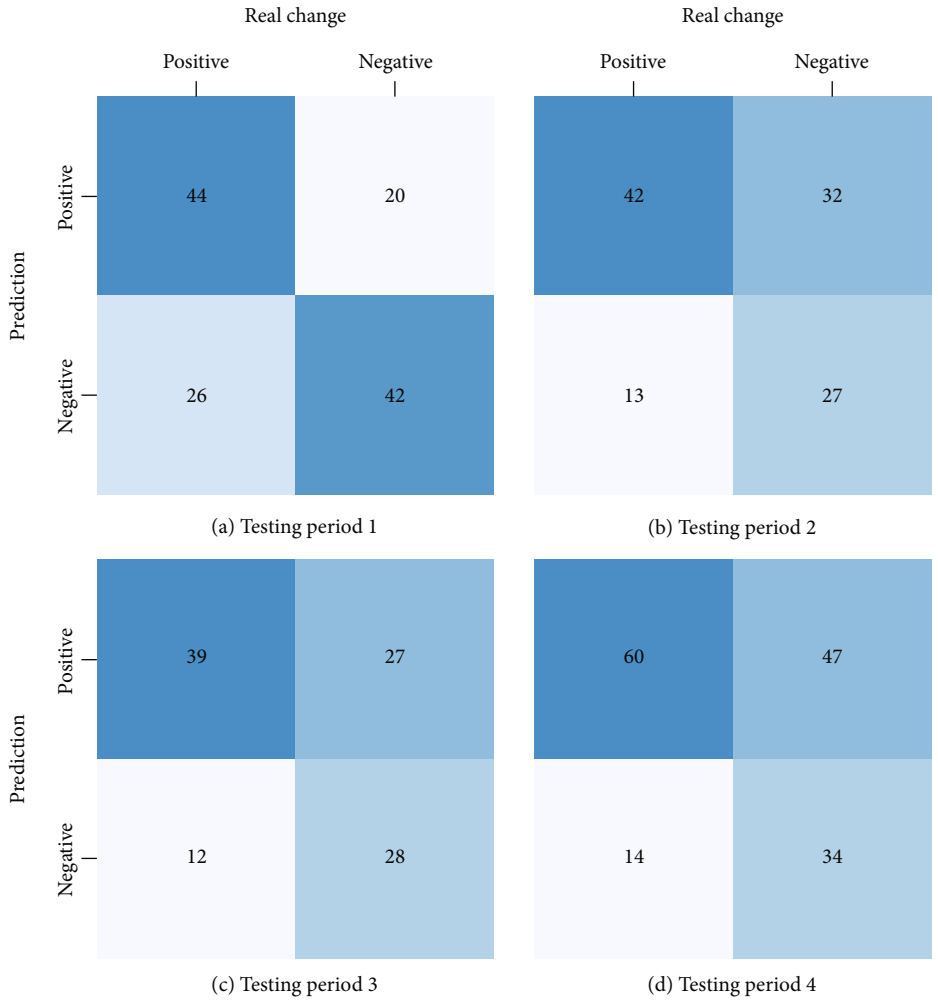

Figure 3: The confusion matrix results of direction prediction for the proposed method in the four testing periods.

Table 6: The F1-measure results of the benchmarks and the proposed method SMOTE-FRS.

Method	SMOTE-SVM	SMOTE-ANN	SMOTE-RF	SMOTE-XGBoost	SMOTE-MLP	FRS-no-SMOTE	SMOTE-FRS
Period 1	68.92%	65.77%	60.53%	61.39%	65.79%	38.10%	65.67%
Period 2	61.31%	51.69%	66.67%	56.10%	62.30%	60.00%	65.12%
Period 3	59.20%	64.58%	61.54%	63.92%	64.46%	60.87%	66.67%
Period 4	53.10%	60.61%	57.63%	66.67%	72.41%	50.00%	66.30%
Average	60.63%	60.66%	61.59%	62.02%	66.24%	52.24%	65.94%

greater than 65% in all four quarters. It can be concluded that although a deep learning-based algorithm may produce a wonderful performance than the traditional machine learning models, while in the case of price trend multiclassification for CSI300 futures, as evidenced by the confusion matrix results in Figure 3, the method proposed in this research successfully produced a more robust performance. Moreover, compared with the F1-measure results of FRS without SMOTE (FRS-no-SMOTE), the proposed method produced a superior prediction performance after adopting the SMOTE-based method to solve the sample imbalance problem.

6.2. Hit Ratio Results. To further evaluate the performance of the proposed method in price change prediction, the hit ratio results produced by the benchmarks and the proposed method are reported in Table 7. First, it could be observed that the average hit ratio of the proposed method in four subtesting periods is 62.39%, which outperforms that of the benchmark methods, including the SMOTE-SVM (59.94%), SMOTE-ANN (59.16%), SMOTE-RF (59.97%), SMOTE-XGBoost (59.57%), and SMOTE-MLP (61.99%). Additionally, the proposed method yielded the best direction prediction accuracy in all of the four subtesting periods,

Table 7: The hit ratio results of the benchmarks and the proposed method SMOTE-FRS.

Method	SMOTE-SVM	SMOTE-ANN	SMOTE-RF	SMOTE-XGBoost	SMOTE-MLP	FRS-no-SMOTE	SMOTE-FRS
Period 1	64.05%	58.96%	61.54%	61.25%	62.60%	35.00%	65.15%
Period 2	58.59%	58.25%	59.32%	57.65%	58.18%	55.56%	60.53%
Period 3	58.54%	60.47%	59.02%	62.37%	61.95%	50.00%	63.21%
Period 4	58.59%	58.95%	60.00%	57.00%	65.22%	33.33%	60.65%
Average	59.94%	59.16%	59.97%	59.57%	61.99%	43.47%	62.39%

Table 8: Friedman test on the hit ratio results for the proposed method SMOTE-FRS against the benchmark methods.

Compared models	Significant level $\alpha = 0.05$
SMOTE-FRS versus SMOTE-SVM	$H_0 : n1 = n2 = n3 = n4 = n5 = n6 = n7$
SMOTE-FRS versus SMOTE-ANN	
SMOTE-FRS versus SMOTE-RF	$F = 15.96$
SMOTE-FRS versus SMOTE-XGBoost	
SMOTE-FRS versus SMOTE-MLP	$p = 0.014$ (reject H_0)
SMOTE-FRS versus FRS-no-SMOTE	

Table 9: The accumulated return results of the benchmarks and the proposed method SMOTE-FRS.

Method	SMOTE-SVM	SMOTE-ANN	SMOTE-RF	SMOTE-XGBoost	SMOTE-MLP	FRS-no-SMOTE	BAH	SAH	SMOTE-FRS
Period 1	3.28%	- 0.35%	- 2.08%	- 11.23%	0.15%	- 1.05%	- 2.62%	2.42%	6.49%
Period 2	- 2.55%	- 3.40%	- 6.38%	- 1.28%	- 14.46%	0.18%	7.98%	- 8.18%	5.90%
Period 3	- 11.63%	4.25%	- 13.16%	0.39%	2.31%	- 4.18%	3.00%	- 3.20%	6.25%
Period 4	- 1.79%	- 7.44%	- 9.67%	- 4.64%	- 3.91%	- 0.53%	4.55%	- 4.75%	6.80%
Average	- 3.17%	- 1.74%	- 7.82%	- 4.19%	- 3.98%	- 1.40%	3.23%	- 3.43%	6.36%

which indicates that compared to the most popular machine learning methods, the proposed method performed better when applied to the price direction prediction of the CSI300 futures. The results of the proposed method are better compared to the FRS without SMOTE (FRS-no-SMOTE), which indicates that the performance of the proposed method can be enhanced after applying the SMOTE-based method to deal with the sample unbalanced problem. Furthermore, the Friedman test [40] is employed to evaluate whether the proposed method performed better than the benchmarks significantly. The Friedman test results of the hit ratio are reported in Table 8, from which we can find that the significance is at the 0.05 level for the one-tailed test, demonstrating that the direction prediction accuracy of the proposed method is significantly better than that of the benchmarks.

6.3. Accumulated Return Result. For market participants, an excellent trading decision support system should not only provide accurate signals of price direction change but also own excellent profit-making ability. Table 9 provides the accumulated return results of the proposed method SMOTE-FRS and all benchmarks. The average return of the proposed method over the four subtesting periods is 6.36%, which is superior to the results of the benchmarks, including SMOTE-SVM (- 3.17%), SMOTE-ANN (- 1.74%), SMOTE-RF (- 7.82%), SMOTE-XGBoost (- 4.19%), FRS-no-SMOTE (- 1.40%), and SMOTE-MLP (- 3.98%). In addition, the return generated by the proposed method in subtesting periods 1-4 is 6.49%, 5.90%, 6.25%, and 6.80%, all of which are positive returns. In contrast, the benchmark methods almost produced negative accumulated return results over the four subtesting periods. Although the classic passive trading strategy BAH produced an outstanding return in the second quarter, the proposed approach was capable of producing a more robust return over four quarters. Therefore, it is evident that the proposed method outperforms benchmark methods in terms of profit-making ability. Furthermore, the Friedman test results for accumulated return are

Table 10: The results of the Friedman test on accumulated return for SMOTE-FRS against the benchmark methods.

Compared models	Significant level $\alpha = 0.1$
SMOTE-FRS versus SMOTE-SVM	$H_0 : n1 = n2 = n3 = n4 = n5 = n6 = n7 = n8 = n9$
SMOTE-FRS versus SMOTE-ANN	
SMOTE-FRS versus SMOTE-RF	
SMOTE-FRS versus SMOTE-XGBoost	$F = 14.8$
SMOTE-FRS versus SMOTE-MLP	
SMOTE-FRS versus BAH	
SMOTE-FRS versus SAH	$p = 0.063$ (reject H_0)
SMOTE-FRS versus FRS-no-SMOTE	

displayed in Table 10. It is observed that the profitability of the proposed method is significantly better than that of the benchmarks at the 0.1 level, demonstrating that the method proposed in this research could be applied as an alternative trading support system for the market participants in the CSI300 futures market.

7. Conclusion

In this paper, we propose a novel approach SMOTE-FRS for high-frequency price prediction and trading simulation of the CSI300 futures. The SMOTE-based method is applied to solve the sample imbalanced problem, while the fuzzy rough set-based approach is employed to generate the movement prediction and simulation trading signal. Moreover, for the purpose of improving the profitability of the proposed method, a predesigned trading strategy was proposed, and one-year simulated trading was carried out for the out-of-sample test. For the proposed method, its average F1-measure was 65.94%, the average hit ratio was 62.39%, and the average accumulated return was 6.36%. In summary, compared to benchmark methods, the proposed method SMOTE-FRS produced the best prediction accuracy and trading profit results. The outstanding performance of the proposed method indicates that the proposed method could be applied as an efficient prediction and trading support system for the market participants. Additionally, employing the SMOTE-based method for solving sample unbalanced problems can effectively improve the performance of the proposed method. In future works, researchers could design a more sophisticated trading strategy to enhance the profitability of the method proposed in this research.

Data Availability

Publicly available datasets were analyzed in this study. This data can be found here: http://choice.eastmoney.com/ accessed on 1st June 2022.

Conflicts of Interest

The authors declare no conflict of interest.

Acknowledgments

This research was sponsored by the Philosophy and Social Science Research Project of Hubei Provincial Department of Education (grant number 21Q035).

References

[1] D. Su and D. Kong, "Research on the regulation of futures market manipulation based on the evolutionary game theory," *Journal of Residuals Science & Technology*, vol. 13, 2016.

[2] J. Ma, Y. Pan, and Y. Zhang, "Selection of short-term investment strategy-judgment based on average adhesion state," *International Journal of Business and Management*, vol. 12, no. 6, p. 165, 2017.

[3] Y. Zhang and Y. Liu, "Risk aversion of stock index futures," *Journal of Beijing Institute of Technology*, vol. 10, no. 3, pp. 69–72, 2008.

[4] X. Wang, Q. Ye, F. Zhao, and Y. Kou, "Investor sentiment and the Chinese index futures market: evidence from the internet search," *Journal of Futures Markets*, vol. 38, no. 4, pp. 468–477, 2018.

[5] N. V. Voinov, M. K. Voroshilov, S. A. Molodyakov, P. D. Drobintsev, O. V. Prokofiev, and I. V. Zajtsev, "Predicting RTS index futures using machine learning," in *2021 XXIV International Conference on Soft Computing and Measurements (SCM)*, pp. 193–196, St. Petersburg, Russia, 2021.

[6] R. Jiang and C. Wen, "A comparison between parametric and nonparametric volatility forecasting of stock index futures in China," *Emerging Markets Finance and Trade*, vol. 58, no. 9, pp. 2522–2537, 2022.

[7] S. Cong, J. Liu, J. Liu, and X. Zhao, "Research on the price of stock index futures with ARIMA model," 2016, DEStech Transactions on Economics, Business and Management, iceme-ebm.

[8] J. C. Reboredo, J. M. Matías, and R. Garcia-Rubio, "Nonlinearity in forecasting of high-frequency stock returns," *Computational Economics*, vol. 40, no. 3, pp. 245–264, 2012.

[9] R. Savani, "High-frequency trading: the faster, the better?," *IEEE Intelligent Systems*, vol. 27, no. 4, pp. 70–73, 2012.

[10] A. Stenfors and M. Susai, "Liquidity withdrawal in the FX spot market: a cross-country study using high- frequency data," *Journal of International Financial Markets Institutions and Money*, vol. 59, pp. 36–57, 2019.

[11] W. Lu, C. Geng, and D. Yu, "A new method for futures price trends forecasting based on BPNN and structuring data,"

IEICE Transactions on Information and Systems, vol. E102.D, no. 9, pp. 1882–1886, 2019.

[12] S. Deng, Y. Zhu, X. Huang, S. Duan, and Z. Fu, "High-frequency direction forecasting of the futures market using a machine-learning-based method," *Future Internet*, vol. 14, no. 6, p. 180, 2022.

[13] S. Deng, C. Wang, Z. Fu, and M. Wang, "An intelligent system for insider trading identification in Chinese security market," *Computational Economics*, vol. 57, no. 2, pp. 593–616, 2021.

[14] J. Ayala, M. García-Torres, J. L. V. Noguera, F. Gómez-Vela, and F. Divina, "Technical analysis strategy optimization using a machine learning approach in stock market indices," *Knowledge-Based Systems*, vol. 225, p. 107119, 2021.

[15] L. I. Yan and Y. A. Jianhui, "Prediction of the price of stock index futures based on SVM and triangular fuzzy information granulation concerning investors sentiment," *Management Science and Engineering*, vol. 10, no. 3, pp. 28–34, 2016.

[16] S. Vluymans, Y. Saeys, L. D'Eer, and C. Cornelis, "Applications of fuzzy rough set theory in machine learning: a survey," *Fundamenta Informaticae*, vol. 142, no. 1-4, pp. 53–86, 2015.

[17] D. Dubois and H. Prade, "Rough fuzzy sets and fuzzy rough sets," *International Journal of General Systems*, vol. 17, no. 2-3, pp. 191–209, 1990.

[18] E. Akyildirim, O. Cepni, S. Corbet, and G. S. Uddin, "Forecasting mid-price movement of bitcoin futures using machine learning," *Annals of Operations Research*, vol. 1-32, pp. 1–32, 2021.

[19] R. Blagus and L. Lusa, "SMOTE for high-dimensional class-imbalanced data," *BMC Bioinformatics*, vol. 14, no. 1, p. 106, 2013.

[20] G. Douzas, F. Bacao, and F. Last, "Improving imbalanced learning through a heuristic oversampling method based on k-means and SMOTE," *Information Sciences*, vol. 465, pp. 1–20, 2018.

[21] Y. Lin, S. Liu, H. Yang, and H. Wu, "Stock trend prediction using candlestick charting and ensemble machine learning techniques with a novelty feature engineering scheme," *IEEE Access*, vol. 9, pp. 101433–101446, 2021.

[22] F. Kamalov, "Forecasting significant stock price changes using neural networks," *Neural Computing and Applications*, vol. 32, no. 23, pp. 17655–17667, 2020.

[23] P. Yu and X. Yan, "Stock price prediction based on deep neural networks," *Neural Computing and Applications*, vol. 32, no. 6, pp. 1609–1628, 2020.

[24] B. Sun, H. Guo, H. R. Karimi, Y. Ge, and S. Xiong, "Prediction of stock index futures prices based on fuzzy sets and multivariate fuzzy time series," *Neurocomputing*, vol. 151, pp. 1528–1536, 2015.

[25] S. Kumar, K. Bisht, and K. K. Gupta, "Intuitionistic fuzzy time series forecasting based on dual hesitant fuzzy set for stock market," in *Exploring Critical Approaches of Evolutionary Computation*, IGI Global, 2019.

[26] D. Chen, W. Zhang, D. S. Yeung, and E. C. Tsang, "Rough approximations on a complete completely distributive lattice with applications to generalized rough sets," *Information Sciences*, vol. 176, no. 13, pp. 1829–1848, 2006.

[27] C. Cornelis, M. De Cock, and A. M. Radzikowska, "Fuzzy rough sets: from theory into practice," *Handbook of Granular Computing*, W. Pedrycz, A. Skowron, and V. Kreinovich, Eds., Wiley, 2008.

[28] R. Jensen, C. Cornelis, and Q. Shen, "Hybrid fuzzy-rough rule induction and feature selection," in *2009 IEEE International Conference on Fuzzy Systems*, pp. 1151–1156, Jeju, Korea (South), 2009.

[29] R. Jensen and Q. Shen, "New approaches to fuzzy-rough feature selection," *IEEE Transactions on Fuzzy Systems*, vol. 17, no. 4, pp. 824–838, 2009.

[30] B. Acharjya and S. Natarajan, "A fuzzy rough feature selection framework for investors behavior towards gold exchange-traded fund," *International Journal of Business Analytics*, vol. 6, no. 2, pp. 46–73, 2019.

[31] A. S. Roy and N. Chatterjee, *Forecasting of Indian stock market using rough set and fuzzy-rough set based models*, IETE Technical Review (Institution of Electronics and Telecommunication Engineers, India), 2021.

[32] N. V. Chawla, K. W. Bowyer, L. O. Hall, and W. P. Kegelmeyer, "SMOTE: synthetic minority over-sampling technique," *Journal of Artificial Intelligence Research*, vol. 16, pp. 321–357, 2002.

[33] D. Elreedy and A. F. Atiya, "A comprehensive analysis of synthetic minority oversampling technique (SMOTE) for handling class imbalance," *Information Sciences*, vol. 505, pp. 32–64, 2019.

[34] H. Guan, Y. Zhang, M. Xian, H. D. Cheng, and X. Tang, "SMOTE-WENN: solving class imbalance and small sample problems by oversampling and distance scaling," *Applied Intelligence*, vol. 51, no. 3, pp. 1394–1409, 2021.

[35] N. Mqadi, N. Naicker, and T. Adeliyi, "A SMOTe based oversampling data-point approach to solving the credit card data imbalance problem in financial fraud detection," *International Journal of Computing and Digital Systems*, vol. 10, no. 1, pp. 277–286, 2021.

[36] X. Huang, C. Zhang, and J. Yuan, "Predicting extreme financial risks on imbalanced dataset: a combined kernel FCM and kernel SMOTE based SVM classifier," *Computational Economics*, vol. 56, no. 1, pp. 187–216, 2020.

[37] R. Diao and Q. Shen, "A harmony search based approach to hybrid fuzzy-rough rule induction," in *2012 IEEE International Conference on Fuzzy Systems*, pp. 1–8, Brisbane, QLD, Australia, 2012.

[38] D. Dubois and H. Prade, "Putting rough sets and fuzzy sets together," in *Intelligent Decision Support*, R. Słowiński, Ed., vol. 11 of Theory and Decision Library, Springer, Dordrecht, 1992.

[39] H. Thiele, *Fuzzy Rough Sets versus Rough Fuzzy Sets - An Interpretation and a Comparative Study Using Concepts of Modal Logics*, Technical Representative-30/98 University, Dortmund, Germany, 1998.

[40] J. Derrac, S. García, D. Molina, and F. Herrera, "A practical tutorial on the use of nonparametric statistical tests as a methodology for comparing evolutionary and swarm intelligence algorithms," *Swarm and Evolutionary Computation*, vol. 1, no. 1, pp. 3–18, 2011.

Hindawi
Advances in Mathematical Physics
Volume 2022, Article ID 2223212, 11 pages
https://doi.org/10.1155/2022/2223212

Research Article

Research on the Measurement of Logistics Capability of Core Cities along "the Belt and Road" in China

Zhichao Sun,[1] Tao Wang,[2] Xinuo Xiao,[1] Qing Zhang,[3] and Huiwen Guo[4]

[1]*Graduate School of Global Business Studies, Changwon National University, Changwon, Republic of Korea*
[2]*Graduate School of International Studies, Hanyang University, Seoul, Republic of Korea*
[3]*Graduate School of Chinese Academy of Fiscal Sciences, Beijing, China*
[4]*School of Public Policy and Administration, Chongqing University, China*

Correspondence should be addressed to Tao Wang; ghwzjj@gmail.com and Huiwen Guo; oucghw@163.com

Received 5 July 2022; Accepted 20 August 2022; Published 6 October 2022

Academic Editor: S. E. Najafi

The B&R strategy came into being to promote the free and orderly flow of economic factors, the efficient allocation of resources, and the depth of market integration. Logistics is the artery of element circulation and the basis of the B&R. The logistics capacity of core cities along the R&B will be an essential factor affecting the strategy. In this context, it is of practical significance to measure the logistics capacity of the core cities along the B&R. Since combing domestic and overseas research, this paper first uses clustering analysis to screen out nine core cities along the B&R and then uses fuzzy matter-element analysis to measure their urban logistics capacity and sort them. The results show that the urban logistics capacity in the eastern coastal areas of China is higher than that in northwest and southwest China. The logistics capacity of cities along "The 21st Century Sea Silk Road" is more robust than that of others and through the urban agglomeration could further achieve economies of scale. The logistics capacity of cities along the "Silk Road Economic Zone" should improve the construction of logistics infrastructure and enhance logistics information in the future.

1. Research Background and Significance

1.1. Research Background. The "Silk Road" is an international channel with a long history, which has played an indispensable role in the economic and cultural exchanges between the East and the West since the Western Han Dynasty. With the deepening of global economic integration, this trading artery has also been given a new meaning to the times.

In 2013, President Xi Jinping puts forward a significant initiative to jointly build the Silk Road Economic Belt and the 21st Century Maritime Silk Road (the Belt and Road). As soon as this initiative was put forward, it attracted wide attention at home and abroad. The initiative was promoted to the top-level national strategy in the following important meetings, such as the Third Plenary Session of the 18th CPC Central Committee and the Central Working Conference. It was mentioned many times on international occasions, such as Boao Forum, APEC, and foreign state visits.

The vital role of "the Belt and Road" is to make the circulation of production factors smoother and more convenient. Therefore, in the process of constructing the circulation system of "the Belt and Road," logistics is both a critical connotation and an indispensable vital means. At the same time, implementing "the Belt and Road" will put higher requirements on the logistics capacity of cities along the route.

China's modern logistics industry rose in the 1990s. Although it started relatively late, it has made significant progress, driven by international logistics. As shown above, China's total social logistics was 38.4 trillion CNY in 2004. In 2012, this index increased to 177.3 trillion CNY, with an average annual growth rate of 21.07%. This shows the development speed of China's logistics industry. In terms of logistics cost, in 2004, China's total social logistics cost accounted for 18.8% of GDP; in 2012, it decreased to 18%. Although it has dropped by 0.8 percentage points, there is still a big gap compared with 10% in developed countries. China's logistics

efficiency has improved, and the overall development speed is relatively slow.

1.2. Research Significance. Logistics is the derived demand for social and economic development. Implementing "the Belt and Road" has linked the fragmented regional economies along the line, thus increasing trade and investment and accelerating the industrial transfer and material flow. Implementing "the Belt and Road" should also consider the logistics capacity of areas along the line and promote its economic growth through logistics first. Therefore, the logistics capacity of the core cities along the "Belt and Road" will also become a key factor affecting the implementation of the national strategy. At the present stage, although "the Belt and Road" has become an academic hotspot, there is research on the logistics capability of areas along "the Belt and Road." Under this background, it is of theoretical and practical significance to measure the logistics capacity of the core cities along "the Belt and Road" in China.

2. Literature Review

This paper reviews the existing literature from two aspects: "the Belt and Road" and logistics capability.

2.1. Literature Review of "the Belt and Road." Since it was put forward, "the Belt and Road" has attracted wide attention from scholars in various fields at home and abroad.

Mackerras [1] conducted relevant research from the perspective of "the Belt and Road" construction. He believed that Xinjiang, China, as the hub connecting China and Kazakhstan, should pay attention to its construction and development. Li et al. [2] studied from the perspective of environmental protection, pointing out that "the Belt and Road" involves many countries along the route, so we should pay attention to the protection of resources and the environment in the implementation process. Scholars from neighboring countries in India think more from the perspective of international relations. Chaturvedy [3], on the one hand, discusses in detail the development opportunities brought by China's "the Belt and Road" policy to countries along the route; on the other hand, it studies the possible responses of relevant countries, including positive responses and relatively negative confrontations. Sakhuja [4] pointed out that the "Belt and Road" policy put India in a dilemma: on the one hand, India expected to benefit from cooperation, but on the other hand, it was worried that the rise of China brought about by "the Belt and Road" would adversely affect India.

Domestic scholars have also done a lot of research on "the Belt and Road." In terms of the regional economy, Wubin [5] used the GTAP model to simulate and analyze the regional economic integration effect between China and 64 countries along the "Belt and Road," and based on this, predicted the FTA (free-trade area) strategic path under China's "the Belt and Road." The results show that implementing free trade under "the Belt and Road" will bring positive economic and trade incentives to China and countries along the route. In contrast, countries that have not participated in it will face negative effects. In terms of international trade, Wu [6] used the random front gravity model and the trade barrier analysis model for empirical analysis. The results show that the average trade efficiency between China and the Belt and Road-related countries is 0.49, and half of the trade potential has not yet been developed.

2.2. Literature Review on Logistics Capability. Under the background of the rapid development of logistics, logistics capability has also become a research hotspot in the academic field. The logistics industry in western countries such as Europe, America, and the like has a high level of development, so the relevant scholars in these countries have done more profound research on logistics capabilities.

The Global Logistics Research Team of Michigan State University (MSUGLRT) (1995) researched the measurement of logistics capability. The team divides logistics capabilities into four types, namely, measurement capability, configuration capability, integration capability, and agility capability. This achievement pioneered the research of logistics capability and laid the foundation for subsequent analysis. Follow-up foreign scholars think more from the perspective of enterprise logistics capability. Bowersox [7] believe that logistics capability is the ability of enterprises to provide the best quality logistics services to minimize costs. Morash et al. [8] divided the strategic logistics capability into two parts: the demand-oriented function, which aims to meet customer needs, such as response to the target market, presales and after-sales service, reliability, and punctuality of delivery. The second is the supply-oriented function, which aims to reduce the cost of enterprises, such as distribution scope and cost. Clinton and Closs [9] put information technology into the elements that affect logistics capability, so they think logistics capability includes five components: alliance, information system, EDI, inventory control, and process reengineering. These five elements comprehensively reflect enterprises' logistics integration, information, and process capability. Daugherty et al. [10] explained the logistics capability of enterprises from the perspective of resources. They believe that logistics capability is part of enterprise resources, including all assets, knowledge, and organizational processes of the enterprise. Pfohl and Buse [11] think that a broader range of logistics capabilities includes four key capabilities: flexibility, trade-off, positioning, and merging. Waters and Liu [12] explained the logistics capability from the supply chain perspective. They believe that the logistics capacity of the supply chain refers to the maximum flow of materials in the supply chain within a certain period, from which the optimal output of the supply chain within a limited period can be determined.

2.3. Literature Review. Combined with the above literature, it can be found that the research on "the Belt and Road" covers a vast field. Among them, the research on logistics focuses on the following two aspects. In the aspect of theoretical analysis, it is mainly the idea of building a new logistics development model under the background of "the Belt and Road." Empirical research focuses on the measurement of logistics efficiency and its influencing factors. However, the

research on the logistics capability of core cities along "the Belt and Road" is rare.

As for the research on logistics capability, the western countries started earlier, and China only started the related research after 2000. In theoretical research, the definition of logistics capability involves enterprise logistics capability, supply chain logistics capability, urban logistics capability, and regional logistics capability. At present, there is no recognized measurement method for urban logistics capacity, and the following three methods are used in related research: (1) the classical comprehensive evaluation method based on AHP and TOPSIS; (2) the multivariate statistical method based on dimensionality reduction based on principal component analysis and factor analysis; and (3) the self-compiled formula method. However, the above calculation methods have some defects. If the analytic hierarchy process (AHP) constructs different judgment matrices within the scope of consistency and validity, different evaluation results may be obtained; the problem of the TOPSIS method is that if the scores of the two indexes are symmetrical, the connection between the best scheme and the worst scheme, it is difficult to get accurate results. Principal component analysis and factor analysis are difficult to reflect all the information of indicators; however, the self-compiled formula method obtains the weight through the Delphi method, so it cannot accurately and objectively evaluate the logistics capacity of the city. In contrast, the fuzzy matter-element analysis method can effectively avoid the above problems to objectively and comprehensively assess the logistics capacity of the city, which provides a brand-new idea for this paper.

3. Research Innovation and Methods

3.1. Innovation of the Paper. The innovation of this paper is mainly reflected in the following two aspects.

Firstly, the core cities along "the Belt and Road" are selected by cluster analysis, which ensures that the core cities can organize urban logistics and drive regional logistics and avoids subjective assumptions.

Secondly, on the empirical method, this paper adopts the fuzzy matter-element analysis method to calculate and evaluate the logistics capacity of core cities objectively and comprehensively, making this paper's research results more scientific and reliable.

3.2. Research Methods. This paper mainly adopts theoretical, empirical, comparative, and other research methods to explore the problem and reach a scientific and reliable conclusion.

First, theoretical analysis: by combing and commenting on the existing literature about "the Belt and Road" and logistics capability at home and abroad, we have mastered the research status and development trends of "the Belt and Road" and logistics capability.

Second, empirical analysis: the core cities along "the Belt and Road" are selected through cluster analysis. Then, the fuzzy matter-element analysis method is used to measure the logistics capacity of the core cities.

Third, comparative analysis: this paper compares each city's logistics capabilities, advantages, and disadvantages and puts forward some pertinent suggestions.

4. A Basic Concept of Urban Logistics Capability and the Analysis of the Current Situation of "the Belt and Road"

4.1. The Basic Concept of Urban Logistics Capability. A city is the center of economy and trade in a region, while logistics is the artery of urban development and the foundation of urban economic growth. A logistics center city should have not only good competitive strength but also provide comprehensive and comprehensive logistics services to its surrounding areas. Therefore, an efficient logistics system must have strong storage capacity, throughput capacity, and radiation capacity, which can meet the needs of modern production mode and management mode.

Based on the research, this paper defines the meaning of urban logistics capability. Urban logistics capability is the comprehensive capability of a city to organize regional logistics and drive the logistics in the surrounding areas. With advanced logistics technology, rational development and utilization of logistics resources can promote the coordinated development of regional overall strength and competitiveness.

4.2. The Development Status of "the Belt and Road" and the Choice of Node Cities along the Route

4.2.1. Development Status of "the Belt and Road." "The Belt and Road" includes "Silk Road Economic Belt" and "21st Century Maritime Silk Road." The two international channels involve 26 countries and regions, covering about 4.5 billion people, accounting for 62.5% of the global population. The regional GDP along the line is about 23 trillion USD, accounting for 29.5% of the worldwide GDP. The implementation of this strategy will significantly promote the free and orderly flow of economic factors along the line, optimize resource allocation, and promote the deep integration of the market. "The Belt and Road" can not only become a new economic growth point in China but also play a significant role in driving the economic development of the areas along the line.

Internationally, the "the Belt and Road" strategy crosses Asia and Europe, connects the Asia-Pacific economic circle in the East, and can enter the European economic process through Central Asia and West Asia in the West. Among them, the Silk Road Economic Belt is supported by the Second Asia-Europe Continental Bridge and the node cities along the route to jointly build international economic cooperation corridors such as New China-Indo-China Peninsula and China-Central Asia-West Asia, and gradually spread to more expansive areas such as Western Europe and North Africa in the later period. In the twenty-first century, the Maritime Silk Road takes ports as its node, further deepening the cooperation between China and ASEAN and extending to countries in Africa, the Mediterranean, and other regions later.

Domestically, the "the Belt and Road" strategy has infiltrated and cooperated with various domestic economic regions. Vision and Action is authorized by the State Council. The location of each region has been clearly defined, which will give full play to the comparative advantages of each region, adjust measures to local conditions, and comprehensively improve the opening level of China's economy. Among them, Xinjiang, as an essential window for opening to the West, has become the core area of the Silk Road Economic Belt with its unique location advantages; as an important gateway to the Indian Ocean and the South Pacific, Fujian has been entrusted with the vital task of building the core area of the 21st Century Maritime Silk Road.

4.2.2. Selection of Node Cities along "the Belt and Road." The Silk Road Economic Belt scope mainly includes five provinces in northwest China, namely, Shaanxi, Gansu, Qinghai, Ningxia, and Xinjiang, and four provinces in southwest China, namely, Chongqing, Sichuan, Yunnan, and Guangxi. This paper selects nine cities, Xi'an, Lanzhou, Xining, Yinchuan, Urumqi, Chongqing, Sichuan, Kunming, and Nanning, as the node cities along the "Belt." In the twenty-first century, the maritime silk road mainly relies on the ports of Shanghai, Tianjin, Ningbo, Guangzhou, Xiamen, and Haikou, so this paper chooses these six cities as the node cities along the "One Road."

Therefore, this paper selects the above 15 cities as the node cities along the "Belt and Road."

5. Measurement of Logistics Capacity Research Methods and Model Building

5.1. Fuzzy Matter-Element Analysis Method. Fuzzy matter-element analysis organically combines fuzzy mathematics with matter-element analysis, describing research problems using three elements: things, characteristics, and values. Its basic idea is to analyze the fuzziness of the values corresponding to the attributes of things and the incompatibility among many factors that affect things to solve the problem of numerous indicators and fuzzy incompatibility.

5.1.1. Matter-Element and Fuzzy Matter-Element. The three elements in the meta-analysis are things, characteristics, and corresponding values (the same below), which are recorded. Suppose a matter-element has something, and each thing corresponds to a feature. In that case, the matter-element has a total of values, which can be called the dimensional compound matter-element of each item, namely,

$$Rm \times n = \begin{bmatrix} x11 & \mathrm{L} & x1n \\ \mathrm{M} & \mathrm{O} & \mathrm{M} \\ xm1 & \mathrm{L} & xmn \end{bmatrix}. \tag{1}$$

If the quantity is fuzzy, and the fuzzy quantity is, then the matter-element represents the dimensional compound fuzzy matter-element of a thing. The fuzzy value is calculated according to the principle of preferential membership, and the specific calculation method is:

$$\text{Benefit} : \mu_{\mathrm{ij}} = \frac{x_{ij} - \min x_{ij}}{\max x_{ij} - \min x_{ij}}, \tag{2}$$

$$\text{Cost} : \mu_{\mathrm{ij}} = \frac{\max x_{ij} - x_{ij}}{\max x_{ij} - \min x_{ij}}, \tag{3}$$

where indicates the maximum (minimum) value of all the quantities under the *i*th characteristic of each thing max *xij* (min *xij*).

By combining formulas (2) and (3), the dimensional compound fuzzy matter element of the corresponding item in formula (1) can be obtained, namely,

$$\tilde{R}m \times n = \begin{bmatrix} \mu 11 & \mathrm{L} & \mu 1n \\ \mathrm{M} & \mathrm{O} & \mathrm{M} \\ \mu m1 & \mathrm{L} & \mu mn \end{bmatrix}. \tag{4}$$

Order, that is, the difference square of each item corresponding to the standard fuzzy matter-element and the dimensional compound fuzzy matter-element is called the difference square compound fuzzy matter-element, that is,$\Delta ij = (\mu oj - \mu ij)^2$.

$$\tilde{R}\Delta = \begin{bmatrix} \Delta 11 & \mathrm{L} & \Delta 1n \\ \mathrm{M} & \mathrm{O} & \mathrm{M} \\ \Delta m1 & \mathrm{L} & \Delta mn \end{bmatrix}. \tag{5}$$

Among them, it is the preferential membership degree of each index calculated according to the preferential membership degree. In this paper, if the maximum value is optimized, the subordination degree of each index is 1.

5.1.2. Composite Fuzzy Matter-Element of Weight and Euclidean Closeness. From the perspective of information theory, information is a measure of the degree of system order; on the contrary, entropy is a measure of the system's disorder. However, in the specific process of evaluating the index system, its entropy value is determined by the variation degree of the index value: the high variation degree indicates that the index system contains comprehensive information, and its contribution to the information of the system is high, so the uncertainty is small, and the entropy value of the index is low, and the weight is significant; on the contrary, if the variation degree is low, the entropy value of the index is high, and the weight is small. In this paper, the entropy method is used to calculate the index weight, and the specific calculation process is as follows.

Step 1: normalize the initial matrix to obtain the normalized judgment matrix. Among them,

$$bij = \frac{xij - \min xij}{\max xij - \min xij}. \tag{6}$$

In formula (6), it represents the most satisfactory value

(the least satisfactory value) among different things under the same feature max xij(min xij).

Step 2: according to the definition of entropy in information theory, calculate the entropy of item features of item events:

$$Hi = -\frac{1}{\ln n}\left[\sum_{j=1}^{n} fij \ln fij\right]. \tag{7}$$

Among them,

$$fij = \frac{bij}{\sum_{j=1}^{n} bij}. \tag{8}$$

At that time, it was 0, and currently, it was infinite, so it was necessary to translate. The revised formula is the correction formula:

$$fij = \frac{A + bij}{\sum_{j=1}^{n}(A + bij)}. \tag{9}$$

In formula (9), the translation amplitude is 1.

Step 3: calculate the entropy weight of features:

$$\omega i = \frac{1 - Hi}{m - \sum_{i=1}^{m} Hi}. \tag{10}$$

Satisfy in formula (10).

Step 4: calculate the European closeness of things and the compound fuzzy matter element:

$$\rho Hj = 1 - \sqrt{\sum_{i=1}^{m} \omega i \Delta ij}, \tag{11}$$

$$R\rho H = \begin{bmatrix} & M1 & M2 & \cdots & Mn \\ \rho Hj & \rho H1 & \rho H2 & \cdots & \rho Hn \end{bmatrix}. \tag{12}$$

The closeness degree is used to measure how close everything is to the best thing, and the larger the value, the closer the measured thing is to the best thing.

5.1.3. Fuzzy Matter Elements of Panel Data. Those mentioned above fuzzy matter-element analysis method can be directly used to process cross-sectional data or time series data, but if it is applied to panel data, the data must be dimension-reduced; that is, things in different years are regarded as new things and incorporated into the original dimension complex element, to construct the following new dimension complex element:

$$Rm \times n(y) = \begin{bmatrix} x11(1) & \mathrm{L} & x1n(t) \\ \mathrm{M} & \mathrm{O} & \mathrm{M} \\ xm1(1) & \mathrm{L} & xmn(t) \end{bmatrix}. \tag{13}$$

It indicates the magnitude corresponding to the first feature of the first thing in a year. $xij(y)$, $(y = 1, 2, \cdots t)$ represents the year y and the I and x.

Because the panel data complex element absorbs the information of time and things, it keeps the differences between groups, which makes the finally calculated European closeness comparable. $Rm \times n(y)$ absorbed the information of time and things, thus keeping the differences between groups and making the finally calculated European style close.

5.2. WARD Cluster Analysis. Clustering analysis divides observation samples into different groups or classes based on their similarities or differences among multiple groups of indicators. Its basic idea is to maximize the homogeneity of objects in the same category by classifying individuals or objects. In contrast, the properties of research objects in different types are pretty other so that the problems can be classified according to the characteristics of research objects. This paper adopts the Ward method, a systematic clustering method, and its specific steps are as follows.

The first step is to measure the correlation.

We should first measure the similarity when extracting a relatively simple class structure from a group of complex data. In this paper, the Ward cluster analysis method is adopted, so its corresponding measurement method is Euclidean distance, which is widely used.

Let (x, y) be two cluster variables that measure similarity, containing values. The specific measurement formula is as follows:

$$d(x, y) = \sqrt{\sum_{i=1}^{m} (xi - yi)^2}. \tag{14}$$

In practice, the index data often have different dimensions, impacting the correlation measurement. Therefore, before measuring the correlation, the data should be dimensionless. This paper adopts an extreme difference method to deal with it. The specific calculation method is as follows:

$$x_i' = \frac{xi - \min xi}{\max xi - \min xi}. \tag{15}$$

The second step is clustering or grouping.

Systematic clustering methods mainly include the aggregation method and decomposition method. The aggregation method is to regard each sample as a class and combine the two classes with the closest properties to form a new class, and then, there are common classes. Then, two types with the closest properties are selected from the new classes and merged to obtain classes, and so on, until all the samples are grouped into one class, and a cluster diagram is obtained. On the contrary, the decomposition method treats all samples as one class at first and then divides them into two classes according to the optimal criterion; then, according to this criterion, each subclass is divided into two classes, and a subclass with better objective function is selected so that the two classes become three classes, and so on, until there is only one sample in each category.

Ward clustering is an aggregation method that uses variance analysis to minimize the differences between groups and maximize the differences between groups. That is, because of Euclidean square distance, when the number of classes is fixed, the sum of squares of intraclass deviation will be minimized. This clustering method is very effective in theory and practice and is widely used.

6. "The Belt and Road" along the Core Cities Logistics Capacity Measurement Empirical Analysis

6.1. Selection of Core Cities. Urban energy level reflects a city's comprehensive ability and influence on the surrounding areas. The stronger the comprehensive strength of a city, the higher its energy level, and the lower the energy level. This part measures the energy levels of the node cities selected in Section 1 by constructing the relevant index system and classifies 15 cities by Ward cluster analysis to screen out the core cities along "the Belt and Road."

6.1.1. Index System and Data Source for Measuring Urban Energy Level. The core city is the hub of the circulation of production factors in "the Belt and Road." This function requires it to have a robust external circulation capacity. An efficient logistics system cannot be separated from the perfect infrastructure, so it needs a particular economic strength as support. Based on the existing research of Lijun and Yaolin [13] and Chhetri et al. [14], this paper selects six indicators from three aspects, urban economic strength, urban investment, and construction capacity and urban external circulation capacity, and constructs a comprehensive measurement system of urban energy level. Among them, the indicators that characterize the city's economic strength are GDP, total retail sales of social goods, and the proportion of GDP of secondary and tertiary industries. The index of urban investment and construction ability is the fixed asset investment of the whole society. The indicators that characterize the external circulation capacity of cities are urban freight volume and urban passenger volume. See the following table for the specific index system and data sources (Tables 1 and 2).

As the statistical caliber of passenger traffic indicators of individual cities was adjusted in 2013 and 2014, it is not comparable with previous years' data. Therefore, this paper selects the panel data of 15 cities from 2010 to 2012 as samples.

6.1.2. Establishment of Core Cities Based on Ward Cluster Analysis. Because cluster analysis cannot directly process panel data, this paper takes the average value according to the year to get the cross-section data of 6 indicators in 15 cities and uses the range method to dimensionless the cross-section data to get the cluster analysis raw data with the distribution interval of [0, 1]. See the following table for details:

Using the above data, 15 node cities along "the Belt and Road" are analyzed by the Ward cluster, and the statistical software used in this part is stata13.1, and the hierarchical tree diagram is obtained.

In this paper, 15 node cities are divided into four categories. Shanghai, Chongqing, Tianjin, Chengdu, and Guangzhou have a robust economic foundation and superior geographical position, which are far ahead of other cities in terms of economic strength and circulation capacity, so they are classified as the first category. Nanning, Kunming, Xi'an, and Ningbo are classified in the second category. Although these cities are relatively backward in the economic aggregate, they play an important role in collection and distribution. Haikou, Urumqi, and Xiamen are divided into the third category. Although Haikou and Xiamen are located in the southeast coastal areas, their economic hinterland is relatively narrow compared with Guangzhou, Shenzhen, and other cities, and their contribution to "the Belt and Road" is limited. Urumqi is the gateway of China to Central Asia and the export station of the new Asia-Europe Continental Bridge, which has an irreplaceable strategic position. However, its infrastructure is weak, and it is difficult to meet the demand of modern circulation. Yinchuan, Xining, and Lanzhou, deep inland in the northwest, are divided into the fourth category. Limited by geographical factors, these three cities are weak in all aspects. To better serve the construction of "the Belt and Road," these three cities still have many places to be improved.

According to the results of cluster analysis, this paper selects the first two types of cities, namely, Shanghai, Chongqing, Tianjin, Chengdu, Guangzhou, Nanning, Kunming, Xi'an, and Ningbo, as the core cities along the "Belt and Road," and calculates the logistics capacity.

6.2. Calculation of Logistics Capacity of Core Cities

6.2.1. Index System and Data Source of Urban Logistics Capability. Combining with the definition of urban logistics capability given in Section 1.1 of this paper and based on previous studies, eight indicators are selected to measure urban logistics capability from three aspects: logistics basic level, transportation volume level, and logistics informatization capability. Among them, the indicators to measure the basic level of logistics are an investment in fixed assets and the number of employees in the logistics industry; the indicators to measure the level of transportation are cargo turnover, passenger turnover, and total freight volume; the indexes to measure logistics information ability are the number of postal marketing outlets, the total amount of postal services, and the length of postal routes. See the following table for the specific index system [15].

The data on the total freight volume and the number of postal marketing network points in this paper come from the National Bureau of Statistics. The data of the other six indicators come from the Statistical Yearbook of Cities, the Statistical Yearbook of Transportation, the Statistical Bulletin of National Economic and Social Development, and the statistical yearbooks of the provinces to which each city belongs [16–18]. The statistical caliber of the total post and telecommunications business in Xi'an, Nanning and other cities changed significantly in 2011, which is not comparable

Table 1: Urban energy level index system and data source.

Primary index	Secondary index	Data source
Urban economic strength	GDP	Wind database
	The total volume of retail sales	National Bureau of Statistics (NBS)
	The proportion of gross product of secondary industry in GDP	Wind database
Urban investment and construction capacity	Investment in fixed assets of the whole society	Wind database
Urban external circulation capacity	Urban freight volume	National Bureau of Statistics (NBS)
	Urban passenger traffic	National Bureau of Statistics (NBS)

Table 2: Cluster analysis of raw data.

City	Urban economic strength			Urban investment and construction capacity	Urban external circulation capacity	
	GDP	The total volume of retail sales	The proportion of secondary and third industry in GDP	Investment in fixed assets of the whole society	Urban freight volume	Urban passenger traffic
Ningbo	0.289	0.257	0.725	0.288	0.330	0.200
Xiamen	0.096	0.076	0.971	0.102	0.099	0.071
Guangzhou	0.635	0.730	0.921	0.424	0.704	0.474
Nanning	0.080	0.119	0.000	0.220	0.241	0.053
Seaport	0.000	0.016	0.487	0.000	0.069	0.231
Chengdu	0.338	0.381	0.717	0.639	0.410	0.718
Kunming	0.101	0.142	0.626	0.255	0.216	0.075
Xi'an	0.171	0.248	0.704	0.443	0.412	0.219
Lanzhou	0.034	0.055	0.820	0.074	0.065	0.004
Xining	0.001	0.000	0.761	0.017	0.000	0.009
Yinchuan	0.014	0.000	0.678	0.048	0.100	0.000
Urumqi	0.053	0.063	0.942	0.041	0.153	0.004
Tianjin	0.575	0.459	0.938	0.925	0.454	0.159
Shanghai	1.000	1.000	1.000	0.644	1.000	0.048
Chongqing	0.500	0.511	0.390	1.000	0.964	1.000

with the relevant data in 2010, so this paper selects the data from 2011 to 2014 for four years.

6.2.2. Estimation of Urban Logistics Capacity Based on Fuzzy Matter-Element Analysis. Taking the above-mentioned panel data as samples, this paper uses fuzzy matter-element analysis to measure the logistics capacity of core cities along "the Belt and Road." The operating software used in this part is MATLAB (R2014a).

Firstly, the 8-dimensional compound fuzzy matter-element matrix is calculated according to formulas (1) to (4). This paper adopts the transposed form of the matrix. The matrix shows the relative values of 36 samples on eight indexes [19–21]. The related data of the transpose matrix are as follows:

Then, calculate the entropy weight of eight indexes. According to formulas (5) to (10), the entropy weight vector is:

$$\omega_i = (0.0955\ 0.0741\ 0.0290\ 0.1141\ 0.0622\ 0.1520\ 0.0948\ 0.1983)^T, \quad (i = 1, 2, \cdots, 8). \tag{16}$$

It can be seen from the entropy weight vector that the entropy weights of the eight indexes are between 0.02 and 0.20, with little difference. Among them, the maximum index of entropy weight is the length of the postal route, and the minimum index of entropy weight is the turnover of goods. Under the index system of this paper, the length of the postal route, postal marketing outlets, and passenger turnover have

strong explanatory power to the urban logistics capacity, contributing 46.44% of the information cumulatively. It should be noted that the entropy weight does not mean the importance of an index to improve the urban logistics capability, but only the amount of practical information provided by the index when measuring the urban logistics capability [22].

Finally, based on the index entropy weight, the logistics capacity values of nine cities are calculated and sorted by combining the formula (11). The specific calculation results are shown in the following table (the values in brackets are the ranking of logistics capacity of cities in the current year).

6.3. Analysis of Empirical Results of Urban Logistics Capacity Measurement. In this part, nine core cities are selected from 15 node cities along "the Belt and Road" by cluster analysis. Then, the logistics capacity of 9 core cities is measured by fuzzy matter-element analysis.

Overall, the average level of logistics capacity of core cities along "the Belt and Road" has been increasing in logarithm in the past four years, with the fastest growth rate in 2012 and then gradually slowing down. In 2012, to alleviate the declining growth rate of imports and export, the Chinese government timely introduced measures to stabilize the growth of foreign trade in September so that the growth rate of foreign trade picked up. According to the data released by the General Department of Commerce, China's trade volume of goods still ranks second in the world in 2012, against the background that the world's total import and export volume only increased by 0.2%. Driven by international trade, the logistics industry of the core cities along the "Belt and Road" in China is also constantly transforming and upgrading, realizing the leap-forward improvement of logistics capability. After two years, the world economy continued its weak recovery, and foreign trade was relatively weak. As a result, the logistics capacity of core cities along "the Belt and Road" was affected, and the growth rate declined.

Except that the logistics capacity of Tianjin declined slightly in 2014, and the fluctuation range of Xi'an was extensive, the logistics capacity of other cities mostly made steady progress.

As China's international trade center, Shanghai's port imports and exports account for about 1/3 of the country's total, and it is a vital hub of the 21st Century Maritime Silk Road. The establishment of Daxiaoshan Port makes up for the shortcomings of Shanghai's deep-water port; the deepening of the Shanghai Pilot Free Trade Zone has attracted many outstanding enterprises and talents. Shanghai's logistics capability ranks first among the nine core cities with a solid economic foundation and modern logistics infrastructure. It is far ahead and the mainstay of China's connection with the Asia-Pacific economic circle [23].

As the largest city in western China, Chongqing ranks second in logistics capacity. Chongqing is an important node city on the southwest line of the Silk Road Economic Belt and a transit center to ASEAN countries via Guangxi and Yunnan. With the help of perfect logistics infrastructure and substantial collection and distribution capacity, Chongqing has played an indispensable role in the outbound transportation of western resources and industrial raw materials. Chengdu is one of the largest railway hubs in southwest China and one of the most important highway hub cities in China, which plays a vital role in land transportation. However, the positioning and development of Chengdu determine that its logistics capability is slightly inferior to that of Chongqing.

Although Guangzhou is a subprovincial city, its logistics capacity ranks third above that of Tianjin, and it has grown rapidly since 2012, approaching Chongqing. Guangdong has a superior geographical position and excellent infrastructure and has the natural advantage of multimodal transport by sea, land, and air; with a vast hinterland adjacent to Hong Kong and Macao, it is a crucial material distribution center and trading port in South China. In addition, Guangzhou pays attention to the innovation and development of the logistics industry, such as the coordinated development of e-commerce and logistics, actively expanding overseas warehouses, etc., constantly improving the modern logistics capability and playing the vanguard role of "the Belt and Road."

Tianjin Binhai New Area, with convenient shipping conditions and developed land transportation, is one of the crucial ports connecting inland areas with Japan and South Korea and also one of the core cities of the 21st Century Maritime Silk Road. However, compared with the Yangtze River Delta, Pearl River Delta, and other regions, Tianjin's logistics cost is higher, and its logistics service is relatively backward, so its logistics capability still has a lot of room for improvement.

As an inland city in northwest China, Xi'an has a weak economic foundation and relatively backward infrastructure compared with the eastern coastal areas. From the table above, the passenger and freight turnover and passenger volume of Xi'an fluctuate considerably, indicating that its logistics capacity is unstable. Kunming and Nanning, which are in the southwest inland, are the gateways of China to ASEAN countries. Still, their development lags, and their logistics capacity is relatively weak. It is undeniable that Kunming's logistics capacity was significantly improved in 2013. Ningbo's economy is small; its logistics capacity is insufficient compared with other municipalities directly under the central government and provincial capital cities and even nearly ten times the gap compared with Shanghai.

To sum up, from 2011 to 2014, the average logistics capacity of the core cities along "the Belt and Road" in China has dramatically improved. From the regional point of view, the overall logistics capacity of the eastern coastal areas is more vital than that of the inland cities in the northwest and southwest. Tianjin and Xi'an and other cities have made different degrees of progress, among which Shanghai's logistics capability is far ahead, Guangzhou and Kunming have made significant progress, while Nanning and Ningbo's development is slightly lagging.

6.4. Policy Recommendations. According to the empirical results of urban logistics capacity measurement, this chapter puts forward the following policy suggestions.

First, strengthen the infrastructure construction of cities along the Silk Road Economic Belt and improve the level of logistics technology to adapt to the modern development of logistics. As seen from Tables 3–5, except for Chongqing,

Table 3: Index system of urban logistics capability.

Primary index	Secondary index	Symbol of this article
Basic level of logistics	Investment in fixed assets of logistics	C1
	Number of employees in the logistics industry	C2
Transportation volume level	Cargo turnover	C3
	The volume of passenger transportation	C4
	Total freight volume	C5
Logistics informatization capability	Postal marketing network	C6
	Total post and telecommunications business	C7
	Length of the postal route	C8

there is still a big gap between the urban logistics capacity in the northwest and southwest regions and that in the eastern coastal areas [24]. With the rapid development of science and technology, the early "Tea-Horse Road" has been unable to meet the needs of modern production and management, and the transportation flow of the route and the transit speed of the hub have become the bottlenecks that limit the improvement of its logistics capacity. Therefore, cities in northwest and southwest China should first strengthen the construction of a transportation network and introduce advanced logistics facilities and professionals to dredge the circulation artery of the Silk Road Economic Belt and enhance the city's logistics capacity.

Second, to build urban agglomerations along the 21st Century Maritime Silk Road and achieve $1 + 1 > 2$ urban logistics capacity through urban agglomeration. Each city's location has its advantages and disadvantages. Still, each element in the same urban agglomeration can learn from each other's strong points to make up for one's weak points, define the urban industrial division of labor, accurately position the urban functions, and realize industrial complementarity and infrastructure sharing. For example, Yangshan Deepwater Port in Zhejiang has solved the problem of insufficient water depth in Shanghai port. Similarly, Xiamen's logistics capacity is limited. Still, it can jointly build an urban agglomeration with Fuzhou, Quanzhou, and other cities to expand the economic hinterland, achieve economies of scale, and work together to create the core area of the 21st Century Maritime Silk Road in Fujian.

Third, to better serve "the Belt and Road," cities should actively carry out reform and innovation and give corresponding policy support. For example, implementing the regional customs clearance mechanism along the "Belt and Road" will eliminate cumbersome customs clearance procedures and reduce trade barriers. Further, improve circulation efficiency and promote upgrading urban logistics capacity.

7. Research Conclusions and Prospects

7.1. Research Conclusion. Based on systematically sorting out the related literature about "the Belt and Road" and logistics capability, this paper calculates the logistics capability of core cities along "the Belt and Road." Firstly, cluster analysis selects nine core cities from 15 nodes in the "Belt and Road." Then, the fuzzy matter-element analysis is used to measure the logistics capacity of these nine cities. The main conclusions of this paper are as follows: first, from 2011 to 2014, the logistics capacity of core cities along China's "Belt and Road" continued to improve, but the growth rate declined slightly. Under the background of the weak recovery of the world economy, China should actively take corresponding measures to cooperate with "the Belt and Road" to stimulate foreign trade to enhance the logistics capacity of cities along the route. For example, the regional customs clearance mechanism is implemented along the "Belt and Road." Secondly, the development of logistics capacity in different regions is uneven, among which the logistics capacity of cities in eastern coastal areas is vital. In contrast, that of cities in northwest and southwest areas is weak. To improve the logistics capacity of a town, we should not only rely on international trade but also strengthen the construction of the city's own logistics infrastructure. Therefore, to better serve the construction of "the Belt and Road," the western region should first improve logistics modernization and introduce advanced technical equipment and logistics professionals. The eastern region can build the 21st Century Maritime Silk Road urban agglomeration and realize the specialized division of urban functions through urban agglomeration to realize the scale effect.

7.2. Research Prospect. There are three main points to be improved in this paper: firstly, when clustering the panel data, the average value of the data by year is adopted. The disadvantage of this operation is that the dynamic information reflected by the panel data is eliminated, and the development of a specific city index in four years cannot be measured in the classification process. Secondly, this paper uses the same index system to measure "Belt and Road." Considering the integrity of the data, there is no subdivision of cargo turnover and passenger turnover by water, land, and air, and it is impossible to compare the respective advantages of inland and coastal cities accurately. Thirdly, when measuring the logistics capacity of the core cities, the radiation range of the core cities is not deeply considered. The "breaking point" model can be used to calculate the radiation range of the core city and further enrich the index system to measure the logistics capacity of the city [25].

Table 4: Transpose matrix of 8-dimensional compound fuzzy matrix.

City	Age	C1	C2	C3	C4	C5	C6	C7	C8
Shanghai	2011	0.235	0.625	0.997	0.508	0.950	1.000	0.511	0.077
	2012	0.137	0.650	1.000	0.473	0.963	0.737	0.702	0.105
	2013	0.133	1.000	0.873	0.523	0.928	0.896	0.821	0.119
	2014	0.147	0.992	0.914	0.557	0.914	0.878	1.000	0.129
Chongqing	2011	0.511	0.567	0.113	0.249	0.993	0.636	0.264	0.073
	2012	0.691	0.610	0.119	0.280	0.866	0.490	0.303	0.073
	2013	0.930	0.664	0.102	0.237	0.876	0.610	0.361	0.080
	2014	1.000	0.710	0.116	0.267	1.000	0.702	0.459	0.067
Tianjin	2011	0.281	0.248	0.489	0.109	0.354	0.105	0.196	0.025
	2012	0.332	0.273	0.366	0.146	0.391	0.180	0.203	0.029
	2013	0.437	0.335	0.255	0.163	0.439	0.252	0.213	0.028
	2014	0.460	0.440	0.154	0.141	0.431	0.245	0.267	0.020
Chengdu	2011	0.193	0.290	0.002	0.286	0.228	0.048	0.185	0.117
	2012	0.178	0.297	0.004	0.310	0.291	0.056	0.232	0.139
	2013	0.231	0.360	0.002	0.262	0.338	0.055	0.274	0.138
Chengdu	2014	0.281	0.385	0.004	0.303	0.150	0.060	0.350	0.120
Guangzhou	2011	0.199	0.398	0.130	0.744	0.602	0.001	0.342	0.089
	2012	0.240	0.399	0.233	0.824	0.739	0.000	0.369	0.041
	2013	0.365	0.482	0.326	0.908	0.899	0.011	0.503	0.075
	2014	0.399	0.445	0.416	1.000	0.990	0.011	0.555	0.076
Nanning	2011	0.021	0.000	0.007	0.044	0.105	0.000	0.088	0.023
	2012	0.080	0.138	0.013	0.051	0.172	0.001	0.101	0.026
	2013	0.064	0.123	0.016	0.056	0.185	0.001	0.108	0.025
	2014	0.073	0.128	0.019	0.014	0.213	0.001	0.137	0.024
Kunming	2011	0.028	0.004	0.001	0.068	0.000	0.023	0.000	0.241
	2012	0.067	0.015	0.000	0.058	0.011	0.023	0.015	0.443
	2013	0.122	0.030	0.002	0.068	0.140	0.023	0.010	1.000
	2014	0.106	0.031	0.003	0.078	0.146	0.023	0.011	0.974
Xi'an	2011	0.000	0.300	0.014	0.101	0.287	0.018	0.218	0.027
	2012	0.073	0.241	0.018	0.108	0.357	0.018	0.235	0.533
	2013	0.065	0.315	0.020	0.118	0.421	0.018	0.270	0.045
	2014	0.108	0.296	0.019	0.095	0.322	0.019	0.319	0.045
Ningbo	2011	0.108	0.092	0.092	0.025	0.228	0.018	0.006	0.000
	2012	0.121	0.099	0.091	0.027	0.206	0.019	0.004	0.000
	2013	0.070	0.095	0.099	0.019	0.240	0.019	0.006	0.008
	2014	0.081	0.094	0.090	0.000	0.302	0.017	0.005	0.009

Table 5: Logistics capacity value of core cities along "the Belt and Road".

Age	Shanghai	Chongqing	Tianjin	Chengdu	Guangzhou	Nanning	Kunming	Xi'an	Ningbo	Mean
2011	0.466 (1)	0.288 (2)	0.204 (4)	0.129 (5)	0.212 (3)	0.027 (9)	0.058 (7)	0.077 (6)	0.055 (8)	0.168
2012	0.462 (1)	0.294 (2)	0.212 (4)	0.144 (6)	0.235 (3)	0.050 (9)	0.092 (7)	0.170 (5)	0.055 (8)	0.191
2013	0.490 (1)	0.311 (2)	0.219 (4)	0.153 (5)	0.295 (3)	0.050 (9)	0.143 (6)	0.102 (7)	0.055 (8)	0.202
2014	0.503 (1)	0.333 (2)	0.204 (4)	0.155 (5)	0.318 (3)	0.051 (9)	0.143 (6)	0.102 (7)	0.054 (8)	0.207

This paper uses the fuzzy matter-element analysis method to preliminarily calculate the logistics capacity of the core cities along the "Belt and Road." The empirical analysis shows that this method is feasible for measuring urban logistics capacity, but there are still three problems. Future research can improve on the above three aspects and accurately calculate urban logistics capacity.

Data Availability

All data, models, and code generated or used during the study appear in the submitted article.

Conflicts of Interest

The authors declare that they have no conflicts of interest.

Authors' Contributions

Zhichao Sun,Tao Wang, Xinuo Xiao, Qing Zhang, and Huiwen Guo contributed to the work equally and should be regarded as co-first authors.

References

[1] C. Mackerras, "Xinjiang in China's foreign relations: part of a New Silk Road or central Asian zone of conflict?," *East Asia*, vol. 32, no. 1, pp. 25–42, 2015.

[2] P. Li, H. Qian, K. W. F. Howard, and J. Wu, "Building a new and sustainable "Silk Road economic belt"," *International Viewpoint and News*, vol. 74, no. 10, pp. 7267–7270, 2015.

[3] R. R. Chaturvedy, "New Maritime Silk Road: converging interests and regional responses," *ISAS Working Paper*, vol. 2, p. 197, 2015.

[4] V. Sakhuja, "Xi Jinping and the Maritime Silk Road: the Indian dilemma," *ISAS, Working Paper*, vol. 2, pp. 48–51, 2015.

[5] S. Wubin, *International Regional Economic Cooperation Under the "the Belt and Road" Strategy and Its Effect Analysis, [Ph.D. Thesis]*, Zhejiang University, 2016.

[6] Q. Wu, *Research on the Trade Potential Between China and "the Belt and Road" Countries, [Ph.D. Thesis]*, Nanjing University, 2016.

[7] D. Bowersox, "World class Logistics: the challenge of managing continuous change," *Council of Logistics Management*, vol. 3, pp. 56–58, 1995.

[8] E. A. Morash, C. L. Droge, and S. K. Vickery, "Strategic logistics Capabilities for competitive advantage and firm success," *Journal of Business Logistics*, vol. 17, no. 1, pp. 1–22, 1996.

[9] S. R. Clinton and D. J. Closs, "Logistics strategy: does it exist?," *Journals of Business Logistics*, vol. 18, no. 1, p. 19, 1997.

[10] P. J. Daugherty, T. P. Stank, and A. E. Elinger, "Leveraging logistics/distribution capabilities: the effect of logistics service on market share," *Journal of Business*, vol. 19, pp. 35–52, 1998.

[11] H. C. Pfohl and H. P. Buse, *The Organisation of the Logistics System in Flexible Production Networks: an Organisational Capabilities Perspective*, Darmstadt Technical University, Department of Business Administration, Economics and Law, Institute for Business Studies (BWL), 1998.

[12] D. Waters and B. Liu, *Translated by Han Yong, Introduction to Logistics Managemen,t [M.S. Thesis]*, Electronic Industry Publishing, Beijing, 2004.

[13] L. Lijun and T. Yaolin, "Comprehensive Agglomeration Degree of Central Zhejiang Urban Agglomeration and Core Cities," *Economic Geography*, vol. 4, pp. 552–556, 2008.

[14] P. Chhetri, M. Nkhoma, K. Peszynski, A. Chhetri, and P. T.-W. Lee, "Global logistics city concept: a cluster-led strategy under the Belt and Road initiative," *Maritime Policy & Management*, vol. 45, no. 3, pp. 319–335, 2018.

[15] S. Wang, L. Lei, and L. Xing, "Urban circular economy performance evaluation: A novel fully fuzzy data envelopment analysis with large datasets," *Journal of Cleaner Production*, vol. 324, p. 129214, 2021.

[16] J. Liu, "Development of regional logistics in the Belt and Road," in *Contemporary Logistics in China*, Springer, Singapore, 2018.

[17] C. Ye, S. Li, L. Zhuang, and X. Zhu, "A comparison and case analysis between domestic and overseas industrial parks of China since the Belt and Road initiative," *Journal of Geographical Sciences*, vol. 30, no. 8, pp. 1266–1282, 2020.

[18] Y. Jiang, G. Qiao, and L. Jing, "Impacts of the new international land-sea trade corridor on the freight transport structure in China, central Asia, the ASEAN countries and the EU," *Research in Transportation Business & Management*, vol. 35, article 100419, 2020.

[19] M. Mohammadi, S. Shahparvari, and H. Soleimani, "Multimodal cargo logistics distribution problem: decomposition of the stochastic risk-averse models," *Computers & Operations Research*, vol. 131, article 105280, 2021.

[20] P. T.-W. Lee, Q. Zhang, K. Suthiwartnarueput, D. Zhang, and Z. Yang, "Research trends in Belt and Road initiative studies on logistics, supply chains, and transportation sector," *International Journal of Logistics Research and Applications*, vol. 23, no. 6, pp. 525–543, 2020.

[21] J. Wang, "Construction of modern logistics system in the Belt and Road economic zone," *China Circulation Economy*, vol. 3, pp. 25–31, 2016.

[22] M. L. Song, S. P. Cao, and S. H. Wang, "The impact of knowledge trade on sustainable development and environment-biased technical progress," *Technological Forecasting and Social Change*, vol. 144, pp. 512–523, 2019.

[23] P. Xu, H. Guan, A. A. Talebi, M. Ghassemi, and H. Rashmanlou, "Certain concepts of interval-valued intuitionistic fuzzy graphs with an application," *Advances in Mathematical Physics*, vol. 2022, Article ID 6350959, 12 pages, 2022.

[24] L. N. Yu, Y. Sun, X. Liu, and T. Wang, "Does regional value chain participation affect global value chain positions? Evidence from China," *Economic Research Ekonomska Istraživanja*, vol. 21, no. 8, p. 474, 2022.

[25] D. Wang, X. Q. Wang, M. S. Liu, H. J. Liu, and B. S. Liu, "Managing public-private partnerships: a transmission pattern of underlying dynamics determining project performance," *Engineering, Construction and Architectural Management*, vol. 28, no. 4, pp. 1038–1059, 2020.

Hindawi
Advances in Mathematical Physics
Volume 2022, Article ID 1113693, 10 pages
https://doi.org/10.1155/2022/1113693

Research Article

Evaluation and Analysis of Land Input-Output Comprehensive Benefit Based on Fuzzy Mathematics and Analytic Hierarchy Process

Xincheng Zhu,[1] Yan Zhang ,[2] Yunzhi Hou,[1] and Minda Jiang[3]

[1]*Anglo Chinese School International 61 Jln Hitam Manis, Singapore 278475*
[2]*School of Management, Guangzhou College of Technology and Business, Guangdong 510850, China*
[3]*Australian International School 1 Lor Chuan, Singapore 556818*

Correspondence should be addressed to Yan Zhang; yanzhanggz@outlook.com

Received 5 June 2022; Accepted 18 July 2022; Published 5 September 2022

Academic Editor: S. E. Najafi

Land use and comprehensive land evaluation are essential. Based on fuzzy mathematics theory and biological heuristic algorithm, the land input-output benefits are evaluated comprehensively. This paper firstly selects six indicators from six aspects of land resource input, capital input, and economic output, and so on. Based on land input and output, this paper constructs the evaluation indicator system of comprehensive benefit for land use. Then, based on the theory of fuzzy mathematics, the improved particle swarm optimization (PSO) algorithm is used to identify the fuzzy density value of the evaluation index. Combined with the analytic hierarchy process (AHP), comprehensive evaluation method, through the combination of subjective and objective methods, is comprehensively evaluating land benefits. Finally, the Tobit model is constructed to further analyze the influencing factors of total factor productivity of urban land use and explore the influencing mechanism of government regulation, land opening, and other factors and land development. The research results of this paper can provide reference for future urban planning, land structure adjustment, land resource utilization and protection, food security, ecological security, economic security, and so on.

1. Research Background

Since the birth of the earth, land resources have been born from it. It is the first natural substance that human beings have been exposed to since its birth, an abstract reflection in the human brain. Its connotation has constantly been changing as human beings have deepened their use and understanding. It is both a natural material form of existence and great material wealth of human society. With the development of human beings, the land has been continuously developed and utilized, which has broadened the space for human activities and improved the quality of human life. The relationship between man and land is constantly evolving, and the contradiction between man and land is also constantly prominent. People began to understand and study the relationship between man and land, the law of change, and development of man and land and looked forward to better playing the function of every inch of land.

In the 19th century, Germany was the first country to study land use. The famous agricultural geographer Duneng (Johann Heinrich-von Thun-en 1783-1850), who selected a piece of land 50 miles away from the city as a research object, analyzed the distribution of farming operations dominated by the level of land rent prices. In 1832, he published the publication of the book "The Relationship of Isolated Countries with Agriculture and The National Economy" which also heralded the birth of the theory of agricultural location. Over the next period, land-use research developed rapidly. In the 1920s, the Americans Thor and Jones proposed the concept of land use, and the British Bona made a rough estimate of the country's land resources. In 1930, the famous geographer Sample studied the quality of land in Britain and compiled a British land use map. After that, large-scale land investigation and research in Europe and the United States, represented by Britain and the United States, and

Japan in Asia, continued to advance. In the later development process, Brazil and Mexico in Latin America also carried out land surveys. By the beginning of this century, all countries have compiled their land use status maps. With the advent of new technologies, especially the widespread use of remote sensing (RS), GIS, and GPS, the rapid development of land survey data collection has been promoted. At the same time, as land resources become increasingly scarce, people are beginning to realize the importance of rational planning of existing land and evaluating the benefits of the original land use. Food and Agriculture Organization of the United Nations published the Outline of Land Valuation to guide land-use master planning. In 1993 published, the Guide to Land-Use Planning set out three goals of sustainability, equity, and acceptability.

By the 1990s, the focus shifted to the impact of land use on the global environment, focusing on land use and cover change (LUCC). In this area, the processes of biological and human social activities intersect most closely. With solid support from the International Union of Sciences and the International Federation of Social Sciences, the focus of research work shifted to how land use affects the regional and global environment, focusing on the integrated evaluation of the drivers of land use and regional and global models. The LUCC research plan, adopted internationally in 1996, is guided by five framework issues: first, how human activity has changed land cover over the past three centuries; second, the causes of the leading human factors that have changed in human land use; third, how land-use change will change land cover over the next 50-100 years.

Moreover, fourth, how humans and biophysics have directly driven sustainable land-use development and the specific types of impacts it has. Fifth is the interplay between land use and cover change, global climate change, and biogeochemical change. In the subsequent research process, the impact of land use on the ecological environment, including the study of environmental problems caused by the process of land reclamation in tropical rainforest areas of South America and the Caribbean, was strengthened. Land development on the island of Madagascar is responsible for nearly 50% of the destruction of forest land, and the adverse consequences are evaluated and predicted. It also includes the ecologically fragile areas of Africa, Sumatra, the Philippine Archipelago, the Indochina Peninsula, and other parts of the world where the contradictions are more serious. In the twenty-first century, LUCC's research focus is still on the relationship between global land cover change and the environment, and the C cycle is one of the research hotspots, which mainly explores the distribution, flow, conversion, storage, loss, and the total amount of C in natural and human activities, which is not only closely related to the biological world but also communicates the atmosphere, hydrosphere, lithosphere, and human activities. Humans are trying to unravel the carbon cycle between organisms and the atmosphere, the exchange of carbon dioxide between the atmosphere and the ocean, and the formation and decomposition of carbonaceous rocks.

At the same time, the emergence of remote sensing, computer mapping, global positioning systems, geographic information systems, various mathematical calculation methods, and new technologies has been of great help to the continuous evolution of land evaluation tools, means, and methods, improve the scope and accuracy of data collection, and the accuracy of evaluation. In these areas, foreign scholars have achieved many research results, such as Stark's analysis of GIS technology in German farm planning, land management, and significant projects for land demand analysis; Canada's M. C Roberts and India's J. C Randolph and J.R. Chiesa, who jointly studied the Monroe lake transport in southern India and applied GIS to analyze spatial properties and their combinations; Moisten Ahmadinejad, Yoshihisa Maruyama, Fungi Yamasaki costudied the Zaja region of Iran, and jointly studied the impact of human factors on the land surface cover in the region through multitemporal satellite imagery and GIS technology; Ademola Braimoh and Paul L.G. Vlek costudied rural land cover change in northern Ghana, showing that human activities also have a more significant impact on rural land use; L. M Paden and K. Venkataramaiah applied satellite imagery to study land use in the Indian state of Boulanger District of Orissa in 1983 [1–4]. E.R. Alexander, Faludi, through a large number of empirical studies, proposed the PPIP evaluation model; the most important research results are that in addition to land use research, it also includes land planning research. At present, the more famous ones are the Canadian Institute of Planners (CIP) and the American Institute of Planners (APA).

2. Related Types of Research

The land is one of the essential factors of production, and improving its total factor productivity (TFP) has also become an important research topic. Foreign scholars' research on TFP began with the economic growth accounting method established by Solow [5]. It mainly analyzes the effects of technological progress and institutions on economic growth [6]. Later, Hansen and Prescott [7] considered the land factor and believed that land, capital, and labor are all critical factors in promoting economic growth. Although different scholars have different research emphases, it has become a consensus in the academic world that land, capital, and labor are regarded as the primary factors affecting the total factor productivity of urban land use. Presently, domestic scholars have conducted in-depth studies on urban land use efficiency, and the research results can be summarized into three aspects: the first is the research on the role of urban land use in economic growth. For example, Du and Cai [8] incorporated land resources as input factors into the analysis framework of economic growth and quantitatively analyzed the role of construction land and other factors in economic growth, providing a possibility for in-depth analysis of the role of land resources in economic growth. The second is the evaluation of urban land use extent. Early scholars mainly used the envelope analysis method [9] and the stochastic frontier method [10] to measure urban land use extent in different regions. With the development of econometrics, improving the extent of urban land evaluation methods, study methods tend to be diversified; SBM [11] and the superefficiency model [12] were gradually applied to the related research of the assessment of urban land. The third is the study on the influencing factors and regional differences

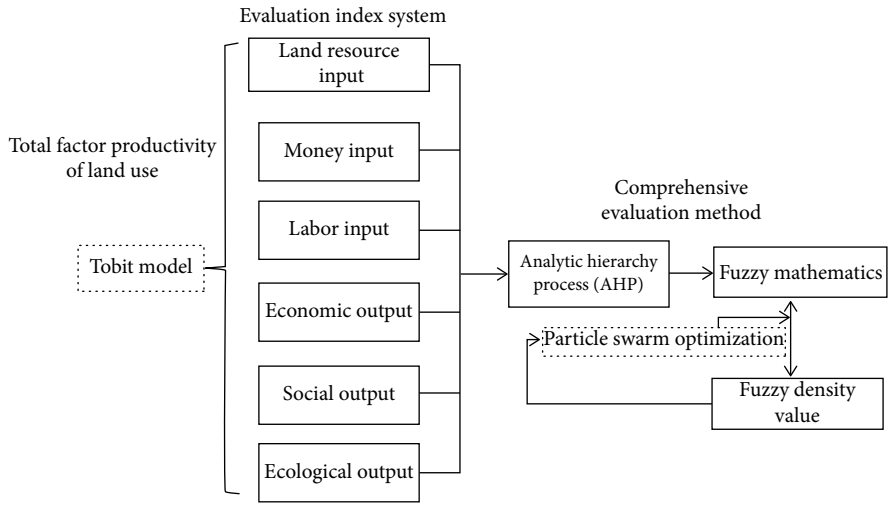

Figure 1: The technology roadmap in this study.

in urban land use extent. In this aspect, the influencing factors and regional differences in urban land use efficiency are analyzed by taking the whole country [13], different regions [14], and different urban agglomerations [15] as case areas [16].

The comprehensive evaluation method uses a more systematic and standardized method to evaluate multiple indexes and units simultaneously. It is an important means to deeply understand and objectively know the evaluated object. It is the decision base for sorting and optimizing the evaluation objects. The evaluation of employees, the finalization of the company's planning scheme, and the rectification of construction projects are inseparable from the comprehensive evaluation method. Therefore, the comprehensive evaluation method is essential for the development of human society. Many comprehensive evaluation models are currently commonly employed in management, economy, society, and education.

The analytic hierarchy process [17] belongs to the system engineering method, entropy value method [18] from the information theory method, and rough sets theory [19] border areas from the fuzzy mathematics thought; fuzzy comprehensive evaluation model is by the method of fuzzy mathematics [20] of evolution; the matter-element analysis method [21] is based on extension set theory; the grey clustering analysis [22] is derived from the gray system theory; TOPSIS model method [23] and cosine decision method [24] are both multiattribute decision methods. In contrast, the catastrophe series method [25] is a mathematical theory derived from topology. The grey-fuzzy safety evaluation method for the antifloating anchor system is established using the grey theory and the relevant theory of fuzzy mathematics [26]. The researcher uses the multilevel fuzzy comprehensive evaluation method to evaluate the human resource performance of enterprises [27]. Researchers construct a method based on data and the model of the analytic hierarchy (AHP) process [28], by using the fuzzy comprehensive evaluation method for water evaluation [29]. Evaluation methods developed rapidly from the 1950s to the 1980s, and various disciplines gradually integrated into evaluation research during this period. AHP, fuzzy comprehensive evaluation method, entropy method, and catastrophe progression method are all produced in this stage. Therefore, with the development of evaluation methods, the application of comprehensive evaluation is increasing. After the evaluation methods are gradually enriched, many scholars also turn their research focus to the evaluation of evaluation methods. The matter-element analysis method, grey clustering analysis method, Technique for Order Preference by Similarity to an Ideal Solution (TOPSIS) model method, rough set multiattribute decision theory, and cosine decision method are developed innovatively based on the formation of essential theories of evaluation methods in the early stage.

With the development of evaluation methods, some combinatorial evaluation methods based on fuzzy mathematics are applied more successfully [30–32]. This paper intends to combine the analytic hierarchy process, particle swarm optimization algorithm, and fuzzy mathematics comprehensive evaluation method, through the subjective and objective mutual combination of methods, a comprehensive evaluation of the comprehensive benefits of the land. In addition, this paper further analyzes the influencing factors of total factor productivity of urban land use by constructing the Tobit model and discusses the influencing mechanism of government regulation, land openness, and other factors and land development. The Tobit model is first proposed by Amemiya [33]. Figure 1 shows the technology roadmap in this study. Fuzzy measure and fuzzy integral are introduced in Section 3, Section 4 introduces the land economic benefit evaluation method based on fuzzy integral, Malmquist index is constructed in Section 5, and Tobit model and APH processing are introduced in Sections 6 and 7.

3. Model Building: Fuzzy Measure and Fuzzy Integral

In 1974, the Japanese scholar Sugeno first defined fuzzy measures and defined the integration of measurable functions concerning fuzzy measures [34]. The fuzzy measure is the scale of subjective measurement of faint objects, the principle of which

is to convert the probability theory generally based on the measurement of things into a possible theory and consider the correlation between evaluation indicators. Generally, when fuzzy measures are applied to decision-making problems, the candidate sets represent evaluation items, and the fuzzy measure is the weight value of the evaluation items [35]. Thus, fuzzy measure refers to the degree to which the object to be measured is sure to belong to the candidate set.

Definition: Let g be a mapping from $P(X)$ (power set of X) to [0,1]; if g satisfies:

Bounded: $g(\varnothing) = 0$, $g(x) = 1$;

Monotonicity: $A, B \in P(X)$, if $A \subseteq B$, so $g(A) \leq g(B)$;

Continuity: if $A_i \in P(X)$ and $\{A_i\}_{i=1}^{\infty}$ are monotonous, that is, $A_1 \subseteq A_2 \subseteq \cdots \subseteq A_n \subseteq \cdots$ or $A_1 \supseteq A_2 \supseteq \cdots \supseteq A_n \supseteq \cdots$, then there is $\lim_{i \longrightarrow \infty} g(A_i) = g(\lim_{i \longrightarrow \infty} A_i)$, then g is said to be a fuzzy measure on $P(X)$.

Three common measures are as follows:

Probabilistic measure: if $A, B \in P(X)$ and $A \cap B = \varnothing$, then $g(A \cup B) = g(A) + g(B)$;

F additive measure: if $A, B \in P(X)$, then $g(A \cup B) = \max\{g(A), g(B)\}$;

(1) λ measure: if $A, B \in P(X)$ and $A \cap B = \varnothing$, then $g(A \cup B) = g(A) + g(B) + \lambda g(A) g(B)$, where $\lambda \in (-1, \infty)$, records as g_λ, When $\lambda = 0$, the g_λ measure is a probabilistic measure

If $X = \{x_1, \cdots, x_n\}$ is a finite set, and each variable x_i corresponds to the fuzzy function g_i, then g_λ can be written as

$$g_\lambda\{x_1, \cdots, x_n\} = \sum_{i=1}^{n} g_i + \lambda \sum_{i_1=1}^{n-1} \sum_{i_2=i_1+1}^{n} g_{i_1} g_{i_2} + \cdots + \lambda^{n-1} g_1 g_2 \cdots g_n = \frac{1}{\lambda} \left| \prod_{i=1}^{n} (1 + \lambda g_i) - 1 \right|, \lambda \in (-1, \infty). \quad (1)$$

When $g(X) = 1$, λ can be calculated as

$$\lambda + 1 = \prod_{i=1}^{n} (1 + \lambda g_i). \quad (2)$$

When calculating the λ fuzzy measure using the above method, the initial fuzzy measure needs to be given by an expert first. If you require a g_λ fuzzy measure of set $A \subseteq X$, you only need to know the fuzzy density g_i of each metric, then find the value of λ from Equation (2), and then get its fuzzy measure according to Equation (1).

Fuzzy integral is a nonlinear function defined based on fuzzy measures. It is not necessary to assume that the evaluation indicators are independent of each other in the comprehensive evaluation. Therefore, it can be applied to situations where there is a correlation between evaluation indicators and is particularly suitable for dealing with the evaluation of subjective values. There are many ways to fuzzy integration, the most commonly used such as Sugeno integrals and Choquet integrals. Choquet integrals describe the degree of interaction between evaluation indicators with fuzzy measures, considering the respective importance of evaluation indicators. Assuming that the question does not lose its generality, $f(x_1^k) \geq \cdots \geq f(x_i) \geq \cdots \geq f(x_n^k)$, $f(x_i)$ represents the normalized evaluation value of the ith evaluation index to evaluate the kth protocol. The fuzzy measure $g(\bullet)$ of $f(\bullet)$ has a Choquet integral on X as [36–38]:

$$\int f dg = f\left(x_n^k\right) g(X_n) + \left[f\left(x_{n-1}^k\right) - f\left(x_n^k\right)\right] g(X_{n-1}) + \cdots + \left[f\left(x_1^k\right) - f\left(x_2^k\right)\right] g(X_1), \quad (3)$$

where $g(X_1) = g(\{x_1\})$, $g(X_2) = g(\{x_1, x_2\})$, $\cdots$, $g(X_n) = g(\{x_1, x_2, \cdots x_n\})$ represents the fuzzy measure of each indicator set. $f = (c) \int f dg$ is the total evaluation value after the fuzzy integral is calculated.

4. Model Building: Land Economic Benefit Evaluation Method Based on Fuzzy Integral

Before evaluating the land economic benefits of the development zone, the fuzzy measure of the evaluation indicators is determined by scoring the importance of each evaluation index and the set of indicators by experts. Suppose the fuzzy measure value given by an expert or determined by other methods does not satisfy the mathematical nature of the λ measure. In that case, it is tough to calculate the λ value from Equation (2). Therefore, the following optimization calculations can be used to go from the fuzzy measure given by the experts to the fuzz measure that meets the requirements of the definition. $\widehat{g}_\lambda(A), A \in P(X)$ represents the λ fuzzy measure given by the expert, and $\widehat{g}_\lambda^i$ represents the fuzzy density value given by the expert. When the set of solutions is a univariate, the optimization equation is as

follows:

$$\min_{\lambda} \sum_{A \in P(X)} \left| \widehat{g}_{\lambda}(A) - \frac{1}{\lambda} \left[\prod_{x_i \in A} \left(1 + \lambda \widehat{g}_{\lambda}^{i}\right) - 1 \right] \right|, \quad \text{s.t.} -1 < \lambda < \infty. \tag{4}$$

When the set of solutions is $(g_{\lambda}^{1}, g_{\lambda}^{2}, \cdots, g_{\lambda}^{n}, \lambda)$, the optimization equation is as follows:

$$\min \sum_{A \in P(X)} \left| \widehat{g}_{\lambda}(A) - \frac{1}{\lambda} \left[\prod_{x_i \in A} \left(1 + \lambda g_{\lambda}^{i}\right) - 1 \right] \right|, \quad \text{s.t.} -1 < \lambda < \infty. \tag{5}$$

In the actual data analysis, an improved PSO is used in this paper to identify the λ value and the fuzzy density value of the evaluation index.

5. Model Building: Malmquist Index

Mquist Productivity Index (from now on referred to as MI) is a unique index used to measure changes in total factor productivity. When the evaluated unit data is panel data containing observed values at multiple time points, the effect of productivity change, technical efficiency, and technological progress on productivity change can be analyzed. The formula is:

$$MI_{t,s} = \left[\frac{d^{t}(x^{s}, y^{s})}{d^{t}(x^{t}, y^{t})} \times \frac{d^{s}(x^{s}, y^{s})}{d^{s}(x^{t}, y^{t})} \right]^{1/2}, \tag{6}$$

where (x^{t}, y^{t}) and (x^{s}, y^{s}) are the input-output relationship of t and s phases, respectively; $d^{t}(x^{t}, \quad)$ is the distance function, representing the distance between the production configuration (x^{t}, y^{t}) and the system frontier at time t. The Malmquist index can be divided into the technological change index and technological efficiency change index under the condition of constant return to scale. After the constraint of constant return to scale is removed, the change index of technical efficiency can be further decomposed into a change of pure technical efficiency and change of scale efficiency.

6. Model Building: Tobit Model

James Tobin first proposed the regression problem that explained variables have an upper limit, lower limit, or extreme value. Then, scholars will be limited in the value of explained variables. There is a choice behavior model called the Tobit model. Because of the urban land measured TFP and decomposition efficiency have been cut and the characteristics of the truncated, traditional least squares estimation method, there is a significant deviation, so using truncation method Tobit regression model analyzes the influencing factors, and the model is:

$$Y_i = \alpha + \beta_i X_i + \varepsilon, \tag{7}$$

where Y_i is the dependent variable; X_i is the independent variable; α is the intercept vector; β_i is the parameter vector; ε is a random vector.

7. Model Building: Weighting by Principal Component Analysis

This article will introduce standardization of evaluation indicators, determination of dataset, and weight hierarchical model building. Hierarchical single ordering and hierarchy total ranking, and its consistency test also will be introduced in detail.

7.1. Standardization of Evaluation Indicators. The data itself should have corresponding units and orders of magnitude differences in the various types of data collected. In order to eliminate the impact of data units on data analysis in the statistical analysis process, it is necessary to standardize the data processing (undimensionization processing, normalization processing). Usually, there are several standardized treatment methods: the power function, the standardized method, the maximum method, the coefficient of variation method, and so on. Therefore, this paper uses the power method in the process of data standardization, and its expression is as follows:

Positive indicators, that is, the bigger the value, the better the indicator, take their upper limit effect:

$$M_{ij} = \frac{(X_i - b_i)}{(a_i - b_i)}. \tag{8}$$

Negative indicators, that is, the smaller the value, the better the indicator, take their lower limit effect:

$$M_{ij} = \frac{(a_i - X_i)}{(a_i - b_i)}, \tag{9}$$

where M_{ij} is the value of the jth indicator in the ith year; a_i and b_i are the dataset's upper and lower limits, respectively; X_i is the data that needs to be standardized.

In practical application, the upper and lower limits of the dataset can be determined according to the relevant policies, statistical standards, and the actual situation of socioeconomic development. For this article, the maximum value of the data is used as the upper bound and the minimum value as the lower limit.

7.2. Model Building: Determination of Dataset Weights. Being able to accurately, reasonably, and effectively determine the weight of each indicator is a crucial step in the overall land efficiency evaluation. The weighting process emphasizes the final effect or contribution of some phenomenon (or dataset) to some aspect. The subjective empowerment method is based on the experience of experts and subjective judgments, such as the analytic hierarchy method (AHP) and Delphi method; these methods were used earlier and have been widely used in economics, management, mathematics, and statistics, more mature. Of course, this method will be affected by subjective factors, but if a large amount of data is collected, the bias caused by subjective factors can be reduced as much as possible. The

objective empowerment method analyzes the data processing process mainly according to the situation of the original data itself and does not rely on people's subjective judgment, for example, coefficient of variation method, entropy method, factor analysis method, and complex correlation coefficient. In this paper, the analytic hierarchy (AHP) method is used to determine the weights according to the actual situation of the data.

The analytic hierarchy method, also known as AHP, was first proposed by Professor T. L SARRTY, who teaches at the University of Pittsburgh. He can analyze and process some uncertain indicators through a combination of qualitative and quantitative methods through mathematical models. This method can use people's subjective judgment to link the elements within the system mathematically and list them layer by layer according to the corresponding hierarchical level by sorting their importance and comparing them with each other (must pass the consistency test), from which to find a way to solve the problem.

7.2.1. Build a Hierarchical Model. First, after data collection, the necessary analysis of the interrelationship between the elements within the data is required to determine their internal correlation. Select the correlation factor as the target layer A, criterion layer B, and factor layer C. Maintain the independence of each factor to form a hierarchical relationship, and finally, establish an evaluation system.

7.2.2. Constructing a Judgment Matrix. In the AHP method, to achieve a comparison between the two pairs of data and to determine the importance relative to each other and their clear level, it is necessary to construct a judgment matrix. This is shown in Table 1.

7.2.3. Method for Determining Matrix Elements A_{ij} Scale. Psychologists believe it is best not to exceed nine levels of comparative factors in comparing the elements. Therefore, the comparison is made on a scale of 1-9.

7.2.4. Hierarchical Single Ordering and Its Consistency Test. According to the results of the expert scoring the importance of each indicator, the judgment matrix is constructed, and the characteristic vector λ max of the most prominent feature root of the corresponding judgment matrix is calculated. Then, the W value is calculated by the corresponding standardized method. W is the weight of the next level in the hierarchy relative to the previous level, and we call this the single hierarchical order.

Once the W weight value is derived, it cannot be used immediately, and it needs to be tested for consistency so that its value falls within the allowable value. Otherwise, the matrix is readjusted until it passes the test. The test can be performed according to the following: theorem 1, the only nonzero feature root of the nth order uniform array is n; the maximum Eigen root of the nth-order positive and negative array A is $\lambda \geq n$, if and only if $\lambda = nA$ is a uniform array.

However, in practical applications, the degree of consistency of A can be measured by the size of the $\lambda - n$ numeric value. Its consistency formula is as follows:

$$\mathrm{CI} = \frac{(\lambda - n)}{(n-1)}. \tag{10}$$

If CI = 0 indicates that the matrix has a firm consistency, which is extremely unlikely; CI is close to 0, it has a satisfactory consistency in most cases; CI is huge, it does not have consistency, and it cannot pass the test. The next step is to find the consistency ratio and define it as CR = CI/RI; when CR < 0.1, if the inconsistency of A is within the allowable range, through the consistency test, it can be normalized as a weight vector. Instead, the judgment matrix needs to be reconstructed to adjust the elements. Table 2 shows the stochastic consistency indicator RI.

Table 1: The judgment matrix.

Factor layer	C1	C2	⋯	C1n
C1	A11	A12	⋯	A1n
C2	A21	A22	⋯	A2n
…	…	…	…	…
Cn	An1	An2	⋯	Ann

Table 2: Stochastic consistency indicator RI.

n	1	2	3	4	5	6	7	8	9
RI	0	0	0.46	0.87	0.98	1.13	1.45	1.61	1.65

7.2.5. Hierarchy Total Ranking and Its Consistency Test. Total hierarchy refers to calculating the weight of the relative importance of all factors at a certain level to the highest level (target layer). It is from the highest layer A to the B layer until the end of the lowest level indicator layer C. The hierarchy is tested for consistency (consistency ratio) by calculating the total hierarchy order:

$$\mathrm{CR} = \frac{\sum w_j \mathrm{CI}_j}{\sum w_j \mathrm{RI}_j}, \quad (j = 1, 2, 3, \cdots, n). \tag{11}$$

When the CR < 0.1, it passes the real hierarchy consistency test. Instead, we need to adjust the values of the CR elements so that the overall hierarchical system passes the test. The weights of each level are derived sequentially, along with their single weight W.

8. Data Using

8.1. Data Description. The data in this paper are mainly from The Statistical Yearbook of Chinese Cities from 2012 to 2021, the Statistical Yearbook of China's Land and Resources, and the Statistical Yearbook of Corresponding Provinces. To ensure comparability, using the CPI will involve revised economic data up to 2012. The indexes selected in this paper are all from the level of municipal districts.

Table 3: Variable descriptive.

Rule layer	Type of indicator	Indicator layer	Unit
Input indicators	Land resource input	Built-up area	Km^2
	Money input	Fixed asset investment	Ten thousand yuan
	Labor input	Workers in the secondary industry	Ten thousand people
		Workers in the tertiary industry	Ten thousand people
Output indicators	Economic output	The added value of the secondary industry	Ten thousand yuan
		The added value of tertiary industry	Ten thousand yuan
	Social output	Per capita disposable income of urban residents	Yuan
	Ecological output	The afforestation coverage area of built-up area	Km^2
Influencing factors	Land relationship	The population density	People/Km^2
	The openness of the city to the outside world	Amount of foreign investment	Ten thousand yuan
	Government regulation	The ratio of fiscal expenditure to GDP	%
	Spatial structure of urban land use	The ratio of built-up area to the municipal area	%
	Land marketization level	"Recruit auction listings" account for the total land offered	%
	The industrial structure	The output value of the tertiary industry accounts for the regional GDP	%

The output value of tertiary industry and gross regional product.

8.2. Variable Description

8.2.1. Evaluation Indicators. Based on reference to previous studies and based on the theory of C-D production function, the investment index is selected from land, capital, and labor. That is, the built-up area (km^2) of the use area represents the investment of urban land resources. Investment in urban fixed assets (ten thousand yuan) represents a capital investment. In contrast, the number of employees in the secondary and tertiary industries (ten thousand people) represents the level of labor investment. Urban land use efficiency is based on urban land use. Urban land output includes three aspects: economy, society, and ecology. Urban land is mainly used to meet the needs of production, living activities, and urban ecological protection. Therefore, the economic output is selected as the added value of the second and third industries (ten thousand yuan) that can directly reflect the output level of urban land use. Social output is expressed as per capita disposable income of urban residents (yuan); the ecological output is expressed by the green coverage area (km^2) of the built-up area.

8.2.2. Influencing Factor Indicators. Man-land relationship: using population density to represent the man-land relationship, good population density can promote urban land use efficiency. Otherwise, the too high or too low population density will lead to overloading or idle urban infrastructure, urban disease, or lack of economic development power, which will reduce urban land use efficiency.

City openness: when the technical efficiency reaches a certain level, the substitution rate between capital and land is high, the scarcity of urban land is insufficient to restrict economic development, and the efficiency of urban land use is improved. On the contrary, the less open we are to the outside world, the more constrained the efficiency of urban land use is.

Government regulation: the ratio of local financial general budget expenditure to GDP represents the level of government regulation. Because the market has blindness and other defects, the government must adjust, and the government increase in financial expenditure can correct the market failure and improve the efficiency of urban land use to a certain extent. However, excessive government regulation and interference with the market will backfire.

Spatial factors of urban land: according to the proportion of built-up area in the area of administrative divisions of municipal districts, generally speaking, under the constraints of urban planning, the higher the proportion of the built-up area is, the less possible it is to strive for a land use index for economic development through urban land expansion, and the more it can force the improvement of existing urban land use efficiency. The lower the proportion of the built-up area is, the lower the cost of land acquisition may be in the process of urban economic development, which reduces the pressure of intensive and economical use of urban land, and, thus is less conducive to improving the efficiency of urban land use.

Marketization level of the land: the ratio of the total area of land transfer with "recruitment, auction, and listing" is expressed. The higher the level of land marketization is, the higher the degree of participation in the market competition is, and the higher the efficiency of urban land use is.

Table 4: Mean value of Malmquist indexes and its decomposing results on urban land use in the land economic zone.

Period	Technical efficiency (TEC = PTEC ∗ SEC)	Technological advancements (TC)	Purely technical efficiency (PE)	Scale efficiency (SE)	TFP (TFP = TEC ∗ TC)
2013	1.111	1.237	0.899	0.962	1.093543
2014	1.166	1.109	0.953	0.963	1.021637
2015	1.113	1.116	0.92	0.943	0.996
2016	1.121	1.158	0.92	0.951	1.038
2017	1.12	1.17	0.913	0.957	1.04265
2018	1.124	1.083	0.935	0.939	0.977445
2019	1.121	1.052	0.919	0.952	0.931068
2020	1.119	1.128	0.915	0.954	1.00296
2021	1.129	1.167	0.928	0.951	1.055376

Table 5: Tobit regression analysis results.

Explanatory variable	TFP		TEC		TC	
	Coefficient	Z-value	Coefficient	Z-value	Coefficient	Z-value
Man-land relationship	0.024	0.560	0.06	2.45^{**}	0.015	0.412
City openness	-0.027	-3.14^{**}	0.006	0.99	-0.02	-2.14^{**}
Government regulation	-0.140	-0.96	-0.031	-0.24	-0.18	-1.012
Spatial factors of urban land	-0.41	-1.13	-0.39	-2.13^{**}	-0.502	-1.542^{**}
Marketization level of land	0.112	1.45 ∗	0.078	0.291	0.069	1.125^{*}
Industrial structure	0.000	0.15	0.002	0.111	0.000	0.113
Constant	1.41	3.8	0.456	2.12	1.24	3.93

Note: "∗∗∗" means passing 1% significance test, "∗∗" means passing 5% significance test, and "∗" means passing 10% significance test.

Table 6: Evaluation accuracy of different optimization algorithms on the test set.

Test sets/total datasets = 0.2		Test sets/total datasets = 0.3	
Accuracy (PSO)	Accuracy (GA)	Accuracy (PSO)	Accuracy (GA)
76.54%	73.56%	75.67%	74.65%

Industrial structure: the proportion of output value of the tertiary industry to GDP is used to represent the status of the urban industrial structure. Under the current situation of high-speed urbanization, the proportion of the output value of the tertiary industry in the GDP of municipal districts can better distinguish the characteristics of urban industrial structures. The descriptive variables are shown in Table 3.

9. Evaluation Analysis Empirical Test

9.1. Spatio-Temporal Analysis of TFP of Urban Land Use. Based on the Malmquist index, the TFP of urban land use in 18 prefecture-level cities in the land Economic Zone was measured with an annual cycle. The results (Table 4) show that from 2013 to 2021, the average TFP of each city fluctuated between [0.993, 1.09].

9.2. Analysis of Influencing Factors of Total Factor Productivity of Urban Land Use. Tobit model was constructed to analyze further the influencing factors of TFP of urban land use. The results (Table 5) show that the influence coefficients of urban land use spatial factors on TFP and decomposition efficiency were negative, and this index's influence on technological progress and efficiency passed the significance test of 5%. The possible explanation is that in the process of urban land expansion, the increase of urban land area alone cannot effectively improve the effectual output and efficiency of urban land use. The land marketization level passes the significance test for the TFP and technological progress of urban land use at the 10% level. The improvement of land marketization management level can promote urban technological progress and thus promote the TFP of urban land use. The influence coefficients of industrial structure on the TFP and decomposition efficiency of urban land use were positive. However, the influence coefficients were minor and did not pass the significance level test, indicating that the proportion of tertiary industry should be increased. The advantages of technology, capital, and information should be utilized to improve the effectual output of urban land use, and there is still plenty of room for improvement.

9.3. Comprehensive Evaluation Results. Table 6 shows the evaluation accuracy of different optimization algorithms on

Table 7: Comprehensive land use benefits of 18 selected regions.

	2013	2014	2015	2016	2017	2018	2019	2020	2021
C1	0.002	0.018	0.022	0.0645	0.0634	0.0591	0.0624	0.0667	0.0829
C2	0.0628	0.0676	0.0662	0.0642	0.059	0.0462	0.0268	0.0175	0.0098
C3	0.0026	0.002	0.0071	0.0038	0.0029	0.0129	0.0055	0.0101	0.0143
C4	0.0687	0.002	0.096	0.0417	0.0675	0.0704	0.0827	0.1168	0.1472
C5	0.002	0.0023	0.0117	0.0105	0.0153	0.0252	0.0459	0.0585	0.0718
C6	0.0046	0.002	0.0053	0.0087	0.0158	0.0162	0.0164	0.0158	0.0158
C7	0.0341	0.055	0.0264	0.031	0.0223	0.0239	0.0228	0.0139	0.0059
C8	0.0032	0.002	0.0031	0.0047	0.0054	0.006	0.006	0.0083	0.0098
C9	0.002	0.0052	0.0079	0.0127	0.0166	0.0209	0.0264	0.0346	0.0463
C10	0.0307	0.002	0.0143	0.0267	0.0297	0.03	0.0297	0.0248	0.0236
C11	0.0278	0.002	0.0125	0.0177	0.0243	0.025	0.0258	0.0222	0.0222
C12	0.002	0.0036	0.0043	0.0046	0.0048	0.0048	0.005	0.005	0.0056
C13	0.002	0.0039	0.0068	0.0097	0.0134	0.0183	0.0241	0.0299	0.039
C14	0.0253	0.0282	0.0253	0.0192	0.0142	0.0078	0.002	0.0049	0.0115
C15	0.0052	0.002	0.0024	0.0159	0.019	0.0277	0.0277	0.0333	0.0325
C16	0.0024	0.0061	0.002	0.0234	0.0234	0.0354	0.0368	0.0378	0.0396
C17	0.003	0.0032	0.002	0.006	0.0145	0.0259	0.0266	0.0291	0.0291
C18	0.0132	0.01322	0.0127	0.0121	0.0111	0.01	0.0089	0.0057	0.002
Comprehensive benefit	0.2936	0.22032	0.328	0.3771	0.4226	0.4657	0.4815	0.5349	0.6089

the test set; as seen from Table 6, the optimization efficiency of the proposed algorithm for the comprehensive evaluation model is higher than that of the benchmark model GA.

Table 7 shows the total benefit evaluation values of land input and output in 18 selected regions from 2010 to 2021 (based on the fuzzy mathematical model optimized by particle swarm optimization). It can be seen from the table that the overall comprehensive evaluation value of land keeps increasing, which indicates that the comprehensive benefit of land keeps expanding.

10. Ending

In this paper, first of all, we select 6 indicators from 6 levels, including land resource input, capital input, and economic output, and build the evaluation index system of land use comprehensive benefit based on land input and output. Then, based on the fuzzy mathematics theory, this paper adopts the improved particle swarm optimization algorithm to identify the fuzzy density value of the evaluation index. This paper, combined with the AHP comprehensive evaluation method, carries out a comprehensive evaluation of the comprehensive benefit of land through the combination of subjective and objective methods. Finally, this paper further analyzes the influencing factors of total factor productivity of urban land use by constructing the Tobit model. It discusses the influencing mechanism of government regulation, land openness, and other factors and land development. The research results of this paper can provide a reference for future urban planning, adjustment of land structure, utilization and protection of land resources, food, and ecological security, and economic security.

Data Availability

The data can be obtained by the corresponding author.

Conflicts of Interest

The authors of this article have no conflicts of interest of any kind.

References

[1] P. Hall and M. Tewdwr-Jones, *Urban and Regional Planning*, Routledge, 2010.

[2] M. C. Roberts, J. C. Randolph, and J. R. Chiesa, "A land suitability model for the evaluation of land-use change," *Environmental Management*, vol. 3, no. 4, pp. 339–352, 1979.

[3] M. Ahmadinejad, Y. Maruyama, and F. Yamazaki, "Evaluation and forecast of human impacts based on land use changes using multi-temporal satellite imagery and GIS: a case study on Zanjan, Iran," *Journal of the Indian Society of Remote Sensing*, vol. 37, no. 4, pp. 659–669, 2009.

[4] A. K. Braimoh, P. Vlek, and A. Stein, "Land evaluation for maize based on fuzzy set and interpolation," *Environmental Management*, vol. 33, no. 2, pp. 226–238, 2004.

[5] R. A. Solow, "A contribution to the theory of economic growth," *Quarterly Journal of Economics*, vol. 70, no. 1, p. 65, 1956.

[6] S. C. Ray and E. Desli, "Productivity growth, technical progress, and efficiency change in industrialized countries: comment," *The American Economic Review*, vol. 87, no. 5, pp. 1033–1039, 1997.

[7] G. D. Hansen and E. C. Prescott, "Malthus to solow," *American economic review*, vol. 92, no. 4, pp. 1205–1217, 2002.

[8] G. Y. Du and Y. L. Cai, "Technical efficiency of built-up land in China's economic growth during 1997-2007," *Progress in Geography, 2010*, vol. 29, no. 6, pp. 693–700, 2010.

[9] J. W. Xu, X. Y. Xu, and M. X. Zhu, "Urban land use efficiency and its change of the Yangtze River delta based on data envelopment analysis," *World Regional Studies*, vol. 22, no. 3, pp. 121–129, 2013.

[10] W. Wei and L. Gang, "Analysis of urban land utilization of cities along the Huaihe River based on PCASFA," *Urban Insight*, vol. 5, pp. 102–112, 2013.

[11] Z. C. Xing, J. G. Wang, and J. Zhang, "Research on regional total-factor ecological efficiency of China: measurement and determinants," *Chinese Journal of Population, Resources and Environment*, vol. 28, pp. 119–126, 2018.

[12] Z. Zhang, C. Lu, X. Chen, B. Xue, and C. Lu, "Urban environmental performance and it's driving factors in China: based on the super-efficiency DEA and panel regressive analysis," *Journal of Arid Land Resources and Environment*, vol. 29, no. 6, pp. 1–7, 2015.

[13] L. Wang, H. Li, and C. Shi, "Urban land-use efficiency, spatial spillover, and determinants in China," *Acta Geographica Sinica*, vol. 70, no. 11, pp. 1788–1799, 2015.

[14] L. T. Liang, Q. L. Zhao, and C. Chen, "Analysis on the characters of spatial disparity of urban land use efficiency and its optimization in China," *China Land Science*, vol. 27, no. 7, pp. 48–52, 2013.

[15] H. Yang, Y. Hu, and Q. Wang, "Evaluation of land use efficiency in three major urban agglomerations of China in 2001-2012," *Scientia Geographica Sinica*, vol. 35, no. 9, pp. 1095–1100, 2015.

[16] Y. Li, B. Shu, and Q. Wu, "Urban land use efficiency in China: spatial and temporal characteristics, regional difference and influence factors," *Economic Geography*, vol. 34, pp. 133–139, 2014.

[17] T. L. Saaty, *Analytic Hierarchy Process*, John Wiley & Sons, Ltd, 2013.

[18] Y. Ji, G. H. Huang, and W. Sun, "Risk assessment of hydropower stations through an integrated fuzzy entropy-weight multiple criteria decision making method: a case study of the Xiangxi River," *Expert Systems with Applications*, vol. 42, no. 12, pp. 5380–5389, 2015.

[19] Z. Pawlak, "Rough set theory and its applications to data analysis," *Cybernetics and Systems*, vol. 29, no. 7, pp. 661–688, 1998.

[20] H. Hong, "Fuzzy mathematics study on evaluating food sensual quality," *Food Science*, vol. 25, no. 6, pp. 185–188, 2004.

[21] H. J. Wu, N. F. Liu, J. He, and W. W. Song, "Comprehensive assessment of ecological environmental by matter element analysis," *Journal of Huazhong University of Science and Technology (Urban Science Edition)*, vol. 23, no. 1, pp. 52–55, 2006.

[22] W. H. Wu, C. T. Lin, K. H. Peng, and C. C. Huang, "Applying hierarchical grey relation clustering analysis to geographical information systems – a case study of the hospitals in Taipei City," *Expert Systems with Applications*, vol. 39, no. 8, pp. 7247–7254, 2012.

[23] Y. Bahrami, H. Hasani, and A. Maghsoudi, "Application of AHP-TOPSIS method to model copper mineral potential in the Abhar 1: 100000 geological map, NW Iran," *Earth Sciences Research Journal*, vol. 12, no. 1, pp. 41–57, 2021.

[24] S. Y. Qu and X. F. Xu, "The evaluation of intercity railway train operation plan based on multi index cosine decision," *Advanced Materials Research*, vol. 598, pp. 130–134, 2012.

[25] L. Chen, X. Gao, S. Gong, and Z. Li, "Regionalization of green building development in China: a comprehensive evaluation model based on the catastrophe progression method," *Sustainability*, vol. 12, no. 15, p. 5988, 2020.

[26] L. Jingwen, Q. Jiangang, D. Yuanming, F. Xu, and L. Xiaoli, "Safety evaluation method of antifloating anchor system based on comprehensive weighting method and gray-fuzzy theory," *Mathematical Problems in Engineering*, vol. 2020, Article ID 3216948, 12 pages, 2020.

[27] L. Wang, "Research on human resource performance and decision-making evaluation based on fuzzy mathematics and clustering model," *Journal of Intelligent & Fuzzy Systems*, vol. 37, no. 1, pp. 171–184, 2019.

[28] T. Chen, D. Shen, Y. Jin et al., "Comprehensive evaluation of environ-economic benefits of anaerobic digestion technology in an integrated food waste-based methane plant using a fuzzy mathematical model," *Applied Energy*, vol. 208, no. 208, pp. 666–677, 2017.

[29] G. Li and C. Jin, "Fuzzy comprehensive evaluation for carrying capacity of regional water resources," *Water Resources Management*, vol. 23, no. 12, pp. 2505–2513, 2009.

[30] C. Cubukcu and C. Cantekin, "Using a combined fuzzy-AHP and topsis decision model for selecting the best firewall alternative," *Journal of fuzzy extension and applications*, vol. 3, no. 3, pp. 192–200, 2022.

[31] J. Li, A. Alburaikan, and R. de Fátima Muniz, "Evaluation of safety-based performance in construction projects with neutrosophic data envelopment analysis," *Management Decision*, 2022.

[32] M. Jatwa and V. Sukhwani, "Fuzzy FMEA model: a case study to identify rejection and losses in fibre industry," *Journal of Fuzzy Extension and Applications*, vol. 3, no. 1, pp. 19–30, 2022.

[33] T. Amemiya, "Tobit models: a survey," *Journal of Econometrics*, vol. 24, no. 1-2, pp. 3–61, 1984.

[34] M. Sugeno, *Theory of Fuzzy Integrals and Its Applications [PhD Thesis]*, Tokyo Institute of Technology, 1974.

[35] K. Ishii and M. Sugeno, "A model of human evaluation process using fuzzy measure," *International Journal of Man-Machine Studies*, vol. 22, no. 1, pp. 19–38, 1985.

[36] J. H. Chiang, "Choquet fuzzy integral-based hierarchical networks for decision analysis," *IEEE Transactions on Fuzzy Systems*, vol. 7, no. 1, pp. 63–71, 1999.

[37] M. Grabisch, "Fuzzy integral in multicriteria decision making," *Fuzzy Sets and Systems*, vol. 69, no. 3, pp. 279–298, 1995.

[38] P. Meyer and M. Rubens, "On the use of the Choquet integral with fuzzy numbers in multiple criteria decision support," *Fuzzy Sets & Systems*, vol. 157, no. 7, pp. 927–938, 2006.

Hindawi
Advances in Mathematical Physics
Volume 2022, Article ID 7057639, 12 pages
https://doi.org/10.1155/2022/7057639

Research Article

A Novel Decision-Making Process in the Environment of Generalized Version of Fuzzy Sets for the Selection of Energy Source

Joseph David Madasi,[1] **Salma Khan**,[2] **Nasreen Kausar**,[3] **Dragan Pamucar**,[4] **Gezahagne Mulat Addis**,[5] **and Muhammad Gulistan**[2]

[1]*College of Mathematics and Computer Science, Zhejiang Normal University, China*
[2]*Department of Mathematics and Statistics Hazara University Mansehra, Pakistan*
[3]*Department of Mathematics, Faculty of Arts and Sciences, Yildiz Technical University, Esenler, 34210 Istanbul, Turkey*
[4]*Faculty of Organizational Sciences, University of Belgrade, Belgrade, Serbia*
[5]*Department of Mathematics, University of Gondar, P.O. Box: 196, Gondar, Ethiopia*

Correspondence should be addressed to Gezahagne Mulat Addis; gezahagne412@gmail.com

Received 4 July 2022; Revised 24 July 2022; Accepted 29 July 2022; Published 23 August 2022

Academic Editor: Ranjan Kumar

In this study, we focus our attention on a kind of generalized fuzzy set. This generalized fuzzy set is known as neutrosophic octahedron sets (NOSs). NOSs are a combination of neutrosophic, intuitionistic fuzzy, and octahedron sets that provide a better platform for dealing with imprecise and ambiguous data. First of all, we analyze uncertainty, for this purpose, we need neutrosophic octahedron set that can also reduce the loss of information about ambiguity and uncertainty. We use NOS over TOPSIS method (technique to order the performance by similarity with the ideal solution). It is a most suitable technique for describing uncertain data in the TOPSIS method in order to allow more imprecision than the neutrosophic, intuitionistic fuzzy, and octahedron set. Thus, the TOPSIS method of NOSs in decision making is used to overcome the problems that arise during decision-making. We use this proposed structure to implement the selection of the energy source by a numerical example as an application. As a result, this model is valuable for decision-making and can be used to choose the most environmentally friendly energy source. Finally, we present an example to demonstrate the validity and effectiveness of the proposed strategy.

1. Introduction

Decision-making is a beneficial method in human activities to consider the appropriate option among alternatives with the highest degree of membership from a group of available possibilities in terms of parameters. In decision-making problems, the evaluated values of alternatives considering the evaluated attribute are often imprecise. The theme of uncertainty and vagueness is difficult, to understand and implement in different areas. So, Zadeh, the developer of fuzzy set theory [1], introduces fuzzy sets in this area to solve the complications and make it more usable. Fuzzy set theory can be applied to evaluate the elements of a set defined by a membership (MM) function in a closed interval $[0, 1]$. After fuzzy set theory, Zadeh [2] also introduced the theme of interval valued fuzzy set in 1975. Atanasove developed the intuitionistic fuzzy set [3] in 1986, with MM and nonmembership (NMM) degrees such that their sum is less than or equal to one. In 1989, Atanassov and Gargov [4] developed a new them with the help of intuitionistic fuzzy set which is known as interval valued intuitionistic fuzzy set. Lee et al. [5] in 2020 introduced octahedron set by combining interval-valued fuzzy set, an intuitionistic fuzzy set and a fuzzy set. The theme of neutrosophic sets developed by Smarandache [6–8] by expanding Atanasove's ideas. He created the term "neutrosophic" because "neutrosophy" is

etymologically related to "neutrosophic." On the other hand, Lupiáñez [9] developed the structure of neutrosophic sets and their topology with basic algebraic operations. In 2005, Wang et al. [10] developed the structure of interval neutrosophic sets. In 2009, Bhowmik and Pal [11] distinguished between truth-based intuitionist neutrosophic sets and intuitionist neutrosophic sets. They established that all intuitionistic neutrosophic sets are neutrosophic sets, but not all neutrosophic sets are intuitionistic neutrosophic sets. In addition, some new INS operations have been defined, as well as illustrations of how the operations could be implemented in real scenarios. Maji [12] developed the structure of neutrosophic soft sets by using Smarandache's idea of neutrosophic sets and also introduced some basic definitions and operation. In 2015, Alkhazaleh and Uluçay [13] initiated the theme of neutrosophic soft expert set with basic operations and also discussed real-life application. Alias et al. [14] established the theme of rough neutrosophic multisets in 2017 with basic operations and properties. The fuzzy sets discussed above are incapable of handling imprecise, uncertain, inconsistent, and incomplete periodic information. To overcome this challenge, Ali and Smarandache [15] expand the idea of neutrosophic sets and developed the structure of complex neutrosophic set. There are some many other applications for solving these uncertainty like [16–19]. In 2012, Balin et al. [20] developed multicriteria decision making model for energy sources. Huang et al. [21] worked on the application used in multicriteria decision making technique in the field of environmental science. TOPSIS is a most useful method. According to certain studies, the TOPSIS technique exhibits a monotonically increasing or decreasing preference for each criterion [22, 23]. Compensatory approaches, like TOPSIS, are widely used in numerous fields of multicriteria decision-making due to the potential of criteria modeling. Some researchers [24, 25] worked on the significance of TOPSIS approach in MADM problem. Pehlivan and Yalçın [26] utilized the TOPSIS approach in a neutrosophic environment to identify sustainable suppliers in a low market chain in 2022. Distinct techniques [27, 28, 30] utilize different versions of neutrosophic sets in decision making challenges, such as single valued neutrosophic sets, single valued neutrosophic type2 fuzzy sets, and type2 neutrosophic model. Jun et al. [29] discovered the cubic set in 2012. Jun et al. [30] studied the concept of cubic subalgebras/ideals in BCK/BCI-algebras and their characteristics. Jun et al. [31] have also presented the neutrosophic cubic set notion (NCS). Gulistan and Khan [32] show the extension of neutrosophic cubic set via complex fuzzy set with application. Some researchers [33, 34] have used the different version of fuzzy sets in the decision-making environment.

Since neutrosophic set provides higher uncertainty and ambiguity than intuitionistic fuzzy set, interval valued fuzzy set and fuzzy set. To further analyze uncertainty, we therefore require a neutrosophic octahedron set. Compared to intuitionistic octahedron sets and octahedron sets, neutrosophic octahedron sets also reduce information loss about ambiguity and uncertainty. So, neutrosophic octahedron set covers broader area as compare to intuitionistic fuzzy set, fuzzy set, and interval valued fuzzy set.

1.1. Contribution of the Study. The following is a list of the planned study's contributions.

(1) Interval number, intuitionistic number, octahedron number, neutrosophic set, and octahedron set are some of the core notions discussed in the literature

(2) This work conceptualises the construction of a NOS with set theoretic operation

(3) In a neutrosophic octahedron environment, the TOPSIS method is proposed

(4) The paper is summarised, along with its scope and future research prospects

1.2. Organization of the Study. The following is a diagram illustrating the study's structure: Section 2: recall some useful information from the previous research. The construction of the NOS is described in Section 3 as a novel mathematical instrument for solving the problem of uncertainty. Introduce the internal and external NOSs, as well as their union and intersection. The NOS's operational features are addressed. Also, the practical element of the suggested structure is developed in this section. Section 4 describes the TOPSIS approach in the context of a NOS as a decision-making problem, and Section 5 describes the comparison, while Section 6 summarises the conclusion and future directions.

2. Materials and Methods

This section of the document reviews the available literature to give some basic materials and methods for a clear understanding of the planned work.

Definition 1 (see [4]). A intuitionistic neutrosophic set is the structure of the form $A = (x, T(x), I(x), F(x))$ such that $T(x) \wedge I(x) \leq 0.5$, $T(x) \wedge F(x) \leq 0.5$, $F(x) \wedge I(x) \leq 0.5$, with $0 \leq T(x) + I(x) + F(x) \leq 2$, for all $x \in X$.

Definition 2 (see [5]). Denote members of $[I] \times (I \oplus I) \times I$ as

$$\tilde{\tilde{x}} = <\tilde{x}, \bar{\lambda}, x> \; = \; < [x-, x-], \left(v^{\epsilon}, x^{\notin}\right), x>, \tag{1}$$

and it is called octahedron number.

Definition 3 (see [5]). Let X be the collection of some elements and let $A^O = [A^-, A^+] \in I]^X$, $B^O = (B^{\epsilon}, B^{\notin}) \in (I \oplus I)^X$, and $\lambda^O \in I^X$. Then, the triplet $O = \langle A^O, B^O, \lambda^O \rangle$ is called an octahedron set in X. The mapping $O : X \longrightarrow I] \times (I \oplus I) \times I$ is known as octahedron.

Definition 4 (see [8]). Let X be the collection of some elements. A neutrsophic set in X is a structure of the type $A = \{x\,; T(x), I(x), F(x) | x \in X\}$, which is characterised by truth-membership (t-MM) T, indeterminacy-membership (i-MM) I, and falsity-membership(f-MM) F, in such a way that $0 \leq T(x) + I(x) + F(l\text{times}) \leq 3$.

3. Neutrosophic Octahedron Sets with Basic Operations

In this section, we introduce new notion of NOS with some interesting properties and basic operations. Also the score function, neutrosophic octahedron weighted average operator, and neutrosophic octahedron order the weighted average operator are discussed.

Definition 5. Let X be the collection of some elements. A structure of the form $A = (A_1, A_2, A_3)$, where $A_1 : X \longrightarrow I]$ denotes the interval valued neutrsophic set, $A_2 : X \longrightarrow (I \oplus I)$ denotes the intuitionistic neutrosophic set, $A_3 : X \longrightarrow I$ denotes the neutrsophic set, is called the neutrosophic octahedron set (NOS) with $A : X \longrightarrow I] \times (I \oplus I) \times I$.

Example 1. Let $X = \{\dot{x}, \ddot{x}, \vec{x}\}$ be a nonempty set and $A = (A_1, A_2, A_3)$: $X \longrightarrow I] \times I \oplus I] \times I$ be the mapping given by

$$A(\dot{x}) = \left\langle \begin{array}{c} A_1(\dot{x}) = ([0.2,0.4], [0.3,0.5], [0.3,0.5]), \\ A_2(\dot{x}) = (0.8,0.2,0.4), \\ A_3(\dot{x}) = (0.6,0.8,0.4) \end{array} \right\rangle, \quad (2)$$

$$A(\ddot{x}) = \left\langle \begin{array}{c} A_1(\ddot{x}) = ([0.3,0.4], [0.4,0.5], [0.4,0.6]), \\ A_2(\ddot{x}) = (0.8,0.2,0.4), \\ A_3(\ddot{x}) = (0.5,0.7,0.6) \end{array} \right\rangle, \quad (3)$$

$$A(\vec{x}) = \left\langle \begin{array}{c} A_1(\vec{x}) = ([0.1,0.3], [0.4,0.6], [0.4,0.5]), \\ A_2(\vec{x}) = (0.8,0.2,0.4), \\ A_3(\vec{x}) = (0.4,0.6,0.5) \end{array} \right\rangle. \quad (4)$$

Then, $A = (A_1, A_2, A_3)$ is NOS.

Definition 6. Let X be the collection of some elements. A structure of the form $A = (A_1, A_2, A_3)$, where $A_1 = \{[A_T^-, A_T^+], [A_I^-, A_I^+], [A_F^-, A_F^+]\} \in I]$, $A_2 = (A_{T^*}, A_{I^*}, A_{F^*}) \in (I \oplus I)^X$, $A_3 = \{A_T, A_I, A_F\} \in I$, is called the NOS in X, with the mapping, $A : X \longrightarrow I] \times (I \oplus I) \times I$. We consider following special NOSs:

$$\langle \hat{0}, \check{0}, 0 \rangle = 0, \quad (5)$$

$$\langle \hat{0}, \check{0}, 1 \rangle, \langle \hat{0}, \check{1}, 0 \rangle, \langle 0, 0, 1 \rangle, \quad (6)$$

$$\langle \hat{0}, \check{1}, 1 \rangle, \langle \hat{1}, 0, 1 \rangle, \langle \hat{1}, \check{1}, 0 \rangle, \quad (7)$$

$$\langle \hat{1}, \check{1}, 1 \rangle = 1. \quad (8)$$

In the above case, 0 (resp., 1) is called a neutrosophic octahedron empty (resp., neutrosophic octahedron whole set) in X.

Remark 7.

(1) Every NOS is an Octahedron set

The set of all NOS of X is denoted by $N^O(X)$.

Definition 8. Let X be the collection of some elements and let $A = (A_1, A_2, A_3)$, and $B = (B_1, B_2, B_3) \in N^O(X)$. Then, we can define the order relations between A and B as follows:

(i) Equality

$$A = B \quad \text{if and only if} \quad A_1 = B_1, \quad A_2 = B_2, \quad A_3 = B_3, \quad (9)$$

(ii) Type 1-order

$$A \subset_1 B \quad \text{if and only if} \quad A_1 \subset B_1, \quad A_2 \subset B_2, \quad A_3 \leq B_3, \quad (10)$$

(iii) Type 2-order

$$A \subset_2 B \quad \text{if and only if} \quad A_1 \subset B_1, \quad A_2 \subset B_2, \quad A_3 \geq B_3, \quad (11)$$

(iv) Type 3-order

$$A \subset_3 B \quad \text{if and only if} \quad A_1 \subset B_1, \quad A_2 \supset B_2, \quad A_3 \leq B_3, \quad (12)$$

(v) Type 4-order

$$A \subset_3 B \quad \text{if and only if} \quad A_1 \subset B_1, \quad A_2 \supset B_2, \quad A_3 \geq B_3. \quad (13)$$

Definition 9. Let X denote a universe of discourse and (A_j) $j \in \bar{J} = \langle A_{1j}, A_{2j}, A_{3j} \rangle j \in \bar{J}$ denote a family of neutrosophic octahedron sets in X. Then, for $(A_j)j \in J(i = 1, 2, 3, 4)$, the type i-union $\cup^i$ and type i-intersection $\cap^i$ are defined as follows:

(i) Type i-union

$$\cup^1_{j \in \bar{J}} A = \left(\cup_{j \in \bar{J}} A_{1j}, \cup_{j \in \bar{J}} A_{2j}, \cup_{j \in \bar{J}} A_{3j} \right), \quad (14)$$

$$\cup^2_{j\in\bar{J}}A = \left(\cup_{j\in\bar{J}}A_{1j}, \cup_{j\in\bar{J}}A_{2j}, \cap_{j\in\bar{J}}A_{3j}\right), \tag{15}$$

$$\cup^3_{j\in\bar{J}}A = \left(\cup_{j\in\bar{J}}A_{1j}, \cap_{j\in\bar{J}}A_{2j}, \cup_{j\in\bar{J}}A_{3j}\right), \tag{16}$$

$$\cup^4_{j\in\bar{J}}A = \left(\cup_{j\in\bar{J}}A_{1j}, \cap_{j\in\bar{J}}A_{2j}, \cap_{j\in\bar{J}}A_{3j}\right). \tag{17}$$

(ii) Type i-intersection

$$\cap^2_{j\in\bar{J}}A = \left(\cap_{j\in\bar{J}}A_{1j}, \cap_{j\in\bar{J}}A_{2j}, \cup_{j\in\bar{J}}A_{3j}\right), \tag{18}$$

$$\cap^3_{j\in\bar{J}}A = \left(\cap_{j\in\bar{J}}A_{1j}, \cup_{j\in\bar{J}}A_{2j}, \cap_{j\in\bar{J}}A_{3j}\right), \tag{19}$$

$$\cap^4_{j\in\bar{J}}A = \left(\cap\cap_{j\in\bar{J}}A_{1j}, \cup_{j\in J}A_{2j}, \cup_{j\in\bar{J}}A_{3j}\right). \tag{20}$$

Proposition 10. *Let X be the collection of some elements and let $A = (A_1, A_2, A_3)$, $B = (B_1, B_2, B_3)$, $C = (C_1, C_2, B_3)$, and $\bar{\alpha} = (\bar{\alpha}_1, \bar{\alpha}_2, \bar{\alpha}_3)$ be neutrosophic octrahedron sets. Then, for each $i = 1, 2, 3, 4$.*

(i) If $A \subset_i B$ and $B \subset_i C$ then $A \subset_i C$

(ii) If $A \subset_i B$ and $A \subset_i C$ then $A \subset_i B \cap C$

(iii) If $A \subset_i B$ and $C \subset_i B$ then $A \cup C \subset_i B$

(iv) If $A \subset_i B$ and $C \subset_i \bar{\alpha}$ then $A \cup C \subset_i B \cup \bar{\alpha}$ and $A \cap C \subset_i B \cap \bar{\alpha}$

Definition 11. Let X be the collection of some elements and let $A = (A_1, A_2, A_3)$ be a neutrosophic octahedron set in X. Then, the complement A^c,[] and $\diamond$ of A are defined as follows:

(i) $A^C = (A_1, A_2, A_3)$

(ii) $[]A = (A_1, []A_2, A_3)$

(iii) $\diamond A = (A_1, \diamond A_2, A_3)$

From Definition 6, we can easily see that the following holds:

$$\hat{\dot{0}}^c = 1, 1^c = 0, \tag{21}$$

$$\left\langle \hat{\dot{0}}, \breve{\dot{0}}, 1 \right\rangle^c = \left\langle \hat{\dot{1}}, \breve{\dot{1}}, 0 \right\rangle, \left\langle \hat{\dot{1}}, \breve{\dot{1}}, 0 \right\rangle^c = \left\langle \hat{\dot{0}}, \breve{\dot{0}}, 1 \right\rangle, \tag{22}$$

$$\left\langle \hat{\dot{0}}, \breve{\dot{1}}, 0 \right\rangle^c = \left\langle \hat{\dot{1}}, \breve{\dot{0}}, 1 \right\rangle, \left\langle \hat{\dot{1}}, \breve{\dot{0}}, 1 \right\rangle^c = \left\langle \hat{\dot{0}}, \breve{\dot{1}}, 0 \right\rangle, \tag{23}$$

$$\left\langle \hat{\dot{1}}, \breve{\dot{0}}, 0 \right\rangle^c = \left\langle 0, \hat{\dot{1}}, \breve{\dot{1}} \right\rangle, \left\langle 0, \hat{\dot{1}}, \breve{\dot{1}} \right\rangle^c = \left\langle \hat{\dot{1}}, \breve{\dot{0}}, 0 \right\rangle, \tag{24}$$

$$\left\langle \hat{\dot{0}}, \breve{\dot{1}}, 1 \right\rangle^c = \left\langle \hat{\dot{1}}, \breve{\dot{0}}, 0 \right\rangle, \left\langle \hat{\dot{1}}, \breve{\dot{0}}, 0 \right\rangle^c = \left\langle \hat{\dot{0}}, \breve{\dot{1}}, 1 \right\rangle, \tag{25}$$

$$\left\langle \hat{\dot{1}}, \breve{\dot{0}}, 1 \right\rangle^c = \left\langle \hat{\dot{0}}, \breve{\dot{1}}, 0 \right\rangle, \left\langle \hat{\dot{0}}, \breve{\dot{1}}, 0 \right\rangle^c = \left\langle \hat{\dot{1}}, \breve{\dot{0}}, 1 \right\rangle, \tag{26}$$

$$\left\langle \hat{\dot{1}}, \breve{\dot{1}}, 0 \right\rangle^c = \left\langle \hat{\dot{0}}, \breve{\dot{0}}, 1 \right\rangle, \left\langle \hat{\dot{0}}, \breve{\dot{0}}, 1 \right\rangle^c = \left\langle \hat{\dot{1}}, \breve{\dot{1}}, 0 \right\rangle. \tag{27}$$

Remark 12. The union, intersection, and complement of NOS does not hold in general, i.e., $A \cup A^c = 1$ and $A \cap A^c = 0$.

Proposition 13. *Let X be the collection of some elements and let $A = (A_1, A_2, A_3)$, and $B = (B_1, B_2, B_3)$ be two neutrosophic octrahedron sets in X. If $A \subset_i B$, then $B^C \subset_i A^C$, for each $i = 1, 2, 3$.*

Proposition 14. *Let $A \in N^O(X)$ and let $(A_J)_j \in J \subset N^O(X)$. Then*

(i) $(A^C)^C = A$

(ii) For each $i = 1, 2, 3$

$$\left(\bigcup_{j\in J}^{i} A_j\right)^C = \bigcap_{j\in J}^{i} A_j^C, \tag{28}$$

$$\left(\bigcap_{j\in J}^{i} A_j\right)^C = \bigcup_{j\in J}^{i} A_j^C. \tag{29}$$

Proposition 15. *Let X be the collection of some elements and let $A = (A_1, A_2, A_3)$, and $B = (B_1, B_2, B_3)$ be two neutrosophic octrahedron sets in X. If $A \subset B$, then $N^N_{CB} \subset N^N_{CA}$ for each $i = 1, 2, 3, 4$.*

Definition 16. Let X be the collection of some elements and let $A = (A_1, A_2, A_3) \in N^O(X)$, then, A is called an internal and external neutrosopic octahedron set if the following are satisfied:

A truth-internal NOS (briefly, INOS) in X, for each $x \in X$,

$$A_{2TA}(x), A_{3TA}(x) \in A_1 = \left([A^-_{TA}, A^+_{TA}], [A^-_{IA}, A^+_{IA}], [A^-_{FA}, A^+_{FA}]\right). \tag{30}$$

An indeterminacy-internal NOS (briefly, INOS) in X, for each $x \in X$,

$$A_{2IA}(x), A_{3IA}(x) \in A_1 = \left([A^-_{TA}, A^+_{TA}], [A^-_{IA}, A^+_{IA}], [A^-_{FA}, A^+_{FA}]\right). \tag{31}$$

A falsity-internal NOS (briefly, INOS) in X, for each $x \in X$,

$$A_{2FA}(x), A_{3FA}(x) \in A_1 = \left([A^-_{TA}, A^+_{TA}], [A^-_{IA}, A^+_{IA}], [A^-_{FA}, A^+_{FA}]\right). \tag{32}$$

A truth-external NOS (briefly, $\notin$–ENOS) in X, for each

Figure 1: Source of solar energy.

Figure 2: Source of wind energy.

$x \in X$,

$$A_{2TA}(x), A_{3TA}(x) \notin A_1 = ([A_{TA}^-, A_{TA}^+], [A_{IA}^-, A_{IA}^+], [A_{FA}^-, A_{FA}^+]). \tag{33}$$

An indeterminacy-external NOS (briefly, INOS) in X, for each $x \in X$,

$$A_{2IA}(x), A_{3IA}(x) \notin A_1 = ([A_{TA}^-, A_{TA}^+], [A_{IA}^-, A_{IA}^+], [A_{FA}^-, A_{FA}^+]). \tag{34}$$

A falsity-external NOS (briefly, INOS) in X, for each $x \in X$,

$$A_{2FA}(x), A_{3FA}(x) \notin A_1 = ([A_{TA}^-, A_{TA}^+], [A_{IA}^-, A_{IA}^+], [A_{FA}^-, A_{FA}^+]). \tag{35}$$

Proposition 17. *Let X be the collection of some elements and let $A = (A_1, A_2, A_3) \in N^O(X)$. If A is not external NOSs, then, there is $x \in X$ such that*

Figure 3: Source of geothermal energy.

Figure 4: Source of hydropower energy.

$$A_2(x) \in ([A_{TA}^-, A_{TA}^+], [A_{IA}^-, A_{IA}^+], [A_{FA}^-, A_{FA}^+]), \tag{36}$$

or

$$1 - A_2(x) \in ([A_{TA}^-, A_{TA}^+], [A_{IA}^-, A_{IA}^+], [A_{FA}^-, A_{FA}^+]), \tag{37}$$

$$A_3(x) \in ([A_{TA}^-, A_{TA}^+], [A_{IA}^-, A_{IA}^+], [A_{FA}^-, A_{FA}^+]). \tag{38}$$

Proposition 18. *Let X be the collection of some elements and let $A = (A_1, A_2, A_3) \in A(X)$. if A is both internal and external NOSs, then, there is $x \in X$,*

$$A_2(x), 1 - A_2(x), A_3(x) \in U(A_1) \cup L(A_1), ([A_{TA}^-, A_{TA}^+], [A_{IA}^-, A_{IA}^+], [A_{FA}^-, A_{FA}^+]), \tag{39}$$

Figure 5: Ranking.

where $U(A_1) = \{A_{TA}^+, A_{IA}^+, A_{FA}^+ : x \in X\}$ *and* $L(A_2) = \{A_{TA}^-, A_{IA}^-, A_{FA}^- : x \in X\}$.

Proposition 19. *Let X be the collection of some elements and let* $A = (A_1, A_2, A_3) \in A(X)$. *if A is an internal (resp., external) NOSs, then,* $\neg A$ *(complement) is external (resp., internal).*

Example 2. Let $A = \langle A_1, A_2, A_3 \rangle$ be a NOS in X given by for each $x \in X$,

$$A(x) = \left\langle \begin{array}{c} \left(\left[\frac{x}{4}, \frac{1+x}{2}\right], \left[\frac{x}{6}, \frac{1+x}{4}\right], \left[\frac{x}{8}, \frac{1+x}{6}\right]\right), \\ \left(\left[\frac{x}{3}, \frac{1+x}{5}\right], \left[\frac{x}{5}, \frac{1+x}{7}\right], \left[\frac{\tilde{a}}{7}, \frac{1+x}{9}\right]\right), \left(\frac{x}{2}, \frac{x}{4}, \frac{x}{6}\right) \end{array} \right\rangle. \tag{40}$$

$A_2(x), A_3(x) \in A_1$ for each $x \in X$ is then easily calculated, but $A_2(x) \notin ([A_{TA}^-, A_{TA}^+], [A_{IA}^-, A_{IA}^+], [A_{FA}^-, A_{FA}^+])$, for each $x \in X$ such that $x > 3/7$. Thus, A is an $\in$–INOS but not a $\notin$–INOS in X.

Proposition 20. *Let X be the collection of some elements and let* $A = (A_1, A_2, A_3)$, *and* $B = (B_1, B_2, B_3)$ *be two neutrosophic octrahedron sets in X. Suppose A and B are internal for each* $x \in X$.

Definition 21. The sum between two NOSs $A = (A_1, A_2, A_3)$, and $B = (B_1, B_2, B_3)$ is defined as

$$A \oplus B = (A_1 + B_1 - A_1.B_1, A_2 + B_2 - A_2.B_2, A_3 + B_3 - A_3.B_3). \tag{41}$$

Definition 22. The product between two NOSs $A = (A_1, A_2, A_3)$, and $B = (B_1, B_2, B_3)$ is defined as $A \otimes B = (A_1.B_1, A_2.B_2, A_3.B_3)$.

Definition 23. Scalar multiplication with a neutrosophic octahedron set of a Scalar $\lambda A = (A_1, A_2, A_3)$, is defined as λA.

Theorem 24. *Let* $A = (A_1, A_2, A_3)$, $B = (B_1, B_2, B_3)$ *and* $C = (C_1, C_2, C_3)$ *be three NOSs of A, where A be a collection of NOSs. Then* $(A, \oplus)$ *is a commutative monoid.*

Proof.

(1) Let $A, B \in A$. Then, we have

$$A \oplus B = \langle (A_1 + B_1 - A_1.B_1, A_2 + B_2 - A_2.B_2, A_3 + B_3 - A_3.B_3) \rangle, \tag{42}$$

which is clearly in A.

(2) Let $A, B, C \in A$. Then, we prove $(A \oplus B) \oplus C = A \oplus (B \oplus C)$

$$\begin{aligned} &\left(N_1^{NC} \oplus N_2^{NC}\right) \oplus N_3^{NC} \\ &= \langle (A_1, A_2, A_3) \oplus (B_1, B_2, B_3) \rangle \oplus \langle C_1, C_2, C_3 \rangle \\ &= \langle (A_1 + B_1 - A_1.B_1, A_2 + B_2 - A_2.B_2, A_3 + B_3 - A_3.B_3) \rangle \\ &\quad \oplus \langle C_1, C_2, C_3 \rangle = (A_1, A_2, A_3) \\ &\quad \oplus \langle (B_1 + C_1 - B_1.C_1, B_2 + C_2 - B_2.C_2, B_3 + C_3 - B_3.C_3) \rangle \\ &= A \oplus (B \oplus C). \end{aligned} \tag{43}$$

(3) Let $A, B \in A$. Then, we have

$$\begin{aligned} A \oplus B &= \langle (A_1, A_2, A_3) \oplus (B_1, B_2, B_3) \rangle \\ &= \langle (A_1 + B_1 - A_1.B_1, A_2 + B_2 - A_2.B_2, A_3 + B_3 - A_3.B_3) \rangle \\ &= \langle (B_1 + A_1 - B_1.A_1, B_2 + A_2 - B_2.A_2, B_3 + A_3 - B_3.A_3) \rangle \\ &= B \oplus A. \end{aligned} \tag{44}$$

Hence, $(A, \oplus)$ is a commutative semigroup. □

Theorem 25. *Let $A = (A_1, A_2, A_3)$, and $B = (B_1, B_2, B_3)$ be any two NOSs. Then, the following holds*

(1) $\ddot{\lambda}(A \oplus B) = \ddot{\lambda}A \oplus \ddot{\lambda}B$

(2) $(\ddot{\lambda}_1 + \ddot{\lambda}_2)A = \ddot{\lambda}_1 A + \ddot{\lambda}_2 A$, *where* $\ddot{\lambda}$ *is any scalar*

Proof.

(1) Let A, B be two NOSs and $\ddot{k}_0$ be any constant. Then, we have

$$\ddot{\lambda}_0(A \oplus B) = \ddot{\lambda}_0(\langle A_1, A_2, A_3 \rangle \oplus \langle B_1, B_2, B_3 \rangle)$$

$$= \ddot{\lambda}_0 \langle (A_1 + B_1 - A_1.B_1, A_2 + B_2 - A_2.B_2, A_3 + B_3 - A_3.B_3) \rangle$$

$$= \left\langle \begin{pmatrix} \left(-1 - (-1 - (A_1 + B_1 - A_1.B_1))^{\ddot{\lambda}_0}\right), \\ \left(-1 - (-1 - (A_2 + B_2 - A_2.B_2))^{\ddot{\lambda}_0}\right), \\ \left(-1 - (-1 - (A_3 + B_3 - A_3.B_3))^{\ddot{\lambda}_0}\right) \end{pmatrix} \right\rangle$$

$$= \left\langle \begin{pmatrix} \left(-1 - (-1 - A_1 - B_1 + A_1.B_1)^{\ddot{\lambda}_0}\right), \\ \left(-1 - (-1 - A_2 - B_2 + A_2.B_2)^{\ddot{\lambda}_0}\right), \\ \left(-1 - (-1 - A_3 - B_3 + A_3.B_3)^{\ddot{\lambda}_0}\right) \end{pmatrix} \right\rangle$$

$$= \left\langle \begin{pmatrix} \left(-1 - (-1 - A_1 - B_1(1 - A_1.B_1))^{\ddot{\lambda}_0}\right), \\ \left(-1 - (-1 - A_2 - B_2(1 - A_2.B_2))^{\ddot{\lambda}_0}\right), \\ \left(-1 - (-1 - A_3 - B_3(1 - A_3.B_3))^{\ddot{\lambda}_0}\right) \end{pmatrix} \right\rangle$$

$$= \left\langle \begin{pmatrix} \left(-1 - (-1 - A_1 - B_1(1 - B_1))^{\ddot{\lambda}_0}\right), \\ \left(-1 - (-1 - A_2 - B_2(1 - B_2))^{\ddot{\lambda}_0}\right), \\ \left(-1 - (-1 - A_3 - B_3(1 - B_3))^{\ddot{\lambda}_0},\right) \end{pmatrix} \right\rangle$$

$$= \left\langle \begin{pmatrix} \left(-1 - ((-1 - A_1)(1 - B_1))^{\ddot{\lambda}_0}\right), \\ \left(-1 - ((-1 - A_2 I)(1 - B_2))^{\ddot{\lambda}_0}\right), \\ \left(-1 - ((-1 - A_3)(1 - B_3))^{\ddot{\lambda}_0}\right) \end{pmatrix} \right\rangle$$

$$= \left\langle \begin{pmatrix} -1 - (-1 - A_1)^{\ddot{\lambda}_0} - (1 + B_2)^{\ddot{\lambda}_0} + 1 + (-1 - A_1)^{\ddot{\lambda}_0} \\ +(1 + B_1)^{\ddot{\lambda}_0} - (-1 - A_1)^{\ddot{\lambda}_0}(1 + B_1)^{\ddot{\lambda}_0}, \end{pmatrix}, \right.$$
$$\left. \begin{pmatrix} -1 - (-1 - A_2)^{\ddot{\lambda}_0} - (1 + B_2)^{\ddot{\lambda}_0} + 1 + (-1 - A_2)^{\ddot{\lambda}_0} \\ +(1 + B_2)^{\ddot{\lambda}_0} - (-1 - A_2)^{\ddot{\lambda}_0}(1 + B_2)^{\ddot{\lambda}_0}, \end{pmatrix}, \right\rangle$$
$$\begin{pmatrix} -1 - (-1 - A_3)^{\ddot{\lambda}_0} - (1 + B_3)^{\ddot{\lambda}_0} + 1 + (-1 - A_3)^{\ddot{\lambda}_0} \\ +(1 + B_3)^{\ddot{\lambda}_0} - (-1 - A_3)^{\ddot{\lambda}_0}(1 + B_3)^{\ddot{\lambda}_0}, \end{pmatrix}$$

$$= \left\langle \begin{pmatrix} 2 - (-1 - A_1)^{\ddot{\lambda}_0} - (1 + B_1)^{\ddot{\lambda}_0} - \left(-1 - (1 + B_1)^{\ddot{\lambda}_0}\right. \\ \left. -(-1 - A_1)^{\ddot{\lambda}_0}\right) + (-1 - A_1)^{\ddot{\lambda}_0}(1 + B_1)^{\ddot{\lambda}_0}, \end{pmatrix}, \right.$$
$$\left. \begin{pmatrix} 2 - (-1 - A_2)^{\ddot{\lambda}_0} - (1 + B_2)^{\ddot{\lambda}_0} - (-1 - (1 + B_2)^{\ddot{\lambda}_0} \\ -(-1 - A_2)^{\ddot{\lambda}_0}) + (-1 - A_2)^{\ddot{\lambda}_0}(1 + B_2)^{\ddot{\lambda}_0}, \end{pmatrix}, \right\rangle$$
$$\begin{pmatrix} 2 - (-1 - A_3)^{\ddot{\lambda}_0} - (1 + B_3)^{\ddot{\lambda}_0} - (-1 - (1 + B_3)^{\ddot{\lambda}_0} \\ -(-1 - A_3)^{\ddot{\lambda}_0}) + -(-1 - A_1)^{\ddot{\lambda}_0}) + (-1 - A_3)^{\ddot{\lambda}_0}(1 + B_3)^{\ddot{\lambda}_0}, \end{pmatrix}$$

$$= \left\langle \begin{pmatrix} -1 - (-1 - A_1)^{\ddot{\lambda}_0} + 1 - (1 - B_1)^{\ddot{\lambda}_0} \\ -\left(1 - (-1 - A_1)^{\ddot{\lambda}_0}\right)\left(1 - (1 - B_1)^{\ddot{\lambda}_0}\right), \end{pmatrix}, \right.$$
$$\left. \begin{pmatrix} -1 - (-1 - A_2)^{\ddot{\lambda}_0} + 1 - (1 - B_2)^{\ddot{\lambda}_0} \\ -\left(1 - (-1 - A_2)^{\ddot{\lambda}_0}\right)\left(1 - (1 - B_2)^{\ddot{\lambda}_0}\right), \end{pmatrix}, \right\rangle$$
$$\begin{pmatrix} -1 - (-1 - A_3)^{\ddot{\lambda}_0} + 1 - (1 - B_3)^{\ddot{\lambda}_0} \\ -\left(1 - (-1 - A_3)^{\ddot{\lambda}_0}\right)\left(1 - (1 - B_3)^{\ddot{\lambda}_0}\right), \end{pmatrix}$$

$$= \left\langle \begin{matrix} -1 - (-1 - A_1)^{\ddot{\lambda}_0}, \\ -1 - (-1 - A_2)^{\ddot{\lambda}_0}, \\ -1 - (-1 - A_3)^{\ddot{\lambda}_0} \end{matrix} \right\rangle \oplus \left\langle \begin{matrix} -1 - (-1 - B_1)^{\ddot{\lambda}_0}, \\ -1 - (-1 - B_2)^{\ddot{\lambda}_0}, \\ -1 - (-1 - B_3)^{\ddot{\lambda}_0} \end{matrix} \right\rangle,$$

$$= \ddot{\lambda}_0 \langle A_1, A_2, A_3 \rangle \oplus \ddot{\lambda}_0 \langle B_1, B_2, B_3 \rangle \tag{45}$$

we have $\ddot{\lambda}_0(A \oplus B) = \lambda A \oplus \ddot{\lambda}_0 B$.

(2) Let $\Omega \in A$ and $\ddot{\lambda}_1, \ddot{\lambda}_2$ be any constant. Then, we have

$$\begin{aligned}
\left(\ddot{\lambda}_1+\ddot{\lambda}_2\right)A &= \left(\ddot{\lambda}_1+\ddot{\lambda}_2\right)\langle A_1,A_2,A_3\rangle \\
&\quad \left(-1-\left(-1-A_1\right)^{\ddot{\lambda}_1+\ddot{\lambda}_2}\right), \\
&= \left\langle \left(-1-\left(-1-A_2\right)^{\ddot{\lambda}_1+\ddot{\lambda}_2}\right), \right\rangle \\
&\quad \left(-1-\left(-1-A_3\right)^{\ddot{\lambda}_1+\ddot{\lambda}_2}\right) \\
&\quad \left(\begin{matrix} -2-\left(1-A_1\right)^{\ddot{\lambda}_1}-\left(1-A_1\right)^{\ddot{\lambda}_2}+\left(1-A_1\right)^{\ddot{\lambda}_1} \\ -1+\left(1-A_1\right)^{\ddot{\lambda}_2}-\left(1-A_1\right)^{\ddot{\lambda}_1+\ddot{\lambda}_2}, \end{matrix}\right), \\
&= \left\langle \left(\begin{matrix} -2-\left(1-A_2\right)^{\ddot{\lambda}_1}-\left(1-A_2\right)^{\ddot{\lambda}_2}+\left(1-A_2\right)^{\ddot{\lambda}_1} \\ -1+\left(1-A_2\right)^{\ddot{\lambda}_2}-\left(1-A_2\right)^{\ddot{\lambda}_1+\ddot{\lambda}_2}, \end{matrix}\right),\right\rangle \\
&\quad \left(\begin{matrix} -2-\left(1-A_3\right)^{\ddot{\lambda}_1}-\left(1-A_3\right)^{\ddot{\lambda}_2}+\left(1-A_3\right)^{\ddot{\lambda}_1} \\ -1+\left(1-A_3\right)^{\ddot{\lambda}_2}-\left(1-A_3\right)^{\ddot{\lambda}_1+\ddot{\lambda}_2}, \end{matrix}\right) \\
&\quad \left(\begin{matrix} -1-\left(-1-A_1\right)^{\ddot{\lambda}_1}+1-\left(-1-A_1\right)^{\ddot{\lambda}_2} \\ -\left(1-\left(1-A_1\right)^{\ddot{\lambda}_1}\right)\left(-1-\left(1-A_1\right)^{\ddot{\lambda}_2}\right) \end{matrix}\right), \\
&= \left\langle \left(\begin{matrix} -1-\left(-1-A_2\right)^{\ddot{\lambda}_1}+1-\left(-1-A_2\right)^{\ddot{\lambda}_2} \\ -\left(1-\left(1-A_2\right)^{\ddot{\lambda}_1}\right)\left(-1-\left(1-A_2\right)^{\ddot{\lambda}_2}\right), \end{matrix}\right),\right\rangle \\
&\quad \left(\begin{matrix} -1-\left(-1-A_3\right)^{\ddot{\lambda}_1}+1-\left(-1-A_3\right)^{\ddot{\lambda}_2} \\ -\left(1-\left(1-A_3\right)^{\ddot{\lambda}_1}\right)\left(-1-\left(1-A_3\right)^{\ddot{\lambda}_2}\right), \end{matrix}\right) \\
&= \left\langle \begin{matrix} 1-\left(1-A_1\right)^{\ddot{\lambda}_1}, \\ 1-\left(1-A_2\right)^{\ddot{\lambda}_1}, \\ 1-\left(1-A_3\right)^{\ddot{\lambda}_1} \end{matrix} \right\rangle \oplus \left\langle \begin{matrix} -1-\left(-1-A_1\right)^{\ddot{\lambda}_2}, \\ -1-\left(-1-A_2\right)^{\ddot{\lambda}_2}, \\ -1-\left(-1-A_3\right)^{\ddot{\lambda}_2} \end{matrix} \right\rangle \qquad (46)
\end{aligned}$$

we have $(\ddot{\lambda}_1+\ddot{\lambda}_2)A_1=\ddot{\lambda}_1A_1+\ddot{\lambda}_2A_1$. □

Definition 26. Let $A=(A_1,A_2,A_3)$ be a NOS, and we define score function as

$$S(A)=\frac{A_1+A_2+A_3}{12}. \qquad (47)$$

Definition 27. Let $A=(A_1,A_2,A_3)_t(t=1,2,\cdots m)$ be the collection of values of neutrosophic octahedron and weighted average operator is defined as $\mathrm{NOWA}:\Omega^n\longrightarrow\Omega$ by $\mathrm{NOWA}_w(A_1,A_2\cdots A_m)=\sum_{Tru=1}^{m}w_tA_1$, where $W=(w_1,w_2,\cdots,w_m)^t$ is the weight vector, such that $w_t\in 0,1]$ and $\sum_{t=1}^{m}w_t=1$.

Definition 28. Let $A=(A_1,A_2,A_3)_t(t=1,2,\cdots m)$ be the collection of values of neutrosophic octahedron and order weighted average operator as $\mathrm{NOOWA}:\Omega^n\longrightarrow\Omega$ by $\mathrm{NOOWA}_w(A_1,A_1\cdots,A_1)=\sum_{t=1}^{m}w_tA_1$, where NOOWA is order weighted average operator A_1 is the the largest, $W=(w_1,w_2\cdots,w_m)^t$ is the weight vector of $A_1(t=1,2,\cdots m)$, such that $w_t\in 0,1]$ and $\sum_{t=1}^{m}w_t=1$.

4. Energy Source Selection by TOPSIS Method

It is essential to select an energy source that has the least impact on the natural environment, and it must take into account crucial factors like as reliability, cost, and maintenance. As a result, selecting the optimal energy source is not a simple task, as this decision may be fraught with uncertainty and ambiguity. To deal with ambiguity and vagueness, Zadeh developed the fuzzy theory. In 1975, he defined interval-valued fuzzy sets as a more general class of fuzzy sets. Intuitionistic fuzzy sets, neutrosophic sets, interval neutrosophic sets, intuitionistic neutrosophic sets, neutrosophic cubic sets, neutrosophic soft sets, rough neutrosophic sets, and octahedron sets are some well-known kinds of fuzzy sets. We use neutrosophic octahedron sets to define decision making problem. The algorithms are proposed in this section. The algorithm shows the procedure of TOPSIS method based on the following terminologies. Some example of energy sources are solar energy, wind energy, geothermal energy, and hydropower energy.

Solar energy: solar power is the conversion of solar energy into thermal or electrical energy. Solar energy is the most abundant and environmentally friendly source of renewable energy available today. The source of solar energy is shown as in Figure 1.

Wind energy: wind is a type of solar energy. Winds are created by the heating of the atmosphere by the sun, the rotation of the Earth, and irregularities in its surface. The source of wind energy is shown as in Figure 2.

Geothermal energy: geothermal energy is the heat that exists in the earth's crust. Geothermal energy is derived from the Greek words geo (earth) and therm (heat). Because heat is constantly produced in the earth, geothermal energy is a renewable energy source. The source of geothermal energy is shown as in Figure 3.

Hydropower energy: the conversion of energy from running water into electricity is known as hydroelectricity. It is the oldest and largest renewable energy source in the world. The source of hydropower energy is shown as in Figure 4.

These energy sources are renewable. These resources do not pollute the environment in any way, and H = human activities have no effect on renewable resources. It is important to choose the best energy source for their country which minimum effects the environment. The important parameter of energy sources is reliability, yields, cost, and maintenance. Where U_1, U_2, U_3, and U_4 stand for solar energy, wind energ, geothermal energy, and hydropower energy. These sources are evaluated against the four parameters which are represented by $\ddot{\lambda}_1$, $\ddot{\lambda}_v$, $\ddot{\lambda}_3$, and $\ddot{\lambda}_4$ where these parameters stand for reliability, yields, cost, and maintenance.

For this purpose, we select a panel which are consist of expertise. The panel assessed the energy sources according to given criteria. The panel gives their judgements in the form of decision matrix. Suppose the decision matrix is represented by $a=[a_{i_j}]m\times n$, where a_{i_j} shows evaluation of ith alternative with respect to jth criteria.

Step 1. Standardize the decision matrix as follows:

$$D = \begin{array}{c} \\ \ddot{\lambda}_1 \\ \ddot{\lambda}_2 \\ \ddot{\lambda}_3 \\ \ddot{\lambda}_4 \end{array} \begin{array}{c} U_1 \\ \left\{\begin{array}{c}(0.1,0.2],\\(0.3,0.1],\\(0.1,0.2],\\(0.5,0.2,0.4),\\(0.2,0.3,0.4)\end{array}\right\} \\ \left\{\begin{array}{c}(0.1,0.1],\\(0.1,0.2],\\(0.1,0.3],\\(0.5,0.2,0.3),\\(0.3,0.4,0.2)\end{array}\right\} \\ \left\{\begin{array}{c}(0.1,0.2],\\(0.1,0.2],\\(0.2,0.1],\\(0.2,0.2,0.5),\\(0.5,0.4,0.3)\end{array}\right\} \\ \left\{\begin{array}{c}(0.1,0.2],\\(0.1,0.2],\\(0.1,0.2],\\(0.8,0.2,0.4),\\(0.6,0.8,0.4)\end{array}\right\} \end{array} \begin{array}{c} U_2 \\ \left\{\begin{array}{c}(0.1,0.1],\\(0.1,0.1],\\(0.1,0.1],\\(0.3,0.2,0.4),\\(0.3,0.5,0.4)\end{array}\right\} \\ \left\{\begin{array}{c}(0.2,0.1],\\(0.3,0.2],\\(0.1,0.2],\\(0.3,0.2,0.4),\\(0.5,0.7,0.6)\end{array}\right\} \\ \left\{\begin{array}{c}(0.1,0.2],\\(0.1,0.1],\\(0.2,0.2],\\(0.3,0.2,0.2),\\(0.4,0.3,0.2)\end{array}\right\} \\ \left\{\begin{array}{c}(0.2,0.1],\\(0.1,0.2],\\(0.3,0.1],\\(0.8,0.2,0.4),\\(0.6,0.8,0.4)\end{array}\right\} \end{array} \begin{array}{c} U_3 \\ \left\{\begin{array}{c}(0.1,0.2],\\(0.1,0.2],\\(0.1,0.2],\\(0.3,0.2,0.4),\\(0.3,0.5,0.4)\end{array}\right\} \\ \left\{\begin{array}{c}(0.1,0.2],\\(0.1,0.2],\\(0.2,0.1],\\(0.5,0.2,0.4),\\(0.2,0.3,0.4)\end{array}\right\} \\ \left\{\begin{array}{c}(0.1,0.2],\\(0.1,0.2],\\(0.2,0.2],\\(0.8,0.2,0.4),\\(0.6,0.8,0.4)\end{array}\right\} \\ \left\{\begin{array}{c}(0.1,0.2],\\(0.2,0.1],\\(0.1,0.1],\\(0.5,0.2,0.4),\\(0.2,0.3,0.4)\end{array}\right\} \end{array} \begin{array}{c} U_4 \\ \left\{\begin{array}{c}(0.1,0.2],\\(0.1,0.1],\\(0.1,0.2],\\(0.3,0.2,0.4),\\(0.3,0.5,0.4)\end{array}\right\} \\ \left\{\begin{array}{c}(0.1,0.1],\\(0.2,0.2],\\(0.2,0.1],\\(0.5,0.2,0.3),\\(0.3,0.4,0.2)\end{array}\right\} \\ \left\{\begin{array}{c}(0.1,0.2],\\(0.2,0.1],\\(0.2,0.2],\\(0.2,0.2,0.5),\\(0.5,0.4,0.3)\end{array}\right\} \\ \left\{\begin{array}{c}(0.2,0.1],\\(0.1,0.1],\\(0.1,0.2],\\(0.2,0.2,0.5),\\(0.5,0.4,0.3)\end{array}\right\} \end{array} \tag{48}$$

Step 2. Construct normalized decision matrix, using the following equation:

$$\mathring{\lambda}_{i_j} = \frac{\mathrm{u}_{i_j}}{\sqrt{\left(\sum \mathrm{u}_{i_j}^2\right)}} \quad \text{for} \quad i = 1, \cdots, m\,; j = 1, \cdots, n. \tag{49}$$

$$\begin{array}{c} \\ \mathring{\lambda}_1 \\ \mathring{\lambda}_2 \\ \mathring{\lambda}_3 \\ \mathring{\lambda}_4 \end{array} \begin{array}{c} U_1 \\ \left\{\begin{array}{c}(0.25,0.29],\\(0.5,0.143],\\(0.2,0.25],\\\left(\begin{array}{c}0.461,0.5,\\0.492\end{array}\right),\\\left(\begin{array}{c}0.233,0.292,\\0.596\end{array}\right)\end{array}\right\} \\ \left\{\begin{array}{c}(0.25,0.143],\\(0.17,0.29],\\(0.2,0.38],\\\left(\begin{array}{c}0.461,0.5,\\0.369\end{array}\right),\\\left(\begin{array}{c}0.349,0.389,\\0.298\end{array}\right)\end{array}\right\} \\ \left\{\begin{array}{c}(0.25,0.29],\\(0.17,0.29],\\(0.5,0.125],\\\left(\begin{array}{c}0.184,0.5,\\0.616\end{array}\right),\\\left(\begin{array}{c}0.581,0.389,\\0.447\end{array}\right)\end{array}\right\} \\ \left\{\begin{array}{c}(0.25,0.29],\\(0.17,0.29],\\(0.2,0.25],\\\left(\begin{array}{c}0.736,0.5,\\0.493\end{array}\right),\\\left(\begin{array}{c}0.698,0.779,\\0.596\end{array}\right)\end{array}\right\} \end{array} \begin{array}{c} U_2 \\ \left\{\begin{array}{c}(0.17,0.1],\\(0.17,0.17],\\(0.143,0.17],\\\left(\begin{array}{c}0.314,0.5,\\0.554\end{array}\right),\\\left(\begin{array}{c}0.6324,0.413,\\0.471\end{array}\right)\end{array}\right\} \\ \left\{\begin{array}{c}(0.33,0.1],\\(0.5,0.33],\\(0.143,0.33],\\\left(\begin{array}{c}0.314,0.5,\\0.554\end{array}\right),\\\left(\begin{array}{c}0.539,0.578,\\0.707\end{array}\right)\end{array}\right\} \\ \left\{\begin{array}{c}(0.17,0.2],\\(0.17,0.17],\\(0.29,0.33],\\\left(\begin{array}{c}0.314,0.5,\\0.277\end{array}\right),\\\left(\begin{array}{c}0.431,0.247,\\0.236\end{array}\right)\end{array}\right\} \\ \left\{\begin{array}{c}(0.33,0.1],\\(0.17,0.33],\\(0.43,0.17],\\\left(\begin{array}{c}0.838,0.5,\\0.554\end{array}\right),\\\left(\begin{array}{c}0.647,0.661,\\0.471\end{array}\right)\end{array}\right\} \end{array} \begin{array}{c} U_3 \\ \left\{\begin{array}{c}(0.25,0.29],\\(0.2,0.25],\\(0.17,0.33],\\\left(\begin{array}{c}0.314,0.5,\\0.554\end{array}\right),\\\left(\begin{array}{c}0.6324,0.413,\\0.471\end{array}\right)\end{array}\right\} \\ \left\{\begin{array}{c}(0.25,0.29],\\(0.2,0.25],\\(0.33,0.17],\\\left(\begin{array}{c}0.461,0.5,\\0.492\end{array}\right),\\\left(\begin{array}{c}0.233,0.292,\\0.596\end{array}\right)\end{array}\right\} \\ \left\{\begin{array}{c}(0.25,0.29],\\(0.2,0.25],\\(0.33,0.33],\\\left(\begin{array}{c}0.838,0.5,\\0.554\end{array}\right),\\\left(\begin{array}{c}0.647,0.661,\\0.471\end{array}\right)\end{array}\right\} \\ \left\{\begin{array}{c}(0.25,0.143],\\(0.4,0.25],\\(0.17,0.17],\\\left(\begin{array}{c}0.461,0.5,\\0.492\end{array}\right),\\\left(\begin{array}{c}0.233,0.292,\\0.596\end{array}\right)\end{array}\right\} \end{array} \begin{array}{c} U_4 \\ \left\{\begin{array}{c}(0.20,0.33],\\(0.17,0.20],\\(0.17,0.29],\\\left(\begin{array}{c}0.314,0.5,\\0.554\end{array}\right),\\\left(\begin{array}{c}0.6324,0.413,\\0.471\end{array}\right)\end{array}\right\} \\ \left\{\begin{array}{c}(0.20,0.17],\\(0.33,0.4],\\(0.33,0.143],\\\left(\begin{array}{c}0.461,0.5,\\0.369\end{array}\right),\\\left(\begin{array}{c}0.349,0.389,\\0.298\end{array}\right)\end{array}\right\} \\ \left\{\begin{array}{c}(0.20,0.33],\\(0.33,0.20],\\(0.33,0.29],\\\left(\begin{array}{c}0.184,0.5,\\0.616\end{array}\right),\\\left(\begin{array}{c}0.581,0.389,\\0.447\end{array}\right)\end{array}\right\} \\ \left\{\begin{array}{c}(0.40,0.17],\\(0.17,0.20],\\(0.17,0.29],\\\left(\begin{array}{c}0.184,0.5,\\0.616\end{array}\right),\\\left(\begin{array}{c}0.581,0.389,\\0.447\end{array}\right)\end{array}\right\} \end{array} \tag{50}$$

Step 3. Create the weighted normalized decision matrix using the equation below

$$\ddot{\lambda}_{i_j} = w_j.\mathring{\lambda}_{i_j}, \tag{51}$$

$$\begin{array}{c} \\ \ddot{\lambda}_1 \\ \ddot{\lambda}_2 \\ \ddot{\lambda}_3 \\ \ddot{\lambda}_4 \end{array} \begin{array}{c} G_1 \\ \left\{\begin{array}{c}(0.075,0.087],\\(0.15,0.043],\\(0.06,0.075],\\\left(\begin{array}{c}0.138,0.15,\\0.148\end{array}\right),\\\left(\begin{array}{c}0.069,0.088,\\0.179\end{array}\right)\end{array}\right\} \\ \left\{\begin{array}{c}(0.075,0.043],\\(0.051,0.087],\\(0.06,0.114],\\\left(\begin{array}{c}0.138,0.15,\\0.1107\end{array}\right),\\\left(\begin{array}{c}0.105,0.117,\\0.089\end{array}\right)\end{array}\right\} \\ \left\{\begin{array}{c}(0.075,0.087],\\(0.051,0.087],\\(0.15,0.038],\\\left(\begin{array}{c}0.055,0.15,\\0.185\end{array}\right),\\\left(\begin{array}{c}0.174,0.117,\\0.134\end{array}\right)\end{array}\right\} \\ \left\{\begin{array}{c}(0.075,0.087],\\(0.051,0.087],\\(0.06,0.075],\\\left(\begin{array}{c}0.221,0.15,\\0.148\end{array}\right),\\\left(\begin{array}{c}0.209,0.234,\\0.179\end{array}\right)\end{array}\right\} \end{array} \begin{array}{c} G_2 \\ \left\{\begin{array}{c}(0.017,0.01],\\(0.017,0.017],\\(0.0143,0.017],\\\left(\begin{array}{c}0.0314,0.05,\\0.0554\end{array}\right),\\\left(\begin{array}{c}0.06324,0.0413,\\0.0471\end{array}\right)\end{array}\right\} \\ \left\{\begin{array}{c}(0.033,0.01],\\(0.05,0.033],\\(0.0143,0.033],\\\left(\begin{array}{c}0.0314,0.05,\\0.0554\end{array}\right),\\\left(\begin{array}{c}0.0539,0.0578,\\0.0707\end{array}\right)\end{array}\right\} \\ \left\{\begin{array}{c}(0.017,0.02],\\(0.017,0.017],\\(0.029,0.033],\\\left(\begin{array}{c}0.0314,0.05,\\0.0277\end{array}\right),\\\left(\begin{array}{c}0.0431,0.0247,\\0.0236\end{array}\right)\end{array}\right\} \\ \left\{\begin{array}{c}(0.033,0.01],\\(0.017,0.033],\\(0.043,0.017],\\\left(\begin{array}{c}0.0838,0.05,\\0.0554\end{array}\right),\\\left(\begin{array}{c}0.0647,0.0661,\\0.0471\end{array}\right)\end{array}\right\} \end{array} \begin{array}{c} G_3 \\ \left\{\begin{array}{c}(0.05,0.06],\\(0.04,0.05],\\(0.034,0.066],\\\left(\begin{array}{c}0.0628,0.1,\\0.1108\end{array}\right),\\\left(\begin{array}{c}0.1265,0.083,\\0.0942\end{array}\right)\end{array}\right\} \\ \left\{\begin{array}{c}(0.05,0.06],\\(0.04,0.05],\\(0.066,0.034],\\\left(\begin{array}{c}0.0922,0.1,\\0.0984\end{array}\right),\\\left(\begin{array}{c}0.0466,0.0584,\\0.1192\end{array}\right)\end{array}\right\} \\ \left\{\begin{array}{c}(0.05,0.06],\\(0.04,0.05],\\(0.066,0.066],\\\left(\begin{array}{c}0.168,0.1,\\0.1108\end{array}\right),\\\left(\begin{array}{c}0.129,0.1322,\\0.0942\end{array}\right)\end{array}\right\} \\ \left\{\begin{array}{c}(0.05,0.143],\\(0.08,0.05],\\(0.034,0.034],\\\left(\begin{array}{c}0.0922,0.1,\\0.0984\end{array}\right),\\\left(\begin{array}{c}0.0466,0.0584,\\0.1192\end{array}\right)\end{array}\right\} \end{array} \begin{array}{c} G_4 \\ \left\{\begin{array}{c}(0.08,0.132],\\(0.07,0.08],\\(0.07,0.12],\\\left(\begin{array}{c}0.1256,0.2,\\0.2216\end{array}\right),\\\left(\begin{array}{c}0.253,0.1652,\\0.1882\end{array}\right)\end{array}\right\} \\ \left\{\begin{array}{c}(0.08,0.07],\\(0.132,0.16],\\(0.132,0.06],\\\left(\begin{array}{c}0.1844,0.2,\\0.1476\end{array}\right),\\\left(\begin{array}{c}0.1396,0.1556,\\0.1192\end{array}\right)\end{array}\right\} \\ \left\{\begin{array}{c}(0.08,0.132],\\(0.132,0.08],\\(0.132,0.12],\\\left(\begin{array}{c}0.0736,0.2,\\0.246\end{array}\right),\\\left(\begin{array}{c}0.2324,0.156,\\0.179\end{array}\right)\end{array}\right\} \\ \left\{\begin{array}{c}(0.40,0.07],\\(0.07,0.08],\\(0.07,0.12],\\\left(\begin{array}{c}0.0736,0.2,\\0.2464\end{array}\right),\\\left(\begin{array}{c}0.2324,0.156,\\0.179\end{array}\right)\end{array}\right\} \end{array} \tag{52}$$

Step 4. Identify the ideal and negative ideal solutions. Ideal solution $\lambda^* = \{\lambda_1^*, \cdots, \lambda_n^*\}$, where

$$\lambda_j^* = \left\{\max\left(\lambda_{i_j}\right) \text{if } j \in J\,; \min\left(\lambda_{i_j}\right) \text{if} j \in J'\right\}. \tag{53}$$

Negative ideal solution

$$\lambda' = \left\{\lambda_1', \cdots, \lambda_n'\right\}, \tag{54}$$

where

$$\lambda_j' = \left\{\max\left(\lambda_{i_j}\right) \text{if} j \in J\,; \min\left(\lambda_{i_j}\right) \text{if} j \in J'\right\}, \tag{55}$$

$$\lambda^{*}\begin{Bmatrix}(0.075,0.087],\\(0.15,0.087],\\(0.15,0.114],\\\begin{pmatrix}0.221,0.15,\\0.185\end{pmatrix},\\\begin{pmatrix}0.209,0.234,\\0.179\end{pmatrix}\end{Bmatrix}\begin{Bmatrix}(0.033,0.02],\\(0.05,0.033],\\(0.029,0.033],\\\begin{pmatrix}0.0838,0.0578,\\0.0554\end{pmatrix},\\\begin{pmatrix}0.0647,0.0661,\\0.0707\end{pmatrix}\end{Bmatrix}\begin{Bmatrix}(0.05,0.143],\\(0.08,0.05],\\(0.066,0.066],\\\begin{pmatrix}0.168,0.1,\\0.1108\end{pmatrix},\\\begin{pmatrix}0.129,0.1322,\\0.1192\end{pmatrix}\end{Bmatrix}\begin{Bmatrix}(0.08,0.07],\\(0.07,0.07],\\(0.07,0.06],\\\begin{pmatrix}0.0736,0.2,\\0.1476\end{pmatrix},\\\begin{pmatrix}0.1396,0.156,\\0.1476\end{pmatrix}\end{Bmatrix},$$
$$\lambda'\begin{Bmatrix}(0.075,0.043],\\(0.051,0.043],\\(0.06,0.038],\\\begin{pmatrix}0.055,0.15,\\0.1107\end{pmatrix},\\\begin{pmatrix}0.069,0.088,\\0.089\end{pmatrix}\end{Bmatrix}\begin{Bmatrix}(0.017,0.01],\\(0.017,0.017],\\(0.0143,0.017],\\\begin{pmatrix}0.0314,0.033,\\0.0277\end{pmatrix},\\\begin{pmatrix}0.0431,0.0247,\\0.0236\end{pmatrix}\end{Bmatrix}\begin{Bmatrix}(0.06,0.05],\\(0.04,0.05],\\(0.034,0.034],\\\begin{pmatrix}0.0628,0.1,\\0.0984\end{pmatrix},\\\begin{pmatrix}0.0466,0.0584,\\0.0942\end{pmatrix}\end{Bmatrix}\begin{Bmatrix}(0.40,0.132],\\(0.132,0.16],\\(0.132,0.12],\\\begin{pmatrix}0.2324,0.2,\\0.246\end{pmatrix},\\\begin{pmatrix}0.253,0.1652,\\0.1882\end{pmatrix}\end{Bmatrix}. \tag{56}$$

Step 5. Calculate the separation measures for each alternatives, with the help of the following equations as

$$s_i^{*}=\sqrt{\left[\sum\left(\lambda_j^{*}-\lambda_{i_j}\right)^2\right]}\, i=1,\cdots,m. \tag{57}$$

Separation from negative ideal alternatives is also expressed as

$$s_i'=\sqrt{\left[\sum\left(\lambda_j'-\lambda_{i_j}\right)^2\right]}\, i=1,\cdots,m, \tag{58}$$

$$\ddot{s}_1^{*}=0.3476, \tag{59}$$

$$\ddot{s}_2^{*}=0.3531, \tag{60}$$

$$\ddot{s}_3^{*}=0.3369, \tag{61}$$

$$\ddot{s}_4^{*}=0.4106, \tag{62}$$

$$\ddot{s}_1'=0.4106, \tag{63}$$

$$\ddot{s}_2'=0.4066, \tag{64}$$

$$\ddot{s}_3'=0.4386, \tag{65}$$

$$\ddot{s}_4'=0.3830. \tag{66}$$

Step 6. Calculate the distance between relative closeness and ideal solution D_i^{*} where

$$D_i^{*}=\frac{s_i'}{\left(s_i^{*}+s_i'\right)}0\le D_i^{*}\le 1, \tag{67}$$

select the option with D_i^{*} closest to 1.

$$\ddot{\lambda}_1=0.4585,\ddot{\lambda}_2=0.4648,\ddot{\lambda}_3=0.4344,\ddot{\lambda}_4=0.5174, \tag{68}$$

$$\ddot{\lambda}_4>\ddot{\lambda}_2>\ddot{\lambda}_1>\ddot{\lambda}_3. \tag{69}$$

The ranking order of $\ddot{\lambda}_1,\ddot{\lambda}_2,\ddot{\lambda}_3$, and $\ddot{\lambda}_4$ is shown as in Figure 5.

5. Comparison

Topsis method is a common technique to handle decision making problems. In a neutrosophic set, a group decision-making procedure was presented by Abdel et al. and Biswas et al. [35, 36]. The several iterations of the neutrosophic set were also used in decision-making issues by Zulqarnain et al. and Dey et al. [37, 38]. All of these techniques are relevant to the ongoing effort. We now contrast the suggested method with two comparable ways to analyze the benefits and drawbacks of the current model in order to demonstrate the technological achievements in this research. The primary distinction between them is that whereas Biswas focused on the hybridization of the two ideas, namely, generalized neutrosophic sets, and soft sets. Abdel examined the truth, indeterminacy, and falsity membership values. As a result, the decision data in the current model is broader. Consequently, the strategy described in this paper is more circumspect.

6. Conclusion

We proposed a new notion known as neutrosophic octahedron set in this article by combining the concepts of neutrosophic set, intuitionistic fuzzy, and octahedron set. The major goal of this concept is to resolve uncertainty in real-world situations. We also look at some basic NOS operations including union, intersection, and complement, as well as their characteristics. Define some operational features as well. We also discussed the fact that the need for energy planning has increased with the development of new energy-related technologies and energy sources. The problem of decision-making is made even more difficult by the need for collaboration between various stakeholders in order to produce effective decisions. In order to quantitatively reflect the ambiguity and imprecision of the data, neutrosophic octahedron sets are a useful tool. Finally, using our proposed method and a numerical example, we presented a decision-making process.

In the future, this structure can be extended in interval neutrosophic octahedron set and can be applied in many real-life applications such as pattern recognition, medical diagnosis, and personal selection. Moreover, one can use this concept and develop a new decision-making technique with VIKOR, ELECTRE, CODAS, and AHP under a neutrosophic octahedron environment.

Data Availability

No data were used to support this study.

Conflicts of Interest

The authors declare that there were no conflicts of interest regarding the publication of this article.

Authors' Contributions

All authors contributed equally to the preparation of this manuscript.

References

[1] L. A. Zadeh, "Fuzzy sets," *Information and Control*, vol. 8, no. 3, pp. 338–353, 1965.

[2] L. A. Zadeh, "The concept of a linguistic variable and its application to approximate reasoning–I," *Information Sciences*, vol. 8, no. 3, pp. 199–249, 1975.

[3] K. Atanassov, "Intuitionistic fuzzy sets," *Fuzzy Sets and Systems*, vol. 20, no. 1, pp. 87–96, 1986.

[4] K. T. Atanassov and G. Gargov, "Interval valued intuitionistic fuzzy sets," *Fuzzy Sets and Systems*, vol. 31, no. 3, pp. 343–349, 1989.

[5] J. G. Lee, G. Senel, P. K. Lim, J. Kim, and K. Hur, "Octahedron sets," *Annals of Fuzzy Mathematics Inform*, vol. 19, no. 3, pp. 211–238, 2020.

[6] F. Smarandache, "Neutrosophic set, a generalization of the intuitionistic fuzzy set," *International Journal of Pure and Applied Mathematics*, vol. 24, no. 3, pp. 287–297, 2005.

[7] F. Smarandache, "Neutrosophic set," in *A Generalization of the Intuitionistic Fuzzy Set in Proceedings of 2006 IEEE International Conference on Granular Computing*, Y.-Q. Zhang and T. Y. Lin, Eds., pp. 38–42, Georgia State University, Atlanta, 2006.

[8] F. Smarandache, *Neutrosophy: neutrosophic probability, set, and logic*, American Research Press, 1998.

[9] F. G. Lupiáñez, "On neutrosophic sets and topology," *Procedia Computer Science*, vol. 120, pp. 975–982, 2017.

[10] H. Wang, F. Smarandache, Y.-Q. Zhang, and R. Sunderraman, *Interval neutrosophic sets and logic: theory and applications in computing: theory and applications in computing*, Hexis, Phoenix, 2005.

[11] M. Bhowmik and M. Pal, "Intuitionistic neutrosophic set," *Journal of Information and Computing Science*, vol. 4, no. 2, pp. 142–152, 2009.

[12] P. Kumar Maji, "Neutrosophic soft set," *Ann. Fuzzy Math. Informatics*, vol. 5, no. 1, pp. 157–168, 2013.

[13] M. Alkhazaleh and S. Uluçay, "Neutrosophic soft expert sets," *Neutrosophic Soft Expert Sets. Appl. Math.*, vol. 6, no. 1, pp. 116–127, 2015.

[14] S. Alias, D. Mohamad, and A. Shuib, "Rough neutrosophic multisets," *Neutrosophic Sets and Systems*, vol. 16, pp. 80–88, 2017.

[15] M. Ali and F. Smarandache, "Complex neutrosophic set," *Neural Comput. Appl.*, vol. 28, no. 7, pp. 1817–1834, 2017.

[16] Z. Xiao, S. Xia, K. Gong, and D. Li, "The trapezoidal fuzzy soft set and its application in MCDM," *Applied Mathematical Modelling*, vol. 36, no. 12, pp. 5844–5855, 2012.

[17] M. Deveci, "Site selection for hydrogen underground storage using interval type-2 hesitant fuzzy sets," *International Journal of Hydrogen Energy*, vol. 43, no. 19, pp. 9353–9368, 2018.

[18] X. Geng, X. Chu, and Z. Zhang, "A new integrated design concept evaluation approach based on vague sets," *Expert Systems with Applications*, vol. 37, no. 9, pp. 6629–6638, 2010.

[19] H. Shidpour, C. Da Cunha, and A. Bernard, "Group multicriteria design concept evaluation using combined rough set theory and fuzzy set theory," *Expert Systems with Applications*, vol. 64, pp. 633–644, 2016.

[20] A. Balin, P. Alcan, and H. Basligil, "Co performance comparison on CCHP systems using different fuzzy multi criteria decision making models for energy sources," *Fuelling the Future*, vol. 2022, pp. 591–595, 2012.

[21] I. B. Huang, J. Keisler, and I. Linkov, "Multi-criteria decision analysis in environmental sciences: ten years of applications and trends," *Science of the Total Environment*, vol. 409, no. 19, pp. 3578–3594, 2011.

[22] Z. Pavić and V. Novoselac, "Notes on TOPSIS method," *International Journal of Research in Engineering and Science*, vol. 1, no. 2, pp. 5–12, 2013.

[23] H. D. Arora and A. Naithani, "Significance of TOPSIS approach to MADM in computing exponential divergence measures for Pythagorean Fuzzy Sets," *Decision Making: Applications in Management and Engineering*, vol. 5, no. 1, pp. 146–163, 2022.

[24] I. Petrovic and M. Kankaras, "A hybridized IT2FS-DEMATEL-AHP-TOPSIS multicriteria decision making approach: case study of selection and evaluation of criteria for determination of air traffic control radar position," *Decision Making: Applications in Management and Engineering.*, vol. 3, no. 1, pp. 134–152, 2020.

[25] I. M. Hezam, A. R. Mishra, R. Krishankumar, K. S. Ravichandran, S. Kar, and D. S. Pamucar, "A single-valued neutrosophic decision framework for the assessment of sustainable transport investment projects based on discrimination measure," in *Management Decision*, Emerald Insight, 2022.

[26] N. Y. Pehlivan and N. Yalçın, "Neutrosophic TOPSIS method for sustainable supplier selection in a discount market chain," in *Handbook of Research on Advances and Applications of Fuzzy Sets and Logic*, pp. 692–715, IGI Global, 2022.

[27] S. Özlü and F. Karaaslan, "Hybrid similarity measures of single-valued neutrosophic type-2 fuzzy sets and their application to MCDM based on TOPSIS," *Soft Computing.*, vol. 26, no. 9, pp. 4059–4080, 2022.

[28] V. Simic, I. Gokasar, M. Deveci, and A. Karakurt, "An integrated CRITIC and MABAC based type-2 neutrosophic model for public transportation pricing system selection," *Socio-Economic Planning Sciences*, vol. 80, p. 101157, 2022.

[29] Y. B. Jun, C. S. Kim, and K. O. Yang, "Cubic sets," *Ann. Fuzzy Math. Inform.*, vol. 4, no. 1, pp. 83–98, 2012.

[30] Y. B. Jun, C. S. Kim, and M. S. Kang, "Cubic sub-algebras and ideals of BCK/BCI-algebras," *Far East Journal of Mathematical Sciences*, vol. 44, pp. 239–250, 2010.

[31] Y. B. Jun, F. Smarandache, and C. S. Kim, "Neutrosophic cubic sets," *New mathematics and natural computation*, vol. 13, no. 1, pp. 41–54, 2017.

[32] M. Gulistan and S. Khan, "Extentions of neutrosophic cubic sets via complex fuzzy sets with application," *Complex & Intelligent Systems*, vol. 6, no. 2, pp. 309–320, 2020.

[33] D. Bozanic, D. Tešić, D. Marinković, and A. Milić, "Modeling of neuro-fuzzy system as a support in decision-making processes," *Reports in Mechanical Engineering*, vol. 2, no. 1, pp. 222–234, 2021.

[34] D. Stanujkić and D. Karabašević, "An extension of the WASPAS method for decision-making problems with intuitionistic fuzzy numbers: a case of website evaluation," *Operational Research in Engineering Sciences: Theory and Applications*, vol. 1, no. 1, pp. 29–39, 2019.

[35] M. Abdel-Basset, G. Manogaran, A. Gamal, and F. Smarandache, "A group decision-making framework based on neutrosophic TOPSIS approach for smart medical device selection," *Journal of medical systems*, vol. 43, no. 2, p. 38, 2019.

[36] P. Biswas, S. Pramanik, and B. C. Giri, "Neutrosophic TOPSIS with group decision making," in *In fuzzy multi-criteria decision-making using neutrosophic sets*, pp. 543–585, Springer, Cham, 2019.

[37] R. M. Zulqarnain, X. L. Xin, M. Saeed, F. Smarandache, and N. Ahmad, *Generalized neutrosophic TOPSIS to solve multi-criteria decision-making problems*, Infinite Study, 2020.

[38] P. P. Dey, S. Pramanik, and B. C. Giri, "Generalized neutrosophic soft multi-attribute group decision making based on TOPSIS," *Critical Review*, vol. 11, pp. 41–55, 2015.

Hindawi
Advances in Mathematical Physics
Volume 2022, Article ID 1550332, 8 pages
https://doi.org/10.1155/2022/1550332

Research Article

On Some New Common Fixed Point Results for Finite Number of Mappings in Fuzzy Metric Spaces

Ayush Bartwal,[1] Junaid Ahmad,[2] R. C. Dimri,[3] Gopi Prasad,[3] and Ebenezer Bonyah[4]

[1]*Department of Mathematics, Himwant Kavi Chandra Kunwar Bartwal Govt. P.G. College, Nagnath Pokhari, Uttarakhand, India*
[2]*Department of Mathematics and Statistics, International Islamic University, H-10, Islamabad 44000, Pakistan*
[3]*Department of Mathematics, HNB Garhwal University, Uttarakhand, India*
[4]*Department of Mathematics Education, Akenten Appiah-Menka University of Skills Training and Entrepreneurial Development, Kumasi 00233, Ghana*

Correspondence should be addressed to Junaid Ahmad; ahmadjunaid436@gmail.com and Ebenezer Bonyah; ebbonya@gmail.com

Received 24 April 2022; Revised 27 June 2022; Accepted 29 July 2022; Published 17 August 2022

Academic Editor: Ranjan Kumar

We essentially suggest the concept of mutual sequences and Cauchy mutual sequence and utilize the same to prove the existence and uniqueness of common fixed point results for finite number of self- and non-self-mappings using fuzzy $\mathbb{Z}^*$-contractive mappings in fuzzy metric spaces. Our main result was obtained under generalized contractive condition in the fuzzy metric spaces. We provide examples to vindicate the claims and usefulness of such investigations. In this way, the present results generalize and enrich the several existing literature of the fuzzy metric spaces.

1. Introduction

In 1975, Kramosil and Michalek [1] introduced the notion of fuzzy metric spaces using the theory of fuzzy sets, which generalizes the metric spaces. Later on, many authors have introduced the notion of fuzzy metric spaces in different ways (see [2–5]). The widely accepted definition is given by George and Veeramani [6]. They presented slight modification on the definition of fuzzy metric spaces initiated by the respective authors by obtaining Hausdorff topology on the same setting. Utilizing the notion of the fuzzy metric, many authors proved various interesting common fixed point result for self- and non-self-mappings using different contraction in this setting. In 1984, Hadžić [7] proved some common fixed point theorems for family of mapping. After that, Bari and Vetro [8] also proved theorems for family of mappings in fuzzy metric spaces. In 1994, Subrahmanyam [9] generalized Jungck's theorem [10] in the setting of fuzzy metric spaces introduced by Kramosil and Michalek [1]. Vasuki [11] proved common fixed point theorems in the same setting. In 2002, Rhoades [12] proved common fixed point theorems for non-self-mappings using quasicontraction.

Jungck and Rhoades [13] introduced the concept of weak compatibility in metric spaces, which was further studied by Singh and Jain [14] in the fuzzy metric settings. Sedghi et al. [15] proved common fixed point theorems for four weakly compatible mappings. For the common fixed point using the notion of common limit range property, we refer common fixed point theorems by Chauhan et al. [16]. In this continuation, Imdad et al. [17] proved common fixed point theorems in fuzzy metric spaces using common property (E.A) and Prasad et al. [18] presented some coincidence point theorems via contractive mappings.

Recently, Roldan and Sintunavarat [19] introduced an important concept of fuzzy metric spaces on the product space $\mathcal{X}^{\mathcal{N}}$ which is induced by a simple fuzzy metric structure and compare the convergence, Cauchy, and completeness between these two structures. They also proved common fixed point results using CLRg property in the same metric setting. On the other hand, Shukla et al. [20] unify classes of different fuzzy contractive mappings

presented in [21–24] and introduced a new class of fuzzy $\mathcal{Z}$-contractive mapping and notions of properties S and S' to prove fixed point results in the fuzzy metric spaces.

In this paper, firstly we define the mutual sequences and Cauchy mutual sequences. The idea behind defining Cauchy mutual sequence is to collect those Cauchy sequences which are converging to the same limit. After that, we utilize this idea to find common fixed points. Indeed, Cauchy mutual sequences in a fuzzy metric space $(\mathcal{X}, \mathcal{M}, *)$ are the special type of Cauchy sequences in fuzzy metric space $(\mathcal{X}^{\mathcal{N}}, \mathcal{M}^{\mathcal{N}}, *)$ which converge to the same limit $\varrho \in \mathcal{X}$, if they are convergent. We also generalize the $\mathbb{Z}$-contraction for finite number of mappings; using these contractive mappings, we will prove some unique common fixed point theorems in fuzzy metric spaces. The main aim of this paper is to prove unique common fixed point theorems using $\mathbb{Z}^*$-contraction (which is the extension of $\mathbb{Z}$-contraction for finite number of mappings) in fuzzy metric spaces for self- and nonself-mappings with the help of mutual sequences. We also give examples for validity of our claims. In this way, our results generalize and improve several existing results.

2. Preliminaries

Throughout this paper, $\mathcal{N}, n, m$ are natural numbers, $i \in (1, 2, .., \mathcal{N})$; $\mathcal{X}^{\mathcal{N}}$ will denote Cartesian product of $\mathcal{N}$-copies of $\mathcal{X}$ and $\mathcal{X}$ is any nonempty set. In the sequel, sometimes $\mathcal{T}(\varrho)$ will be denoted by $\mathcal{T}\varrho$.

Definition 1 (see [6]). An ordered triple $(\mathcal{X}, \mathcal{M}, *)$ is called a fuzzy metric space if $\mathcal{X}$ is a (nonempty) set, $\mathcal{M}$ is a fuzzy set on $\mathcal{X}^2 \times (0,\infty)$, and $*$ is a continuous t-norm satisfying the following conditions, for all $\varrho, \rho, z \in \mathcal{X}$ and $t, s > 0$:

(1) $\mathcal{M}(\varrho, \rho, t) > 0$

(2) $\mathcal{M}(\varrho, \rho, t) = 1$, if and only if $\varrho = \rho$

(3) $\mathcal{M}(\varrho, \rho, t) = \mathcal{M}(\rho, \varrho, t)$

(4) $\mathcal{M}(\varrho, z, t + s) \geq \mathcal{M}(\varrho, \rho, t) * \mathcal{M}(\rho, z, s)$

(5) $\mathcal{M}(\varrho, \rho, .)$: $(0,\infty) \longrightarrow (0, 1]$ is continuous

Definition 2 (see [6]).

(i) Let $(\mathcal{X}, \mathcal{M}, *)$ be a fuzzy metric space. A sequence (ϱ_n) is said to be converge to ϱ in $\mathcal{X}$ if and only if $\lim_{n\longrightarrow\infty} \mathcal{M}(\varrho_n, \varrho, t) = 1$ for all $t > 0$, i.e., for each $r \in (0, 1)$ and $t > 0$, there exists $n_0 \in \mathbb{N}$ such that $\mathcal{M}(\varrho_n, \varrho, t) > 1 - r$ for all $n \geq n_0$

(ii) A sequence (ϱ_n) in a fuzzy metric space $(\mathcal{X}, \mathcal{M}, *)$ is a Cauchy sequence if and only if for each $\epsilon > 0$, $t > 0$ there exists $n_0 \in \mathcal{N}$ such that $\mathcal{M}(\varrho_n, \varrho_m, t) > 1 - \epsilon$ for all $n, m > n_0$. On the other hand, (ϱ_n) is called a Cauchy sequence if $\lim_{n\longrightarrow\infty} \mathcal{M}(\varrho_n, \varrho_{n+m}, t) = 1$ for all $m \in \mathbb{N}$ and $t > 0$

(iii) A fuzzy metric space $(\mathcal{X}, \mathcal{M}, *)$ is said to be complete if every Cauchy sequence in $\mathcal{X}$ is convergent to some $\varrho \in \mathcal{X}$

Lemma 3 (see [19]). *Let $(\mathcal{X}, \mathcal{M}, *)$ be a fuzzy metric space and $\mathcal{X}^{\mathcal{N}} = \underbrace{\mathcal{X} \times \mathcal{X} \times \cdots \times \mathcal{X}}_{\mathcal{N} \text{ times}}$, where $\mathcal{N} \in \mathbb{N}$ and define a fuzzy set $\mathcal{M}^{\mathcal{N}}$ on $\mathcal{X}^{\mathcal{N}} \times \mathcal{X}^{\mathcal{N}} \times [0,\infty) \longrightarrow [0, 1]$ such that*

$$\mathcal{M}^{\mathcal{N}}(\mathcal{P}, \mathcal{Q}, t) = *_{i=1}^{\mathcal{N}} \mathcal{M}(p_i, q_i, t), \quad \text{for all } \mathcal{P} = (p_1, p_2, \cdots, p_{\mathcal{N}}), \ \mathcal{Q} = (q_1, q_2, \cdots, q_{\mathcal{N}}) \in \mathcal{X}^{\mathcal{N}}, t > 0. \tag{1}$$

Then, the following hold:

(i) $(\mathcal{X}^{\mathcal{N}}, \mathcal{M}^{\mathcal{N}}, *)$ is also a fuzzy metric space

(ii) Let $(\mathcal{P}_n = (p_n^1, p_n^2, \cdots, p_n^{\mathcal{N}}))$ be a sequence on $\mathcal{X}^{\mathcal{N}}$ and $\mathcal{P} = (p^1, p^2, \cdots, p^{\mathcal{N}}) \in \mathcal{X}^{\mathcal{N}}$; then, sequence $(\mathcal{P}_n)$ converges to $\mathcal{P}$ on $(\mathcal{X}^{\mathcal{N}}, \mathcal{M}^{\mathcal{N}}, *)$ if and only if all sequences (p_n^i) converge to (p_i) on $(\mathcal{X}, \mathcal{M}, *)$, for all $i \in (1, 2, \cdots, \mathcal{N})$

(iii) Let $(\mathcal{P}_n = (p_n^1, p_n^2, \cdots, p_n^{\mathcal{N}}))$ be a sequence on $\mathcal{X}^{\mathcal{N}}$; then, $(\mathcal{P}_n)$ is Cauchy sequence on $(\mathcal{X}^{\mathcal{N}}, \mathcal{M}^{\mathcal{N}}, *)$ if and only if (p_n^i) is Cauchy sequence on $(\mathcal{X}, \mathcal{M}, *)$, for all $i \in (1, 2, \cdots, \mathcal{N})$

(iv) $(\mathcal{X}, \mathcal{M}, *)$ is complete if and only if $(\mathcal{X}^{\mathcal{N}}, \mathcal{M}^{\mathcal{N}}, *)$ is complete

Definition 4 (see [20]). Let $\mathcal{Z}$ denote the family of all functions $\zeta : (0, 1] \times (0, 1] \longrightarrow \mathbb{R}$ satisfying the following condition: $\zeta(t, s) > s$, for all $t, s \in (0, 1)$.

Definition 5 (see [20]). Let $\mathcal{T}$ be a self-mapping and $(\mathcal{X}, \mathcal{M}, *)$ a fuzzy metric space. If there exists $\zeta \in \mathcal{Z}$ such that

$$\mathcal{M}(\mathcal{T}\varrho, \mathcal{T}\rho, t) \geq \zeta(\mathcal{M}(\mathcal{T}\varrho, \mathcal{T}\rho, t), \mathcal{M}(\varrho, \rho, t)), \tag{2}$$

for all $\varrho, \rho \in \mathcal{X}$, $\mathcal{T}\varrho \neq \mathcal{T}\rho$, $t > 0$, then $\mathcal{T}$ is called a fuzzy $\mathcal{Z}$-contractive mapping with respect to the function $\zeta \in \mathcal{Z}$.

Definition 6 (see [20]). Let $\mathcal{T}$ be any self-mapping in $\mathcal{X}$, $\zeta \in \mathcal{Z}$ and $(\mathcal{X}, \mathcal{M}, *)$ a fuzzy metric space then quadruplet $(\mathcal{X}, \mathcal{M}, \mathcal{T}, \zeta)$ has the property (S'), if there exists $\varrho_n \in \mathcal{X}$ such that $\varrho_n = \mathcal{T}^n\varrho$, for all $n \in \mathbb{N}$ and $\inf_{m>n} \mathcal{M}(\varrho_n, \varrho_m, t) \leq \inf_{m>n} \mathcal{M}(\varrho_{n+1}, \varrho_{m+1}, t)$, for all $n \in \mathbb{N}$, $t > 0$ and $0 < \lim_{n\longrightarrow\infty} \inf_{m>n} \mathcal{M}(\varrho_n, \varrho_m, t) < 1$, for all $t > 0$ implies that

$$\lim_{n\longrightarrow\infty} \inf_{m>n} \zeta(\mathcal{M}(\varrho_{n+1}, \varrho_{m+1}, t), \mathcal{M}(\varrho_n, \varrho_m, t)) = 1, \quad \text{for all } t > 0. \tag{3}$$

3. Proposed Results

For brevity, we observe that Definitions 4 and 6 can be unified as follows.

Definition 7. Let $\mathbb{Z}^*$ denote the set of all functions $\zeta : (0,1] \times (0,1]$ to $\mathbb{R}$ satisfying the following conditions:

(i) $\zeta(p,q) > q$, for all~$p, q \in (0,1)$

(ii) Let (p_n) and (q_n) be two sequences in $(0,1]$ such that $p_n \le q_n$, for all $n \in \mathbb{N}$ and $\lim_{n\longrightarrow\infty} p_n \in (0,1]$ and then $\lim_{n\longrightarrow\infty} \inf_{m>n} \zeta(q_n, p_n) = 1$

Example 1. Define $\zeta : (0,1] \times (0,1] \longrightarrow \mathbb{R}$ such that $\zeta(p,q) = q/p$ and $q_n = (1/2) - (1/3n)$, $p_n = (1/2) + (1/3n)$, we observe that $\zeta \in \mathbb{Z}^*$ as $\lim_{n\longrightarrow\infty} ((1/2) - (1/3n))/((1/2) + (1/3n)) = 1$.

Definition 8. Let $(\mathcal{X}, \mathcal{M}, *)$ be a fuzzy metric space and $\mathcal{T}_1, \mathcal{T}_2, \cdots, \mathcal{T}_{\mathcal{N}}$ are $\mathcal{N}$-mapping on $\mathcal{X}$ satisfying following condition:

$$\begin{aligned}&\mathcal{M}^{\mathcal{N}}\left(\left(\mathcal{T}_1\varrho^1, \mathcal{T}_2\varrho^2, \cdots, \mathcal{T}_{\mathcal{N}}\varrho^{\mathcal{N}}\right), \left(\mathcal{T}_2\rho^2, \mathcal{T}_3\rho^3, \cdots, \mathcal{T}_{\mathcal{N}}\rho^{\mathcal{N}}, \mathcal{T}_1\rho^1\right), t\right)\\ &\quad \ge \zeta\left(\mathcal{M}^{\mathcal{N}}\left(\left(\mathcal{T}_1\varrho^1, \mathcal{T}_2\varrho^2, \cdots, \mathcal{T}_{\mathcal{N}}\varrho^{\mathcal{N}}\right), \left(\mathcal{T}_2\rho^2, \mathcal{T}_3\rho^3, \cdots, \mathcal{T}_{\mathcal{N}}\rho^{\mathcal{N}}, \mathcal{T}_1\rho^1\right), t\right), \mathcal{M}^{\mathcal{N}}\right.\\ &\qquad \left.\times\left(\left(\varrho^1, \varrho^2, \cdots, \varrho^{\mathcal{N}}\right), \left(\rho^2, \rho^3, \cdots, \rho^{\mathcal{N}}, \rho^1\right), t\right)\right),\end{aligned} \tag{4}$$

for all $t > 0$, $(\varrho^1, \varrho^2, \cdots, \varrho^{\mathcal{N}}) \ne (\rho^1, \rho^2, \cdots, \rho^{\mathcal{N}}) \in \mathcal{X}$, $(\mathcal{T}_1\varrho^1, \mathcal{T}_2\varrho^2, \cdots, \mathcal{T}_{\mathcal{N}}\varrho^{\mathcal{N}}) \ne (\mathcal{T}_1\rho^1, \mathcal{T}_2\rho^2, \cdots, \mathcal{T}_{\mathcal{N}}\rho^{\mathcal{N}})$, where $\mathcal{N} \in \mathbb{N}, \zeta \in \mathbb{Z}^*$ and $(\mathcal{X}^{\mathcal{N}}, \mathcal{M}^{\mathcal{N}}, *)$ is a fuzzy metric space induced by $(\mathcal{X}, \mathcal{M}, *)$. Then, $\mathcal{T}_1, \mathcal{T}_2, \cdots, \mathcal{T}_{\mathcal{N}}$ are said to be fuzzy $\mathbb{Z}^*$-contractive mappings.

Observe that for "$\mathcal{N} = 1$," Definition 5 is a particular case of Definition 8.

Definition 9. A sequence $(\varrho_n^1, \varrho_n^2, \cdots, \varrho_n^{\mathcal{N}}) \in \mathcal{X}^{\mathcal{N}} = \underbrace{\mathcal{X} \times \mathcal{X} \times \cdots \times \mathcal{X}}_{\mathcal{N} \text{ times}}$ is said to be a mutual sequence in a fuzzy metric space $(\mathcal{X}, \mathcal{M}, *)$.

Definition 10. Let $(\varrho_n^1, \varrho_n^2, \cdots, \varrho_n^{\mathcal{N}}) \in \mathcal{X}^{\mathcal{N}} = \underbrace{\mathcal{X} \times \mathcal{X} \times \cdots \times \mathcal{X}}_{\mathcal{N} \text{ times}}$ be a mutual sequence in a fuzzy metric space $(\mathcal{X}, \mathcal{M}, *)$ and all sequences (ϱ_n^i), $i \in (1, 2, \cdots \mathcal{N})$ converge, then the sequence $(\varrho_n^1, \varrho_n^2, \cdots, \varrho_n^{\mathcal{N}})$ is said to be convergent mutual sequence. If the sequence (ϱ_n^i), for all $i \in (1, 2, \cdots, \mathcal{N})$ converge to the unique limit $\varrho \in \mathcal{X}$, then the mutual sequence is said to be coconvergent mutual sequence and limit ϱ is said to be the mutual limit.

Definition 11. A mutual sequence $(\varrho_n^1, \varrho_n^2, \cdots, \varrho_n^{\mathcal{N}}) \in \mathcal{X}^N = \underbrace{\mathcal{X} \times \mathcal{X} \times \cdots \times \mathcal{X}}_{\mathcal{N} \text{ times}}$ is said to be a Cauchy mutual sequence in a fuzzy metric space $(\mathcal{X}, \mathcal{M}, *)$, if for each $\epsilon > 0$, there exists $n_0 \in \mathbb{N}$ such that for all $n, m \ge n_0 (n, m \in \mathbb{N})$, we have

$$\mathcal{M}^{\mathcal{N}}\left(\left(\varrho_n^1, \varrho_n^2, \cdots, \varrho_n^{\mathcal{N}}\right), \left(\varrho_m^2, \varrho_m^3, \cdots, \varrho_m^{\mathcal{N}}, \varrho_m^1\right), t\right) > 1 - \epsilon, \tag{5}$$

for all $t > 0$, i.e., a mutual sequence is said to be a Cauchy mutual sequence if as $n, m \longrightarrow \infty$,

$$\mathcal{M}^{\mathcal{N}}\left(\left(\varrho_n^1, \varrho_n^2, \cdots, \varrho_n^{\mathcal{N}}\right), \left(\varrho_m^2, \varrho_m^3, \cdots, \varrho_m^{\mathcal{N}}, \varrho_m^1\right), t\right) \longrightarrow 1, \tag{6}$$

for all $t > 0$, where $(\mathcal{X}^{\mathcal{N}}, \mathcal{M}^{\mathcal{N}}, *)$ is fuzzy metric spaces induced by $(\mathcal{X}, \mathcal{M}, *)$.

Now, we are considering the following lemmas to prove the existence and uniqueness of common fixed points.

Lemma 12. *Every Cauchy mutual sequence in $(\mathcal{X}, \mathcal{M}, *)$ is a Cauchy sequence in $(\mathcal{X}^{\mathcal{N}}, \mathcal{M}^{\mathcal{N}}, *)$.*

Proof. Let $\{(\varrho_n^1, \varrho_n^2, \cdots, \varrho_n^{\mathcal{N}})\}$ be a mutual sequence. By Definition 1 and Lemma 3, we have

$$\begin{aligned}&\mathcal{M}^{\mathcal{N}}\left(\left(\varrho_n^1, \varrho_n^2, \cdots, \varrho_n^{\mathcal{N}}\right), \left(\varrho_m^1, \varrho_m^2, \cdots, \varrho_m^{\mathcal{N}}\right), t\right)\\ &\quad \ge \mathcal{M}^{\mathcal{N}}\left(\left(\varrho_n^1, \varrho_n^2, \cdots, \varrho_n^{\mathcal{N}}\right), \left(\varrho_k^2, \varrho_k^3, \cdots, \varrho_k^{\mathcal{N}}, \varrho_k^1\right), \frac{t}{2}\right)\\ &\qquad * \mathcal{M}^{\mathcal{N}}\left(\left(\varrho_k^2, \varrho_k^3, \cdots, \varrho_k^{\mathcal{N}}, \varrho_k^1\right), \left(\varrho_m^1, \varrho_m^2, \cdots, \varrho_m^{\mathcal{N}}\right), \frac{t}{2}\right).\end{aligned} \tag{7}$$

Now, we have sequence $\{(\varrho_n^1, \varrho_n^2, \cdots, \varrho_n^{\mathcal{N}})\}$ a Cauchy mutual sequence. So, as $n, m, k \longrightarrow \infty$, we get

$$\mathcal{M}^{\mathcal{N}}\left(\left(\varrho_n^1, \varrho_n^2, \cdots, \varrho_n^{\mathcal{N}}\right), \left(\varrho_m^1, \varrho_m^2, \cdots, \varrho_m^{\mathcal{N}}\right), t\right) \longrightarrow 1. \tag{8}$$

Hence, $\{(\varrho_n^1, \varrho_n^2, \cdots, \varrho_n^{\mathcal{N}})\}$ is a Cauchy sequence in $(\mathcal{X}^{\mathcal{N}}, \mathcal{M}^{\mathcal{N}}, *)$.

The following example shows that the converse of Lemma 12 may not be true. □

Example 2. Let $\mathcal{X} = [1,\infty)$ define a fuzzy metric space $(\mathcal{X}, \mathcal{M}, *)$, where

$$\mathcal{M}(\varrho, \rho, t) = \begin{cases} 1, & \text{if } \varrho = \rho \\ \dfrac{2}{2 + \max\{\varrho, \rho\}}, & \text{otherwise} \end{cases} \quad \text{for all } \varrho, \rho \in \mathbb{R}^+,\ t > 0, \tag{9}$$

and $*$ be a continuous t-norm defined as $a * b = \min\{a, b\}$. Consider a mutual sequence $\{(1 - (1/n), 2 - (1/n), 3 - (1/n))\}$ on fuzzy metric space $(\mathcal{X}^{\mathcal{N}}, \mathcal{M}^{\mathcal{N}}, *)$, then mutual sequence is a Cauchy sequence in $(\mathcal{X}^{\mathcal{N}}, \mathcal{M}^{\mathcal{N}}, *)$ but not

Cauchy mutual sequence because as $n, m \longrightarrow \infty$, we have

$$\mathscr{M}^3\left(\left(1-\frac{1}{n}, 2-\frac{1}{n}, 3-\frac{1}{n}\right), \left(2-\frac{1}{m}, 3-\frac{1}{m}, 1-\frac{1}{m}\right), t\right) \longrightarrow \frac{2}{5}, \tag{10}$$

for all $t > 0$.

Lemma 13. *In a fuzzy metric space, every convergent Cauchy mutual sequence is coconvergent.*

Proof. Let $\{(\varrho_n^1, \varrho_n^2, \cdots, \varrho_n^{\mathscr{N}})\}$ be a convergent mutual sequence which converges to $(\varrho^1, \varrho^2, \cdots, \varrho^{\mathscr{N}})$, where $\varrho^i \in \mathscr{X}$, for $i \in (1, 2, \cdots, \mathscr{N})$. Since $\{(\varrho_n^1, \varrho_n^2, \cdots, \varrho_n^{\mathscr{N}})\}$ is a convergent Cauchy mutual sequence, as $n, m \longrightarrow \infty$, we have

$$\mathscr{M}^{\mathscr{N}}\left(\left(\varrho_n^1, \varrho_n^2, \cdots, \varrho_n^{\mathscr{N}}\right), \left(\varrho_m^2, \varrho_m^3, \cdots, \varrho_m^{\mathscr{N}}, \varrho_m^1\right), t\right) \longrightarrow 1, \tag{11}$$

for all $t > 0$, which implies that

$$\mathscr{M}^{\mathscr{N}}\left(\left(\varrho^1, \varrho^2, \cdots, \varrho^{\mathscr{N}}\right), \left(\varrho^2, \varrho^3, \cdots, \varrho^{\mathscr{N}}, \varrho^1\right), t\right) = 1, \tag{12}$$

for all $t > 0$. Hence, $\varrho^1 = \varrho^2 = \cdots = \varrho^{\mathscr{N}}$. □

Theorem 14. *Let $(\mathscr{X}, \mathscr{M}, *)$ be a complete fuzzy metric space; $\mathscr{T}_1, \mathscr{T}_2, \cdots, \mathscr{T}_{\mathscr{N}}$ are $\mathscr{N}$-self mappings on $\mathscr{X}$ satisfying*

(a) fuzzy $\mathbb{Z}^*$-contraction

(b) $\lim_{n\longrightarrow\infty} \inf_{m>n} \mathscr{M}^{\mathscr{N}}((\mathscr{T}_1^m(\varrho), \mathscr{T}_2^m(\varrho), \cdots, \mathscr{T}_{\mathscr{N}}^n(\varrho)), (\mathscr{T}_2^m(\varrho), \mathscr{T}_3^m(\varrho), \cdots, \mathscr{T}_{\mathscr{N}}^n(\varrho), \mathscr{T}_1^m(\varrho)), t) > 0$, *for all* $t > 0$, $\varrho \in \mathscr{X}$

Then, $\mathscr{T}_1, \mathscr{T}_2, \cdots, \mathscr{T}_{\mathscr{N}}$ have unique common fixed point.

Proof. Let $\varrho_0^i \in \mathscr{X}$ and $\mathscr{T}_i(\varrho_n^i) = \varrho_{n+1}^i$, for all $n \in \mathbb{N} \cup \{0\}$ and $i \in (1, 2, \cdots \mathscr{N})$. We get $(\varrho_n^1, \varrho_n^2, \cdots, \varrho_n^{\mathscr{N}})$ as a mutual sequence on $(\mathscr{X}, \mathscr{M}, *)$ and according to Lemma 3, $(\mathscr{X}^{\mathscr{N}}, \mathscr{M}^{\mathscr{N}}, *)$ is also a fuzzy metric space.

If $\varrho_n^i = \varrho_{n-1}^i$, for all $i \in (1, 2, \cdots, \mathscr{N})$ and for any $n \in \mathbb{N}$, then $\mathscr{T}_i(\varrho_n^i) = \varrho_{n-1}^i = \varrho_n^i$, i.e., ϱ_n^i is the fixed point of $\mathscr{T}_{i'}s$, for every i and a fixed n. Suppose that $\varrho_n^1 \neq \varrho_n^2 \neq \cdots \neq \varrho_n^{\mathscr{N}}$, for fixed n. From, Definitions 8 and 7

$$\begin{aligned}
&\mathscr{M}^{\mathscr{N}}\left(\left(\varrho_n^1, \varrho_n^2, \cdots, \varrho_n^{\mathscr{N}}\right), \left(\varrho_{n-1}^2, \varrho_{n-1}^3, \cdots, \varrho_{n-1}^{\mathscr{N}}, \varrho_{n-1}^1\right), t\right) \\
&= \mathscr{M}^{\mathscr{N}}\left(\left(\mathscr{T}_1\varrho_n^1, \mathscr{T}_2\varrho_n^2, \cdots, \mathscr{T}_{\mathscr{N}}\varrho_n^{\mathscr{N}}\right), \left(\mathscr{T}_2\varrho_{n-1}^2, \mathscr{T}_3\varrho_{n-1}^3, \cdots, \mathscr{T}_{\mathscr{N}}\varrho_{n-1}^{\mathscr{N}}, \mathscr{T}_1\varrho_{n-1}^1\right), t\right) \\
&\geq \zeta\left(\mathscr{M}^{\mathscr{N}}\left(\left(\mathscr{T}_1\varrho_n^1, \mathscr{T}_2\varrho_n^2, \cdots, \mathscr{T}_{\mathscr{N}}\varrho_n^{\mathscr{N}}\right), \left(\mathscr{T}_2\varrho_{n-1}^2, \mathscr{T}_3\varrho_{n-1}^3, \cdots, \mathscr{T}_{\mathscr{N}}\varrho_{n-1}^{\mathscr{N}}, \mathscr{T}_1\varrho_{n-1}^1\right), t\right), \mathscr{M}^{\mathscr{N}}\right. \\
&\quad \left.\times \left(\left(\varrho_n^1, \varrho_n^2, \cdots, \varrho_n^{\mathscr{N}}\right), \left(\varrho_{n-1}^2, \varrho_{n-1}^3, \cdots, \varrho_{n-1}^{\mathscr{N}}, \varrho_{n-1}^1\right), t\right)\right) \\
&> \mathscr{M}^{\mathscr{N}}\left(\left(\varrho_n^1, \varrho_n^2, \cdots, \varrho_n^{\mathscr{N}}\right), \left(\varrho_{n-1}^2, \varrho_{n-1}^3, \cdots, \varrho_{n-1}^{\mathscr{N}}, \varrho_{n-1}^1\right), t\right),
\end{aligned} \tag{13}$$

for all $t > 0$. So, $\varrho_n^1 = \varrho_n^2 = \cdots = \varrho_n^{\mathscr{N}} = \varrho$ (say) is a common fixed point of $\mathscr{T}_{i'}s$.

Now, assume that no consecutive terms of the sequence $(\varrho_n^1, \varrho_n^2, \cdots, \varrho_n^{\mathscr{N}})$ are the same and $(\varrho_n^1, \varrho_n^2, \cdots, \varrho_n^{\mathscr{N}}) = (\varrho_m^1, \varrho_m^2, \cdots, \varrho_m^{\mathscr{N}})$ for some $n < m$, i.e.,

$$\varrho_{n+1}^i = \mathscr{T}_i\varrho_n^i = \mathscr{T}_i\varrho_m^i = \varrho_{m+1}^i, \tag{14}$$

for some $n < m$ and for all i. From Definition 8 and 7, we have

$$\begin{aligned}
&\mathscr{M}^{\mathscr{N}}\left(\left(\varrho_{n+2}^1, \varrho_{n+2}^2, \cdots, \varrho_{n+2}^{\mathscr{N}}\right), \left(\varrho_{n+1}^2, \varrho_{n+1}^3, \cdots, \varrho_{n+1}^{\mathscr{N}}, \varrho_{n+1}^1\right), t\right) \\
&= \mathscr{M}^{\mathscr{N}}\left(\left(\mathscr{T}_1\varrho_{n+1}^1, \mathscr{T}_2\varrho_{n+1}^2, \cdots, \mathscr{T}_{\mathscr{N}}\varrho_{n+1}^{\mathscr{N}}\right),\right. \\
&\quad \left.\times \left(\mathscr{T}_2\varrho_n^2, \mathscr{T}_3\varrho_n^3, \cdots, \mathscr{T}_{\mathscr{N}}\varrho_n^{\mathscr{N}}, \mathscr{T}_1\varrho_n^1\right), t\right) \\
&\geq \zeta\left(\mathscr{M}^{\mathscr{N}}\left(\left(\mathscr{T}_1\varrho_{n+1}^1, \mathscr{T}_2\varrho_{n+1}^2, \cdots, \mathscr{T}_{\mathscr{N}}\varrho_{n+1}^{\mathscr{N}}\right),\right.\right. \\
&\quad \left.\times \left(\mathscr{T}_2\varrho_n^2, \mathscr{T}_3\varrho_n^3, \cdots, \mathscr{T}_{\mathscr{N}}\varrho_n^{\mathscr{N}}, \mathscr{T}_1\varrho_n^1\right), t\right), \mathscr{M}^{\mathscr{N}} \\
&\quad \left.\times \left(\left(\varrho_{n+1}^1, \varrho_{n+1}^2, \cdots, \varrho_{n+1}^{\mathscr{N}}\right), \left(\varrho_n^2, \varrho_n^3, \cdots, \varrho_n^{\mathscr{N}}, \varrho_n^1\right), t\right)\right) \\
&> \mathscr{M}^{\mathscr{N}}\left(\left(\varrho_{n+1}^1, \varrho_{n+1}^2, \cdots, \varrho_{n+1}^{\mathscr{N}}\right), \left(\varrho_n^2, \varrho_n^3, \cdots, \varrho_n^{\mathscr{N}}, \varrho_n^1\right), t\right),
\end{aligned} \tag{15}$$

for all $t > 0$. Similarly, we get

$$\begin{aligned}
&\mathscr{M}^{\mathscr{N}}\left(\left(\varrho_{n+1}^1, \varrho_{n+1}^2, \cdots, \varrho_{n+1}^{\mathscr{N}}\right), \left(\varrho_n^2, \varrho_n^3, \cdots, \varrho_n^{\mathscr{N}}, \varrho_n^1\right), t\right) \\
&< \mathscr{M}^{\mathscr{N}}\left(\left(\varrho_{n+2}^1, \varrho_{n+2}^2, \cdots, \varrho_{n+2}^{\mathscr{N}}\right), \left(\varrho_{n+1}^2, \varrho_{n+1}^3, \cdots, \varrho_{n+1}^{\mathscr{N}}, \varrho_{n+1}^1\right), t\right) \\
&< \cdots < \mathscr{M}^{\mathscr{N}}\left(\left(\varrho_{m+1}^1, \varrho_{m+1}^2, \cdots, \varrho_{m+1}^{\mathscr{N}}\right), \left(\varrho_m^2, \varrho_m^3, \cdots, \varrho_m^{\mathscr{N}}, \varrho_m^1\right), t\right),
\end{aligned} \tag{16}$$

for all $t > 0$, which is a contradiction in light of the inequality (14). Therefore, $(\varrho_n^1, \varrho_n^2, \cdots, \varrho_n^{\mathscr{N}}) \neq (\varrho_m^1, \varrho_m^2, \cdots, \varrho_m^{\mathscr{N}})$, for some $n < m$.

Now consider, $(\varrho_n^1, \varrho_n^2, \cdots, \varrho_n^{\mathscr{N}}) \neq (\varrho_m^1, \varrho_m^2, \cdots, \varrho_m^{\mathscr{N}})$, for all $n \neq m (\in \mathbb{N})$. Then, from Definitions 8 and 7, we have

$$\begin{aligned}
&\mathscr{M}^{\mathscr{N}}\left(\left(\varrho_{m+1}^1, \varrho_{m+1}^2, \cdots, \varrho_{m+1}^{\mathscr{N}}\right), \left(\varrho_{n+1}^2, \varrho_{n+1}^3, \cdots, \varrho_{n+1}^{\mathscr{N}}, \varrho_{n+1}^1\right), t\right) \\
&= \mathscr{M}^{\mathscr{N}}\left(\left(\mathscr{T}_1\varrho_m^1, \mathscr{T}_2\varrho_m^2, \cdots, \mathscr{T}_{\mathscr{N}}\varrho_m^{\mathscr{N}}\right),\right. \\
&\quad \left.\times \left(\mathscr{T}_2\varrho_n^2, \mathscr{T}_3\varrho_n^3, \cdots, \mathscr{T}_{\mathscr{N}}\varrho_n^{\mathscr{N}}, \mathscr{T}_1\varrho_n^1\right), t\right) \\
&\geq \zeta\left(\mathscr{M}^{\mathscr{N}}\left(\left(\mathscr{T}_1\varrho_m^1, \mathscr{T}_2\varrho_m^2, \cdots, \mathscr{T}_{\mathscr{N}}\varrho_m^{\mathscr{N}}\right),\right.\right. \\
&\quad \left.\times \left(\mathscr{T}_2\varrho_n^2, \mathscr{T}_3\varrho_n^3, \cdots, \mathscr{T}_{\mathscr{N}}\varrho_n^{\mathscr{N}}, \mathscr{T}_1\varrho_n^1\right), t\right) \mathscr{M}^{\mathscr{N}} \\
&\quad \left.\times \left(\left(\varrho_m^1, \varrho_m^2, \cdots, \varrho_m^{\mathscr{N}}\right), \left(\varrho_n^2, \varrho_n^3, \cdots, \varrho_n^{\mathscr{N}}, \varrho_n^1\right), t\right)\right) \\
&> \mathscr{M}^{\mathscr{N}}\left(\left(\varrho_m^1, \varrho_m^2, \cdots, \varrho_m^{\mathscr{N}}\right), \left(\varrho_n^2, \varrho_n^3, \cdots, \varrho_n^{\mathscr{N}}, \varrho_n^1\right), t\right),
\end{aligned} \tag{17}$$

for all $t > 0$ and $n < m$. Taking infimum (over $m > n$) in the

above inequality, we have

$$\inf_{m>n}\mathscr{M}^{\mathscr{N}}\left(\left(\varrho_m^1,\varrho_m^2,\cdots,\varrho_m^{\mathscr{N}}\right),\left(\varrho_n^2,\varrho_n^3,\cdots,\varrho_n^{\mathscr{N}},\varrho_n^1\right),t\right) \le \inf_{m>n}\mathscr{M}^{\mathscr{N}}\left(\left(\varrho_{m+1}^1,\varrho_{m+1}^2,\cdots,\varrho_{m+1}^{\mathscr{N}}\right),\left(\varrho_{n+1}^2,\varrho_{n+1}^3,\cdots,\varrho_{n+1}^{\mathscr{N}},\varrho_{n+1}^1\right),t\right), \tag{18}$$

for all $t>0$. Therefore, $(\inf_{m>n}\mathscr{M}^{\mathscr{N}}((\varrho_m^1,\varrho_m^2,\cdots,\varrho_m^{\mathscr{N}}),(\varrho_n^2,\varrho_n^3,\cdots,\varrho_n^{\mathscr{N}},\varrho_n^1),t))$ is a monotonic and bounded sequence, for all $t>0$. So, there exist some $s(t)\le 1$ such that

$$\lim_{n\longrightarrow\infty}\inf_{m>n}\mathscr{M}^{\mathscr{N}}\left(\left(\varrho_m^1,\varrho_m^2,\cdots,\varrho_m^{\mathscr{N}}\right),\left(\varrho_n^2,\varrho_n^3,\cdots,\varrho_n^{\mathscr{N}},\varrho_n^1\right),t\right)=s(t), \tag{19}$$

for all $t>0$.

Denote

$$p_n=\mathscr{M}^{\mathscr{N}}\left(\left(\varrho_m^1,\varrho_m^2,\cdots,\varrho_m^{\mathscr{N}}\right),\left(\varrho_n^2,\varrho_n^3,\cdots,\varrho_n^{\mathscr{N}},\varrho_n^1\right),t\right), \tag{20}$$

$$q_n=\mathscr{M}^{\mathscr{N}}\left(\left(\varrho_{m+1}^1,\varrho_{m+1}^2,\cdots,\varrho_{m+1}^{\mathscr{N}}\right),\left(\varrho_{n+1}^2,\varrho_{n+1}^3,\cdots,\varrho_{n+1}^{\mathscr{N}},\varrho_{n+1}^1\right),t\right), \tag{21}$$

for all $t>0$.

Now, our claim is $s(t)=1$, for every $t>0$. Letting on contrary that $s(t_1)<1$, for some $t_1>0$. In light of (3), we have $p_n\le q_n$ and by condition (b), $\lim_{n\longrightarrow\infty}p_n\in(0,1]$. Applying Definition 7, we get

$$\lim_{n\longrightarrow\infty}\inf_{m>n}\zeta\left(\mathscr{M}^{\mathscr{N}}\left(\left(\varrho_m^1,\varrho_m^2,\cdots,\varrho_m^{\mathscr{N}}\right),\left(\varrho_n^2,\varrho_n^3,\cdots,\varrho_n^{\mathscr{N}},\varrho_n^1\right),t_1\right),\mathscr{M}^{\mathscr{N}} \times\left(\left(\varrho_{m+1}^1,\varrho_{m+1}^2,\cdots,\varrho_{m+1}^{\mathscr{N}}\right),\left(\varrho_{n+1}^2,\varrho_{n+1}^3,\cdots,\varrho_{n+1}^{\mathscr{N}},\varrho_{n+1}^1\right),t_1\right)\right)=1. \tag{22}$$

From (2), we have

$$\begin{aligned}&\inf_{m>n}\mathscr{M}^{\mathscr{N}}\left(\left(\varrho_{m+1}^1,\varrho_{m+1}^2,\cdots,\varrho_{m+1}^{\mathscr{N}}\right),\left(\varrho_{n+1}^2,\varrho_{n+1}^3,\cdots,\varrho_{n+1}^{\mathscr{N}},\varrho_{n+1}^1\right),t_1\right)\\ &\ge\inf_{m>n}\zeta\left(\mathscr{M}^{\mathscr{N}}\left(\left(\mathscr{T}_1\varrho_m^1,\mathscr{T}_2\varrho_m^2,\cdots,\mathscr{T}_{\mathscr{N}}\varrho_m^{\mathscr{N}}\right),\right.\right.\\ &\quad\left.\times\left(\mathscr{T}_2\varrho_n^2,\mathscr{T}_3\varrho_n^3,\cdots,\mathscr{T}_{\mathscr{N}}\varrho_n^{\mathscr{N}},\mathscr{T}_1\varrho_n^1\right),t_1\right),\mathscr{M}^{\mathscr{N}}\\ &\quad\left.\times\left(\left(\varrho_m^1,\varrho_m^2,\cdots,\varrho_m^{\mathscr{N}}\right),\left(\varrho_n^2,\varrho_n^3,\cdots,\varrho_n^{\mathscr{N}},\varrho_n^1\right),t_1\right)\right)\\ &>\inf_{m>n}\mathscr{M}^{\mathscr{N}}\left(\left(\varrho_m^1,\varrho_m^2,\cdots,\varrho_m^{\mathscr{N}}\right),\left(\varrho_n^2,\varrho_n^3,\cdots,\varrho_n^{\mathscr{N}},\varrho_n^1\right),t_1\right).\end{aligned} \tag{23}$$

By (22) and as $n\longrightarrow\infty$, we get

$$\inf_{m>n}\mathscr{M}^{\mathscr{N}}\left(\left(\varrho_m^1,\varrho_m^2,\cdots,\varrho_m^{\mathscr{N}}\right),\left(\varrho_n^2,\varrho_n^3,\cdots,\varrho_n^{\mathscr{N}},\varrho_n^1\right),t_1\right)=s(t_1)=1, \tag{24}$$

which is a contradiction. We conclude that

$$\lim_{n\longrightarrow\infty}\lim_{n,m\longrightarrow\infty}\mathscr{M}^{\mathscr{N}}\left(\left(\varrho_m^1,\varrho_m^2,\cdots,\varrho_m^{\mathscr{N}}\right),\left(\varrho_n^2,\varrho_n^3,\cdots,\varrho_n^{\mathscr{N}},\varrho_n^1\right),t\right)=1, \tag{25}$$

for all $t>0$. Hence, the mutual sequence $(\varrho_n^1,\varrho_n^2,\cdots,\varrho_n^{\mathscr{N}})$ is a Cauchy mutual sequence. Completeness of $\mathscr{X}$ and Lemma 12 ensure that there exists $(\varrho^1,\varrho^2,\cdots,\varrho^{\mathscr{N}})\in\mathscr{X}$ such that

$$\lim_{n\longrightarrow\infty}\mathscr{M}^{\mathscr{N}}\left(\left(\varrho_n^1,\varrho_n^2,\cdots,\varrho_n^{\mathscr{N}}\right),\left(\left(\varrho^1,\varrho^2,\cdots,\varrho^{\mathscr{N}}\right),t\right)\right)=1, \tag{26}$$

for all $t>0$. From Lemma 13, sequence $(\varrho_n^1,\varrho_n^2,\cdots,\varrho_n^{\mathscr{N}})$ is coconvergent sequence, i.e., $\varrho^1=\varrho^2=\cdots=\varrho^{\mathscr{N}}=\varrho$ (say). Now, we have to prove that ϱ is a common fixed point of $\mathscr{T}_1,\mathscr{T}_2,\cdots,\mathscr{T}_{\mathscr{N}}$. Suppose that $\mathscr{T}_i\varrho\ne\varrho$, $i\in(1,2,\cdots,\mathscr{N})$. Without loss of generality, let us assume that $(\varrho_n^1,\varrho_n^2,\cdots,\varrho_n^{\mathscr{N}})\ne(\varrho,\varrho,\cdots,\varrho)$ and $(\varrho_n^1,\varrho_n^2,\cdots,\varrho_n^{\mathscr{N}})\ne(\mathscr{T}_2\varrho,\mathscr{T}_3\varrho,\cdots,\mathscr{T}_{\mathscr{N}}\varrho,\mathscr{T}_1\varrho)$, for all $n\in\mathscr{N}$. So, there exists $t_1>0$ such that $\mathscr{M}^{\mathscr{N}}((\varrho,\varrho,\cdots,\varrho),(\mathscr{T}_2\varrho,\mathscr{T}_3\varrho,\cdots,\mathscr{T}_{\mathscr{N}}\varrho,\mathscr{T}_1\varrho),t_1)<1$, $\mathscr{M}^{\mathscr{N}}((\varrho_n^1,\varrho_n^2,\cdots,\varrho_n^{\mathscr{N}}),(\varrho,\varrho,\cdots,\varrho),t_1)<1$ and

$$\begin{aligned}&\mathscr{M}^{\mathscr{N}}\left(\left(\mathscr{T}_1\varrho_n^1,\mathscr{T}_2\varrho_n^2,\cdots,\mathscr{T}_{\mathscr{N}}\varrho_n^{\mathscr{N}}\right),(\mathscr{T}_2\varrho,\mathscr{T}_3\varrho,\cdots,\mathscr{T}_{\mathscr{N}}\varrho,\mathscr{T}_1\varrho),t_1\right)\\ &=\mathscr{M}^{\mathscr{N}}\left(\left(\varrho_{n+1}^1,\varrho_{n+1}^2,\cdots,\varrho_{n+1}^{\mathscr{N}}\right),(\mathscr{T}_2\varrho,\mathscr{T}_3\varrho,\cdots,\mathscr{T}_{\mathscr{N}}\varrho,\mathscr{T}_1\varrho),t_1\right)<1,\end{aligned} \tag{27}$$

for all $n\in\mathbb{N}$. Then, we have

$$\begin{aligned}&\mathscr{M}^{\mathscr{N}}\left(\left(\varrho_n^1,\varrho_n^2,\cdots,\varrho_n^{\mathscr{N}}\right),(\varrho,\varrho,\cdots,\varrho),t_1\right)<\zeta\left(\mathscr{M}^{\mathscr{N}}\left(\left(\mathscr{T}_1\varrho_n^1,\mathscr{T}_2\varrho_n^2,\cdots,\mathscr{T}_{\mathscr{N}}\varrho_n^{\mathscr{N}}\right),\right.\right.\\ &\quad\left.\left.\times(\mathscr{T}_2\varrho,\mathscr{T}_3\varrho,\cdots,\mathscr{T}_{\mathscr{N}}\varrho,\mathscr{T}_1\varrho,t_1),\mathscr{M}^{\mathscr{N}}\left(\left(\varrho_n^1,\varrho_n^2,\cdots,\varrho_n^{\mathscr{N}}\right),(\varrho,\varrho,\cdots,\varrho),t_1\right)\right)\right.\\ &=\mathscr{M}^{\mathscr{N}}\left(\left(\mathscr{T}_1\varrho_n^1,\mathscr{T}_2\varrho_n^2,\cdots,\mathscr{T}_{\mathscr{N}}\varrho_n^{\mathscr{N}}\right),(\mathscr{T}_2\varrho,\mathscr{T}_3\varrho,\cdots,\mathscr{T}_{\mathscr{N}}\varrho,\mathscr{T}_1\varrho),t_1\right)\\ &=\mathscr{M}^{\mathscr{N}}\left(\left(\varrho_{n+1}^1,\varrho_{n+1}^2,\cdots,\varrho_{n+1}^{\mathscr{N}}\right),(\mathscr{T}_2\varrho,\mathscr{T}_3\varrho,\cdots,\mathscr{T}_{\mathscr{N}}\varrho,\mathscr{T}_1\varrho),t_1\right),\end{aligned} \tag{28}$$

as $n\longrightarrow\infty$; from (5) and Lemma 13, we get

$$\mathscr{M}^{\mathscr{N}}((\mathscr{T}_1\varrho,\mathscr{T}_2\varrho,\cdots\mathscr{T}_{\mathscr{N}}\varrho),(\varrho,\varrho,\cdots,\varrho),t_1)\ge 1, \tag{29}$$

which is a contradiction. Hence, $\mathscr{M}^{\mathscr{N}}((\mathscr{T}_1\varrho,\mathscr{T}_2\varrho,\cdots\mathscr{T}_{\mathscr{N}}\varrho),(\varrho,\varrho,\cdots,\varrho),t)=1$, for all $t>0$. Hence, ϱ is the common fixed point of $\mathscr{T}_{i'}s$, for all $i\in(1,2,\cdots\mathscr{N})$.

Now, we have to prove the uniqueness of the common fixed point of $\mathscr{T}_{i'}s$. Assume on contrary that $\varrho,\rho\in\mathscr{X}$ be two distinct common fixed points of $\mathscr{T}_{i'}s$, for all $i\in(1,2,\cdots,\mathscr{N})$ and there exists $t_1>0$ such that $\mathscr{M}^{\mathscr{N}}((\varrho,\varrho,\cdots,\varrho),(\rho,\rho,\cdots,\rho),t_1)<1$. Then, from Definitions 8 and 7, we get

$$\begin{aligned}&\mathscr{M}^{\mathscr{N}}((\varrho,\varrho,\cdots,\varrho),(\rho,\rho,\cdots,\rho),t_1)\\ &=\mathscr{M}^{\mathscr{N}}((\mathscr{T}_1\varrho,\mathscr{T}_2\varrho,\cdots,\mathscr{T}_{\mathscr{N}}\varrho),(\mathscr{T}_2\rho,\mathscr{T}_3\rho,\cdots,\mathscr{T}_{\mathscr{N}}\rho,\mathscr{T}_1\rho),t_1)\\ &=\zeta\left(\mathscr{M}^{\mathscr{N}}((\mathscr{T}_1\varrho,\mathscr{T}_2\varrho,\cdots,\mathscr{T}_{\mathscr{N}}\varrho),(\mathscr{T}_2\rho,\mathscr{T}_3\rho,\cdots,\mathscr{T}_{\mathscr{N}}\rho,\mathscr{T}_1\rho),t_1),\mathscr{M}^{\mathscr{N}}\right.\\ &\quad\left.\times((\varrho,\varrho,\cdots,\varrho),(\rho,\rho,\cdots,\rho),t_1))>\mathscr{M}^{\mathscr{N}}((\varrho,\varrho,\cdots,\varrho),(\rho,\rho,\cdots,\rho),t_1),\end{aligned} \tag{30}$$

implying thereby $\mathscr{M}^{\mathscr{N}}((\varrho,\varrho,\cdots,\varrho),(\rho,\rho,\cdots,\rho),t)=1$, for all $t>0$. Hence, $\varrho=\rho$. □

Remark 15. On putting $\mathscr{N}=1$, in Theorem 14, it reduces to Theorem 3.19 presented in [20].

Example 3. Let $\mathcal{X} = \{0, 1/5, 1/3, 1/2, 1, 2, 12, 17, 31, 45, 60, 71, 91, 100, 111\}$ and $(\mathcal{X}, \mathcal{M}, *)$ be a fuzzy metric space in which $\mathcal{M}$ is a fuzzy set defined on $\mathcal{X}^2 \times (0,\infty)$ such that $\mathcal{M} = t/(t + |\varrho - \rho|)$ for all $\varrho, \rho \in \mathcal{X}$ and $t > 0$, $*$ is a continuous t-norm defined as $\varrho * \rho = \varrho.\rho$, then $(\mathcal{X}, \mathcal{M}, *)$ is a complete metric space. Now, let us define 5-maps $\mathcal{T}_1, \mathcal{T}_2, \cdots \mathcal{T}_5 : \mathcal{X} \longrightarrow \mathcal{M}$ as

$$\begin{aligned}
\mathcal{T}_1(\varrho) &= \begin{cases} 1, & \text{if } \varrho \in \{12, 17, 31\}, \\ 0, & \text{otherwise,} \end{cases} \\
\mathcal{T}_2(\varrho) &= \begin{cases} \frac{1}{2}, & \text{if } \varrho \in \{45, 60, 71\}, \\ 0, & \text{otherwise,} \end{cases} \\
\mathcal{T}_3(\varrho) &= \begin{cases} 2, & \text{if } \varrho \in \{91, 100, 111\}, \\ 0, & \text{otherwise,} \end{cases} \\
\mathcal{T}_4(\varrho) &= \begin{cases} 0, & \varrho \in \left\{1, \frac{1}{2}, \frac{1}{3}, \frac{1}{5}, 0\right\}, \\ \frac{1}{3}, & \text{otherwise,} \end{cases} \\
\mathcal{T}_5(\varrho) &= \begin{cases} 0, & \text{if } \varrho \in \left\{\frac{1}{2}, \frac{1}{3}, \frac{1}{5}, 0\right\}, \\ \frac{1}{5}, & \text{otherwise,} \end{cases}
\end{aligned} \tag{31}$$

and a function $\zeta : (0, 1] \times (0, 1] \longrightarrow \mathbb{R}$ such that $\zeta(p, q) = q/p$ for all $p, q \in (0, 1]$.

Let $(\varrho_0^1, \varrho_0^2, \varrho_0^3, \varrho_0^4, \varrho_0^5) = (31, 60, 91, 1, 2)$ and $\mathcal{T}_i(\varrho_n^i) = \varrho_{n+1}^i$ for all $n \in \mathbb{N} \cup \{0\}$, we get $\{(31, 60, 91, 1, 2), (1, 1/2, 2, 0, 1/5), (0, 0, 0, 0, 0), \cdots\}$ as a mutual sequence. We can easily observe that conditions (a) and (b) of Theorem 14 are satisfied. Hence, 0 is the unique common fixed point of $\mathcal{T}_1, \mathcal{T}_2, \cdots \mathcal{T}_5$.

Now, we present the fixed point theorem for non-self-mappings.

Theorem 16. *Let $(\mathcal{X}, \mathcal{M}, *)$ be a fuzzy metric space, $\mathcal{Y}_1, \mathcal{Y}_2, \cdots, \mathcal{Y}_\mathcal{N}$ are $\mathcal{N}$ subset of $\mathcal{X}$. Let $\mathcal{T}_1 : \mathcal{Y}_1 \longrightarrow \mathcal{Y}_2, \mathcal{T}_2 : \mathcal{Y}_2 \longrightarrow \mathcal{Y}_3, \cdots, \mathcal{T}_{\mathcal{N}-1} : \mathcal{Y}_{\mathcal{N}-1} \longrightarrow \mathcal{Y}_\mathcal{N}$ and $\mathcal{T}_\mathcal{N} : \mathcal{Y}_\mathcal{N} \longrightarrow \mathcal{Y}_1$ are $\mathcal{N}$ mappings satisfying the following conditions:*

(i) $\mathcal{T}_i(\mathcal{Y}_i)$ *are complete subspace of* $\mathcal{X}$

(ii) $\mathcal{M}^\mathcal{N}((\mathcal{T}_1\varrho^1, \mathcal{T}_2\varrho^2, \cdots, \mathcal{T}_\mathcal{N}\varrho^\mathcal{N}), (\mathcal{T}_1\rho^1, \mathcal{T}_2\rho^2, \cdots, \mathcal{T}_\mathcal{N}\rho^\mathcal{N}), t) \geq \zeta(\mathcal{M}^\mathcal{N}((\mathcal{T}_1\varrho^1, \mathcal{T}_2\varrho^2, \cdots, \mathcal{T}_\mathcal{N}\varrho^\mathcal{N}), (\mathcal{T}_1\rho^1, \mathcal{T}_2\rho^2, \cdots, \mathcal{T}_\mathcal{N}\rho^\mathcal{N}), t), \mathcal{M}^\mathcal{N}((\varrho^1, \varrho^2, \cdots, \varrho^\mathcal{N}), (\rho^2, \rho^3, \cdots, \rho^\mathcal{N}, \rho^1), t))$ *for all* $t > 0$, $\varrho^i \neq \rho^i (\in \mathcal{Y}_i)$, $i \in (1, 2, \cdots \mathcal{N})$, $(\mathcal{T}_1\varrho^1, \mathcal{T}_2\varrho^2, \cdots, \mathcal{T}_\mathcal{N}\varrho^\mathcal{N}) \neq (\mathcal{T}_1\rho^1, \mathcal{T}_2\rho^2, \cdots, \mathcal{T}_\mathcal{N}\rho^\mathcal{N})$, *where* $\mathcal{N} \in \mathbb{N}, \zeta \in \mathbb{Z}^*$ *and* $(\mathcal{X}^\mathcal{N}, \mathcal{M}^\mathcal{N}, *)$ *is fuzzy metric spaces induced by* $(\mathcal{X}, \mathcal{M}, *)$

(iii) $\lim_{n\longrightarrow\infty} \inf_{m>n} \mathcal{M}^\mathcal{N}((\mathcal{T}_1^m(\varrho^1), \mathcal{T}_2^m(\varrho^2), \cdots, \mathcal{T}_\mathcal{N}^n(\varrho^\mathcal{N})), (\mathcal{T}_2^m(\varrho^2), \mathcal{T}_3^m(\varrho^3), \cdots, \mathcal{T}_\mathcal{N}^n(\varrho^\mathcal{N}), \mathcal{T}_1^m(\varrho^1)), t) > 0$ *for all* $t > 0$, $\varrho^i \in \mathcal{Y}_i$, $i \in (1, 2, \cdots, \mathcal{N})$

Then, $\mathcal{T}_1, \mathcal{T}_2, \cdots, \mathcal{T}_\mathcal{N}$ have unique common fixed point.

Proof. Let $\varrho_1^1 \in \mathcal{Y}_1$ and $\mathcal{T}_1(\varrho_n^1) = \varrho_n^2$, $\mathcal{T}_2(\varrho_n^2) = \varrho_n^3$,..., $\mathcal{T}_{\mathcal{N}-1}(\varrho_n^{\mathcal{N}-1}) = \varrho_n^\mathcal{N}$ and $\mathcal{T}_\mathcal{N}(\varrho_n^\mathcal{N}) = \varrho_{n+1}^1$, for all $n \in \mathbb{N}$. We get $(\varrho_m^1, \varrho_m^2, \cdots, \varrho_m^\mathcal{N}) \in \mathcal{X}^\mathcal{N}$ as a mutual on $(\mathcal{X}, \mathcal{M}, *)$.

If $\varrho_n^i = \varrho_{n+1}^i$, for all $1 \leq i \leq \mathcal{N} \in \mathbb{N}$ and for any $n \in \mathbb{N}$, then $\mathcal{T}_1(\varrho_n^1) = \varrho_n^2 = \varrho_{n+1}^2$, $\mathcal{T}_2(\varrho_n^2) = \varrho_n^3 = \varrho_{n+1}^3$, ..., $\mathcal{T}_{\mathcal{N}-1}(\varrho_n^{\mathcal{N}-1}) = \varrho_n^\mathcal{N} = \varrho_{n+1}^\mathcal{N}$ and $\mathcal{T}_\mathcal{N}(\varrho_n^\mathcal{N}) = \varrho_{n+1}^1 = \varrho_{n+1}^1$. Now, from Lemma 3, Definition 7, and condition (ii), we have

$$\begin{aligned}
&\mathcal{M}^\mathcal{N}\left(\left(\varrho_n^1, \varrho_n^2, \cdots, \varrho_n^\mathcal{N}\right), \left(\varrho_{n+1}^2, \varrho_{n+1}^3, \cdots, \varrho_{n+1}^\mathcal{N}, \varrho_{n+1}^1\right), t\right) \\
&= \mathcal{M}^\mathcal{N}\left(\left(\varrho_{n+1}^1, \varrho_n^2, \cdots, \varrho_n^\mathcal{N}\right), \left(\varrho_{n+1}^2, \varrho_{n+1}^3, \cdots, \varrho_{n+1}^\mathcal{N}, \varrho_{n+1}^1\right), t\right) \\
&= \mathcal{M}^\mathcal{N}\left(\left(\mathcal{T}_\mathcal{N}\varrho_n^\mathcal{N}, \mathcal{T}_1\varrho_n^1, \cdots, \mathcal{T}_{\mathcal{N}-1}\varrho_n^{\mathcal{N}-1}\right),\right. \\
&\quad \left.\times \left(\mathcal{T}_1\varrho_{n+1}^1, \mathcal{T}_2\varrho_{n+1}^2, \cdots, \mathcal{T}_{\mathcal{N}-1}\varrho_{n+1}^{\mathcal{N}-1}, \mathcal{T}_\mathcal{N}\varrho_n^\mathcal{N}\right), t\right) \\
&\geq \zeta\left(\mathcal{M}^\mathcal{N}\left(\left(\mathcal{T}_\mathcal{N}\varrho_n^\mathcal{N}, \mathcal{T}_1\varrho_n^1, \cdots, \mathcal{T}_{\mathcal{N}-1}\varrho_n^{\mathcal{N}-1}\right),\right.\right. \\
&\quad \times \left(\mathcal{T}_1\varrho_{n+1}^1, \mathcal{T}_2\varrho_{n+1}^2, \cdots, \mathcal{T}_{\mathcal{N}-1}\varrho_{n+1}^{\mathcal{N}-1}, \mathcal{T}_\mathcal{N}\varrho_n^\mathcal{N}\right), t\Big), \mathcal{M}^\mathcal{N} \\
&\quad \left.\left.\times \left(\left(\varrho_n^\mathcal{N}, \varrho_n^1, \cdots, \varrho_n^{\mathcal{N}-1}\right), \left(\varrho_{n+1}^1, \varrho_{n+1}^2, \cdots, \varrho_{n+1}^{\mathcal{N}-1}, \varrho_n^\mathcal{N}\right), t\right)\right) \right. \\
&> \mathcal{M}^\mathcal{N}\left(\left(\varrho_n^\mathcal{N}, \varrho_n^1, \cdots, \varrho_n^{\mathcal{N}-1}\right), \left(\varrho_{n+1}^1, \varrho_{n+1}^2, \cdots, \varrho_{n+1}^{\mathcal{N}-1}, \varrho_n^\mathcal{N}\right), t\right) \\
&= \mathcal{M}^\mathcal{N}\left(\left(\varrho_n^1, \varrho_n^2, \cdots, \varrho_n^\mathcal{N}\right), \left(\varrho_{n+1}^2, \varrho_{n+1}^3, \cdots, \varrho_{n+1}^\mathcal{N}, \varrho_{n+1}^1\right), t\right),
\end{aligned} \tag{32}$$

for all $t > 0$, a contradiction, which implies that $\mathcal{M}^\mathcal{N}((\varrho_n^1, \varrho_n^2, \cdots, \varrho_n^\mathcal{N}), (\varrho_{n+1}^2, \varrho_{n+1}^3, \cdots, \varrho_{n+1}^\mathcal{N}, \varrho_{n+1}^1), t) = 1$, i.e., $\varrho_n^1 = \varrho_n^2 = \cdots = \varrho_n^\mathcal{N} = \varrho$ (say) is a common fixed point of $\mathcal{T}_i$'s.

From Lemma 3, Definition 7, and condition (ii), for all $t > 0$, we have

$$\begin{aligned}
&\mathcal{M}^\mathcal{N}\left(\left(\varrho_{n+2}^1, \varrho_{n+2}^2, \cdots, \varrho_{n+2}^\mathcal{N}\right), \left(\varrho_{n+1}^2, \varrho_{n+1}^3, \cdots, \varrho_{n+1}^\mathcal{N}, \varrho_{n+1}^1\right), t\right) \\
&= \mathcal{M}^\mathcal{N}\left(\left(\mathcal{T}_\mathcal{N}\varrho_{n+1}^\mathcal{N}, \mathcal{T}_1\varrho_{n+2}^1, \cdots, \mathcal{T}_{\mathcal{N}-1}\varrho_{n+2}^{\mathcal{N}-1}\right),\right. \\
&\quad \left.\times \left(\mathcal{T}_1\varrho_{n+1}^1, \mathcal{T}_2\varrho_{n+1}^2, \cdots, \mathcal{T}_{\mathcal{N}-1}\varrho_{n+1}^{\mathcal{N}-1}, \mathcal{T}_\mathcal{N}\varrho_n^\mathcal{N}\right), t\right) \\
&\geq \zeta\left(\mathcal{M}^\mathcal{N}\left(\left(\mathcal{T}_\mathcal{N}\varrho_{n+1}^\mathcal{N}, \mathcal{T}_1\varrho_{n+2}^1, \cdots, \mathcal{T}_{\mathcal{N}-1}\varrho_{n+2}^{\mathcal{N}-1}\right),\right.\right. \\
&\quad \times \left(\mathcal{T}_1\varrho_{n+1}^1, \mathcal{T}_2\varrho_{n+1}^2, \cdots, \mathcal{T}_{\mathcal{N}-1}\varrho_{n+1}^{\mathcal{N}-1}, \mathcal{T}_\mathcal{N}\varrho_n^\mathcal{N}\right), t\Big), \mathcal{M}^\mathcal{N} \\
&\quad \left.\left.\times \left(\left(\varrho_{n+1}^\mathcal{N}, \varrho_{n+2}^1, \cdots, \varrho_{n+2}^{\mathcal{N}-1}\right), \left(\varrho_{n+1}^1, \varrho_{n+1}^2, \cdots, \varrho_{n+1}^{\mathcal{N}-1}, \varrho_n^\mathcal{N}\right), t\right)\right) \right. \\
&> \mathcal{M}^\mathcal{N}\left(\left(\varrho_{n+1}^\mathcal{N}, \varrho_{n+2}^1, \cdots, \varrho_{n+2}^{\mathcal{N}-1}\right), \left(\varrho_{n+1}^1, \varrho_{n+1}^2, \cdots, \varrho_{n+1}^{\mathcal{N}-1}, \varrho_n^\mathcal{N}\right)t\right) \\
&= \mathcal{M}^\mathcal{N}\left(\left(\mathcal{T}_{\mathcal{N}-1}\varrho_{n+1}^{\mathcal{N}-1}, \mathcal{T}_\mathcal{N}\varrho_{n+1}^\mathcal{N}, \cdots, \mathcal{T}_{\mathcal{N}-2}\varrho_{n+2}^{\mathcal{N}-2}\right),\right. \\
&\quad \left.\times \left(\mathcal{T}_\mathcal{N}\varrho_n^\mathcal{N}, \mathcal{T}_1\varrho_{n+1}^1, \cdots, \mathcal{T}_{\mathcal{N}-1}\varrho_n^{\mathcal{N}-1}\right), t\right) \\
&\geq \zeta\left(\mathcal{M}^\mathcal{N}\left(\left(\mathcal{T}_{\mathcal{N}-1}\varrho_{n+1}^{\mathcal{N}-1}, \mathcal{T}_\mathcal{N}\varrho_{n+1}^\mathcal{N}, \cdots, \mathcal{T}_{\mathcal{N}-2}\varrho_{n+2}^{\mathcal{N}-2}\right),\right.\right. \\
&\quad \times \left(\mathcal{T}_\mathcal{N}\varrho_n^\mathcal{N}, \mathcal{T}_1\varrho_{n+1}^1, \cdots, \mathcal{T}_{\mathcal{N}-1}\varrho_n^{\mathcal{N}-1}\right), t\Big), \mathcal{M}^\mathcal{N} \\
&\quad \left.\left.\times \left(\left(\varrho_{n+1}^{\mathcal{N}-1}, \varrho_{n+1}^\mathcal{N}, \cdots, \varrho_{n+2}^{\mathcal{N}-2}\right), \left(\varrho_n^\mathcal{N}, \varrho_{n+1}^1, \cdots, \varrho_{n+1}^{\mathcal{N}-2}, \varrho_n^{\mathcal{N}-1}\right), t\right)\right) \right. \\
&> \mathcal{M}^\mathcal{N}\left(\left(\varrho_{n+1}^{\mathcal{N}-1}, \varrho_{n+1}^\mathcal{N}, \cdots, \varrho_{n+2}^{\mathcal{N}-2}\right), \left(\varrho_n^\mathcal{N}, \varrho_{n+1}^1, \cdots, \varrho_{n+1}^{\mathcal{N}-2}, \varrho_n^{\mathcal{N}-1}\right), t\right) \\
&> \cdots > \mathcal{M}^\mathcal{N}\left(\left(\varrho_{n+1}^1, \varrho_{n+1}^2, \cdots, \varrho_{n+1}^\mathcal{N}\right), \left(\varrho_n^2, \varrho_n^3, \cdots, \varrho_n^\mathcal{N}, \varrho_n^1\right), t\right).
\end{aligned} \tag{33}$$

In the light of inequality (6), we observe that the behavior of mutual sequence in the proof of Theorem 14 and

mutual sequence as above is alike. The proof of sequence $(\varrho_m^1, \varrho_m^2, \cdots, \varrho_m^{\mathcal{N}})$ to be a Cauchy mutual sequence is immediate from Theorem 14.

From (i) and Lemma 12, there exist $\varrho^i \in \mathcal{T}_i(\mathcal{Y}_i)$ such that $(\varrho_m^1, \varrho_m^2, \cdots, \varrho_m^{\mathcal{N}})$ converges to $(\varrho^1, \varrho^2, \cdots, \varrho^{\mathcal{N}})$, and from Lemma 13, sequence $(\varrho_m^1, \varrho_m^2, \cdots, \varrho_m^{\mathcal{N}})$ is coconvergent to some point $\varrho \in \mathcal{X}$.

Now, we have to prove that ϱ is a common fixed point of $\mathcal{T}_i$'s. Without loss of generality, let us assume that $(\varrho_n^1, \varrho_n^2, \cdots, \varrho_n^{\mathcal{N}}) \neq (\varrho, \varrho, \cdots, \varrho)$ and

$$\left(\varrho_n^1, \varrho_n^2, \cdots, \varrho_n^{\mathcal{N}}\right) \neq (\mathcal{T}_2\varrho, \mathcal{T}_3\varrho, \cdots, \mathcal{T}_{\mathcal{N}}\varrho, \mathcal{T}_1\varrho), \quad \text{for all } n \in \mathcal{N}. \tag{34}$$

So, there exists $t_1 > 0$ such that $\mathcal{M}^{\mathcal{N}}((\varrho, \varrho, \cdots, \varrho), (\mathcal{T}_2\varrho, \mathcal{T}_3\varrho, \cdots, \mathcal{T}_{\mathcal{N}}\varrho, \mathcal{T}_1\varrho), t_1) < 1$,

$$\mathcal{M}^{\mathcal{N}}\left(\left(\varrho_n^1, \varrho_n^2, \cdots, \varrho_n^{\mathcal{N}}\right), (\varrho, \varrho, \cdots, \varrho), t_1\right) < 1, \tag{35}$$

$$\begin{aligned}&\mathcal{M}^{\mathcal{N}}\left((\mathcal{T}_1\varrho, \mathcal{T}_2\varrho, \cdots, \mathcal{T}_{\mathcal{N}}\varrho), \left(\mathcal{T}_2\varrho_{n+1}^2, \mathcal{T}_3\varrho_{n+1}^3, \cdots, \mathcal{T}_{\mathcal{N}}\varrho_{n+1}^{\mathcal{N}}, \mathcal{T}_1\varrho_n^1\right), t_1\right)\\ &\quad = \mathcal{M}^{\mathcal{N}}\left((\mathcal{T}_1\varrho, \mathcal{T}_2\varrho, \cdots, \mathcal{T}_{\mathcal{N}}\varrho), \left(\varrho_{n+1}^1, \varrho_{n+1}^2, \cdots, \varrho_{n+1}^{\mathcal{N}}\right), t_1\right) < 1,\end{aligned} \tag{36}$$

for all $n \in \mathbb{N}$. Then, we have

$$\begin{aligned}&\mathcal{M}^{\mathcal{N}}\left((\varrho, \varrho, \cdots, \varrho), \left(\varrho_{n+1}^2, \cdots, \varrho_{n+1}^{\mathcal{N}}, \varrho_n^1\right), t_1\right)\\ &< \zeta\left(\mathcal{M}^{\mathcal{N}}\left((\mathcal{T}_1\varrho, \mathcal{T}_2\varrho, \cdots, \mathcal{T}_{\mathcal{N}}\varrho), \left(\mathcal{T}_2\varrho_{n+1}^2, \mathcal{T}_3\varrho_{n+1}^3, \cdots, \mathcal{T}_{\mathcal{N}}\varrho_{n+1}^{\mathcal{N}}, \mathcal{T}_1\varrho_n^1\right), t_1\right), \mathcal{M}^{\mathcal{N}}\right.\\ &\quad \left.\times\left((\varrho, \varrho, \cdots, \varrho), \left(\varrho_{n+1}^2, \varrho_{n+1}^3, \cdots, \varrho_{n+1}^{\mathcal{N}}, \varrho_n^1\right), t_1\right)\right)\\ &= \mathcal{M}^{\mathcal{N}}\left((\mathcal{T}_1\varrho, \mathcal{T}_2\varrho, \cdots, \mathcal{T}_{\mathcal{N}}\varrho), \left(\mathcal{T}_2\varrho_{n+1}^2, \mathcal{T}_3\varrho_{n+1}^3, \cdots, \mathcal{T}_{\mathcal{N}}\varrho_{n+1}^{\mathcal{N}}, \mathcal{T}_1\varrho_n^1\right), t_1\right)\\ &= \mathcal{M}^{\mathcal{N}}\left((\mathcal{T}_1\varrho, \mathcal{T}_2\varrho, \cdots, \mathcal{T}_{\mathcal{N}}\varrho), \left(\varrho_{n+1}^1, \varrho_{n+1}^2, \cdots, \varrho_{n+1}^{\mathcal{N}}\right), t_1\right),\end{aligned} \tag{37}$$

as $n \longrightarrow \infty$, and from (5), we get $\mathcal{M}^{\mathcal{N}}((\mathcal{T}_1\varrho, \mathcal{T}_2\varrho, \cdots \mathcal{T}_{\mathcal{N}}\varrho), (\varrho, \varrho, \cdots, \varrho), t_1) \geq 1$, a contradiction. Hence, $\mathcal{M}^{\mathcal{N}}((\mathcal{T}_1\varrho, \mathcal{T}_2\varrho, \cdots \mathcal{T}_{\mathcal{N}}\varrho), (\varrho, \varrho, \cdots, \varrho), t) = 1$, for all $t > 0$. Therefore, ϱ is the common fixed point of $\mathcal{T}_i$'s, for all $i \in (1, 2, \cdots \mathcal{N})$.

The proof of uniqueness of common fixed point runs similar to the proof of Theorem 14. Hence, we are through. □

Example 4. Let $\mathcal{X} = (0, 1]$ and $(\mathcal{X}, \mathcal{M}, *)$ be a fuzzy metric space where

$$\mathcal{M}(\varrho, \rho, t) = \begin{cases} 1, & \text{if } \varrho = \rho \\ \min\{\varrho, \rho\}, & \text{otherwise} \end{cases} \quad \text{for all } \varrho, \rho \in \mathcal{X},\ t > 0, \tag{38}$$

$*$ is continuous t-norm defined as $a * b = \min\{a, b\}$. Let

$$\begin{aligned}\mathcal{Y}_1 &= \left\{\frac{1}{1000}, \frac{1}{600}, \frac{1}{200}, \frac{1}{70}, 1\right\},\\ \mathcal{Y}_2 &= \left\{\frac{1}{900}, \frac{1}{500}, \frac{1}{100}, \frac{1}{50}, 1\right\},\\ \mathcal{Y}_3 &= \left\{\frac{1}{800}, \frac{1}{400}, \frac{1}{90}, \frac{1}{30}, 1\right\},\\ \mathcal{Y}_4 &= \left\{\frac{1}{700}, \frac{1}{300}, \frac{1}{80}, \frac{1}{20}, 1\right\},\end{aligned} \tag{39}$$

be subset of $\mathcal{X}$; we define $\mathcal{T}_1 : \mathcal{Y}_1 \longrightarrow \mathcal{Y}_2, \mathcal{T}_2 : \mathcal{Y}_2 \longrightarrow \mathcal{Y}_3, \mathcal{T}_3 : \mathcal{Y}_3 \longrightarrow \mathcal{Y}_4$ and $\mathcal{T}_4 : \mathcal{Y}_4 \longrightarrow \mathcal{Y}_1$ such that

$$\begin{aligned}&\mathcal{T}_1(1) = \mathcal{T}_2(1) = \mathcal{T}_3(1) = \mathcal{T}_4(1) = 1,\\ &\mathcal{T}_1\left(\frac{1}{1000}\right) = \frac{1}{900}, \mathcal{T}_1\left(\frac{1}{600}\right) = \frac{1}{500}, \mathcal{T}_1\left(\frac{1}{200}\right) = \frac{1}{100}, \mathcal{T}_1\left(\frac{1}{70}\right) = \frac{1}{50},\\ &\mathcal{T}_2\left(\frac{1}{900}\right) = \frac{1}{800}, \mathcal{T}_2\left(\frac{1}{500}\right) = \frac{1}{400}, \mathcal{T}_2\left(\frac{1}{100}\right) = \frac{1}{90}, \mathcal{T}_2\left(\frac{1}{50}\right) = \frac{1}{30},\\ &\mathcal{T}_3\left(\frac{1}{800}\right) = \frac{1}{700}, \mathcal{T}_3\left(\frac{1}{400}\right) = \frac{1}{300}, \mathcal{T}_3\left(\frac{1}{90}\right) = \frac{1}{80}, \mathcal{T}_3\left(\frac{1}{30}\right) = \frac{1}{20},\\ &\mathcal{T}_4\left(\frac{1}{700}\right) = \frac{1}{600}, \mathcal{T}_4\left(\frac{1}{300}\right) = \frac{1}{200}, \mathcal{T}_4\left(\frac{1}{80}\right) = \frac{1}{70}, \mathcal{T}_4\left(\frac{1}{20}\right) = 1.\end{aligned} \tag{40}$$

Now, define function ζ similar to Example 3. We can easily verify that all conditions of Theorem 16 are satisfied. If $\varrho_1^1 = 1/1000$ and $\mathcal{T}_1(\varrho_n^1) = \varrho_n^2$, $\mathcal{T}_2(\varrho_n^2) = \varrho_n^3$,..., $\mathcal{T}_{\mathcal{N}-1}(\varrho_n^{\mathcal{N}-1}) = \varrho_n^{\mathcal{N}}$ and $\mathcal{T}_{\mathcal{N}}(\varrho_n^{\mathcal{N}}) = \varrho_{n+1}^1$ for all $n \in \mathcal{N}$. We get $\{(1/1000, 1/900, 1/800, 1/700), (1/600, 1/500, 1/400, 1/300), \cdots\}$ as mutual sequence, 1 as unique common fixed point of $\mathcal{T}_1$, $\mathcal{T}_2$, $\mathcal{T}_3$, and $\mathcal{T}_4$.

4. Conclusion

In this paper, the concept of mutual sequences in $(\mathcal{X}, \mathcal{M}, *)$ is given, and with the help of induced fuzzy metric structure $(\mathcal{X}^{\mathcal{N}}, \mathcal{M}^{\mathcal{N}}, *)$, we define Cauchy mutual sequences in simple fuzzy metric structure $(\mathcal{X}, \mathcal{M}, *)$. For brevity, Definitions 2.6 and 2.4 (presented in [20]) are unified as Definition 7. We also present $\mathbb{Z}^*$ contraction, which is an extension of $\mathbb{Z}$-contraction for finite number of mappings. With the help of mutual sequences, we proved unique common fixed point theorems for finite numbers of mappings using $\mathbb{Z}^*$ contraction. We also provide many examples to show that our results are meaningful and to support our theorems. The given results generalize and extend several results in the existing literature. As perspectives, it would be interesting that the results presented in this paper proved for other contractive conditions and extend to other nonclassical metric structure, like bipolar fuzzy metric spaces [5] and relational fuzzy metric spaces [25].

Data Availability

No data were used to support this study.

Conflicts of Interest

All the authors declare that they have no conflict of interest.

Authors' Contributions

Each author contributed equally and significantly to every part of this article. All authors read and approved the final version of the paper.

References

[1] I. Kramosil and J. Michalek, "Fuzzy metric and statistical metric spaces," *Kybernetika*, vol. 11, no. 5, pp. 336–344, 1975.

[2] D. Zi-ke, "Fuzzy pseudo-metric spaces," *Journal of Mathematical Analysis and Applications*, vol. 86, no. 1, pp. 74–95, 1982.

[3] M. A. Erceg, "Metric spaces in fuzzy set theory," *Journal of Mathematical Analysis and Applications*, vol. 69, no. 1, pp. 205–230, 1979.

[4] O. Kaleva and S. Seikkala, "On fuzzy metric spaces," *Fuzzy Sets and Systems*, vol. 12, no. 3, pp. 215–229, 1984.

[5] A. Bartwal, R. C. Dimri, and G. Prasad, "Some fixed point theorems in fuzzy bipolar metric spaces," *Journal of Nonlinear Science Applied*, vol. 13, no. 4, pp. 196–204, 2020.

[6] A. George and P. Veeramani, "On some results in fuzzy metric spaces," *Fuzzy Sets and Systems*, vol. 64, no. 3, pp. 395–399, 1994.

[7] O. Hadzic, "Common fixed point theorems for families of mapping in complete metric space," *Math Japon*, vol. 9, pp. 127–134, 1984.

[8] C. Di Bari and C. Vetro, "A fixed point theorem for a family of mappings in a fuzzy metric space," *Rendiconti del Circolo Matematico di Palermo*, vol. 52, no. 2, pp. 315–321, 2003.

[9] P. V. Subrahmanyam, "A common fixed point theorem in fuzzy metric spaces," *Information Sciences*, vol. 83, no. 3-4, pp. 109–112, 1995.

[10] G. Jungck, "Commuting mappings and fixed points," *The American Mathematical Monthly*, vol. 83, no. 4, pp. 261–263, 1976.

[11] R. Vasuki, "A common fixed point theorem in a fuzzy metric space," *Fuzzy Sets and Systems*, vol. 97, no. 3, pp. 395–397, 1998.

[12] B. E. Rhoades, "Common fixed point theorems for nonself quasi-contraction mappings," *Varohmihir Journal of Mathematical Sciences*, vol. 2, no. 1, pp. 11–14, 2002.

[13] G. Jungck and B. E. Rhoades, "Fixed point for set valued functions without continuity," *Indian Journal of Pure and Applied Mathematics*, vol. 29, no. 3, pp. 227–238, 1998.

[14] B. Singh and S. Jain, "Weak compatibility and fixed point theorems in fuzzy metric spaces," *Ganita*, vol. 56, no. 2, pp. 167–176, 2005.

[15] S. Sedghi, B. S. Choudhury, and N. Shobe, "Unique common fixed point theorem for four weakly compatible mappings in complete fuzzy metric spaces," *Journal of Fuzzy Mathematics*, vol. 18, pp. 161–170, 2010.

[16] S. Chauhan, M. A. Khan, and W. Sintunavarat, "Common fixed point theorems in fuzzy metric spaces satisfying ϕ-contractive condition with common limit range property," *Abstract and Applied Analysis*, vol. 2013, Article ID 735217, 14 pages, 2013.

[17] M. Imdad, J. Ali, and M. Hasan, "Common fixed point theorems in fuzzy metric spaces employing common property (E.A.)," *Mathematical and Computer Modelling*, vol. 55, no. 3-4, pp. 770–778, 2012.

[18] G. Prasad, A. Tomar, R. C. Dimri, and A. Bartwal, "Coincidence theorems via contractive mappings in ordered non-Archimedean fuzzy metric spaces," *Pure and Applied Mathematics*, vol. 27, no. 7-8, pp. 1475–1490, 2020.

[19] A. Roldan and W. Sintunavarat, "Common fixed point theorems in fuzzy metric spaces using the CLRg property," *Fuzzy Sets and Systems*, vol. 282, pp. 131–142, 2016.

[20] S. Shukla, D. Gopal, and W. Sintunavarat, "A new class of fuzzy contractive mappings and fixed point theorems," *Fuzzy Sets and Systems*, vol. 350, pp. 85–94, 2018.

[21] V. Gregori and A. Sapena, "On fixed-point theorems in fuzzy metric spaces," *Fuzzy Sets and Systems*, vol. 125, no. 2, pp. 245–252, 2002.

[22] P. Tirado, "Contraction mappings in fuzzy quasi-metric spaces and [0, 1]-fuzzy posets," *Fixed Point Theory*, vol. 13, no. 1, pp. 273–283, 2012.

[23] D. Mihet, "Fuzzy Ψ-contractive mappings in non-Archimedean fuzzy metric spaces," *Fuzzy Sets and Systems*, vol. 159, no. 6, pp. 739–744, 2008.

[24] D. Wardowski, "Fuzzy contractive mappings and fixed points in fuzzy metric spaces," *Fuzzy Sets and Systems*, vol. 222, pp. 108–114, 2013.

[25] A. Bartwal, R. C. Dimri, and S. Rawat, "Fixed point results via altering distance functions in relational fuzzy metric spaces with application," *Mathematica Moravica*, vol. 25, no. 2, pp. 109–124, 2021.

Hindawi
Advances in Mathematical Physics
Volume 2022, Article ID 1776150, 12 pages
https://doi.org/10.1155/2022/1776150

Research Article

Jewelry Packaging User Demand Analysis Based on Fuzzy Kano Model

Zhanmei Hu

Shaanxi Institute of International Trade & Commerce Xianyang, Shaanxi, China

Correspondence should be addressed to Zhanmei Hu; 719883537@qq.com

Received 22 April 2022; Revised 15 June 2022; Accepted 8 July 2022; Published 13 August 2022

Academic Editor: S. E. Najafi

China's jewelry sales maintain a good momentum of annual growth, and consumption potential is huge. However, jewelry packaging design faced many problems. Even through China has many jewelry brands, the packaging is poorly designed. The fundamental reason lies in the lack of targeted design of jewelry packaging and the lack of detailed analysis and research, only to meet the functional use. Fuzzy front-end is suitable for the initial stage of product design and determines the success or failure of product design. In view of the uncertain factors, such as consumer demand, technical characteristics, and competitive environment that need to be considered in jewelry packaging design, this paper takes jewelry packaging products, jewelry brands, and fuzzy front-end as research objects, analyzes the existing problems, and makes quantitative analysis by using methods such as questionnaire survey, brainstorming, and scenario analysis. Rough set theory and Kano Model are used to classify and analyze user demand information and determine the realization opportunity. Finally, the research ideas of this topic are formed, and the corresponding research methods and models for ring packaging in jewelry are put forward and verified by examples, so as to form a research method suitable for fuzzy front-end design of jewelry packaging and improve the quality of jewelry packaging design.

1. Introduction

In 2020, the sales volume of precious metal jewelry in China has exceeded 200 billion yuan. It can be seen that Chinese people's consumption demand for jewelry products is extremely strong. As the carrier and bridge between consumers and jewelry brands, jewelry packaging also embodies the practical functions of protection, display, and collection. Therefore, jewelry packaging design occupies an important position in the gold and silver jewelry sales market. At present, jewelry packaging design in the market generally has problems such as lack of aesthetic feeling, brand difference, less correlation between packaging and jewelry, and single function [1]. The occurrence of these problems shows that the current jewelry packaging does not consider the consumers, brands, and product characteristics for creative design, which needs to be analyzed based on the comprehensive factors of consumer psychology, science, technology, culture, and processing technology.

The design process can be divided into fuzzy front-end (FFE) stages according to the chronological order of design, new product development (NPD), and commercialization stage. Among them, the fuzzy front-end (FFE) is the initial stage of product design, which determines the success or failure of product design [2]. Since there are a series of unknown and unclear factors in this stage, such as consumer needs, technical characteristics, and market conditions, this stage is also the most critical and difficult to control of the entire product design process.

2. Fuzzy Front-End Design Theory and Method

Scholars have done a lot of research on fuzzy front-end theory which is mainly used in the field of management. Therefore, there are relatively few fuzzy front-end theories and application methods for product packaging. Scholars such as Moenaert and Meyer [3] summarized the fuzzy front-end as the enterprise determines the concept for the new

product development and whether it needs to invest the resources owned by the enterprise in the detailed product development process. This paper uses the fuzzy front-end theory to solve the problems existing in jewelry packaging. The first person to introduce the concept of fuzzy front-end in China should be Professor Chen Jin and his team from Zhejiang University, and they elaborated on the content and procedures of fuzzy front-end management in detail [4].

Ashish Dutta and Ajay Pal Singh Rathore published an article saying: Ergonomic attributes play an important role in cars and passengers. Identify 20 important attributes, obtain user needs, and build a new framework combining quality functions [5].

Dou and Li point out in their article: The degree of satisfaction improvement of each product attribute is measured from two aspects of customer perception and competitor performance, and House of Quality (HoQ) is used to calculate the optimal improvement scheme [6].

Kim and Hong mainly studied the analysis of fruit packaging quality with Fuzzy Kano Model [7].

Fuzzy front-end (FFE) refers to the first stage of product design. Many factors need to be considered, including consumers, materials, technologies, and markets. Fuzzy uncertainty increases the failure rate of new product development. It is easy to cause blind design and lack of classification, generalization, and analysis of influencing factors. Through the analysis of relevant literature, several common methods for fuzzy front-end design are summarized: (1) brainstorming method: it is a kind of "group thinking," emphasizing unlimited creativity, focusing on quantity, and problem guidance, highlighting the thinking of seeking differences. (2) Scenario analysis method: scenario analysis method requires centralized analysis of component users and use environment, to find problems and solutions in the design. (3) Cluster analysis: cluster analysis is a multivariate statistical technique that performs cluster analysis on similar samples or indicators. (4) Rough set theory: this theory analyzes inaccurate, inconsistent, and incomplete information and forms complementary with fuzzy theory. (5) Quality function deployment: quality function deployment is a systematic decision-making technique based on satisfying user requirement [8], which helps researchers to accurately construct the demand matrix.

Quantitative analysis was carried out by means of brainstorming, scenario analysis, cluster analysis, rough set theory, etc., and the information was classified and analyzed by using Analytic Hierarchy Process (AHP) and Kano Model and realized the opportunity. Finally, the research of this paper is formed the corresponding methods and combined with specific design examples to verify.

3. Analysis of Jewelry Packaging Design

Jewelry packaging products revolve around the types of jewelry, mainly including the following: ring box, paired ring box, pendant box, bracelet box, long chain box, watch box, and suit box. Commonly used processes include the following: hot stamping, hot silver, embossing, embroidery, silk screen, UV, and other more than 10 kinds of processes. Optional materials include the following: paper, PU leather, leather, microfiber, cotton, linen, and flannel. Common shapes are as follows: square, rectangle, circle, heart shape, and irregular shape [9].

There are many problems in jewelry packaging design. The biggest difference between jewelry products and other products is the small in size and high in value, and jewelry, as a form of gifts, may exist between buyers and users who are not the same one. Therefore, the objects to be considered are also different. On the one hand, analyze the type of jewelry and design according to the size parameters of the jewelry. On the other hand, consider increasing the value of jewelry through packaging design artistically. It also has the function of general packaging and needs to have the function of emotional transmission. If it can reflect the emotional expression of the gifter, will be more favored by consumer groups.

Another important problem of jewelry packaging is that the production of jewelry packaging and jewelry product brand enterprises are in mostly cases are separated. The packaging is designed and produced by the packaging company, and there are many cases of general packaging, which are mainly customized by brand.

4. Research Content of Jewelry Packaging Based on Kano Model

4.1. Opportunity Identification: Obtaining User Demand. Opportunity identification is the first stage of fuzzy front-end design. The sources of opportunity identification include the following: brainstorming method, scenario analysis method, and questionnaire survey method. This paper selects jewelry entrepreneurs, salespersons, and consumers as questionnaires and interview objects, uses scenario analysis to improve consumer needs, and uses brainstorming to obtain N requirements of customers [10]. This paper takes the new product of a jewelry packaging and processing enterprise as the research event object and applies the research theory of product fuzzy front-end design to verify the results. The specific implementation steps are as follows:

4.1.1. Determine the Perceptual Vocabulary. Collect perceptual words from advertisements, Internet, magazines, and other channels, use semantic differential [11] to formulate an evaluation form, make questionnaire, and select six groups of the most representative words describing jewelry packaging as shown in Table 1.

4.1.2. Evaluate Perceptual Vocabulary against Product Samples. Combined with the survey samples, a semantic difference scale was established, formed a questionnaire to obtain the perceptual cognition of the test on the product and to obtain the priority planning of various functions of the jewelry packaging product.

Through the analysis of consumers' requirement for products, the keywords of the problem are extracted, and the requirements of jewelry packaging in terms of function,

Table 1: Describes the most representative words for jewelry packaging.

Forward feature	Reverse feature	Forward feature	Reverse feature
Beautiful	Ugly	Expensive	Cheap
Rich	Monotone	Transparent	Opaque
Unique	Featureless	Hard	Soft

appearance, and performance are obtained as the main concerns; the specific function points are displayed in Figure 1.

4.1.3. Determine Design Elements. The sample pictures of jewelry packaging are adopted color removal process, which does not affect consumers' evaluation. As shown in Figure 2, select 20 groups for analysis:

Select 20 representative jewelry packaging samples for designed jewelry packaging products. Combined with consumer perceptual vocabulary analysis, we can better analyze the functional requirements of packaging.

4.2. Assumption Screening. Through the above methods, obtain the consumers' data acquisition of products, the information is disordered and chaotic, the hierarchical structure of information needs integrated, and the cluster analysis method and AHP analysis method are used to process the relevant information. Combined with the above research, enterprises can obtain the most core "concerns" of consumers' products, to obtain the importance of customer needs and new "selling points" of products [12]. Make the final product plan designed by the enterprise in line with the research conclusions, get the sales results to verify the success of the plan by putting it in the market, improve the profit rate of the enterprise and the satisfaction of consumers, and expand the brand influence, thus proving the fuzzy front-end design method applied in this paper as feasible and scientific.

4.2.1. Analysis of the Customer Demand. On the basis of jewelry packaging three requirements, use Likert scale method to form the consumer's satisfaction with certain requirement [13]. The specific methods are as follows:

Firstly, define the demand evaluation set $V = \{V_1, V_2, V_3, V_4, V_5\}$, V is the name of the set, and there are five elements in the set, from V_1 to V_5, respectively, representing the satisfaction of a certain demand for jewelry packaging. Specifically, $V_1 = 1$ means that consumers are very dissatisfied with this demand, $V_2 = 2$ means that consumers are dissatisfied with this demand, $V_3 = 3$ means that consumers are generally satisfied with this demand, $V_4 = 4$ means satisfied, and $V_5 = 5$ means very satisfied with this requirement.

Secondly, according to the survey of consumer set $L = \{L_1, L_2, L_3\}$ for the fifteen items of demand results of jewelry packaging in three aspects: function, appearance, and performance, create a consumer demand evaluation gradient table based on rough set theory [14]. The evaluation gradient of consumers is shown in Tables 2 and 3.

Among them, T is the set of different conditional demand properties defined in the evaluation form, consumers fill in the satisfaction value CS according to different demand properties, the combination of consumer demand properties is represented by A, and the combination of satisfaction properties is represented by B.

According to the Relative Positive Field Theory, the Relative Positive Field of consumer L_1's requirement CR_1 can be expressed by the following formula:

$$\begin{aligned} \mathrm{POS}_{A-\{\mathrm{CR}_1\}}(B) = {} & \{T_4, T_{26}\}, \{T_6, T_{15}, T_{38}\}, \{T_8, T_{16}, T_{24}\}, \\ & \cdot \{T_9.T_{17}\}, \{T_{10}, T_{18}\}, \{T_{13}, T_{21}\}, \\ & \cdot \{T_{22}, T_{37}\}, \{T_{28}, T_{39}\}, \{T_{31}, T_{35}\}. \end{aligned} \tag{1}$$

The Relative Positive domain of consumer L_1's demand CR_2 can be expressed by the following formula:

$$\mathrm{POS}_{A-\{\mathrm{CR}_2\}}(B) = \{T_9, T_{11}\}, \{T_{33}, T_{37}\}, \{T_{34}, T_{38}\}. \tag{2}$$

The Relative Positive domain of consumer L_1's demand CR_3 can be expressed by the following formula:

$$\begin{aligned} \mathrm{POS}_{A-\{\mathrm{CR}_3\}}(B) = {} & \{T_1, T_2, T_5\}, \{T_3, T_4\}, \{T_9, T_{10}\}, \{T_{17}, T_{18}\}, \\ & \cdot \{T_{22}, T_{23}\}, \{T_{29}, T_{30}\}, \{T_{33}, T_{34}\}. \end{aligned} \tag{3}$$

For consumer L_1, because it satisfies the positive constraint of formula (4), it can be concluded that the three requirements CR_1, CR_2, and CR_3 of consumer L_1 cannot be simplified relative to the satisfaction value CS. The same conclusion can be drawn for consumers L_2 and L_3.

$$\begin{aligned} \mathrm{POS}_{A-\{\mathrm{CR}_1\}}(B) &\neq \mathrm{POS}_A(B), \\ \mathrm{POS}_{A-\{\mathrm{CR}_2\}}(B) &\neq \mathrm{POS}_A(B), \\ \mathrm{POS}_{A-\{\mathrm{CR}_3\}}(B) &\neq \mathrm{POS}_A(B). \end{aligned} \tag{4}$$

Then, calculate the importance of each demand to consumers λ_{iL}, where i represents the demand variable, CR_i, $(i = 1, 2, 3)$, and L is the set of consumers. For the consumer L_1, the importance of the three requirements CR_1, CR_2, and CR_3 is expressed by the following formula:

$$\begin{cases} \lambda_{1L_1} = \dfrac{|\mathrm{POS}_A(B)|}{|T|} - \dfrac{\mathrm{POS}_{A-\{\mathrm{CR}_1\}}(B)}{|T|} = 1\text{-}\dfrac{20}{40} = 0.5, \\ \lambda_{2L_1} = \dfrac{|\mathrm{POS}_A(B)|}{|T|} - \dfrac{\mathrm{POS}_{A-\{\mathrm{CR}_2\}}(B)}{|T|} = 1\text{-}\dfrac{6}{40} = 0.85, \\ \lambda_{3L_1} = \dfrac{|\mathrm{POS}_A(B)|}{|T|} - \dfrac{\mathrm{POS}_{A-\{\mathrm{CR}_3\}}(B)}{|T|} = 1\text{-}\dfrac{15}{40} == 0.625. \end{cases} \tag{5}$$

According to the contents of Tables 3 and 4, calculate the importance degree of demand of consumers L_2 and L_3,

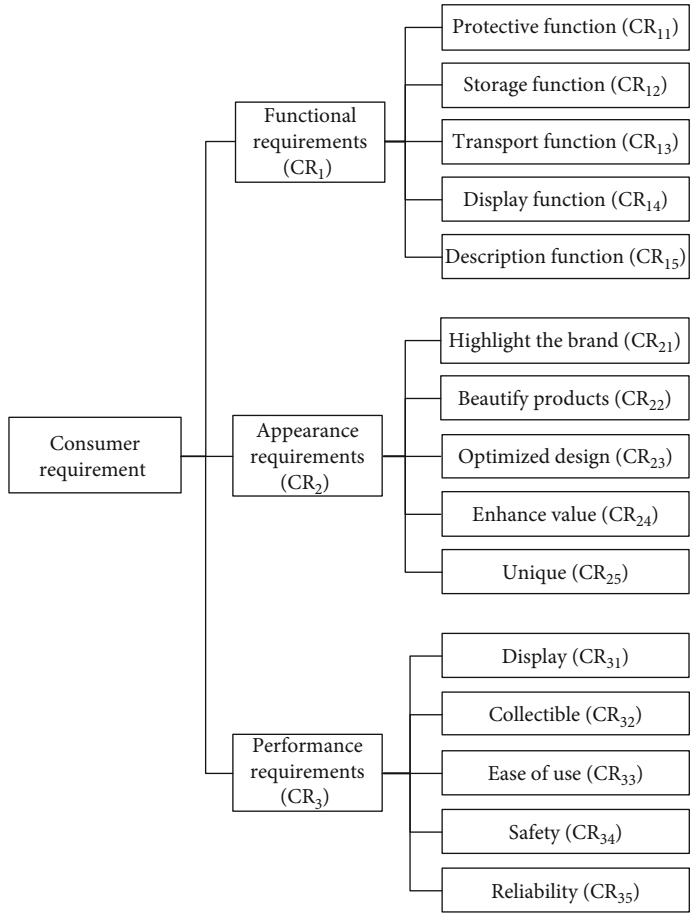

Figure 1: Three consumer demands for jewelry packaging.

and calculate the average value of all demand importance degrees in the consumer set L to obtain the average degree of importance of basic needs, as shown in the formulas (6)–(8).

$$\lambda_1 = \frac{\sum_{L=L_1}^{3} \lambda_{1L}}{\text{count}(L)} = \frac{\lambda_{1L_1} + \lambda_{1L_2} + \lambda_{1L_3}}{3} = \frac{0.5 + 0.6 + 0.575}{3} = 0.558, \tag{6}$$

$$\lambda_2 = \frac{\sum_{L=L_1}^{3} \lambda_{2L}}{\text{count}(L)} = \frac{\lambda_{2L_1} + \lambda_{2L_2} + \lambda_{2L_3}}{3} = \frac{0.85 + 0.6 + 0.575}{3} = 0.675, \tag{7}$$

$$\lambda_3 = \frac{\sum_{L=L_1}^{3} \lambda_{3L}}{\text{count}(L)} = \frac{\lambda_{3L_1} + \lambda_{3L_2} + \lambda_{3L_3}}{3} = \frac{0.625 + 0.4 + 0.625}{3} = 0.55. \tag{8}$$

According to the above calculation results, $\lambda_2 > \lambda_1 > \lambda_3$, it can be concluded that consumers pay the most attention to the appearance requirements of jewelry packaging, followed by the functional requirements, and the performance requirements are the least concerned.

Finally, after obtaining the importance of the requirements of the first layer (CR_1, CR_2, and CR_3), the importance of the second layer of requirement attributes is obtained according to quantitative statistics as shown in Table 5, λ'_{CR} as CR represents the number of layers of requirements and the serial number of specific requirements.

The importance of the first layer of demand calculated by formulas (6)–(8) and the calculation method of calculating the importance of the second layer of demand in formula (9) can be concluded that consumers have quantitative statistics on each layer of jewelry packaging. The importance of each requirement is shown in Table 6.

$$\lambda_{i\text{CR}} = \lambda_i \cdot \lambda'_{\text{CR}}. \tag{9}$$

4.2.2. Correction and Quantification of Requirement Importance Based on Competitive Product Analysis. On the basis of obtaining the importance of various needs of jewelry packaging through consumer survey results, it is also necessary to consider the evaluation and scoring of other competing products, so as to obtain more comprehensive analysis conclusion of the market competitive advantage of jewelry packaging needs.

Firstly, define $G = \{G_1, G_2, \cdots, G_j\}$, and $j = 1, 2, 3, 4, 5$ to quantify the pros and cons of consumers' requirements for the product compared with similar products in the market. Specifically, G_1 means that the product has no

(a) (b) (c) (d) (e) (f) (g) (h) (i) (j) (k) (l) (m) (n) (o) (p)

Figure 2: Continued.

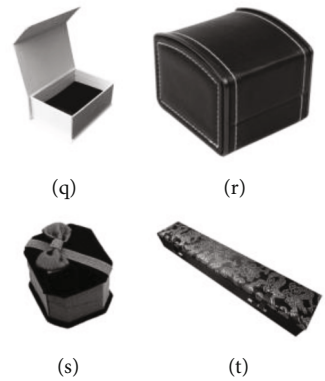

Figure 2: 20 representative jewelry packaging samples.

Table 2: Evaluation gradient of consumer L_1.

T	CR_1	CR_2	CR_3	CS	T	CR_1	CR_2	CR_3	CS	T	CR_1	CR_2	CR_3	CS
1	1	2	3	1	15	2	4	5	4	29	4	1	3	3
2	1	2	5	1	16	3	1	1	1	30	4	1	5	3
3	1	3	2	1	17	3	1	3	2	31	4	2	1	3
4	1	3	5	1	18	3	1	5	2	32	5	1	1	2
5	1	2	4	1	19	3	2	1	2	33	5	1	3	4
6	1	4	5	4	20	3	3	2	2	34	5	1	5	4
7	1	5	4	2	21	3	3	5	3	35	5	2	1	3
8	2	1	1	1	22	3	5	3	4	36	5	3	2	4
9	2	1	3	2	23	3	5	5	4	37	5	5	3	4
10	2	1	5	2	24	4	1	1	1	38	5	4	5	4
11	2	2	3	2	25	4	3	2	3	39	5	4	5	5
12	2	3	4	2	26	4	3	5	1	40	5	5	3	5
13	2	3	5	3	27	4	4	2	4					
14	2	4	2	2	28	4	4	5	5					

Table 3: Evaluation gradient of consumer L_3.

T	CR_1	CR_2	CR_3	CS	T	CR_1	CR_2	CR_3	CS	T	CR_1	CR_2	CR_3	CS
1	1	1	1	1	15	2	4	2	2	29	4	2	3	3
2	1	1	2	1	16	2	4	5	3	30	4	2	5	3
3	1	1	3	1	17	2	5	3	3	31	4	3	2	3
4	1	2	3	1	18	2	5	5	4	32	4	3	5	4
5	1	2	5	1	19	3	1	5	3	33	4	5	3	4
6	1	2	4	1	20	3	2	1	2	34	4	5	5	5
7	1	4	5	1	21	3	2	3	3	35	5	1	1	2
8	1	3	4	2	22	3	2	5	3	36	5	1	3	4
9	2	2	3	2	23	3	4	2	3	37	5	2	3	3
10	1	5	4	2	24	3	4	5	4	38	5	3	5	4
11	2	1	1	1	25	3	5	3	4	39	5	3	2	4
12	2	2	5	3	26	3	5	5	4	40	5	5	3	4
13	2	3	4	2	27	4	1	1	3					
14	2	3	5	3	28	4	2	1	3					

Table 4: Evaluation gradient of consumer L_2.

T	CR_1	CR_2	CR_3	CS	T	CR_1	CR_2	CR_3	CS	T	CR_1	CR_2	CR_3	CS
1	1	1	1	1	15	2	5	3	3	29	4	2	3	3
2	1	1	2	1	16	2	5	5	4	30	4	2	5	3
3	1	1	3	1	17	3	1	1	2	31	4	4	2	4
4	1	3	2	1	18	3	1	3	2	32	4	4	5	4
5	1	3	5	1	19	3	1	5	3	33	4	5	3	4
6	1	3	4	2	20	3	2	1	2	34	4	5	5	5
7	1	5	5	2	21	3	3	2	2	35	5	1	5	4
8	1	5	4	2	22	3	3	5	3	36	5	2	1	3
9	2	1	1	1	23	3	4	2	3	37	5	2	3	3
10	2	1	3	2	24	3	4	5	4	38	5	3	5	4
11	2	1	5	2	25	3	5	3	4	39	5	5	3	5
12	2	2	3	2	26	4	1	3	3	40	5	5	5	5
13	2	2	4	2	27	4	1	5	3					
14	2	2	5	3	28	4	2	1	3					

Table 5: The importance of peer-level requirements of the second-level requirements.

Contents of the second layer requirements	The importance of peer requirements	Contents of the second layer requirements	The importance of peer requirements
Protective function	0.245	Enhance value	0.195
Storage function	0.09	Unique value	0.265
Transport function	0.215	Display	0.235
Display function	0.255	Collectible	0.225
Description function	0.195	Ease of use	0.175
Highlight the brand	0.29	Safety	0.2
Beautify products	0.125	Reliability	0.165
Optimized design	0.125		

Table 6: Importance of consumers' requirements for jewelry packaging.

First floor requirements	Basic importance	Second floor requirements	Basic importance
Functional requirements CR_1	0.558	Protective function	0.137
		Storage function	0.05
		Transport function	0.119
		Display function	0.143
		Description function	0.109
Appearance requirements CR_2	0.675	Highlight the brand	0.196
		Beautify products	0.084
		Optimized design	0.084
		Enhance value	0.132
Performance requirements CR_3	0.55	Unique	0.179
		Display	0.129
		Collectible	0.124
		Ease of use	0.096
		Safety	0.11
		Reliability	0.090

Table 7: Market competitive advantages of each requirement.

Consumer requirement		Market competitiveness evaluation			
First floor requirements	Second floor requirements	Similar product in the market (G) Zhou**	Northwest**	Requirement functional relevance (F)	Market competitiveness (H)
	CR_{11}	4	3	4	0.733
	CR_{12}	3	3	3	0.600
CR_1	CR_{13}	4	3	2	0.600
	CR_{14}	3	3	2	0.533
	CR_{15}	3	4	3	0.667
	CR_{21}	5	4	5	0.933
	CR_{22}	4	4	3	0.733
CR_2	CR_{23}	4	3	3	0.667
	CR_{24}	2	2	2	0.400
	CR_{25}	4	3	4	0.733
	CR_{31}	2	2	3	0.467
	CR_{32}	4	5	5	0.933
CR_3	CR_{33}	2	3	2	0.467
	CR_{34}	2	3	3	0.533
	CR_{35}	2	4	3	0.600

Table 8: Market competitive advantages of each requirement.

Consumer requirement		Basic importance correction			
First floor requirements	Second floor requirements	Selling point Existing products	New products	Standard increase rate (L)	Kano correction factor (K)
	CR_{11}	4	5	1.25	1.2
	CR_{12}	3	3	1.00	1
CR_1	CR_{13}	3	3	1.00	1
	CR_{14}	3	3	1.00	1.3
	CR_{15}	3	4	1.33	1
	CR_{21}	3	5	1.67	1
	CR_{22}	4	5	1.25	1
CR_2	CR_{23}	4	5	1.25	1.4
	CR_{24}	3	3	1.00	1
	CR_{25}	3	4	1.33	1
	CR_{31}	3	3	1.00	1.3
	CR_{32}	3	4	1.33	1
CR_3	CR_{33}	2	2	1.00	1.2
	CR_{34}	3	3	1.00	1
	CR_{35}	3	3	1.00	1

competitive advantage; G_2 means that the advantage is lacking; G_3 means that it has a general advantage; G_4 means that the advantage is strong; G_5 means that the product has a strong advantage.

Secondly, define $F = \{F_1, F_2, \cdots, F_f\}$, $f = 1, 2, 3, 4, 5$ as the quantitative rating of the product designer on whether a certain requirement of the product is related to similar products in the market. Specifically, F_1 means that the requirement is not related to the existing product; F_2 means that it is generally related; F_3 means that it is relatively related; F_4 means that it is closely related; F_5 means that it is very related.

Table 9: Final importance correction results.

Consumer requirement First floor requirements	Second floor requirements	Basic importance (λ)	Basic importance correction			
			Market competitiveness (H)	Kano correction factor (K)	Standard increase rate (L)	Final importance indicator (P)
Functional requirements CR_1	Protective function CR_{11}	0.137	0.733	1.2	1.25	0.150
	Storage function CR_{12}	0.050	0.600	1	1.00	0.030
	Transport function CR_{13}	0.120	0.600	1	1.00	0.072
	Display function CR_{14}	0.142	0.533	1.3	1.00	0.099
	Description function CR_{15}	0.109	0.667	1	1.33	0.097
Appearance requirements CR_2	Highlight the brand CR_{21}	0.196	0.933	1	1.67	0.305
	Beautify products CR_{22}	0.084	0.733	1	1.25	0.077
	Optimized design CR_{23}	0.084	0.667	1.4	1.25	0.098
	Enhance value CR_{24}	0.132	0.400	1	1.00	0.053
	Unique CR_{25}	0.179	0.733	1	1.33	0.175
Performance requirements CR_3	Display CR_{31}	0.129	0.467	1.3	1.00	0.078
	Collectible CR_{32}	0.124	0.933	1	1.33	0.154
	Ease of use CR_{33}	0.096	0.467	1.2	1.00	0.054
	Safety CR_{34}	0.110	0.533	1	1.00	0.059
	Reliability CR_{35}	0.091	0.600	1	1.00	0.054

Figure 3: Ruby ring packaging design renderings.

Then, define the variable set $H = \{H_1, H_2, \cdots, H_h\}$, $h = 1, 2, 3 \cdots$ for the analysis of the product market competitive advantage of h consumers surveyed, and compare N related similar competing products; then, for specific consumer, the following calculation formula can be obtained.

$$H_h = \frac{\sum_{n=1}^{N} G + \sum_{n=1}^{N} F}{(i+f)\cdot(N+1)}. \tag{10}$$

In this paper, we compared the packaging design of two similar brand products in the market: Zhou** and Northwest**, scored the competitive evaluation of each demand, to obtain the market competitive advantage table of each demand, such as shown in Table 7.

4.2.3. The Final Quantification of the Importance of Consumer Requirements Based on the Kano Model. According to the consumer requirement hierarchy chart for jewelry packaging, the functional demand is protection function, the appearance demand is to highlight the brand and beautify the product, it is unique, and the performance requirement is highly collectible. Brand, uniqueness, and collectability will be the main "selling points" of jewelry packaging development and design, and the company's existing products will be compared with the new products to be developed and designed; the horizontal growth rate of each requirements will be obtained. Specific data is shown in Table 8.

The calculation of the final importance degree $P_{\mathrm{CR}i}$ of each consumer demand is defined as formula (11), $\lambda_{i\mathrm{CR}}$ is the basic importance degree of the consumer to the requirements CR_i, and its value is obtained from Section 4.2.1; H_i is the market competitiveness of the requirement CR_i. Its value is given by formula (10); K_i is the modified quantitative parameter of the requirements; L_i is the horizontal growth value of the market demand of the demand.

$$P_{\mathrm{CR}i} = \lambda_{\mathrm{CR}i} \cdot H_i \cdot K_i \cdot L_i, i = 1, 2, 3, \cdots, n. \tag{11}$$

In this paper, according to the quantitative formula, the basic importance of comprehensive consumer requirements, the market competitiveness of consumer requirements, the use of Kano Model to correct various requirements quantitative parameters and the horizontal growth value [15], the final importance of customer demand for jewelry packaging products is obtained. The quantification results are shown in Table 9.

4.3. Realization Opportunities. After the abovementioned stages, it can be seen from Table 6 that consumers are more concerned about the three requirements of jewelry packaging, namely, "brand highlighting CR_{21}," "unique CR_{25}," and "display function CR_{14}." After the above market competition analysis, it can be concluded from Table 9: adding the influencing factors between the market and competing products, the "collectible CR_{32}" of jewelry packaging has replaced "display function CR_{14}" as the third content of concern, the two needs of "highlighting the brand CR_{21}" and "unique C R_{25}" are still the focus of consumers' attention, so it can be concluded that for the field of jewelry packaging design, attention should be paid to the innovation of appearance design needs, and packaging needs to be considered at the same time, providing new selling points for jewelry sales.

5. Ruby Ring Packaging Design Practice Based on Kano Model

5.1. Appearance Design. The design drawing shown in Figure 3 is based on the theme of ruby rings. The ring shape is relatively small, and the structure is stable [16]. Combined with the design process and conclusion of the Fuzzy Kano Model, first of all, the consumer demand for ruby rings is analyzed to understand the weight of consumer demand for each part, appearance demand more than function requirements more than performance requirements, focusing on the analysis of appearance design. This packaging design adopts the expression form of leather material, hexagon, and red. Leather material is a high-grade material in the selection of jewelry packaging materials. The hexagon is a design in the shape of a turtle shell and a honeycomb. The red hue is consistent with the ruby ring of the package contents and is highly ornamental. The auspicious ornamentation in the outer packaging echoes the inner wall of the ring, increasing the relevance [17] and cultural nature of the packaging in the details.

5.2. Functional Design. According to the analysis of functional requirements of jewelry packaging, it is mainly reflected in the following: protection function, storage function, transportation function, display function, and explanation function. This packaging design has a rigorous packaging structure, which can protect the interior well. The regular hexagonal design is convenient for storage and transportation, and the transparent setting on the top can better display the jewelry.

5.3. Dimensional Analysis. As a ring packaging box, the packaging size should not be too large. The height of ring packaging currently on the market is generally between 1.8 cm and 3.5 cm. Therefore, this packaging design adopts 3.5 cm and hexagonal diameter 6 cm, which is more in line with the grip of the hand. The size is easy to carry, and the specific product size chart is shown in Figure 4.

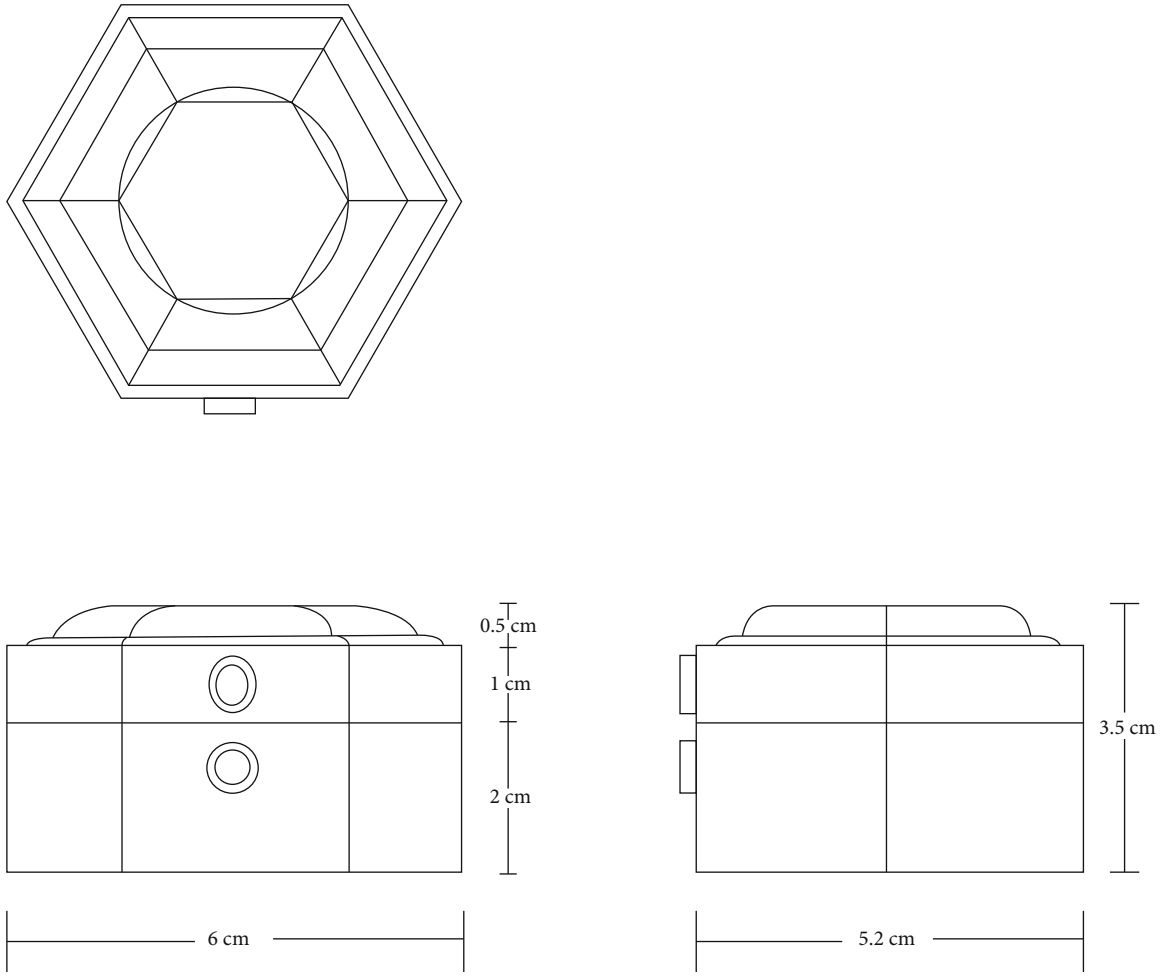

Figure 4: Packaging design dimensions.

5.4. Unique Analysis. Based on the Kano Model summary, obtain the unique design requirements for jewelry packaging. This packaging design has a dark pattern on the surface of the packaging, which has good unified echo with the inner wall pattern of the ring. It is customized packaging design and has certainly collection [18], to satisfy the consumer requirement for high-end jewelry packaging design.

6. Conclusion

Jewelry packaging products, as the "clothing" of jewelry, have many important functions. In view of the fact that domestic enterprises currently not pay much attention to the front-end development of jewelry packaging, it is hoped that through the research content of this article, enterprises can understand the demands of jewelry packaging. Regarding the weight relationship of various needs of jewelry packaging, we design products that satisfy consumers. Through the research on the fuzzy front-end design theory, combined with the specific placement, the weight analysis of the demand layer, and functional layer of jewelry packaging, in addition to highlighting the brand and unique characteristics, the front-end designer of jewelry packaging also needs to consider adding collection design; research in this aspect can continue to combine fuzzy front-end theory and semiotic theory to analyze specific design plans in the future.

Through research and the implementation of the fuzzy front-end theoretical feasibility plan, the randomness in the design process of the enterprise can be avoided, the experience value of jewelry can be improved, the sales and packaging innovation of the enterprise can be better promoted, the market share of the enterprise can be increased, and the brand influence can be expanded.

Data Availability

All data, models, and code generated or used during the study appear in the submitted article.

Conflicts of Interest

The author declares no conflicts of interest.

Acknowledgments

The article is one of the phased achievements of the 2021 general special scientific research project of the Education

Department of Shaanxi Province, "Research on Ruby Jewelry Packaging Based on Fuzzy Front End Theory" (21JK0514).

References

[1] M. X. Chen, *The Packageing Design Strategy Research of Jewelry Brand Based on Emotional Experience*, D. Wuhan University, 2017.

[2] L. M. Liu, R. H. Tan, and W. Liu, "Identification of Innovation Opportunities in Fuzzy Front End Based on Scenario," *Computer Integrated Manufacturing System*, 2021.

[3] R. K. Moenaert and A. D. Meyer, "R & D/marketing communication during the fuzzy front-end," *IEEE transactions on Engineering Management*, vol. 42, no. 3, pp. 243–258, 1995.

[4] Y. L. Wei, X. X. Li An, and X. Q. Jiang, "Usability Optimization Design of Cloud Pet APP Based on Kano-QFD," *Journal of Packaging Engineering*, vol. 43, no. 2, pp. 378–386, 2022.

[5] A. Dutta and A. P. Rathore, "A novel method to prioritise the ergonomic attributes of a passenger car using fuzzy approach," *International Journal of Business and Systems Research*, vol. 15, no. 5, pp. 601–628, 2021.

[6] R. Dou, W. Li, and G. Nan, "An integrated approach for dynamic customer requirement identification for product development," *Enterprise Information Systems*, vol. 13, no. 4, pp. 448–466, 2019.

[7] K. S. Jun and H. S. Jin, "A study on the analysis of fruit packaging quality using a fuzzy Kano model," *Journal of Korean Institute of Intelligent*, vol. 28, no. 1, pp. 77–82, 2018.

[8] J. Chen and J. Y. Gao, "The influence of fuzzy front end on innovation performance of complex product systems," *Chinese Journal of Management.*, vol. 2, no. 3, pp. 281–290, 2005.

[9] H. S. Zhang, J. Chen, and J. Y. Gao, *The study about FEE of radical product innovation*, vol. 16, no. 6, 2005J. R&D Management, 2005.

[10] Y. M. Chen, *Research on Jewelry Packaging Design Based on Custom Consumption Trend*, D. Wuhan Textile University., 2020.

[11] J. X. Bing, *The Public Art Deisign Strategy of Airport Terminal Space Based on the Method of Semantic Differential*, Harbin Institute of Technology, 2020.

[12] L. J. Feng, C. S. Li, J. F. Wang, and K. Zhang, *Research on product innovation path based on lead user demand*, vol. 1, Industrial Engineering and Management, 2022.

[13] D. Zhang, G. R. Wang, and Z. G. Li, "Customer demand analysis model of takeaway packaging design based on QFD," *Journal of Packaging Engineering*, vol. 42, no. 5, pp. 216–222, 2021.

[14] K. Zhou, H. Y. Sun, H. Jiang, and J. J. Yi, "The evaluation method of green packaging based on rough set theory and TOPSIS," *Journal of Packaging Engineering*, vol. 39, no. 17, pp. 142–146, 2018.

[15] W. B. Deng, Z. J. Zhang, and Q. Wang, *Modular office storage product design based on fuzzy Kano model*, China Academic Journals (CD Edition) Electronic Publishing House, Packaging Engineering, 2021.

[16] B. Q. Wang, "Analysis for Design Elements of Rings–Based on Kansei Engineering Aimed at Post-90s Group," China University of Geosciences, Beijing, 2020.

[17] Y. Xie, X. N. Mou, and R. R. Zhao, "Analysis on the Emotional Design of Ring Packaging box," *Chinese Journal of Green Package*, vol. 9, pp. 94–97, 2021.

[18] W. X. Zhai, *Research and Deisign of Personalized Jewelry Customization Service–Taking Meeding Technology Jewelry Customization Platform as an Example*, East China University of Science and Technology, 2019.

Hindawi
Advances in Mathematical Physics
Volume 2022, Article ID 2946497, 8 pages
https://doi.org/10.1155/2022/2946497

Research Article

Adaptive Fuzzy Control of Sludge Conditioning and Pressing

Luo Long

Mechanical & Electrical Department, Guangzhou Institute of Technology, Guangzhou 510075, China

Correspondence should be addressed to Luo Long; gtluolong@163.com

Received 26 May 2022; Revised 24 June 2022; Accepted 14 July 2022; Published 9 August 2022

Academic Editor: S. E. Najafi

The basic technological process of sludge conditioning and pressing is introduced in this paper. The purpose is to set up an adaptive fuzzy control algorithm to treat the problems of conditioning, mixing, feeding, and pressing control, so that the equipment used to process the sludge can run on demand. The algorithm is verified by MATLAB simulation. The results show that the control accuracy of the fuzzy adaptive control system is significantly improved compared with the original PID (proportion integration differentiation) control algorithm. The upper computer program is compiled with VB (visual basic) and applied to industry control to save the energy consumption.

1. Preface

Urban sewage treatment will inevitably produce sludge, and many harmful substances will remain in the sludge, so it is necessary to treat and dispose of excess sludge [1]; otherwise, it will pollute the environment. Sludge treatment and disposal follow the reduction, stabilization, harmlessness, and resource utilization. It is necessary to reduce the amount of sludge in the sewage treatment plant before connecting to the next stage [2]. It can be seen that dehydration and volume reduction are the most urgent needs at present, no matter what the disposal method is. The sludge conditioning and pressing technology is widely used and has become an important sludge dewatering treatment technology [3]. According to the needs of customers, the moisture content range after dehydration can be adjusted, and it has a very high degree of matching with various subsequent sludge disposal outlets. Due to the uncertainty of the organic matter content, moisture content, and process environment of the sludge drying treatment, the sludge volume and various parameters of the sludge quality of each batch are uncertain, resulting in the inconsistency of the sludge conditioning formula and control strategy [4]. Due to the lack of self-adaptive adjustment system, the current domestic process schemes often adopt the method of adding more chemicals and amplifying the insurance factor to standardize the water content of the mud; however, it cannot realize the on-demand distribution of chemicals and process operations, which increase the operating costs. In addition, it is difficult to obtain an accurate mathematical model and control accurately for traditional method; there are many input parameters and control objects in the whole process system and still problems of nonlinearity and large time delay [5]. Therefore, a more reasonable and complicated algorithm needs to be proposed. The fuzzy adaptive control technology was used to dynamically control and adjust the feeding time, pressing pressure, and time in the filtering and pressing process [6], so as to realize on-demand operation, and achieve the goal of reducing the overall energy consumption of the system and saving operating costs. For uncertain nonlinear systems, indirect and direct adaptive fuzzy control (AFC) approaches have been intensively developed in the past decades [7]. Javanbakht and Chakravorty propose a new application of the prediction of human behavior using TOPSIS as an appropriate tool for data optimization [8]. Garg et al. presented a novel idea about the continuous possibilistic cooperative static game. The proposed Poss-CCSTG is a continuous cooperative static game (CCSTG) in which parameter associated with the cost functions of the players involves the possibility measures [9]. Bulut and Ozceylan developed a fuzzy inference system (FIS) to use six criteria as inputs, 144 rules were created, and the linguistic variables of air

textured yarn (ATY) samples of a textile manufacturer were used as well [10]. The quality level of the products according to the different membership functions is identified with the proposed FIS generated by MATLAB version 2015a, and recommendations are made to the manufacturer. Arora et al. use the Mamdani fuzzy inference system to predict COVID-19. The timely prognosis of the disease at home isolation or at the security checks can help the patient to seek the medical treatment as early as possible [11]. Chen et al. introduce the basic concepts of fuzzy theory and several common types of fuzzy application examples such as fuzzy washing machine and fuzzy control of incinerator plant in China illustrating the application of fuzzy theory in real society [12]. In this paper, for the uncertainty of pressure control in the process of sludge conditioning and pressing, an adaptive fuzzy control algorithm is proposed, and a control model is established to dynamically control and adjust the process of conditioning and pressing, so as to realize the operation of equipment on demand, and achieve the goal of reducing the overall energy consumption of the system and saving the operation cost.

2. Sludge Conditioning and Pressing Process

The residual sludge in the secondary sedimentation tank of the sewage treatment plant was used as analyte by the sludge conditioning and pressing process. [13]. The volume or weight of the sludge is reduced by two-thirds, and then, the remaining one-third of the concentrated sludge is reduced by more than 90% through the "chemical conditioning and pressing process," and the sludge becomes a granules with moisture content less than 60% [14], which can initially reduce the amount of sludge treatment and reduce subsequent equipment investment and operating costs. After preconcentration, the sludge is quantitatively added with a suitable proportion of conditioner to improve the dewatering performance of the sludge, kill the pathogenic bacteria in the sludge and solidify the heavy metals in the sludge, and then press, and the moisture content of the pressed mud cake is below 60%. The corresponding sludge volume will be reduced by 8 to 13 times [15]. The mud cake can be disposed by various methods such as landfill, land use, and incineration. The entire process is shown in Figure 1.

In this process, the core equipment is the diaphragm filter press, which is composed of a filter plate and a filter frame with filtrate passages. It consists of five parts [16] as shown in Figure 2. A filter cloth is sandwiched between each group of filter plates and filter frames, and the filter plates and filter frames are pressed tightly with the movable end, so that a filter press chamber is formed between the filter plates and the filter frame. The sludge flows in from the feed liquid inlet, and the water flows through the filter plate out from the filtrate discharge port [17]. During this procedure, the filter cake will be squeezed and accumulated on the frame filter cloth. After the filter plate and the filter frame are loosened, the mud cake can be easily peeled off from the filter frame or removed from the filter cloth with a shovel.

Diaphragm filter press realizes a complete cycle of sludge deep dewatering procedure which mainly includes the following processes [18]: filling and filtration, diaphragm pressing, feeding hole core blowing, automatic pulling plate, and unloading cake, as shown in Figure 3. (1) Filling and filtration: the sludge is injected into all the filter chambers through the feeding pipeline. At the same time, the newly injected sludge squeezes the previous sludge to discharge the filtrate through the filter cloth. (2) Diaphragm pressing: after the feeding is finished, the extrusion medium (high pressure water) enters, and the diaphragm enters the filter chamber from the stop position under pressure. Through the movement of the diaphragm, the volume of the filter chamber is reduced, and the filter cake is squeezed and mechanically dried. (3) Core blowing in the feeding hole: use compressed air to blow the sludge in the feeding pipeline back to the feeding direction, so that the feeding hole and its surroundings are kept drying [19]. (4) Automatically pulling the plate and unloading the cake: the flap is opened, the hydraulic system drives the filter plate moving device to open the filter chamber one by one, and the filter cake is discharged into the downstream equipment.

In the actual production process, the key parameters of the machine are the pressing pressure and pressing time, which lead to the mud cake produced by the plate and frame filter press fulfill the criterion or not. If the pressing pressure is insufficient, no matter how long the pressing time is, the mud cake cannot fulfill the criterion [20]; if the pressing pressure is sufficient and the pressing time is not enough, the standard water content of mud cannot be produced. In terms of cost control, on the one hand, it is necessary to find a suitable pressing pressure to prevent it is too low to exceed the standard of mud production, further more causes energy waste in long-term pressing. On the other hand, when the pressing pressure is determined [21], it is necessary to find out appropriate pressing time, in order to achieve qualified water content of the mud, and the pressing time should not be too long to waste energy. In addition, if the water content of the sludge entering the diaphragm plate and frame sludge filter press is too high, in order to maintain the process stability, the dosing ratio of chemical additives must be slightly increased, thereby increasing the cost and the water content of the sludge, and the amount of mud entering the plate and frame will be increased too [22]. If the residence time of the leaching tank is shortened, the biological reaction is affected when the moisture content is too high, then the feeding needs to be completed within the specified time, and the flow rate of the sludge screw pump needs to be increased, which will inevitably increase the power of the sludge screw pump, thereby increasing the power consumption. In this paper, in order to keep the mud quality and conditioning conditions of each batch, the fuzzy adaptive control algorithm is used to dynamically control and adjust the feeding time, pressing pressure, and time of the filtration and pressing process, so as to realize on-demand operation, and achieve the goal of reducing the overall energy consumption of the system and saving operating costs [23].

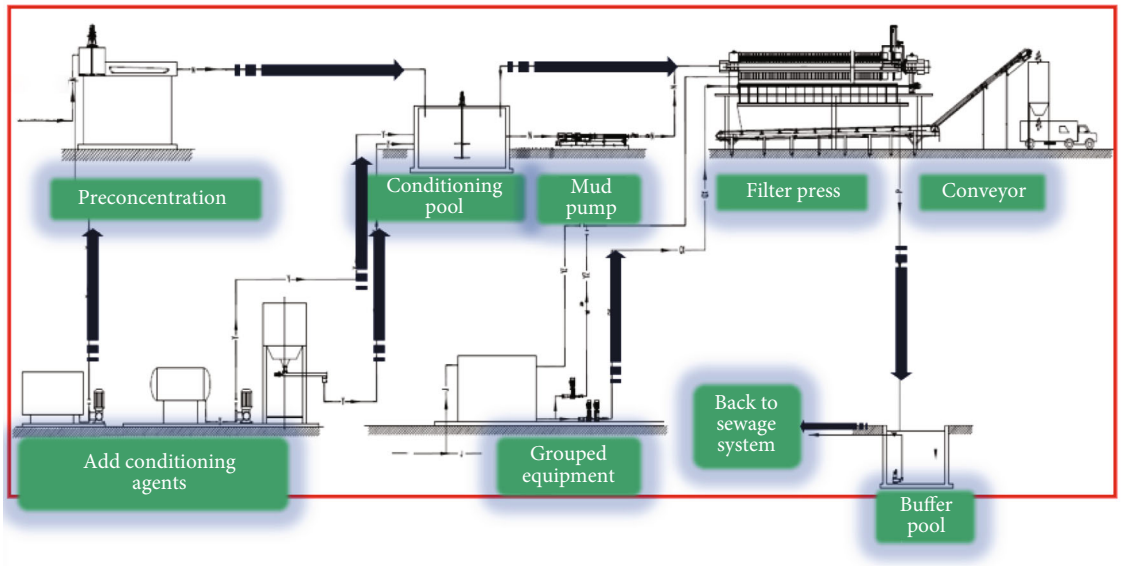

Figure 1: Sludge deep dewatering process flow chart.

Figure 2: Diaphragm filter press.

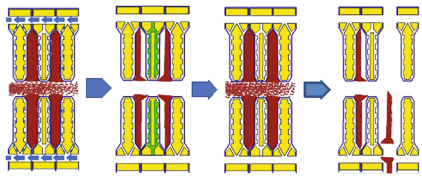

Figure 3: Sludge deep dewatering process.

3. Design of Fuzzy Adaptive Control Algorithm

In the early 1990s, Liu et al. proved that the fuzzy controller is a universal nonlinear approximator; that is, the fuzzy controller can realize the function approximation under arbitrary precision for any kind of continuous nonlinear equation defined under the density [24]. It is an important theoretical foundation for the universal application of fuzzy technology. In 1993, Yang et al. first proposed a stable adaptive fuzzy control method. Based on the Lyapunov function, they gave the adaptive rate of the parameters in the fuzzy system and strictly proved the stability of the control system. The derived closed-loop control system is globally stable, and the tracking error of the system converges to zero asymptotically under the condition that the minimum approximation error is square integrable [25]. Yang et al.'s work has made a breakthrough in the research of adaptive fuzzy control theory. Under their promotion, the analysis methods of the stability, robustness, and control performance of fuzzy control systems have been developed rapidly. The stable adaptive fuzzy control method proposed by Yang et al. opens up a new way to study the control problems of unknown nonlinear systems with fuzzy logic systems.

3.1. System Description. Consider the object of study described by the following equation:

$$\begin{cases} x^{(n)} = f\left(x, \dot{x}, \cdots, x^{(n-1)}\right) + bu, \\ y = x. \end{cases} \tag{1}$$

In the formula, f is an unknown function, and b is an unknown constant. Direct adaptive fuzzy control uses the following IF-THEN fuzzy rules to describe the control knowledge:

$$\text{IF } x_1 \text{ is } P_1^r \text{ and } x_n \text{ is } P_n^r, \text{ THEN } u \text{ is } Q^r. \tag{2}$$

In the formula, P_i^r, Q^r is a fuzzy set in R, and $r = 1, 2, \cdots, L_n$.

Suppose the position command is y_m; make

$$e = y_m - y = y_m - x, e = \left(e, \dot{e}, \cdots, e^{(n-1)}\right)^T. \tag{3}$$

Choose $k = (k_n, \cdots, k_1)^T$ so that all the roots of the polynomial $s^n + k_1 s^{(n-1)} + \cdots + k_n$ lie in the left half-open of the complex plane. Because b in the system is uncertain, in order to ensure the stability of the fuzzy controller, another controller can be designed and added to the fuzzy controller to

maintain the stability, which is called the supervisory controller. Take the control law as

$$u^* = \frac{1}{b}\left[-f(x) + y_m^{(n)} + K^T e\right]. \tag{4}$$

Substitute equation (4) into equation (1) to obtain the equation of the closed-loop control system:

$$e^{(n)} + k_1 e^{(n-1)} + \cdots + k_n e = 0. \tag{5}$$

Through the selection of K, when $t \longrightarrow \infty$, $\mathrm{e(t)} \longrightarrow 0$, that is the output y of the system gradually converges to the ideal output.

Direct type fuzzy adaptive control is based on fuzzy system to design a feedback controller $u = u(x|\theta)$ and an adaptive law of adjusting parameter vector θ, so that the system output y can track the ideal output y_m as much as possible.

3.2. Design of Fuzzy Controller. The direct adaptive fuzzy controller is

$$u = u_D(x|\theta), \tag{6}$$

where is a fuzzy system andθ is a set of adjustable parameters.

The fuzzy system u_D can be constructed by the following two steps:

Step 1. For variable $x_i (i = 1, 2, \cdots, n)$, define m_i fuzzy sets $A_i^{l_i}$ $(l_i = 1, 2, \cdots, m_i)$.

Step 2. Construct a fuzzy system $\prod_{i=1}^{n} m_i$ with the following $u_D(x|\theta)$ fuzzy rules:

$$\text{IF } x_1 \text{ is } A_1^{l_1} \text{ and } x_n \text{ is } A_n^{l_n}, \text{ THEN } u_D \text{ is } S^{l_1 \cdots l_n}, \tag{7}$$

where $l_1 = 1, 2, \cdots, m_i$ and $i = 1, 2, \cdots, n$.

A product inference engine, a single-valued fuzzer, and a center-averaged defuzzifier are used to design the controller.

$$u_D\left(\frac{x}{\theta}\right) = \frac{\sum_{l_{1=1}}^{m_1} \cdots \sum_{l_{n=1}}^{m_n} y_u^{-l_1 \cdots l_n} \left(\prod_{i=1}^{n} u_{A_i}^{l_i}(x_i)\right)}{\sum_{l_{1=1}}^{m_1} \cdots \sum_{l_{n=1}}^{m_n} \left(\prod_{i=1}^{n} u_{A_i}^{l_i}(x_i)\right)}. \tag{8}$$

Let $y_u^{-l_1 \cdots l_n}$ be a free parameter and put them in the set $\theta \in R \prod_{i=1}^{n} m_i$, respectively; then, the fuzzy controller is

$$u_D(x|\theta) = \theta^T \xi(x), \tag{9}$$

where $\xi(x)$ is a $\prod_{i=1}^{n} m_i$ dimensional vector whose $l_1, \cdots, l_n$ element is

$$\xi_{l_1 \cdots l_n}(x) = \frac{\prod_{i=1}^{n} u_{A_i}^{l_i}(x_i)}{\sum_{l_{1=1}}^{m_1} \cdots \sum_{l_{n=1}}^{m_n} \left(\prod_{i=1}^{n} u_{A_i}^{l_i}(x_i)\right)}. \tag{10}$$

The fuzzy control rule (2) is embedded in the fuzzy controller by setting its initial parameters.

3.3. Design of the Adaptive Law. Substitute equations (4) and (6) into equation (1), and get

$$e^{(n)} = -K^T e + b\left[u^* - u_D\left(\frac{x}{\theta}\right)\right]. \tag{11}$$

Make

$$\Lambda = \begin{pmatrix} 0 & 1 & 0 & 0 & \cdots & 0 & 0 \\ 0 & 0 & 1 & 0 & \cdots & 0 & 0 \\ \vdots & \vdots & \vdots & \vdots & \ddots & \vdots & \vdots \\ 0 & 0 & 0 & 0 & \cdots & 0 & 1 \\ -k_n & -k_{n-1} & & & \cdots & & -k_1 \end{pmatrix} b = \begin{pmatrix} 0 \\ 0 \\ \vdots \\ 0 \\ b \end{pmatrix}. \tag{12}$$

Then, the closed-loop system dynamic equation (11) can be written in vector form:

$$\dot{e} = \Lambda e + b\left[u^* - u_D\left(\frac{x}{\theta}\right)\right]. \tag{13}$$

The optimal parameters are defined as

$$\theta^* = \arg \min_{\prod_{\theta \in R_i=1}^{n} m_i} \left[\sup_{x \in R^n} |u_D(x|\theta) - u^*|\right]. \tag{14}$$

The minimum approximation error is defined as

$$\omega = u_D(x|\theta^*) - u^*. \tag{15}$$

From formula (13), we can get

$$\dot{e} = \Lambda e + b(u_D(x|\theta^*) - u_D(x|\theta)) - b(u_D(x|\theta^*) - u^*). \tag{16}$$

From equation (9), the error equation (16) can be rewritten as

$$\dot{e} = \Lambda e + b(\theta^* - \theta)^T \xi(x) - b\omega. \tag{17}$$

Define the Lyapunov function:

$$V = \frac{1}{2} e^T P e + \frac{b}{2r} (\theta^* - \theta)^T (\theta^* - \theta), \tag{18}$$

where parameter γ is a positive constant.

P is a positive definite matrix and satisfies the Lyapunov equation:

$$\Lambda^T P + P\Lambda = -Q, \tag{19}$$

where Q is an arbitrary positive definite matrix $n \times n$ given by equation (12).

Take $V_1 = (1/2)e^T Pe$ and $V_2 = (b/2r)(\theta^* - \theta)^T(\theta^* - \theta)$, let $M = b(\theta^* - \theta)^T \xi(x) - b\omega$, and then formula (17) becomes

$$\dot{e} = \Lambda e + M,$$

$$\begin{aligned}\dot{V} &= \frac{1}{2}\dot{e}^T Pe + \frac{1}{2}e^T P\dot{e} = \frac{1}{2}\left(e^T\Lambda^T + M^T\right)Pe + \frac{1}{2}e^T P(\Lambda e + M)\\ &= \frac{1}{2}e^T\left(\Lambda^T P + P\Lambda\right)e + \frac{1}{2}M^T Pe + \frac{1}{2}e^T PM\\ &= -\frac{1}{2}e^T Qe + \frac{1}{2}\left(M^T Pe + \frac{1}{2}e^T PM\right) = -\frac{1}{2}e^T Qe + e^T PM,\end{aligned} \tag{20}$$

which is $\dot{V}_1 = -(1/2)e^T Qe + e^T Pb[(\theta^* - \theta)^T\xi(x) - \omega]$ and $\dot{V}_2 = -(b/r)(\theta^* - \theta)^T\dot{\theta}$.

The derivative of V is

$$\dot{V} = -\frac{1}{2}e^T Qe + e^T Pb\left[(\theta^* - \theta)^T\xi(x) - \omega\right] - \frac{b}{r}(\theta^* - \theta)^T\dot{\theta}. \tag{21}$$

Let p_n be the last column of P, it can be $e^T Pb = e^T p_n b$ known from $b = [0,\cdots,0, b]^T$, and then, formula (21) becomes

$$\dot{V} = -\frac{1}{2}e^T Qe + \frac{b}{r}(\theta^* - \theta)^T\left[\gamma e^T p_n\xi(x) - \dot{\theta}\right] - e^T p_n b\omega. \tag{22}$$

Make adaptive law:

$$\begin{aligned}\dot{\theta} &= \gamma e^T p_n\xi(x),\\ \dot{V} &= -\frac{1}{2}e^T Qe - e^T p_n b\omega.\end{aligned} \tag{23}$$

Since $Q > 0$ and ω are the minimum approximation errors, by designing a fuzzy system$u_D(x|\theta)$ with enough rules, ω can be made sufficiently small and satisfy $|e^T p_n b\omega| \langle (1/2)e^T Q$, so that $\dot{V}\langle 0$.

The structure of the direct adaptive fuzzy control system is shown in Figure 4.

3.4. Simulation Discussion. The simulation of sludge conditioning and pressing can generally be defined as a first-order inertia plus pure lag link model. The sludge screw pressing process is affected by the fluctuation of sludge concentration, the different viscosity of materials in the wastewater, the structural characteristics of variable pitch and diameter, and the dewatering process. Therefore, the control system of the dewatering machine is nonlinear and time-lag, which can easily lead to the blockage of the dewatering machine and the unstable concentration of the discharged sludge.

This paper studies the sludge dewatering process and designs an adaptive fuzzy control algorithm suitable for sludge dewatering. The transfer function of the controlled object and the disturbance channel is $P_1 = P_{d1} = e^{-10s}/100s + 1$ and $P_2 = P_{d2} = 2e^{-2s}/20s + 1$. The input pressure is $x_d(t) = \sin(t)$. Take the following five membership functions to fuzzify the input x_i of the fuzzy system:$\mu_{NM}(x_i) = \exp[-((x_i + \pi/3)/(\pi/12))^2]$, $\mu_{NS}(x_i) = \exp[-((x_i + \pi/6)/(\pi/12))^2]$, $\mu_Z(x_i) = \exp[-(x_i/(\pi/12))^2]$, $\mu_{PS}(x_i) = \exp[-((x_i - \pi/6)/(\pi/12))^2]$, and $\mu_{PM}(x_i) = \exp[-((x_i - \pi/3)/(\pi/12))^2]$. Then, there are 25 fuzzy rules for approximating f. According to the membership function design program, the membership function diagram can be obtained, as shown in Figure 5.

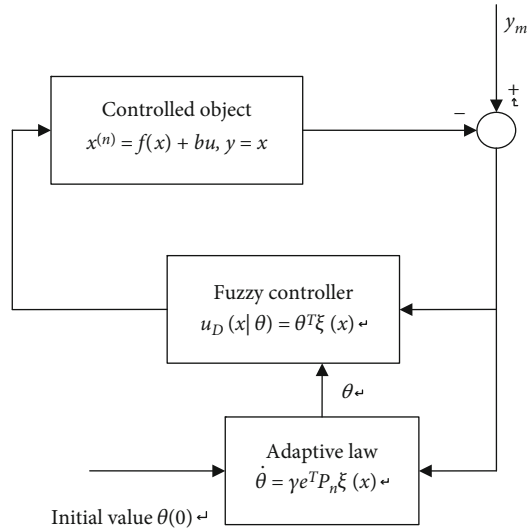

Figure 4: Direct type adaptive fuzzy control.

After analyzing the input and output characteristics of the actual control system, it is concluded that the transfer function of sludge conditioning and pressing is approximated as a first-order inertia plus pure lag link model. The step response curve of the above fuzzy control system is shown in Figure 6. For analysis and comparison, the control effect of the above system and the traditional PID control effect are placed in a coordinate system. From the system simulation curve, the system response curve of the PID controller has overshoot and the transition time is relatively long, while the system response curve of the fuzzy controller is relatively stable and has no overshoot.

Using the adaptive fuzzy algorithm above, real-time control is realized by computer. According to the deviation and the fluctuation, the fuzzy control rules are used to determine the electrical output, so as to obtain a good control effect, which has the following characteristics:

(1) Compared with the control effect of the ordinary PID controller, the system response overshoot is small after the adaptive fuzzy controller is adopted, and the response curve is stable

(2) The system has good response speed, stability, and accuracy and has strong robustness

(3) The three parameters determined by the fuzzy control rules are dynamic, which is more in line with the control characteristics of the system

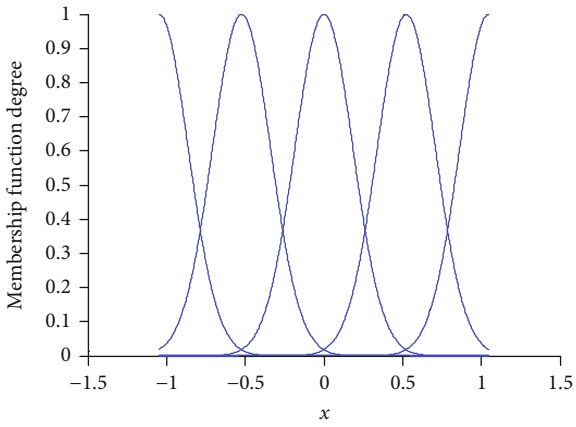

Figure 5: Membership function of x_i.

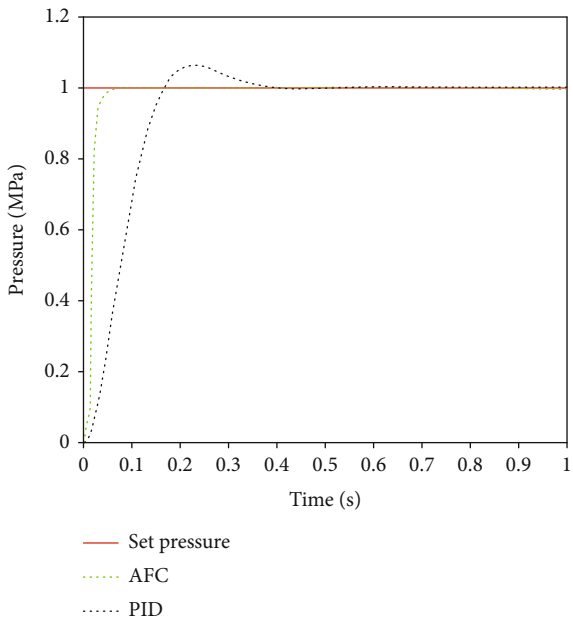

Figure 6: Pressure control response curve.

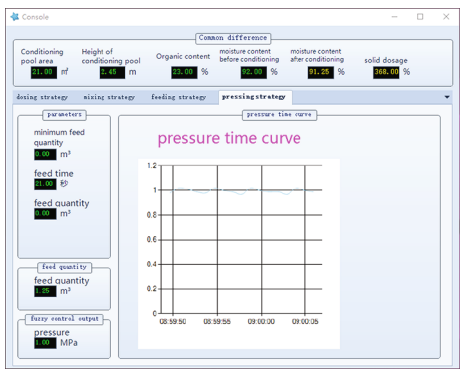

Figure 7: Press interface and time pressure curve.

4. Control System Composition

The adaptive fuzzy control algorithm of this project is developed by the host computer using high-level language programming. The entire control system consists of two parts: measurement and control subsystem and execution subsystem. The measurement and control subsystem is responsible for completing the collection of on-site data and generating dynamically adjustable dosing amount and feeding pressure according to the adaptive fuzzy control algorithm and sends the speed regulation command to the frequency converter for control. The execution subsystem is composed of PLC and control motor, to communicate between fuzzy control software and field PLC through standard Ethernet communication protocol.

The main pressure control is divided into feeding control and pressing control. Generally, the feeding pressure shall not exceed 0.45 MPa, and the thickness or volume of the filter cake formed by the feeding shall not exceed the specified value.

4.1. Feed Control Strategy. Collect the organic substance content of each batch after treating the sludge, and calculate the feed volume according to the measured sludge moisture content, dosing amount, and the water content of the batch of sludge after dosing. The feeding time is set (usually 90 minutes), and the adaptive fuzzy control is used for subfeeding according to the actual feeding pressure, and the feeding pressure is automatically adjusted to reduce the energy consumption of the system. Input the parameters required by the system: minimum feeding amount, feeding time, feeding material, running time, and other parameters. The fuzzy control system will output the segmented feeding control pressure according to the input parameters.

4.2. Squeeze Control Strategy. By monitoring the liquid level of the conditioning tank in real time, when the liquid level drops to the set value after the feeding is completed, the water content of the sludge after dosing can be used to calculate the liquid level that needs to be lowered in the conditioning tank. The amount of material to choose the controlled pressing pressure and pressing time, to control the press, and the pressure control curve is shown in Figure 7.

In the process of sludge adjustment and pressing, the traditional PID automatic control mode and adaptive fuzzy control mode are used to control the operation of the sludge treatment equipment, and the power consumption during the operation of the equipment is evaluated and compared. The power consumption of the equipment mainly includes sludge feeding process, conditioning process, pressing process, and sludge conveying process. The comparative analysis is shown in Table 1.

According to the statistics in the above table, when the complete set of sludge treatment equipment is operated under the traditional PID control mode and the adaptive fuzzy control mode, except for the sludge conveying system, the latter save nearly 11% of the total cost of electricity.

Table 1: Comparative analysis of power consumption.

Category	Technological process	PID control	Adaptive fuzzy control	Saving ratio
Power consumption (kW·h/batch)	Sludge feeding	0.60	0.52	13.3%
	Conditioning	8.02	7.14	11.0%
	Press	7.6	6.72	11.6%
	Sludge transportation	0.80	0.80	0.0%
	Total	17.02	15.18	10.8%
Electricity cost (RMB yuan/t)	Total	18.24	16.26	10.9%

Note: the unit price of electricity is calculated as 0.75 yuan/kw · h, the treatment capacity of each batch is calculated as 0.70 t, and the sludge volume is calculated as 80% moisture content.

5. Summary

In this paper, the design and implementation of an adaptive fuzzy control system for the sludge conditioning and pressing process is completed, which is superior to the traditional PID control method. Fuzzy control is controlled according to the experience of experts, the control is intelligent and flexible, and it can control the system in real time accurately. The control process is simple and effective. Compared with the traditional controller, it has the advantages of small overshoot and small steady-state error. And for different control objects, without changing the parameters, all achieved better control effect. Through real-time dynamic detection and self-adaptive control of each batch of sludge volume and mud quality and use of fuzzy expert control technology to establish a control model to dynamically control and adjust the conditioning process, the equipment can be operated on demand, so as to reduce the overall energy consumption of the system and save energy. With the continuous in-depth research and development of fuzzy control technology, it will definitely open up new application prospects for industrial process control, environmental protection, and control in the fields of sewage sludge.

This paper studies the self-adaptive fuzzy control method of sludge conditioning and pressing in sewage plant, in order to reduce production energy consumption. On the other hand, the historical data of the operation of the sewage treatment system is accumulating, and many important information is hidden behind these data. It is important to understand the hidden knowledge, potential relationships, and rules behind the data from a large number of highly coupled historical data. In the next step, we will deeply study the coupling relationship between dissolved oxygen and total sludge, combine the control of dissolved oxygen with the control of total sludge, and then study the sludge reduction control method in the sewage treatment process.

Data Availability

All data, models, and code generated or used during the study appear in the submitted article.

Conflicts of Interest

The author declares no conflicts of interest.

Acknowledgments

This work was supported by the Guangzhou Youth Science and Technology Education Project (KP 2022157) and a support from the Intelligent Control Application Innovation Team in Guangzhou Vocational Colleges.

References

[1] H. Wei, B. Gao, J. Ren, A. Li, and H. Yang, "Coagulation/flocculation in dewatering of sludge: a review," *Water Research*, vol. 143, pp. 608–631, 2018.

[2] Y. Li, L. Pan, Y. Zhu et al., "How does zero valent iron activating peroxydisulfate improve the dewatering of anaerobically digested sludge?," *Water Research*, vol. 163, article 114912, 2019.

[3] S. Skinner, L. J. Studer, D. R. Dixon et al., "Quantification of wastewater sludge dewatering," *Water Research*, vol. 82, pp. 2–13, 2015.

[4] M. L. Christensen, K. Keiding, P. H. Nielsen, and M. K. Jørgensen, "Dewatering in biological wastewater treatment: a review," *Water Research*, vol. 82, pp. 14–24, 2015.

[5] A. G. Sheik, S. M. Mohan, and A. S. Rao, "Fuzzy logic control of active sludge-based wastewater treatment plants," in *Soft Computing Techniques in Solid Waste and Wastewater Management*, R. R. Karri, G. Ravindran, and M. H. Dehghani, Eds., pp. 409–422, Elsevier, 2021.

[6] M. Wójcik and F. Stachowicz, "Influence of physical, chemical and dual sewage sludge conditioning methods on the dewatering efficiency," *Powder Technology*, vol. 344, pp. 96–102, 2019.

[7] L. X. Wang, *Adaptive Fuzzy Systems and Control: Design and Stability Analysis*, Prentice-Hall, New Jersey, USA, 1994.

[8] T. Javanbakht and S. Chakravorty, "Prediction of human behavior with TOPSIS," *Journal of Fuzzy Extension and Applications*, vol. 3, no. 2, pp. 109–125, 2022.

[9] H. Garg, S. A. Edalatpanah, S. El-Morsy, and H. A. El-Wahed Khalifa, "On stability of continuous cooperative static games with possibilistic parameters in the objective functions," *Computational Intelligence and Neuroscience*, vol. 2022, Article ID 6979075, 10 pages, 2022.

[10] U. Bulut and E. Ozceylan, "Application of the fuzzy inference system to evaluate the quality of air textured warp yarn," *Journal of Fuzzy Extension and Applications*, vol. 3, no. 1, pp. 31–44, 2022.

[11] S. Arora, R. Vadhera, and B. Chugh, "A decision-making system for Corona prognosis using fuzzy inference system," *Journal of Fuzzy Extension and Applications*, vol. 2, no. 4, pp. 344–354, 2021.

[12] T. Chen, I. Karimov, J. Chen, and A. Constantinovitc, "Computer and fuzzy theory application: review in home appliances," *Journal of Fuzzy Extension and Applications*, vol. 1, no. 2, pp. 133–138, 2020.

[13] S. V. Patil and B. N. Thorat, "Mechanical dewatering of red mud," *Separation and Purification Technology*, 2022.

[14] H. Budiarto and A. Dafid, "Design and development of fuzzy logic control systems on bottled drinking water pressing equipment," *IOP Conference Series Materials Science and Engineering*, vol. 1125, no. 1, article 012057, 2021.

[15] L. Swierczek, B. M. Cieślik, and P. Konieczka, "The potential of raw sewage sludge in construction industry - a review," *Journal of Cleaner Production*, vol. 200, pp. 342–356, 2018.

[16] B. Bień and J. D. Bień, "Dewatering of sewage sludge treated by the combination of ultrasonic field and chemical methods," *Desalination and Water Treatment*, vol. 199, pp. 72–78, 2020.

[17] B. Bień and J. D. Bień, "Analysis of reject water formed in the mechanical dewatering process of digested sludge conditioned by physical and chemical methods," *Energies*, vol. 15, no. 5, p. 1678, 2022.

[18] J. T. Novak, "Dewatering of sewage sludge," *Drying Technology*, vol. 24, no. 10, pp. 1257–1262, 2006.

[19] G. Feng, W. Tan, Y. Geng, Z. He, and L. Liu, "Optimization study of municipal sludge conditioning, filtering, and expressing dewatering by partial least squares regression," *Drying Technology*, vol. 32, no. 7, pp. 841–850, 2014.

[20] M. Kowalczyk and T. Kamizela, "Artificial neural networks in modeling of dewaterability of sewage sludge," *Energies*, vol. 14, no. 6, p. 1552, 2021.

[21] G. Raman, M. S. Klima, and J. M. Bishop, "Pressure filtration: bench-scale evaluation and modeling using multivariable regression and artificial neural network," *International Journal of Mineral Processing*, vol. 158, pp. 76–84, 2017.

[22] T. Zhang, S. S. Ge, and C. C. Hang, "Stable adaptive control for a class of nonlinear systems using a modified Lyapunov function," *IEEE Transactions on Automatic Control*, vol. 45, no. 1, pp. 129–132, 2000.

[23] G. Mininni, L. Spinosa, and V. Lotito, "Cost optimization of sewage sludge filterpressing," *Water Science and Technology*, vol. 23, no. 10-12, pp. 2001–2009, 1991.

[24] Y. Liu, S. Tong, and W. Wang, "Adaptive fuzzy output tracking control for a class of uncertain nonlinear systems," *Fuzzy Sets and Systems*, vol. 160, no. 19, pp. 2727–2754, 2009.

[25] L. Yang, G. Wang, H. Zhang, J. Liu, and Y. Zhang, "Pressing speed stability control of a special ceramic roller bearing press based on fuzzy adaptive PID," *Journal of Computational Methods in Sciences and Engineering*, vol. 2, pp. 1–16, 2021.

Hindawi
Advances in Mathematical Physics
Volume 2022, Article ID 9431846, 12 pages
https://doi.org/10.1155/2022/9431846

Research Article

A Stochastic Approach Analysing Enterprises' Investment following Financing Reform in China

Shuxing Xiao,[1,2] Guangliang Li,[3] Weikun Zhang,[4] Mingming Zhou,[5] and Wolin Zheng[6]

[1]*School of Public Administration and Law, Hunan Agricultural University, Changsha, China*
[2]*School of Teacher Education, Shaoguan University, Shaoguan, China*
[3]*School of Economics & Management, Shanghai Ocean University, Shanghai, China*
[4]*Mangrove Institute, Lingnan Normal University, Zhanjiang, China*
[5]*School of Economics, Jiaxing University, Jiaxing, China*
[6]*School of Credit Management, Guangdong University of Finance, Guangzhou, China*

Correspondence should be addressed to Weikun Zhang; weikunz@sids.org.cn and Mingming Zhou; zhoumingming66@126.com

Received 16 May 2022; Revised 13 June 2022; Accepted 6 July 2022; Published 1 August 2022

Academic Editor: S. E. Najafi

This paper explores the change of enterprises' investment following the financing system reform through the established stochastic investment model. In this constructed model, financing property, market-oriented reform, and government intervention are regarded as a stochastic process. Furthermore, the modern China's economic situation is interpreted to analyze the enterprises' investment by government intervention plan combined with he deduced proposition from the stochastic investment model. The results provide a depth understanding for characteristics of the enterprise in China that the steady capital of state-owned enterprises' investment is higher than that of non-state-owned enterprises without government intervention before completing financing reform. Although government intervention can increase the investment level of state-owned enterprises, doing so increases the turbulence of the market economy. Additionally, the impact of government-led financing reform on enterprises' investment is asymmetrical. Promoting market-oriented, clear-cut financing reform, and reducing government-led investment plans will improve enterprises' investment efficiency and stabilize China's economic development. The present paper provides a specific future orientation of China's financing reform determining the level of enterprises' investment.

1. Introduction

China is a country with consumer power shortage, and its economic growth mainly depends on corporate investment. China can increase corporate investment through financing reform so as to get through the crisis smoothly, when the market environment is in a slump. The financing reform increased the potential output of enterprises and made economic development more resistant to economic shocks [1]. But financing reform also has some shortcomings such as placing some enterprises lacking political connection under huge financial burden due to unfair institutional contracts [2]. Yet, existing studies on enterprise investments have not identified the mechanism by which financing reform changes enterprise investment behavior.

Previous studies have shown that the financing reform by government might distort the level of enterprises' investment due to political intervention, resulting in inefficient investment [3–5]. Enterprise managers may abuse freer cash flow for overinvestment, leading to more inefficient investments [6, 7]. Other studies have shown that the financing reform was valuable in promoting efficient enterprises' investment during the financial crisis [8–11], which can better remedy market failures and compensate for inefficient market allocation [12, 13]. Financing reform can better ensure reform in enterprises' investment and economic growth faced with economic recession and external shocks,

which may result in a national fiscal deficit in the short term, but improve the output of enterprises and employment in the medium term and generate a huge fiscal surplus in the long run [14]. With the development of a market-oriented system, the rewarding priority of reform would bring the knowledge transfer spillovers [15].

This paper first attempts to build a new stochastic investment model to evaluate the consequence of the government-based financing reform. When the economic institution is relatively simple, the level can be adjusted through financing reform if something goes wrong. However, when the economic institution is more complicated, this transaction cost of correcting course is too large. In the past, many economic problems and social contradictions have been solved by massive investment expansion. If the economic growth rate declines, many contradictions and problems were revealed due to declining capital returns from enterprises' investment. The enterprise investment is related to the state administrative institution [16]. So, due to the random volatility of China's policy plan, China's financing reform defers to the Markov process containing the correction mechanism with independent increments; that is, the factor of this reform consists of the institutional constant, correction mechanism, and white noise, making deterministic quantization of financing reform difficult.

An answer to identify the enterprises' investment efficiency is relevant to the considerations for China's external capital and the government intervention-oriented plan. Based on the assumption that external capital has infinite flexibility, enterprise financing has depended to some extent on its demand for debt [17]. Unfortunately, China's capital markets, especially the stock market and bond market, were relatively unsophisticated, and bank credit has been the main source of financing for Chinese enterprises [18, 19]. If the Chinese central government intervened in enterprises' investment in response to economic depression, it would loosen the bank credit supply by implementing economic stimulus plans and release more liquidity to the market to remedy the failure of the capital market [9, 10, 11, 20]. However, Liu et al. pointed out that this policy mechanism is of great significance to the investment of state-owned enterprises, but not significant in non-state-owned enterprises' investment [21]. Despite increasing the investment in state-owned enterprises, the financing system may fail to maintain the effectiveness of these investments from state-owned ones, thus leading to overcapacity from expanding production due to government intervention. In China, there are double atrophy of output and investment in state-owned enterprises and double rise in output and investment in non-state-owned enterprises [22]

Also, the paper differentiates the state- and non-state-owned enterprises' investment function from macroenterprise investments. In China, non-state-owned enterprise is subject to unfair discrimination compared to state-owned one with which the state power has a good relationship. Although individual non-state-owned enterprises maintain a relationship with state-owned banks or governments, their ability to obtain information is less than that of state-owned enterprises; they also suffer from the discriminatory treatment of bank credit, in which banks are reluctant to lend to non-state-owned enterprises for investment [23, 24]. Even if non-state-owned enterprises is lent based on reliable business judgments [25], depending on their reputation, most of the credit goes to state-owned enterprises [21, 26]. In the case of incomplete social information, state-owned enterprises increase their level of investment, and more investments are based on private interests or the trend to crony capitalism rather than economies of scale. Wang et al. pointed out that the government may use political power to control state-owned enterprises to achieve private goals [27]. Government intervention creates market distortions under certain circumstances and leads to improper allocation of market resources [28, 29].

This paper relaxes the assumption for the certainty of the economic situation, namely, the accurate known and predicted economic status, and views the financing as a Brownian movement condition. There are inherent unobservable noneconomic fluctuations [30, 31]; that is, an economic entity cannot predict the fluctuation of economic conditions caused by disturbances in the process of economic development, and such disturbances change the information set of enterprises for future economic investment output. Truly, there are macroeconomic uncertainties in the process of financing institution reform. If the reform decision-making adjustment cost function is nonconvex, some irreversible government-led investment projects will increase the real option value of enterprise investment [32]. The uncertainty in institutional reforms, namely, the unknown and unpredicted economic consequence resulting from financing reform, can lead to an increase in the market risk premium, so that a rise in risk premiums increases corporate financing costs or difficulties and has a significant negative impact on enterprise investment [33]. In addition, the return on capital also increases with the rise in the financing cost, so the drive to perform the investment will decline, and cash holdings will tend to increase, resulting in a liquidity preference or ambiguity aversion behavior [34, 35].

This paper contributes to the growing body of literature on enterprise investment following financing reform by providing novel insights into the mechanism of enterprises' investment. The enterprises' investment effect by financing reform is reconstructed to investigate the role of government intervention through the built stochastic investment model with the consideration for the uncertainty from the economic consequence produced by institutional arrangement. Existing researches are based on the influence mechanism of financing reform and enterprise investment in developed Western capitalist countries and rarely consider the relationship between the financing reform in this particular economy and enterprise investment. The central role of China's state-owned enterprises means that its economic development is very different from western developed capitalist countries. Opportunistic behaviors such as political corruption and rent-seeking are inevitable, and distortion of market resource allocation may lead to biased corporate investment. Therefore, this paper focuses on the financing system and the random fluctuation of the reform process

and explores the relationship between the financing reform and the enterprise investment level in China.

The rest of the paper is organized as follows. The second part establishes the stochastic investment model following the financing reform; the third part solves the model and obtains the investment level of the enterprise in the steady state and the enterprise investment in the process of financing reform. The fourth part further explores changes in levels of investment in combination with China's economic development and provides a deeper deconstruction of the "structural imbalance" of the current depressed Chinese economy using propositions derived from the third part. The fifth part is the conclusion.

2. Model

2.1. The Basic Model of Enterprises' Investment. Enterprises in China, especially state-owned enterprises, have different business objectives due to the special arrangement of the property rights system, which goes beyond the maximization of profits (i.e., the sales income of enterprises minus the operating cost of raw materials) as in the West, or the maximization of outputs. It is a common practice to expand investment scale and production capacity to win political benefits because of the objectives of state-owned enterprise management (since the equilibrium prices of market commodities were unknown during China's planned economy era, the SOEs chose a quantitative index with the maximizations of their output instead of a market profit or income. Furthermore, SOE managers with correlated administrative levels at the company level sought a strong incentive to maximize productions due to the returns on companies' control property rights. For the SOE, expanding the investment scale is the common method winning the political asset (Li, 2006)). Considering that state-owned enterprises with output maximization as their quantitative objective have the dual objective of profits and production, the profit function of state-owned enterprises expressed as an instantaneous profit function is $pf(K,L) - C(K,L,I)$, where $f(\cdot)$ and $C(\cdot)$ represent production function and cost function, with p, K, L, and I representing relative prices, capital, labor, and investment related to product production. $(\theta - 1)pf(K,L)$ represents the production objective of enterprises. $\theta \geq 1$ measures the impact of property rights on firms' operations. When $\theta = 1$, property rights reform is completed. The bigger θ is, the lower the marketization from property rights reform. The actual financing cost can be characterized by the relative price of finished goods to capital goods implicit in China. We modeled χ ($\chi \geq 1$) as the commercialization of banks. When $\chi = 1$, the commercialization of banks is complete, and soft constraints are gone. The bigger the χ, the lower the commercialization of banks and the stronger the impact of soft constraints.

Of course, every aspect of economic life in China, especially dependence on government's top-down planning, involves government intervention. The government in China, according to its judgment of the economic situation, exercises its management power over state-owned enterprises and intervenes in their operation at its discretion either through administration or direction. State-owned enterprises in China are at present still subordinate to the administrative management of SASAC (State-owned Assets Supervision and Administration Commission), so the intervention of government administrative power will inevitably affect the operation of enterprises. If the government wishes to pursue rapid national economic development and requires the cooperation of state-owned enterprises, state-owned enterprises need to accomplish certain quantitative tasks, although doing so may violate the interests of state-owned enterprises. λ ($\lambda > 0$) is used for the measurement of government intervention. If $\lambda > 1$, the government hopes to expand its capacity; otherwise, the government imposes limitations over the operation of enterprises. Therefore, we have the following decision objective:

$$\lambda\chi\theta pf(K,L) - C(K,L,I), \quad \lambda > 0, \chi \geq 1, \theta \geq 1. \tag{1}$$

The difference in state- and non-state-owned enterprises is their business objectives and financing costs, so the specific modeling must be carried out in different areas for state- and non-state-owned enterprises. If two types of enterprises are assumed to have the same production technology, the investment behavior of non-state-owned enterprises could be regarded as a special case of the state-owned enterprise model; for instance, $\lambda = \chi = \theta \equiv 1$. Because non-state-owned enterprises are not administratively regulated by the Chinese government, which holds surplus control over many banks, they without the benefits of low-interest bank credit have only one profit goal to make market profits rather than political profits. Therefore, we discuss non-state-owned enterprises as a special case of state-owned enterprises, when $\lambda = \chi = \theta \equiv 1$.

2.2. The Stochastic Process Setting. A continuous time uncertain investment model is usually characterized by a random process. This paper divides the randomness into two parts: the stochastic process setting and its correlation.

It is necessary to analyze the characteristics of China's economic transformation, among which gradual reform is China's overall reform idea, including reform of the property rights system and the commercialization of banks. The miracle of China in the past 40 years of reform and opening-up demonstrates that the most worthwhile reform approach is at exploring methods guided by asymptotic market-oriented reform through government intervention. China's reform process, in fact, includes random disturbances called stochastic deviations. The benchmark, under the condition of complete marketization with the relative price of finished goods to capital goods, property rights reform, and bank commercialization reform through government intervention, is analyzed in accordance with the following geometric Brownian motion equations.

$$dp_t = \mu_p p_t dt + \sigma_p p_t dz_p, \tag{2}$$

$$d\theta_t = \mu_\theta \theta_t dt + \sigma_\theta \theta_t dz_\theta, \tag{3}$$

$$d\chi_t = \mu_\chi \chi_t dt + \sigma_\chi \chi_t dz_\chi, \tag{4}$$

$$d\lambda_t = \mu_\lambda \lambda_t dt + \sigma_\lambda \lambda_t dz_\lambda, \tag{5}$$

where μ_p, μ_θ, μ_χ, and μ_λ and σ_p, σ_θ, σ_χ, and σ_λ are constants that represent drift rate and variance rate concerning relative price, property design, commercialization of bank reform, and government intervention. dz_p, dz_θ, dz_χ, and dz_λ are set in accordance with standard Brownian motion. It is worth noting that there may be uncertainties about labor productivity in a real-life economy, but to simplify this model, stochastic changes are reflected in the random process of relative price of finished goods to capital goods variable p. It is a kind of "real price" with labor productivity or that of "relative price" compared with cost price. If China's economic transformation still adheres to reform and opening up over the long term, μ_θ and μ_χ should be less than 0, which indicates that property rights reform for state-owned enterprises has improved in the direction of the modern enterprise system, with state-owned commercial banks more and more commercialized but less affected by institutional factors. The government has no policy rules in the early stages of reform, only depending on history in the formulation and operation of policies according the actual situation, so μ_λ can be arbitrary, positive or negative, and its sign can be heterogeneous at different times.

The profits of enterprises in Equation (1) mainly come from the following three aspects:

(1) $\theta\chi$, the institutional arrangement

(2) λ, government policy decisions based on its financial status

(3) p, pure economic factors

Parameter correlations in Equations (2)–(5) can be classified into four categories. On one hand, assuming that dz_λ, dz_χ, and dz_θ have no correlation with dz_p, if $X \in (\lambda, \chi, \theta)$, the correlation coefficient is $\rho(dz_X, dz_p) = E[(dz_X - E(dz_X))(dz_p - E(dz_p))]/(\text{var}\,(dz_X)\,\text{var}\,(dz_p))^{1/2} \equiv E(dz_X dz_p)/dt$ with $E(dz_X) = E(dz_p) \equiv 0$ and $\text{var}\,(dz_X) = \text{var}\,(dz_p) \equiv dt$ due to dz in accordance with standard Brownian motion. On another hand, given that the property rights system will affect the dual goal decision-making of state-owned enterprises, and government intervention is defined as the direct administrative meddling of the government in enterprises, there is a relationship between voluntary decision-making and administrative order with $\rho(dz_\theta, dz_\lambda) = 0$, but it is possible that state-owned enterprises remain "loyal" to the government with $\rho(dz_\theta, dz_\lambda) > 0$, and we do not set $\rho(dz_\theta, dz_\lambda) > 0$ to avoid reinforcing the latter conclusion. There are still some positive correlations between λ and χ due to government management between state-owned enterprises and state-owned banks. If the outcome of the government's discretion is to stimulate investment and the economy, it would require the cooperation of state-owned enterprises and state-owned banks. When state-owned enterprises hope to stabilize product returns with the increase of λ, the state-owned banks will provide more credit under government pressure and also will be motivated to ease credit for state-owned enterprises with the increase of χ, so $\rho(dz_\lambda, dz_\chi) > 0$. The current state of the Chinese economy in the Sino-US trade war proves that the central bank has lowered its benchmark to implement a looser monetary policy, with the main credit flowing to state-owned enterprises.

(1) θ depends on the arrangement of the property rights of state-owned enterprises and the behavior characteristics of state-owned enterprises themselves

(2) χ depends on the mechanism of "rotten meat in the pot" and state-owned banks themselves

So, $\rho(dz_\chi, dz_\theta) = 0$.

In general, relaxing this assumption does not affect the conclusion of mathematical derivation in this paper, and we can conclude the following:

$$\rho_{\chi,p} = \rho_{\theta,p} = \rho_{\lambda,p} = \rho_{\theta,\lambda} = \rho_{\theta,\chi} \equiv 0\, \rho_{\lambda,\chi} > 0, \text{ where } \rho_{X,Y} = \frac{E(dz_X, dz_Y)}{dt}. \tag{6}$$

3. Model Solution and Related Propositional Deduction

3.1. Model Solution. Consider a representative state-owned enterprise whose production function is Cob-Douglas, $F_s L_s^a K_s^{1-a}$, while the cost of investment is $C(I) = \gamma I^\beta$ and $\beta > 1$ with no correlation between investment cost and investment stock, $C_K{}' = 0$. Following Equations (1)–(6), let $F \equiv \lambda\theta\chi p$. Given state variable K_t (capital stock) and F_t (including current institutional arrangement $\theta_t\chi_t$, government intervention λ_t, and pure economic factor p_t), state-owned enterprises make investment decisions to maximize the expected discounted present value $V(\cdot)$ of the income stream or investment under their dual objectives. Therefore, the maximum value function in the case of uncertainty is

$$V(K_t, F_t) = \max_{I_s, L_s} E_t \int_t^{+\infty} e^{-r(s-t)} \left[F_s L_s^a K_s^{1-a} - wL_s - \gamma I_s^\beta \right] ds, \tag{7}$$

$$\text{s.t.} dK_t = (I - \delta K_t)dt, \tag{8}$$

where w is wages and r is interest rate. δ is capital discount rate, and E_t is the expectation operator of this value function. The stochastic Bellman equation for this optimization problem is

$$rV(K_t, F_t)dt = \max_{I_t, L_t} \left[F_t L_t^a K_t^{1-a} - wL_t - \gamma I_t^\beta \right] dt + E_t(dV). \tag{9}$$

Using Ito's Lemma, we obtain

$$dV = V_K dK + V_F dF + \left(\frac{1}{2}\right) V_{KK}(dK)^2 + \left(\frac{1}{2}\right) V_{FF}(dF)^2 + V_{FK}(dF)(dK). \tag{10}$$

V_K and V and V_{KK} and V_{FF} are the first and second derivatives of subscript variables, and $V_{FK} = \partial^2 V/(\partial F \partial K)$.

Because $F \equiv \lambda\theta\chi$p, we can obtain with Ito's Lemma:

$$\begin{aligned} dF = {} & F_\lambda d\lambda + F_\theta d\theta + F_\chi d\chi + F_p dp + \left(\frac{1}{2}\right) \\ & \cdot \left[F_{\lambda\lambda}(d\lambda)^2 + F_{\theta\theta}(d\theta)^2 + F_{\chi\chi}(d\chi)^2 + F_{pp}(\mathrm{dp})^2\right] \\ & + F_{\lambda\theta}(d\lambda)(d\theta) + F_{\chi\lambda}(d\lambda)(d\chi) + F_{\lambda p}(d\lambda)(dp) \\ & + F_{\theta\chi}(d\theta)(dp) + F_{\chi P}(d\chi)(dp). \end{aligned} \tag{11}$$

$F_X = \partial F/\partial X$, with Equations (3)–(5), we obtain:

$$F_X dX = F\mu_X dt + F\sigma_X dz_X. \tag{12}$$

Because $(dt)^2 = (dt)(dz_X) \equiv 0$ and $(dz_X)^2 = dt$,

$$\begin{aligned} F_{XX}(dX)(dY) &= \frac{F}{(XY)}(\mu_X X_t dt + \sigma_X X_t dz_X) \\ &\quad \cdot (\mu_Y Y_t dt + \sigma_Y Y_t dz_Y) \\ &= F\sigma_X\sigma_Y dz_X dz_Y. \end{aligned} \tag{13}$$

With $F_{XX} = 0$, Equation (12) and equation (13) can be substituted into Equation (11), and we obtain:

$$\begin{aligned} dF = {} & F\left(\mu_\lambda + \mu_\theta + \mu_\chi + \mu_p\right) dt + F\left(\sigma_\lambda dz_\lambda + \sigma_\theta dz_\theta \right. \\ & \left. + \sigma_\chi dz_\chi + \sigma_p dz_p\right) + F\left(\sigma_\lambda\sigma_\chi dz_\lambda dz_\chi \right. \\ & \left. + \sigma_\lambda\sigma_p dz_\lambda dz_p + \sigma_\theta\sigma_\chi dz_\theta dz_\chi + \sigma_\chi\sigma_p dz_\chi dz_p\right). \end{aligned} \tag{14}$$

With $(dt)^2 = (dt)(dz_X) = 0$, $(dz_X)^2 = dt$

$$\begin{aligned} (dF)^2 &= F^2\left(\sigma_\lambda dz_\lambda + \sigma_\theta dz_\theta + \sigma_\chi dz_\chi + \sigma_p dz_p\right)^2 \\ &= F^2\left(\sigma_\lambda^2 + \sigma_\theta^2 + \sigma_\chi^2 + \sigma_p^2\right) dt + 2F\left(\sigma_\lambda\sigma_\theta dz_\lambda dz_\theta \right. \\ &\quad + \sigma_\lambda\sigma_\chi dz_\lambda dz_\chi + \sigma_\lambda\sigma_p dz_\lambda dz_p + \sigma_\chi\sigma_\theta dz_\chi dz_\theta \\ &\quad \left. + \sigma_p\sigma_\theta dz_p dz_\theta + \sigma_\chi\sigma_p dz_\chi dz_p\right). \end{aligned} \tag{15}$$

According to Equation (8), $dK = (I - \delta K)dt$, $(dK)^2 = (I - \delta K)^2(dt)^2 = 0$, and $(dK)(dF) = (I_t - \delta K_t)(dt)(dF) = 0$.

With Equation (8), Equation (14) and Equation (15) can be substituted into Equation (10), and using $E_t(dz_X) = (dt)^2 = (dt)(dz_X) = 0$, we obtain:

$$\begin{aligned} E_t(dV) = {} & \left[(I_t - \delta K_t)V_K + F\left(\mu + \rho_{\lambda,\chi}\sigma_\lambda\sigma_\chi\right)V_F \right. \\ & \left. + \left(\frac{1}{2}\right)F_t^2\left(\sigma^2 + 2\rho_{\lambda,\chi}\sigma_\lambda\sigma_\chi\right)V_{FF}\right] dt, \end{aligned} \tag{16}$$

where $\mu \equiv \mu_\lambda + \mu_\theta + \mu_\chi + \mu_p$ and $\sigma^2 \equiv \sigma_\lambda^2 + \sigma_\theta^2 + \sigma_\chi^2 + \sigma_p^2$. If Equation (16) is substituted into Equation (9), eliminating dt, we get

$$\begin{aligned} rV(K_t, F_t) = \max_{L_t, I_t}\Big\{ & \left(F_t L_t^a K_t^{1-a} - wL_t - \gamma I_t^\beta\right) \\ & + (I_t - \delta K_t)V_K + \left(\mu + \rho_{\lambda,\chi}\sigma_\lambda\sigma_\chi\right)FV_F \\ & + \left(\frac{1}{2}\right)F^2\left(\sigma^2 + 2\rho_{\lambda,\chi}\sigma_\lambda\sigma_\chi\right)V_{FF}\Big\}, \end{aligned} \tag{17}$$

where $\mu \equiv \mu_\lambda + \mu_\theta + \mu_\chi + \mu_p$ and $\sigma^2 \equiv \sigma_\lambda^2 + \sigma_\theta^2 + \sigma_\chi^2 + \sigma_p^2$.

The first-order condition for in Equation (7) is

$$\gamma\beta I^{\beta\text{-}1} = V_K. \tag{18}$$

And the first-order condition for L in Equation (7) is

$$aF_t L_t^{a-1} K_t^{1-a} = w. \tag{19}$$

So,

$$\max_{L_t}\left\{F_t L_t^a K_t^{1-a} - wL_t\right\} = hF_t^{1/(1-a)}K_t,, \tag{20}$$

where $h = (1-a)(a/w)^{a/(1-a)}$. Substituting into Equation (17) with Equation (18) and Equation (20), we obtain

$$\begin{aligned} rV(K_t, F_t) = {} & hF_t^{1/(1-a)}K_t + (\beta - 1)\gamma I_t^\beta - \delta K_t V_K \\ & + \left(\mu + \rho_{\lambda,\chi}\sigma_\lambda\sigma_\chi\right)F_t V_F \\ & + \left(\frac{1}{2}\right)F_t^2\left(\sigma^2 + 2\rho_{\lambda,\chi}\sigma_\lambda\sigma_\chi\right)V_{FF}. \end{aligned} \tag{21}$$

Let $V_K \equiv q$ represents the shadow price of capital, and we obtain the second-order partial differential equation of

$$V(K_t, F_t) = q(F)K + G(F), \tag{22}$$

where $q(F)$ and $G(F)$ is the function of F. With Equation (22) and $V_K \equiv q$ substituted into Equation (21), we obtain

$$\begin{aligned} rq(F)K_t + rG(F) = {} & hF_t^{1/(1-a)}K_t + (\beta - 1)\gamma I_t^\beta - \delta K_t q + \Big(\mu \\ & + \rho_{\lambda,\chi}\sigma_\lambda\sigma_\chi\Big)F(q_F(F)K + G_F(F)) + \left(\frac{1}{2}\right) \\ & \cdot \left(\sigma^2 + 2\rho_{\lambda,\chi}\sigma_\lambda\sigma_\chi\right)(q_{FF}(F)K + G_{FF}(F)). \end{aligned} \tag{23}$$

First order of Equation (23) related to K_t:

$$rq = hF^{1/(1-a)} - \delta q + \left(\mu + \rho_{\lambda,\chi}\sigma_\lambda\sigma_\chi\right) + Fq_F + \left(\frac{1}{2}\right)F^2\left(\sigma^2 + 2\rho_{\lambda,\chi}\sigma_\lambda\sigma_\chi\right)q_{FF}. \tag{24}$$

Equation (24) is the nonlinear second-order differential equation, called the Euler Equation, whose general solution is:

$$q(F) = BF^{1/(1-a)} + A_1F^{\eta_1} + A_2F^{\eta_2}, \tag{25}$$

where B, A_1, and A_2 are the undetermined parameters, and $\eta_1 > \eta_2$ are the two roots of $r + \delta - (\mu - \rho_{\lambda,\chi}\sigma_\lambda\sigma_\chi)\eta - (1/2)(\sigma^2 + 2\rho_{\lambda,\chi}\sigma_\lambda\sigma_\chi)\eta(\eta - 1) = 0$. In fact, q is the shadow price of capital, and we make sure this equation does not diverge, $A_1 = A_2 = 0$

$$q(F) = BF^{1/(1-a)}. \tag{26}$$

If Equation (26) is substituted into Equation (24), we obtain:

$$B \equiv \frac{h}{r + \delta - \left(\left(\mu + \rho_{\lambda,\chi}\sigma_\lambda\sigma_\chi\right)/(1-a)\right) - \left(\left(\sigma^2 + 2\rho_{\lambda,\chi}\sigma_\lambda\sigma_\chi\right)a/2(1-a)^2\right)}. \tag{27}$$

If Equation (27) is substituted into Equation (26), we obtain:

$$qt = \frac{hF_t^{1/(1-a)}}{r + \delta - \left(\left(\mu + \rho_{\lambda,\chi}\sigma_\lambda\sigma_\chi\right)/(1-a)\right) - \left(\left(\sigma^2 + 2\rho_{\lambda,\chi}\sigma_\lambda\sigma_\chi\right)a/2(1-a)^2\right)}. \tag{28}$$

With Equation (18) and $q_t \equiv V_K$, we can obtain the optimal investment level of state-owned enterprises:

$$I_t = [q_t/\gamma\beta]^{1/(\beta-1)} = \frac{h^{1/(\beta-1)}F_t^{1/[(1-a)(\beta-1)]}}{(\gamma\beta)^{1/(\beta-1)}\left[r + \delta - \left(\mu + \rho_{\lambda,\chi}\sigma_\lambda\sigma_\chi/(1-a)\right) - \left(\left(\sigma^2 + 2\rho_{\lambda,\chi}\sigma_\lambda\sigma_\chi\right)a/2(1-a)^2\right)\right]^{1/(\beta-1)}}. \tag{29}$$

With the differential of Equation (28) based on Ito's Lemma, we obtain:

$$\frac{dq_t}{q_t} = \frac{1}{1-a}\frac{dF_t}{F_t} + \frac{a}{2(1-a)^2}\left(\frac{dF_t}{F_t}\right)^2. \tag{30}$$

With the differential of Equation (29) based on Ito's Lemma, we obtain:

$$\frac{dI_t}{I_t} = \frac{1}{\beta-1}\frac{dq_t}{q_t} + \frac{2-\beta}{2(\beta-1)^2}\left(\frac{dq_t}{q_t}\right)^2. \tag{31}$$

With Equation (30) substituted into Equation (31), we obtain:

$$\begin{aligned}\frac{dI_t}{I_t} &= \frac{1}{\beta-1}\left(\frac{1}{1-a}\frac{dF_t}{F_t} + \frac{a}{2(1-a)^2}\left(\frac{dF_t}{F_t}\right)^2\right) + \frac{2-\beta}{2(\beta-1)^2}\left(\frac{1}{1-a}\frac{dF_t}{F_t} + \frac{a}{2(1-a)^2}\left(\frac{dF_t}{F_t}\right)^2\right)^2 \\ &= \frac{1}{\beta-1}\left(\frac{1}{1-a}\frac{dF_t}{F_t} + \frac{a}{2(1-a)^2}\left(\frac{dF_t}{F_t}\right)^2\right) + \frac{2-\beta}{2(\beta-1)^2}\left(\frac{1}{1-a}\frac{dF_t}{F_t}\right)^2.\end{aligned} \tag{32}$$

With Equation (14) and $E_t dz_X = E_t dz_p = 0$, we obtain:

$$E_t = \left(\frac{dF_t}{F_t}\right) = \left(\mu_\lambda + \mu_\theta + \mu_\chi + \mu_p\right)dt \equiv \mu dt. \tag{33}$$

With Equation (6), Equation (33), and $(dt)^2 = (dt)(dz_X) = 0$, we obtain:

$$\begin{aligned}\left(\frac{dF_t}{F_t}\right)^2 &= \left(\sigma_\lambda^2 + \sigma_\theta^2 + \sigma_\chi^2 + \sigma_p^2\right)dt + 2\sigma_\lambda\sigma_\chi\rho_{\lambda,\chi}dt \\ &\equiv \sigma^2 dt + 2\sigma_\lambda\sigma_\chi\rho_{\lambda,\chi}dt.\end{aligned} \tag{34}$$

With Equation (33) and Equation (34) substituted into Equation (32), we obtain the expected growth rate of investment in state-owned enterprises:

$$\begin{aligned}\frac{1}{dt}E\left(\frac{dI_t}{I_t}\right) = \frac{\mu}{(\beta-1)(1-a)} + \frac{a(\beta-1)+2-\beta}{2(\beta-1)^2(1-a)^2} \\ \cdot\left(\sigma^2 + 2\rho_{\lambda,\chi}\sigma_\lambda\sigma_\chi\right),\end{aligned} \tag{35}$$

where $F_t \equiv \lambda_t\theta_t\chi_t p_t$, $\mu \equiv \mu_\lambda + \mu_\theta + \mu_\chi + \mu_p$, and $\sigma^2 \equiv \sigma_\lambda^2 + \sigma_\theta^2 + \sigma_\chi^2 + \sigma_p^2$.

The investment function of non-state-owned enterprises is only a special case of the function of state-owned enterprises when $\lambda_t = \theta_t = \chi_t \equiv 1$. The optimal investment level of non-state-owned enterprises is:

$$\widehat{I}_t = \frac{h^{1/(\beta-1)}p_t^{1/[(1-a)(\beta-1)]}}{(\gamma\beta)^{1/(\beta-1)}\left[r+\delta-\left(\mu_p/(1-a)\right)-\left(\sigma_p^2 a/2(1-a)^2\right)\right]^{1/(\beta-1)}}. \tag{36}$$

The expected growth rate of investment in non-state-owned enterprises is:

$$\frac{1}{dt}E\left(\frac{d\widehat{I}_t}{\widehat{I}_t}\right) = \frac{\mu_p}{(\beta-1)(1-a)} + \frac{a(\beta-1)+2-\beta}{2(\beta-1)(1-a)^2}\sigma_p^2. \tag{37}$$

3.2. Related Propositional Deduction

3.2.1. The Advancement of the Reform of Financing Institutions and Enterprises' Investment

Proposition 1. *Without government intervention, the steady capital of state-owned enterprises is higher than that of non-state-owned enterprises before the reform of investment institutions is completed. State-owned enterprises will always accumulate excessive capital, triggering a new round of "national advancement and civil retreat," which is not conducive to sustainable economic development.*

Proof. See Appendix A.1. □

Proposition 2. *The investment drive of state-owned enterprises can be alleviated by the reform of market-oriented financing institutions.*

Proof. See Appendix A.2. □

3.2.2. Government Intervention and Investment of Enterprises

Proposition 3. *Government intervention increases investment turbulence when it effectively regulates the investment of state-owned enterprises.*

Proof. See Appendix A.3. □

In other words, government intervention can regulate the investment level of state-owned enterprises efficiently and also increase investment turbulence, consistent with the conclusion of Gulen et al. (2016), which is not conducive to the sustainability of investment by state-owned enterprises.

Proposition 4. *The impact of government intervention behavior on enterprises' investment level is asymmetric in terms of promotion or restraint.*

Proof. See Appendix A.4. □

Given in Proposition 3, no matter whether government intervention is one-time or continuous, $dz_\lambda > 0$, $\mu_\lambda = 0$, or $dz_\lambda > 0$, $\mu_\lambda > 0$, the sustainability of state-owned enterprises' investment will increase. In addition, if the reform of financing institutions is complete, $Ed\theta_t/\theta_t = \mu_\theta = 0$, and $Ed\chi_t/\chi_t = \mu_\chi = 0$, Equation (38) can be transformed:

$$E_t g_{It} = \frac{\mu_\lambda + \mu_p}{(\beta-1)(1-a)} + \frac{[2(\beta-1)+2-\beta]\left(\sigma^2 + 2\rho_{\lambda,\chi}\sigma_\lambda\sigma_\chi\right)}{2[(\beta-1)(1-a)]^2}. \tag{38}$$

The difference in investment growth rate between state-owned enterprises and non-state-owned enterprises is (Equations (37) and (38))

$$\begin{aligned}E_t g_{It} - E_t g_{\widehat{I}_t} = \frac{\mu_\lambda + \mu_p}{(\beta-1)(1-a)} \\ + \frac{[a(\beta-1)+2-\beta]\left(\sigma_\theta^2 + \sigma_\chi^2 + \sigma_\lambda^2 + 2\rho_{\lambda,\chi}\sigma_\lambda\sigma_\chi\right)}{2[(\beta-1)(1-a)]^2}.\end{aligned} \tag{39}$$

If $\beta < (2-a)/(1-a)$, the latter item in Equation (28) would be greater than 0. No matter whether $\mu_\lambda > 0$ or $\mu_\lambda = 0$, the investment growth rate of state-owned enterprises is higher than that of non-state-owned enterprises because $E_t g_{It} - E_t g_{\widehat{I}_t} > 0$. Therefore, we obtain Proposition 5.

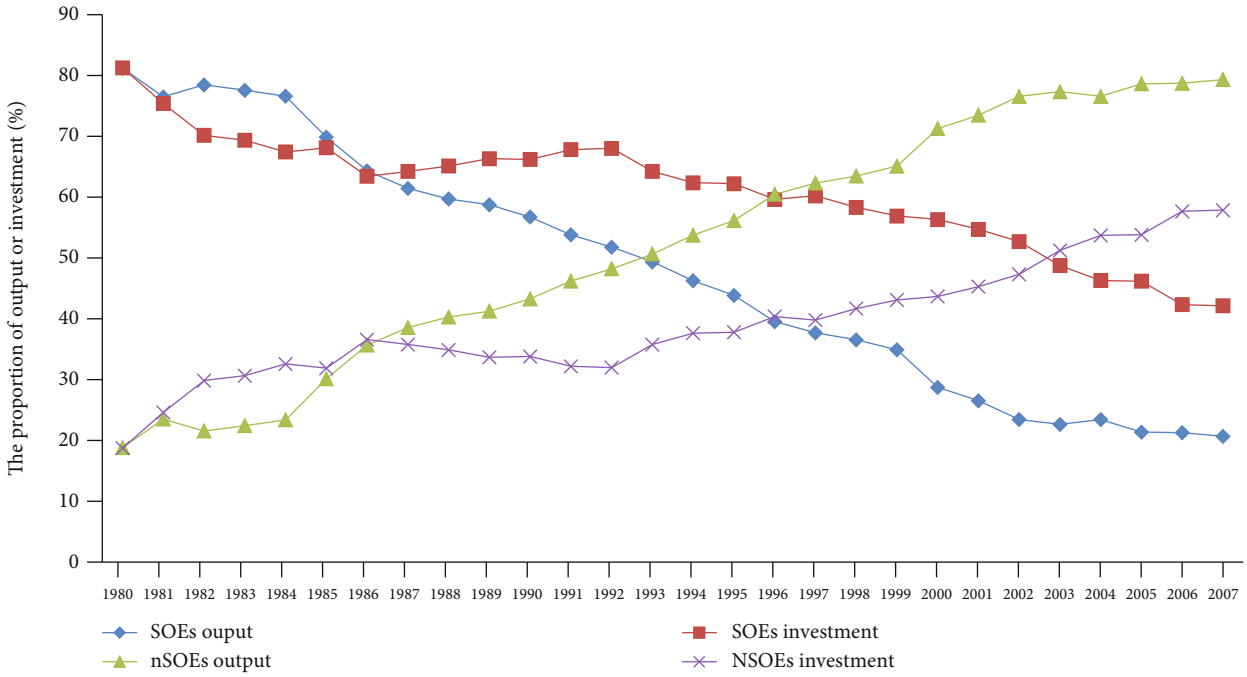

Figure 1: The proportion of output or investment of state-owned and non-state-owned enterprises. Data source: China Statistical Yearbook: 1981–2008.

Proposition 5. *If the effect of government intervention is positive, the investment drive and investment growth rate of state-owned enterprises are higher than those of non-state-owned enterprises. However, if the reform of financing institutions is stopped with* $\beta < (2-a)/(1-a)$*, the investment growth rate of state-owned enterprises is increasingly higher than that of non-state-owned enterprises.*

4. Further Discussion for China's Economic Downturn

Combined with the concrete practice of China's economic transformation and current financing institutions, the characteristic trend in enterprises' investment levels in China is analyzed in this section, with several propositions put forward based on the preceding theoretical model.

Bank loans in China are the main source of external financing for enterprises, because of the underdeveloped stock and bond market in China (Cull & Xu, 2000; Firth et al., 2008; Firth et al., 2012). State-owned enterprises accounted for 78% of new corporate loans in 2016, while non-state-owned enterprises accounted for only 17%. Deeper reform of financing institutions was implemented in the second half of 2016 by China's central government to foster a better external financing environment. However, the financing scale of non-state-owned enterprises declined from 0.86 million dollars in 2015 to 0.66 million dollars in 2017, while that of state-owned enterprises rose from 1 million dollars to 3.2 million dollars, which is a typical case of "the state advancing and the people retreating."

The emergence of a Sino-US trade war in 2018 has had a devastating impact on China's enterprises, especially for non-state-enterprise operations, due to a sharp drop in foreign demand with the decrease of μ_p. Moreover, the absolute level and growth rate of business investment will decrease, which will cause a greater economic decline such as the thunderstorm on current P2P platform in accordance with Equations (29), (35), (36), and (37). The central government in China may decide to adopt a large-scale positive economic stimulus package such as the "New 0.682 Billion Dollars Economic Stimulus Plan" announced in August 2018 to deal with the economic decline the Sino-US trade war triggered, when $dz_\lambda > 0$ and maybe $\mu_\lambda > 0$. At the same time, when local governments face a decline in their economies, they carried out 1 billion dollar leading investment plan in September 2018, and thus, dz_λ and μ_λ would be on the rise continuously. This economic stimulus package implemented in 2018, which points that state-owned enterprises and non-state-owned enterprises with politically connected and local governments must be saved, is a directional rescue compared with the plan in 2008. Revenue from local state-owned enterprises has become the main financing source of local governments since the implementation of fiscal and tax decentralization in 1994. Local governments' economic stimulus packages mainly benefit local state-owned enterprises controlled by local political power, which to a certain extent distorts resource allocation. Of course, state-owned banks also take the initiative to develop robust positive loan policies, such as the targeted cuts to required reserve ratios that release 1,081 billion dollars in credit in October 2018, when $\rho_{\lambda,\chi} > 0$ brings $dz_\chi > 0$ and $d\chi/(\chi dt)$

> 0. When the central government grants property rights to state-owned enterprises, it also gives them political advantages, scale advantages, and market advantages. State-owned bank loan credit might give first place to state-owned enterprises, especially central enterprises, due to their national political power from their soft constraints on credit, meaning that the investment level of state-owned enterprises may increase. The result may be another example of "the state advancing and the people retreating." The outcome of excessive accumulation of capital and rapid investment of state-owned enterprises would further strengthen the inefficiency of their investment, based on Propositions 1 and 5. When the government realized the problem of inefficient investment, it decided to "restructure" to maintain efficiency. The difficulty and complexity of hindering enterprises' investment and economic growth largely outweigh its positive ability, unless it again deepens the reform of financing institutions, due to the asymmetry explained by Proposition 4 and Proposition 5.

According to Proposition 5, although the past evolution of the investment system would lead to "the state retreating and the people advancing," the reverse would happen with massive government intervention, especially if the financing reform is suspended. We also contribute to the current debate on whether "the state is advancing and the people retreating" or not: the development in China is bound to be "the state retreating and the people advancing" as stated by Liu et al. (2016), in contrast to before 1978, but it is "the state advancing and the people retreating" surely in response to recent economic circumstances. Hence, the "state advancing and the people retreating" due to government intervention has a number of costs, including the low efficiency of state-owned enterprise investment and greater instability in the national economy. We thus obtain Proposition 6.

Proposition 6. *The implementation of market-oriented reform of investment institutions and the reduction of government-led economic stimulus plans will improve the efficiency of investments and reduce volatility.*

To be clear, we are not opposed to a stimulus package to deal with the recent economic decline, but we need to know its purpose. The implementation of a robust positive economic stimulus plan in regard to this depression would further aggravate the inefficiency of state-owned enterprises' investment level, as suggested by Proposition 5. Although the current administrative and investment intervention of the Chinese government may achieve good results in the short term, it could also be accompanied by huge costs, such as the low efficiency of investment, repeated construction (the supply of products or services whose quality is not as good as the existing products or services is greater than the social demand) in the long term, and nonperforming loans. The government should focus on domestic demand such as increasing household income and guiding household consumption, which may be more and more effective than the leading positive financing policy.

σ^2 and $\rho_{\lambda,\chi}\sigma_\lambda\sigma_\chi$ in Equation (29) provide the impact for uncertainty (second order) of financing reform on state-owned enterprises' investment. If uncertainty about the financing reform ($\sigma_\theta\sigma_\chi\sigma_\lambda$) increases, state-owned enterprises' investment level will increase as the denominator in Equation (29) decreases. In addition, an increase in uncertainty of reform of financial institutions will improve the expected investment growth rate of state-owned enterprises only with $\beta < (2-a)/(1-a)$. That is, if the central government in China carries out regular and normative reform of financial institutions (conforming to objective criteria defining the scope of powers and responsibilities of local government and enterprises), the variance rate (σ_θ, σ_λ, and σ_χ) in Equations (3)–(5) will drop, which means that the investment and expected growth rate of state-owned enterprises will decline. Hence, we obtain Proposition 7.

Proposition 7. *Poor financing reform may increase the investment level of state-owned enterprises, but regular and normative reforms that are fair and just can reduce economic volatility.*

Using enterprises' investment to stimulate economic growth has become our "conventional weapon" for macrocontrol. Because the financing reform involves a great deal of uncertainty, it may result in excessive investment among state-owned enterprises and thus have consequences such as waste of resources, environmental pollution, and economic overheating. When these consequences emerge, unless social planners under the financing reform (which could cause economic upheaval), it will be much more difficult to regulate the economic system, in accordance with propositions (5) and (6). Proposition 7 indicates that the evolution of systemic reform and financing reform will reduce price fluctuation and the overinvestment of state-owned enterprises, which will stabilize market supply and alleviate the "distortion" of economic structure.

5. Conclusion

The financing reform in China in connection with enterprises' investment behavior is generally advancing in the direction of marketization. The reform is gradual, in which government intervention is of a "discretionary" nature. In this paper, we establish the stochastic investment to explore the change of enterprises' (especially state-owned enterprises) investment and interpret the modern China's economy. We can transform the evolution of the financing reform and government intervention into a stochastic process and implant it into a classical enterprise investment model to construct a stochastic theory investment model to analyze the trend of enterprises' investment level in China's transition period, which suggests the following conclusions. First, the advancement of property rights and the financing reform before 2008 may have reduced state-owned enterprises' investment level and outputs in contrast with non-state-owned enterprises, to some extent bringing about "the state retreating and the people advancing." Second, if

the government does not intervene economically and the financing reform remains incomplete, the stable capital accumulation of state-owned enterprises is higher than that of nonstate enterprises. However, it could aggravate this economic instability, resulting in "the state advancing and the people retreating," though government intervention and random reform of financing institutions could increase state-owned enterprises' investment level. The promoting or restraining effect of government intervention on enterprises' investment level appears to be asymmetric. Third, the decrease of government-led investment and market-oriented or normative reform of financing institutions could improve the efficiency of enterprises' investment levels and reduce economic turmoil and promoting social welfare.

For the record, the regular and normative reform of financing institution this paper proposes is an updated version of the top-down design suggested by China's social planners in 2011. It is a pity that this design has not been carried out by China's local governments, and the policy has been implemented through mandatory monopoly plan directives such as the circuit breaker in 2016. Deepening reform of financing institutions has been mentioned in the "opinions on deepening financing reform" published by the CPC Central Committee and State Council in 2016 and in the report of the nineteenth national congress of the CPC in 2017. However, this statement only refers to a specific target, without mentioning a standard, specific implementation plan and specific institutional guarantee. "Shouting slogans" and "singing with high voices" will not develop China's economy and improve the efficiency of social investment. The market-oriented reform of financing institutions regulates the relationship between local government and enterprises, through contract law protected by legal institutions, though the antimonopoly law of 2007 and the law on unfair competition in commodities of 2018 were promulgated without exact criteria for "monopoly" and "unfair competition," and are thus unenforceable. A market-oriented reform of financing institutions needs fair, clear, and equitable rules to balance the interests of local governments and enterprises.

The article only discusses "what should be done," but the question of "how to do it" still needs more in-depth and systematic analysis. Its conclusion could help deepen the understanding of enterprises' investment behavior in response to the reform of financing institutions and current investment phenomena in China's transition period. Of course, this paper also has some shortcomings, which should be supplemented by future research. It has focused its analysis on China's state-owned enterprises and adopted a general setting for non-state-owned enterprises. Non-state-owned enterprises in China also have some irrational characteristics, which should be the focus of future research. In addition, the short-term and long-term effects of China's economic depression as a result of the Sino-US trade war have not been discussed in this paper. What intervention should the government make, such as intervening in the hiring practices or investment of enterprises, especially state-owned enterprises? This question might be the focus of our future research.

Appendix

A. Proof of Proposition

A.1. Proof of Proposition 1. When capital reaches a steady state, capital stock remains unchanged: $dK_t = (I - \delta K_t)dt \equiv 0$, $I \equiv \delta K_t$. That is to say, steady-state investment is used to offset capital discount. The value objective function of Equation (7) for state-owned enterprises with $I \equiv \delta K_t$ and Equation (18) is transformed into

$$\max_{K_s} E_t \int_t^{+\infty} \left[hF_s^{1/(1-a)} K_s - \gamma(\delta K_s)^{\beta} \right] \exp\left(-r(s-t)\right) ds. \tag{A.1}$$

The equilibrium value of this objective function of Equation (A.1) relative to K_s is

$$K_s^{st} = \left(\frac{hF_s^{1/(1-a)}}{\gamma\beta\delta^{\beta}} \right)^{1/(\beta-1)}. \tag{A.2}$$

If there is no government intervention, then $\lambda_2 \equiv 1$, and the equilibrium value of the objective function of Equation (A.1) relative to K_s is

$$K_s^{st} = \left(\frac{h(\theta_s \chi_s p_s)^{1/(1-a)}}{\gamma\beta\delta^{\beta}} \right)^{1/(\beta-1)}. \tag{A.3}$$

The stable capital for state-owned enterprises $(\theta_s \chi_s > 1)$ before the reform of financial institution is complete is higher than that of non-state-owned enterprises $(\theta_s = \chi_s \equiv 1)$. Therefore, state-owned enterprises always accumulate capital in excess.

In addition, the financing reform from mainly occurred after the worldwide financial crisis in 2008. Because SOE output is lower than nSOE output and the former's investment higher than the latter's, the former's investment efficiency (e.g., output divided by investment) is higher than the latter's, as shown in Figure 1.

A.2. Proof of Proposition 2. The reform of market-oriented financing institutions can reduce θ_t and χ_t. F_t will decrease over time due to $F_t = \lambda_t \theta_t \chi_t p_t$. The optimal investment level of state-owned enterprises in Equation (29) also decreases with time. After the reform of market-oriented financing institutions, $\mu_\theta < 0$, and $\mu_\chi < 0$, but if this reform has not been accomplished, $\mu_\theta = \mu_\chi = 0$. The denominator of the investment function in reform becomes larger with $\mu_\theta = \mu_\chi = 0$, $\mu_\theta < 0$, and $\mu_\chi < 0$ substitutes into Equation (29); that is, $I|_{\mu_\theta<0\mu_\chi<0} < I|_{\mu_\theta=\mu_\chi=0}$. Let $(1/dt)E(dI/I_t) \equiv E_t g_{It}$. Then, the reform of market-oriented institutions reduces the expected rate of enterprises with $E_t g_{It}|_{\mu_\theta<0\mu_\chi<0} < E_t g_{It}|_{\mu_\theta=\mu_\chi=0}$.

In sum, the sustainability of investment by state-owned enterprises could be reduced by the reform of market-oriented institutions through institutional design F_t, the

impact of drift rate $\mu_{\theta \text{ or } \chi}$, and the change of expected growth rate. Above all, the impact of $\mu_\theta < 0$ and $\mu_\chi < 0$ changes the expectation of institutional design F_t and that of the income discount in the enterprise objective function. Furthermore, institutional design F_t and $\mu_\theta < 0$ or $\mu_\chi < 0$ both decrease the expected growth rate of enterprises, whereas $\mu_{\theta \text{ or } \chi}$ mostly decreases the absolute level of enterprises' investment. Therefore, the reform of China's marketization is effective at present.

A.3. Proof of Proposition 3. If the government decides to get involved in expanding or reducing all-over social production capacity, μ_λ and dz_λ in Equation (5) will change. If government intervention is short-term, $dz_\lambda > 0$ and $\mu_\lambda = 0$; but if it continues for a long time, $dz_\lambda > 0$, and $\mu_\lambda > 0$.

Whatever the government intervention, it will greatly affect the investment behavior of state-owned enterprises. If the government hopes that state-owned enterprises will expand their investment level, this will affect the real investment sustainability of state-owned enterprises. As long as the government engages in intervention behavior, $dz_\lambda > 0$, $d\lambda_t/(\lambda_t dt)$ in Equation (5) will increase, because $\rho_{\lambda,\chi} > 0$, $dz_\lambda > 0$, and $d\chi_t/(\chi_t dt)$ in Equation (4) will increase. I_t in Equation (29) will increase as λ_t and χ_t increase. When $dz_\lambda > 0$, $\mu_\lambda > 0$ will make the denominator in Equation (29) decrease and increase the investment level; in addition, $E_t g_{1t}$ increases. Thus, continuous government intervention changes the absolute investment level of enterprises and their expected growth rate of investment.

A.4. Proof of Proposition 4. The effect of continuous government intervention behavior on state-owned enterprises' investment level appears to be asymmetric. We obtain this result by substituting $\mu \equiv \mu_\lambda + \mu_\theta + \mu_\chi + \mu_p$ into Equation (35):

$$E_t g_{1t} = \frac{\mu_\lambda}{(\beta-1)(1-a)} + \phi, \phi \equiv \frac{\mu_\theta + \mu_\chi + \mu_p}{(\beta-1)(1-a)} + \frac{[a(\beta-1)+2-\beta]\left(\sigma^2 + 2\rho_{\lambda,\chi}\sigma_\lambda\sigma_\chi\right)}{2[(\beta-1)(1-a)]^2}. \tag{A.4}$$

The effect μ_λ between positive change (Δ) and negative change $(-\Delta)$ has the same strength over the expected investment growth rate of state-owned enterprises unless $\phi = 0$ is different; that is, $E_t g_{It}|_{\mu_\lambda=\Delta} \neq -E_t g_{It}|_{\mu_\lambda=-\Delta}$. Of course, $\phi = 0$ is only a coincidental situation. Therefore, government intervention has an asymmetrical impact on the promotion or restraint of enterprises' investment levels.

Data Availability

The data used to support the findings of this study are included within the article.

Conflicts of Interest

The authors declare that they have no competing interest.

Acknowledgments

This work was supported by the Open Project of Mangrove Institute, Lingnan Normal University (grant number: PYXM03), and 2022 Annual Planning Topic, Qingyuan Philosophy and Social Sciences (grant number: QYSK2022018).

References

[1] M. Campello, R. P. Ribas, and A. Wang, "Is the stock market just a side show? Evidence from a structural reform," *NBER Working Papers*, vol. 3, no. 1-2, pp. 1–38, 2014.

[2] Q. Gou, Y. Huang, and J. Xu, "Does ownership matter in access to bank credit in China?," *European Journal of Finance*, vol. 24, no. 16, pp. 1409–1427, 2018.

[3] A. D. R. Atahau and T. Cronje, "Bank lending: the bank ownership focus in the pre- and post-global financial crisis periods," *Economic Systems*, vol. 44, no. 4, p. 100813, 2020.

[4] T. Arifin, I. Hasan, and R. Kabir, "Transactional and relational approaches to political connections and the cost of debt," *Journal of Corporate Finance*, vol. 65, p. 101768, 2020.

[5] L. A. Mariani, "Government-owned banks and development: on unintended consequences of bank privatizations," *Job Market Paper*, vol. 9, 2020.

[6] M. C. Jensen and W. H. Meckling, "Theory of the firm: managerial behavior, agency costs and ownership structure," *Corporate Governance. Gower*, vol. 4, pp. 77–132, 2019.

[7] J. Ha and M. Feng, "Tax avoidance and over-investment: the role of the information environment," *Journal of Corporate Accounting & Finance*, vol. 32, no. 1, pp. 48–77, 2021.

[8] H. Tong and S.-J. Wei, "Did unconventional interventions unfreeze the credit market?," *American Economic Journal: Macroeconomics*, vol. 12, no. 2, pp. 284–309, 2020.

[9] M. Giannetti and A. Simonov, "On the real effects of bank bailouts: micro evidence from Japan," *American Economic Journal: Macroeconomics*, vol. 5, no. 1, pp. 135–167, 2013.

[10] Y. Lin, A. Srinivasan, and T. Yamada, *The effect of government bank lending: evidence from the financial crisis in Japan*, Social Science Electronic Publishing, 2015.

[11] Y. S. Chen, Y. Chen, I. Hasan, and C. Y. Lin, "Is there a bright side to government banks? Evidence from the global financial crisis," *Journal of Financial Stability*, vol. 26, no. 8, pp. 128–143, 2016.

[12] M. Bachmann, *Market Illiquidity, Credit Freezes and Endogenous Funding Constraints*, no. 255, 2018Department of Economics Working Paper, 2018.

[13] L. Agnello, V. Castro, J. T. Jalles, and R. M. Sousa, "What determines the likelihood of structural reforms," *European Journal of Political Economy*, vol. 37, no. 10, pp. 129–145, 2015.

[14] T. Krebs and M. Scheffel, *Structural Reform in Germany*, no. 1, 2014Social Science Electronic Publishing, 2014.

[15] E. Dablanorris, G. Ho, and A. Kyobe, "Structural reforms and productivity growth in emerging market and developing economies," *IMF Working Papers*, vol. 16, no. 15, pp. 1–11, 2016.

[16] D. Castellani, E. Giaretta, and R. Staglianò, "Early-stage financing diversity and firms' export intensity: a cross-

country analysis," *Finance Research Letters*, vol. 44, no. 1, p. 102030, 2021.

[17] G. Fraser-Sampson, *The Pillars of Finance: The Misalignment of Finance Theory and Investment Practice*, Springer, 2014.

[18] H. Shen, H. Wu, W. Long, and L. Luo, "Environmental performance of firms and access to bank loans," *The International Journal of Accounting*, vol. 56, no. 2, p. 2150007, 2021.

[19] M. Firth, P. H. Malatesta, Q. Xin, and L. Xu, "Corporate investment, government control, and financing channels: evidence from China's listed companies," *Journal of Corporate Finance*, vol. 18, no. 3, pp. 433–450, 2012.

[20] H. Tong and S. J. Wei, "Did unconventional interventions unfreeze the credit market? Some international evidence," *SSRN Electronic Journal*, p. 1742014, 2011.

[21] Q. Liu, X. Pan, and G. Tian, "To what extent did the economic stimulus package influence bank lending and corporate investment decisions? Evidence from China," *Journal of Banking & Finance*, vol. 86, no. 4, pp. 177–193, 2018.

[22] Y. Zhang, M. Zhang, Y. Liu, and R. Nie, "Enterprise investment, local government intervention and coal overcapacity: the case of China," *Energy Policy*, vol. 101, no. 11, pp. 162–169, 2017.

[23] A. Popov, "Evidence on finance and economic growth," *Handbook of Finance and Development*, vol. 7, pp. 63–104, 2018.

[24] Y. Chen, M. Liu, and J. Su, "Greasing the wheels of bank lending: evidence from private firms in China," *Journal of Banking & Finance*, vol. 37, no. 7, pp. 2533–2545, 2013.

[25] N. Azevedo, M. Mateus, and Á. Pina, "Bank credit allocation and productivity: stylised facts for Portugal," *Studies in Economics and Finance*, vol. 39, no. 4, pp. 644–674, 2022.

[26] C. Wong, "The fiscal stimulus programme and public governance issues in China," *OECD Journal on Budgeting*, vol. 11, no. 3, pp. 1–22, 2011.

[27] Y. Wang, G. Luo, and Y. Guo, "Why is there overcapacity in China's PV industry in its early growth stage?," *Renewable Energy*, vol. 72, no. 7, pp. 188–194, 2014.

[28] J. Wang, Y. Dong, J. Wu, R. Mu, and H. Jiang, "Coal production forecast and low carbon policies in china," *Energy Policy*, vol. 39, no. 10, pp. 5970–5979, 2011.

[29] S. Wu, K. X. Li, W. Shi, and Z. Yang, "Influence of local government on port investment: implications of China's decentralized port governance system," *Maritime Policy & Management*, vol. 43, no. 7, pp. 777–797, 2016.

[30] N. Bloom, "Fluctuations in uncertainty," *Journal of Economic Perspectives*, vol. 28, no. 2, pp. 153–176, 2014.

[31] G. Segal, I. Shaliastovich, and A. Yaron, "Good and bad uncertainty: macroeconomic and financial market implications," *Journal of Financial Economics*, vol. 117, no. 2, pp. 369–397, 2015.

[32] B. Kelly, Ľ. Pástor, and P. Veronesi, "The price of political uncertainty: theory and evidence from the option market," *The Journal of Finance*, vol. 71, no. 5, pp. 2417–2480, 2016.

[33] S. Gilchrist, J. W. Sim, and E. Zakrajšek, "Uncertainty, financial frictions, and investment dynamics," *Finance and Economics Discussion Series*, vol. 2014, no. 69, pp. 1–58, 2014.

[34] L. Pastor and P. Veronesi, "Uncertainty about government policy and stock prices," *Journal of Finance*, vol. 67, no. 4, pp. 1219–1264, 2012.

[35] H. Kim and H. Kung, "The asset redeployability channel: how uncertainty affects corporate investment," *Review of Financial Studies*, vol. 30, no. 1, pp. 245–280, 2017.

Hindawi
Advances in Mathematical Physics
Volume 2022, Article ID 8737448, 15 pages
https://doi.org/10.1155/2022/8737448

Research Article

A New Type-3 Fuzzy PID for Energy Management in Microgrids

Weiping Fan,[1] **Ardashir Mohammadzadeh**,[2] **Nasreen Kausar**,[3,4] **Dragan Pamucar**,[5] **and Nasr Al Din Ide**[6]

[1]*Swan College, Central South University of Forestry and Technology, Changsha, 410210 Hunan, China*
[2]*Multidisciplinary Center for Infrastructure Engineering, Shenyang University of Technology, Shenyang 110870, China*
[3]*Department of Mathematics and Statistics, Quaid e Azam university, Islamabad, Pakistan*
[4]*Department of Mathematics, Faculty of Arts and Sciences, Yildiz Technical University, Esenler, 34210 Istanbul, Turkey*
[5]*Faculty of Organizational Sciences, University of Belgrade, Belgrade, Serbia*
[6]*Department of Mathematics, University of Aleppo, Aleppo, Syria*

Correspondence should be addressed to Nasr Al Din Ide; ide1112002@yahoo.ca

Received 3 June 2022; Accepted 4 July 2022; Published 29 July 2022

Academic Editor: S. E. Najafi

More recently, type-3 (T3) fuzzy logic systems (FLSs) with better learning ability and uncertainty modeling have been presented. On other hand, the proportional-integral-derivative (PID) is commonly employed in most industrial control systems, because of its simplicity and efficiency. The measurement errors, nonlinearities, and uncertainties degrade the performance of conventional PIDs. In this study, for the first time, a new T3-FLS-based PID scheme with deep learning approach is introduced. In addition to rules, the parameters of fuzzy sets are also tuned such that a fast regulation efficiency is obtained. Unlike the most conventional approaches, the suggested tuning approach is done in an online scheme. Also, a nonsingleton fuzzification is suggested to reduce the effect of sensor errors. The proposed scheme is examined on a case-study microgrid (MG), and its good frequency stabilization performance is demonstrated in various hard conditions such as variable load, unknown dynamics, and variation in renewable energy (RE) sources.

1. Introduction

Today, as technology advances and the consumerist population grows, providing sustainable, safe, and clean energy is one of the human's core concerns. Regarding limitation of non-RE resources and the environmental problems caused by their consumption, different countries have decided to choose other energy sources, including renewable sources, as a future and sustainable energy source. Although RE sources are available worldwide, many of these sources are not available seven days a week, 24 hours a day. Some days may be windier than others, the sun does not shine at night, and droughts may occur for a period of time. It can be unpredictable weather events that disrupt these technologies. To improve the sustainability, some energy storage systems and modern controllers should be used to make a balance between consumption and germination [1, 2].

Because of its simplicity and capacity, PID control systems are extensively employed in most industrial problems such as mechanical engineering, chaotic systems, and electrical engineering [3]. In proportional control mode of PID, the output is proportional to the amount of error (hence, it is called proportional). If the error is large, the controller output is large, and if the error is small, the controller output is small. The adjustable parameter of proportional control is called controller gain. The higher the controller gain leads to the higher the proportional error. If the gain is adjusted too high, the control loop will start to oscillate and become unstable [4]. On the other hand, if the gain is too low, responding to disturbances or changes in the setpoint will not be effective enough. There is one major drawback to using a proportional controller alone, and that is offset. Offset is a persistent error that cannot be eliminated by proportional control alone. The integrated control mode continuously

increases or decreases the controller output to minimize error. By the larger error, the integral mode increases or decreases the output rapidly, and by the smaller error, changes will be occur more slowly. The output of the derivative controller is directly related to the error rate over time. Derivative controllers are generally used when process variables start to fluctuate or change at very high speeds. Derivative controllers are also used to predict the future performance of the error by means of an error curve. In this mode, when the error changes are large, the derivative mode will produce more control action. When the error does not change, the derivative operation will be zero. When the derivative time is too long, fluctuations occur in this mode and the closed loop becomes unstable. Then, in real-world applications, the PID parameters should be carefully tuned [5–7].

2. Literature Review

The main approach that has been frequently used for PID tuning is the use of evolutionary based methods. For example, the fractional PID is investigated in [8], and by the use of grasshopper optimization algorithm, the parameters of PID are tuned. In [9], a predictive controller is used to improve the performance of PI controller. In [10], a regulator is constructed using a reinforcement method, and it is evaluated on an isolated MG. The developed genetic algorithm (GA) by the use of nondominated sorting approach is suggested in [11], to design a frequency regulator. The application of FLSs in designing of voltage controller is studied in [12]. The particle swarm optimization (PSO) is used in [13] for optimization, and it is examined on an inverter-based MG. In [14], the various approaches are reviewed.

One of main approaches to tune the PIDs is the use of FLSs and neural networks [15, 16]. The FLSs are widely used for approximation problems [17, 18]. For example, in [19], a PID is designed using type-1 FLSs, and it is applied for temperature control. In [20], a defuzzification is suggested for FLSs to decrease the computations, and then, a PID is designed based on the simplified FLS. The backstepping PID is studied in [21], and a FLS is formulated to estimate the uncertainties. Similar to classical PIDs that are reviewed in the above paragraph, some evolutionary-based algorithms have also been developed for tuning of FLS-PIDs. In these methods, the evolutionary-based techniques are used to tune FLS rules, and the output of FLSs determines the gains of PID [22]. In [23], a fractional-order version of PID is designed, and one FLS is used to optimize all gains. In [24], the frequency control in MG is studied, and a FLS-based PID is schemed. In [25], the efficiency of FLS-PID is examined on a power system, and the accuracy improvement by FLSs is shown. A comparative study in [26] shows that FLSs well amend the accuracy of PIDs in versus of disturbances and uncertainties.

The type-2 FLSs have been rarely used in MG. For example, in [27], a deep-learned T2-FLS-based control technique is developed, and the good efficiency of T2-FLSs is verified. In [28], a T2-FLS is formulated for optimizing a PID, and its performance is examined by a stabilization problem in MGs. In [29], the membership functions of a generalized IT2FS are optimized, and a controller is designed for both frequency and voltage management. The equilibrium optimization scheme is used in [30] for tuning the parameters of PID controller on the basis of T2-FLSs. In [31], a type-2 PID is developed, and its efficiency is compared by applying on MG. In [32], the efficiency of the T2-FLS-based control systems is evaluated on the basis of Harris approach. A PID is developed in [33] using T2-FLSs, and it is demonstrated that high-order FLSs enhance the accuracy.

More recently, it has been shown that high-order FLSs such as type-3 FLSs and generalized FLSs give better efficiency in real-world engineering problems. For example, in [34], a T3-FLS is used for energy management, and by various comparisons, the superiority of T3-FLSs is shown. In [35], a T3-FLS-based controller is designed for MGs and the fluctuation of solar energies is tackled by the use of T3-FLSs. The capability of T3-FLSs in a real-world 5G telecom application is tested in [36], and it is verified that T3-FLSs result in better stabilization efficiency. Similarly, in [37], the better estimation efficiency and stabilization performance of T3-FLSs are examined in an experimental DC power system.

3. Motivations

The literature review shows that in most of PID tuning approaches, trial-and-error methods and some evolutionary algorithms are commonly used. However, the uncertainties, nonlinearities, and changes in dynamic parameters decrease the performance of conventional approaches. Also, the evolutionary-based approaches are not suitable for practical systems, due to the high computational process of these algorithms. Furthermore, in most of investigated methods, the tuning is done in an off-line schedule, and then, the unpredictable online disturbances are not supported. Although some FLS-based PIDs have been presented, most of the conventional FLSs are vulnerable to the plant's uncertainties, sensor errors, and nonlinearities.

4. Novelettes

The basic advantages of the designed regulator are as follows:

(i) A type-3 FLS-based PID with higher capability and using fractional-order calculus is introduced

(ii) There is no need for MG dynamics

(iii) Unlike most FLS-based PIDs, the structure of the suggested approach is nonlinear

(iv) In addition to rules, the MFs are also tuned to speed up the learning

(v) The tuning is done in an online approach, and the suggested PID is updated, at each sample time

(vi) All gains are tuned simultaneously

(vii) Nonsingleton fuzzification decreases the effect of sensor error

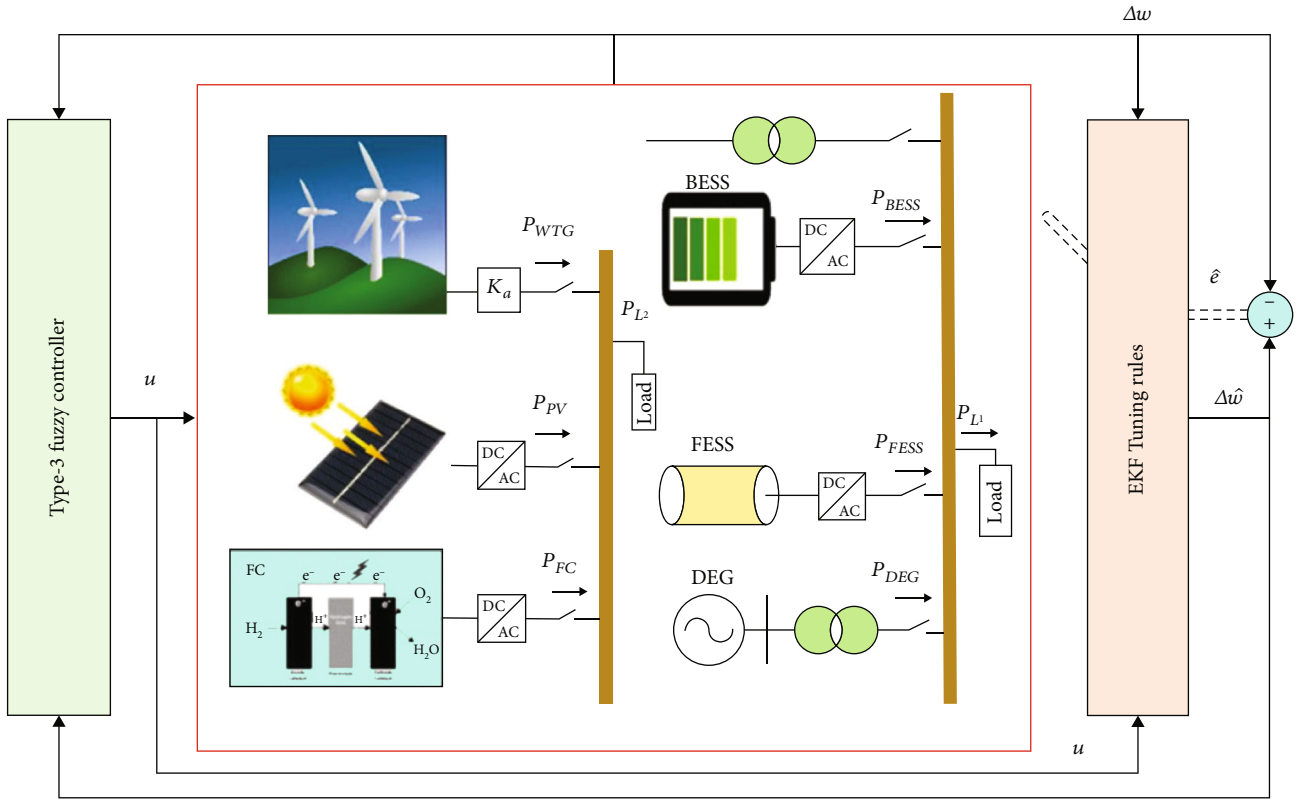

Figure 1: General diagram.

(viii) In various hard conditions, such as considering load changes, variation of wind/solar powers, and dynamic disturbances, the better efficiency of the suggested approach is demonstrated

5. Problem Formulation

Power imbalance is felt by its effect on the speed or frequency of the generator. If the load is reduced and the output is increased, the generator tends to enhance its speed/frequency. By increasing load and production shortage, the speed/frequency of the generator decreases. The variation of frequency from its nominal value is chosen as a signal to excite the automatic controller. Then, a power balance at a constant frequency is an important problem [38, 39].

The load frequency control (LFC) loop responds only to small amplitude and slow load and frequency changes and is unable to control in emergencies and the resulting power imbalance. System control in emergencies and sudden changes is examined by studying the transient stability and protection of systems.

A general view is shown in Figure 1. The designed control scheme does not use the mathematical models. The suggested control technique is well optimized and tackles the effect of perturbations such as variation of weather conditions and output lead.

The main purposes of LFC are as follows: maintaining the frequency uniformly, dividing the system load between the generators optimally and preferably economically, and regulating the power exchanged from the communication lines in the planned values. In fact, the change in the frequency of the system and the actual power of the communication lines must be eliminated by changing the output.

6. Fuzzy PID Controller

PIDs are commonly employed in most industrial control systems because of their simplicity and capacity. The control performance of conventional PIDs degrades under nonlinearities, uncertainties, and parameter changes. In the conventional FLS-based PIDs, FLSs are used to alter the PID gains. The closed-loop error and its derivative are commonly used as inputs of FLSs. The output of FLS determines the gains of PIDs. In the suggested approach, the output of designed type-3 FLS directly determines the output. The input variables are error and its fractional derivative and integral. Rules of FLS are tuned such that an error-based cost function is minimized. The general scheme is shown in Figure 2.

7. Type-3 FLS

The type-3 FLS [40] is a more capable version of the type-2 FLS. Figure 3 depicts a broad overview of the hypothesized T3-FLS. In T3-FLSs, secondary membership function (MF) is likewise a type-2 MF, as illustrated in Figure 4. In contrast to conventional MFs, the top/lower boundaries of memberships are not constant. Because of these characteristics, type-3 MFs can manage a higher amount of uncertainty. The computations are discussed in this section:

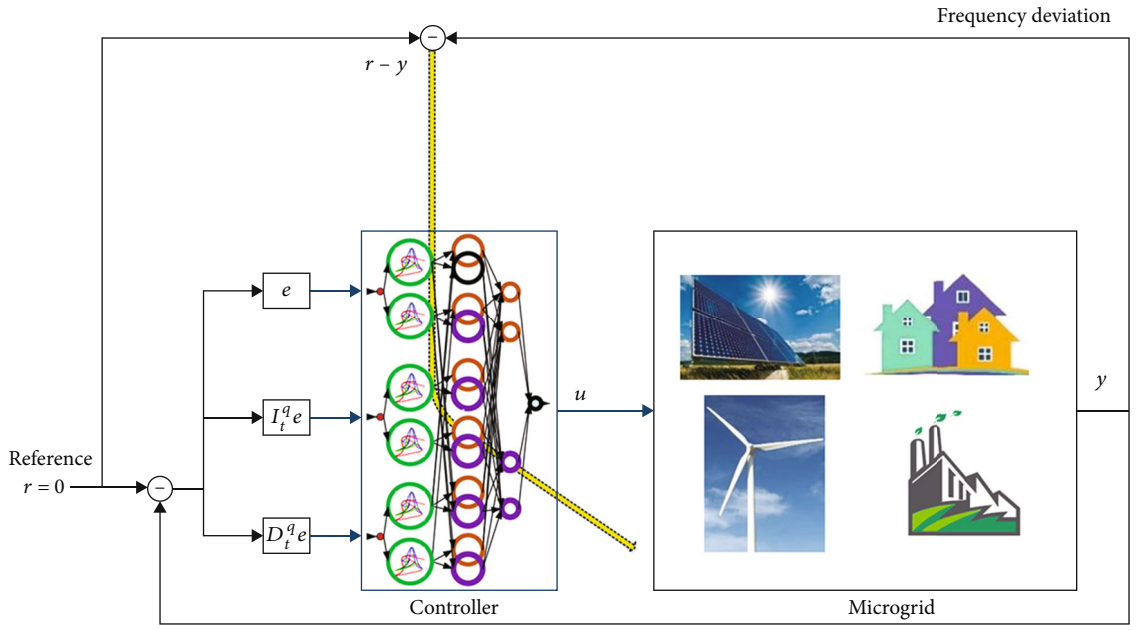

Figure 2: General view.

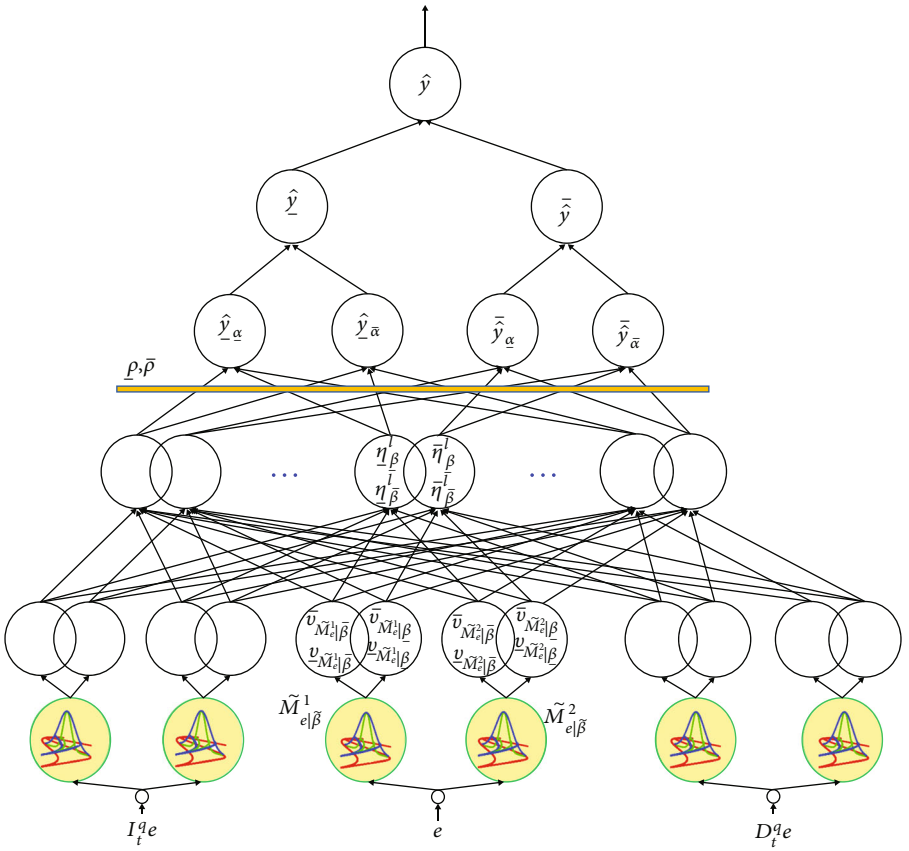

Figure 3: A general view on T3-FLS.

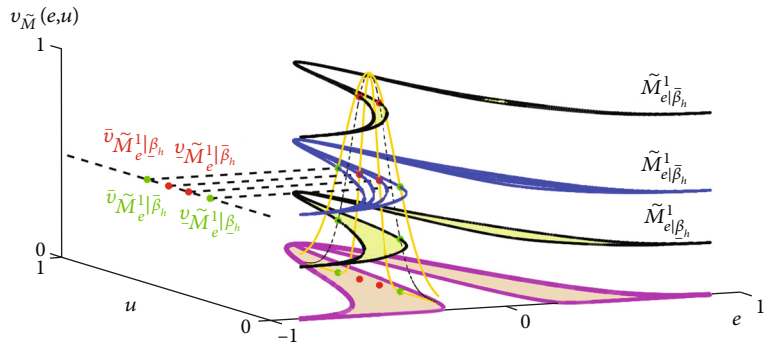

Figure 4: Type-3 MF.

(1) The input variables are e, $I_t^q e$, and $D_t^q e$, where

$$D_t^q e(t) = \frac{\int_0^t (e(x)/(t-x)^q)dx}{\Gamma(1-q)},$$
$$I_t^q e(t) = \frac{\int_0^t (t-x)^{q-1} e(x)dx}{\Gamma(q)} \quad (1)$$

(2) For inputs e, $I_t^q e$, and $D_t^q e$, MFs are considered as $\tilde{M}_e^1 - \tilde{M}_e^2$, $M_{I_t^q e}^1 - \tilde{M}_{I_t^q e}^2$, and $M_{D_t^q e}^1 - \tilde{M}_{D_t^q e}^2$, respectively. As illustrated in Figure 4, each MF is horizontally split into n levels. The memberships for horizontal slice level β_h are calculated for each input, as illustrated in Figure 4. A Gaussian MF is considered for inputs to handle the sensor errors. The upper/lower memberships at level β_h for input e are calculated as follows:

$$\bar{\upsilon}_{\tilde{M}_e^j|\bar{\beta}_h} = \exp\left(-\frac{\left(\bar{e}_{\bar{\beta}_h} - c_{\tilde{M}_e^j|\bar{\beta}_h}\right)^2}{\bar{\vartheta}^2_{\tilde{M}_e^j|\bar{\beta}_h}}\right),$$
$$\bar{\upsilon}_{\tilde{M}_e^j|\underline{\beta}_h} = \exp\left(-\frac{\left(\bar{e}_{\underline{\beta}_h} - c_{\tilde{M}_e^j|\underline{\beta}_h}\right)^2}{\bar{\vartheta}^2_{\tilde{M}_e^j|\underline{\beta}_h}}\right),$$
$$\underline{\upsilon}_{\tilde{M}_e^j|\bar{\beta}_h} = \exp\left(-\frac{\left(\underline{e}_{\bar{\beta}_h} - c_{\tilde{M}_e^j|\bar{\beta}_h}\right)^2}{\underline{\vartheta}^2_{\tilde{M}_e^j|\bar{\beta}_h}}\right),$$
$$\underline{\upsilon}_{\tilde{M}_e^j|\underline{\beta}_h} = \exp\left(-\frac{\left(\underline{e}_{\underline{\beta}_h} - c_{\tilde{M}_e^j|\underline{\beta}_h}\right)^2}{\underline{\vartheta}^2_{\tilde{M}_e^j|\underline{\beta}_h}}\right), \quad (2)$$

where

$$\bar{e}_{\bar{\beta}_h} = \frac{e\bar{\vartheta}^2_{\tilde{M}_e^j|\bar{\beta}_h} + \sigma_s^2 c_{\tilde{M}_e^j|\bar{\beta}_h}}{\bar{\vartheta}^2_{\tilde{M}_e^j|\bar{\beta}_h} + \sigma_s^2},$$
$$\bar{e}_{\underline{\beta}_h} = \frac{e\bar{\vartheta}^2_{\tilde{M}_e^j|\underline{\beta}_h} + \sigma_s^2 c_{\tilde{M}_e^j|\underline{\beta}_h}}{\bar{\vartheta}^2_{\tilde{M}_e^j|\underline{\beta}_h} + \sigma_s^2},$$
$$\underline{e}_{\bar{\beta}_h} = \frac{e\underline{\vartheta}^2_{\tilde{M}_e^j|\bar{\beta}_h} + \sigma_s^2 c_{\tilde{M}_e^j|\bar{\beta}_h}}{\underline{\vartheta}^2_{\tilde{M}_e^j|\bar{\beta}_h} + \sigma_s^2},$$
$$\underline{e}_{\underline{\beta}_h} = \frac{e\underline{\vartheta}^2_{\tilde{M}_e^j|\underline{\beta}_h} + \sigma_s^2 c_{\tilde{M}_e^j|\underline{\beta}_h}}{\underline{\vartheta}^2_{\tilde{M}_e^j|\underline{\beta}_h} + \sigma_s^2}, \quad (3)$$

where, $h = 1, \cdots, n$, $j = 1, 2$, $c_{\tilde{M}_e^j|\bar{\beta}_h}$ is the center of MF $\tilde{M}_e^j|\bar{\beta}_h$, and $\bar{\vartheta}_{\tilde{M}_e^j|\bar{\beta}_h}$ and $\underline{\vartheta}_{\tilde{M}_e^j|\bar{\beta}_h}$ are the upper/lower standard-divisions (SD) for $\tilde{M}_e^j|\bar{\beta}_h$. For input $I_t^q e$, we have

$$\bar{\upsilon}_{\tilde{M}^j_{I_t^q e}|\bar{\beta}_h} = \exp\left(-\frac{\left(I_t^q\bar{e}_{\bar{\beta}_h} - c_{\tilde{M}^j_{I_t^q e}|\bar{\beta}_h}\right)^2}{\bar{\vartheta}^2_{\tilde{M}^j_{I_t^q e}|\bar{\beta}_h}}\right),$$
$$\bar{\upsilon}_{\tilde{M}^j_{I_t^q e}|\underline{\beta}_h} = \exp\left(-\frac{\left(I_t^q\bar{e}_{\underline{\beta}_h} - c_{\tilde{M}^j_{I_t^q e}|\underline{\beta}_h}\right)^2}{\bar{\vartheta}^2_{\tilde{M}^j_{I_t^q e}|\underline{\beta}_h}}\right),$$
$$\underline{\upsilon}_{\tilde{M}^j_{I_t^q e}|\bar{\beta}_h} = \exp\left(-\frac{\left(I_t^q\underline{e}_{\bar{\beta}_h} - c_{\tilde{M}^j_{I_t^q e}|\bar{\beta}_h}\right)^2}{\underline{\vartheta}^2_{\tilde{M}^j_{I_t^q e}|\bar{\beta}_h}}\right),$$
$$\underline{\upsilon}_{\tilde{M}^j_{I_t^q e}|\underline{\beta}_h} = \exp\left(-\frac{\left(I_t^q\underline{e}_{\underline{\beta}_h} - c_{\tilde{M}^j_{I_t^q e}|\underline{\beta}_h}\right)^2}{\underline{\vartheta}^2_{\tilde{M}^j_{I_t^q e}|\underline{\beta}_h}}\right), \quad (4)$$

where

$$
\begin{aligned}
I_t^q \bar{e}_{\bar{\beta}_h} &= \frac{I_t^q e \bar{\vartheta}^2_{\tilde{M}_e^j|\bar{\beta}_h} + \sigma_s^2 c_{\tilde{M}_e^j|\bar{\beta}_h}}{\bar{\vartheta}^2_{\tilde{M}_e^j|\bar{\beta}_h} + \sigma_s^2},\\
I_t^q \bar{e}_{\underline{\beta}_h} &= \frac{I_t^q e \bar{\vartheta}^2_{\tilde{M}_e^j|\underline{\beta}_h} + \sigma_s^2 c_{\tilde{M}_e^j|\underline{\beta}_h}}{\bar{\vartheta}^2_{\tilde{M}_e^j|\underline{\beta}_h} + \sigma_s^2},\\
I_t^q \underline{e}_{\bar{\beta}_h} &= \frac{I_t^q e \underline{\vartheta}^2_{\tilde{M}_e^j|\bar{\beta}_h} + \sigma_s^2 c_{\tilde{M}_e^j|\bar{\beta}_h}}{\underline{\vartheta}^2_{\tilde{M}_e^j|\bar{\beta}_h} + \sigma_s^2},\\
I_t^q \underline{e}_{\underline{\beta}_h} &= \frac{I_t^q e \underline{\vartheta}^2_{\tilde{M}_e^j|\underline{\beta}_h} + \sigma_s^2 c_{\tilde{M}_e^j|\underline{\beta}_h}}{\underline{\vartheta}^2_{\tilde{M}_e^j|\underline{\beta}_h} + \sigma_s^2},
\end{aligned}
\tag{5}
$$

where $h = 1, \cdots, n$, $j = 1, 2$, $c_{\tilde{M}^j_{I_t^q e}|\bar{\beta}_h}$ denotes center of $\tilde{M}^j_{I_t^q e}|\bar{\beta}_h$, and $\bar{\vartheta}_{\tilde{M}^j_{I_t^q e}|\bar{\beta}_h}$ and $\underline{\vartheta}_{\tilde{M}^j_{I_t^q e}|\bar{\beta}_h}$ are the upper/lower SD for $\tilde{M}^j_{I_t^q e}|\bar{\beta}_h$. Similarly, for $D_t^q e$, we have

$$
\begin{aligned}
\bar{\upsilon}_{\tilde{M}^j_{D_t^q e}|\bar{\beta}_h} &= \exp\left(-\frac{\left(D_t^q \bar{e}_{\bar{\beta}_h} - c_{\tilde{M}^j_{D_t^q e}|\bar{\beta}_h}\right)^2}{\bar{\vartheta}^2_{\tilde{M}^j_{D_t^q e}|\bar{\beta}_h}}\right),\\
\bar{\upsilon}_{\tilde{M}^j_{D_t^q e}|\underline{\beta}_h} &= \exp\left(-\frac{\left(D_t^q \bar{e}_{\underline{\beta}_h} - c_{\tilde{M}^j_{D_t^q e}|\underline{\beta}_h}\right)^2}{\bar{\vartheta}^2_{\tilde{M}^j_{D_t^q e}|\underline{\beta}_h}}\right),\\
\underline{\upsilon}_{\tilde{M}^j_{D_t^q e}|\bar{\beta}_h} &= \exp\left(-\frac{\left(D_t^q \underline{e}_{\bar{\beta}_h} - c_{\tilde{M}^j_{D_t^q e}|\bar{\beta}_h}\right)^2}{\underline{\vartheta}^2_{\tilde{M}^j_{D_t^q e}|\bar{\beta}_h}}\right),\\
\underline{\upsilon}_{\tilde{M}^j_{D_t^q e}|\underline{\beta}_h} &= \exp\left(-\frac{\left(D_t^q \underline{e}_{\underline{\beta}_h} - c_{\tilde{M}^j_{D_t^q e}|\underline{\beta}_h}\right)^2}{\underline{\vartheta}^2_{\tilde{M}^j_{D_t^q e}|\underline{\beta}_h}}\right),
\end{aligned}
\tag{6}
$$

where

$$
\begin{aligned}
D_t^q \bar{e}_{\bar{\beta}_h} &= \frac{I_t^q e \bar{\vartheta}^2_{\tilde{M}_e^j|\bar{\beta}_h} + \sigma_s^2 c_{\tilde{M}_e^j|\bar{\beta}_h}}{\bar{\vartheta}^2_{\tilde{M}_e^j|\bar{\beta}_h} + \sigma_s^2},\\
D_t^q \bar{e}_{\underline{\beta}_h} &= \frac{D_t^q e \bar{\vartheta}^2_{\tilde{M}_e^j|\underline{\beta}_h} + \sigma_s^2 c_{\tilde{M}_e^j|\underline{\beta}_h}}{\bar{\vartheta}^2_{\tilde{M}_e^j|\underline{\beta}_h} + \sigma_s^2},
\end{aligned}
$$

$$
\begin{aligned}
D_t^q \underline{e}_{\bar{\beta}_h} &= \frac{D_t^q e \underline{\vartheta}^2_{\tilde{M}_e^j|\bar{\beta}_h} + \sigma_s^2 c_{\tilde{M}_e^j|\bar{\beta}_h}}{\underline{\vartheta}^2_{\tilde{M}_e^j|\bar{\beta}_h} + \sigma_s^2},\\
D_t^q \underline{e}_{\underline{\beta}_h} &= \frac{D_t^q e \underline{\vartheta}^2_{\tilde{M}_e^j|\underline{\beta}_h} + \sigma_s^2 c_{\tilde{M}_e^j|\underline{\beta}_h}}{\underline{\vartheta}^2_{\tilde{M}_e^j|\underline{\beta}_h} + \sigma_s^2},
\end{aligned}
\tag{7}
$$

where $h = 1, \cdots, n$, $j = 1, 2$, $c_{\tilde{M}^j_{D_t^q e}|\bar{\beta}_h}$ denotes the center of $\tilde{M}^j_{D_t^q e}|\bar{\beta}_h$, and $\bar{\vartheta}_{\tilde{M}^j_{D_t^q e}|\bar{\beta}_h}$ and $\underline{\vartheta}_{\tilde{M}^j_{D_t^q e}|\bar{\beta}_h}$ are the upper/lower SD for $\tilde{M}^j_{D_t^q e}|\bar{\beta}_h$.

(3) The rule firing at $\bar{\beta}_h$ is obtained as

$$
\begin{aligned}
\bar{\eta}^1_{\bar{\beta}_h} &= \bar{\upsilon}_{\tilde{M}_e^1|\bar{\beta}_h} \bar{\upsilon}_{\tilde{M}^1_{I_t^q e}|\bar{\beta}_h} \bar{\upsilon}_{\tilde{M}^1_{D_t^q e}|\bar{\beta}_h},\\
\bar{\eta}^2_{\bar{\beta}_h} &= \bar{\upsilon}_{\tilde{M}_e^1|\bar{\beta}_h} \bar{\upsilon}_{\tilde{M}^1_{I_t^q e}|\bar{\beta}_h} \bar{\upsilon}_{\tilde{M}^2_{D_t^q e}|\bar{\beta}_h},\\
\bar{\eta}^3_{\bar{\beta}_h} &= \bar{\upsilon}_{\tilde{M}_e^1|\bar{\beta}_h} \bar{\upsilon}_{\tilde{M}^2_{I_t^q e}|\bar{\beta}_h} \bar{\upsilon}_{\tilde{M}^1_{D_t^q e}|\bar{\beta}_h},\\
\bar{\eta}^4_{\bar{\beta}_h} &= \bar{\upsilon}_{\tilde{M}_e^1|\bar{\beta}_h} \bar{\upsilon}_{\tilde{M}^2_{I_t^q e}|\bar{\beta}_h} \bar{\upsilon}_{\tilde{M}^2_{D_t^q e}|\bar{\beta}_h},\\
\bar{\eta}^5_{\bar{\beta}_h} &= \bar{\upsilon}_{\tilde{M}_e^2|\bar{\beta}_h} \bar{\upsilon}_{\tilde{M}^1_{I_t^q e}|\bar{\beta}_h} \bar{\upsilon}_{\tilde{M}^1_{D_t^q e}|\bar{\beta}_h},\\
\bar{\eta}^6_{\bar{\beta}_h} &= \bar{\upsilon}_{\tilde{M}_e^2|\bar{\beta}_h} \bar{\upsilon}_{\tilde{M}^1_{I_t^q e}|\bar{\beta}_h} \bar{\upsilon}_{\tilde{M}^2_{D_t^q e}|\bar{\beta}_h},\\
\bar{\eta}^7_{\bar{\beta}_h} &= \bar{\upsilon}_{\tilde{M}_e^2|\bar{\beta}_h} \bar{\upsilon}_{\tilde{M}^2_{I_t^q e}|\bar{\beta}_h} \bar{\upsilon}_{\tilde{M}^1_{D_t^q e}|\bar{\beta}_h},\\
\bar{\eta}^8_{\bar{\beta}_h} &= \bar{\upsilon}_{\tilde{M}_e^2|\bar{\beta}_h} \bar{\upsilon}_{\tilde{M}^2_{I_t^q e}|\bar{\beta}_h} \bar{\upsilon}_{\tilde{M}^2_{D_t^q e}|\bar{\beta}_h}
\end{aligned}
\tag{8}
$$

For $\underline{\beta}_h$, we have

$$
\begin{aligned}
\bar{\eta}^1_{\underline{\beta}_h} &= \bar{\upsilon}_{\tilde{M}_e^1|\underline{\beta}_h} \bar{\upsilon}_{\tilde{M}^1_{I_t^q e}|\underline{\beta}_h} \bar{\upsilon}_{\tilde{M}^1_{D_t^q e}|\underline{\beta}_h},\\
\bar{\eta}^2_{\underline{\beta}_h} &= \bar{\upsilon}_{\tilde{M}_e^1|\underline{\beta}_h} \bar{\upsilon}_{\tilde{M}^1_{I_t^q e}|\underline{\beta}_h} \bar{\upsilon}_{\tilde{M}^2_{D_t^q e}|\underline{\beta}_h},\\
\bar{\eta}^3_{\underline{\beta}_h} &= \bar{\upsilon}_{\tilde{M}_e^1|\underline{\beta}_h} \bar{\upsilon}_{\tilde{M}^2_{I_t^q e}|\underline{\beta}_h} \bar{\upsilon}_{\tilde{M}^1_{D_t^q e}|\underline{\beta}_h},\\
\bar{\eta}^4_{\underline{\beta}_h} &= \bar{\upsilon}_{\tilde{M}_e^1|\underline{\beta}_h} \bar{\upsilon}_{\tilde{M}^2_{I_t^q e}|\underline{\beta}_h} \bar{\upsilon}_{\tilde{M}^2_{D_t^q e}|\underline{\beta}_h},\\
\bar{\eta}^5_{\underline{\beta}_h} &= \bar{\upsilon}_{\tilde{M}_e^2|\underline{\beta}_h} \bar{\upsilon}_{\tilde{M}^1_{I_t^q e}|\underline{\beta}_h} \bar{\upsilon}_{\tilde{M}^1_{D_t^q e}|\underline{\beta}_h},\\
\bar{\eta}^6_{\underline{\beta}_h} &= \bar{\upsilon}_{\tilde{M}_e^2|\underline{\beta}_h} \bar{\upsilon}_{\tilde{M}^1_{I_t^q e}|\underline{\beta}_h} \bar{\upsilon}_{\tilde{M}^2_{D_t^q e}|\underline{\beta}_h},\\
\bar{\eta}^7_{\underline{\beta}_h} &= \bar{\upsilon}_{\tilde{M}_e^2|\underline{\beta}_h} \bar{\upsilon}_{\tilde{M}^2_{I_t^q e}|\underline{\beta}_h} \bar{\upsilon}_{\tilde{M}^1_{D_t^q e}|\underline{\beta}_h},\\
\bar{\eta}^8_{\underline{\beta}_h} &= \bar{\upsilon}_{\tilde{M}_e^2|\underline{\beta}_h} \bar{\upsilon}_{\tilde{M}^2_{I_t^q e}|\underline{\beta}_h} \bar{\upsilon}_{\tilde{M}^2_{D_t^q e}|\underline{\beta}_h}.
\end{aligned}
\tag{9}
$$

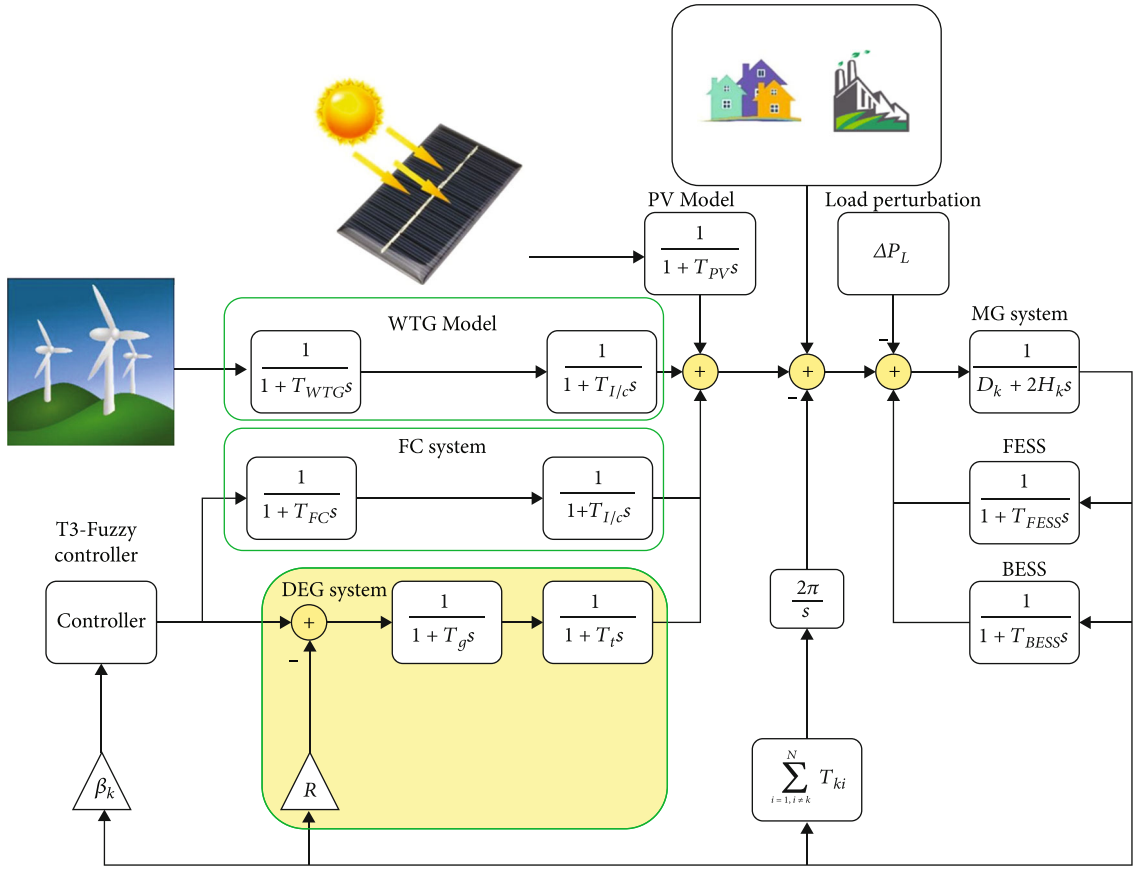

Figure 5: Case-study MG.

The lower firing degree of rules at upper/lower slice levels is obtained as

$$\underline{\eta}^1_{\bar{\beta}_h} = \bar{\upsilon}_{\tilde{M}^1_e|\bar{\beta}_h} \bar{\upsilon}_{\tilde{M}^1_{I^q_t e}|\bar{\beta}_h} \bar{\upsilon}_{\tilde{M}^1_{D^q_t e}|\bar{\beta}_h},$$

$$\underline{\eta}^2_{\bar{\beta}_h} = \bar{\upsilon}_{\tilde{M}^1_e|\bar{\beta}_h} \bar{\upsilon}_{\tilde{M}^1_{I^q_t e}|\bar{\beta}_h} \bar{\upsilon}_{\tilde{M}^2_{D^q_t e}|\bar{\beta}_h},$$

$$\underline{\eta}^3_{\bar{\beta}_h} = \bar{\upsilon}_{\tilde{M}^1_e|\bar{\beta}_h} \bar{\upsilon}_{\tilde{M}^2_{I^q_t e}|\bar{\beta}_h} \bar{\upsilon}_{\tilde{M}^1_{D^q_t e}|\bar{\beta}_h},$$

$$\underline{\eta}^4_{\bar{\beta}_h} = \bar{\upsilon}_{\tilde{M}^1_e|\bar{\beta}_h} \bar{\upsilon}_{\tilde{M}^2_{I^q_t e}|\bar{\beta}_h} \bar{\upsilon}_{\tilde{M}^2_{D^q_t e}|\bar{\beta}_h},$$

$$\underline{\eta}^5_{\bar{\beta}_h} = \bar{\upsilon}_{\tilde{M}^2_e|\bar{\beta}_h} \bar{\upsilon}_{\tilde{M}^1_{I^q_t e}|\bar{\beta}_h} \bar{\upsilon}_{\tilde{M}^1_{D^q_t e}|\bar{\beta}_h},$$

$$\underline{\eta}^6_{\bar{\beta}_h} = \bar{\upsilon}_{\tilde{M}^2_e|\bar{\beta}_h} \bar{\upsilon}_{\tilde{M}^1_{I^q_t e}|\bar{\beta}_h} \bar{\upsilon}_{\tilde{M}^2_{D^q_t e}|\bar{\beta}_h},$$

$$\underline{\eta}^7_{\bar{\beta}_h} = \bar{\upsilon}_{\tilde{M}^2_e|\bar{\beta}_h} \bar{\upsilon}_{\tilde{M}^2_{I^q_t e}|\bar{\beta}_h} \bar{\upsilon}_{\tilde{M}^1_{D^q_t e}|\bar{\beta}_h},$$

$$\underline{\eta}^8_{\bar{\beta}_h} = \bar{\upsilon}_{\tilde{M}^2_e|\bar{\beta}_h} \bar{\upsilon}_{\tilde{M}^2_{I^q_t e}|\bar{\beta}_h} \bar{\upsilon}_{\tilde{M}^2_{D^q_t e}|\bar{\beta}_h},$$

$$\underline{\eta}^1_{\underline{\beta}_h} = \bar{\upsilon}_{\tilde{M}^1_e|\underline{\beta}_h} \bar{\upsilon}_{\tilde{M}^1_{I^q_t e}|\underline{\beta}_h} \bar{\upsilon}_{\tilde{M}^1_{D^q_t e}|\underline{\beta}_h},$$

$$\underline{\eta}^2_{\underline{\beta}_h} = \bar{\upsilon}_{\tilde{M}^1_e|\underline{\beta}_h} \bar{\upsilon}_{\tilde{M}^1_{I^q_t e}|\underline{\beta}_h} \bar{\upsilon}_{\tilde{M}^2_{D^q_t e}|\underline{\beta}_h},$$

Table 1: System parameter description (powers are in (KW)).

e_{BESS}	0.20 (s)	e_g	0.10 (s)	DEG	161	$I^q_t e_{L_2} =$
e_{PV}	1.84 (s)	e_{WTG}	1.44 (s)	PV	32	$I^q_t e_{L_1} =$
H	0.18 (pu)	e_{FESS}	0.20 (s)	FC	71	
e_t	0.41 (s)	$e_{I/c}$	0.0035 (s)	FESS	47	220
e_{IN}	0.050 (s)	n_r	0.320 (pu/Hz)	BESS	45	

$$\underline{\eta}^3_{\underline{\beta}_h} = \bar{\upsilon}_{\tilde{M}^1_e|\underline{\beta}_h} \bar{\upsilon}_{\tilde{M}^2_{I^q_t e}|\underline{\beta}_h} \bar{\upsilon}_{\tilde{M}^1_{D^q_t e}|\underline{\beta}_h},$$

$$\underline{\eta}^4_{\underline{\beta}_h} = \bar{\upsilon}_{\tilde{M}^1_e|\underline{\beta}_h} \bar{\upsilon}_{\tilde{M}^2_{I^q_t e}|\underline{\beta}_h} \bar{\upsilon}_{\tilde{M}^2_{D^q_t e}|\underline{\beta}_h},$$

$$\underline{\eta}^5_{\underline{\beta}_h} = \bar{\upsilon}_{\tilde{M}^2_e|\underline{\beta}_h} \bar{\upsilon}_{\tilde{M}^1_{I^q_t e}|\underline{\beta}_h} \bar{\upsilon}_{\tilde{M}^1_{D^q_t e}|\underline{\beta}_h},$$

$$\underline{\eta}^6_{\underline{\beta}_h} = \bar{\upsilon}_{\tilde{M}^2_e|\underline{\beta}_h} \bar{\upsilon}_{\tilde{M}^1_{I^q_t e}|\underline{\beta}_h} \bar{\upsilon}_{\tilde{M}^2_{D^q_t e}|\underline{\beta}_h},$$

$$\underline{\eta}^7_{\underline{\beta}_h} = \bar{\upsilon}_{\tilde{M}^2_e|\underline{\beta}_h} \bar{\upsilon}_{\tilde{M}^2_{I^q_t e}|\underline{\beta}_h} \bar{\upsilon}_{\tilde{M}^1_{D^q_t e}|\underline{\beta}_h},$$

$$\underline{\eta}^8_{\underline{\beta}_h} = \bar{\upsilon}_{\tilde{M}^2_e|\underline{\beta}_h} \bar{\upsilon}_{\tilde{M}^2_{I^q_t e}|\underline{\beta}_h} \bar{\upsilon}_{\tilde{M}^2_{D^q_t e}|\underline{\beta}_h}. \quad (10)$$

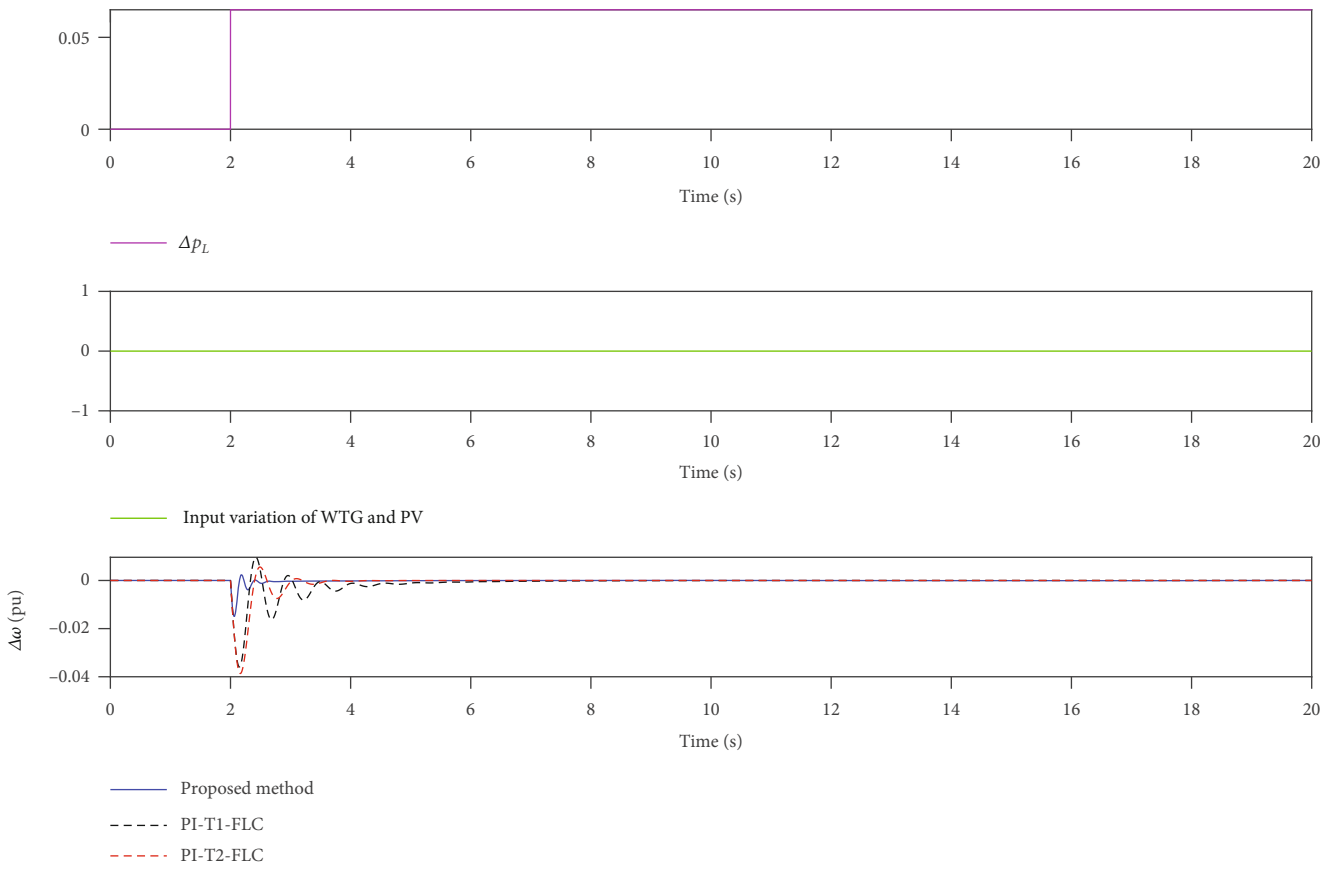

Figure 6: Scenario 1: load changes.

Considering the type reduction, the upper/lower bounds of control signal is computed as

$$\begin{aligned}
\bar{\bar{y}}_{\bar{\beta}_h} &= \frac{\sum_{l=1}^{n_r} \bar{\eta}^l_{\bar{\beta}_h} \bar{\rho}_l}{\sum_{l=1}^{n_r} \left(\bar{\eta}^l_{\bar{\beta}_h} + \underline{\eta}^l_{\bar{\beta}_h}\right)}, \\
\bar{\bar{y}}_{\underline{\beta}_h} &= \frac{\sum_{l=1}^{n_r} \bar{\eta}^l_{\underline{\beta}_h} \bar{\rho}_l}{\sum_{l=1}^{n_r} \left(\bar{\eta}^l_{\underline{\beta}_h} + \underline{\eta}^l_{\underline{\beta}_h}\right)}, \\
\underline{\hat{y}}_{\bar{\beta}_h} &= \frac{\sum_{l=1}^{n_r} \underline{\eta}^l_{\bar{\beta}_h} \underline{\rho}_l}{\sum_{l=1}^{n_r} \left(\bar{\eta}^l_{\bar{\beta}_h} + \underline{\eta}^l_{\bar{\beta}_h}\right)}, \\
\underline{\hat{y}}_{\underline{\beta}_h} &= \frac{\sum_{l=1}^{n_r} \bar{\eta}^l_{\underline{\beta}_h} \underline{\rho}_l}{\sum_{l=1}^{n_r} \left(\underline{\eta}^l_{\underline{\beta}_h} + \underline{\eta}^l_{\underline{\beta}_h}\right)},
\end{aligned} \tag{11}$$

where n_r denotes the number of rules and $\underline{\rho}_l$ and $\bar{\rho}_l$ are the lower/upper of lth rule parameters.

The second type reduction is computed as

$$\begin{aligned}
\bar{\bar{y}} &= \frac{\sum_{h=1}^{n} \bar{\beta}_h \bar{\bar{y}}_{\bar{\beta}_h}}{\sum_{h=1}^{n} \left(\bar{\beta}_h + \underline{\beta}_h\right)} + \frac{\sum_{h=1}^{n} \underline{\beta}_h \bar{\bar{y}}_{\underline{\beta}_h}}{\sum_{h=1}^{n} \left(\bar{\beta}_h + \underline{\beta}_h\right)}, \\
\underline{\hat{y}} &= \frac{\sum_{h=1}^{n} \bar{\beta}_h \underline{\hat{y}}_{\bar{\beta}_h}}{\sum_{h=1}^{n} \left(\bar{\beta}_h + \underline{\beta}_h\right)} + \frac{\sum_{h=1}^{n} \underline{\beta}_h \underline{\hat{y}}_{\underline{\beta}_h}}{\sum_{h=1}^{n} \left(\bar{\beta}_h + \underline{\beta}_h\right)}.
\end{aligned} \tag{12}$$

The output $\hat{y}$ (control signal) is computed as

$$\hat{y} = \frac{\bar{\bar{y}} + \underline{\hat{y}}}{2}. \tag{13}$$

8. Learning Algorithm

The rule and MFs are tuned in this part.

8.1. Tuning of Rule Parameters. The EKF method tunes the rule parameters such that (14) is minimized:

$$J = \frac{1}{2}(\hat{y})^2, \tag{14}$$

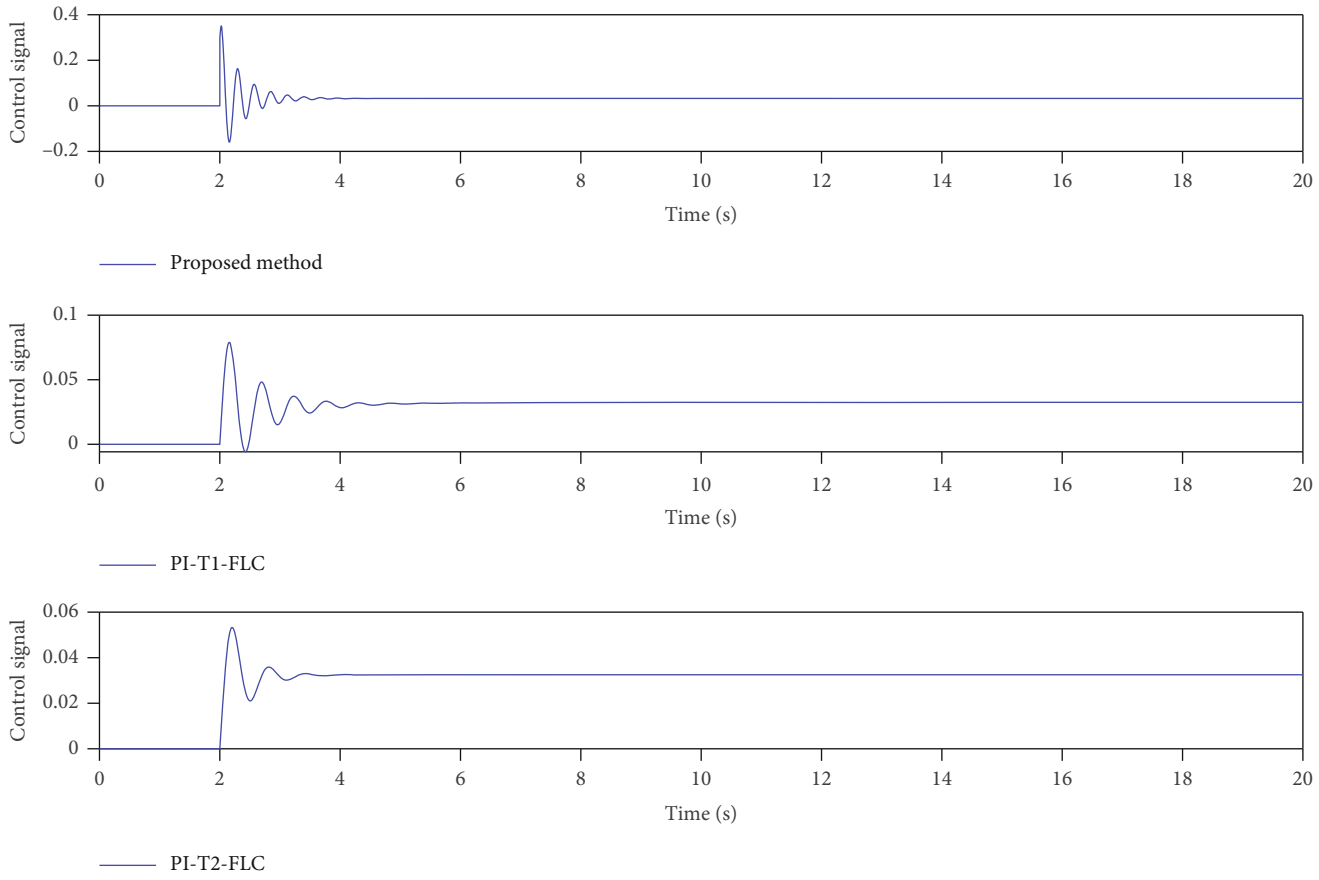

Figure 7: Scenario 1: control signals.

where $\hat{y}$ is the output T3-FLS that denotes control signal. The adjusting laws for $\bar{\rho}$ and $\underline{\rho}$ are computed as

$$\begin{aligned}\bar{\rho}(t) &= \bar{\rho}(t-1) + \bar{\xi}(t)\bar{\chi}(t)(-\hat{y}),\\ \underline{\rho}(t) &= \underline{\rho}(t-1) + \underline{\xi}(t)\underline{\chi}(t)(-\hat{y}),\end{aligned} \tag{15}$$

where $\bar{\xi}$ and $\underline{\xi}(t)$ are covariance matrices for $\bar{\rho}$ and $\underline{\rho}$, respectively. $\bar{\chi}(t)$ and $\underline{\chi}(t)$ are

$$\begin{aligned}\bar{\chi} &= \left[\bar{\chi}_1, \cdots, \bar{\chi}_l, \cdots, \bar{\chi}_{n_r}\right]^T,\\ \underline{\chi} &= \left[\underline{\chi}_1, \cdots, \underline{\chi}_l, \cdots, \underline{\chi}_{n_r}\right]^T,\end{aligned} \tag{16}$$

where $\bar{\chi}_l$ and $\underline{\chi}_l$ are

$$\begin{aligned}\bar{\chi}_l &= \frac{\partial \hat{y}}{\partial \bar{\rho}_l} = \frac{\partial \hat{y}}{\partial \bar{\hat{y}}}\frac{\partial \bar{\hat{y}}}{\partial \bar{\rho}_l} = \frac{\partial \hat{y}}{\partial \bar{\hat{y}}}\frac{\partial \bar{\hat{y}}}{\partial \bar{\hat{y}}_{\bar{\beta}_h}}\frac{\partial \bar{\hat{y}}_{\bar{\beta}_h}}{\partial \bar{\rho}_l} + \frac{\partial \hat{y}}{\partial \bar{\hat{y}}}\frac{\partial \bar{\hat{y}}}{\partial \bar{\hat{y}}_{\underline{\beta}_h}}\frac{\partial \bar{\hat{y}}_{\underline{\beta}_h}}{\partial \bar{\rho}_l}\\ &= 0.5\frac{1}{\sum_{h=1}^{n}\left(\bar{\beta}_h + \underline{\beta}_h\right)}\sum_{h=1}^{n}\bar{\beta}_h\frac{\bar{\eta}^l_{\bar{\beta}_h}}{\sum_{l=1}^{n_r}\left(\bar{\eta}^l_{\underline{\beta}_h} + \underline{\eta}^l_{\underline{\beta}_h}\right)} +\\ &\quad 0.5\frac{1}{\sum_{h=1}^{n}\left(\bar{\beta}_h + \underline{\beta}_h\right)}\sum_{h=1}^{n}\underline{\beta}_h\frac{\bar{\eta}^l_{\underline{\beta}_h}}{\sum_{l=1}^{n_r}\left(\bar{\eta}^l_{\underline{\beta}_h} + \underline{\eta}^l_{\underline{\beta}_h}\right)},\\ \underline{\chi}_l &= \frac{\partial \hat{y}}{\partial \underline{\rho}_l} = \frac{\partial \hat{y}}{\partial \underline{\hat{y}}}\frac{\partial \underline{\hat{y}}}{\partial \underline{\rho}_l} = \frac{\partial \hat{y}}{\partial \underline{\hat{y}}}\frac{\partial \underline{\hat{y}}}{\partial \underline{\hat{y}}_{\bar{\beta}_h}}\frac{\partial \underline{\hat{y}}_{\bar{\beta}_h}}{\partial \underline{\rho}_l} + \frac{\partial \hat{y}}{\partial \underline{\hat{y}}}\frac{\partial \underline{\hat{y}}}{\partial \underline{\hat{y}}_{\underline{\beta}_h}}\frac{\partial \underline{\hat{y}}_{\underline{\beta}_h}}{\partial \underline{\rho}_l}\\ &= 0.5\frac{1}{\sum_{h=1}^{n}\left(\bar{\beta}_h + \underline{\beta}_h\right)}\sum_{h=1}^{n}\bar{\beta}_h\frac{\underline{\eta}^l_{\bar{\beta}_h}}{\sum_{l=1}^{n_r}\left(\bar{\eta}^l_{\underline{\beta}_h} + \underline{\eta}^l_{\underline{\beta}_h}\right)} +\\ &\quad 0.5\frac{1}{\sum_{h=1}^{n}\left(\bar{\beta}_h + \underline{\beta}_h\right)}\sum_{h=1}^{n}\underline{\beta}_h\frac{\underline{\eta}^l_{\underline{\beta}_h}}{\sum_{l=1}^{n_r}\left(\bar{\eta}^l_{\underline{\beta}_h} + \underline{\eta}^l_{\underline{\beta}_h}\right)}.\end{aligned} \tag{17}$$

8.2. Tuning of MF Parameters. The centers of MFs are adjusted using the gradient descent. The tuning laws are therefore written as follows:

$$c_{\tilde{M}^j_e}(t) = c_{\tilde{M}^j_e}(t-1) - \gamma\frac{\partial J}{\partial c_{\tilde{M}^j_e}}, \quad j = 1, 2,$$

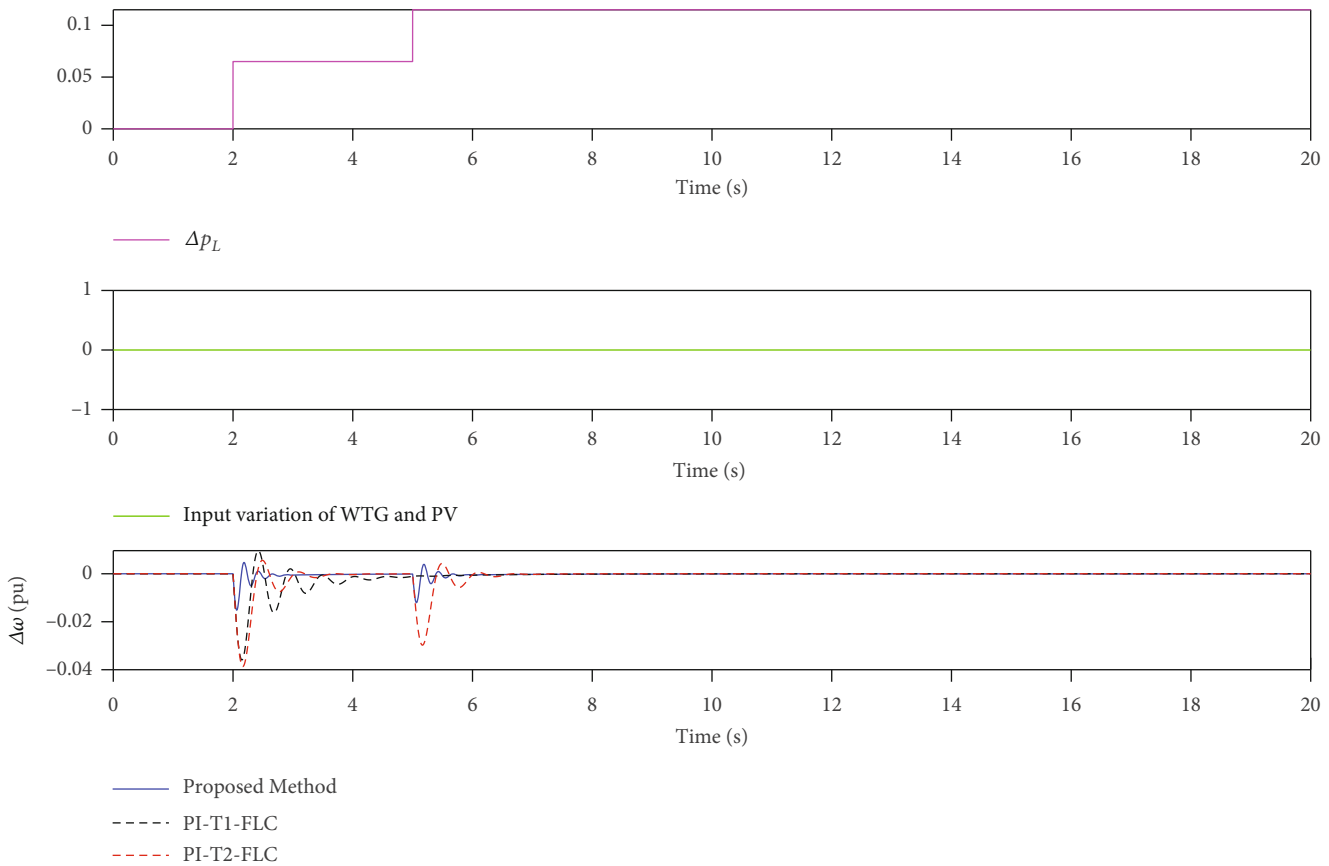

Figure 8: Scenario 2: multiple load changes.

$$c_{\tilde{M}^j_{I^{q_e}_t}}(t) = c_{\tilde{M}^j_{I^{q_e}_t}}(t-1) - \gamma \frac{\partial J}{\partial c_{\tilde{M}^j_{I^{q_e}_t}}}, j = 1, 2,$$
$$c_{\tilde{M}^j_{D^{q_e}_t}}(t) = c_{\tilde{M}^j_{D^{q_e}_t}}(t-1) - \gamma \frac{\partial J}{\partial c_{\tilde{M}^j_{D^{q_e}_t}}}, j = 1, 2, \tag{18}$$

where γ is a constant rate. $\partial J/\partial c_{\tilde{M}^1_e}$ is

$$\begin{aligned}
\frac{\partial J}{\partial c_{\tilde{M}^1_e}} &= \frac{\partial J}{\partial \hat{y}}\frac{\partial \hat{y}}{\partial \bar{\hat{y}}}\frac{\partial \bar{\hat{y}}}{\partial \bar{\hat{y}}_{\bar{\beta}_h}}\left(\sum_{l=1}^{n_r}\bar{\varsigma}_e^l\frac{\partial \bar{\hat{y}}_{\bar{\beta}_h}}{\partial \bar{\eta}^l_{\bar{\beta}_h}}\frac{\partial \bar{\eta}^l_{\bar{\beta}_h}}{\partial c_{\tilde{M}^1_e}} + \sum_{l=1}^{n_r}\bar{\varsigma}_e^l\frac{\partial \bar{\hat{y}}_{\bar{\beta}_h}}{\partial \underline{\eta}^l_{\bar{\beta}_h}}\frac{\partial \underline{\eta}^l_{\bar{\beta}_h}}{\partial c_{\tilde{M}^1_e}}\right) + \\
&= \frac{\partial J}{\partial \hat{y}}\frac{\partial \hat{y}}{\partial \bar{\hat{y}}}\frac{\partial \bar{\hat{y}}}{\partial \bar{\hat{y}}_{\underline{\beta}_h}}\left(\sum_{l=1}^{n_r}\bar{\varsigma}_e^l\frac{\partial \bar{\hat{y}}_{\underline{\beta}_h}}{\partial \bar{\eta}^l_{\underline{\beta}_h}}\frac{\partial \bar{\eta}^l_{\underline{\beta}_h}}{\partial c_{\tilde{M}^1_e}} + \sum_{l=1}^{n_r}\bar{\varsigma}_e^l\frac{\partial \bar{\hat{y}}_{\underline{\beta}_h}}{\partial \underline{\eta}^l_{\underline{\beta}_h}}\frac{\partial \underline{\eta}^l_{\underline{\beta}_h}}{\partial c_{\tilde{M}^1_e}}\right) + \\
&= \frac{\partial J}{\partial \hat{y}}\frac{\partial \hat{y}}{\partial \underline{\hat{y}}}\frac{\partial \underline{\hat{y}}}{\partial \underline{\hat{y}}_{\underline{\beta}_h}}\left(\sum_{l=1}^{n_r}\bar{\varsigma}_e^l\frac{\partial \underline{\hat{y}}_{\underline{\beta}_h}}{\partial \bar{\eta}^l_{\underline{\beta}_h}}\frac{\partial \bar{\eta}^l_{\underline{\beta}_h}}{\partial c_{\tilde{M}^1_e}} + \sum_{l=1}^{n_r}\bar{\varsigma}_e^l\frac{\partial \underline{\hat{y}}_{\underline{\beta}_h}}{\partial \underline{\eta}^l_{\underline{\beta}_h}}\frac{\partial \underline{\eta}^l_{\underline{\beta}_h}}{\partial c_{\tilde{M}^1_e}}\right) + \\
&= \frac{\partial J}{\partial \hat{y}}\frac{\partial \hat{y}}{\partial \underline{\hat{y}}}\frac{\partial \underline{\hat{y}}}{\partial \underline{\hat{y}}_{\bar{\beta}_h}}\left(\sum_{l=1}^{n_r}\bar{\varsigma}_e^l\frac{\partial \underline{\hat{y}}_{\bar{\beta}_h}}{\partial \bar{\eta}^l_{\bar{\beta}_h}}\frac{\partial \bar{\eta}^l_{\bar{\beta}_h}}{\partial c_{\tilde{M}^1_e}} + \sum_{l=1}^{n_r}\bar{\varsigma}_e^l\frac{\partial \underline{\hat{y}}_{\bar{\beta}_h}}{\partial \underline{\eta}^l_{\bar{\beta}_h}}\frac{\partial \underline{\eta}^l_{\bar{\beta}_h}}{\partial c_{\tilde{M}^1_e}}\right),
\end{aligned} \tag{19}$$

where $\bar{\varsigma}_e^l$ denotes the lth element of $\bar{\varsigma}_e$. $\bar{\varsigma}_e$ is written as

$$\bar{\varsigma}_e = [1, 1, 1, 1, 0, 0, 0, 0], \tag{20}$$

where the components of $\bar{\varsigma}_e$ in rules that contain $c_{\tilde{M}^1_e}$ are one. $\partial \bar{\hat{y}}_{\bar{\beta}_h}/\partial \bar{\eta}^l_{\bar{\beta}_h}$, $\partial \bar{\hat{y}}_{\bar{\beta}_h}/\partial \underline{\eta}^l_{\bar{\beta}_h}$, $\partial \bar{\hat{y}}_{\underline{\beta}_h}/\partial \bar{\eta}^l_{\underline{\beta}_h}$, $\partial \bar{\hat{y}}_{\underline{\beta}_h}/\partial \underline{\eta}^l_{\underline{\beta}_h}$, $\partial \underline{\hat{y}}_{\bar{\beta}_h}/\partial \bar{\eta}^l_{\bar{\beta}_h}$, $\partial \underline{\hat{y}}_{\bar{\beta}_h}/\partial \underline{\eta}^l_{\bar{\beta}_h}$, $\partial \underline{\hat{y}}_{\underline{\beta}_h}/\partial \bar{\eta}^l_{\underline{\beta}_h}$, and $\partial \underline{\hat{y}}_{\underline{\beta}_h}/\partial \underline{\eta}^l_{\underline{\beta}_h}$ are written as

$$\begin{aligned}
\frac{\partial \bar{\hat{y}}_{\bar{\beta}_h}}{\partial \bar{\eta}^l_{\bar{\beta}_h}} &= \bar{\rho}_l\frac{\sum_{l=1}^{n_r}\left(\bar{\eta}^l_{\bar{\beta}_h} + \underline{\eta}^l_{\bar{\beta}_h}\right) - \bar{\eta}^l_{\bar{\beta}_h}}{\left(\sum_{l=1}^{n_r}\left(\bar{\eta}^l_{\bar{\beta}_h} + \underline{\eta}^l_{\bar{\beta}_h}\right)\right)^2}, \\
\frac{\partial \bar{\hat{y}}_{\bar{\beta}_h}}{\partial \underline{\eta}^l_{\bar{\beta}_h}} &= \bar{\rho}_l\frac{-1}{\left(\sum_{l=1}^{n_r}\left(\bar{\eta}^l_{\bar{\beta}_h} + \underline{\eta}^l_{\bar{\beta}_h}\right)\right)^2}, \\
\frac{\partial \bar{\hat{y}}_{\underline{\beta}_h}}{\partial \bar{\eta}^l_{\underline{\beta}_h}} &= \bar{\rho}_l\frac{\sum_{l=1}^{n_r}\left(\bar{\eta}^l_{\underline{\beta}_h} + \underline{\eta}^l_{\underline{\beta}_h}\right) - \bar{\eta}^l_{\underline{\beta}_h}}{\left(\sum_{l=1}^{n_r}\left(\bar{\eta}^l_{\underline{\beta}_h} + \underline{\eta}^l_{\underline{\beta}_h}\right)\right)^2}, \\
\frac{\partial \bar{\hat{y}}_{\underline{\beta}_h}}{\partial \underline{\eta}^l_{\underline{\beta}_h}} &= \bar{\rho}_l\frac{-1}{\left(\sum_{l=1}^{n_r}\left(\bar{\eta}^l_{\underline{\beta}_h} + \underline{\eta}^l_{\underline{\beta}_h}\right)\right)^2},
\end{aligned}$$

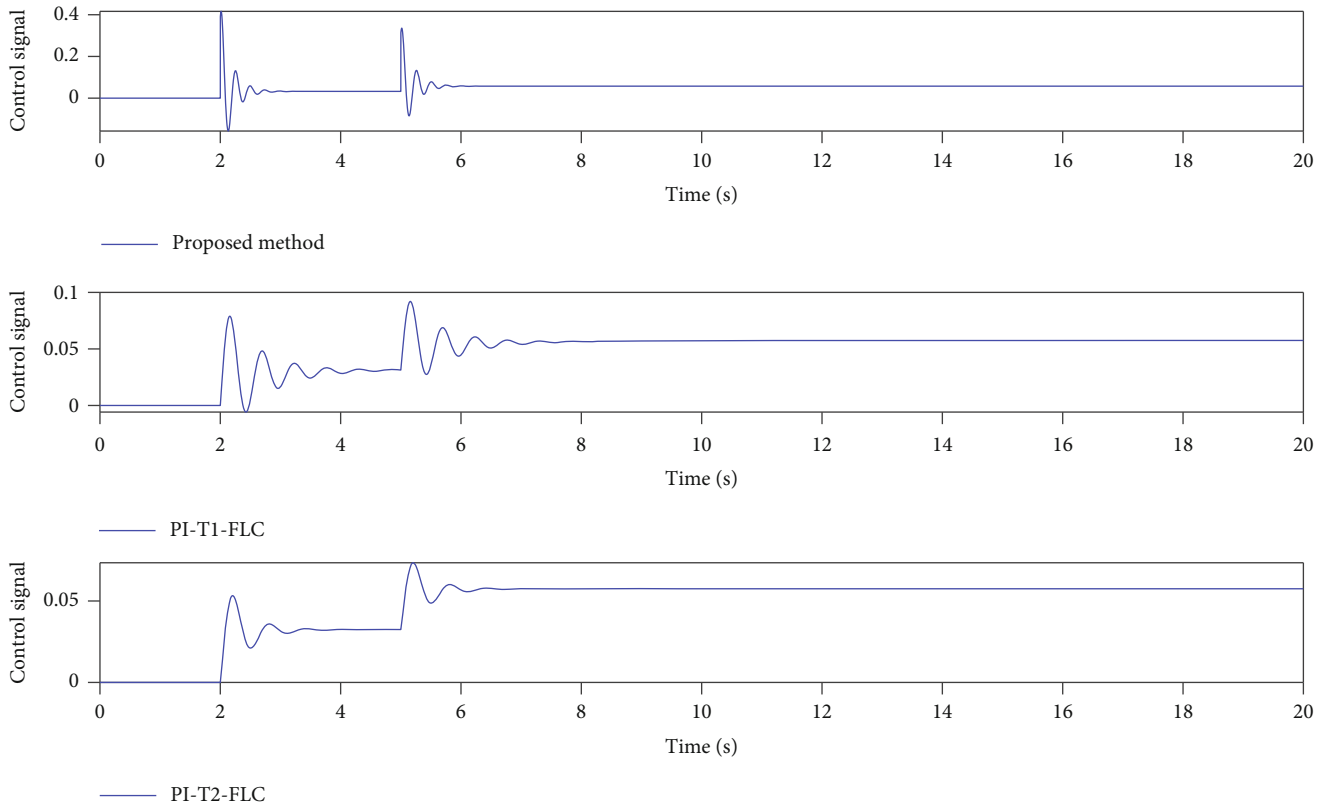

Figure 9: Scenario 2: control signals.

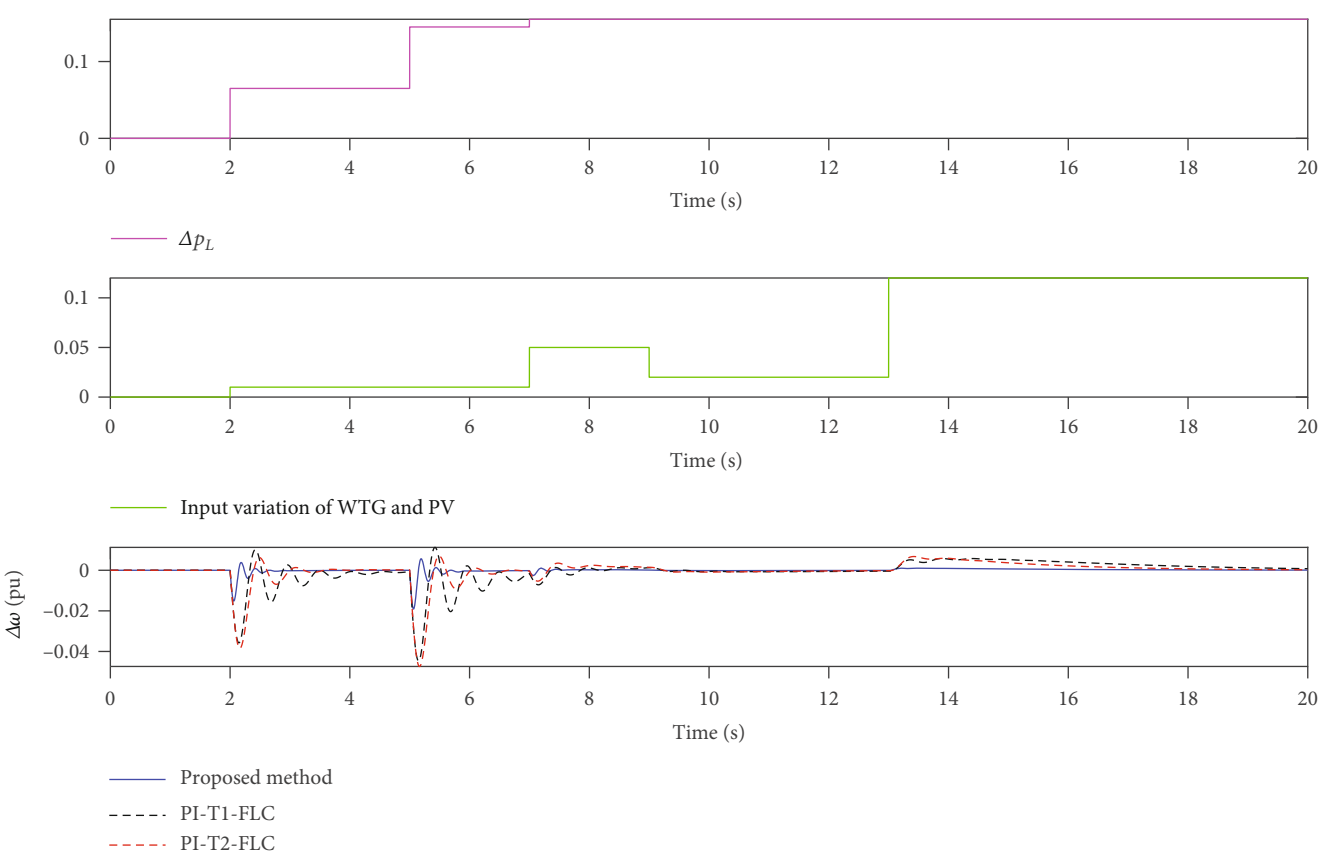

Figure 10: Scenario 3: multiple changes in load and irradiation wind power.

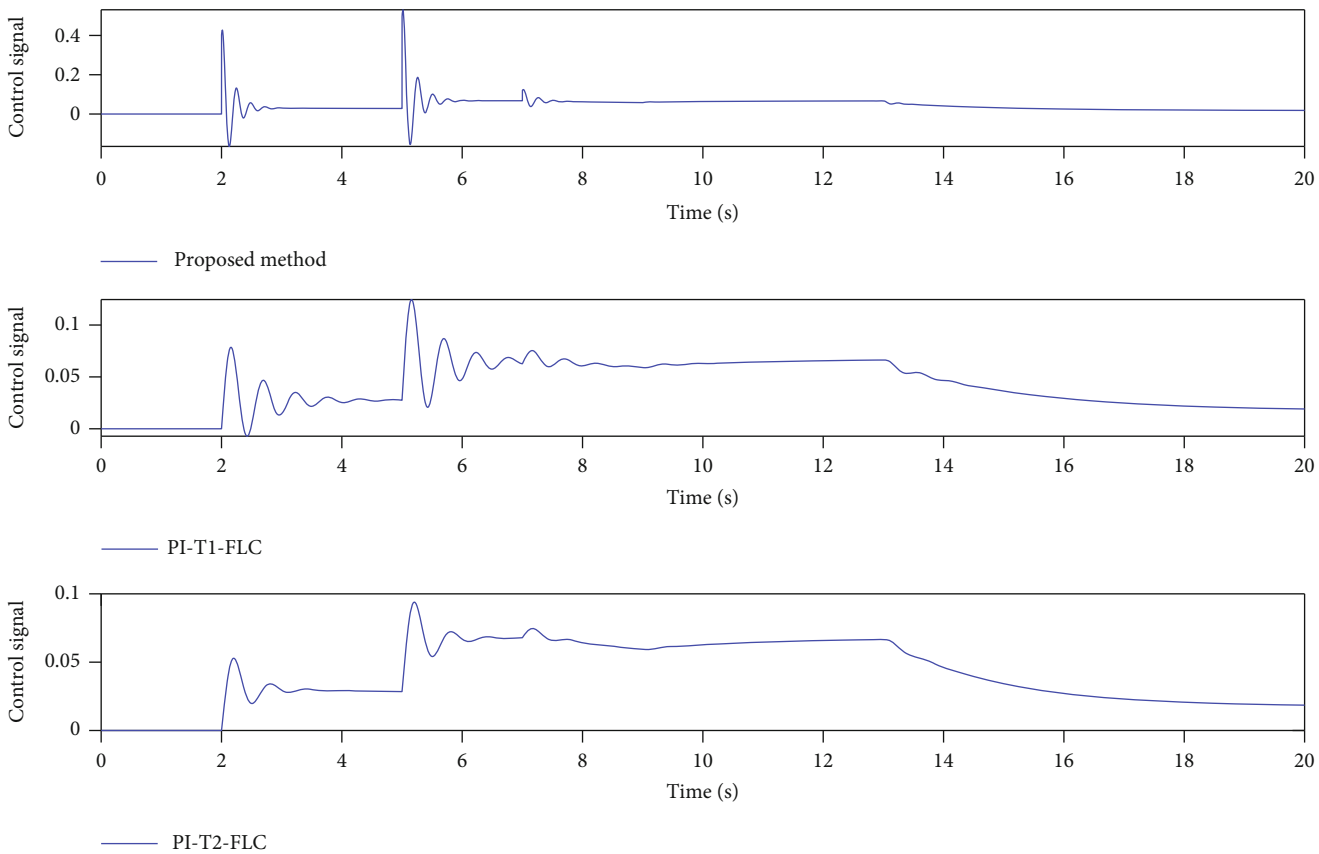

Figure 11: Scenario 3: control signals.

Table 2: RMSE comparison.

Scenarios	Designed controller	PI-T1-FLC [41]	PI-T2-FLC [42]	GT2-FLC [29]
	0.0012	0.0124	0.0106	0.0052
	0.0014	0.0065	0.0062	0.0035
	0.0016	0.0079	0.0074	0.0018

$$\begin{aligned}
\frac{\partial \underline{\widehat{y}}_{\bar{\beta}_h}}{\partial \bar{\eta}^l_{\bar{\beta}_h}} &= \underline{\rho}_l \frac{\sum_{l=1}^{n_r}\left(\bar{\eta}^l_{\bar{\beta}_h}+\underline{\eta}^l_{\bar{\beta}_h}\right)-\bar{\eta}^l_{\bar{\beta}_h}}{\left(\sum_{l=1}^{n_r}\left(\bar{\eta}^l_{\bar{\beta}_h}+\underline{\eta}^l_{\bar{\beta}_h}\right)\right)^2},\\
\frac{\partial \underline{\widehat{y}}_{\bar{\beta}_h}}{\partial \underline{\eta}^l_{\bar{\beta}_h}} &= \underline{\rho}_l \frac{-1}{\left(\sum_{l=1}^{n_r}\left(\bar{\eta}^l_{\bar{\beta}_h}+\underline{\eta}^l_{\bar{\beta}_h}\right)\right)^2},\\
\frac{\partial \underline{\widehat{y}}_{\underline{\beta}_h}}{\partial \bar{\eta}^l_{\underline{\beta}_h}} &= \underline{\rho}_l \frac{\sum_{l=1}^{n_r}\left(\bar{\eta}^l_{\underline{\beta}_h}+\underline{\eta}^l_{\underline{\beta}_h}\right)-\bar{\eta}^l_{\underline{\beta}_h}}{\left(\sum_{l=1}^{n_r}\left(\bar{\eta}^l_{\underline{\beta}_h}+\underline{\eta}^l_{\underline{\beta}_h}\right)\right)^2},\\
\frac{\partial \underline{\widehat{y}}_{\underline{\beta}_h}}{\partial \underline{\eta}^l_{\underline{\beta}_h}} &= \underline{\rho}_l \frac{-1}{\left(\sum_{l=1}^{n_r}\left(\bar{\eta}^l_{\underline{\beta}_h}+\underline{\eta}^l_{\underline{\beta}_h}\right)\right)^2}.
\end{aligned} \tag{21}$$

For $\partial\bar{\eta}^l_{\bar{\beta}_h}/\partial c_{\tilde{M}^1_e}$, $\partial\bar{\eta}^l_{\underline{\beta}_h}/\partial c_{\tilde{M}^1_e}$, $\partial\underline{\eta}^l_{\bar{\beta}_h}/\partial c_{\tilde{M}^1_e}$, and $\partial\underline{\eta}^l_{\underline{\beta}_h}/\partial c_{\tilde{M}^1_e}$, one has

$$\begin{aligned}
\frac{\partial\bar{\eta}^l_{\bar{\beta}_h}}{\partial c_{\tilde{M}^1_e}} &= \frac{2\left(e-c_{\tilde{M}^1_e|\bar{\beta}_h}\right)}{\bar{\vartheta}^2_{\tilde{M}^1_e|\bar{\beta}_h}}\bar{\eta}^l_{\bar{\beta}_h},\\
\frac{\partial\bar{\eta}^l_{\underline{\beta}_h}}{\partial c_{\tilde{M}^1_e}} &= \frac{2\left(e-c_{\tilde{M}^1_e|\underline{\beta}_h}\right)}{\bar{\vartheta}^2_{\tilde{M}^1_e|\underline{\beta}_h}}\bar{\eta}^l_{\underline{\beta}_h},\\
\frac{\partial\underline{\eta}^l_{\bar{\beta}_h}}{\partial c_{\tilde{M}^1_e}} &= \frac{2\left(e-c_{\tilde{M}^1_e|\bar{\beta}_h}\right)}{\bar{\vartheta}^2_{\tilde{M}^1_e|\bar{\beta}_h}}\underline{\eta}^l_{\bar{\beta}_h},\\
\frac{\partial\underline{\eta}^l_{\underline{\beta}_h}}{\partial c_{\tilde{M}^1_e}} &= \frac{2\left(e-c_{\tilde{M}^1_e|\underline{\beta}_h}\right)}{\bar{\vartheta}^2_{\tilde{M}^1_e|\underline{\beta}_h}}\underline{\eta}^l_{\underline{\beta}_h}.
\end{aligned} \tag{22}$$

The computation of $\partial J/\partial c_{\tilde{M}^2_e}$, $\partial J/\partial c_{\tilde{M}^1_{D^q_t e}}$, $\partial J/\partial c_{\tilde{M}^2_{D^q_t e}}$, $\partial J/\partial c_{\tilde{M}^1_{I^q_t e}}$, and $\partial J/\partial c_{\tilde{M}^2_{I^q_t e}}$ are the same as $\partial J/\partial c_{\tilde{M}^1_e}$, with just difference that $\bar{\varsigma}_e$ is replaced with $\underline{\varsigma}_e$, $\bar{\varsigma}_{D^q_t e}$, $\underline{\varsigma}_{D^q_t e}$, $\bar{\varsigma}_{I^q_t e}$, and $\underline{\varsigma}_{I^q_t e}$, respectively. Also, $c_{\tilde{M}^1_e|\bar{\beta}_h}$, $c_{\tilde{M}^1_e|\underline{\beta}_h}$, $\bar{\vartheta}_{\tilde{M}^1_e|\bar{\beta}_h}$, and $\bar{\vartheta}^2_{\tilde{M}^1_e|\underline{\beta}_h}$ must be

replaced with the corresponding terms. The vectors $\underline{\varsigma}_e$, $\bar{\varsigma}_{D_t^q e}$, $\underline{\varsigma}_{D_t^q e}$, $\bar{\varsigma}_{I_t^q e}$, and $\underline{\varsigma}_{I_t^q e}$ are as

$$\begin{aligned}
\underline{\varsigma}_e &= [0, 0, 0, 0, 1, 1, 1, 1], \\
\bar{\varsigma}_{D_t^q e} &= [1, 0, 1, 0, 1, 0, 1, 0], \\
\underline{\varsigma}_{D_t^q e} &= [0, 1, 0, 1, 0, 1, 0, 1], \\
\bar{\varsigma}_{I_t^q e} &= [1, 1, 0, 0, 1, 1, 0, 0], \\
\underline{\varsigma}_{I_t^q e} &= [0, 0, 1, 1, 0, 0, 1, 1].
\end{aligned} \tag{23}$$

9. Simulations

The designed controller is applied on a case-study MG that is shown in Figure 5 [29] and is described in Table 1 [29]. Time-varying dynamics, rapid power changes and solar irradiation, multiple load changes, and so on are all considered in the evaluation of the LFC's regulatory performance.

Scenario 1: a single load perturbation is taken into account in the initial set of parameters. Also, the model information of all units is unknown. Figure 6 shows the regulation performance. Figure 7 shows the controller signal. Comparison with type-1 fuzzy controller (PI-T1-FLC) [41] and type-2 FLC (PI-T2-FLC) [42] shows that the suggested approach is superior in terms of overall performance and accuracy. An observer can clearly tell that the designed control system is able to outperform.

Scenario 2: in addition to the perturbation of previous scenario, in the second case, the values of all unit parameters are considered to be time-varying as $p = (1 + \cos(t))p$. Figure 8 depicts the system's regulation outcome. Figure 9 show the controller signal. It is clear from Figure 8 that the proposed FLC performs exceptionally well.

Scenario 3: the solar/wind powers are also time-varying in the third scenario, in addition to the numerous fluctuations in the load. Also, a sensor error is added to output signals as a Gaussian noise with variance 0.01. Figure 10 shows the frequency's performance in this situation. Figure 11 shows the controller signal. One can see that the proposed technique holds up well in the face of solar variation, wind turbine mechanical power disturbance, and various load variations. In comparison to the other controllers, the suggested method's frequency trajectory shows less variance. Table 2 contains the RMSE values for each of the various cases. The performance is compared with PI-T1-FLC [41], PI-T2-FLC [42], and general type-2 FLC (GT2-FLC) [29]. The suggested method's RMSE in all circumstances appear to be significantly lower than those of the other techniques.

10. Conclusion

The applications of renewable energies (REs) in meeting the energy needs of human societies are extended, because the use of RE sources can prevent the emission of greenhouse gases and pollutants, reduce water consumption, and ultimately help sustainable security. One of the main drawbacks is the natural fluctuation of voltage/frequency in microgrids (MGs) that include RE sources. In this paper, a new scheme is developed for frequency management in MGs. A new T3-FLS-based controller is designed, and an online optimization scheme is proposed. The designed controller is applied for an MG, and its performance is evaluated under various practical conditions. In the first scenario, in addition to unknown dynamics, an abrupt change is considered in the output load. It is shown that the suggested controller well handles the disturbances, and the output is stabilized in a finite time. For the second examination, another is added to the previous one, and the parameters of the MG dynamics are considered to be time-varying. The simulation results are verified that the suggested approach well resists against dynamic perturbations. Finally, for the last examination, beside the dynamic uncertainties and load perturbations, the solar/wind powers are also changed, and a sensor error is added to signals as a Gaussian noise with variance 0.01. The results and comparisons with other approaches demonstrate that the suggested controller has a good regulation outcome with the least steady-state error and good transient performance.

Nomenclature

FLSs: Fuzzy logic systems
PI: Proportional-integral
T3: Type 3
MG: Microgrid
RE: Renewable energies
GA: Genetic algorithm
PSO: Particle swarm optimization
LFC: Load frequency control
MF: Membership function
SD: Standard divisions
FLC: Fuzzy controller.

Data Availability

All the numerical simulation parameters are mentioned in the respective text part, and there are no additional data requirements for the simulation results.

Conflicts of Interest

The authors declare that there is no conflict of interest.

References

[1] A. H. T. Yabr, S. E. Najafi, Z. Moghaddas, and P. S. Shahrezaei, "Interval cross efficiency measurement for general two-stage systems," *Mathematical Problems in Engineering*, vol. 2022, Article ID 5431358, 19 pages, 2022.

[2] T. Xiao, C. Gan, and Q. Zhang, "The existence of least energy sign-changing solution for Kirchhoff-type problem with potential vanishing at infinity," *Advances in Mathematical Physics*, vol. 2021, Article ID 6690204, 10 pages, 2021.

[3] H.-A. Trinh, H.-V.-A. Truong, and K. K. Ahn, "Development of fuzzy-adaptive control based energy management strategy for PEM fuel cell hybrid tramway system," *Applied Sciences*, vol. 12, no. 8, p. 3880, 2022.

[4] H. V. A. Truong, H. A. Trinh, D. T. Tran, and K. K. Ahn, "A robust observer for sensor faults estimation on n-DOF

manipulator in constrained framework environment," *IEEE Access*, vol. 9, pp. 88439–88451, 2021.

[5] C. Zhu, Q. Tu, C. Jiang, M. Pan, H. Huang, and Z. Tu, "Mean deviation coupling control for multimotor system via global fast terminal sliding mode control," *Advances in Mathematical Physics*, vol. 2021, Article ID 9200267, 16 pages, 2021.

[6] H. Salahuddin, K. Imdad, M. U. Chaudhry, D. Nazarenko, V. Bolshev, and M. Yasir, "Induction machine-based EV vector control model using Mamdani fuzzy logic controller," *Applied Sciences*, vol. 12, no. 9, p. 4647, 2022.

[7] R. Ashraf, M. A. Habib, M. Akram et al., "Deep convolution neural network for big data medical image classification," *IEEE Access*, vol. 8, pp. 105659–105670, 2020.

[8] A. Tabak, "Fractional order frequency proportional-integral-derivative control of microgrid consisting of renewable energy sources based on multi-objective grasshopper optimization algorithm," *Transactions of the Institute of Measurement and Control*, vol. 44, no. 2, pp. 378–392, 2022.

[9] R. Tripathi and O. Singh, "An analysis on frequency control of microgrid including diverse renewable energy sources," in *Advances in Energy Technology*, pp. 81–95, Springer, 2022.

[10] H. M. El Zoghby and H. S. Ramadan, "Isolated microgrid stability reinforcement using optimally controlled STATCOM," *Sustainable Energy Technologies and Assessments*, vol. 50, article 101883, 2022.

[11] G. K. Suman, J. M. Guerrero, and O. P. Roy, "Stability of microgrid cluster with diverse energy sources: a multi-objective solution using NSGA-II based controller," *Sustainable Energy Technologies and Assessments*, vol. 50, article 101834, 2022.

[12] K. A. Al Sumarmad, N. Sulaiman, N. I. A. Wahab, and H. Hizam, "Energy management and voltage control in microgrids using artificial neural networks, PID, and fuzzy logic controllers," *Energies*, vol. 15, no. 1, p. 303, 2022.

[13] H. K. Vanashi, F. D. Mohammadi, V. Verma, J. Solanki, and S. K. Solanki, "Hierarchical multi-agent based frequency and voltage control for a microgrid power system," *International Journal of Electrical Power & Energy Systems*, vol. 135, article 107535, 2022.

[14] M. Ranjan and R. Shankar, "A literature survey on load frequency control considering renewable energy integration in power system: recent trends and future prospects," *Journal of Energy Storage*, vol. 45, article 103717, 2022.

[15] R. Kumar, S. Jha, and R. Singh, "A different approach for solving the shortest path problem under mixed fuzzy environment," *International Journal of Fuzzy System Applications*, vol. 9, no. 2, pp. 132–161, 2020.

[16] S. Deng, C. Wang, Z. Fu, and M. Wang, "An intelligent system for insider trading identification in Chinese security market," *Computational Economics*, vol. 57, no. 2, pp. 593–616, 2021.

[17] M. Vilela, G. Oluyemi, and A. Petrovski, "A fuzzy inference system applied to value of information assessment for oil and gas industry," *Decision Making: Applications in Management and Engineering*, vol. 2, no. 2, pp. 1–18, 2019.

[18] E. K. Zavadskas, V. Gediminas, Z. Turskis, Ž. Stević, and A. Mardani, "Modelling procedure for the selection of steel pipes supplier by applying fuzzy AHP method," *Operational Research in Engineering Sciences: Theory and Applications*, vol. 3, no. 2, pp. 39–53, 2020.

[19] Q. Bu, J. Cai, Y. Liu et al., "The effect of fuzzy PID temperature control on thermal behavior analysis and kinetics study of biomass microwave pyrolysis," *Journal of Analytical and Applied Pyrolysis*, vol. 158, article 105176, 2021.

[20] D. Sain and B. Mohan, "Modeling, simulation and experimental realization of a new nonlinear fuzzy PID controller using center of gravity defuzzification," *ISA Transactions*, vol. 110, pp. 319–327, 2021.

[21] T. A. Mai, T. S. Dang, D. T. Duong, V. C. Le, and S. Banerjee, "A combined backstepping and adaptive fuzzy PID approach for trajectory tracking of autonomous mobile robots," *Journal of the Brazilian Society of Mechanical Sciences and Engineering*, vol. 43, no. 3, pp. 1–13, 2021.

[22] O. Karahan, "Design of optimal fractional order fuzzy PID controller based on cuckoo search algorithm for core power control in molten salt reactors," *Progress in Nuclear Energy*, vol. 139, article 103868, 2021.

[23] D. Sain and B. Mohan, "A simple approach to mathematical modelling of integer order and fractional order fuzzy PID controllers using one-dimensional input space and their experimental realization," *Journal of the Franklin Institute*, vol. 358, no. 7, pp. 3726–3756, 2021.

[24] P. C. Nayak, B. P. Nayak, R. C. Prusty, and S. Panda, "Sunflower optimization based fractional order fuzzy PID controller for frequency regulation of solar-wind integrated power system with hydrogen aqua equalizer-fuel cell unit," *Energy Sources, Part A: Recovery, Utilization, and Environmental Effects*, pp. 1–19, 2021.

[25] A. Aftab and X. Luan, "A fuzzy-PID series feedback self-tuned adaptive control of reactor power using nonlinear multipoint kinetic model under reference tracking and disturbance rejection," *Annals of Nuclear Energy*, vol. 166, article 108696, 2022.

[26] Y. Liu, K. Fan, and Q. Ouyang, "Intelligent traction control method based on model predictive fuzzy PID control and online optimization for permanent magnetic maglev trains," *IEEE Access*, vol. 9, pp. 29032–29046, 2021.

[27] M. G. Gafar, R. A. El-Sehiemy, and S. Sarhan, "A hybrid fuzzy-crow optimizer for unconstrained and constrained engineering design problems," *Human-centric Computing and Information Sciences*, vol. 12, pp. 1–24, 2022.

[28] G. Sahoo, R. K. Sahu, N. R. Samal, and S. Panda, "Analysis of type-2 fuzzy fractional-order PD-PI controller for frequency stabilisation of the micro-grid system with real-time simulation," *International Journal of Sustainable Energy*, vol. 41, no. 5, pp. 412–433, 2022.

[29] A. Mohammadzadeh, M. H. Sabzalian, A. Ahmadian, and N. Nabipour, "A dynamic general type-2 fuzzy system with optimized secondary membership for online frequency regulation," *ISA Transactions*, vol. 112, pp. 150–160, 2021.

[30] R. K. Khadanga, A. Kumar, and S. Panda, "Application of interval type-2 fuzzy PID controller for frequency regulation of ac islanded microgrid using modified equilibrium optimization algorithm," *Arabian Journal for Science and Engineering*, vol. 46, no. 10, pp. 9831–9847, 2021.

[31] K. Sabahi, M. Tavan, and A. Hajizadeh, "Adaptive type-2 fuzzy PID controller for LFC in AC microgrid," *Soft Computing*, vol. 25, no. 11, pp. 7423–7434, 2021.

[32] P. Jekan and C. Subramani, "The performance analysis of type-2 fuzzy fractional-order tilt integral derivative controller with enhanced Harris hawks optimization," *Transactions of the Institute of Measurement and Control*, vol. 43, no. 12, pp. 2818–2834, 2021.

[33] S. Rawat, B. Jha, M. K. Panda, and J. Kanti, "Interval type-2 fuzzy logic control-based frequency control of hybrid power system using DMGS of PI controller," *Applied Sciences*, vol. 11, no. 21, p. 10217, 2021.

[34] Y. Cao, A. Raise, A. Mohammadzadeh, S. Rathinasamy, S. S. Band, and A. Mosavi, "Deep learned recurrent type-3 fuzzy system: application for renewable energy modeling/prediction," *Energy Reports*, vol. 7, pp. 8115–8127, 2021.

[35] Z. Liu, A. Mohammadzadeh, H. Turabieh, M. Mafarja, S. S. Band, and A. Mosavi, "A new online learned interval type-3 fuzzy control system for solar energy management systems," *IEEE Access*, vol. 9, pp. 10498–10508, 2021.

[36] M. Gheisarnejad, A. Mohammadzadeh, H. Farsizadeh, and M.-H. Khooban, "Stabilization of 5G telecom converter-based deep type-3 fuzzy machine learning control for telecom applications," *IEEE Transactions on Circuits and Systems II: Express Briefs*, vol. 69, no. 2, pp. 544–548, 2022.

[37] M. Gheisarnejad, A. Mohammadzadeh, and M. Khooban, "Model predictive control-based type-3 fuzzy estimator for voltage stabilization of DC power converters," *IEEE Transactions on Industrial Electronics*, vol. 69, no. 12, pp. 13849–13858, 2022.

[38] M. Li, H. S. Dizaji, S. Asaadi, F. Jarad, A. E. Anqi, and M. Wae-hayee, "Thermo-economic, exergetic and mechanical analysis of thermoelectric generator with hollow leg structure; impact of leg cross-section shape and hollow-to-filled area ratio," *Case Studies in Thermal Engineering*, vol. 27, article 101314, 2021.

[39] J. Li, J. Geng, and T. Yu, "Grid-area coordinated load frequency control strategy using large-scale multi- agent deep reinforcement learning," *Energy Reports*, vol. 8, pp. 255–274, 2022.

[40] A. Mohammadzadeh, M. H. Sabzalian, and W. Zhang, "An interval type-3 fuzzy system and a new online fractional-order learning algorithm: theory and practice," *IEEE Transactions on Fuzzy Systems*, vol. 28, no. 9, pp. 1940–1950, 2019.

[41] M. Mokhtar, M. I. Marei, M. A. Sameh, and M. A. Attia, "An adaptive load frequency control for power systems with renewable energy sources," *Energies*, vol. 15, no. 2, p. 573, 2022.

[42] A. D. Shakibjoo, M. Moradzadeh, S. U. Din, A. Mohammadzadeh, A. H. Mosavi, and L. Vandevelde, "Optimized type-2 fuzzy frequency control for multi-area power systems," *IEEE Access*, vol. 10, pp. 6989–7002, 2022.

Hindawi
Advances in Mathematical Physics
Volume 2022, Article ID 6368110, 20 pages
https://doi.org/10.1155/2022/6368110

Research Article

Research on Fuzzy Decision-Making Method of Task Allocation for Ship Multiagent Collaborative Design

Jinghua Li,[1] Yiying Wang,[2] Boxin Yang,[1] Qinghua Zhou,[1] and Feihui Yuan[3]

[1]*College of Mechanical and Electrical Engineering, Harbin Engineering University, Harbin, China*
[2]*College of Shipbuilding Engineering, Harbin Engineering University, Harbin, China*
[3]*Design Department I, Shanghai Waigaoqiao Shipbuilding Co., Ltd., Shanghai, China*

Correspondence should be addressed to Boxin Yang; yangboxin@foxmail.com

Received 5 May 2022; Accepted 13 June 2022; Published 18 July 2022

Academic Editor: S. E. Najafi

Since task allocation is one of the core tasks of ship design, the choice of its allocation strategy is a key factor that affects whether the task and the design agent can be beneficially matched. Different from the traditional one-way assignment mode of assigning tasks to designers, in the task assignment strategy of modern ship collaborative design mode, designers' ability and benefit ratio is getting higher and higher. Therefore, in order to improve the efficiency and quality of task design, this paper proposes a multidesign agent-task allocation decision-making method. In this paper, the task attributes and designers' attributes are introduced into the task allocation strategy model, and the fuzzy linguistic variable method is used to build the evaluation index matrix of the design agent, and the task timeliness function is established. Secondly, the multidesign agent-task benefit function is established and solved to obtain the best allocation strategy. Finally, through example verification and comparative analysis with the Round-Robin algorithm (RR) and the Weighted Round-Robin (WRR) algorithm, the validity, feasibility, and stability of the multidesign agent-task allocation decision-making method proposed in this paper are verified, and it is proved that the task allocation method takes the bilateral needs of the task and the design agent into account, solves the optimal allocation strategy of collaborative design tasks, and realizes the balanced allocation between the ship collaborative design task and the design agent.

1. Introduction

Ship product design is an extremely complex process that requires the participation of multiple departments and professionals. In order to shorten the ship design cycle, meet the coordination and communication between designers, and improve the quality of ship design, domestic ships are gradually turning to a collaborative design model. The collaborative design of modern ships is jointly completed by design institutes, shipyards, shipowners, classification societies, suppliers, subcontractors, and other entities. Due to the large volume of ships and a large number of design tasks, the agents participating in the design have different fields, knowledge background, and cooperation efficiency. How to choose a plan with appropriate design task granularity and optimal benefit between multiple design agents and tasks from many task allocation schemes is one of the key problems in the current research of ship collaborative design.

Task assignment is an important stage and link of collaborative design, and it is the communication between task assignor and task receiver. Reasonable task allocation can make full use of resources and assign tasks to the most appropriate executors, so that task executors can complete collaborative design tasks efficiently, low cost, and high quality, and finally improve the efficiency of collaborative design product design. At present, scholars at home and abroad have done a lot of research on the rational allocation of tasks and personnel. Some scholars take task assigners or task recipients as the research objects and take factors such as the skill level of personnel or the preference of task assigners as the research background to study how to improve the efficiency of task assignment and the degree of task completion. Gui et al. [1]

considered two task allocation situations of initial personnel alliance and joining new personnel to form a new alliance and established a task allocation strategy of task priority satisfaction and performance reward to meet the characteristics of task timeliness, stability, and dynamics. Jiang et al. [2] considered the user's learning ability, modeled the user's skill update method in the process of performing tasks, proposed a user skill update mechanism, established a task allocation function that maximizes the number of tasks completed, and applied an improved whale algorithm. Solve task allocation problems. Wang et al. [3] introduced a minimum perceived quality threshold for tasks in the context of a multitasking assignment problem, which improves the perceived quality of individual tasks by considering the maximum number of tasks allowed for the personnel, thus improving the overall utility of the task. Wu et al. [4] proposed an algorithm capable of real-time task assignment and budget awareness based on personnel maximization of desired outcomes with a finite task budget in the context of spatial task package assignment, which was verified to be effective in improving task assignment efficiency. Jiang et al. [5] proposed a group-oriented approach to measure the ability of a group to complete a task in terms of contextual crowdsourcing value and constructed a task allocation algorithm to rationally allocate tasks and people. Li and Zhang [6] considered two types of time-constrained properties, task timeliness, and personnel availability and designed two types of evolutionary algorithms to solve the multitask assignment problem with time constraints. Most of the above scholars take the maximum ability or quantity limit of task recipients as the realistic constraints and take improving the efficiency of task allocation as the ultimate goal. Some scholars also take the skill level of task recipients as the influencing factor of task quality. While choosing different research subjects, scholars design corresponding functional relations to measure the timeliness and quality of task completion in combination with the specific environmental background of task allocation.

In task allocation, resources are an important element that affects the balance of task allocation. Many scholars have carried out research on the impact of resources on task allocation. Huang at al. [7] used idle vehicle resources as the background to construct the coordinated task processing calculation paradigm CVEC for parked vehicles and MEC servers and studied how to perform effective workload distribution and maximize user center utility in a dynamic environment to optimize network task scheduling. Xu et al. [8] aimed at the low utilization rate of collaborative logistics task resource allocation and the conflict of interest between operators and customers. Based on the multidistribution hybrid collaborative network, considering factors such as task delay penalties and capacity limitations, they formulated a multiobjective and multilogistics task scheduling strategy and designed an immune genetic algorithm with a three-layer coding mechanism to solve the model. Rajakumari et al. [9] introduced cloud computing resources, system throughput, and execution time in the context of cloud computing task scheduling problem, maximized resource utilization, minimized system throughput, and minimized execution waiting time as objective functions, thus designing a cloud computing fuzzy hybrid particle swarm parallel ant colony optimization algorithm. Baroudi et al. [10] studied the online dynamic multirobot task assignment problem and constructed a distributed multiobjective task assignment method with the task quality level as the optimization objective, while considering task distance and load balancing. Lee [11] proposed a resource-based multirobot task allocation algorithm with task completion timeliness and resource consumption effectiveness as the research objectives, so as to improve task efficiency and effectiveness. Yang et al. [12] designed a node affinity-based task assignment method for the wireless sensor task assignment problem under resource constraints and also to reduce node task redundancy. Most of the task assignment problems related to resource influencing factors focus on multiuser system application fields such as logistics, cloud computing, and multirobot system. In view of the task allocation problem in the above multiuser system application fields, scholars also limited the types of key resources. In the above study, resources were limited to network computing resources, robot use resources, logistics vehicles, and other consumable resources, and allocation constraints were applied to the application of system resources.

At the same time, some scholars focus their research on task allocation decision-making methods and use different algorithms to innovate problem solving methods. Song et al. [13] took the multirobot system in the medical and nursing environment as the application background and proposed a group intelligent allocation scheme based on the near-field task subset division. Firstly, the tasks are arranged orderly by ant colony algorithm to determine an optimal task chain, and then, the task chain is divided into subsets by genetic algorithm. Hu et al. [14] proposed a multiobjective reinforced greedy iterative algorithm to solve the task allocation and scheduling among mobile smart users. At the macro level of the algorithm, the Q-learning reinforcement learning algorithm is used to optimize learning, and at the micro level, the greedy algorithm is used to select the iterative optimal solution, and it is verified that the proposed algorithm has fast convergence speed and low energy consumption. Feng et al. [15] proposed a group intelligence-aware user task allocation mechanism, which combines vehicle user trajectory characteristics with combinatorial multiarmed bandit (CMAB) algorithm to improve the accuracy of task allocation. Ye et al. [16] used the cooperative multitask assignment of the UAV to perform the suppression of enemy air defense (SEAD) mission on the ground stationary target as the research goal. In order to solve the problems faced in task allocation, such as large scale, heterogeneity of UAV, different task coupling, and task priority constraints, an improved genetic algorithm with multitype gene chromosome coding strategy is proposed, and the optimization performance of the algorithm is verified by simulation. Shi et al. [17] proposed a dynamic auction approach for differentiated tasks under cost rigidities (DAACR) in the context of a multirobot system, which was validated to reduce the task assignment delay time of a multirobot system, while the algorithm can be applied to multirobot systems with different work contexts, thus improving the overall utilization of the robot system. Zhang et al. [18] extended their research on the existing status of UAV swarm task preprocessing to construct a discrete particle swarm algorithm that introduces a market auction mechanism to study the dynamic task assignment problem during

task execution, with the objective of real-time task assignment for UAV swarms. Yin et al. [19] constructed a group intelligent software development task assignment method based on the heterogeneity of software development tasks in the context of software development task assignment in P2P networks by transforming the task assignment problem into an optimization problem and modeling the task assignment process through Hidden Markov models. Zhang et al. [20] combined cloud computing and smart grid and constructed a new smart grid cloud task scheduling strategy to solve the cloud task scheduling problem with minimizing task completion time and minimizing task execution cost as the objectives. Gong et al. [21] constructed the eco-friendly task assignment algorithm (EFTA) to solve the task assignment problem of minimizing carbon emissions under constraints such as task duration and road traffic constraints. Wu et al. [22] constructed an unmanned submersible-mission matching matrix while introducing temporal path and voyage impact constraints to design a dynamic extended consistency set algorithm based on the consistency algorithm. Nedjah et al. [23] proposed a clustered dynamic task assignment algorithm in order to improve the efficiency of robot population task assignment coordination, which guides the robot to complete the exploration of the assigned space at an adaptive rate. Zhao et al. [24] proposed a fast task assignment algorithm based on Q-learning algorithm to solve the task assignment problem of heterogeneous UAVs in uncertain environments. There are a variety of algorithm innovations in task allocation, most of which are based on heuristic algorithms such as particle swarm algorithm and genetic algorithm. According to the actual environment background of task allocation, new algorithms are introduced to update and improve strategies. Some scholars apply reinforcement learning algorithms to obtain better task allocation strategies through the expansibility of reinforcement learning.

The above literature studies task allocation strategies from different perspectives but only discusses one type of task recipients and does not consider the existence of multiagent task recipients, that is, the task recipients come from different units and have different fields and disciplines. And the collaboration efficiency between task recipients is also different. In addition, the literature has more research on the number and quality of task completion, task completion efficiency, and other issues, and less consideration is given to the relationship between task completion timeliness, task completion benefits and personnel attributes, and task attributes. That is to say, there is less research on the attributes of both tasks and personnel at the same time. At present, most of the research in the field of ship collaborative design focuses on how to apply computer technology and digital technology to improve the parallelism and professionalism of ship design process and finally improve the design quality and efficiency, for example, the secondary development of modeling software to enable the integration of complex and large span of expertise or to explore the application and verification of the ship design field of the full three-dimensional model and simulation of the full coverage system. These studies mainly focus on the design itself, while task management is also very important to improve the design efficiency as the first step of design. At present, the task management level of ship field is in the development stage, and the assignment of design task mainly adopts the way of combining manual and computer. The task manager selects the task and the task receiver and centrally distributes the task through the computer system. When task managers assign tasks, most of them consider the professional suitability of designers and the time occupation of designers, and less consider the collaboration between designers in task collaboration. At the same time, the literature has less research on the problems in the field of ship design task allocation. As a complex product, ship design tasks are complex, design tasks are time-sensitive, oriented to many professions, and require high skills for designers. At the same time, designers usually come from different units. Reasonably allocate tasks so that tasks can be assigned to the most suitable personnel at the first time, so that designers with different specialties and abilities can coordinate their work in a unified way and improve the task execution rate. To sum up, it is very important to take intelligent research on ship design task allocation strategy.

The designer's ability attribute is an important factor that affects the result of task assignment decision. Competent and efficient designers tend to have low rework rates and high-quality tasks. In general, the description of designer capability attributes is inaccurate and vague. For example, terms such as general, good, and very good can be used to evaluate the designer's negotiation and communication ability, but it cannot be expressed by precise value. How to quantitatively measure the attribute value of ability is also a problem that needs to be explored and solved in this paper. A practical method is to replace numerical evaluation with fuzzy linguistic variable evaluation and to solve complex, unstructured, and nonquantitative problems by taking the words and sentences as the value of fuzzy linguistic variable. Some scholars use fuzzy sets, fuzzy soft sets, and other theories to solve group decision-making and multiobjective decision-making problems. Garg et al. [25] combined with the advantages of interval valued spherical fuzzy sets and complex numbers and proposed complex interval valued t-sphere fuzzy sets (CIVTSFS); Siddique et al. [26] introduced algebraic operation into Pythagorean fuzzy soft set (PFSS) and proposed a PFSS decision method based on score matrix; Akram et al. [27] extended and generalized the q-order graph fuzzy set (q-RPFS) to solve the multi-objective decision-making problem. Some scholars have also extended the fuzzy super soft set. Ihsan et al. [28] introduced a new extended fuzzy parameterization model in the Pythagorean fuzzy super soft expert set; Rahman et al. [29] proposed two new structures: fuzzy parameterized intuitionistic fuzzy hypersoft set (fpifhs-set) and fuzzy parameterized neutrosophic hypersoft set (fpnhs-set); Debnath [30] describes the related operations of fuzzy super soft sets.

To sum up, through the above literature analysis and discussion, based on the background of ship collaborative design, this paper selects a certain stage of ship production design, considering that the recipient of the design task is multiple design agents from different units such as shipyard design department, suppliers, design subcontractors, and classification societies. The professional attributes and collaboration rate between design agents are introduced into the problem-solving model, and a task assignment decision algorithm for ship multiagent collaborative design based on the design agent's professional

attributes, ability attributes, design efficiency, design rework rate, and collaboration rate between design agents is proposed. This paper constructs the task timeliness function, sets the design agent evaluation index matrix by introducing the fuzzy linguistic variable method, then constructs the multidesign agent-task benefit function, and obtains the task allocation strategy by solving the benefit function value, so as to realize the distribution balance between multidesign agents and tasks, improve the design efficiency, and shorten the design cycle.

The chapters of this paper are arranged as follows. In Section 2, we set up a five-tuple allocation decision model including design task elements, design agent elements, design task attribute elements, design agent attribute elements, and benefit function elements. In Section 3, we set the value range or value set of each attribute in the design agent attribute matrix, construct the evaluation matrix through the fuzzy linguistic variable method, establish the task timeliness function, and finally establish the benefit function. In Section 4, we take a certain stage of ship collaborative design as an example to verify and take polling algorithm and weighted polling algorithm as comparison methods to verify the effectiveness and stability of the multiagent task allocation decision-making method for ship collaborative design proposed in this paper. Finally, Section 5 summarizes this paper and discusses the future work.

2. Multidesign Agent-Task Allocation Decision Model

Based on the task allocation in the subdesign stage of ship production design, the collaborative units in this design stage include shipyards, suppliers, design subcontractors, and classification societies. The production design tasks at this stage involve structure, piping, outfitting, hull, interior installation, and other majors. In the ship design business, a hull section design project is used as a design task package, which includes tasks for various design agents in various disciplines and types.

The distribution decision model should have the characteristics of being able to completely describe the problem background and abstract the content of the problem. Based on the above design objectives, it is defined as follows.

Definition 1. Set the distribution decision model elements and specifies the distribution decision model as a five-tuple:

$$\text{Model} = \langle T, D, Q_T, Q_D, V \rangle. \tag{1}$$

The specific meanings of allocation decision model elements and their decomposition elements are shown in Table 1.

2.1. Design Task Model Elements. T represents the design task matrix. m represents the number of all hull section design tasks in the task set, and T_i represents a hull section design project, including various professional design tasks for multiple design agents. n represents the number of design tasks in a design project. In summary, the design tasks are defined as follows.

$$\begin{aligned} T &= [T_1, T_2 \cdots T_m]^T, \\ T_i &= [T_{i1}, T_{i2} \cdots T_{\text{in}}]. \end{aligned} \tag{2}$$

A design task matrix T contains all design tasks.

$$T = \begin{bmatrix} T_{11} & T_{12} & \cdots & T_{1n} \\ T_{21} & T_{22} & \cdots & T_{2n} \\ \vdots & \vdots & \cdots & \vdots \\ T_{m1} & T_{m2} & \cdots & T_{mn} \end{bmatrix}. \tag{3}$$

Among them, T_{ij} is the subtask j in the task item i,

$$\begin{cases} i = 1, 2, \cdots, m, \\ j = 1, 2, \cdots, n. \end{cases} \tag{4}$$

That is, after the task is decomposed, it is the most fine-grained subtask suitable for task allocation.

2.2. Model Elements of the Design Agent. D represents the design agent matrix. Designers are divided based on unit departments, such as shipyard structural design department, shipyard piping design department or suppliers, and design subcontractors, with a unit department as a design agent.

k represents the number of design agents involved in the task, and D_i represents a design agent, including multiple designers who can receive design tasks. l represents the number of designers who can accept tasks in a design agent. In summary, the design agent is defined as follows.

$$\begin{aligned} D &= [D_1 D_2 \cdots D_k]^T, \\ D_1 &= [D_{i1} D_{i2} \cdots D_{il}]. \end{aligned} \tag{5}$$

A design agent matrix D that contains all designers.

$$D = \begin{bmatrix} D_{11} & D_{12} & \cdots & D_{1l} \\ D_{21} & D_{22} & \cdots & D_{2l} \\ \vdots & \vdots & \cdots & \vdots \\ D_{k1} & D_{k2} & \cdots & D_{kl} \end{bmatrix}, \tag{6}$$

where D_{pq} is the designer q in the design agent p.

2.3. Model Elements for Design Task Attributes.

$$Q_T = \{Q_{TA}, , Q_{TC}, Q_{TE}\}. \tag{7}$$

Q_T represents a collection of design task attributes.

Table 1: Model elements definition.

Elements	Meaning
$\boldsymbol{T}$	The design task matrix
$\boldsymbol{D}$	The design agent matrix
Q_T	Collection of design task attributes
Q_D	Collection of design agent attributes
$\boldsymbol{V}$	The benefit function matrix
$\boldsymbol{m}$	The number of all hull section design tasks in the task set
$\boldsymbol{n}$	The number of design tasks in a design project
T_{ij}	The subtask j in the task item i, $1 \le i \le m$; $1 \le j \le n$
$\boldsymbol{k}$	The number of design agents involved in the task
$\boldsymbol{l}$	The number of designers who can accept tasks in a design agent
D_{pq}	The designer q in the design agent p, $1 \le p \le k$; $1 \le q \le l$
Q_{TA}	The matrix of the number of designers
$Q_{TA_i^j}$	The number of designers required to complete the task T_{ij}
Q_{TC}	The rated completion time matrix required to complete the task
$Q_{TC_i^j}$	The rated time required to complete the task T_{ij}
Q_{TE}	Represents the average amount of tasks
$Q_{TE_i^j}$	The average amount of tasks occupied by a single designer in completing the T_{ij} task
Q_{Df}	The professional attribute matrix of the design agent
$\widehat{Q}_{Df_i^j}$	The professional attribute value matrix of all design agents D for the design task T_{ij}
${}_p^q\widehat{Q}_{Df_i^j}$	The professional attribute value of a single designer D_{pq} for the design task T_{ij}
Q_{Dgx}	The attribute matrix of negotiation and communication ability of the design agent
$Q_{Dgx_p^q}$	The attribute value of the negotiation and communication ability of the designer D_{pq}
Q_{Dgy}	The analysis and planning ability attribute matrix of the design agent
$Q_{Dgy_p^q}$	The attribute value of the analysis and planning ability of the designer D_{pq}
Q_{Dgz}	The attribute matrix of the design agent's practical execution ability
$Q_{Dgz_p^q}$	The attribute value of the practical execution ability of the designer D_{pq}
Q_{Dh}	The design efficiency matrix of the design agent
$Q_{Dh_p^q}$	The task design efficiency of the designer D_{pq}
Q_{Dl}	The design rework rate matrix of the main body of the design
$Q_{Dl_p^q}$	The design rework rate of the designer D_{pq}
Q_{Do}	The coordination rate matrix of the design agent
$Q_{Do_p^q}$	The value of the synergy rate of the designer D_{pq}
U_{ij}^{pq}	The timeliness function of the designer D_{pq} to the design task T_{ij}
Φ	The task quantity evaluation matrix that defines the design task
V_{ij}^{pq}	The T_{ij} benefit function of selecting the designer D_{pq}

(1)Q_{TA} represents the matrix of the number of designers required by the task specification

$$Q_{TA} = \begin{bmatrix} Q_{TA_1^1} & Q_{TA_1^2} & \cdots & Q_{TA_1^n} \\ Q_{TA_2^1} & Q_{TA_2^2} & \cdots & Q_{TA_2^n} \\ \vdots & \vdots & \cdots & \vdots \\ Q_{TA_m^1} & Q_{TA_m^2} & \cdots & Q_{TA_m^n} \end{bmatrix}. \tag{8}$$

$Q_{TA_i^j}$ represents the number of designers required to complete the task T_{ij}.

(2)Q_{TC} represents the rated completion time matrix required to complete the task

$$Q_{TC} = \begin{bmatrix} Q_{TC_1^1} & Q_{TC_1^2} & \cdots & Q_{TC_1^n} \\ Q_{TC_2^1} & Q_{TC_2^2} & \cdots & Q_{TC_2^n} \\ \vdots & \vdots & \cdots & \vdots \\ Q_{TC_m^1} & Q_{TC_m^2} & \cdots & Q_{TC_m^n} \end{bmatrix}. \tag{9}$$

$Q_{TC_i^j}$ represents the rated time required to complete the task T_{ij}. This task needs to be completed within the specified time; otherwise, the task is overdue and requires corresponding overdue penalties.

(3)Q_{TE} represents the average amount of tasks

$$Q_{TE} = \begin{bmatrix} Q_{TE_1^1} & Q_{TE_1^2} & \cdots & Q_{TE_1^n} \\ Q_{TE_2^1} & Q_{TE_2^2} & \cdots & Q_{TE_2^n} \\ \vdots & \vdots & \cdots & \vdots \\ Q_{TE_m^1} & Q_{TE_m^2} & \cdots & Q_{TE_m^n} \end{bmatrix}, \tag{10}$$

$$Q_{TE_i^j} = \frac{1 \times Q_{TC_i^j}}{Q_{TA_i^j}}. \tag{11}$$

$Q_{TE_i^j}$ represents the average amount of tasks occupied by a single designer in completing the T_{ij} task. The larger the value, the greater the average workload of the task.

$$\begin{cases} \mathrm{MAX}Q_{TE} = \max \sum_{j=1}^{n} \sum_{i=1}^{m} Q_{TE_i^j}, \\ \mathrm{MIN}Q_{TE} = \min \sum_{j=1}^{n} \sum_{i=1}^{m} Q_{TE_i^j}, \\ q_{te_i^j} = \dfrac{Q_{TE_i^j} - \mathrm{MIN}Q_{TE}}{\mathrm{MAX}Q_{TE} - \mathrm{MIN}Q_{TE}}, q_{te_i^j} = [0, 1], \\ i = 1, 2, \cdots, m, j = 1, 2, \cdots, n. \end{cases} \tag{12}$$

The average task load is normalized and dimensionless, and its value range is [0,1].

2.4. Model Elements for Design Agent Attributes.

$$Q_D = \left\{ Q_{Df}, Q_{Dg}, Q_{Dh}, Q_{Dl}, Q_{Do} \right\}. \tag{13}$$

Q_D represents a collection of design agent attributes.

(1) Q_{Df} is the professional attribute matrix of the design agent. It indicates the degree of professional Matching between the design agent and the design task.

$$\begin{aligned} Q_{Df} &= \left[\widehat{Q}_{Df_i^j} \right]_{m \times n}; \widehat{Q}_{Df_i^j} = \left[{}_p^q \widehat{Q}_{Df_i^j} \right]_{k \times l}, \\ Q_{Df} &= \begin{bmatrix} \widehat{Q}_{Df_1^1} & \widehat{Q}_{Df_1^2} & \cdots & \widehat{Q}_{Df_1^n} \\ \widehat{Q}_{Df_2^1} & \widehat{Q}_{Df_2^2} & \cdots & \widehat{Q}_{Df_2^n} \\ \vdots & \vdots & \cdots & \vdots \\ \widehat{Q}_{Df_m^1} & \widehat{Q}_{Df_m^2} & \cdots & \widehat{Q}_{Df_m^n} \end{bmatrix}, \\ \widehat{Q}_{Df_i^j} &= \begin{bmatrix} {}_1^1\widehat{Q}_{Df_i^j} & {}_1^2\widehat{Q}_{Df_i^j} & \cdots & {}_1^l\widehat{Q}_{Df_i^j} \\ {}_2^1\widehat{Q}_{Df_i^j} & {}_2^2\widehat{Q}_{Df_i^j} & \cdots & {}_2^l\widehat{Q}_{Df_i^j} \\ \vdots & \vdots & \cdots & \vdots \\ {}_k^1\widehat{Q}_{Df_i^j} & {}_k^2\widehat{Q}_{Df_i^j} & \cdots & {}_k^l\widehat{Q}_{Df_i^j} \end{bmatrix}. \end{aligned} \tag{14}$$

Among them, $\widehat{Q}_{Df_i^j}$ represents the professional attribute value matrix of all design agents D for the design task T_{ij}. ${}_p^q\widehat{Q}_{Df_i^j}$ represents the professional attribute value of a single designer D_{pq} for the design task T_{ij}.

(2)Q_{Dg} represents the set of design main body's ability attributes

$$Q_{Dg} = \left\{ Q_{Dgx}, Q_{Dgy}, Q_{Dgz} \right\} \tag{15}$$

(a)Q_{Dgx} is the attribute matrix of negotiation and communication ability of the design agent

$$Q_{Dgx} = \begin{bmatrix} Q_{Dgx_1^1} & Q_{Dgx_1^2} & \cdots & Q_{Dgx_1^l} \\ Q_{Dgx_2^1} & Q_{Dgx_2^2} & \cdots & Q_{Dgx_2^l} \\ \vdots & \vdots & \cdots & \vdots \\ Q_{Dgx_k^1} & Q_{Dgx_k^2} & \cdots & Q_{Dgx_k^l} \end{bmatrix}. \tag{16}$$

Among them, $Q_{Dgx_p^q}$ represents the attribute value of the negotiation and communication ability of the designer D_q^p.

(b)Q_{Dgy} is the analysis and planning ability attribute matrix of the design agent

$$Q_{Dgy} = \begin{bmatrix} Q_{Dgy_1^1} & Q_{Dgy_1^2} & \cdots & Q_{Dgy_1^l} \\ Q_{Dgy_2^1} & Q_{Dgy_2^2} & \cdots & Q_{Dgy_2^l} \\ \vdots & \vdots & \cdots & \vdots \\ Q_{Dgy_k^1} & Q_{Dgy_k^2} & \cdots & Q_{Dgy_k^l} \end{bmatrix}. \tag{17}$$

Among them, $Q_{Dgy_p^q}$ represents the attribute value of the analysis and planning ability of the designer D_{pq}.

(c)Q_{Dgz} is the attribute matrix of the design agent's practical execution ability

$$Q_{Dgz} = \begin{bmatrix} Q_{Dgz_1^1} & Q_{Dgz_1^2} & \cdots & Q_{Dgz_1^l} \\ Q_{Dgz_2^1} & Q_{Dgz_2^2} & \cdots & Q_{Dgz_2^l} \\ \vdots & \vdots & \cdots & \vdots \\ Q_{Dgz_k^1} & Q_{Dgz_k^2} & \cdots & Q_{Dgz_k^l} \end{bmatrix}. \tag{18}$$

Among them, $Q_{Dgz_p^q}$ represents the attribute value of the practical execution ability of the designer D_{pq}.

(3)Q_{Dh} is the design efficiency matrix of the design agent

$$Q_{Dh} = \begin{bmatrix} Q_{Dh_1^1} & Q_{Dh_1^2} & \cdots & Q_{Dh_1^l} \\ Q_{Dh_2^1} & Q_{Dh_2^2} & \cdots & Q_{Dh_2^l} \\ \vdots & \vdots & \cdots & \vdots \\ Q_{Dh_k^1} & Q_{Dh_k^2} & \cdots & Q_{Dh_k^l} \end{bmatrix}. \tag{19}$$

Among them, $Q_{Dh_p^q}$ is the task design efficiency of the designer D_{pq}.

(4)Q_{Dl} is the design rework rate matrix of the main body of the design

$$Q_{Dl} = \begin{bmatrix} Q_{Dl_1^1} & Q_{Dl_1^2} & \cdots & Q_{Dl_1^l} \\ Q_{Dl_2^1} & Q_{Dl_2^2} & \cdots & Q_{Dl_2^l} \\ \vdots & \vdots & \cdots & \vdots \\ Q_{Dl_k^1} & Q_{Dl_k^2} & \cdots & Q_{Dl_k^l} \end{bmatrix}. \tag{20}$$

Among them, $Q_{Dl_p^q}$ is the design rework rate of the designer D_{pq}.

(5)Q_{Do} is the coordination rate matrix of the design agent

$$Q_{Do} = \begin{bmatrix} Q_{Do_1^1} & Q_{Do_1^2} & \cdots & Q_{Do_1^l} \\ Q_{Do_2^1} & Q_{Do_2^2} & \cdots & Q_{Do_2^l} \\ \vdots & \vdots & \cdots & \vdots \\ Q_{Do_k^1} & Q_{Do_k^2} & \cdots & Q_{Do_k^l} \end{bmatrix}. \tag{21}$$

Among them, $Q_{Do_p^q}$ represents the value of the synergy rate of the designer D_{pq}.

2.5. Model Elements of Benefit Function. V represents the benefit function matrix.

$$V = \begin{bmatrix} V_{11} & V_{12} & \cdots & V_{1n} \\ V_{21} & V_{22} & \cdots & V_{2n} \\ \vdots & \vdots & \cdots & \vdots \\ V_{m1} & V_{m2} & \cdots & V_{mn} \end{bmatrix}, V = \left[V_{ij}^{pq}\right]_{k\times l}. \tag{22}$$

Among them, V_{ij} is the benefit function of the subtask T_{ij}. The benefit function is constructed by selecting different designers and qualitatively processing their design attributes. The value of V_{ij} is calculated by selecting the task allocation strategy. The larger the value is, the more suitable the designer selected in the task allocation scheme is to the design task, and the stronger the balance between the design agent and the task.

The decomposition logic diagram of the multidesign agent-task allocation decision-making method proposed in this paper is shown in Figure 1.

3. Multidesign Agent-Task Allocation Decision-Making Strategy

The decision-making process of ship collaborative design task allocation is a complex coordinated decision-making process, and the bilateral needs between tasks and designers need to be considered at the same time. This paper is aimed at matching and balancing between design tasks and designers, taking the requirements of task allocation and the design needs of designers into account, and establishing a multiagent-task allocation decision-making model.

Through the above description of the multiagent-task allocation decision-making model, the model elements of design task, design agent, design task attribute, design agent attribute, and benefit function are set. The following will analyze in detail the process of establishing the benefit function based on the given model and its value.

Firstly, this paper sets the value range or value set of each attribute in the main design attribute matrix, then constructs the evaluation matrix through the fuzzy linguistic variable method, establishes the task timeliness function, and finally establishes the benefit function.

3.1. Evaluation Matrix Based on Fuzzy Linguistic Variables. In the process of assigning tasks and personnel, the character attributes of personnel and the task attributes of tasks are important influencing factors that affect the task assignment strategy and determine the effect of task completion. At present, scholars have conducted some researches on personnel and task attributes in task allocation. Jiang et al. [31] considered the staff's experience value and current load value of the task, matched the staff's role and skills with the task, and designed a task assignment algorithm based on the task and the staff's attributes. Wu et al. [32] introduced the concept of task personnel's personality ability attributes and comprehensive technical ability attributes in the task personnel matching process to provide decision support for task assignment. Tu

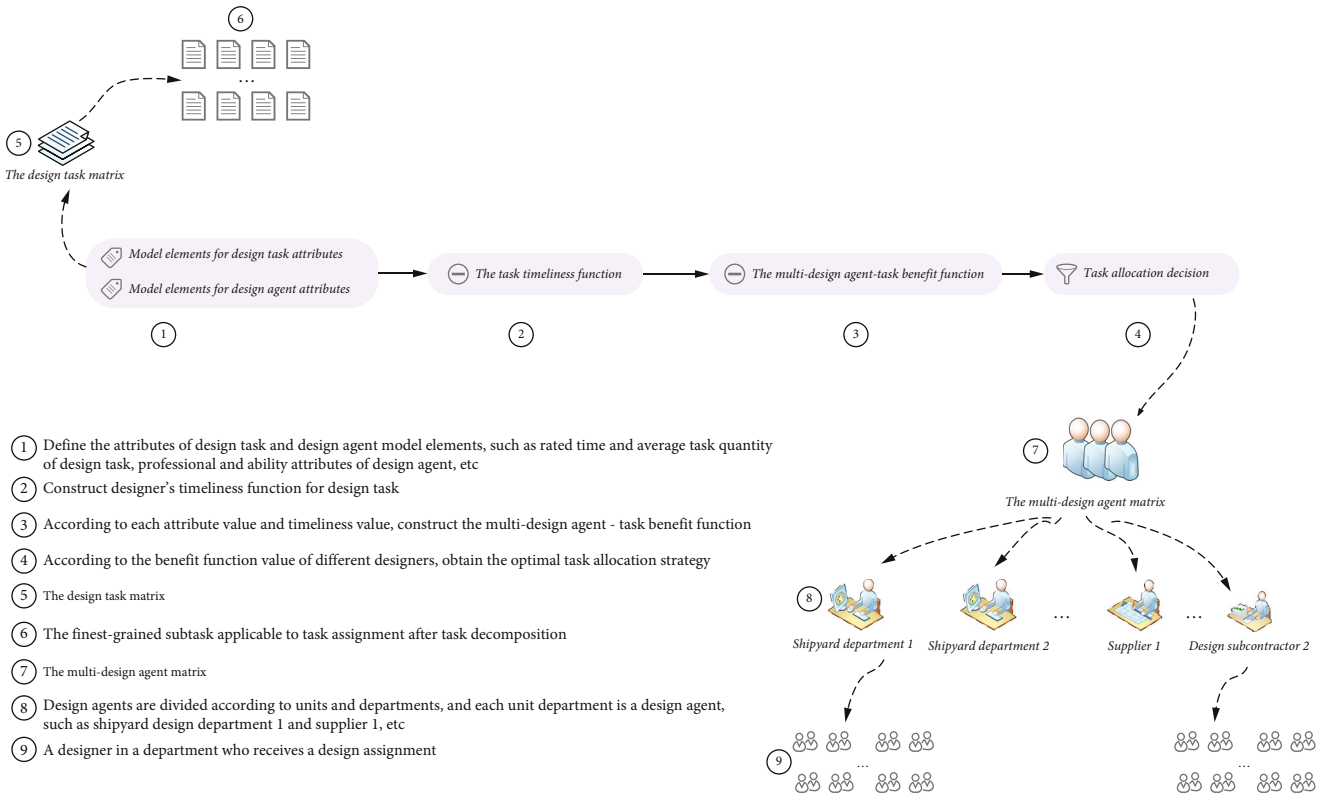

Figure 1: The decomposition logic diagram of the multidesign agent-task allocation decision-making method.

et al. [33] proposed a task allocation strategy that can capture complex interactions between tasks and personnel by constructing a personnel bias model that includes personnel bias, task basic facts, and character characteristics. Wei et al. [34] took the aircraft assembly coordination task and personnel balance as the background, comprehensively considered the factors such as task granularity, equalization degree, and personnel ability attribute, and constructed the task personnel evaluation matrix based on the fuzzy linguistic variable method. Huang et al. [35] constructed a time-dependent task assignment algorithm in the context of the task assignment problem for mobile groups with time constraints and considered the time-dependent task assignment problem with personnel time perception capability and perceived duration. Park et al. [36] studied the multirobot task allocation problem by applying cross-attentive machines to compute robot preferences for tasks and constructing deep reinforcement learning algorithms to solve the task optimal allocation time problem. Xu et al. [37] took the characteristics of the tasks, system features, and the randomness of personnel requirements and other attributes into account and constructed a multiobjective task scheduling model in the context of the cloud task assignment problem. Ji et al. [38] proposed an evolutionary multitasking allocation method with the goal of maximizing the perceived quality of the task while considering three types of constraint attributes: task budget, perceived quality of the task, and personnel workload. Zhao et al. [39] combined mobile crowdsourcing with social networks to consider the important influence of personnel relationship attributes in task assignment.

Therefore, a conclusion can be drawn from the literature: only by constructing a task allocation decision-making strategy on the basis of taking the bilateral attribute requirements of personnel and tasks into account can the subjective initiative of personnel be fully utilized and the balance of task allocation can be maximized. This paper analyzes the professional attributes, ability attributes, design efficiency, design rework rate, and personnel collaboration rate of ship collaborative designers. These attributes are a generalized concept, and the determination of their values is an uncertain problem. In order to qualitatively analyze its value, this paper first uses Delphi expert consultation method and empirical investigation method to determine the evaluation information of designers' ability attributes; Secondly, this paper uses the fuzzy linguistic variable method to quantify its value and get the capability attribute evaluation matrix through weight calculation.

Delphi expert consultation method and experience investigation method are both investigation methods that obtain a large number of actual data through various investigation methods, integrate and analyze the data with the knowledge and experience of experts, and finally obtain the characteristics of the research object. This paper combines Delphi expert consultation method and experience investigation method, through the investigation, analysis and statistics of the completion time, quality, feedback of tasks, others' evaluation and other contents of the designers to complete the task, finally obtains the description information of the evaluation size of the ship designers' ability attributes. For example, for the collaborative ability of designers, the collaborative ability

is described as follows: general synergy rate, higher synergy rate, and high synergy rate. Another example is to describe the attribute size of the designer's negotiation and communication ability, analysis and planning ability, and practice and execution ability as follows: poor, average, better, and very good.

The fuzzy linguistic variable method is applied to the problems that cannot be evaluated with accurate numerical values in the decision-making process. The semantics of elements in a fuzzy linguistic set are usually represented by fuzzy numbers defined on [0,1]. The capability attribute information fuzzy set with three description elements is represented by a triangular fuzzy number, and the capability attribute information fuzzy set with four description elements is represented by a trapezoidal fuzzy number. For example, the designer collaboration rate is quantified as (0.5, 0.75, 1), and the negotiation and communication ability of designers is quantified as (0.25, 0.5, 0.75, 1). Finally, the ability attribute evaluation matrix is obtained by calculating the weight. At the same time, the fuzzy linguistic variable method is used to construct the task quantity evaluation matrix. Fuzzy decision-making method can be applied to the selection and evaluation of various fields. Hakim Nik Badrul Alam et al. [40] proposed a novel multicriteria decision-making (MCDM) model based on IZN and applied it to the selection of automobile suppliers. Venugopal et al. [41] constructed the fuzzy Decision-Making Trial and Evaluation Laboratory (DEMATEL) approach and applied it to the stock selection of investors and traders in the financial field. Imeni [42] believes that it is also very necessary to apply the fuzzy decision-making method to economic decisions such as accounting and auditing. Sirbiladze [43] introduced various operators used in fuzzy decision-making. Sorourkhah and Edalatpanah [44] also extended their research.

The ability attribute description of designers and its quantitative processing with fuzzy linguistic variables and the specific process of constructing the ability attribute matrix are shown below.

(1) Quantify Q_{Df}

For the design task T_{ij}, the professional attribute value of a single designer D_{pq} for the task ${}_{p}^{q}\widehat{Q}_{Df_i^j}$, the professional attribute size is described as follows: {Professional mismatch, Major match, Professional match}..

Through the Delphi expert consultation method and empirical survey method, the attribute evaluation set of the ability is summarized. The above description of the ability is fuzzy and uncertain and cannot be qualitatively analyzed, so it is quantified. The capacity of designers is reflected by specific numerical values. The quantized values of ${}_{p}^{q}\widehat{Q}_{Df_i^j}$ are as Table 2.

$$ {}_{p}^{q}\widehat{Q}_{Df_i^j} \in \{0, 0.5, 1\}. \tag{23} $$

Designer selection strategy: avoid choosing designers who do not match the task's specialty, consider choosing designers who are more suitable for the task, and give priority to designers who match the task's specialty.

Table 2: Quantification of personnel professional match description.

	Property description		
	Professional mismatch	Major match	Professional match
Quantified value	0	0.5	1

(2)Quantitative analysis of Q_{Dgx}, Q_{Dgy}, and Q_{Dgz}

Among the many types of ability attributes, this paper selects representative three types of attributes that are also important to the task completion effect as the research points. The three types of ability attributes are as follows: negotiation and communication ability, analysis and planning ability, and practical execution ability. The ability attribute evaluation set is as Table 3.

To sum up, design the main body ability attribute matrix Q_{Dg}, and the values of the elements are as follows.

$$ \begin{cases} Q_{Dgx_p^q} \in \{0.25, 0.5, 0.75, 1\}, \\ Q_{Dgy_p^q} \in \{0.25, 0.5, 0.75, 1\}, \\ Q_{Dgz_p^q} \in \{0.25, 0.5, 0.75, 1\}. \end{cases} \tag{24} $$

The larger the value, the better the designer's ability. It is defined as follows:

$$ \begin{cases} N_{dgx}^{0.25}, N_{dgx}^{0.5}, N_{dgx}^{0.75}, N_{dgx}^{1} = \\ \text{the number of elements in the matrix } Q_{Dgx} \\ \text{with the value } 0.25, 0.5, 0.75, 1, \end{cases} \tag{25} $$

$$ \begin{cases} N_{dgy}^{0.25}, N_{dgy}^{0.5}, N_{dgy}^{0.75}, N_{dgy}^{1} = \\ \text{the number of elements in the matrix } Q_{Dgy} \\ \text{with the value } 0.25, 0.5, 0.75, 1, \end{cases} \tag{26} $$

$$ \begin{cases} N_{dgz}^{0.25}, N_{dgz}^{0.5}, N_{dgz}^{0.75}, N_{dgz}^{1} = \\ \text{the number of elements in the matrix } Q_{Dgz} \\ \text{with the value } 0.25, 0.5, 0.75, 1. \end{cases} \tag{27} $$

For example, $N_{dgx}^{0.25}$ represents the number of attribute values with a value of 0.25 in the attribute matrix Q_{Dgx} of the negotiation and communication ability of the design agent.

In order to calculate the attribute weight of the design agent's ability, according to formulas (25)–(27), there are the following definitions.

Table 3: Personnel ability description quantitative table.

	Property description			
	Poor	General	Better	Very good
Quantified value	0.25	0.5	0.75	1

Table 4: Staff design efficiency description quantitative table.

	Property description			
	Very low rework rate	Low rework rate	Higher rework rate	High rework rate
Quantified value	0.05	0.1	0.15	0.2

$$\begin{cases} I\left(Q_{Dg}\right) = 1 - \dfrac{1}{kl}, \\ I\left(Q_{Dgx}\right) = \displaystyle\sum_{t=0.25,0.5,0.75,1} \frac{N_{dgx}^{t}}{kl}\left(1 - \frac{N_{dgx}^{t}}{kl}\right), \\ I\left(Q_{Dgy}\right) = \displaystyle\sum_{t=0.25,0.5,0.75,1} \frac{N_{dgy}^{t}}{kl}\left(1 - \frac{N_{dgy}^{t}}{kl}\right), \\ I\left(Q_{Dgz}\right) = \displaystyle\sum_{t=0.25,0.5,0.75,1} \frac{N_{dgz}^{t}}{kl}\left(1 - \frac{N_{dgz}^{t}}{kl}\right). \end{cases} \tag{28}$$

Define the weight of each attribute of the evaluation matrix as $\bar{\omega}_{gx}$, $\bar{\omega}_{gy}$, and $\bar{\omega}_{gz}$. Then through the above calculation formula (28), the weight calculation formula can be obtained as follows.

$$\begin{cases} \bar{\omega}_{gx} = \dfrac{I\left(Q_{Dg}\right) - I\left(Q_{Dgx}\right)}{3I\left(Q_{Dg}\right) - \left(I\left(Q_{Dgx}\right) + I\left(Q_{Dgy}\right) + I\left(Q_{Dgz}\right)\right)} \\ \bar{\omega}_{gy} = \dfrac{I\left(Q_{Dg}\right) - I\left(Q_{Dgy}\right)}{3I\left(Q_{Dg}\right) - \left(I\left(Q_{Dgx}\right) + I\left(Q_{Dgy}\right) + I\left(Q_{Dgz}\right)\right)} \\ \bar{\omega}_{gz} = \dfrac{I\left(Q_{Dg}\right) - I\left(Q_{Dgz}\right)}{3I\left(Q_{Dg}\right) - \left(I\left(Q_{Dgx}\right) + I\left(Q_{Dgy}\right) + I\left(Q_{Dgz}\right)\right)} \end{cases} \tag{29}$$

In summary, according to formula (29), the calculation formula for the ability attribute matrix of the design agent can be obtained.

$$Q_{Dg} = \bar{\omega}_{gx}Q_{Dgx} + \bar{\omega}_{gy}Q_{Dgy} + \bar{\omega}_{gz}Q_{Dgz}. \tag{30}$$

Designer selection strategy: priority is given to selecting designers with high personnel ability attribute values to complete design tasks.

(3)Quantitative analysis Q_{D_l}

The design rework rate value $Q_{Dl_p^q}$ of the designer D_{pq} for the task is quantified as Table 4.

$$Q_{Dl_p^q} \in \{0.05, 0.1, 0.15, 0.2\}. \tag{31}$$

Designer selection strategy: prioritize designers with extremely low rework rates or low rework rates, and avoid designers with high rework rates.

(4)Quantitative analysis of Q_{Dh} and Q_{Do}

The design efficiency value $Q_{Dh_p^q}$ of the designer D_{pq} for the task is quantified as Table 5.

$$Q_{Dh_p^q} \in \{0.5, 0.75, 1\}. \tag{32}$$

For the designer D_{pq}, the synergy rate value $Q_{Do_p^q}$ is quantified as Table 6.

$$Q_{Do_p^q} \in \{0.5, 0.75, 1\}. \tag{33}$$

Define the timeliness evaluation matrix Q_{Dho} as follows.

$$Q_{Dho} = \left[Q_{Dho_p^q}\right]_{k\times l}, \tag{34}$$

$$\left\{N_{dh}^{0.5}, N_{dh}^{0.75}, N_{dh}^{1}\right. = \text{the number of elements in the matrix } Q_{Dh} \text{ with the value } 0.5, 0.75, 1, \tag{35}$$

$$\left\{N_{do}^{0.5}, N_{do}^{0.75}, N_{do}^{1}\right. = \text{the number of elements in the matrix } Q_{Do} \text{ with the value } 0.5, 0.75, 1, \tag{36}$$

$$\begin{cases} I(Q_{Dho}) = 1 - \dfrac{1}{kl}, \\ I(Q_{Dh}) = \displaystyle\sum_{t=0.5,0.75,1} \frac{N_{dh}^{t}}{kl}\left(1 - \frac{N_{dh}^{t}}{kl}\right), \\ I(Q_{Do}) = \displaystyle\sum_{t=0.5,0.75,1} \frac{N_{do}^{t}}{kl}\left(1 - \frac{N_{do}^{t}}{kl}\right). \end{cases} \tag{37}$$

Table 5: Staff design efficiency description quantitative table.

	Property description		
	Average efficiency	Higher efficiency	High efficiency
Quantified value	0.5	0.75	1

Table 6: Personnel collaboration rate description quantitative table.

	Property description		
	General synergy rate	Higher synergy rate	High synergy rate
Quantified value	0.5	0.75	1

Define the weight of each attribute of the timeliness evaluation matrix as $\bar{\omega}_{dh}$, $\bar{\omega}_{do}$. According to formulas (35)–(37), the following formulas can be obtained.

$$\begin{cases} \bar{\omega}_{dh} = \dfrac{I(Q_{Dho}) - I(Q_{Dh})}{2I(Q_{Dho}) - (I(Q_{Dh}) + I(Q_{Do}))}, \\ \bar{\omega}_{do} = \dfrac{I(Q_{Dho}) - I(Q_{Do})}{2I(Q_{Dho}) - (I(Q_{Dh}) + I(Q_{Do}))}. \end{cases} \tag{38}$$

In summary, according to formula (38), the calculation formula of the timeliness evaluation matrix of the main body of the design can be obtained.

$$Q_{Dho} = \bar{\omega}_{dh} * Q_{Dh} + \bar{\omega}_{do} * Q_{Do}. \tag{39}$$

3.2. Construct Task Timeliness Function. Define the timeliness function of the designer D_{pq} to the design task T_{ij} as U_{ij}^{pq}. According to formulas (12) and (39), the following formulas can be obtained.

$$U_{ij}^{pq} = \sqrt{1 + \lambda * q_{te_i^j} * Q_{Dho_p^q}}. \tag{40}$$

In the formula, λ is the time-dependent coefficient, $\lambda \in (0, 1)$. The greater the timeliness coefficient, the more timeliness of completion of the tasks of designers with the higher design efficiency and collaboration rate under the same task conditions. For different designers, the task timeliness function values are different. The higher the weight of designer efficiency and collaboration rate, the stronger the task timeliness.

3.3. Construct Multidesign Agent-Task Benefit Function. (1)Task capacity evaluation matrix

There are many professions involved in ship collaborative design tasks. This article takes the three majors of structure $\tilde{A}$, piping $\tilde{B}$, and electrical $\tilde{C}$ as examples.

$$\begin{cases} NT_i^{\tau} = \text{number of tasks with type } \tau \text{ in set } T_i, \\ \tau \in \left\{\tilde{A}, \tilde{B}, \tilde{C}\right\}, \\ 1 \le i \le m. \end{cases} \tag{41}$$

$$m\tilde{A} = \sum_{i=1}^{m} NT_i^{\tilde{A}}, m\tilde{B} = \sum_{i=1}^{m} NT_i^{\tilde{B}}, m\tilde{C} = \sum_{i=1}^{m} NT_i^{\tilde{C}}, \tag{42}$$

$$m\tilde{A} + m\tilde{B} + m\tilde{C} = m * n, \tag{43}$$

$$\begin{aligned} \tilde{M}\tilde{A} &= \left[\frac{NT_1^{\tilde{A}}}{m\tilde{A}}, \frac{NT_2^{\tilde{A}}}{m\tilde{A}}, \cdots, \frac{NT_m^{\tilde{A}}}{m\tilde{A}}\right], \tilde{M}\tilde{B} = \left[\frac{NT_1^{\tilde{B}}}{m\tilde{B}}, \frac{NT_2^{\tilde{B}}}{m\tilde{B}}, \cdots, \frac{NT_m^{\tilde{B}}}{m\tilde{B}}\right] \\ \tilde{M}\tilde{C} &= \left[\frac{NT_1^{\tilde{C}}}{m\tilde{C}}, \frac{NT_2^{\tilde{C}}}{m\tilde{C}}, \cdots, \frac{NT_m^{\tilde{C}}}{m\tilde{C}}\right]. \end{aligned} \tag{44}$$

Among them, $NT_i^{\tilde{A}}$ represents the number of structure $\tilde{A}$ tasks in the task item T_i, $m\tilde{A}$ represents the number of structure $\tilde{A}$ tasks in all tasks, $NT_i^{\tilde{A}}/m\tilde{A}$ represents the ratio of the number of tasks of structure $\tilde{A}$ in the subtask T_i to the number of tasks of structure $\tilde{A}$ in all tasks. The other matrix elements are similar. According to formulas (41)–(44), the following formulas can be obtained.

$$I\left(\tilde{M}\right) = 1 - \frac{1}{m}, \tag{45}$$

$$\begin{cases} I\left(\tilde{M}\tilde{A}\right) = \sum_{i=1}^{m} \dfrac{NT_i^{\tilde{A}}}{m}\left(1 - \dfrac{NT_i^{\tilde{A}}}{m}\right), I\left(\tilde{M}\tilde{B}\right) = \sum_{i=1}^{m} \dfrac{NT_i^{\tilde{B}}}{m}\left(1 - \dfrac{NT_i^{\tilde{B}}}{m}\right) \\ I\left(\tilde{M}\tilde{C}\right) = \sum_{i=1}^{m} \dfrac{NT_i^{\tilde{C}}}{m}\left(1 - \dfrac{NT_i^{\tilde{C}}}{m}\right). \end{cases} \tag{46}$$

Define the weight of each attribute of the task load evaluation matrix as $\bar{\omega}_{\tilde{M}\tilde{A}}, \bar{\omega}_{\tilde{M}\tilde{B}}$, and $\bar{\omega}_{\tilde{M}\tilde{C}}$. Then, through the above calculation, formulas (45) and (46), the weight calculation formula can be obtained as follows.

$$\begin{cases} \bar{\omega}_{\tilde{M}\tilde{A}} = \dfrac{I\left(\tilde{M}\right) - I\left(\tilde{M}\tilde{A}\right)}{3I\left(\tilde{M}\right) - \left(I\left(\tilde{M}\tilde{A}\right) + I\left(\tilde{M}\tilde{B}\right) + I\left(\tilde{M}\tilde{C}\right)\right)}, \\ \bar{\omega}_{\tilde{M}\tilde{B}} = \dfrac{I\left(\tilde{M}\right) - I\left(\tilde{M}\tilde{B}\right)}{3I\left(\tilde{M}\right) - \left(I\left(\tilde{M}\tilde{A}\right) + I\left(\tilde{M}\tilde{B}\right) + I\left(\tilde{M}\tilde{C}\right)\right)}, \\ \bar{\omega}_{\tilde{M}\tilde{C}} = \dfrac{I\left(\tilde{M}\right) - I\left(\tilde{M}\tilde{C}\right)}{3I\left(\tilde{M}\right) - \left(I\left(\tilde{M}\tilde{A}\right) + I\left(\tilde{M}\tilde{B}\right) + I\left(\tilde{M}\tilde{C}\right)\right)}. \end{cases} \tag{47}$$

It is defined as follows:

$$\Gamma = [\Gamma_1, \Gamma_2, \cdots, \Gamma_m], \tag{48}$$

$$\Gamma_i = \bar{\omega}_{\tilde{M}\tilde{A}}\tilde{M}\tilde{A}_i + \bar{\omega}_{\tilde{M}\tilde{B}}\tilde{M}\tilde{B}_i + \bar{\omega}_{\tilde{M}\tilde{C}}\tilde{M}\tilde{C}_i. \tag{49}$$

In summary, the task quantity evaluation matrix that defines the design task is Φ. According to formulas (11) and (49), the following formulas can be obtained.

Table 7: Design task.

Task item	Subtasks (professional classification)				
	1	2	3	4	5
1	Structure 1	Structure 1	structure2	Pipe system 3	Electrical 1
2	Structure 1	Pipe system 2	Electrical 2	Pipe system 1	Electrical 1
3	Structure 1	Structure 2	Pipe system 1	Pipe system 2	Electrical 3
4	Structure 3	Pipe system 3	Pipe system 3	Electrical 2	Electrical 3

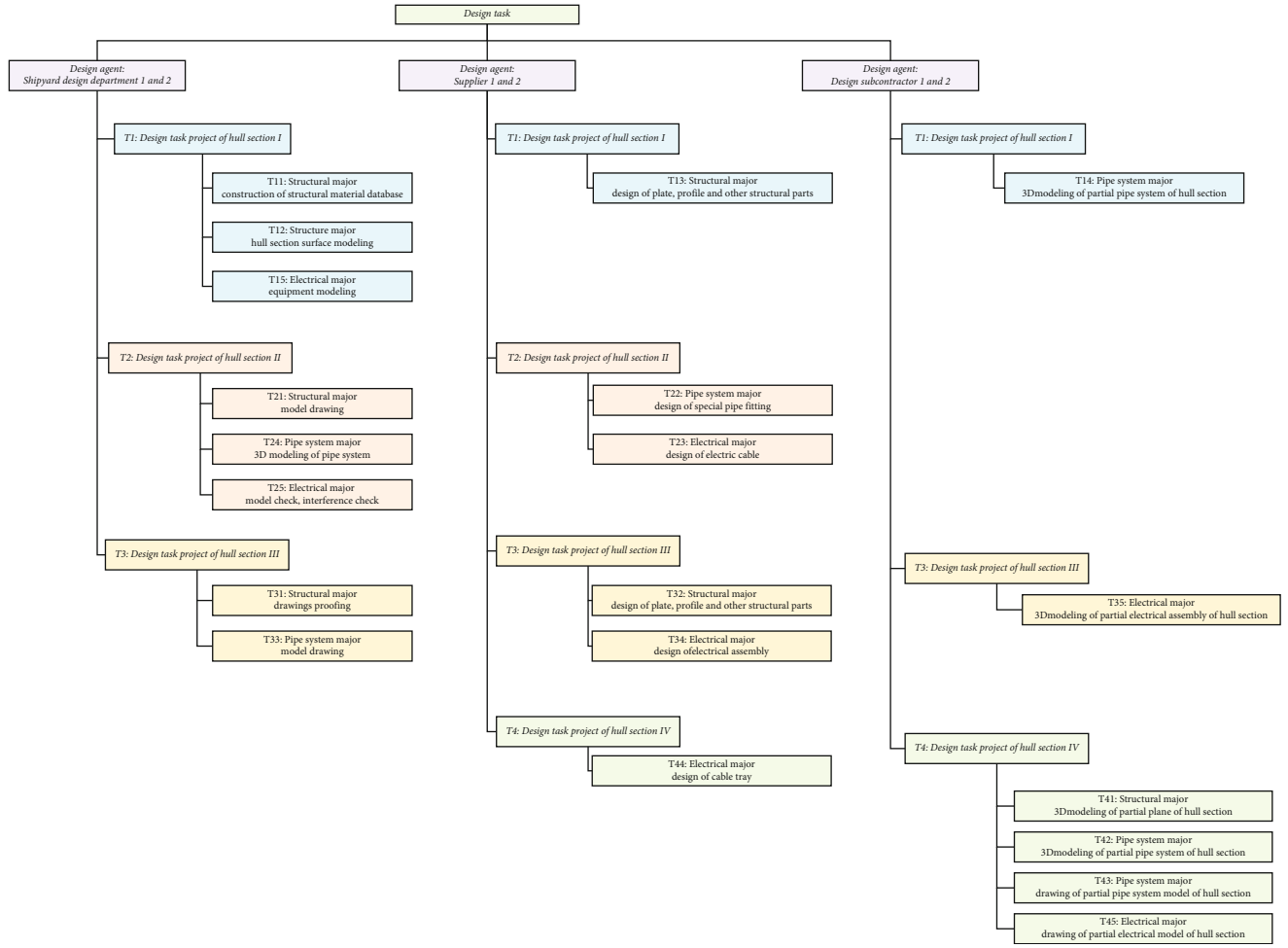

Figure 2: Task item decomposition and specific contents of subtasks.

$$\Phi = \left[\Gamma_i Q_{TE_i^j}\right]_{m\times n}. \tag{50}$$

(2)Construct multidesign agent-task benefit function

Taking a single task T_{ij} as an example, the T_{ij} benefit function of selecting the designer D_{pq} is defined as V_{ij}^{pq}. According to formulas (30), (40), and (50) and the relevant attribute values ${}_p^q\widehat{Q}_{Df_i^j}$ and $Q_{Dl_p^q}$ of the designer, the following formulas can be obtained.

Table 8: Design task-number of rated personnel.

Task item	Subtasks (number of rated personnel)				
	1	2	3	4	5
1	2	1	1	2	2
2	1	1	2	2	1
3	3	1	1	2	1
4	2	2	1	2	2

Table 9: Design task-rated completion time.

Task item	Subtasks (rated completion time)				
	1	2	3	4	5
1	10	6	5	12	8
2	8	5	6	8	8
3	15	4	5	10	6
4	12	8	4	8	8

Table 10: Design task-average task amount.

Task item	Subtasks (average task amount)				
	1	2	3	4	5
1	5	6	5	6	4
2	8	5	3	4	8
3	5	4	5	5	6
4	6	4	4	4	4

$$\begin{cases} V_{ij}^{pq} = \dfrac{\sum_{p}^{q} \widehat{Q}_{DJ_i^j} * U_{ij}^{pq} * \left[\theta * Q_{Dg_p^q} - (1-\theta) * Q_{DI_p^q}\right]}{\Gamma_i Q_{TE_i^j}}, \\ i = 1, 2, \cdots, m \quad j = 1, 2, \cdots, n, \\ p = 1, 2, \cdots, k \quad q = 1, 2, \cdots, l. \end{cases} \tag{51}$$

Among them, θ is the designer's evaluation weight, $\theta \epsilon [0, 1]$. The larger the value, the greater the impact of designers' negotiation and communication ability, analysis and planning ability, and practical execution ability on task allocation in the benefit function. The benefit value calculated by the above formula, the larger the value, the better the selection strategy.

(3)Expected completion time of the task

Define the expected completion time of the subtask T_{ij} as t_{ij}: it indicates the expected time required for the assigned designer to complete the subtask after the designer assigns the task.

Define the average attribute value Q of designers: it means the ability attribute value $Q_{Dg_p^q}$ of all designers, the value of timeliness function $Q_{Dho_p^q}$, and the value of design rework rate $Q_{DI_p^q}$.

$$Q = \frac{\sum_{p=1}^{k}\sum_{q=1}^{l} Q_{Dg_p^q} + \sum_{p=1}^{k}\sum_{q=1}^{l} Q_{Dho_p^q} - \sum_{p=1}^{k}\sum_{q=1}^{l} Q_{DI_p^q}}{3 * k * l}. \tag{52}$$

Definition Π is the set of designers assigned to the subtask T_{ij}, and the size of Π is $Q_{TA_i^j}$, that is, the rated number of personnel for the subtask T_{ij}.

The definition X_{ij} is the average value of the original attributes of the designer assigned to the subtask T_{ij}.

$$X_{ij} = \frac{\sum_{\Pi} Q_{Dgx_p^q} + \sum_{\Pi} Q_{Dgy_p^q} + \sum_{\Pi} Q_{Dgz_p^q} + \sum_{\Pi} Q_{Dh_p^q} + \sum_{\Pi} Q_{Do_p^q} - \sum_{\Pi} Q_{DI_p^q}}{6 * Q_{TA_i^j}}. \tag{53}$$

In summary, the calculation formula for the expected completion time t_{ij} of the subtask T_{ij} is as follows.

$$t_{ij} = Q_{TC_i^j} - Q_{TC_i^j}\left(X_{ij} - Q\right). \tag{54}$$

Among them, $Q_{TC_i^j}$ represents the rated time required to complete the subtask T_{ij}.

4. Instance Verification

4.1. Multidesign Agent-Task Benefit Function Example Verification. Taking a certain stage of ship collaborative design as an example, the multiagent-task allocation strategy proposed in this paper is applied. This paper sets the design agent as shipyard department 1, shipyard department 2, supplier 1, supplier 2, design subcontractor 1, and design subcontractor 2.

It is stipulated that different subtasks are distinguished by professional classification in Table 7. This paper takes the three types of majors of structure, pipe system, and electrical as examples and distinguishes design tasks applicable to different design agents by 1, 2, and 3, 1 for shipyard departments, 2 for suppliers, and 3 for design subcontracting. For example, structure 1 represents the structural design tasks that can be assigned to the shipyard department, and the others are the same.

T_i represents a hull section design project, which includes various professional design tasks for multiple design agents. The ship design is different from the work in other fields such as the construction industry. The hull structure is complex, and there are many tasks such as three-dimensional (3D) model establishment, inspection, and drawing. At the same time, it is necessary to carry out interference, balance, and weight center of gravity inspection, so that the model structures of various disciplines do not collide, and the designed hull meets the requirements of stability and rigidity. In this paper, the typical tasks of each major in hull sections I, II, III, and IV are selected for example analysis, that is, four task items are selected, and each task item contains five subtasks. The breakdown of task items and the specific content of subtasks are shown in Figure 2.

The rated number of personnel and the rated time of the design task are set as Tables 8–10.

This article selects six types of design agents, each of which contains four designers. These six design agents are shipyard department 1, shipyard department 2, supplier 1, supplier 2, design subcontractor 1, and design subcontractor 2. This article sets up the designer's ability attribute table, which contains the ability attribute values of the designer's negotiation and communication, analysis and planning, practice execution, design efficiency, collaboration rate, and design rework rate.

Table 11: Designer capability attribute.

Design agent	Designer	Capability attribute					
		Negotiation and communication	Analysis and planning	Practice execution	Design efficiency	Collaboration rate	Design rework rate
Shipyard department 1	1	0.75	0.5	0.75	1	0.75	0.05
	2	1	1	1	0.75	1	0.05
	3	0.5	1	0.75	1	1	0.15
	4	0.75	0.75	0.5	0.5	0.75	0.1
Shipyard department 2	1	1	1	0.75	0.75	0.5	0.1
	2	1	1	1	0.5	1	0.05
	3	0.75	0.75	0.75	0.75	0.75	0.1
	4	0.5	0.5	0.5	1	0.5	0.05
Supplier 1	1	0.25	1	1	1	1	0.15
	2	0.75	0.75	0.75	0.5	0.75	0.1
	3	0.75	1	1	1	1	0.05
	4	1	1	1	1	0.5	0.1
Supplier 2	1	1	1	1	0.75	0.75	0.1
	2	0.75	0.75	0.75	1	0.5	0.05
	3	0.5	0.75	0.5	0.5	1	0.1
	4	0.75	0.25	1	1	1	0.2
Design subcontractor 1	1	0.5	0.5	0.5	1	0.5	0.1
	2	1	1	1	0.75	0.75	0.05
	3	0.25	1	0.25	0.75	1	0.2
	4	1	0.5	1	1	1	0.05
Design subcontractor 2	1	1	1	1	1	1	0.1
	2	1	1	1	0.5	0.75	0.05
	3	0.75	0.75	0.75	1	0.5	0.1
	4	1	0.5	1	0.75	0.75	0.05

Table 12: Designer's ability attribute matrix-Q_{Dg}.

	Design agent	Designer (ability attribute matrix)			
		1	2	3	4
1	Shipyard department 1	0.663825758	1	0.760416667	0.661931818
2	Shipyard department 2	0.911931818	1	0.75	0.5
3	Supplier 1	0.772727273	0.75	0.924242424	1
4	Supplier 2	1	0.75	0.586174242	0.665719697
5	Design subcontractor 1	0.5	1	0.508522727	0.827651515
6	Design subcontractor 2	1	1	0.75	0.827651515

Table 13: Designer timeliness matrix-Q_{Dho}.

	Design agent	Designer (timeliness matrix)			
		1	2	3	4
1	Shipyard department 1	0.881081081	0.868918919	1	0.618918919
2	Shipyard department 2	0.631081081	0.737837838	0.75	0.762162162
3	Supplier 1	1	0.618918919	1	0.762162162
4	Supplier 2	0.75	0.762162162	0.737837838	1
5	Design subcontractor 1	0.762162162	0.75	0.868918919	1
6	Design subcontractor 2	1	0.618918919	0.762162162	0.75

The ability attribute description information of designers in each design agent is finally obtained through investigation, sorting, analysis, and statistics and combined with Delphi expert consultation method and experience investigation method. At the same time, according to the setting in Section 3.1, the description of capability attribute information corresponds to its semantic fuzzy number one by one. Finally, the ability attribute description information of each designer is quantized into Table 11 after numerical expression.

The designer's ability attribute matrix and timeliness matrix are calculated by formulas (30) and (39), as shown in Tables 12 and 13.

This article assumes that similar professions include different types of tasks such as drawing, modeling, review, and modification. However, because the specific content of the subtasks is different, the same designer has different professional attribute values for the subtasks of the same professional type. For example, the subtasks T_{11} and T_{12} belong to the structure 1 professional type, but the subtask T_{11} represents the construction of structural material database to the shipyard department, and the subtask T_{12} represents the structure professional modeling task applicable to the shipyard department. The professional attribute values of each subtask are different, and the others are the same.

Taking the assignment of the subtask T_{11} to the designer as an example, the designer's professional attribute value ${}_{p}^{q}\widehat{Q}_{Df_1^1}$ for the subtask T_{11} is set, and the benefit function is used to calculate the benefit function value of each designer for the subtask T_{11}. The details are shown in Table 14.

The timeliness coefficient $\lambda = 0.6$ in the benefit function formula and the personnel evaluation weight $\theta = 0.75$ are set. Through calculation, the designer's benefit function value V_{11}^{pq} for the subtask T_{11} can be obtained as follows. Through formula (51), the calculation results are shown in Table 15.

Based on the calculation result of the above benefit function and combined with the rated number of subtasks, designers D_{21} and D_{22} are finally assigned to subtask T_{11}.

After assigning a designer to the subtask T_{11}, the expected completion time is calculated by formulas (52)–(54):

$$\begin{aligned} Q &= \frac{36.3040}{3 * 6 * 4} = 0.5042, \\ X_{11} &= \frac{8.35}{6 * 2} = 0.6958, \\ t_{11} &= 10 - 10(0.6958 - 0.5042) = 8.08. \end{aligned} \tag{55}$$

It can be obtained that $t_{11} = 8.08$. Compared with its rated time, it can be seen that through the multidesigner-task allocation strategy proposed in this paper, the task time of ship collaborative design is reduced, the ability of designers is greatly utilized, and the matching degree between tasks and designers is improved.

In the same way, through the task allocation decision-making method for ship multiagent collaborative design proposed in this paper, other design tasks are allocated, and the task allocation strategy is shown in Table 16.

Table 14: Designer on subtask T_{11}-professional attribute-${}_{p}^{q}\widehat{Q}_{Df_1^1}$.

	Design agent	Designer (professional attribute matrix)			
		1	2	3	4
1	Shipyard department 1	1	0.5	1	0.5
2	Shipyard department 2	0.5	1	1	0.5
3	Supplier 1	0	0	0	0
4	Supplier 2	0	0	0	0
5	Design subcontractor 1	0	0	0	0
6	Design subcontractor 2	0	0	0	0

Table 15: Subtask T_{11}-designer benefit function value V_{11}^{pq}.

	Design agent	Designer (benefit function value)			
		1	2	3	4
1	Shipyard department 1	1.346	1.022	1.495	0.637
2	Shipyard department 2	0.891	2.016	1.471	0.497
3	Supplier 1	0	0	0	0
4	Supplier 2	0	0	0	0
5	Design subcontractor 1	0	0	0	0
6	Design subcontractor 2	0	0	0	0

Table 16: Design allocation strategy.

Task item	Subtasks (design allocation strategy)				
	1	2	3	4	5
1	D_{21}, D_{22}	D_{11}	D_{33}	D_{52}, D_{62}	D_{14}, D_{24}
2	D_{21}	D_{41}	D_{42}	D_{12}, D_{13}	D_{14}
3	D_{11}, D_{21}, D_{23}	D_{31}	D_{12}	D_{32}, D_{34}	D_{53}
4	D_{54}, D_{63}	D_{52}, D_{64}	D_{64}	D_{43}, D_{44}	D_{51}, D_{61}

Table 17: Expected completion time-t_{ij}.

Task item	Subtasks (expected completion time)				
	1	2	3	4	5
1	8.08	5.33	3.60	9.40	7.97
2	6.83	3.85	5.33	6.47	7.83
3	13.12	3.28	3.60	8.54	5.98
4	8.90	6.43	3.38	7.40	6.83

Based on the above task allocation strategy, the expected completion time of the task is calculated, and the results are shown in Table 17.

Comparing the rated completion time $Q_{TC_i^j}$ of the collaborative design task with the expected completion time t_{ij}, the analysis diagram is as Figure 3.

From the comparative analysis of the design task's rated completion time and the expected completion time, it can be seen that the use of the ship multidesign agent-task allocation

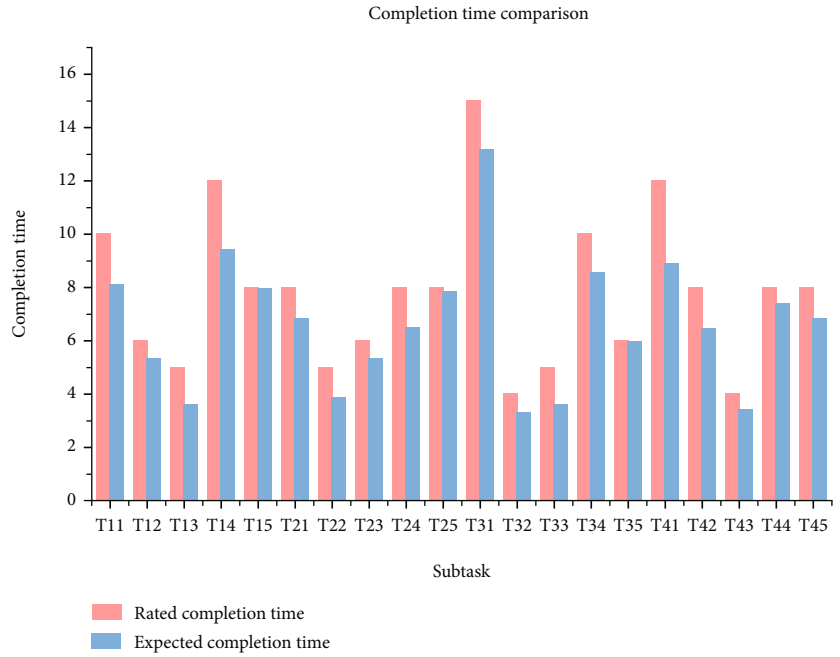

Figure 3: Completion time comparison chart.

Table 18: RR-design allocation strategy.

Task item	Subtasks (RR-design allocation strategy)				
	1	2	3	4	5
1	D_{11}, D_{12}	D_{12}	D_{31}	D_{51}, D_{63}	D_{11}, D_{13}
2	D_{14}	D_{32}	D_{33}, D_{43}	D_{13}, D_{21}	D_{22}
3	D_{14}, D_{21}, D_{23}	D_{34}	D_{24}	D_{41}, D_{44}	D_{52}
4	D_{53}, D_{64}	D_{51}, D_{54}	D_{61}	D_{31}, D_{42}	D_{52}, D_{62}

Table 19: RR-expected completion time.

Task item	Subtasks (RR-expected completion time)				
	1	2	3	4	5
1	8.04	4.33	4.10	11.50	6.83
2	7.83	4.69	5.10	6.70	6.10
3	13.65	3.08	5.06	8.21	Professional mismatch
4	11.05	7.13	2.75	6.83	Professional mismatch

Table 20: WRR-design allocation strategy.

Task item	Subtasks (WRR-design allocation strategy)				
	1	2	3	4	5
1	D_{12}, D_{13}	D_{21}	D_{34}	D_{51}, D_{63}	D_{12}, D_{13}
2	D_{22}	D_{41}	D_{31}, D_{43}	D_{14}, D_{21}	D_{24}
3	D_{11} D_{14}, D_{23}	D_{42}	D_{11}	D_{32}, D_{44}	D_{61}
4	D_{52}, D_{64}	D_{51}, D_{53}	D_{62}	D_{31}, D_{33}	D_{52}, D_{54}

Table 21: WRR-expected completion time.

Task item	Subtasks (WRR-expected completion time)				
	1	2	3	4	5
1	7.71	5.13	3.85	11.50	6.17
2	6.10	3.85	5.40	7.33	8.10
3	13.81	3.55	4.44	9.04	Professional mismatch
4	9.65	8.07	3.22	6.17	6.10

strategy proposed in this paper shortens the task completion time.

4.2. Algorithm Comparison Analysis. In order to verify the stability of the multidesign agent-task allocation decision-making method for ship collaborative design proposed in this paper, the Round-Robin (RR) algorithm and Weighted Round-Robin (WRR) algorithm are used as the experimental comparison objects. The RR and the WRR are applied to design task allocation, solve the corresponding task allocation strategy, and calculate the expected completion time of the task according to formula (54). By comparing the expected completion time of the task calculated by different methods, the stability of the proposed method, the RR, and the WRR in the task allocation problem is analyzed.

Both the RR and the WRR are a load balancing algorithm. The RR assumes that the processing performance of all servers is the same and allocates requests from users to internal servers in turn.

When the algorithm is applied to the task allocation problem, the RR is a task allocation method of stateless scheduling. This algorithm treats users as no difference and assigns tasks to users in turn in a Round-Robin manner.

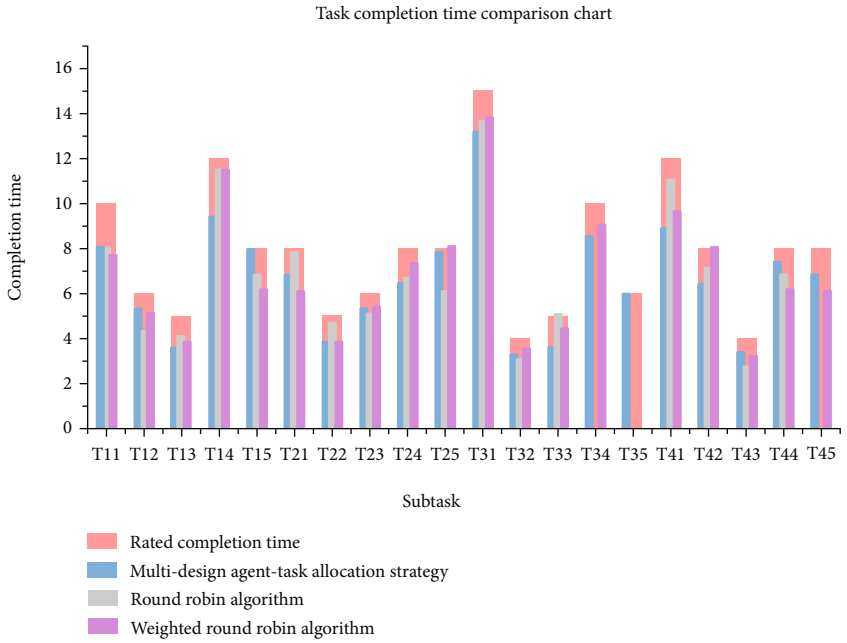

Figure 4: Task completion time comparison chart.

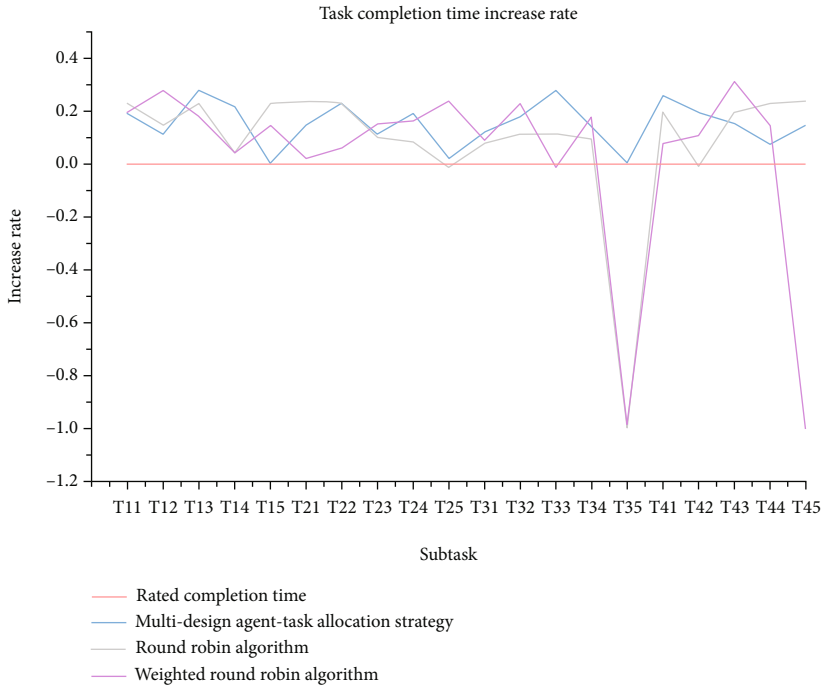

Figure 5: Task completion time increase rate chart.

Using the RR to calculate the task allocation strategy table and taking the corresponding professional attribute values of the personnel into account, the expected completion schedule of the calculation task is as Tables 18 and 19.

The WRR assigns different weights to each server according to the different processing capabilities of the server, so that it can accept service requests with corresponding weights. When the algorithm is applied to the task allocation problem, the rated number of tasks completed is used as the weight, so that the task can be allocated to the designer of the specified number of completed tasks. The WRR is used to calculate the task allocation strategy table, and the corresponding

Table 22: Task allocation method stability.

	Task allocation method stability		
	Multidesign agent-task allocation decision-making method	RR	WRR
Stability value	100%	85%	85%

professional attribute values of the personnel are considered at the same time. The expected completion schedule of the task is as Tables 20 and 21.

The expected completion time of tasks calculated by the multidesign agent-task allocation decision-making method and the RR and the WRR are compared. The comparison and analysis diagram is as Figure 4.

Comparing the multidesign agent-task allocation decision-making method and the RR and the WRR proposed in this paper, the designer's task completion time increase rate is calculated, and the comparison and analysis diagram is as Figure 5.

The stability values of the three task allocation methods are shown in Table 22.

Through the above analysis, the multidesign agent-task allocation decision-making method proposed in this paper has advantages in the balance and stability of task and personnel allocation. The specific advantages are as follows.

(i) The multidesign agent-task allocation decision-making method fully considers the task attributes of the task, the professional attributes of the personnel, the ability attributes, the design rework rate, and other character attributes and can take the bilateral needs of the task and the personnel into account at the same time. The RR and the WRR do not consider the attributes of tasks and personnel when assigning tasks and treat all objects as indistinguishable

(ii) The task-agent allocation strategy obtained by applying the multidesign agent-task allocation decision-making method improves the designer's task completion efficiency and reduces the task completion time. With the task allocation strategy solved by the RR and the WRR, there is a mismatch between the task and the designer's profession, which makes the designer unable to complete the task. The stability of these two algorithms is significantly lower than that of the multidesign agent-task allocation decision-making method

(iii) Comprehensive analysis shows that the multidesign agent-task allocation decision-making method proposed in this article has more advantages in terms of balance and stability of task and designer allocation, makes full use of design resources, and is more in line with the current situation of multispecialty parallelism in ship collaborative design. It is more in line with the task distribution requirements of ship collaborative design

5. Conclusion

This paper presents a multidesign agent-task allocation decision-making method for multidesign agents, which takes into account the task attributes and the ability attributes of designers. The purpose is to formulate a reasonable task allocation strategy for ship collaborative design, achieve resource balance, and improve design efficiency. This paper verifies the effectiveness, feasibility, and stability of the multidesign agent-task allocation decision-making method through the example verification analysis and the comparison analysis of RR and WRR algorithms.

The theoretical contributions of the multidesign agent-task allocation decision-making method are as follows: (1) This method expands the types of design agents in the task allocation process, considers the multiagent task recipients from different regions and units such as shipyards, suppliers, and design subcontractors, improves the flexibility and multiscalability of multidesign agents, and further deepens the concept of multiagent theory. (2) This method considers the task attribute, the specialty attribute, and the capability attribute of the design subject and constructs the task timeliness function and the multidesign subject task benefit function, so that designers with different specialties and abilities can coordinate and allocate based on the unified and reasonable theory, and further deepens the concept of collaboration in ship collaborative design. (3) In this method, Delphi expert consultation method and experience investigation method are used to determine the ability attribute evaluation information of designers. Secondly, fuzzy linguistic variable method is used to quantify its value, and the ability attribute evaluation matrix is obtained through weight calculation, which further expands the application method of personnel evaluation decision. The practical significance is as follows: (1) The enterprise decision-makers can make full use of and reasonably allocate resources by using the multidesign agent task allocation decision-making method to allocate tasks to the most appropriate executors, so that the task executors can complete the collaborative design tasks with high efficiency, low cost, and high quality and finally improve the design efficiency of collaborative design products and enhance the core competitiveness of enterprises. (2) The application of the multidesign agent-task allocation decision-making method satisfies the multidesign agent task benefit function and can simultaneously take into account the bilateral needs of tasks and personnel. It is helpful for shipyards, suppliers, design subcontractors, and other enterprises to participate in the project management and personnel management of ship collaborative design.

It is a very complicated work to balance the assignment of tasks and personnel in ship collaborative design. This paper selects and studies several typical representatives of design agent attributes that need to be considered in task assignment. At the same time, it is set that the assigned design tasks have reached the most fine-grained for task assignment. In addition to the task attributes and personnel attributes set in this paper, there are many factors that affect the task designer allocation strategy, such as task decomposition granularity, task context,

and designer reward and punishment mechanism. In future research, we will refine the personnel attributes that affect the task allocation strategy, consider the impact of personnel reward and punishment measures on the ability of designers to perform tasks, further explore the impact of fine-grained task decomposition on task allocation, and continue to expand the collaborative design task scheduling strategy of shipyards, suppliers, design subcontractors, and other multidesign agents.

Data Availability

All data, models, and code generated or used during the study appear in the submitted article.

Disclosure

The authors are responsible for the contents of this publication.

Conflicts of Interest

The authors declare that they have no conflicts of interest.

Acknowledgments

This research was funded by the Ministry of Industry and Information Technology of the People's Republic of China (Nos. 2018473 and 2019331) and the Fundamental Research Funds for the Central Universities (3072022CFJ0703).

References

[1] H. Gui, B. Zhao, G. Zhang, Z. Su, and J. Jiang, "Payoff distribution of overlapping coalitions for task priority satisfaction and performance rewards," *Journal of Systems Engineering*, vol. 36, no. 3, pp. 302–313, 2021.

[2] W. Jiang, W. Zhang, P. Chen, J. Chen, Y. Sun, and Q. Liu, "Quantity sensitive task allocation method based on IWOA in group intelligence perception," *Acta Electronica Sinica*, pp. 1–16, 2021.

[3] J. Wang, Y. Wang, D. Zhang et al., "Multi-task allocation in Mobile crowd sensing with individual task quality assurance," *IEEE Transactions on Mobile Computing*, vol. 17, no. 9, pp. 2101–2113, 2018.

[4] P. Wu, E. W. T. Ngai, and Y. Wu, "Toward a real-time and budget-aware task package allocation in spatial crowdsourcing," *Decision Support Systems*, vol. 110, pp. 107–117, 2018.

[5] J. Jiang, B. An, Y. Jiang, C. Zhang, Z. Bu, and J. Cao, "Group-oriented task allocation for crowdsourcing in social networks," *IEEE Transactions on Systems, Man, and Cybernetics: Systems*, vol. 51, no. 7, pp. 4417–4432, 2021.

[6] X. Li and X. Zhang, "Multi-task allocation under time constraints in mobile crowdsensing," *IEEE Transactions on Mobile Computing*, vol. 20, no. 4, pp. 1494–1510, 2021.

[7] X. Huang, R. Yu, D. Ye, L. Shu, and S. Xie, "Efficient workload allocation and user-centric utility maximization for task scheduling in collaborative vehicular edge computing," *IEEE Transactions on Vehicular Technology*, vol. 70, no. 4, pp. 3773–3787, 2021.

[8] X. Xu, Y. Sun, and J. Wang, "Multi-task transportation scheduling model with backhauls based on hub and spoke in collaborative logistics network," *Journal of Ambient Intelligence and Humanized Computing*, vol. 10, no. 1, pp. 333–343, 2019.

[9] K. Rajakumari, M. V. Kumar, G. Verma, S. Balu, D. K. Sharma, and S. Sengan, "Fuzzy based ant colony optimization scheduling in cloud computing," *Computer Systems Science and Engineering*, vol. 40, no. 2, pp. 581–592, 2022.

[10] U. Baroudi, M. Alshaboti, A. Koubaa, and S. Trigui, "Dynamic multi-objective auction-based (DYMO-auction) task allocation," *Applied Sciences*, vol. 10, no. 9, p. 3264, 2020.

[11] D.-H. Lee, "Resource-based task allocation for multi-robot systems," *Robotics and Autonomous Systems*, vol. 103, pp. 151–161, 2018.

[12] G. Yang, Z. Zhang, J. Wang, and X. He, "Task allocation based on node pair intimacy in wireless sensor networks," *IET Communications*, vol. 14, no. 12, pp. 1902–1909, 2020.

[13] W. Song, Y. Gao, L. Shen, and Y. Zhang, "A multi-robot task allocation algorithm based on near-field subset partition," *Robot*, vol. 43, no. 5, pp. 629–640, 2021.

[14] H. Hu, Q. Zhang, H. Hu, J. Chen, and Z. Li, "Q-learning based sensing task assignment algorithm for mobile crowd sensing system," *Computer Integrated Manufacturing Systems*, vol. 24, no. 7, pp. 1774–1783, 2018.

[15] X. Feng, D. Guo, Z. Liu, and H. Zheng, "Task allocation in IoV-based crowdsensing combing clustering and CMAB," *Chinese Journal on Internet of Things*, vol. 5, no. 3, pp. 86–96, 2021.

[16] F. Ye, J. Chen, Y. Tian, and T. Jiang, "Cooperative multiple task assignment of heterogeneous UAVs using a modified genetic algorithm with multi-type-gene chromosome encoding strategy," *Journal of Intelligent and Robotic Systems*, vol. 100, no. 2, pp. 615–627, 2020.

[17] J. Shi, Z. Yang, and J. Zhu, "An auction-based rescue task allocation approach for heterogeneous multi-robot system," *Multimedia Tools and Applications*, vol. 79, no. 21–22, pp. 14529–14538, 2020.

[18] J. Zhang, Y. Chen, Q. Yang et al., "Dynamic task allocation of multiple UAVs based on improved A-QCDPSO," *Electronics*, vol. 11, no. 7, p. 1028, 2022.

[19] X. Yin, J. Huang, W. He, W. Guo, H. Yu, and L. Cui, "Group task allocation approach for heterogeneous software crowdsourcing tasks," *Peer-to-Peer Networking and Applications*, vol. 14, no. 3, pp. 1736–1747, 2021.

[20] H. Zhang, J. Shi, B. Deng, G. Jia, G. Han, and L. Shu, "MCTE: minimizes task completion time and execution cost to optimize scheduling performance for smart grid cloud," *IEEE Access*, vol. 7, pp. 134793–134803, 2019.

[21] W. Gong, X. Huang, B. Zhang, and Y. Zhao, "Task allocation in eco-friendly mobile crowdsensing: problems and algorithms," *Mobile Networks and Applications*, vol. 25, no. 2, pp. 491–504, 2020.

[22] X. Wu, Z. Gao, S. Yuan, Q. Hu, and Z. Dang, "A dynamic task allocation algorithm for heterogeneous UUV swarms," *Sensors*, vol. 22, no. 6, p. 2122, 2022.

[23] N. Nedjah, L. M. Ribeiro, and L. de Macedo Mourelle, "Communication optimization for efficient dynamic task allocation in swarm robotics," *Applied Soft Computing*, vol. 105, article 107297, 2021.

[24] X. Zhao, Q. Zong, B. Tian, B. Zhang, and M. You, "Fast task allocation for heterogeneous unmanned aerial vehicles through reinforcement learning," *Aerospace Science and Technology*, vol. 92, pp. 588–594, 2019.

[25] H. Garg, K. Ullah, T. Mahmood, Z. Ali, and H. Khalifa, "Multi-attribute decision-making problems based on aggregation operators with complex interval-valued T-spherical fuzzy information," *Maejo International Journal of Science and Technology*, vol. 16, no. 1, pp. 51–65, 2022.

[26] I. Siddique, R. M. Zulqarnain, R. Ali, A. Alburaikan, A. Iampan, and H. A. E.-W. Khalifa, "A decision-making approach based on score matrix for Pythagorean fuzzy soft set," *Computational Intelligence and Neuroscience*, vol. 2021, Article ID 5447422, 16 pages, 2021.

[27] M. Akram, A. Bashir, and S. A. Edalatpanah, "A hybrid decision-making analysis under complex q-rung picture fuzzy Einstein averaging operators," *Computational and Applied Mathematics*, vol. 40, no. 8, p. 305, 2021.

[28] M. Ihsan, M. Saeed, A. Alburaikan, and H. A. E.-W. Khalifa, "Product evaluation through multi-criteria decision making based on fuzzy parameterized Pythagorean fuzzy hypersoft expert set," *AIMS Math.*, vol. 7, no. 6, pp. 11024–11052, 2022.

[29] A. U. Rahman, M. Saeed, A. Alburaikan, and H. A. E.-W. Khalifa, "An intelligent multiattribute decision-support framework based on parameterization of neutrosophic hypersoft set," *Computational Intelligence and Neuroscience*, vol. 2022, Article ID 6229947, 20 pages, 2022.

[30] S. Debnath, "Fuzzy hypersoft sets and its weightage operator for decision making," *Journal of Fuzzy Extension and Applications*, vol. 2, no. 2, pp. 163–170, 2021.

[31] J. Jiang, B. Yang, Z. Miao, and B. Zhu, "A workflow task assignment method based on the properties of task and user," *Computer Simulation*, vol. 32, no. 12, pp. 222–225, 2015.

[32] A. Wu, L. Xie, and J. Xiao, "An optimised task-personnel matching method supporting software project resources scheduling," *Computer Applications and Software*, vol. 28, no. 3, pp. 20–25, 2011.

[33] J. Tu, G. Yu, J. Wang, C. Domeniconi, M. Guo, and X. Zhang, "CrowdWT: crowdsourcing via joint modeling of workers and tasks," *ACM Transactions on Knowledge Discovery from Data*, vol. 15, no. 1, pp. 1–24, 2020.

[34] M. Wei, X. Tian, J. Geng, and M. Zhang, "A balanced task-personnel matching method for aircraft assembly coordination planning," *Xibei Gongye Daxue Xuebao/Journal of Northwestern Polytechnical University*, vol. 38, no. 1, pp. 130–138, 2020.

[35] Y. Huang, H. Chen, G. Ma et al., "OPAT: optimized allocation of time-dependent tasks for mobile crowdsensing," *IEEE Transactions on Industrial Informatics*, vol. 18, no. 4, pp. 2476–2485, 2022.

[36] B. Park, C. Kang, and J. Choi, "Cooperative multi-robot task allocation with reinforcement learning," *Applied Sciences*, vol. 12, no. 1, p. 272, 2022.

[37] J. Xu, Z. Zhang, Z. Hu, L. Du, and X. Cai, "A many-objective optimized task allocation scheduling model in cloud computing," *Applied Intelligence*, vol. 51, no. 6, pp. 3293–3310, 2021.

[38] J. Ji, Y. Guo, D. Gong, and X. Shen, "Evolutionary multi-task allocation for mobile crowdsensing with limited resource," *Swarm and Evolutionary Computation*, vol. 63, p. 100872, 2021.

[39] B. Zhao, Y. Wang, Y. Li, Y. Gao, and X. Tong, "Task allocation model based on worker friend relationship for mobile crowdsourcing," *Sensors*, vol. 19, no. 4, p. 921, 2019.

[40] N. M. F. H. N. B. Alam, K. M. N. K. Khalif, N. I. Jaini, A. S. A. Bakar, and L. Abdullah, "Intuitive multiple centroid defuzzification of intuitionistic Z-numbers," *Journal of Fuzzy Extension and Applications*, vol. 3, no. 2, pp. 126–139, 2022.

[41] R. Venugopal, C. Veeramani, and S. A. Edalatpanah, "Analysis of fuzzy DEMATEL approach for financial ratio performance evaluation of NASDAQ exchange," *Proceedings of International Conference on Data Science and Applications*, M. Saraswat, S. Roy, C. Chowdhury, and A. H. Gandomi, Eds., , pp. 637–648, Springer, Singapore, 2022.

[42] M. Imeni, "Fuzzy logic in accounting and auditing," *Journal of Fuzzy Extension and Applications*, vol. 1, no. 1, pp. 66–72, 2020.

[43] G. Sirbiladze, "New view of fuzzy aggregations. part I: general information structure for decision-making models," *Journal of Fuzzy Extension and Applications*, vol. 2, no. 2, pp. 130–143, 2021.

[44] A. Sorourkhah and S. A. Edalatpanah, "Using a combination of matrix approach to robustness analysis (MARA) and fuzzy DEMATEL-based ANP (FDANP) to choose the best decision," *International Journal of Mathematical, Engineering and Management Sciences*, vol. 7, no. 1, pp. 68–80, 2022.

Hindawi
Advances in Mathematical Physics
Volume 2022, Article ID 8479433, 10 pages
https://doi.org/10.1155/2022/8479433

Research Article

Differential Quadrature Method to Examine the Dynamical Behavior of Soliton Solutions to the Korteweg-de Vries Equation

Shubham Mishra,[1] Geeta Arora,[1] Homan Emadifar,[2] Soubhagya Kumar Sahoo,[3] and Afshin Ghanizadeh[4]

[1]*Department of Mathematics, Lovely Professional University, Phagwara, Punjab, India*
[2]*Department of Mathematics, Hamedan Branch, Islamic Azad University, Hamedan, Iran*
[3]*Department of Mathematics, Institute of Technical Education and Research, Siksha 'O' Anusandhan University, Bhubaneswar, 751030 Odisha, India*
[4]*Department of Statistics, Kermanshah Branch, Islamic Azad University, Kermanshah, Iran*

Correspondence should be addressed to Homan Emadifar; homan_emadi@yahoo.com

Received 13 May 2022; Revised 13 June 2022; Accepted 20 June 2022; Published 9 July 2022

Academic Editor: Ghulam Rasool

Nonlinear evolution equations are crucial for understanding the phenomena in science and technology. One such equation with periodic solutions that has applications in various fields of physics is the Korteweg-de Vries (KdV) equation. In the present work, we are concerned with the implementation of a newly defined quintic B-spline basis function in the differential quadrature method for solving the Korteweg-de Vries (KdV) equation. The results are presented using four experiments involving a single soliton and the interaction of solitons. The accuracy and efficiency of the method are presented by computing the L_2 and L_∞ norms along with the conservational quantities in the forms of tables. The results show that the proposed scheme not only gives acceptable results but also consumes less time, as shown by the CPU for the elapsed time in two examples. The graphical representations of the obtained numerical solutions are compared with the exact solution to discuss the nature of solitons and their interactions for more than one soliton.

1. Introduction

While performing studies to identify the most effective design for canal boats on the Edinburgh-Glasgow canal in 1844, John Scott Russell noticed a phenomenon. He noticed that after one or two miles, the height of water in the canal steadily decreases as it travels along the watercourse. He invented the term "wave of translation" to describe this unique and wonderful phenomenon [1]. This gives rise to the soliton defined as a wave with a defined shape traveling at a constant speed through a given medium. The first wave to exhibit characteristics similar to a soliton was observed by Yuliawati et al. [2]. This was the beginning of an absolutely specific field of research to which scientists and mathematicians have contributed a lot over time. Nowadays, it is known that many equations have soliton solutions. Some of the equations having soliton solution are the KdV equation, Fisher equation, NLS equation, etc.

The Korteweg-de Vries (KdV) equation is a nonlinear partial differential equation developed by Gardner and Morikawa in 1895 with respect to plasma waves [3] and then again by Washimi and Taniuti [4] to study acoustic waves in a cold plasma. The KdV equation is used to examine the propagation of low-amplitude water waves in shallow water bodies. The solution to this equation produces solitary waves [5].

The KdV equation is given by

$$\frac{\partial U}{\partial t}(x,t) + \varepsilon U(x,t)\frac{\partial U}{\partial x}(x,t) + \mu\frac{\partial^3 U}{\partial x^3}(x,t) = 0, \quad a \le x \le b, t > 0, \tag{1}$$

where ε and μ are positive parameters and a, b represents the range under consideration. The KdV equation is a third-order nonlinear evolution equation that characterizes long waves and is widely used in physical and engineering disciplines. For example, it is used in modeling ionic-acoustic solitons in plasma physics [6], in the study of a long wave in subsurface oceans, and shallow sols in geophysical fluid dynamics [7, 8]. It also describes the phenomenon in cluster physics and superdeformed nuclei [9, 10], quantum field theory, and classical general relativity [11]. The solution of the KdV equation has opened enormous possibilities for mathematical concepts.

The solutions of nonlinear equations are always of interest to researchers as they are studied using various approaches [12, 13]. In most cases, an analytical solution is not accessible, so numerical aspects are always necessary [14]. Gardner et al. [15] proved both the existence and uniqueness of solutions to the KdV equation. Liu [16] provided an elliptic Jacobi function solution for the KdV equation. In the same research paper, Hufford and Xing [17] reported a numerical solution for the linearized version of the problem as well as superconvergence for the approach used. Trogdon and Deconinck [18] presented a finite-genus solution to the equation. Grava and Klein [19] solved the KdV equation numerically and asymptotically for a small dispersion limit. Leach [20] gives the large-time evolution of the generalized Korteweg-de Vries equation. The wavelet Galerkin approach is used by Kumar and Mehra [21] to find a time-accurate solution of this equation. To solve this equation, Bahadir [22] uses an exponential finite difference technique. Aksan and Özdeş [23] use the Galerkin finite element approach with B-spline functions. This equation was solved numerically and analytically by Özer and Kutluay [24]. Ascher and McLachlan [25] provided a multisymplectic box technique for the KdV equation. Small time solutions of the equation were given by Kutluay et al. [26]. Idrees et al. [27] use the optimal homotopic asymptotic technique to solve this equation. To solve the KdV equation numerically, Gücüyenen and Tanoğlu [28] used the iterative splitting approach. Sarma [29] provided a solitary wave solution for this equation. Van de Fliert and Groesen [30] used a variational methodology, which was further investigated by Yuliawati et al. using the steepest descent approach, to study the solution of the KDV equation in the Hamiltonian condition. In addition, there have been several other successful numerical approaches to the KdV equation, including the spectral method [31], the pseudospectral method, and the collocation method [32].

This paper is divided into the following sections. In Section 2, the numerical scheme with the weight coefficient calculation procedure is discussed. Section 3 discusses numerical experiments and results, and Section 4 presents the final conclusion.

2. Numerical Scheme

Bellman et al. [33] first introduced the differential quadrature method (DQM) for the numerical solution of partial differential equations in 1972. Due to its simplicity, the approach has recently attracted much attention. The concept of the method is to use basis functions whose derivatives at the nodes are known [34]. Numerous researchers have used various test functions to construct different types of DQMs [35–38].

The differential quadrature method involves estimating a derivative of a given function using linear summation of its components at different nodes of the problem domain. The domain $[a, b]$ can be simply partitioned into uniformly distributed finite nodes x_i with distance h, such that

$$a = x_0 < x_1 < x_2 < \cdots < x_{n-1} < x_n = b. \tag{2}$$

Let $B_i(x)$ be the quintic B-splines with knots at points x_n, $n = 0, 1, 2, \cdots, N$. The arrangement of splines $\{B_{-1}, B_0, B_1, \cdots, B_N, B_{N+1}\}$ forms the basis for any function on $[a, b]$. For $i = 1, 2, \cdots, N$, the solution at each time point of the node x_i is $U(x_i, t)$. The estimated derivative parameters are calculated as follows:

$$\begin{aligned} U_x &= \sum_{j=1}^{N} p_{ij} u(x_j, t), \\ U_{xx} &= \sum_{j=1}^{N} q_{ij} u(x_j, t), \\ U_{xxx} &= \sum_{j=1}^{N} r_{ij} u(x_j, t), \end{aligned} \tag{3}$$

for $i = 1, 2, \cdots, N$. The derivatives are approximated by p_{ij}, q_{ij}, and r_{ij}. Once the values of p_{ij} are fixed as described in the next section, the weighting coefficients q_{ij} and r_{ij} can be easily calculated. The method for calculating the other coefficients is as follows:

$$\begin{aligned} \frac{\partial^2 u_i}{\partial x^2} &= \frac{\partial}{\partial x}\left(\frac{\partial u}{\partial x}\right) = \sum_{k=1}^{N} p_{ik} \left(\frac{\partial u}{\partial x}\right)_{x=x_k} \\ &= \sum_{k=1}^{N} p_{ik} \left(\sum_{j=1}^{N} \mathrm{p}_{kj} u(x_j, t)\right) = \sum_{k=1}^{N} \sum_{j=1}^{N} p_{ik} p_{kj} u(x_j, t) \\ &= \sum_{j=1}^{N} q_{ij} u(x_j, t), \quad i = 1, 2, 3, \cdots, N. \end{aligned} \tag{4}$$

Since q_{ij} is calculated using p_{ij},r_{ij} can be calculated in a similar manner.

For $i = -2, -1, 0, \cdots, N + 2$, $B_i(x)$, the quintic B-spline basis function, describes a piecewise-defined function with the properties of continuity and division of unity.

Table 1: Values of $B_i(x)$ and its derivatives at the nodes [34].

x	x_{i-3}	x_{i-2}	x_{i-1}	x_i	x_{i+1}	x_{i+2}	x_{i+3}
$B_i(x)$	0	1	26	66	26	1	0
$B_i'(x)$	0	$5/h$	$50/h$	0	$-50/h$	$5/h$	0
$B_i''(x)$	0	$20/h^2$	$40/h^2$	$-120/h^2$	$40/h^2$	$20/h^2$	0
$B_i'''(x)$	0	$60/h^3$	$-120/h^3$	0	$120/h^3$	$-60/h^3$	0
$B_i^{iv}(x)$	0	$120/h^4$	$-480/h^4$	$720/h^4$	$-480/h^4$	$120/h^4$	0

Table 2: Experimental evaluation of single soliton: $\Delta t = 0.0005$.

Method	N	T	L_2	L_∞	I_1	I_2	I_3
Present scheme	151	0.25	2.3524×10^{-6}	6.4229×10^{-6}	0.1446	0.0868	0.0469
		0.50	4.0430×10^{-6}	1.2235×10^{-5}	0.1446	0.0868	0.0469
		0.75	6.0076×10^{-6}	1.9232×10^{-5}	0.1446	0.0868	0.0469
		1.00	8.1958×10^{-6}	2.5869×10^{-5}	0.1446	0.0868	0.0469
		2.00	4.3005×10^{-5}	9.0073×10^{-5}	0.1446	0.0868	0.0469
		3.00	8.3086×10^{-4}	0.0022×10^{-6}	0.1444	0.0868	0.0469
MQ_DQM [41]	201	0.25	1.01×10^{-5}	2.66×10^{-5}	0.1445	0.0867	0.0468
		0.50	1.11×10^{-5}	2.59×10^{-5}	0.1445	0.0867	0.0468
		0.75	1.33×10^{-5}	3.94×10^{-5}	0.1445	0.0867	0.0468
		1.00	1.43×10^{-5}	4.08×10^{-5}	0.1445	0.0867	0.0468
		2.00	2.14×10^{-5}	6.74×10^{-5}	0.1445	0.0867	0.0468
		3.00	2.86×10^{-5}	8.15×10^{-5}	0.1446	0.0867	0.0468

Table 3: Experimental evaluation of single soliton: $\Delta t = 0.001$.

Method	N	T	L_2	L_∞	I_1	I_2	I_3
Present scheme	91	0.25	6.2478×10^{-5}	2.1816×10^{-4}	0.1446	0.0868	0.0469
		0.50	9.6636×10^{-5}	2.0265×10^{-4}	0.1446	0.0868	0.0469
		0.75	1.9160×10^{-4}	3.0993×10^{-4}	0.1446	0.0868	0.0469
		1.00	4.4543×10^{-4}	7.0164×10^{-4}	0.1446	0.0868	0.0469
MQ_DQM [41]	201	0.25	0.000010	0.000027	0.1445	0.0867	0.0468
		0.50	0.000010	0.000021	0.1445	0.0867	0.0468
		0.75	0.000012	0.000034	0.1445	0.0867	0.0468
		1.00	0.000012	0.000032	0.1445	0.0867	0.0468
[42]	200	0.25	0.00522	—			
		0.50	0.01200	—	0.144590	0.086759	0.046871
		0.75	0.01220	—			
		1.00	0.02220	—	0.144590	0.086759	0.046873

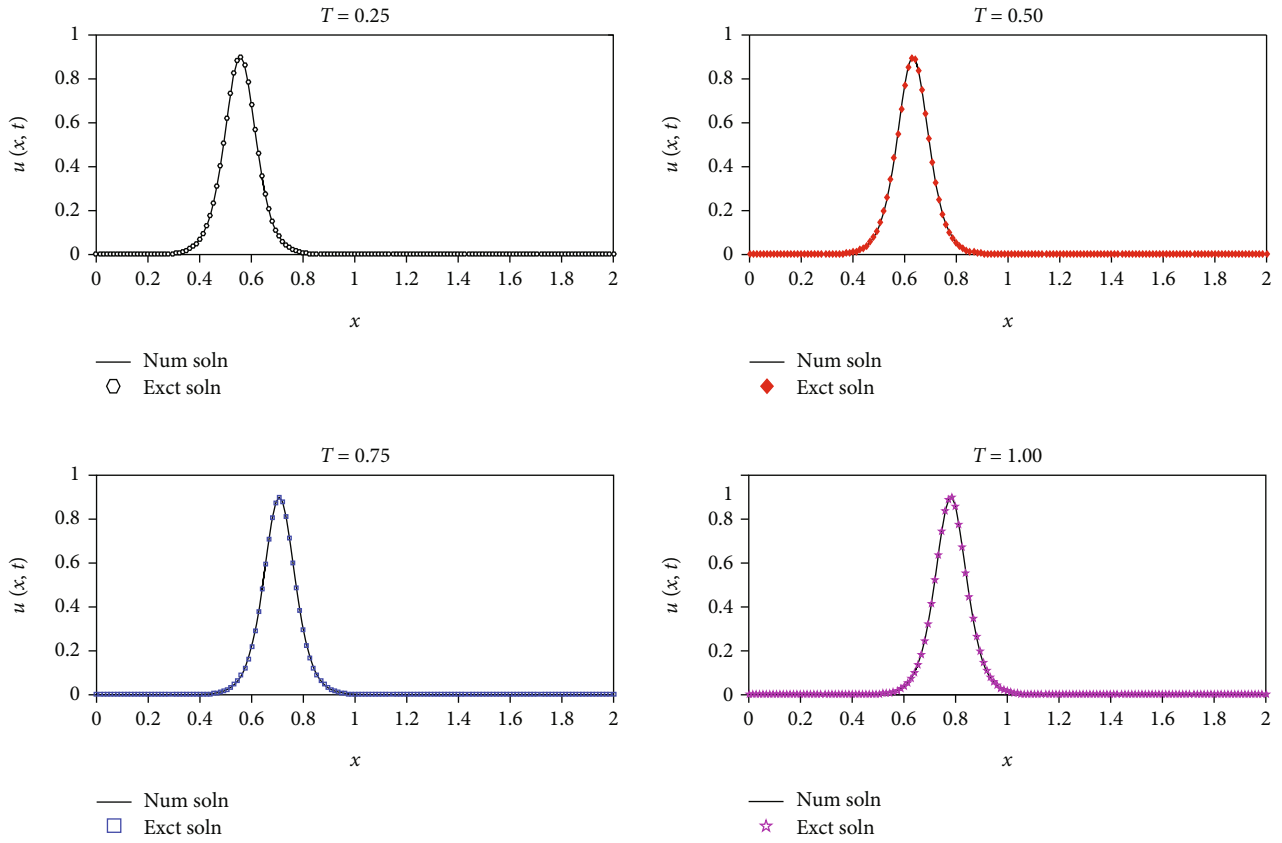

Figure 1: Simulations of single solitons: $\Delta t = 0.0005$.

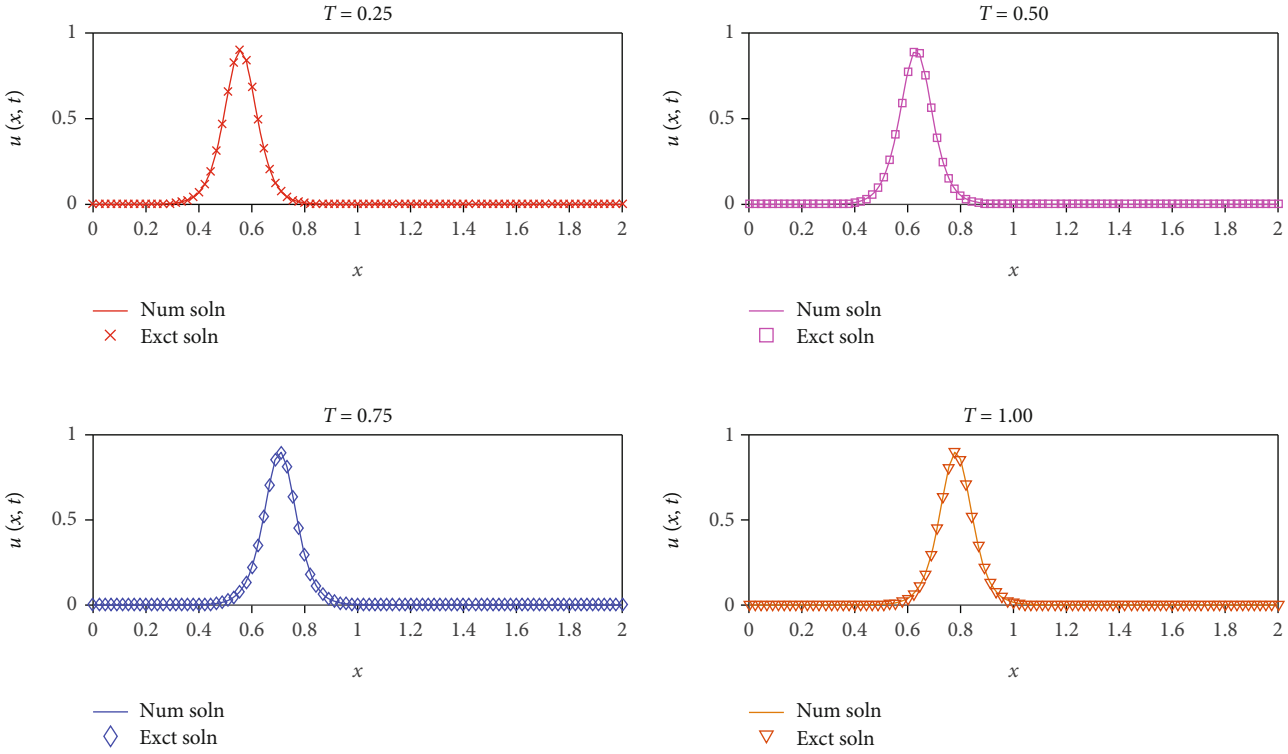

Figure 2: Simulations of single solitons: $\Delta t = 0.001$.

Table 4: Experimental evaluation of interaction of two solitons: $\Delta t = 0.005$.

Method	N	T	I_1	I_2	I_3	CPU time (sec)
Present scheme	91	0.75	0.2281	0.1071	0.0533	0.208
		1.50	0.2279	0.1071	0.0533	0.244
		2.25	0.2278	0.1071	0.0533	0.283
		3.00	0.2238	0.1074	0.0533	0.316
MQ_DQM [41]	91	0.75	0.2281	0.1070	0.0533	
		1.50	0.2280	0.1070	0.0533	
		2.25	0.2279	0.1070	0.0533	
		3.00	0.2277	0.1070	0.0533	
	200	0.75	0.2280	0.1070	0.0535	
		1.50	0.2280	0.1070	0.0534	
		3.00	0.2279	0.1070	0.0532	

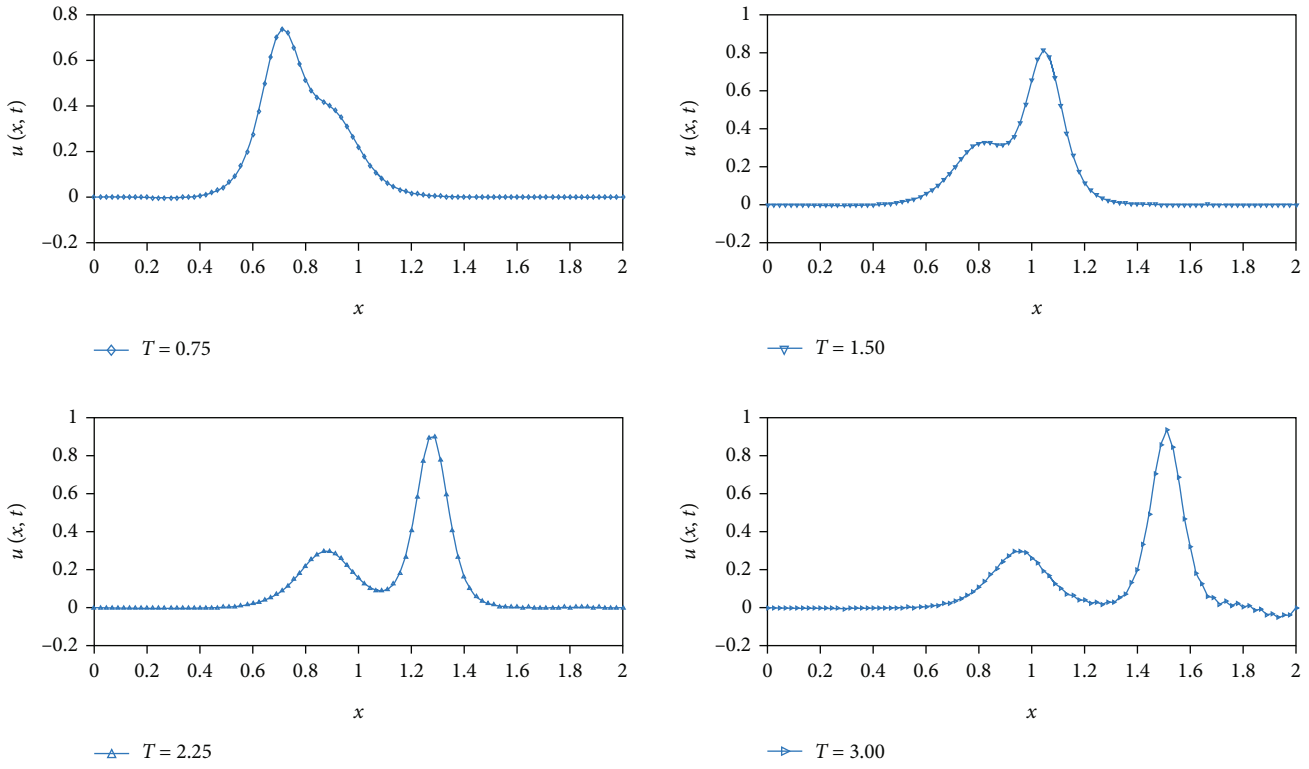

Figure 3: Simulations of two solitons: $\Delta t = 0.005$.

The following equations can be used to calculate the basis functions.

$$B_i(x) = \frac{1}{h^5}\begin{cases} (x - x_{i-3})^5, & x \in [x_{i-3}, x_{i-2}), \\ (x - x_{i-3})^5 - 6(x - x_{i-2})^5, & x \in [x_{i-2}, x_{i-1}), \\ (x - x_{i-3})^5 - 6(x - x_{i-2})^5 + 15(x - x_{i-1})^5, & x \in [x_{i-1}, x_i), \\ (x_{i+3} - x)^5 - 6(x_{i+2} - x)^5 + 15(x_{i+1} - x)^5, & x \in [x_i, x_{i+1}), \\ (x_{i+3} - x)^5 - 6(x_{i+2} - x)^5, & x \in [x_{i+1}, x_{i+2}), \\ (x_{i+3} - x)^5, & x \in [x_{i+2}, x_{i+3}), \\ 0, & \text{otherwise}, \end{cases} \tag{5}$$

where $B_{-2}, B_{-1}, B_0, B_1, \cdots, 0_{i+1}, B_{i+2}$ are the bases formed over the region $a \le x \le b$. Each quintic B-spline covers six elements, so that a total of six quintic B-splines cover one element. Table 1 summarizes the values of $B_i(x)$ and the first four derivatives.

The first-order approximation of the derivative can be estimated using the following relation:

$$B_i'(x_i) = \sum_{j=1}^{N} p_{ij} B_i(x_j), \quad \text{for } i = 1, 2, \cdots, N. \tag{6}$$

Table 5: Experimental evaluation of interaction of three solitons: $\Delta t = 0.1$.

Method	N	T	I_1	I_2	I_3
Present scheme	251	56	18.0004	9.8274	5.2615
		112	17.9991	9.8275	5.2633
		168	18.0029	9.8275	5.2627
		224	18.0098	9.8276	5.2624
		280	18.1445	9.8989	5.2627
MQ_DQM [41]	481	56	18.0002	9.8273	5.2622
		112	17.9994	9.8273	5.2621
		168	17.9989	9.8274	5.2623
		224	17.9988	9.8274	5.2623
		280	18.0006	9.8274	5.2623
MQ	2000	56	18.0018	9.5936	5.0328
		112	17.9974	9.5138	4.9651
		168	17.9971	9.3228	4.7808
		224	17.9985	9.0697	4.5362
		280	17.9995	8.8327	4.3141

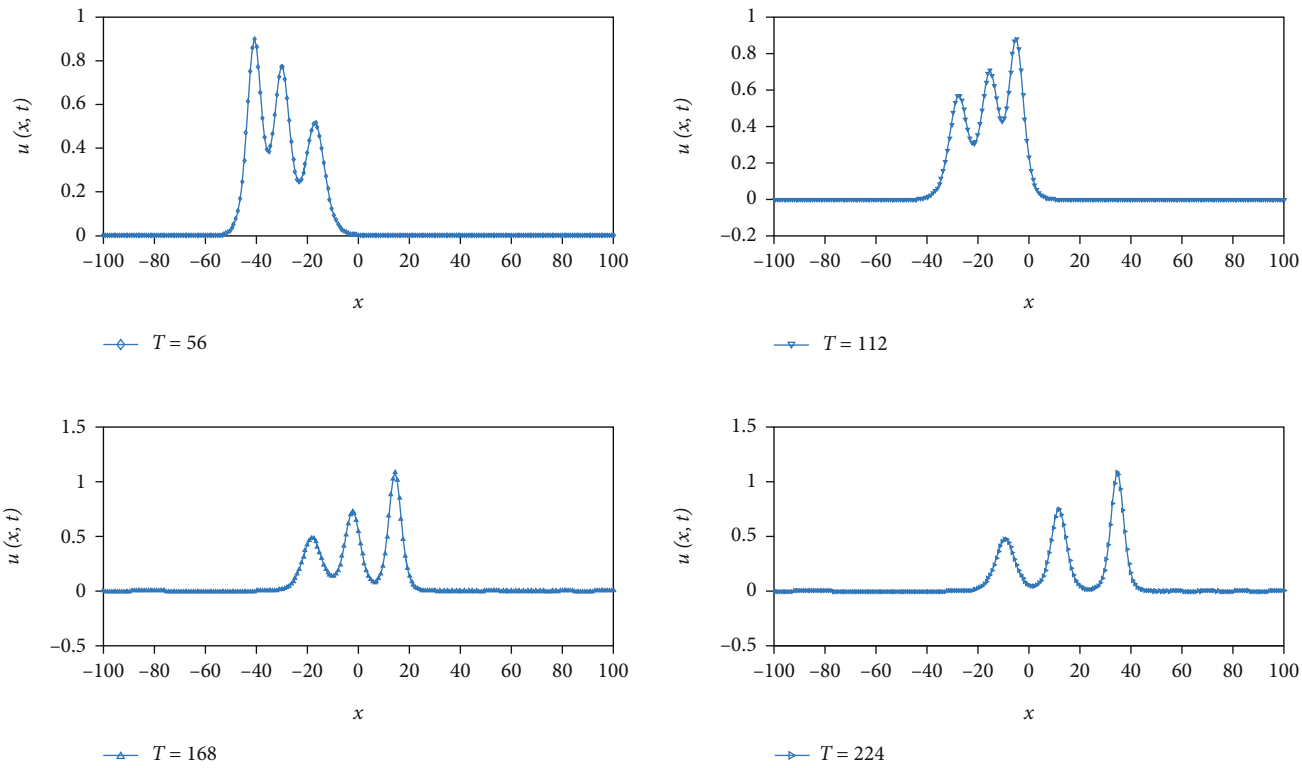

Figure 4: Simulations of three solitons: $\Delta t = 0.1$.

Table 6: Experimental evaluation of the interaction of four solitons: $\Delta t = 0.1$.

Method	N	T	I_1	I_2	I_3	CPU time (sec)
Present scheme	401	80	21.6000	10.3887	5.2687	2.225
		160	21.5999	10.3887	5.2683	3.819
		240	21.6002	10.3887	5.2702	5.316
		320	21.5992	10.3887	5.2691	7.263
		400	21.5360	10.3973	5.2707	9.173
MQ_DQM [41]	451	80	21.6000	10.3887	5.2688	
		160	21.6000	10.3886	5.2687	
		240	21.6000	10.3886	5.2688	
		320	21.5998	10.3887	5.2688	
		400	21.6000	10.3887	5.2688	
	1500	80	2.16028	9.9723	4.8594	
		160	21.6049	9.7448	4.6426	
		240	21.6011	9.7023	4.6035	
		320	21.6007	9.4774	4.3943	
		400	21.6074	9.1922	4.1368	

As a result, a matrix system emerges as follows:

$$A\vec{p}[i] = \vec{s}[i]. \tag{7}$$

Here, A is the coefficient matrix given by

$$\begin{bmatrix} 66 & 26 & 1 & 0 & 0 & 0 & \cdot & 0 \\ 26 & 66 & 26 & 1 & 0 & 0 & \cdot & 0 \\ 1 & 26 & 66 & 26 & 1 & 0 & \cdot & 0 \\ \cdot & \cdot & \cdot & \cdot & \cdot & \cdot & \cdot & \cdot \\ 0 & \cdot & 0 & 1 & 26 & 66 & 26 & 1 \\ 0 & \cdot & 0 & 0 & 1 & 26 & 66 & 26 \\ 0 & \cdot & 0 & 0 & 0 & 1 & 26 & 66 \end{bmatrix}, \tag{8}$$

representing the vector, corresponding to node point x_i. The unknown coefficients are $\vec{p}\,[i] = [p_{i1}, p_{i2}, \cdots, p_{\mathrm{iN}}]^T$, $i = 1, 2, \cdots, N$, with the right-hand side given as follows:

$$\begin{aligned} \vec{s}[1] &= [0, f, g, 0, \cdots, 0]^T, \\ \vec{s}[2] &= [-f, 0, f, g, 0, \cdots, 0]^T, \\ \vec{s}[3] &= [-g, -f, 0, f, g, \cdots, 0]^T, \\ &\cdot \\ &\cdot \\ \vec{s}[N-2] &= [0, \cdots, -g, -f, 0, f, g]^T, \\ \vec{s}[N-1] &= [0, \cdots, 0, -g, -f, 0, f]^T, \\ \vec{s}[N] &= [0, \cdots, 0, -g, -f, 0]^T. \end{aligned} \tag{9}$$

Here, $f = 50/h$ and $g = 5/h$.

The coefficients $p_{i1}, p_{i2}, \cdots, p_{\mathrm{iN}}$ for $i = 1, 2, \cdots, N$ were calculated using MATLAB 2014 to solve the given five-band matrix system. Substituting approximate values for the derived first- and third-order spatial derivatives in equation (1) yields the following system:

$$u_t = -\epsilon u \sum_{j=1}^{N} p_{ij} u_j - \mu \sum_{j=1}^{N} r_{ij} u_j. \tag{10}$$

The SSP-RK43 scheme [39] is then used to solve this system of ordinary differential equations, which offers numerical solutions at various time levels.

3. Numerical Experiments

In this section, the accuracy of the proposed method is shown by calculating the L_2 and L_∞ errors defined as follows:

$$\begin{aligned} L_2 &= \|U^{ex} - U_N\|_2 \simeq \sqrt{h \sum_{j=1}^{N} \left| U_j^{ex.} - (U_N)_j \right|^2}, \\ L_\infty &= \|U^{ex} - U_N\|_\infty \approx \max_j \left| U_j^{ex.} - (U_N)_j \right|, \quad j = 1, 2, \cdots, N-1. \end{aligned} \tag{11}$$

The lowest three invariants related to mass, momentum, and energy conservation are also calculated by the following equations:

$$I_1 = \int_a^b U dx, I_2 = \int_c^b U^2 dx, I_3 = \int_a^b \left[U^3 - \frac{3\mu}{\varepsilon} \left(U' \right)^2 \right] dx. \tag{12}$$

3.1. Experimental of Evaluation of a Single Soliton. Consider

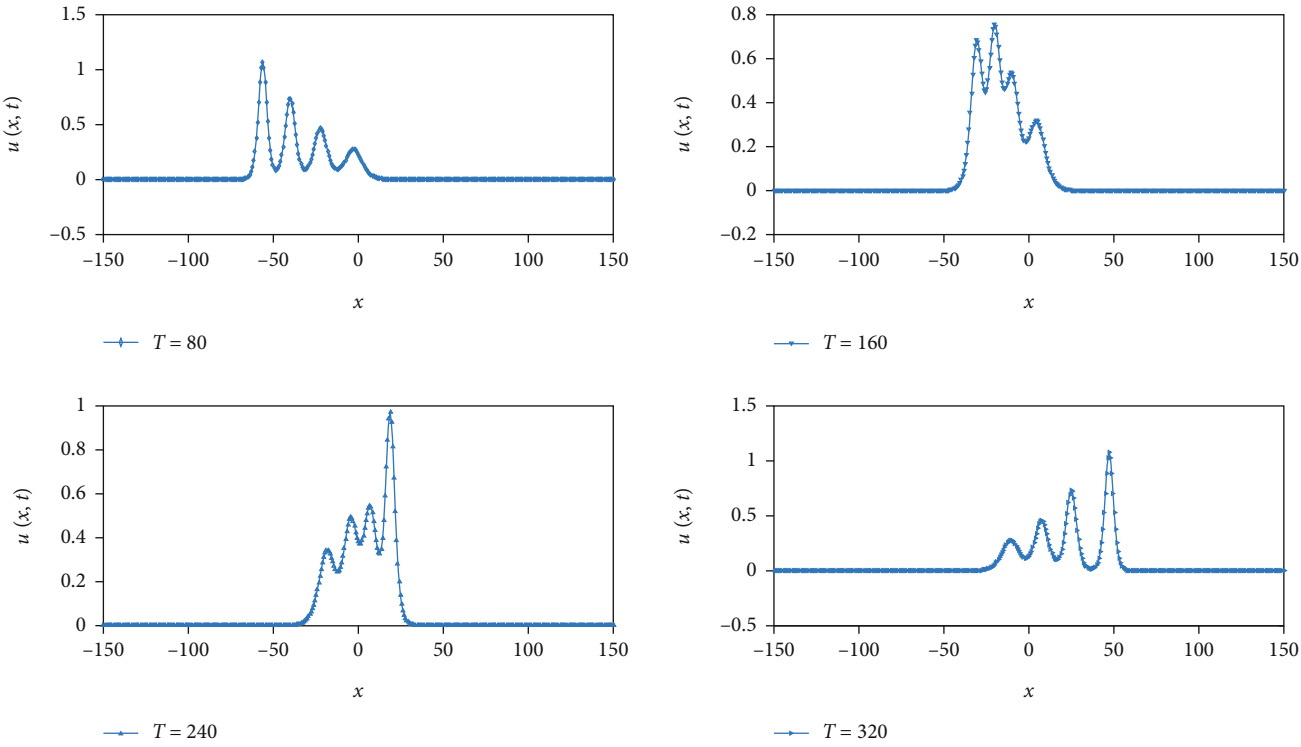

Figure 5: Simulations of four solitons at $\Delta t = 0.1$.

the KdV equation with the exact solution given as [40] follows:

$$U(x,t) = 3C \sec h^2(Ax - Bt + D), \tag{13}$$

Here,

$$A = \frac{1}{2}\left(\frac{\varepsilon C}{\mu}\right)^{1/2}, \qquad B = \frac{1}{2}\varepsilon C\left(\frac{\varepsilon C}{\mu}\right)^{1/2}, \tag{14}$$

so that (13) offers a single soliton with amplitude $3C$ and velocity εC moving towards the right.

The equation is solved with the initial state taken from analytic solution (13) as follows:

$$U(x,0) = 3C \sec h^2(Ax + D), \tag{15}$$

and the boundary conditions $U(0,t) = U(2,t) = 0$ for $t \geq 0$. $\varepsilon = 1, \mu = 4.84 \times 10^{-4}, C = 0.3, D = -6$ is employed in order to create a comparison with other investigations. To demonstrate the evolution of the current technique using a modified quintic B-spline DQM, Tables 2 and 3 show the error norm and invariant values, respectively. Moreover, at different values of $\Delta t = 0.0005$ and 0.001, numerical and exact solutions are represented by Figures 1 and 2, respectively.

3.2. Experimental Evaluation of the Interaction of Two Solitons. Consider this second experiment [43] with the initial condition stated as follows:

$$U = \sum_{i=1}^{2} 3C_i \sec h^2(A_i x + x_i), \quad A_i = \frac{1}{2}\left(\frac{\varepsilon C_i}{\mu}\right)^{1/2}, i = 1, 2, \tag{16}$$

with boundary conditions

$$U(0,t) = U(2,t) = 0, \tag{17}$$

where $\varepsilon = 1, \mu = 4.84 \times 10^{-4}, C_1 = 0.3, C_2 = 0.1, x_1 = x_2 = -6$ is considered in all simulations. The same parameters as in the previous study [43] are used for numerical calculations using MATLAB R2015b (32 bit) in Windows 10 version 21H2 for 64x, with $N = 91$ and $\Delta t = 0.005$. Table 4 displays the error norm and invariant value. Moreover, Figure 3 demonstrates the numerical solution at different values of T.

3.3. Experimental Evaluation of Interaction of Three Solitons. The numerical solution is calculated for the interaction of three solitons having the initial condition [44] given as follows:

$$U(x,0) = \sum_{i=1}^{3} 12C_i^2 \sec h^2(C_i(x - x_i)), \tag{18}$$

with the zero boundary conditions for domain [−100,100]

with $\varepsilon = 1.0, \mu = 1.0, C_1 = 0.3, C_2 = 0.25, C_3 = 0.2, x_1 = -60, x_2 = -44, x_3 = -26$. The same parameters as in the previous study [44] at $\Delta t = 0.1$ and a much smaller number of grid points $N = 251$ than those in the previous study [44] $N = 481$ were used in the numerical computations. Table 5 displays the error norm and invariant value, and the numerical solution at different values of T is presented in Figure 4.

3.4. Experimental Evaluation of Interaction of Four Solitons. In this example, the interaction of four solitons is presented with initial condition [44] given as follows:

$$U = \sum_{i=1}^{4} 12C_i^2 \sec h^2(C_i(x - x_i)), \tag{19}$$

along with zero boundary conditions for domain [−150,150] with $\varepsilon = 1.0, \mu = 1.0, C_1 = 0.3, C_2 = 0.25, C_3 = 0.2, C_4 = 0.15, x_1 = -85, x_2 = -60, x_3 = -35, x_4 = -10$.

The considered parameters are the same as those in the previous study [44] at $\Delta t = 0.1$, and a much smaller number of grid points $N = 401$ than that in the previous study [44] $N = 451$ were used in the numerical computations. Table 6 displays the error norm and invariant value at different time levels with the physical behavior being shown in Figure 5 for different values of T.

4. Conclusion

Due to the numerous applications of the KDV equation in the physical phenomena, in recent years, this equation has become a point of attraction for the researchers who want to find a numerical solution for this equation using various methods. In this paper, the newly defined quintic B-spline basis function is presented to solve the equation using the differential quadrature method. The advantage of this approach is involved in transforming the partial differential equation to an ordinary differential equation which can be solved by any numerical technique for the solution of the ordinary differential equation. In the present work, the SSP-RK43 is implemented to solve the obtained system of the ordinary differential equation which is a combination of the RK method of orders four and five that is a strong-stability-preserving scheme. Numerical results in terms of conservation variables and errors are calculated for the single soliton and extended till interaction of four solitons. The results are compared with numerical solutions from the literature. The obtained results agree well with those obtained earlier. The advantage of the proposed method is its ease of implementation compared to the previous methods. Thus, the present approach can be utilized to solve a variety of nonlinear physical models with extension and application to two-dimensional problems.

Data Availability

The (data type) data used to support the findings of this study are available from the corresponding author upon request.

Conflicts of Interest

The authors declare that there is no conflict of interest.

References

[1] J. S. Russell, "Fourteenth meeting of the British Association for the Advancement of Science," *Report on Waves: Made to the Meetings of the British Association in 1842-43*, London, 1845.

[2] L. Yuliawati, W. S. Budhi, and D. Adytia, "Numerical studying of soliton in the Korteweg-de Vries (KdV) equation," *Journal of Physics: Conference Series*, vol. 1127, no. 1, article 012065, 2019.

[3] C. S. Gardner and G. K. Morikawa, *Courant Institute of Mathematical Sciences Ref*, 1960.

[4] H. Washimi and T. Taniuti, "Propagation of ion-acoustic solitary waves of small amplitude," *Physical Review Letters*, vol. 17, no. 19, pp. 996–998, 1966.

[5] O. Kolebaje and O. Oyewande, "Numerical solution of the korteweg de vries equation by finite difference and adomian decomposition method," *International Journal of Basic and Applied Sciences*, vol. 1, no. 3, pp. 321–335, 2012.

[6] G. C. Das and J. Sarma, "Response to "comment on 'a new mathematical approach for finding the solitary waves in dusty plasma". [Phys. Plasmas 6, 4392 (1999)]," *Physics of Plasmas*, vol. 6, no. 11, pp. 4394–4397, 1999.

[7] A. R. Osborne, "The inverse scattering transform: tools for the nonlinear Fourier analysis and filtering of ocean surface waves," *Chaos, Solitons & Fractals*, vol. 5, no. 12, pp. 2623–2637, 1995.

[8] L. A. Ostrovsky and Y. A. Stepanyants, "Do internal solitions exist in the ocean?," *Reviews of Geophysics*, vol. 27, no. 3, pp. 293–310, 1989.

[9] L. Reatto and D. Galli, "What is a roton?," *International Journal of Modern Physics B*, vol. 13, no. 5n06, pp. 607–616, 1999.

[10] A. Ludu and J. P. Draayer, "Nonlinear modes of liquid drops as solitary waves," *Physical Review Letters*, vol. 80, no. 10, pp. 2125–2128, 1998.

[11] D. G. Crighton, "Applications of KdV," *Acta Applicandae Mathematicae*, vol. 39, no. 1-3, pp. 39–67, 1995.

[12] Z. Yan and H. Zhang, "New explicit solitary wave solutions and periodic wave solutions for Whitham- Broer-Kaup equation in shallow water," *Physics Letters A*, vol. 285, no. 5-6, pp. 355–362, 2001.

[13] Y. Lei, Z. Fajiang, and W. Yinghai, "The homogeneous balance method, lax pair, Hirota transformation and a general fifth-order KdV equation," *Chaos, Solitons & Fractals*, vol. 13, no. 2, pp. 337–340, 2002.

[14] A. Rashid, "Numerical solution of Korteweg-de Vries equation by the Fourier pseudospectral method," *Bulletin of the Belgian Mathematical Society*, vol. 14, no. 4, pp. 709–721, 2007.

[15] C. S. Gardner, J. M. Greene, M. D. Kruskal, and R. M. Miura, "Method for solving the Korteweg-deVries equation," *Physical Review Letters*, vol. 19, no. 19, pp. 1095–1097, 1967.

[16] H. Z. Liu, "A note on "Jacobi elliptic function solutions for the modified Korteweg-de Vries equation"," *Journal of King Saud University-Science*, vol. 26, no. 2, pp. 159-160, 2014.

[17] C. Hufford and Y. Xing, "Superconvergence of the local discontinuous Galerkin method for the linearized Korteweg-de Vries equation," *Journal of Computational and Applied Mathematics*, vol. 255, pp. 441–455, 2014.

[18] T. Trogdon and B. Deconinck, "Numerical computation of the finite-genus solutions of the Korteweg-de Vries equation via Riemann-Hilbert problems," *Applied Mathematics Letters*, vol. 26, no. 1, pp. 5–9, 2013.

[19] T. Grava and C. Klein, "A numerical study of the small dispersion limit of the Korteweg-de Vries equation and asymptotic solutions," *Physica D: Nonlinear Phenomena*, vol. 241, no. 23-24, pp. 2246–2264, 2012.

[20] J. A. Leach, "The large-time development of the solution to an initial-value problem for the generalized Korteweg-de Vries equation," *Applied Mathematics Letters*, vol. 24, no. 2, pp. 214–218, 2011.

[21] B. R. Kumar and M. Mehra, "Time-accurate solutions of Korteweg-de Vries equation using wavelet Galerkin method," *Applied Mathematics and Computation*, vol. 162, no. 1, pp. 447–460, 2005.

[22] A. R. Bahadır, "Exponential finite-difference method applied to Korteweg-de Vries equation for small times," *Applied Mathematics and Computation*, vol. 160, no. 3, pp. 675–682, 2005.

[23] E. N. Aksan and A. Özdeş, "Numerical solution of Korteweg-de Vries equation by Galerkin B-spline finite element method," *Applied Mathematics and Computation*, vol. 175, no. 2, pp. 1256–1265, 2006.

[24] S. Özer and S. Kutluay, "An analytical-numerical method for solving the Korteweg-de Vries equation," *Applied Mathematics and Computation*, vol. 164, no. 3, pp. 789–797, 2005.

[25] U. M. Ascher and R. I. McLachlan, "Multisymplectic box schemes and the Korteweg-de Vries equation," *Applied Numerical Mathematics*, vol. 48, no. 3-4, pp. 255–269, 2004.

[26] S. Kutluay, A. R. Bahadir, and A. Özdeş, "A small time solutions for the Korteweg-de Vries equation," *Applied Mathematics and Computation*, vol. 107, no. 2-3, pp. 203–210, 2000.

[27] M. Idrees, S. Islam, S. I. A. Tirmizi, and S. Haq, "Application of the optimal homotopy asymptotic method for the solution of the Korteweg-de Vries equation," *Mathematical and Computer Modelling*, vol. 55, no. 3-4, pp. 1324–1333, 2012.

[28] N. Gücüyenen and G. Tanoğlu, "On the numerical solution of Korteweg-de Vries equation by the iterative splitting method," *Applied Mathematics and Computation*, vol. 218, no. 3, pp. 777–782, 2011.

[29] J. Sarma, "Solitary wave solution of higher-order Korteweg-de Vries equation," *Chaos, Solitons & Fractals*, vol. 39, no. 1, pp. 277–281, 2009.

[30] B. W. Van de Fliert and E. V. Groesen, "On variational principles for coherent vortex structures," *Advances in Turbulence IV*, vol. 51, pp. 399–403, 1993.

[31] H. P. Ma and B. Y. Guo, "The Fourier pseudospectral method with a restrain operator for the Korteweg-de Vries equation," *Journal of Computational Physics*, vol. 65, no. 1, pp. 120–137, 1986.

[32] M. Dehghan and A. Shokri, "A numerical method for KdV equation using collocation and radial basis functions," *Nonlinear Dynamics*, vol. 50, no. 1-2, pp. 111–120, 2007.

[33] R. Bellman, B. G. Kashef, and J. Casti, "Differential quadrature: a technique for the rapid solution of nonlinear partial differential equations," *Journal of Computational Physics*, vol. 10, no. 1, pp. 40–52, 1972.

[34] A. Başhan, S. B. G. Karakoc, and T. Geyikli, "Approximation of the KdVB equation by the quintic B-spline differential quadrature method," *Kuwait Journal of Science*, vol. 42, no. 2, pp. 67–92, 2015.

[35] R. Bellman, B. Kashef, E. S. Lee, and R. Vasudevan, "Differential quadrature and splines," *Computers & Mathematics with Applications*, vol. 1, no. 3-4, pp. 371–376, 1975.

[36] J. R. Quan and C. T. Chang, "New insights in solving distributed system equations by the quadrature method –I. Analysis," *Computers & Chemical Engineering*, vol. 13, no. 7, pp. 779–788, 1989.

[37] J. R. Quan and C. T. Chang, "New sightings in involving distributed system equations by the quadrature methods-II," *Computers and Chemical Engineering*, vol. 13, pp. 717–724, 1989.

[38] C. Shu and B. E. Richards, "Application of generalized differential quadrature to solve two-dimensional incompressible Navier-Stokes equations," *International Journal for Numerical Methods in Fluids*, vol. 15, no. 7, pp. 791–798, 1992.

[39] R. J. Spiteri and S. J. Ruuth, "A new class of optimal high-order strong-stability-preserving time discretization methods," *SIAM Journal on Numerical Analysis*, vol. 40, no. 2, pp. 469–491, 2002.

[40] M. E. Alexander and J. L. Morris, "Galerkin methods applied to some model equations for non-linear dispersive waves," *Journal of Computational Physics*, vol. 30, no. 3, pp. 428–451, 1979.

[41] A. Başhan, "Modification of quintic B-spline differential quadrature method to nonlinear Korteweg-de Vries equation and numerical experiments," *Applied Numerical Mathematics*, vol. 167, pp. 356–374, 2021.

[42] A. A. Soliman, A. H. A. Ali, and K. R. Raslan, "Numerical solution for the KdV equation based on similarity reductions," *Applied Mathematical Modelling*, vol. 33, no. 2, pp. 1107–1115, 2009.

[43] İ. Dağ and Y. Dereli, "Numerical solutions of KdV equation using radial basis functions," *Applied Mathematical Modelling*, vol. 32, no. 4, pp. 535–546, 2008.

[44] D. Kong, Y. Xu, and Z. Zheng, "A hybrid numerical method for the KdV equation by finite difference and sinc collocation method," *Applied Mathematics and Computation*, vol. 355, pp. 61–72, 2019.

Hindawi
Advances in Mathematical Physics
Volume 2022, Article ID 2412012, 15 pages
https://doi.org/10.1155/2022/2412012

Research Article

A Novel Description of Some Concepts in Interval-Valued Intuitionistic Fuzzy Graph with an Application

Xiaoli Qiang,[1] Saeed Kosari,[1] Xiang Chen,[1] Ali Asghar Talebi,[2] Ghulam Muhiuddin,[3] and Seyed Hossein Sadati[2]

[1]*Institute of Computing Science and Technology, Guangzhou University, Guangzhou 510006, China*
[2]*Department of Mathematics, University of Mazandaran, Babolsar, Iran*
[3]*Department of Mathematics, University of Tabuk, Tabuk 71491, Saudi Arabia*

Correspondence should be addressed to Saeed Kosari; saeedkosari38@gzhu.edu.cn

Received 22 April 2022; Revised 7 June 2022; Accepted 21 June 2022; Published 8 July 2022

Academic Editor: Ranjan Kumar

Covering, matching, and domination are the basic concepts in graphs that play a decisive role in the properties of graphs. Calculating these parameters is one of the difficulties in fuzzy graphs when it is not possible to accurately determine the values of the vertices of a graph. The interval-valued intuitionistic fuzzy graph (IVIFG) is one of the fuzzy graphs which can play an important role in solving uncertain problems in different sciences such as psychology, biological sciences, medicine, and social networks. The necessity of using a range of value instead of one number caused them to help researchers in optimizing and saving time and cost. In this study, we introduce some of the specific concepts such as covering, matching, and paired domination using strong arc or effective edges by giving appropriate examples. In addition, we have calculated strong node covering number, strong independent number, and other parameters of complete bipartite IVIFGs with several examples. Finally, we have presented an application of IVIFG in social networks.

1. Introduction

Graphs are an inevitable tool in applied mathematics. Among the various concepts in graphs, some concepts are more important such as covering, matching, and domination. These concepts are closely related to vertices, as one of the most important components of the graph, and cause them to participate in many analyses related to vertices. Many studies have been done by researchers on various graphs. It is difficult to examine these concepts when the exact values for the vertices cannot be considered.

In 1965, Zadeh [1] presented the basic idea of fuzzy set (FS) where its prominent feature was the allocation of membership degree between 0 and 1 to each element in a set. Zadeh [2] also introduced the interval-valued fuzzy set (IVFS) in 1975, in which membership degrees were intervals of numbers. Roselfeld [3] defined a new concept called the fuzzy graph (FG) by employing fuzzy relations on FS. FGs were considered by researchers in the fields related to ambiguous and uncertain problems. They were able to find numerous applications in solving and modeling problems in computer science, engineering, system analysis, economics, network routing, transportation, and so on. With the advent of new indefinite problems, it became clear that a membership function could not well express the ambiguity in subjective perceptions and the complexity of data. To overcome this shortcoming of the FS, Atanassov [4] proposed an extension of FS by introducing nonmembership function and defined intuitionistic fuzzy set (IFS). IFGs were first introduced by Atanassov [5] in 1999 and was further discussed in [6]. Mahapatra et al. [7–9] explored concepts on fuzzy graphs. Rashmanlou and Pal [10, 11] studied different kinds of FGs. Kosari et al. [12] presented vague graph structure with an application in medical diagnosis. Kou et al. [13] studied some properties of vague graph (VG). Krishna et al. [14] studied new results in cubic graphs. Talebi et al. [15, 16] defined Cayley-FGs and some operations on level graphs of bipolar FGs. Atanassov [17] recently introduced some new

topological operators over IFSs. Mathew et al. [18] conducted research on vertex rough graphs. Some concepts in IVFGs and neutrosophic graphs are studied by Jan et al. [19]. Voskoglou [20] used a combination of soft sets and gray numbers in decision-making. Mahapatra et al. [21–23] introduced concepts of neutrosophic graphs used in social networks.

The decision to determine accurate numerical values in uncertain and inaccurate evaluations of information, which often occur in practical situations, is associated with difficulties. Thus, in 1989, Atanassov and Gargov [24] introduced the idea of the interval-valued intuitionistic fuzzy set (IVIFS) in order to unify perceptions and quantify the uncertain nature of the mind. This concept is defined by a membership function, a nonmembership function, and a hesitant function whose values are intervals between 0 and 1 instead of exact numbers. IVIFS has been widely used in many areas, such as decision-making [25], pattern recognition [26], medical diagnosis [27], and graph theory [28]. The concept of interval-valued fuzzy graphs (IVFGs) is presented by Hongmei and Lianhua in [29]. Akram et al. [30, 31] defined certain types of IVFGs. The product of IVIFGs was proposed by Mishra and Pal in [32]. The strong IVIFG concept is described by Ismayil and Ali [33]. Rashmanlou et al. [25, 34–36] studied some IVIFG concepts.

The purpose of this paper is to find a way to determine the concepts of vertex covering, matching, and paired domination in IVIFGs where we are dealing with interval-valued numbers instead of fuzzy numbers. The previous definition limitations in the vertex covering, matching, and paired domination of FGs have directed us to offer new classifications in terms of IVIFG. These concepts have already been studied by some researchers in a variety of FGs. Sahoo et al. [37] investigated covering and paired domination in IFGs.

The rest of this article is organized as follows: Section 2 briefly reviews related basic concepts to IVIFGs. In Section 3, we introduced the concepts of strong vertex covering, independent vertex covering, and perfect strong matching in an IVIFG by strong edges and defined some of its properties in specific types of IVIFGs. In this section, we introduce paired domination in IVIFG and examine its implications. Finally, we present an application of IVIFG on social networks in Section 4.

2. Preliminaries

In this section, we briefly define some of the basic concepts for entering the main discussion.

Definition 1 (see [24]). An IVIFS A in X can be described as

$$A = \left\{ \left\langle x, \left[\mu_A^L(x), \mu_A^U(x)\right], \left[\nu_A^L(x), \nu_A^U(x)\right] \right\rangle | x \in X \right\}, \quad (1)$$

where $0 \le \mu_A^L(x) \le \mu_A^U \le 1$, $0 \le \nu_A^L(x) \le \nu_A^U \le 1$, and $0 \le \mu_A^U(x) + \nu_A^U(x) \le 1$, for all $x \in X$.

Similarly, the intervals $[\mu_A^L(x), \mu_A^U(x)]$ and $[\nu_A^L(x), \nu_A^U(x)]$ denoted the MV and non-MV of an element x, respectively. If each of the intervals contains only one value for each $x \in X$, we have

$$\mu_A(x) = \mu_A^L(x) = \mu_A^U(x), \nu_A(x) = \nu_A^L(x) = \nu_A^U(x). \quad (2)$$

Furthermore, the hesitancy degree of each element x is as follows:

$$\left[1 - \mu_A^L(x) - \nu_A^L(x), 1 - \mu_A^U(x) - \nu_A^U(x)\right]. \quad (3)$$

Definition 2 (see [33]). An IVIFG of an underlying graph $G^* = (V, E)$ is a pair $G = (V, A, B)$ so that

$$A = \left\{ \left\langle \left[\mu_A^L(x), \mu_A^U(x)\right], \left[\nu_A^L(x), \nu_A^U(x)\right] \right\rangle | x \in V \right\}, \quad (4)$$

is an IVIFS in V and

$$B = \left\{ \left\langle \left[\mu_B^L(xy), \mu_B^U(xy)\right], \left[\nu_B^L(xy), \nu_B^U(xy)\right] \right\rangle | xy \in E \right\}, \quad (5)$$

is an interval-valued intuitionistic fuzzy relation (IVIFR) $V \times V$ so that

$$\begin{aligned} \mu_B &: E \subseteq V \times V \longrightarrow D[0,1], \\ \nu_B &: E \subseteq V \times V \longrightarrow D[0,1], \\ \mu_B^L(xy) &\le \min\left\{\mu_A^L(x), \mu_A^L(y)\right\}, \\ \mu_B^U(xy) &\le \min\left\{\mu_A^U(x), \mu_A^U(y)\right\}, \\ \nu_B^L(xy) &\ge \max\left\{\nu_A^L(x), \nu_A^L(y)\right\}, \\ \nu_B^U(xy) &\ge \max\left\{\nu_A^U(x), \nu_A^U(y)\right\}, \end{aligned} \quad (6)$$

and $\mu_B^U(xy) + \nu_B^U(xy) \le 1$, for each $xy \in E$.

Definition 3 (see [34]). An edge xy of an IVIFG, G is named a strong arc (SA) or effective edge if

$$\begin{aligned} \mu_B^L(xy) &= \min\left\{\mu_A^L(x), \mu_A^L(y)\right\}, \\ \mu_B^U(xy) &= \min\left\{\mu_A^U(x), \mu_A^U(y)\right\}, \\ \nu_B^L(xy) &= \max\left\{\nu_A^L(x), \nu_A^L(y)\right\}, \\ \nu_B^U(xy) &= \max\left\{\nu_A^U(x), \nu_A^U(y)\right\}. \end{aligned} \quad (7)$$

Definition 4 (see [34]). An IVIFG is complete, if

$$\begin{aligned} \mu_B^L(xy) &= \min\left\{\mu_A^L(x), \mu_A^L(y)\right\}, \\ \nu_B^L(xy) &= \max\left\{\nu_A^L(x), \nu_A^L(y)\right\}, \\ \mu_B^U(xy) &= \min\left\{\mu_A^U(x), \mu_A^U(y)\right\}, \\ \nu_B^U(xy) &= \max\left\{\nu_A^U(x), \nu_A^U(y)\right\}, \end{aligned} \quad (8)$$

for all $xy \in V \times V$.

As a result of the above definition, the following definition can be provided.

Definition 5. An IVIFG G is named bipartite whenever the vertex set V can be partitioned into two nonempty sets V_1

and V_2 so that $\mu_B^L(xy) = \mu_B^U(xy) = 0$ and $\nu_B^L(xy) = \nu_B^U(xy) = 0$, for $xy \in V_1$ or $xy \in V_2$. If

$$\begin{aligned}\mu_B^L(xy) &= \min\left\{\mu_A^L(x), \mu_A^L(y)\right\},\\ \mu_B^U(xy) &= \min\left\{\mu_A^U(x), \mu_A^U(y)\right\},\\ \nu_B^L(xy) &= \max\left\{\nu_A^L(x), \nu_A^L(y)\right\},\\ \nu_B^U(xy) &= \max\left\{\nu_A^U(x), \nu_A^U(y)\right\},\end{aligned} \tag{9}$$

for all $x \in V_1$ and $y \in V_2$; then, G is named a complete bipartite IVIFG (CB-IVIFG) and is shown by K_{σ_1,σ_2}.

All the basic notations are shown in Table 1.

3. Covering, Matching, and Paired Domination in the IVIFGs

In this section, we introduce covering, matching, and paired domination in the IVIFGs by the weight of strong edges and examine some of its properties and results.

Definition 6. Let $G = (V, A, B)$ be an IVIFG. An SNC in an IVIFG G is the set D of nodes that cover all SAs of G. The weight of an SNC D is denoted as

$$\begin{aligned}W_{nc} &= \left\langle \left[W_{nc}^{L_\mu}(D), W_{nc}^{U_\mu}(D)\right], \left[W_{nc}^{L_\nu}(D), W_{nc}^{U_\nu}(D)\right]\right\rangle,\\ W_{nc} &= \left\langle \left[\sum_{x\in D}\mu_B^L(xy), \sum_{x\in D}\mu_B^U(xy)\right], \left[\sum_{x\in D}\nu_B^L(xy), \sum_{x\in D}\nu_B^U(xy)\right]\right\rangle,\end{aligned} \tag{10}$$

so that $\mu_B^L(xy)$ and $\mu_B^U(xy)$ are the minimum of the lower and upper of IVMBs and $\nu_B^L(xy)$ and $\nu_B^U(xy)$ are the maximum of the lower and upper of IVNMBs of all SAs incident on x, respectively.

An SNCN of an IVIFG G is shown as follows $\alpha_{s_0}(G) = \alpha_{s_0} = \langle[\alpha_{s_0}^{L_\mu}, \alpha_{s_0}^{U_\mu}], [\alpha_{s_0}^{L_\nu}, \alpha_{s_0}^{U_\nu}]\rangle$ so that

$$\begin{aligned}\alpha_{s_0}^{L_\mu} &= \min\left\{W_{nc}^{L_\mu} \middle| D \text{ is the weight of SNCs of } G\right\},\\ \alpha_{s_0}^{U_\mu} &= \min\left\{W_{nc}^{U_\mu} \middle| D \text{ is the weight of SNCs of } G\right\},\\ \alpha_{s_0}^{L_\nu} &= \max\left\{W_{nc}^{L_\nu} \middle| D \text{ is the weight of SNCs of } G\right\},\\ \alpha_{s_0}^{U_\nu} &= \max\left\{W_{nc}^{U_\nu} \middle| D \text{ is the weight of SNCs of } G\right\}.\end{aligned} \tag{11}$$

A minimum SNC in an IVIFG G is an SNC of minimum IVMBs and maximum IVNMBs.

Table 1: Some basic notations.

Notation	Meaning
IVFS	Interval-valued fuzzy set
IFG	Intuitionistic fuzzy graph
IVIFS	Interval-valued intuitionistic fuzzy set
IVIFG	Interval-valued intuitionistic fuzzy graph
CIVIFG	Complete interval-valued intuitionistic fuzzy graph
SA	Strong arc
CB	Complete bipartite
SC	Strong cover
SCN	Strong covering number
SNC	Strong node cover
ISA	Incident strong arc
SNCN	Strong node covering number
IVMB	Interval-valued membership bound
IVNMB	Interval-valued nonmembership bound
SI	Strong independent
SIS	Strong independent set
SIN	Strong independent number
IN	Isolated node
SAC	Strong arc cover
PD	Paired domination
SPDN	Strong paired domination number
SM	Strong matching
SMN	Strong matching number
SIAC	Strong independent arc cover
PSM	Perfect strong matching
SDS	Strong dominating set
SPDS	Strong paired dominating set

Theorem 7. *Let $G = (V, A, B)$ be a CIVIFG. Then,*

$$\begin{aligned}\alpha_{s_0}^{L_\mu} &= (r-1)\mu_B^L(xy),\\ \alpha_{s_0}^{L_\nu} &= (r-1)\nu_B^L(xy),\\ \alpha_{s_0}^{U_\mu} &= (r-1)\mu_B^U(xy),\\ \alpha_{s_0}^{U_\nu} &= (r-1)\nu_B^U(xy),\end{aligned} \tag{12}$$

where $\mu_B^L(xy)$ and $\mu_B^U(xy)$ are the lower and upper of IVMBs and $\nu_B^L(xy)$ and $\nu_B^U(xy)$ are the lower and upper of IVNMBs of the weakest arc in G. Note that r is the number of vertex in G.

Proof. Since G is a CIVIFG, all arcs are strong, and every node is neighbor to all other vertices. So, any set includes $(r-1)$ nodes forming an SNC of G.

Let x be a vertex having minimum of IVMBs and maximum of IVNMBs in G. Suppose $y_1, y_2 \cdots, y_{n-1}$ is the node neighbor to x. Then, the $(r-1)$ arcs $xy_1, xy_2, \cdots, xy_{r-1}$ are all weakest arcs of G, and strength of each arcs is equal to $\langle[\mu_B^L(xy), \mu_B^U(xy)], [\nu_B^L(xy), \nu_B^U(xy)]\rangle$, which $y \in \{y_1, y_2, \cdots, y_{r-1}\}$.

Hence, the set $D=\{y_1, y_2, \cdots, y_{r-1}\}$ of $(r-1)$ vertices forms an SNC of G with

$$W_{nc}^{L_\mu}(D)=\sum_{y_i\in D}\mu_B^L(xy_i)=\mu_B^L(xy_1)+\mu_B^L(xy_2)+\cdots+\mu_B^L(xy_{r-1}),$$
$$W_{nc}^{U_\mu}(D)=\sum_{y_i\in D}\mu_B^U(xy_i)=\mu_B^U(xy_1)+\mu_B^U(xy_2)+\cdots+\mu_B^U(xy_{r-1}), \tag{13}$$

where $\mu_B^L(xy_i), i=1,2,\cdots,(r-1)$ is the minimum lower of IVMB and $\mu_B^U(xy_i), i=1,2,\cdots,(r-1)$ is the minimum upper of IVNMB of SAs incident on y_i. Then,

$$\alpha_{s_0}^{L_\mu}=\mu_B^L(xy)+\mu_B^L(xy)+\cdots+\mu_B^L(xy),$$
$$\alpha_{s_0}^{U_\mu}=\mu_B^U(xy)+\mu_B^U(xy)+\cdots+\mu_B^U(xy), \tag{14}$$

where $\mu_B^L(xy)$ and $\mu_B^U(xy)$ are the lower and upper of IVMBs of a weakest arc in G.

Hence, $\alpha_{s_0}^{L_\mu}=(r-1)\mu_B^L(xy)$ and $\alpha_{s_0}^{U_\mu}=(r-1)\mu_B^U(xy)$. Similarly,

$$W_{nc}^{L_\nu}(D)=\sum_{y_i\in D}\nu_B^L(xy_i)=\nu_B^L(xy_1)+\nu_B^L(xy_2)+\cdots+\nu_B^L(xy_{r-1}),$$
$$W_{nc}^{U_\nu}(D)=\sum_{y_i\in D}\nu_B^U(xy_i)=\nu_B^U(xy_1)+\nu_B^U(xy_2)+\cdots+\nu_B^U(xy_{r-1}), \tag{15}$$

where $\nu_B^L(xy_i)$ and $\nu_B^U(xy_i)$, $i=1,2,\cdots,(r-1)$ are the maximum lower and upper of IVNMBs of all SAs incident on y_i. Then,

$$\alpha_{s_0}^{L_\nu}=\nu_B^L(xy)+\nu_B^L(xy)+\cdots+\nu_B^L(xy),$$
$$\alpha_{s_0}^{U_\nu}=\nu_B^U(xy)+\nu_B^U(xy)+\cdots+\nu_B^U(xy), \tag{16}$$

where $\nu_B^L(xy)$ and $\nu_B^U(xy)$ are the lower and upper of IVNMBs of a weakest arc in G. Hence, $\alpha_{s_0}^{L_\nu}=(r-1)\nu_B^L(xy)$ and $\alpha_{s_0}^{U_\nu}=(r-1)\nu_B^U(xy)$. □

Theorem 8. *For a CB-IVIFG K_{σ_1,σ_2} with partite set V_1 and V_2,*

$$\alpha_{s_0}^{L_\mu}\left(K_{\sigma_1,\sigma_2}\right)=\min\left\{W_{nc}^{L_\mu}(V_1), W_{nc}^{L_\mu}(V_2)\right\},$$
$$\alpha_{s_0}^{U_\mu}\left(K_{\sigma_1,\sigma_2}\right)=\min\left\{W_{nc}^{U_\mu}(V_1), W_{nc}^{U_\mu}(V_2)\right\},$$
$$\alpha_{s_0}^{L_\nu}\left(K_{\sigma_1,\sigma_2}\right)=\max\left\{W_{nc}^{L_\nu}(V_1), W_{nc}^{L_\nu}(V_2)\right\},$$
$$\alpha_{s_0}^{U_\nu}\left(K_{\sigma_1,\sigma_2}\right)=\max\left\{W_{nc}^{U_\nu}(V_1), W_{nc}^{U_\nu}(V_2)\right\}. \tag{17}$$

Proof. All arcs in K_{σ_1,σ_2} are strong, and each node in V_1 is neighbor with all nodes in V_2 and contrariwise. The set of all arcs of K_{σ_1,σ_2} is a set of all arcs incident on each node of V_1 or a set of all arcs incident on each node of V_2. Hence, all SNCs in K_{σ_1,σ_2} are V_1, V_2, and $V_1\cup V_2$. Clearly, $W_{nc}^{L_\mu}(V_1\cup V_2)$ is greater than $W_{nc}^{L_\mu}(V_1)$ and $W_{nc}^{L_\mu}(V_2)$. Hence,

$$\alpha_{s_0}^{L_\mu}\left(K_{\sigma_1,\sigma_2}\right)=\min\left\{W_{nc}^{L_\mu}(V_1), W_{nc}^{L_\mu}(V_2)\right\}. \tag{18}$$

Similarly, $\alpha_{s_0}^{U_\mu}(K_{\sigma_1,\sigma_2})=\min\{W_{nc}^{U_\mu}(V_1), W_{nc}^{U_\mu}(V_2)\}$. Also, $W_{nc}^{L_\nu}(V_1\cup V_2)$ is less than $W_{nc}^{L_\nu}(V_1)$ and $W_{nc}^{L_\nu}(V_2)$. So,

$$\alpha_{s_0}^{L_\nu}\left(K_{\sigma_1,\sigma_2}\right)=\max\left\{W_{nc}^{L_\nu}(V_1), W_{nc}^{L_\nu}(V_2)\right\}. \tag{19}$$

In the same way, we have $\alpha_{s_0}^{U_\nu}(K_{\sigma_1,\sigma_2})=\max\{W_{nc}^{U_\nu}(V_1), W_{nc}^{U_\nu}(V_2)\}$. □

Definition 9. In an IVIFG G, two nodes are said to be SI if there is no SA between them. A set of nodes in G is an SI if and only if two nodes are in an SI set.

Definition 10. The weight of an SIS D in an IVIFG G is described as

$$W_{\text{is}}(D)=\left\langle\left[W_{\text{is}}^{L_\mu}(D), W_{\text{is}}^{U_\mu}(D)\right], \left[W_{\text{is}}^{L_\nu}(D), W_{\text{is}}^{U_\nu}(D)\right]\right\rangle, \tag{20}$$

i.e.,

$$W_{\text{is}}(D)=\left\langle\left[\sum_{x\in D}\mu_B^L(xy), \sum_{x\in D}\mu_B^U(xy)\right], \left[\sum_{x\in D}\nu_B^L(xy), \sum_{x\in D}\nu_B^U(xy)\right]\right\rangle, \tag{21}$$

where $\mu_B^L(xy)$ and $\mu_B^U(xy)$ are minimum of the lower and upper of IVMBs and $\nu_B^L(xy)$ and $\nu_B^U(xy)$ are maximum of the lower and upper of IVNMBs of all SAs incident on x, respectively.

An SIN of an IVIFG G is shown by $\beta_{s_0}(G)=\beta_{s_0}=\langle[\beta_{s_0}^{L_\mu}, \beta_{s_0}^{U_\mu}], [\beta_{s_0}^{L_\nu}, \beta_{s_0}^{U_\nu}]\rangle$, which

$$\beta_{s_0}^{L_\mu}=\max\left\{W_{\text{is}}^{L_\mu}(D)\middle| D \text{ is the SISs of nodes in } G\right\},$$
$$\beta_{s_0}^{U_\mu}=\max\left\{W_{\text{is}}^{U_\mu}(D)\middle| D \text{ is the SISs of nodes in } G\right\},$$
$$\beta_{s_0}^{L_\nu}=\min\left\{W_{\text{is}}^{L_\nu}(D)\middle| D \text{ is the SISs of nodes in } G\right\},$$
$$\beta_{s_0}^{U_\nu}=\min\left\{W_{\text{is}}^{U_\nu}(D)\middle| D \text{ is the SISs of nodes in } G\right\}. \tag{22}$$

A maximum SIS in an IVIFG G is an SIS with the maximum IVMBs and minimum IVNMBs.

Theorem 11. *Let G be a CIVIFG. Then,*

$$\beta_{s_0}(G) = \left\langle \left[\mu_B^L(xy), \mu_B^U(xy)\right], \left[\nu_B^L(xy), \nu_B^U(xy)\right] \right\rangle, \tag{23}$$

where $\mu_B^L(xy)$ and $\mu_B^U(xy)$ are the lower and upper of IVMBs and $\nu_B^L(xy)$ and $\nu_B^U(xy)$ are the lower and upper of IVNMBs of a weakest arc in G.

Proof. Since G is a CIVIFG, so all arcs are strong, and also, each arc is neighbor to all other nodes. Hence, $D = \{x\}$ is the only SIS for each $x \in V$. Thus, the result is true. □

Theorem 12. *Let K_{σ_1,σ_2} be a CB-IVIFG with partite set V_1 and V_2. Then,*

$$\begin{aligned}
\beta_{s_0}^{L_\mu}\left(K_{\sigma_1,\sigma_2}\right) &= \max\left\{W_{is}^{L_\mu}(V_1), W_{is}^{L_\mu}(V_2)\right\},\\
\beta_{s_0}^{U_\mu}\left(K_{\sigma_1,\sigma_2}\right) &= \max\left\{W_{is}^{U_\mu}(V_1), W_{is}^{U_\mu}(V_2)\right\},\\
\beta_{s_0}^{L_\nu}\left(K_{\sigma_1,\sigma_2}\right) &= \min\left\{W_{is}^{L_\nu}(V_1), W_{is}^{L_\nu}(V_2)\right\},\\
\beta_{s_0}^{U_\nu}\left(K_{\sigma_1,\sigma_2}\right) &= \min\left\{W_{is}^{U_\nu}(V_1), W_{is}^{U_\nu}(V_2)\right\}.
\end{aligned} \tag{24}$$

Proof. In K_{σ_1,σ_2} all arcs are strong. Also, each node in V_1 is neighbor with all nodes in V_2 and contrariwise. Therefore, all SISs in K_{σ_1,σ_2} are V_1 and V_2. Hence, the result is true. □

Example 1. Consider an IVIFG G is drawn in Figure 1.

Clearly, all arcs are strong, and all SNCs of G are as follows:

$$\begin{aligned}
D_1 &= \{y, t\},\\
D_2 &= \{x, y, z\},\\
D_3 &= \{x, z, t\},\\
D_4 &= \{y, z, t\},\\
D_5 &= \{x, y, t\},\\
D_6 &= \{x, y, z, t\}.
\end{aligned} \tag{25}$$

Table 2 shows the method of calculating the weight of SISs.

Thus, $\alpha_{s_0} = \langle[0.2,0.4], [0.8,2]\rangle$.

Example 2. Consider a strong IVIFG G is drawn in Figure 2. All SISs in G are $D_1 = \{x, z\}, D_2 = \{y, t\}$. The calculation of the weight of SIS is shown in Table 3. Therefore, $\beta_{s_0} = \langle[0.4,1], [0.7,0.9]\rangle$.

Definition 13. Let G be an IVIFG without INs. The weight of an SAC Y is described as $W_{ac}(Y) = \langle[W_{ac}^{L_\mu}(Y), W_{ac}^{U_\mu}(Y)], [W_{ac}^{L_\nu}(Y), W_{ac}^{U_\nu}(Y)]\rangle$, which $W_{ac}(Y) = \langle[\sum_{xy\in Y}\mu_B^L(xy), \sum_{xy\in Y}\mu_B^U(xy)], [\sum_{xy\in Y}\nu_B^L(xy), \sum_{xy\in Y}\nu_B^U(xy)]\rangle$.

An SACN of an IVIFG G is denoted by $\alpha_{s_1}(G) = \alpha_{s_1} = \langle[\alpha_{s_1}^{L_\mu}, \alpha_{s_1}^{U_\mu}], [\alpha_{s_1}^{L_\nu}, \alpha_{s_1}^{U_\nu}]\rangle$, where

$$\begin{aligned}
\alpha_{s_1}^{L_\mu} &= \min\left\{W_{ac}^{L_\mu}(Y)\,\middle|\, Y \text{ is the SACs of } G\right\},\\
\alpha_{s_1}^{U_\mu} &= \min\left\{W_{ac}^{U_\mu}(Y)\,\middle|\, Y \text{ is the SACs of } G\right\},\\
\alpha_{s_1}^{L_\nu} &= \max\left\{W_{ac}^{L_\nu}(Y)\,\middle|\, Y \text{ is the SACs of } G\right\},\\
\alpha_{s_1}^{U_\nu} &= \max\left\{W_{ac}^{U_\nu}(Y)\,\middle|\, Y \text{ is the SACs of } G\right\}.
\end{aligned} \tag{26}$$

A minimum SAC in an IVIFG G is an SAC with minimum IVMBs and maximum IVNMBs.

Theorem 14. *If G is a complete IVIFG, then*

$$\begin{aligned}
\alpha_{s_1}^{L_\mu} &= \min\left\{W_{ac}^{L_\mu}(Y)\,\middle|\, Y \textit{ is a SAC in } G \textit{ with } |Y| \geq \left\lceil\frac{n}{2}\right\rceil\right\},\\
\alpha_{s_1}^{U_\mu} &= \min\left\{W_{ac}^{U_\mu}(Y)\,\middle|\, Y \textit{ is a SAC in } G \textit{ with } |Y| \geq \left\lceil\frac{n}{2}\right\rceil\right\},\\
\alpha_{s_1}^{L_\nu} &= \max\left\{W_{ac}^{L_\nu}(Y)\,\middle|\, Y \textit{ is a SAC in } G \textit{ with } |Y| \geq \left\lceil\frac{n}{2}\right\rceil\right\},\\
\alpha_{s_1}^{U_\nu} &= \max\left\{W_{ac}^{U_\nu}(Y)\,\middle|\, Y \textit{ is a SAC in } G \textit{ with } |Y| \geq \left\lceil\frac{n}{2}\right\rceil\right\}.
\end{aligned} \tag{27}$$

Proof. Since G is a CIVIFG, so all arcs are SA, and each vertex is neighbor to all others vertices. Also, the number of arcs in SAC of both G and G^* is identical because each arc in both graphs is strong. Now, the SACN of G^* is $\lceil n/2\rceil$. Therefore, the minimum number of arcs in an SAC of G is $\lceil n/2\rceil$. This completes the proof. □

Theorem 15. *If K_{σ_1,σ_2} is a CB-IVIFG with partite set V_1 and V_2. Then,*

$$\begin{aligned}
\alpha_{s_1}^{L_\mu}\left(K_{\sigma_1,\sigma_2}\right) &= \min\left\{W_{ac}^{L_\mu}(Y)\,\middle|\, Y \textit{ is a SAC in } K_{\sigma_1,\sigma_2} \textit{ with } |Y| \geq \max\{|V_1|, |V_2|\}\right\},\\
\alpha_{s_1}^{U_\mu}\left(K_{\sigma_1,\sigma_2}\right) &= \min\left\{W_{ac}^{U_\mu}(Y)\,\middle|\, Y \textit{ is a SAC in } K_{\sigma_1,\sigma_2} \textit{ with } |Y| \geq \max\{|V_1|, |V_2|\}\right\},\\
\alpha_{s_1}^{L_\nu}\left(K_{\sigma_1,\sigma_2}\right) &= \max\left\{W_{ac}^{L_\nu}(Y)\,\middle|\, Y \textit{ is a SAC in } K_{\sigma_1,\sigma_2} \textit{ with } |Y| \geq \max\{|V_1|, |V_2|\}\right\},\\
\alpha_{s_1}^{U_\nu}\left(K_{\sigma_1,\sigma_2}\right) &= \max\left\{W_{ac}^{U_\nu}(Y)\,\middle|\, Y \textit{ is a SAC in } K_{\sigma_1,\sigma_2} \textit{ with } |Y| \geq \max\{|V_1|, |V_2|\}\right\}.
\end{aligned} \tag{28}$$

Proof. In K_{σ_1,σ_2}, all arcs are strong. Also, each node in V_1 is neighbor with all nodes in V_2 and contrariwise. Also, the number of arcs in an SAC of both G and G^* is identical because each arc in both graph is strong. Now, the arc

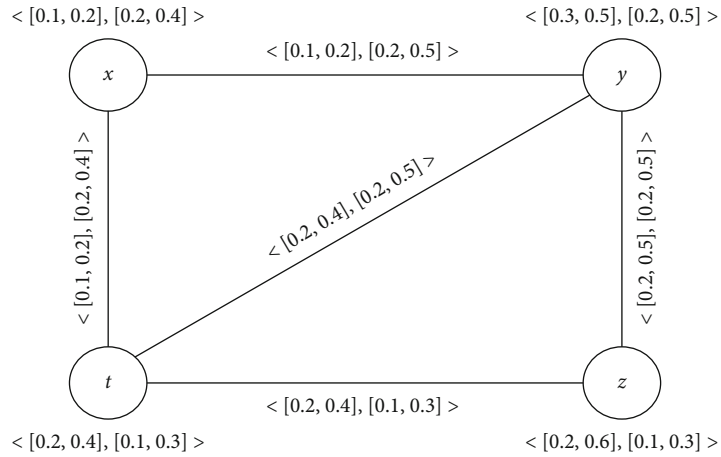

Figure 1: An IVIFG G for a strong node cover (SNC).

Table 2: Calculating the weight of SISs.

D	$W_{nc}^{L_\mu}(D)$	$W_{nc}^{U_\mu}(D)$	$W_{nc}^{L_\nu}(D)$	$W_{nc}^{U_\nu}(D)$	$W_{nc}(D)$
$\{y,t\}$	0.1 + 0.1	0.2 + 0.2	0.2 + 0.2	0.5 + 0.5	$\langle$[0.2,0.4], [0.4,1]$\rangle$
$\{x,y,z\}$	0.1 + 0.1 + 0.2	0.2 + 0.2 + 0.4	0.2 + 0.2 + 0.2	0.5 + 0.5 + 0.5	$\langle$[0.4,0.8], [0.6,1.5]$\rangle$
$\{x,z,t\}$	0.1 + 0.1 + 0.2	0.2 + 0.2 + 0.4	0.2 + 0.2 + 0.2	0.5 + 0.5 + 0.5	$\langle$[0.4,0.8], [0.6,1.5]$\rangle$
$\{y,z,t\}$	0.1 + 0.2 + 0.1	0.2 + 0.4 + 0.2	0.2 + 0.2 + 0.2	0.5 + 0.5 + 0.5	$\langle$[0.4,0.8], [0.6,1.5]$\rangle$
$\{x,y,t\}$	0.1 + 0.1 + 0.1	0.2 + 0.2 + 0.2	0.2 + 0.2 + 0.2	0.5 + 0.5 + 0.5	$\langle$[0.3,0.6], [0.6,1.5]$\rangle$
$\{x,y,z,t\}$	0.1 + 0.1 + 0.2 + 0.1	0.2 + 0.2 + 0.4 + 0.2	0.2 + 0.2 + 0.2 + 0.2	0.5 + 0.5 + 0.5 + 0.5	$\langle$[0.5,1], [0.8,2]$\rangle$

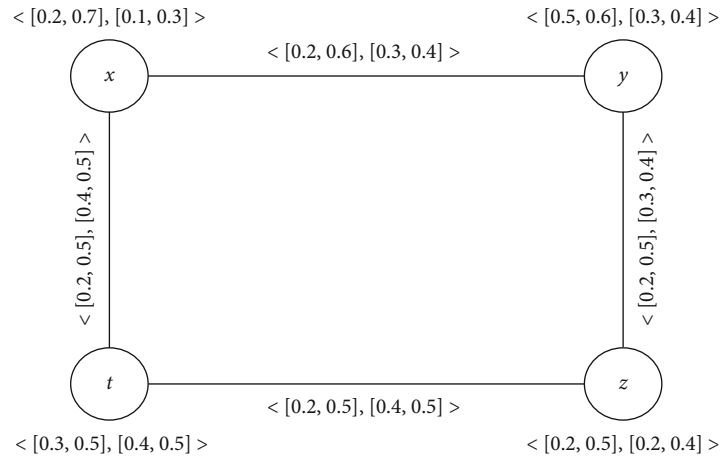

Figure 2: A strong IVIFG G for a strong independent set (SIS).

Table 3: Calculating the weight of SISs.

D	$W_{nc}^{L_\mu}(D)$	$W_{nc}^{U_\mu}(D)$	$W_{nc}^{L_\nu}(D)$	$W_{nc}^{U_\nu}(D)$	$W_{nc}(D)$
$\{x,t\}$	0.2 + 0.2	0.5 + 0.4	0.4 + 0.4	0.5 + 0.5	$\langle$[0.4,0.9], [0.8,1]$\rangle$
$\{y,t\}$	0.2 + 0.2	0.5 + 0.5	0.3 + 0.4	0.4 + 0.5	$\langle$[0.4,1], [0.7,0.9]$\rangle$

covering number of $K^*_{\sigma_1,\sigma_2}$ is max $\{|V_1|, |V_2|\}$. Therefore, the minimum number of arcs in an SAC of K_{σ_1,σ_2} is max $\{|V_1|, |V_2|\}$. Thus, the result is obtained. □

Definition 16. Let G be an IVIFG. A set T of SAs in G so that no two arcs in T have a common node is named an SIS of arcs or an SM in G.

Definition 17. Let T be an SM in IVIFG G. If $xy \in T$, then, we say that T strongly matches x to y. The weight of an SM is described as

$$W_{sm}(T) = \left\langle \left[W^{L_\mu}_{sm}(T), W^{U_\mu}_{sm}(T)\right], \left[W^{L_\nu}_{sm}(T), W^{U_\nu}_{sm}(T)\right]\right\rangle,$$
$$W_{sm}(T) = \left\langle \left[\sum_{xy\in T}\mu^L_B(xy), \sum_{xy\in T}\mu^U_B(xy)\right], \left[\sum_{xy\in T}\nu^L_B(xy), \sum_{xy\in T}\nu^U_B(xy)\right]\right\rangle. \tag{29}$$

An SMN of an IVIFG G is shown by $\beta_{s_1}(G) = \beta_{s_1} = \langle[\beta^{L_\mu}_{s_1}, \beta^{U_\mu}_{s_1}], [\beta^{L_\nu}_{s_1}, \beta^{U_\nu}_{s_1}]\rangle$, which

$$\begin{aligned}
\beta^{L_\mu}_{s_1} &= \max\left\{W^{L_\mu}_{sm}(T)\middle| T \text{ is the SM of } G\right\},\\
\beta^{U_\mu}_{s_1} &= \max\left\{W^{U_\mu}_{sm}(T)\middle| T \text{ is the SM of } G\right\},\\
\beta^{L_\nu}_{s_1} &= \min\left\{W^{L_\nu}_{sm}(T)\middle| T \text{ is the SM of } G\right\},\\
\beta^{U_\nu}_{s_1} &= \min\left\{W^{U_\nu}_{sm}(T)\middle| T \text{ is the SM of } G\right\}.
\end{aligned} \tag{30}$$

A maximum SM in an IVIFG G is an SM of maximum IVMBs and minimum IVNMBs.

Theorem 18. *If G is a CIVIFG, then*

$$\begin{aligned}
\beta^{L_\mu}_{s_1} &= \max\left\{W^{L_\mu}_{sm}(T)\middle| T \textit{ is a SM with } |T| \le \left\lfloor\frac{n}{2}\right\rfloor\right\},\\
\beta^{U_\mu}_{s_1} &= \max\left\{W^{U_\mu}_{sm}(T)\middle| T \textit{ is a SM with } |T| \le \left\lfloor\frac{n}{2}\right\rfloor\right\},\\
\beta^{L_\nu}_{s_1} &= \min\left\{W^{L_\nu}_{sm}(T)\middle| T \textit{ is a SM with } |T| \le \left\lfloor\frac{n}{2}\right\rfloor\right\},\\
\beta^{U_\nu}_{s_1} &= \min\left\{W^{U_\nu}_{sm}(T)\middle| T \textit{ is a SM with } |T| \le \left\lfloor\frac{n}{2}\right\rfloor\right\}.
\end{aligned} \tag{31}$$

Proof. Since G is a CIVIFG, all arcs are strong, and each node is neighbor to all other nodes. Also, the number of arcs in an SM of both G and G^* is identical because each arc in both graph is strong. Now, the SMN of G^* is $\lfloor n/2\rfloor$. Therefore, the maximum number of arcs in an SM of G is $\lfloor n/2\rfloor$. Hence, the result follows. □

Theorem 19. *For a CB-IVIFG K_{σ_1,σ_2} with partite set V_1 and V_2,*

$$\begin{aligned}
\beta^{L_\mu}_{s_1}(K_{\sigma_1,\sigma_2}) &= \max\left\{W^{L_\mu}_{sm}(T)\middle| T \textit{ is a SM in } K_{\sigma_1,\sigma_2} \textit{ with } |T| \le \min\{|V_1|, |V_2|\}\right\},\\
\beta^{U_\mu}_{s_1}(K_{\sigma_1,\sigma_2}) &= \max\left\{W^{U_\mu}_{sm}(T)\middle| T \textit{ is a SM in } K_{\sigma_1,\sigma_2} \textit{ with } |T| \le \min\{|V_1|, |V_2|\}\right\},\\
\beta^{L_\nu}_{s_1}(K_{\sigma_1,\sigma_2}) &= \min\left\{W^{L_\nu}_{sm}(T)\middle| T \textit{ is a SM in } K_{\sigma_1,\sigma_2} \textit{ with } |T| \le \min\{|V_1|, |V_2|\}\right\},\\
\beta^{U_\nu}_{s_1}(K_{\sigma_1,\sigma_2}) &= \min\left\{W^{U_\nu}_{sm}(T)\middle| T \textit{ is a SM in } K_{\sigma_1,\sigma_2} \textit{ with } |T| \le \min\{|V_1|, |V_2|\}\right\}.
\end{aligned} \tag{32}$$

Proof. In K_{σ_1,σ_2}, all arcs are strong. Also, each node in V_1 is neighbor with all nodes in V_2 and contrariwise. Thus, the number of arcs in an SM of both K_{σ_1,σ_2} and $K^*_{\sigma_1,\sigma_2}$ is identical because each arc in both graphs is strong. Now, the SMN of $K^*_{\sigma_1,\sigma_2}$ is max $\{|V_1|, |V_2|\}$. Therefore, the maximum number of arcs in an SM of K_{σ_1,σ_2} is max $\{|V_1|, |V_2|\}$.

Hence, the result is obtained. □

Example 3. Consider a strong IVIFG G is drawn in Figure 3. All arcs are strong, and the SACs are as follows:

$$\begin{aligned}
Y_1 &= \{xy, tz\},\\
Y_2 &= \{xt, yz\},\\
Y_3 &= \{yt, tx, yz\},\\
Y_4 &= \{yt, xy, tz\},\\
Y_5 &= \{xy, yz, zt\},\\
Y_6 &= \{xy, xt, tz\},\\
Y_7 &= \{xt, xy, yz\},\\
Y_8 &= \{xt, zt, yz\}.
\end{aligned} \tag{33}$$

The calculation of the weight of SACs is shown in Table 4.

So, $\alpha_{s_1} = \langle[0.3,0.6], [0.6,1.4]\rangle$.

Again, the two sets Y_1 and Y_2 are the only SAC and SM in G. So,

$$\begin{aligned}
W_{sm}(Y_1) &= \langle[0.3,0.6], [0.3,0.8]\rangle,\\
W_{sm}(Y_2) &= \langle[0.3,0.7], [0.4,0.9]\rangle.
\end{aligned} \tag{34}$$

Hence, $\beta_{s_1} = \langle[0.3,0.7], [0.3,0.8]\rangle$.

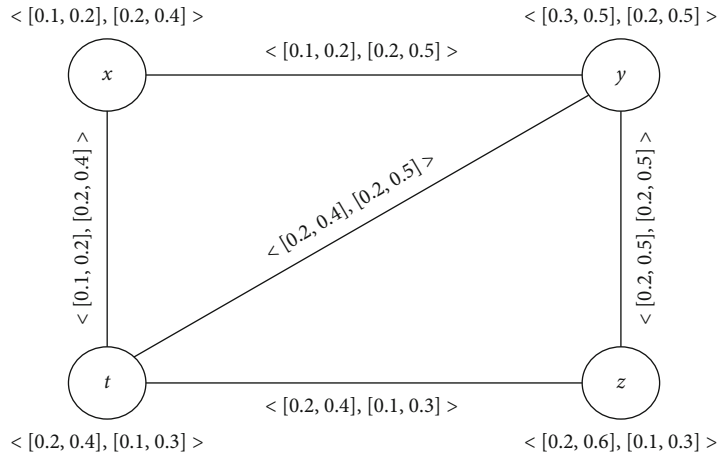

Figure 3: A strong IVIFG G for strong maching (SM).

Table 4: Calculating the weight of strong arc cover sets Y.

Y	$W_{ac}^{L_\mu}(Y)$	$W_{ac}^{U_\mu}(Y)$	$W_{ac}^{L_\nu}(Y)$	$W_{ac}^{U_\nu}(Y)$	$W_{ac}(Y)$
Y_1	0.1 + 0.2	0.2 + 0.4	0.2 + 0.1	0.5 + 0.3	⟨[0.3,0.6], [0.3,0.8]⟩
Y_2	0.1 + 0.2	0.2 + 0.5	0.2 + 0.2	0.4 + 0.5	⟨[0.3,0.7], [0.4,0.9]⟩
Y_3	0.2 + 0.1 + 0.2	0.4 + 0.2 + 0.5	0.2 + 0.2 + 0.2	0.5 + 0.4 + 0.5	⟨[0.5,1.1], [0.6,1.4]⟩
Y_4	0.2 + 0.1 + 0.2	0.4 + 0.2 + 0.4	0.2 + 0.2 + 0.1	0.5 + 0.5 + 0.3	⟨[0.5,1], [0.5,1.3]⟩
Y_5	0.1 + 0.2 + 0.2	0.2 + 0.5 + 0.4	0.2 + 0.2 + 0.1	0.5 + 0.5 + 0.3	⟨[0.5,1.1], [0.5,1.3]⟩
Y_6	0.1 + 0.1 + 0.2	0.2 + 0.2 + 0.4	0.2 + 0.2 + 0.1	0.5 + 0.4 + 0.3	⟨[0.4,0.8], [0.5,1.2]⟩
Y_7	0.1 + 0.1 + 0.2	0.2 + 0.2 + 0.5	0.2 + 0.2 + 0.2	0.4 + 0.5 + 0.5	⟨[0.4,0.9], [0.6,1.4]⟩
Y_8	0.1 + 0.2 + 0.2	0.2 + 0.4 + 0.5	0.2 + 0.1 + 0.2	0.4 + 0.3 + 0.5	⟨[0.4,1.1], [0.5,1.2]⟩

Example 4. Consider an IVIFG G is drawn in Figure 4.

All SAs are xt, zt, and yz, and all SACs are as follows:

$$\begin{aligned} Y_1 &= \{xt, yz\}, \\ Y_2 &= \{xt, tz, yz\}. \end{aligned} \tag{35}$$

The calculation of the weight of SACs is shown in Table 5. So, $\alpha_{s_1} = \langle[0.4,1], [1.1,1.4]\rangle$.

The set $Y_1 = \{xt, yz\}$ is the only SIAC. So, $\beta_{s_1} = W_{sm}(Y_1) = \langle[0.4,1], [0.7,0.9]\rangle$.

Theorem 20. *Let G be an IVIFG containing no IN. Then,*

$$\begin{aligned} \alpha_{s_0}^{L_\mu} + \beta_{s_0}^{L_\mu} &= W^{L_\mu}(V), \\ \alpha_{s_0}^{L_\nu} + \beta_{s_0}^{L_\nu} &= W^{L_\nu}(V), \\ \alpha_{s_0}^{U_\mu} + \beta_{s_0}^{U_\mu} &= W^{U_\mu}(V), \\ \alpha_{s_0}^{U_\nu} + \beta_{s_0}^{U_\nu} &= W^{U_\nu}(V). \end{aligned} \tag{36}$$

Proof. Let M_{s_0} be a minimum SNC of G, which

$$\begin{aligned} \alpha_{s_0}^{L_\mu} &= W^{L_\mu}\left(M_{s_0}\right), \\ \alpha_{s_0}^{L_\nu} &= W^{L_\nu}\left(M_{s_0}\right), \\ \alpha_{s_0}^{U_\mu} &= W^{U_\mu}\left(M_{s_0}\right), \\ \alpha_{s_0}^{U_\nu} &= W^{U_\nu}\left(M_{s_0}\right). \end{aligned} \tag{37}$$

Then, $V - M_{s_0}$ is an SIS of nodes. In other words, the nodes in $V - M_{s_0}$ are incident on SAs of G. Thus,

$$\begin{aligned} &\beta_{s_0}^{L_\mu} \geq W^{L_\mu}\left(V - M_{s_0}\right) = W^{L_\mu}(V) - \alpha_{s_0}^{L_\mu} \Rightarrow \alpha_{s_0}^{L_\mu} + \beta_{s_0}^{L_\mu} \geq W^{L_\mu}(V), \\ &\beta_{s_0}^{U_\mu} \geq W^{U_\mu}\left(V - M_{s_0}\right) = W^{U_\mu}(V) - \alpha_{s_0}^{U_\mu} \Rightarrow \alpha_{s_0}^{U_\mu} + \beta_{s_0}^{U_\mu} \geq W^{U_\mu}(V), \\ &\beta_{s_0}^{L_\nu} \leq W^{L_\nu}\left(V - M_{s_0}\right) = W^{L_\nu}(V) - \alpha_{s_0}^{L_\nu} \Rightarrow \alpha_{s_0}^{L_\nu} + \beta_{s_0}^{L_\nu} \leq W^{L_\nu}(V), \\ &\beta_{s_0}^{U_\nu} \leq W^{U_\nu}\left(V - M_{s_0}\right) = W^{U_\nu}(V) - \alpha_{s_0}^{U_\nu} \Rightarrow \alpha_{s_0}^{U_\nu} + \beta_{s_0}^{U_\nu} \leq W^{U_\nu}(V). \end{aligned} \tag{38}$$

Let $\beta_{s_0}^{L_\mu} = W(Q_{s_0})$, where Q_{s_0} is a maximum SIS of nodes in G. That is, no two nodes in Q_{s_0} are neighbor to each other

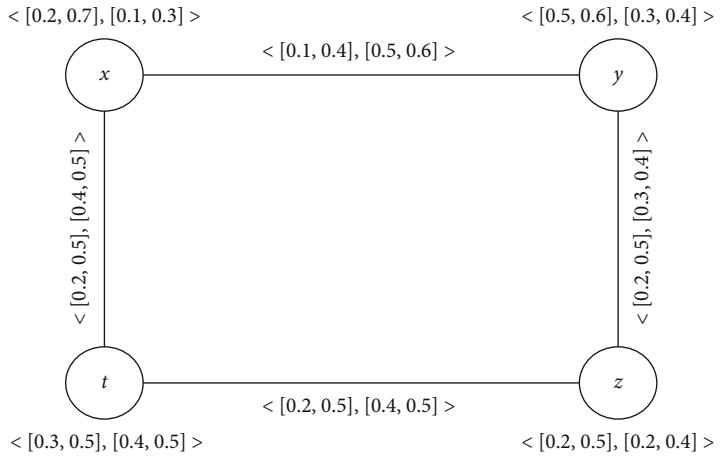

Figure 4: An IVIFG G for strong independent arc cover (SIAC).

Table 5: Calculating the weight of strong arc cover sets Y.

Y	$W_{ac}^{L_\mu}(Y)$	$W_{ac}^{U_\mu}(Y)$	$W_{ac}^{L_\nu}(Y)$	$W_{ac}^{U_\nu}(Y)$	$W_{ac}(Y)$
Y_1	0.2 + 0.2	0.5 + 0.5	0.4 + 0.3	0.5 + 0.4	$\langle[0.4,1], [0.7,0.9]\rangle$
Y_2	0.2 + 0.2 + 0.2	0.5 + 0.5 + 0.5	0.4 + 0.4 + 0.3	0.5 + 0.5 + 0.4	$\langle[0.6,1.5], [1.1,1.4]\rangle$

by an SA, and thus, the node in $V - Q_{s_0}$ strongly covers all SAs of G. Hence, $V - Q_{s_0}$ is an SNC of G, and $\alpha_{s_0}^{L_\mu}$ and $\alpha_{s_0}^{U_\mu}$ are the minimum lower and upper of IVMBs, and $\alpha_{s_0}^{L_\nu}$ and $\alpha_{s_0}^{U_\nu}$ are the maximum lower and upper of IVNMBs. So,

$$\begin{aligned}
\alpha_{s_0}^{L_\mu} &\le W^{L_\mu}\left(V - Q_{s_0}\right) = W^{L_\mu}(V) - \beta_{s_0}^{L_\mu} \Rightarrow \alpha_{s_0}^{L_\mu} + \beta_{s_0}^{L_\mu} \le W^{L_\mu}(V),\\
\alpha_{s_0}^{U_\mu} &\le W^{U_\mu}\left(V - Q_{s_0}\right) = W^{U_\mu}(V) - \beta_{s_0}^{U_\mu} \Rightarrow \alpha_{s_0}^{U_\mu} + \beta_{s_0}^{U_\mu} \le W^{U_\mu}(V),\\
\alpha_{s_0}^{L_\nu} &\ge W^{L_\nu}\left(V - Q_{s_0}\right) = W^{L_\nu}(V) - \beta_{s_0}^{L_\nu} \Rightarrow \alpha_{s_0}^{L_\nu} + \beta_{s_0}^{L_\nu} \ge W^{L_\nu}(V),\\
\alpha_{s_0}^{U_\nu} &\ge W^{U_\nu}\left(V - Q_{s_0}\right) = W^{U_\nu}(V) - \beta_{s_0}^{U_\nu} \Rightarrow \alpha_{s_0}^{U_\nu} + \beta_{s_0}^{U_\nu} \ge W^{U_\nu}(V).
\end{aligned} \tag{39}$$

From (38) and (39), we have

$$\begin{aligned}
&\alpha_{s_0}^{L_\mu} + \beta_{s_0}^{L_\mu} = W^{L_\mu}(V), \alpha_{s_0}^{U_\mu} + \beta_{s_0}^{U_\mu} = W^{U_\mu}(V),\\
&\alpha_{s_0}^{L_\nu} + \beta_{s_0}^{L_\nu} = W^{L_\nu}(V), \alpha_{s_0}^{U_\nu} + \beta_{s_0}^{U_\nu} = W^{U_\nu}(V).
\end{aligned} \tag{40}$$

□

Definition 21. Let G be an IVIFG and M be an SM in G. Then, M is named a PSM if M strongly matches each node of G to some nodes of G.

Example 5. Consider an IVIFG G is drawn in Figure 5. All arcs are strong, and the sets M_1 and M_2 are PSMs. The calculation of the weight of PSMs is given in Table 6.

$$\begin{aligned}
M_1 &= \{xt, yz\},\\
M_2 &= \{xz, yt\},\\
M_3 &= \{xt, xz, yz\},\\
M_4 &= \{xt, ty, yz\}.
\end{aligned} \tag{41}$$

So, $\beta_{s_1} = \langle[0.6,1.3], [0.7,0.9]\rangle$.

Hence, $\alpha_{s_1} = \langle[0.3,0.7], [1.2,1.6]\rangle$.

Now, we introduced PD in IVIFGs using SAs based on PSM. Also, some useful results are established.

Definition 22. A set D of nodes of IVIFG G is an SDS of G if every node of $V - D$ is a strong neighbor of some nodes in D.

Definition 23. The weight of an SDS D is defined as

$$W_{sd}(D) = \left\langle \left[W_{sd}^{L_\mu}(D), W_{sd}^{U_\mu}(D)\right], \left[W_{sd}^{L_\nu}(D), W_{sd}^{U_\nu}(D)\right] \right\rangle, \tag{42}$$

or

$$W_{sd}(D) = \left\langle \left[\sum_{x\in D} \mu_B^L(xy), \sum_{x\in D} \mu_B^U(xy)\right], \left[\sum_{x\in D} \nu_B^L(xy), \sum_{x\in D} \nu_B^U(xy)\right] \right\rangle, \tag{43}$$

where $\mu_B^L(xy)$ and $\mu_B^U(xy)$ are the minimum lower and upper of IVMBs and $\nu_B^L(xy)$ and $\nu_B^U(xy)$ are the maximum lower and upper of IVNMBs of SAs incident on x, respectively.

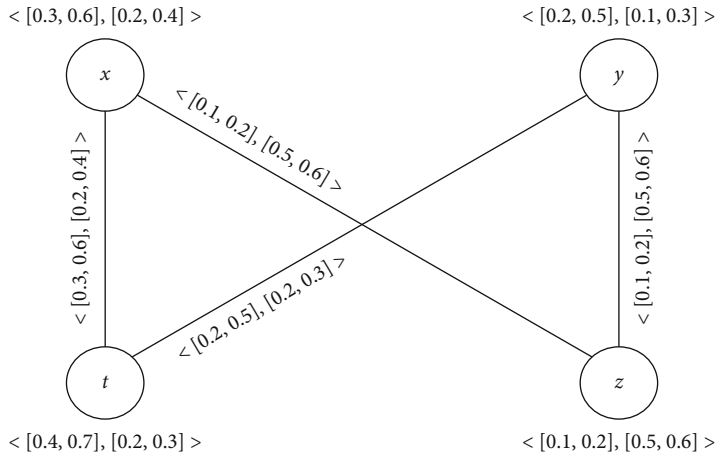

Figure 5: An IVIFG G for perfect strong matching (PSM).

Table 6: Calculating the weight of perfect strong matchings M.

M	$W_{sm}^{L_\mu}(M)$	$W_{sm}^{U_\mu}(M)$	$W_{sm}^{L_\nu}(M)$	$W_{sm}^{U_\nu}(M)$	$W_{sm}(M)$
M_1	0.3 + 0.1	0.6 + 0.2	0.2 + 0.5	0.4 + 0.6	$\langle[0.4,0.8], [0.7,1]\rangle$
M_2	0.1 + 0.2	0.2 + 0.5	0.5 + 0.2	0.6 + 0.3	$\langle[0.3,0.7], [0.7,0.9]\rangle$
M_3	0.3 + 0.1 + 0.1	0.6 + 0.2 + 0.2	0.2 + 0.5 + 0.5	0.4 + 0.6 + 0.6	$\langle[0.5,1], [1.2,1.6]\rangle$
M_4	0.3 + 0.2 + 0.1	0.6 + 0.5 + 0.2	0.2 + 0.2 + 0.5	0.4 + 0.3 + 0.6	$\langle[0.6,1.3], [0.9,1.3]\rangle$

An SDN of an IVIFG G is denoted by $\gamma_s(G) = \gamma_s = \langle[\gamma_s^{L_\mu}, \gamma_s^{U_\mu}], [\gamma_s^{L_\nu}, \gamma_s^{U_\nu}]\rangle$, where

$$\begin{aligned}
\gamma_s^{L_\mu} &= \min\left\{W_{sd}^{L_\mu}(D)\,\middle|\, D \text{ is the SDSs of } G\right\},\\
\gamma_s^{U_\mu} &= \min\left\{W_{sd}^{U_\mu}(D)\,\middle|\, D \text{ is the SDSs of } G\right\},\\
\gamma_s^{L_\nu} &= \max\left\{W_{sd}^{L_\nu}(D)\,\middle|\, D \text{ is the SDSs of } G\right\},\\
\gamma_s^{U_\nu} &= \max\left\{W_{sd}^{U_\nu}(D)\,\middle|\, D \text{ is the SDSs of } G\right\}.
\end{aligned} \tag{44}$$

Definition 24. Let G be an IVIFG. A set D of nodes is named to be an SPDS if D is an SDS and the IVIF-subgraph induced by D has a PSM. The weight of an SPDS D is described as $W_{spd}(D) = \langle[W_{spd}^{L_\mu}(D), W_{spd}^{U_\mu}(D)], [W_{spd}^{L_\nu}(D), W_{spd}^{U_\nu}(D)]\rangle$, which

$$W_{spd}(D) = \left\langle \left[\sum_{x\in D}\mu_B^L(xy), \sum_{x\in D}\mu_B^U(xy)\right], \left[\sum_{x\in D}\nu_B^L(xy), \sum_{x\in D}\nu_B^U(xy)\right]\right\rangle. \tag{45}$$

An SPDN of an IVIFG G is denoted by $\gamma_{spd}(G) = \gamma_{spd} = \langle[\gamma_{spd}^{L_\mu}, \gamma_{spd}^{U_\mu}], [\gamma_{spd}^{L_\nu}, \gamma_{spd}^{U_\nu}]\rangle$, that

$$\begin{aligned}
\gamma_{spd}^{L_\mu} &= \min\left\{W_{spd}^{L_\mu}(D)\,\middle|\, D \text{ is the SPDSs of } G\right\},\\
\gamma_{spd}^{U_\mu} &= \min\left\{W_{spd}^{U_\mu}(D)\,\middle|\, D \text{ is the SPDSs of } G\right\},\\
\gamma_{spd}^{L_\nu} &= \max\left\{W_{spd}^{L_\nu}(D)\,\middle|\, D \text{ is the SPDSs of } G\right\},\\
\gamma_{spd}^{U_\nu} &= \max\left\{W_{spd}^{U_\nu}(D)\,\middle|\, D \text{ is the SPDSs of } G\right\}.
\end{aligned} \tag{46}$$

Example 6. Consider an IVIFG G is drawn in Figure 6. All SAs are xt, zt, and yz. The PDs in G are D_1, D_2, and D_3. The weights of these sets are calculated as follows:

$$\begin{aligned}
D_2 &= \{x, y\},\\
D_2 &= \{z, t\},\\
D_3 &= \{x, y, z, t\}.
\end{aligned} \tag{47}$$

Table 7 shows the calculation of the weight of PDs. Hence, $\gamma_{spd}(G) = \langle[0.4,1], [1.4,1.9]\rangle$.

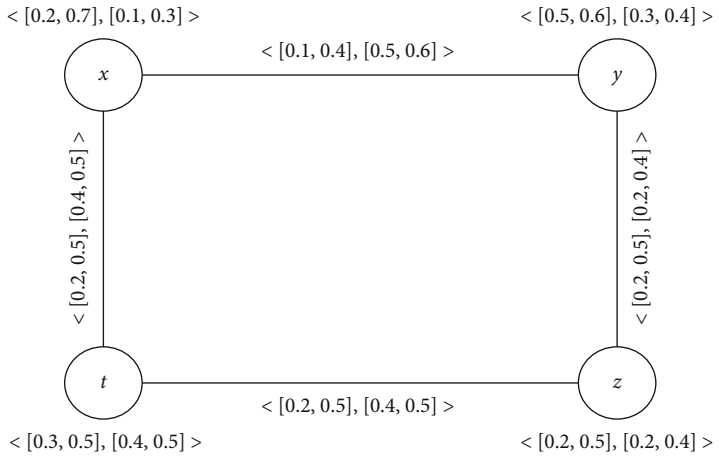

Figure 6: An IVIFG G for strong paired dominating set (SPDS).

Table 7: Calculating the weight of paired dominating sets.

D	$W_{spd}^{L_\mu}(D)$	$W_{spd}^{U_\mu}(D)$	$W_{spd}^{L_\nu}(D)$	$W_{spd}^{U_\nu}(D)$	$W_{spd}(D)$
D_1	0.2 + 0.2	0.5 + 0.5	0.4 + 0.2	0.5 + 0.4	⟨[0.4,1], [0.6,0.9]⟩
D_2	0.2 + 0.2	0.5 + 0.5	0.4 + 0.4	0.5 + 0.5	⟨[0.4,1], [0.8,1]⟩
D_3	0.2 + 0.2 + 0.2 + 0.2	0.5 + 0.5 + 0.5 + 0.5	0.4 + 0.2 + 0.4 + 0.4	0.5 + 0.4 + 0.5 + 0.5	⟨[0.8,2], [1.4,1.9]⟩

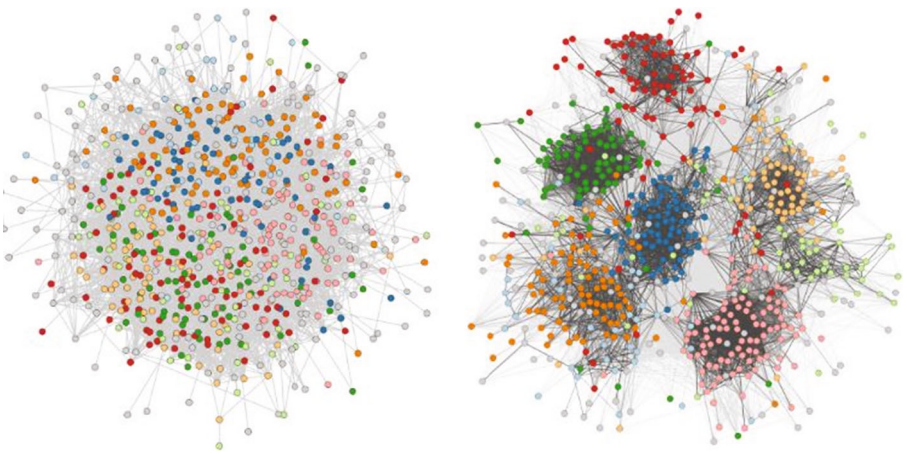

Figure 7: Scientific community network of researchers.

Theorem 25. *Let G be a CIVIFG. Then,*

$$\begin{aligned}\gamma_{spd}^{L_\mu} &= 2\mu_B^L(xy),\\ \gamma_{spd}^{L_\nu} &= 2\nu_B^L(xy),\\ \gamma_{spd}^{U_\mu} &= 2\mu_B^U(xy),\\ \gamma_{spd}^{U_\nu} &= 2\nu_B^U(xy),\end{aligned} \tag{48}$$

where $\mu_B^L(xy)$ and $\mu_B^U(xy)$ are the lower and upper of IVMB and $\nu_B^L(xy)$ and $\nu_B^U(xy)$ are the lower and upper of IVNMB of any weakest arc in G, respectively.

Proof. Since G is a CIVIFG, all arcs are strong, and every vertex is neighbor to all other vertices. Then, any set consisting of two nodes $\{x_1, x_2\}$ in G forms an SPDS. Hence,

$$\begin{aligned}\gamma_{spd}^{L_\mu} &= \mu_B^L(xy) + \mu_B^L(xy) = 2\mu_B^L(xy),\\ \gamma_{spd}^{U_\mu} &= \mu_B^U(xy) + \mu_B^U(xy) = 2\mu_B^U(xy),\\ \gamma_{spd}^{L_\nu} &= \nu_B^L(xy) + \nu_B^L(xy) = 2\nu_B^L(xy),\\ \gamma_{spd}^{U_\nu} &= \nu_B^U(xy) + \nu_B^U(xy) = 2\nu_B^U(xy),\end{aligned} \tag{49}$$

where xy is the weakest arc in G. □

Table 8: Data set.

Vertices	Communities	Number of members	Average attendance of members
a	Biology	35	30
b	Chemistry	25	21
c	Engineering	55	45
d	Information technology (IT)	75	60
e	Mathematics	40	32
f	Medicine	50	45
g	Physics	30	24
h	Social sciences	45	37

4. Application

Social networks are a group of individuals or organizations with common tastes or interests that come together to achieve specific goals. Each member is named an actor. Social networks are characterized by complex relationships and interactions between actors. The main reasons for creating social networks are individual relationships, labor relations, scientific relations, shared tastes, interests and hobbies, sociopolitical motives, and virtual network analysis.

Graphs are used as a mathematical tool to represent and analyze a social network by visually representing social networks. In these graphs, the actors are considered as vertices of the graph, and the connections between them are displayed by the edges of the graph. Intuitively, the edges are distributed on social networks locally. This means that the number of edges distributed among a group of vertices is much greater than the number of distribution edges among this group of vertices and the rest of the vertices of the graph. This feature, which can be seen in graphs related to real data, is called a community. In some sources, the community is also called a cluster or module. In other words, communities are a set of vertices that are more likely to share common features than the rest of the graph. Since people in forums on a social network are more likely to have common interests, this information can be used to promote specific products by finding their interests. Most online social networks have overlapping communities. This means that these networks are made up of overlapping communities, and one vertex can belong to more than one community. Figure 7 illustrates the social network of researchers in a country that is a member of different scientific communities according to the subjects under study. These communities include chemistry, biology, engineering, information technology (IT), mathematics, medicine, physics, and social sciences. Table 8 shows the number of members of each community and the average number of members present at the meetings.

In the evaluations made by the members on the effect of community on the scientific promotion of members, since the mentioned variables have uncertain values, so for each community, we considered an interval-valued intuitionistic fuzzy number as the amount of influence of community on its members. Since the presence of

Table 9: The IVIFNs of scientific communities.

Vertices	Communities	The IVIFNs corresponding to each community.
a	Biology	⟨[0.80,0.90], [0.05,0.10]⟩
b	Chemistry	⟨[0.79,0.89], [0.11,0.21]⟩
c	Engineering	⟨[0.76,0.86], [0.14,0.16]⟩
d	Information technology (IT)	⟨[0.75,0.85], [0.10,0.15]⟩
e	Mathematics	⟨[0.75,0.85], [0.10,0.15]⟩
f	Medicine	⟨[0.80,0.90], [0.5,0.10]⟩
g	Physics	⟨[0.75,0.85], [0.10,0.15]⟩
h	Social sciences	⟨[0.77,0.87], [0.10,0.13]⟩

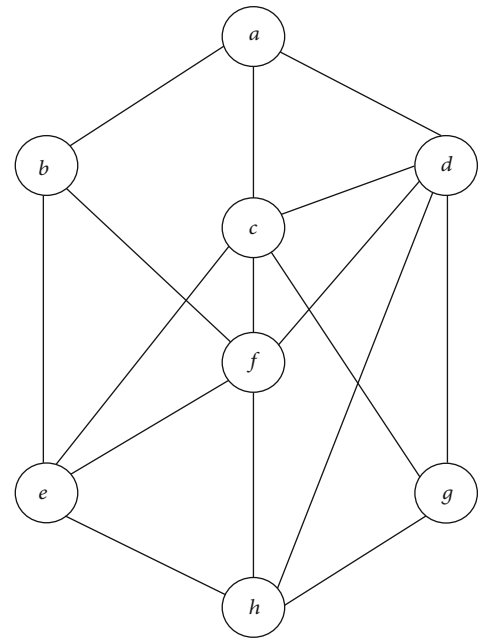

Figure 8: The scientific communities IVIFG.

Table 10: IVIFNs of relations between scientific communities.

Edges	IVIFNs	Edges	IVIFNs
ab	⟨[0.97,0.89], [0.11,0.21]⟩	df	⟨[0.75,0.85], [0.10,0.15]⟩
ac	⟨[0.76,0.86], [0.14,0.16]⟩	dg	⟨[0.75,0.85], [0.10,0.15]⟩
ad	⟨[0.75,0.85], [0.10,0.15]⟩	dh	⟨[0.75,0.85], [0.10,0.15]⟩
be	⟨[0.75,0.85], [0.11,0.21]⟩	ef	⟨[0.75,0.85], [0.10,0.15]⟩
bf	⟨[0.79,0.89], [0.11,0.21]⟩	eh	⟨[0.75,0.85], [0.10,0.15]⟩
cd	⟨[0.75,0.85], [0.14,0.16]⟩	fh	⟨[0.77,0.87], [0.10,0.13]⟩
cf	⟨[0.76,0.86], [0.14,0.16]⟩	gh	⟨[0.75,0.85], [0.10,0.15]⟩
ce	⟨[0.75,0.85], [0.14,0.16]⟩	cg	⟨[0.75,0.85], [0.14,0.16]⟩

Step 1. Consider vertex x as a member of F. Then, remove all adjacent vertices of x.
Step 2. Consider another arbitrary vertex in the remaining graph as a new member of F.
Depending on which member of the remaining vertex set is selected, different independent sets, including x, are obtained.
Step 3. Repeat Step 2 to select all possible vertices.

Algorithm 1: Finding the maximal SISs F of G containing an arbitrary vertex x.

Table 11: Calculations for finding maximal SISs in the IVIFG of Figure 8.

Step 1	Step 2	Step 3	SISs
	e	g	{a,e,g}
	f	g	{a, f, g}
a	g	f	{a,g,f}
		e	{a,g,e}
	h		{a,h}
	c	h	{b,c,h}
b	d		{b,d}
	g		{b,g}
	h	c	{b,h,c}
	b	h	{c,b,h}
c	h	b	{c,h,b}
	b		{d,b}
d	e		{d,e}
	a	g	{e,a,g}
e	d		{e,d}
	g	a	{e,g,a}
	a	g	{f,a,g}
f	g	a	{f,g,e}
	a	f	{g,a,f}
		e	{g,a,e}
g	b		{g,b}
	e	a	{g,e,a}
	f	a	{g,f,a}
	a		{h,a}
h	b	c	{h, b, c}
	c	b	{h,c,b}

members in the meetings of the community is effective on the scientific promotion of members, we introduced the ratio of the average number of members present in the meetings to the total number as an IVIFN. For example, studies have shown that the biology community is 80 to 90 percent effective in advancing the science of its members and 5 to 10 percent ineffective. These values are specified in Table 9.

The strong relationships between scientific communities are illustrated in the form of an IVIFG in Figure 8. In this IVIFG, the membership values of the edges are the effect that the members of the two communities have on their scientific advancement. For example, the collaboration between the two communities of chemistry and medicine is about 79 to 89 percent effective in the scientific advancement of the members of each community and 11 to 21 percent ineffective. These values are shown in Table 10.

In general, there is no polynomial algorithm for finding a maximum independent set for an arbitrary graph. This means that it is not possible to access such a collection in a short time. To obtain the maximal SISs in IVIFG with a small number of vertices, we use the following instructions.

Since all edges are SA, so by applying the above steps for all vertices on the IVIFG of Figure 8, all maximal SISs and cardinalities can be seen in Table 11. Now, by calculating the cardinal of all the SISs obtained from the above steps, we can also determine the maximum SISs.

The maximum SISs are $D_1 = \{a, e, g\}$, $D_2 = \{a, f, g\}$, and $D_3 = \{b, c, h\}$.

After calculating the weight of the above sets, we have $W(D_1) = \langle[2.25,2.55], [0.42,0.58]\rangle$, $W(D_2) = \langle[2.25,2.55], [0.42,0.53]\rangle$, and $W(D_3) = \langle[2.25,2.55], [0.35,0.52]\rangle$.

Therefore, D_3 has the maximum weight of membership and the minimum weight of nonmembership, so it can be chosen as the best option. It is interesting to know that D_3 also has the maximum number of members in scientific communities. That is, strong independent scientific communities include chemistry, engineering, and social sciences.

Suppose knowledge-based companies intend to organize an exhibition at the meeting place of scientific communities to acquaint researchers with their scientific products. Researchers at the knowledge-based companies can be members of various scientific communities. The goal is to hold as many exhibitions as possible at the same time provided that each knowledge-based company has a maximum of one exhibition in a specific time period and to hold another exhibition at different time intervals. In this case, the maximum independent set is the maximum number of exhibitions that can be held at one time in scientific communities.

5. Conclusion

Analysis of uncertain problems by IVIFG is important because it gives more integrity and flexibility to the system. An IVIFG, as an extension of FGs, has good capabilities in dealing with problems that cannot be explained by FGs. They have been able to have wide applications even in fields such as psychology and identifying people based on cancerous behaviors. In this paper, covering and matching have been defined in IVIFGs using strong arcs. These concepts are introduced as an interval-valued intuitionistic number. One of the advantages of this method is that the amount of defined parameters can be expressed and compared in terms of membership and nonmembership. Also, the

concepts of SNC, SIN, SAC, and SM in IVIFGs are determined, and the relations among them have been obtained. Furthermore, we have introduced the PD and SPDN in CIVIFG and CB-IVIFG. Since the parameters being studied are interval values, comparisons of these parameters may be limited in an IVIFG. Finally, we have presented an application of IVIFG in social networks. In their future work, the authors try to study the concepts of m-polar IVIFGs.

Data Availability

No data were used in this study.

Conflicts of Interest

The authors declare that they have no conflicts of interest.

Acknowledgments

This work was supported by the Natural Science Foundation of Guangdong Province of China (2022A1515011468).

References

[1] A. Zadeh, "Fuzzy sets," *Information and Control*, vol. 8, no. 3, pp. 338–353, 1965.

[2] A. Zadeh, "The concept of a linguistic variable and its application to approximate reasoning–I," *Information Sciences*, vol. 8, no. 3, pp. 199–249, 1975.

[3] A. Roselfeld, "Fuzzy graphs," in *Fuzzy Sets and Their Applications*, L. A. Zadeh, K. S. Fu, and M. Shimura, Eds., pp. 77–95, Academic Press, New York, NY, USA, 1975.

[4] K. T. Atanassov, "Intuitionistic fuzzy sets," *Fuzzy Sets and Systems*, vol. 20, no. 1, pp. 87–96, 1986.

[5] K. T. Atanassov, *Intuitionistic Fuzzy Sets*, Physica-Verlag, Heidelberg, New York, NY, USA, 1999.

[6] M. Akram and B. Davvaz, "Strong intuitionistic fuzzy graphs," *Univerzitet u Nišu*, vol. 26, pp. 177–196, 2012.

[7] R. Mahapatra, S. Samanta, T. Allahviranloo, and M. Pal, "Radio fuzzy graphs and assignment of frequency in radio stations," *Computational and Applied Mathematics*, vol. 38, no. 3, pp. 1–20, 2019.

[8] R. Mahapatra, S. Samanta, and M. Pal, "Applications of edge colouring of fuzzy graphs," *Informatica*, vol. 31, no. 2, pp. 313–330, 2020.

[9] R. Mahapatra, S. Samanta, M. Pal et al., "Colouring of COVID-19 affected region based on fuzzy directed graphs," *Computers, Materials & Continua*, vol. 68, no. 1, pp. 1219–1233, 2021.

[10] H. Rashmanlou and M. Pal, "Antipodal interval-valued fuzzy graphs," *International Journal of Applications of Fuzzy Sets and Artificial Intelligence*, vol. 3, pp. 107–130, 2013.

[11] H. Rashmanlou and M. Pal, "Balanced interval-valued fuzzy graph," *Journal of Physical Sciences*, vol. 17, pp. 43–57, 2013.

[12] S. Kosari, Y. Rao, H. Jiang, X. Liu, P. Wu, and Z. Shao, "Vague graph structure with application in medical diagnosis," *Symmetry*, vol. 12, no. 10, p. 1582, 2020.

[13] Z. Kou, S. Kosari, and M. Akhoundi, "A novel description on vague graph with application in transportation systems," *Journal of Mathematics*, vol. 2021, Article ID 4800499, 11 pages, 2021.

[14] K. K. Krishna, Y. Talebi, H. Rashmanlou, A. A. Talebi, and F. Mofidnakhaei, "New concept of cubic graph with application," *Journal of Multiple Valued Logic and Soft Computing*, vol. 33, pp. 135–154, 2019.

[15] A. A. Talebi, "Cayley fuzzy graphs on the fuzzy groups," *Computational and Applied Mathematics*, vol. 37, no. 4, pp. 4611–4632, 2018.

[16] A. A. Talebi and W. A. Dudek, "Operations on level graphs of bipolar fuzzy graphs," *Bulletin Academiel De Stiinte A Republic Moldova Mathematica*, vol. 2, no. 81, pp. 107–124, 2016.

[17] K. T. Atanassov, "New topological operator over intuitionistic fuzzy sets," *Journal of Computational and Cognitive Engineering*, 2022.

[18] B. Mathew, S. J. John, and H. Garg, "Vertex rough graphs," *Complex and Intelligent Systems*, vol. 6, no. 2, pp. 347–353, 2020.

[19] N. Jan, K. Ullah, T. Mahmood et al., "Some root level modifications in interval valued fuzzy graphs and their generalizations including neutrosophic graphs," *Mathematics*, vol. 7, no. 1, p. 72, 2019.

[20] M. G. Voskoglou, "A combined use of softs sets and grey numbers in decision making," *Journal of Computational and Cognitive Engineering*, 2022.

[21] R. Mahapatra, S. Samanta, M. Pal, and Q. Xin, "Link prediction in social networks by neutrosophic graph," *International Journal of Computational Intelligence Systems*, vol. 13, no. 1, pp. 1699–1713, 2020.

[22] R. Mahapatra, S. Samanta, and M. Pal, "Generalized neutrosophic planar graphs and its application," *Journal of Applied Mathematics and Computing*, vol. 65, no. 1, pp. 693–712, 2021.

[23] R. Mahapatra, S. Samanta, M. Pal, and Q. Xin, "RSM index: a new way of link prediction in social networks," *Journal of Intelligent and Fuzzy Systems*, vol. 37, no. 2, pp. 2137–2151, 2019.

[24] K. T. Atanassov and G. Gargov, "Interval valued intuitionistic fuzzy sets," *Fuzzy Sets and Systems*, vol. 31, no. 3, pp. 343–349, 1989.

[25] H. Rashmanlou and R. A. Borzooei, "New concepts of interval-valued intuitionistic (S, T)-fuzzy graphs," *Journal of Intelligent and Fuzzy Systems*, vol. 30, no. 4, pp. 1893–1901, 2016.

[26] M. Dgenci, "A new distance measure for interval valued intuitionistic fuzzy sets and its application to group decision making problems with incomplete weights information," *Applied Soft Computing*, vol. 41, pp. 120–134, 2016.

[27] Z. Zhang, M. Wang, Y. Hu, J. Yang, Y. Ye, and Y. Li, "A dynamic interval-valued intuitionistic fuzzy sets applied to pattern recognition," *Mathematical Problems in Engineering*, vol. 2013, Article ID 408012, 16 pages, 2013.

[28] J. Y. Ahn, K. S. Han, and C. D. Lee, "An application of interval-valued intuitionistic fuzzy sets for medicdl diagnosis of headache," *International Journal of Innovative Computing, Information and Control*, vol. 7, no. 5, pp. 2755–2762, 2011.

[29] J. Hongmei and W. Lianhua, "Interval-valued fuzzy subsemigroups and subgroups associated by interval-valued fuzzy graphs," in *2009 WRI Global Congress on Intelligent System*, pp. 484–487, Xiamen, China, 2009.

[30] M. Akram and W. A. Dudek, "Interval-valued fuzzy graphs," *Computers and Mathematics with Applications*, vol. 61, no. 2, pp. 289–299, 2011.

[31] M. Akram, N. O. Alshehri, and W. A. Dudek, "Certain types of interval-valued fuzzy graphs," *Journal of Applied Mathematics*, vol. 2013, Article ID 857070, 11 pages, 2013.

[32] S. N. Mishra and A. Pal, "Product of interval-valued intuitionistic fuzzy graph," *Annals of Pure and Applied Mathematics*, vol. 5, no. 1, pp. 37–46, 2013.

[33] A. M. Ismayil and A. M. Ali, "On strong interval-valued intuitionistic fuzzy graph," *International Journal of Fuzzy Mathematics and Systems*, vol. 4, no. 2, pp. 161–168, 2014.

[34] A. A. Talebi, H. Rashmanlou, and S. H. Sadati, "Interval-valued intuitionistic fuzzy competition graph," *Journal of Multiple-Valued Logic & Soft Computing*, vol. 34, pp. 335–364, 2020.

[35] A. A. Talebi, H. Rashmanlou, and S. H. Sadati, "New concepts on m-polar interval-valued intuitionistic fuzzy graph," *Journal of Applied and Engineering Mathematics*, vol. 10, no. 3, pp. 806–818, 2020.

[36] P. Xu, H. Guan, A. A. Talebi, M. Ghassemi, and H. Rashmanlou, "Certain concepts of interval-valued intuitionistic fuzzy graphs with an application," *Advances in Mathematical Physics*, vol. 2022, Article ID 6350959, 12 pages, 2022.

[37] S. Sahoo, M. Pal, H. Rashmanlou, and R. A. Borzooei, "Covering and paired domination in intuitionistic fuzzy graphs," *Journal of Intelligent and Fuzzy Systems*, vol. 33, no. 6, pp. 4007–4015, 2017.

Hindawi
Advances in Mathematical Physics
Volume 2022, Article ID 5314322, 8 pages
https://doi.org/10.1155/2022/5314322

Research Article

A New Methodology for Solving Piecewise Quadratic Fuzzy Cooperative Continuous Static Games

He Xiao,[1] **Xiaoju Zhang**,[1] **Dong Lin**,[2] **Hamiden Abd El- Wahed Khalifa**,[3,4] **and S. A. Edalatpanah**[5]

[1]*Xi'an Traffic Engineering Institute, Xi'an, Shaanxi 710300, China*
[2]*Scientific Research Department, Xijing University, Xi'an, Shaanxi 710123, China*
[3]*Department of Operations Research, Faculty of Graduate Studies for Statistical Research, Cairo University, Giza 12613, Egypt*
[4]*Department of Mathematics, College of Science and Arts, Qassim University, Al-Badaya 51951, Saudi Arabia*
[5]*Department of Applied Mathematics, Ayandegan Institute of Higher Education, Tonekabon, Iran*

Correspondence should be addressed to Dong Lin; lindong@xijing.edu.cn and S. A. Edalatpanah; s.a.edalatpanah@aihe.ac.ir

Received 26 April 2022; Accepted 3 June 2022; Published 22 June 2022

Academic Editor: Shangkun Deng

This paper deals with n-players fuzzy cooperative continuous static games (FCCSGs). The cost function coefficients are characterized by piecewise quadratic fuzzy numbers. One of the best approximate intervals, namely, the inexact interval of the piecewise quadratic fuzzy number is used. Furthermore, we proposed a new methodology based on the weighted Tchebycheff method to solve CCSG with n-players. The advantages of the approach are the ability to enable the decision-maker to have satisfactory solution and applied for different real-world problems with various types of fuzzy numbers. There is also a stability set of the first kind without differentiability for the optimal compromise solution that was found. In the future, the proposed methodology could be used in different types of real-world problems and multiple decision-makers. This proposed work can also be extended to hypersoft set, fuzzy hypersoft sets, intuitionistic hypersoft sets, bipolar hypersoft sets, and pythagorean hypersoft sets. At the end, a numerical example is given to demonstrate the computational efficiency of the proposed method.

1. Introduction

Game theory has enormous applications in real-world problems as in economics, engineering, biology, etc. The crucial types of games are differential games, matrix games, and continuous static games. Matrix games are named after the discrete relationship between a finite or countable set of alternative decisions and the resulting costs. In terms of a matrix (or two-player games), one player's decision corresponds to the selection of a row, and the other player's decision relates to the selection of a column, with the accompanying entries signifying the costs. It is evident that cooperative games do not necessitate the use of decision probabilities. As a result, there is no interplay between costs and decisions in games that are purely static. Differential games are distinguished by a dynamic system regulated by ordinary differential equations and costs that are always changing. There are a variety of approaches to solving the problem of continuous, static games. The player's own personality also has a role on how he or she employs these notions in the context of the game. Depending on the circumstances, a player may or may not be able to play logically, cheat, cooperate, bargain, and so on. All of these considerations must be taken into account by a player when deciding on a control vector.

Although the mentioned approaches are very suitable, however, in the real-world problems, all or some of parameters are vague and uncertain. Therefore, these techniques cannot handle CSG with uncertain problem. There are numerous works in the field of fuzzy and fuzzy extension set optimization; for example, see [1–15]. However, these models cannot solve CSG.

Vincent and Grantham [16] introduced different formulations in continuous static games (CSG). This game uses

three essential concepts: min-max solutions (MMS), Nash equilibrium solution, (NES), and Pareto minimum solutions (PMS). Vincent and Leitmann [17] investigated the control-space features of cooperative solutions for all types of games. Mallozzi and Morgan [18] introduced ε-mixed approaches for CSG. El Shafei [19] proposed a new formulation of large scale CSG and explained how they can solve the mentioned problem by the concept of PMS and in [20] suggested an interactive compromise programming for a kind of Cooperative CSG (CCSG). Kenneth et al. [21] designated some methods for solving all solutions of polynomial systems and then using these compute the equilibrium manifold of a kind of CSG, see also [22–27].

Continuous static games with fuzzy parameters can be solved using the Stackelberg leader and min-max follower's solution presented by Osman et al. [28]. Osman et al. [29] also created the Nash equilibrium solution for large-scale continuous static games with parameters in all cost functions and constraints, where players are autonomous and do not participate with any other players, and each player strives to minimize their cost functions. In addition, the information that is available to every player contains the cost functions and constraints. Khalifa and Zeineldin [30] introduced a fuzzy version of CSG and using α-level sets, and reference attainable point technique suggested a solution for it. Kenneth et al. [21] using the solution of multiobjective nonlinear programming problems proposes a solution for CCSG. She also in [31] studied a CCSG with k players in fuzzy environment and presented an algorithmic approach for it. Elnaga et al. [32] focused on hybrid CSGs that contain several players playing autonomously using the NES and others playing under a secure concept using MMS in fuzzy environment, see also [33–40]. Khalifa et al. [41, 42] studied continuous static games and applied different approaches for solving this problem. Garg et al. [43] have introduced CCSG having possibilistic parameters in the cost functions.

In this paper, we proposed a new methodology based on the weighted Tchebycheff method to solve CCSG with n -players that have piecewise quadratic fuzzy number (PQFN) in the cost functions of the players. Moreover, the stability set of the first kind corresponding to the α-optimal compromise solution has been determined. One of the main advantages of our approach is that this method enables the decision-maker to have satisfactory solution and therefore can applied it for different real-world problems with various types of fuzzy numbers.

2. Research Gap and Motivation

(i) The phrase" pentagonal fuzzy number" is actually meant for dispensing the fuzzy value to each attribute/subattribute in the domain of singleargument/ multiargument approximate function

(1) Many researchers discussed the fuzzy set-like structures under soft set environment with fuzzy set-like settings

(2) Along these lines, another construction requests its place in writing for tending to such obstacle; so, fuzzy set is conceptualized to handle such situations

The rest of the paper is arranged as follows: Section 3 offers some necessary prerequisites for this work. The mathematical model for continuous cooperative static games is presented in Section 4. Section 5 presents a method for finding the best compromise solution. Section 6 illustrates the concept with a numerical example. A comparison of existing algorithms and our suggested technique is shown in Section 7. Finally, in section 8, some findings are presented.

3. Basic Concepts

Here, we study some basic concepts that is need for other sections; for more details, see [44, 45].

Definition 1. (Zadeh [44]). A fuzzy set $\tilde{W}$ characterized by real line $\mathfrak{R}$ is referred as fuzzy number, provided the function: $\mu_{\tilde{Q}}(x)$: $\mathfrak{R} \longrightarrow [0, 1]$ and confirms the below conditions:

(1) The mapping $\mu_{\tilde{W}}(x)$ is an upper semicontinuous

(2) The set $\tilde{W}$ is convex, i.e., $\mu_{\tilde{W}}(\delta x + (1-\delta) y) \geq \min\{\mu_{\tilde{W}}(x), \mu_{\tilde{W}}(y)\} \forall x, y \in \mathfrak{R}; 0 \leq \delta \leq 1$

(3) The set $\tilde{W}$ is normal, i.e., there exists a point $x_0 \in \mathfrak{R}$, so that $\mu_{\tilde{W}}(x_0)$ equals to 1

(4) $\text{Supp}(\tilde{W}) = \{x \in \mathfrak{R} : \mu_{\tilde{Q}}(x) > 0\}$ is treated as support of $\tilde{W}$, and the set "closure $\text{cl}(\text{Supp}(\tilde{W}))$" is compact

Definition 2. (Jain [45]). A PQFN is denoted by $\tilde{W}_{PQ} = (w_1, w_2, w_3, w_4, w_5)$, where $w_1 \leq w_2 \leq w_3 \leq w_4 \leq w_5$ are real numbers, and is defined by if its membership function $\mu_{\tilde{W}_{PQ}}$ is given by

$$\mu_{\tilde{W}_{PQ}} = \begin{cases} 0, x < w_1; \\ \frac{1}{2}\frac{1}{(w_2 - w_1)^2}(x - u_1)^2, w_1 \leq x \leq w_2; \\ \frac{1}{2}\frac{1}{(w_3 - w_2)^2}(x - w_2)^2 + 1, w_2 \leq x \leq w_3; \\ \frac{1}{2}\frac{1}{(w_4 - w_3)^2}(x - w_3)^2 + 1, w_3 \leq x \leq w_4; \\ \frac{1}{2}\frac{1}{(w_5 - w_4)^2}(x - w_4)^2, w_4 \leq x \leq w_5; \\ 0, x > w_5. \end{cases}$$

$$\mu_{\tilde{W}_{PQ}} \tag{1}$$

Figure 1 shows a graphical view of PQFN.

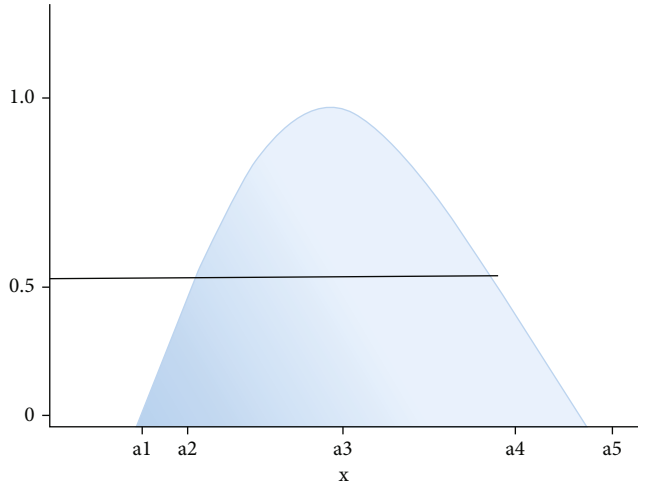

Figure 1: Graphical representation of PQFN.

Definition 3. (Jain [45]). Let $\tilde{U}_{PQ} = (u_1, u_2, u_3, u_4, u_5)$ and $\tilde{V}_{PQ} = (v_1, v_2, v_3, v_4, v_5)$ be two piecewise quadratic fuzzy numbers. The arithmetic operations on $\tilde{U}_{PQ}$ and $\tilde{V}_{PQ}$ are as follows:

(i) Addition: $\tilde{U}_{PQ}(+)\tilde{V}_{PQ} = (u_1 + v_1, u_2 + v_2, u_3 + v_3, u_4 + v_4, u_5 + v_5)i)$

(ii) Subtraction: $\tilde{U}_{PQ}(-)\tilde{V}_{PQ} = (u_1 - v_5, u_2 - v_4, u_3 - v_3, u_4 - v_2, u_5 - v_1)$

(iii) Scalar multiplication:

$$k\tilde{U}_{PQ} = \begin{cases} (ku_1, ku_2, ku_3, ku_4, ku_5), k > 0, \\ (ku_5, ku_4, ku_3, ku_2, ku_1), k < 0. \end{cases} \tag{2}$$

Definition 4. (Jain [45]). For the close interval approximation of PQFN of $[U] = [U_\alpha^-, U_\alpha^+]$, we called $\hat{U} = \mathrm{U}_\alpha^- + \mathrm{U}_\alpha^+/2$ as the associated real number of $[U]$.

Definition 5. (Jain [45]). For $[U] = [U_\alpha^-, U_\alpha^+]$, and $[V] = [V_\alpha^-, V_\alpha^+]$, we have the following properties:

(1) Addition: $[U](+)[V] = [U_\alpha^- + Vb_\alpha^-, U_\alpha^+ + V_\alpha^+]$

(2) Subtraction: $[U](-)[V] = [U_\alpha^- - V_\alpha^+, U_\alpha^+ - V_\alpha^-]$

(3) Scalar multiplication: $\mathrm{k[U]} = \begin{cases} [kU_\alpha^-, kU_\alpha^+], k > 0 \\ [kU_\alpha^+, kU_\alpha^-], k < 0 \end{cases}$

(4) Multiplication: $[U](\times)[V]$

$$\left[\frac{\mathrm{U}_\alpha^+\mathrm{V}_\alpha^- + \mathrm{U}_\alpha^-\mathrm{V}_\alpha^+}{2}, \frac{\mathrm{U}_\alpha^-\mathrm{Vb}_\alpha^- + \mathrm{U}_\alpha^+\mathrm{V}_\alpha^+}{2}\right]. \tag{3}$$

(5) Division: $[U](\div)[V]$

$$\begin{cases} \left[2\left(\frac{U_\alpha^-}{V_\alpha^- + V_\alpha^+}\right), 2\left(\frac{U_\alpha^+}{V_\alpha^- + V_\alpha^+}\right)\right], [V] > 0, V_\alpha^- + V_\alpha^+ \neq 0, \\ \left[2\left(\frac{U_\alpha^+}{V_\alpha^- + V_\alpha^+}\right), 2\left(\frac{U_\alpha^-}{V_\alpha^- + V_\alpha^+}\right)\right], [V] < 0, V_\alpha^- + V_\alpha^+ \neq 0. \end{cases} \tag{4}$$

(6) The order relations:

(i) $[U](\lesssim)[V]$ if $U_\alpha^- \leq V_\alpha^-$ and $U_\alpha^+ \leq V_\alpha^+$ or $U_\alpha^- + U_\alpha^+ \leq V_\alpha^- + V_\alpha^+$

(ii) $[U]$ is preferred to $[V]$ if and only if $U_\alpha^- \geq V_\alpha^-, U_\alpha^+ \geq V_\alpha^+$

4. Problem Formulation and Solution Concepts

A fuzzy cooperative continuous static game (F-CCSG) with n – players having piecewise quadratic fuzzy parameters in the cost functions of the players can be formulated as

$$(F - \mathrm{CCSG}) \quad G_1(b, ,\xi, \tilde{a}_1), G_2(b, \xi, \tilde{a}_1), \cdots, G_m(b, \xi, \tilde{a}_m) \quad \text{Subject to} \tag{5}$$

$$g_j(b, \xi) = 0, j = \bar{1, n}, \tag{6}$$

$$\xi \in \Omega = \left\{\xi \in \mathfrak{R}^s : h_l(b, \xi) \geq 0, l = \bar{1, r}\right\}, \tag{7}$$

where $G_i(b, \xi, \tilde{a}_i), ji = \bar{1, m}$ are convex functions on $\mathfrak{R}^n \times \mathfrak{R}^s$, $h_l(b, \xi), l = \bar{1, r}$ are concave functions on $\mathfrak{R}^n \times \mathfrak{R}^s$, and $g_j(b, \xi), j = \bar{1, n}$ are convex functions on $\mathfrak{R}^n \times \mathfrak{R}^s$. Assume that there exists a function $b = f(\xi)$, if the function $\mathrm{g_j(b, \xi)} = 0$ is of class $\mathfrak{C}^{(1)}$, then the Jacobian $|\partial \mathrm{g_j(b, \xi)}/\partial \mathrm{b_q}| \neq 0, \mathrm{j; q = \bar{1, n}}$ in the neighborhood of a solution point (b, ξ) to (6), $b = f(\xi)$, is the solution to (6) generated by $\xi \in \Omega$; differentiability assumptions are not needed her for all the functions $G_i(b, \gamma, \tilde{a}_i), i = \bar{1, n}$, and $h_l(b, \xi)$, Ω is a regular and compact set. $\tilde{a}_i, i = \bar{1, m}$ represents a vector of PQFNs. Let $\tilde{a}_1, \tilde{a}_2, \cdots, \tilde{a}_m$; $\mu_{\tilde{a}_1}(a_1), \mu_{\tilde{a}_2}(a_2) \cdots, \mu_{\tilde{a}_m}(a_m)$ be the PQFNs in F-CCSG problem with convex membership functions, respectively.

The following fuzzy form [46, 47] can be used to rewrite the F-CCSG problem:

$$(\alpha - \mathrm{CCSG}) \quad G_1(b, \xi, a_1), G_2(b, \xi, a_2), \cdots, G_n(b, \gamma, a_m) \quad s.t: \tag{8}$$

$$g_j(b, \xi) = 0, j = 1, 2, \cdots, n, \tag{9}$$

$$\Omega = \left\{\xi \in \mathfrak{R}^s : h_l(b, \xi) \geq 0, \mathrm{l} = \bar{1, r}\right\}, \tag{10}$$

$$a_i \in L_\alpha(\tilde{a}_i), i = 1,\bar{m} \tag{11}$$

Definition 6. Let $b = f(\xi)$ be the solution to (9) generated by $\xi \in \Omega$. A point $\xi^* \in \Omega$, is called a α – Pareto optimal solution to the α-CCSG problem, if and only if there does not exist $(\xi, a) \in \Omega \times L_\alpha(\tilde{a}_i)$ such that

$$\begin{aligned} G_i(f(\xi), \xi, a_i) &\le G_i\left(f\left(\xi^*\right), \xi^*, a_i^*\right); \forall i \\ &= 1,\bar{m} \text{ and } G_i(f(\xi), \xi, a_i) \\ &< G_i\left(f\left(\bar{\xi}\right), \xi^*, a_i^*\right) \text{ for some } i \in \{1, 2, \cdots, m\}. \end{aligned} \tag{12}$$

Based on the optimality of α-CCSG problem concept, we can show that a point $\xi^* \in \Omega$ is a solution to the α-CCSG problem if and only if ξ^* is solution to the following α – multiobjective optimization problem:

$$(\alpha - \text{MOP}) \quad \min \left(\bar{G}_1(\xi, a_1), \bar{G}_2(\xi, a_2), \cdots, \bar{G}_m(\xi, a_m)\right)^{\mathrm{T}}, \quad \text{Subject to} \tag{13}$$

$$\Omega = \left\{\xi \in \Re^{\mathrm{s}} : \bar{h}_l(b, \xi) \ge 0, \mathrm{l} = 1,\bar{r}\right\}, \tag{14}$$

$$a_i \in L_\alpha(\tilde{a}_i), i = 1,\bar{m}, \tag{15}$$

where $\bar{h}_l(\xi), l = 1,\bar{r}$ is concave functions on $\Re^s$, $\bar{G}_i(\xi, a_i), i = 1,\bar{m}$ are convex functions on $\Re^n \times \Re^t$, $\bar{G}_i(\xi, a_i) = G_i(f(\xi), \xi, a_i)$, and $\bar{h}_l(\xi) = h_l(f(\xi), \xi)$. Assume that the α-MOP is to be stable [48], problem (13) will be solved by the weighting Tchebycheff method:

$$\min_{\xi \in \Omega a_i \in L_\alpha(\tilde{a}_i)} \max_{1 \le i \le m} \left\{w_i\left(\bar{G}_i(\xi, a_i) - \bar{G}_i\left(\xi^*, a_i^*\right)\right), a_i \in L_\alpha(\tilde{a}_i), i = 1,\bar{m}\right\}, \tag{16}$$

$$\min \left\{\lambda : w_i\left(\bar{G}_i(\xi, a_i) - \bar{G}_i\left(\xi^*, a_i^*\right)\right) \le \lambda, \xi \in \Omega, a_i \in L_\alpha(\tilde{a}_i), i = 1,\bar{m}\right\}, \tag{17}$$

where $w_i \ge , \mathrm{i} = 1,\bar{m}$, and $\bar{G}_i\left(\xi^*, a_i^*\right), i = 1,\bar{m}$ are the ideal targets. It is noted that stability of (α-MOP) implies to the stability of problem (17).

In addition, problem (13) can be treated using the weighting method as

$$\min \left\{\sum_{i=1}^{m} w_i \bar{G}_i(\xi, a_i) : x \in \Omega, a_i \in L_\alpha(\tilde{a}_i), i = 1,\bar{m}\right\}, \text{where } w \ge 0, w \ne 0. \tag{18}$$

We can see that if there is $w^* \ge 0$ such that (ξ^*, a^*) is the unique optimal solution of issue (18) corresponding to the α – level, then, (ξ^*, a^*) is an α – Pareto optimal solution of Eq. (13).

Remark 7. The stability of Eqs. (17) and (18) is inextricably linked to the stability of Eq. (13).

5. Solution Procedure

The solution method based on determining the to the α – best compromise solution within the inexact interval of PQFNs has the minimum deviation from the $\bar{G}_{\mathrm{i}}(\xi^*, a_i^*)$, where

$$\bar{G}_i\left(\xi^*, a_i^*\right) = \min_{\xi \in \Omega, a_i \in L_\alpha(\tilde{a}_i)} \bar{G}_i(\xi, a_i), i = 1,\bar{m}. \tag{19}$$

Step 1. Calculate $\bar{G}_i^{\min}$, and $\bar{G}_i^{\max}$ (i.e., individual minimum and maximum) at $\alpha = 0$ and $\alpha = 1$; separately.

Step 2. Calculate the weight from the following:

$$w_i = \frac{\bar{G}_i^{\max} - \bar{G}_i^{\min}}{\sum_{i=1}^{m}\left(\bar{G}_i^{\max} - \bar{G}_i^{\min}\right)}. \tag{20}$$

Step 3. Formulate and solve Eq. (21).

$$\min \lambda, \quad \text{Subject to} \tag{21}$$

$$W_i\left(\bar{G}_i(\xi, a_i) - \bar{G}_i\left(\xi^*, a_i^*\right)\right) \le \lambda, i = 1,\bar{m}, \tag{22}$$

$$\xi \in \Omega, a_i = \left[(a_i)_\alpha^-, (a_i)_\alpha^+\right], i = 1,\bar{m}, \tag{23}$$

where $\mathrm{W_i} \ge 0, i = 1,\bar{m}$, $\sum_{i=1}^{m} w_i = 1$, $[(a_{1i})_\alpha^-, (a_{2i})_\alpha^+] = \mathrm{L}_\alpha(\tilde{\mathrm{a}}_{\mathrm{i}}), \mathrm{i} = 1,\bar{\mathrm{m}}$

Let (ξ°, a_i°) be the α – optimal compromise solution.

Step 4. Determine $S(\xi^\circ, a_i^\circ)$

Let $\mathrm{d} = (d_1, d_2) \in \Re^{2\mathrm{m}}$, where $d_1 = (d_{11}, \cdots, d_{im})^T$, $d_2 = (d_{21}, \cdots, d_{2m})^T$. Assume that problem (21) can be solved for $(w^\circ, \mathrm{d}^\circ) \in \Re^{3m}$ and that an α – Pareto optimum solution (ξ°, a_i°) can be found, then $S(\xi^\circ, a_i^\circ)$ is determined by applying the following conditions:

$$\begin{aligned} \zeta_i^\circ(a_i^\circ - d_{2i}) &= 0, i = 1,\bar{m}, \\ \eta_i^\circ(d_{1i} - \mathrm{a}_{\mathrm{i}}^\circ) &= 0, i = 1,\bar{m}, \\ \zeta_i^\circ, \eta_i^\circ \ge 0, d_{1i}, d_{2i} \in \Re, &\left[(a_{1i})_\alpha^-, (a_{2i})_\alpha^+\right] = L_\alpha(\tilde{a}_i), i = 1,\bar{m} \end{aligned} \tag{24}$$

6. A Numerical Example

Consider the following two-player game with

$$\begin{aligned} \bar{G}_1(\xi, \tilde{\mathrm{a}}_1) &= (\xi_1 - \tilde{\mathrm{a}}_1)^2 + (\xi_2 - 1)^2, \\ \bar{G}_2(\xi, \tilde{\mathrm{a}}_2) &= (\xi_1 - 1)^2 + \tilde{\mathrm{a}}_2(\xi_2 - 2)^2, \end{aligned} \tag{25}$$

where player 1 controls $\xi_1 \in \Re$, and player 2 controls $\xi_2 \in \Re$ with

$$\xi_1 - 4 \le 0, \xi_2 - 4 \le 0, -\xi_1 \le 0, -\xi_2 \le 0. \tag{26}$$

Let $\tilde{\mathrm{a}}_1 = (1, 2, 3, 4, 5,)$ and $\tilde{\mathrm{a}}_1 = (1, 3, 5, 9, 10)$ with the

close interval approximation be $[(\tilde{a}_1)_\alpha] = [2, 4]$ and $[(\tilde{a}_2)_\alpha] = [3, 9]$.

Step 1. Solve the following:

$$\min (\xi_1 - 1)^2 + (\xi_2 - 1)^2,$$
$$\text{Subject to}$$
$$\xi_1 - 4 \le 0, \xi_2 - 4 \le 0, -\xi_1 \le 0, -\xi_2 \le 0, \mu_{\tilde{a}_1}(a_1) = 0, \mu_{\tilde{a}_2}(a_2) = 0. \tag{27}$$

Let $(\xi_1, \xi_2, a_1 = 1) = (1, 1, 1)$ with $\bar{G}_1^{\min} = 0$.
Solve

$$\min (\xi_1 - 1)^2 + 10(\xi_2 - 2)^2,$$
$$\text{Subject to}$$
$$\xi_1 - 4 \le 0, \xi_2 - 4 \le 0, -\xi_1 \le 0, -\xi_2 \le 0, \mu_{\tilde{a}_1}(a_1) = 0, \mu_{\tilde{a}_2}(a_2) = 0. \tag{28}$$

Let $(\xi_1, \xi_2, a_2 = 1) = (1, 2, 1)$ with $\bar{G}_2^{\min} = 0$.
Solve

$$\max (\xi_1 - 3)^2 + (\xi_2 - 1)^2,$$
$$\text{Subject to}$$
$$\xi_1 - 4 \le 0, \xi_2 - 4 \le 0, -\xi_1 \le 0, -\xi_2 \le 0, \mu_{\tilde{a}_1}(a_1) = 1, \mu_{\tilde{a}_2}(a_2) = 1. \tag{29}$$

Let $(\xi_1, \xi_2, a_1 = 3) = (0, 4, 3)$ with $\bar{G}_1^{\max} = 18$.
Solve

$$\max (\xi_1 - 1)^2 + 5(\xi_2 - 2)^2,$$
$$\text{Subject to}$$
$$\xi_1 - 4 \le 0, \xi_2 - 4 \le 0, -\xi_1 \le 0, -\xi_2 \le 0, \mu_{\tilde{a}_1}(a_1) = 1, \mu_{\tilde{a}_2}(a_2) = 1. \tag{30}$$

Let $(\xi_1, \xi_2, a_2 = 5) = (4, 0, 5)$ with $\bar{G}_2^{\max} = 29$.

Step 2. $w_1 = \bar{G}_1^{\max} - \bar{G}_1^{\min} / (\bar{G}_1^{\max} - \bar{G}_1^{\min}) + (\bar{G}_2^{\max} - \bar{G}_2^{\min}) = 0.383$ and $w_2 = \bar{G}_2^{\max} - \bar{G}_2^{\min} / (\bar{G}_1^{\max} - \bar{G}_1^{\min}) + (\bar{G}_2^{\max} - \bar{G}_2^{\min}) = 0.617$.

Step 3. Solve the following:

$$\begin{gathered} \min \lambda, \\ \text{Subject to} \\ (\xi_1 - a_1)^2 + (\xi_2 - 1)^2 - \frac{47}{18}\lambda \le 0, \\ (\xi_1 - 1)^2 + a_2(\xi_2 - 2)^2 - \frac{47}{29}\lambda \le 0, \\ 2 \le a_1 \le 4, = [2, 4], \text{and } 3 \le a_2 \le 9, \\ \xi_1 - 4 \le 0, \xi_2 - 4 \le 0, -\xi_1 \le 0, -\xi_2 \le 0, \end{gathered} \tag{31}$$

and yields $\xi_1^\circ = 1.440665, \xi_2^\circ = 1, a_1^\circ = 2, a_2^\circ = 3$ and $\lambda^\circ = 0.1198169$.

Step 4. Determine $S(1.440665, 1, 2, 3)$ by applying the following conditions:

$$\begin{gathered} \zeta_1^\circ(2 - d_{21}) = 0, \zeta_2^\circ(3 - d_{22}) = 0, \\ \eta_1^\circ(d_{11} - 2) = 0, \eta_2^\circ(3 - d_{12}) = 0, \\ \zeta_1^\circ, \zeta_2^\circ; \eta_1^\circ, \eta_2^\circ \ge 0, [c_{1i}, c_{2i}] = \mathrm{L}_\alpha(\tilde{a}_i), i = 1, 2. \end{gathered} \tag{32}$$

We have $J_{1k}; J_{2k} \subseteq \{1, 2\}$, for $J_{11} = \{1\}, \zeta_1^\circ, > 0\, \zeta_2^\circ = 0$.
For $J_{21} = \{2\}, \eta_1^\circ = 0, \eta_2^\circ = 0$, then

$$S_{J_{11}, J_{21}}(1.440665, 1, 2, 3) = \{(d_1, d_2) \in \mathfrak{R}^4 : d_{21} = 2, d_{22} \ge 3, d_{11} \le 2, d_{12} = 3\}. \tag{33}$$

For $J_{12} = \{2\}, \zeta_1^\circ = 0, \zeta_2^\circ > 0$. For $J_{22} = \{1\}, \eta_1^\circ > 0, \eta_2^\circ = 0$, then

$$S_{J_{12}, J_{22}}(1.440665, 1, 2, 3) = \{(d_1, d_2) \in \mathfrak{R}^4 : d_{21} \ge 2, d_{22} = 3, d_{11} = 2, d_{12} \le 3\}. \tag{34}$$

For $J_{13} = \{1, 2\}, \zeta_1^\circ > 0, \zeta_2^\circ > 0$. For $J_{23} = \varnothing, \eta_1^\circ = 0, \eta_2^\circ = 0$, then

$$S_{J_{13}, J_{23}}(1.440665, 1, 2, 3) = \{(d_1, d_2) \in \mathfrak{R}^4 : d_{21} = 2, d_{22} = 3, d_{11} \le 2, d_{12} \le 3\}. \tag{35}$$

For $J_{14} = \varnothing, \zeta_1^\circ = 0, \zeta_2^\circ = 0$. For $J_{24} = \{1, 2\}, \eta_1^\circ > 0, \eta_2^\circ > 0$, then

$$S_{J_{14}, J_{24}}(1.440665, 1, 2, 3) = \{(d_1, d_2) \in \mathfrak{R}^4 : d_{21} \ge 2, d_{22} \ge 3, d_{11} = 2, d_{12} = 3\}. \tag{36}$$

Hence,

$$S(1.440665, 1, 2, 3) = \bigcup_{k=1}^{4} S_{J_{1k}, J_{2k}}(1.440665, 1, 2, 3). \tag{37}$$

7. Comparative Study

In order to highlight the merits of the proposed approach, Table 1 compares the suggested strategy to some current literature.

8. Conclusions and Future Works

In this paper, the weighted Tchebycheff method has applied to solve cooperative continuous static games with piecewise quadratic fuzzy numbers, and then the stability set of the

Table 1: Comparisons of the contributions of various researchers.

Author's name	Weighted Tchebycheff method	α – Pareto optimal solution	Optimal compromise solution	Parametric study	Environment
Zaichenko [49]	↓	↓	↑	↓	Fuzzy
Donahue et al. [50]	↓	↓	↓	↓	Crisp
Zhou et al. [51]	↓	↓	↑	↓	Fuzzy
Our investigation	↑	↑	↑	↑	Fuzzy

The symbols "↓" and "↑" shown in Table 1 represent whether the associated feature satisfy or not.

first kind corresponding to the α – optimal compromise solution has determined. The advantages of the approach are the ability to enable the decision-maker to have satisfactory solution and applied for different real-world problems with various types of fuzzy numbers. The key features of this work can be summarized as follows:

(i) The fundamental theory of fuzzy set is developed and its decision constructed. A real-world problem is discussed with the support of proposed algorithm and decision support of fuzzy set

(ii) The rudiments of f fuzzy set are characterized and

(iii) The proposed model and its decision-making based system are developed. A real-life problem is studied with the help of proposed algorithm, and decision system of fuzzy set is compared professionally via strategy with some existing relevant models keeping in view important evaluating features

(iv) The particular cases of proposed models of fuzzy set are discussed with the generalization of these structures

(v) As the proposed model is inadequate with the situation in the domain of multiargument approximate function, it is mandatory. Therefore, future work may include the addressing of this limitation and the determination

Data Availability

No data were used to support this study.

Consent

This article does not contain any studies with human participants or animals performed by any of the authors.

Conflicts of Interest

The authors declare that they have no conflicts of interest to report regarding the present study.

Acknowledgments

The researchers would like to thank the Deanship of Scientific Research, Qassim University for support the publication of this project.

References

[1] R. E. Bellman and L. A. Zadeh, "Decision-making in a fuzzy environment," *Management Science*, vol. 17, no. 4, p. 141, 1970.

[2] M. Tayyab and B. Sarkar, "An interactive fuzzy programming approach for a sustainable supplier selection under textile supply chain management," *Computers & Industrial Engineering*, vol. 155, article 107164, 2021.

[3] D. Behera, K. Peters, S. A. Edalatpanah, and D. Qiu, "New methods for solving imprecisely defined linear programming problem under trapezoidal fuzzy uncertainty," *Journal of Information and Optimization Sciences*, vol. 42, no. 3, pp. 603–629, 2021.

[4] P. Peykani, M. Nouri, F. Eshghi, M. Khamechian, and H. Farrokhi-Asl, "A novel mathematical approach for fuzzy multi-period multi-objective portfolio optimization problem under uncertain environment and practical constraints," *Journal of Fuzzy Extension and Applications*, vol. 2, no. 3, pp. 191–203, 2021.

[5] M. Akram, I. Ullah, T. Allahviranloo, and S. A. Edalatpanah, "Fully Pythagorean fuzzy linear programming problems with equality constraints," *Computational and Applied Mathematics*, vol. 40, no. 4, pp. 1–30, 2021.

[6] W. A. Lodwick and J. Kacprzyk, Eds., *Fuzzy Optimization: Recent Advances and Applications*, vol. 254, Springer, 2010.

[7] H. Chen, H. Qiao, L. Xu, Q. Feng, and K. Cai, "A fuzzy optimization strategy for the implementation of RBF LSSVR model in vis–NIR analysis of pomelo maturity," *IEEE Transactions on Industrial Informatics*, vol. 15, no. 11, pp. 5971–5979, 2019.

[8] S. Zhang, M. Chen, W. Zhang, and X. Zhuang, "Fuzzy optimization model for electric vehicle routing problem with time windows and recharging stations," *Expert Systems with Applications*, vol. 145, article 113123, 2020.

[9] H. J. Zimmermann, "Fuzzy programming and linear programming with several objective functions," *Fuzzy Sets and Systems*, vol. 1, no. 1, pp. 45–55, 1978.

[10] A. Ebrahimnejad and S. H. Nasseri, "Linear programmes with trapezoidal fuzzy numbers: a duality approach," *International Journal of Operational Research*, vol. 13, no. 1, pp. 67–89, 2012.

[11] A. Ebrahimnejad, "An effective computational attempt for solving fully fuzzy linear programming using MOLP problem," *Journal of Industrial and Production Engineering*, vol. 36, no. 2, pp. 59–69, 2019.

[12] A. Ebrahimnejad, "Fuzzy linear programming approach for solving transportation problems with interval-valued trapezoidal fuzzy numbers," *Sadhana - Academy Proceedings in Engineering Sciences*, vol. 41, no. 3, pp. 299–316, 2016.

[13] A. Ebrahimnejad and J. L. Verdegay, "A novel approach for sensitivity analysis in linear programs with trapezoidal fuzzy numbers," *Journal of Intelligent & Fuzzy Systems*, vol. 27, no. 1, pp. 173–185, 2014.

[14] S. H. Nasseri, H. Attari, and A. Ebrahimnejad, "Revised simplex method and its application for solving fuzzy linear programming problems," *European Journal of Industrial Engineering*, vol. 6, no. 3, pp. 259–280, 2012.

[15] M. Bagheri, A. Ebrahimnejad, S. Razavyan, F. Hosseinzadeh Lotfi, and N. Malekmohammadi, "Fuzzy arithmetic DEA approach for fuzzy multi-objective transportation problem," *Operational Research*, vol. 22, no. 2, pp. 1479–1509, 2022.

[16] T. L. Vincent and W. J. Grantham, *Optimality in Parametric Systems*, John Wiley& Sons, New York, 1981.

[17] T. L. Vincent and G. Leitmann, "Control-space properties of cooperative games," *Journal of Optimization Theory and Applications*, vol. 6, no. 2, pp. 91–113, 1970.

[18] L. Mallozzi and J. Morgan, "ε-mixed strategies for static continuous-kernel Stackelberg games," *Journal of Optimization Theory and Applications*, vol. 78, no. 2, pp. 303–316, 1993.

[19] K. M. M. El Shafei, "Pareto-minimal solutions for large scale continuous static games (LSCSG)," *Opsearch*, vol. 42, no. 3, pp. 228–237, 2005.

[20] M. M. K. Elshafei, "An interactive approach for solving Nash cooperative continuous static games (NCCSG)," *International journal of contemporary mathematical sciences*, vol. 2, pp. 1147–1162, 2007.

[21] L. Kenneth, P. Renner, and K. Schmedders, "Finding all pure-strategy equilibria in games with continuous strategies," *Quantitative Economics*, vol. 10-45, 2010.

[22] S. D. Flåm, L. Mallozzi, and J. Morgan, "A new look for Stackelberg-Cournot equilibria in oligopolistic markets," *Economic Theory*, vol. 20, no. 1, pp. 183–188, 2002.

[23] L. Mallozzi and J. Morgan, "Mixed strategies for hierarchical zero-sum games," in *Advances in Dynamic Games and Applications*, pp. 65–77, Birkhäuser, Boston, MA, 2001.

[24] A. Matsumoto, F. Szidarovszky, A. Matsumoto, and F. Szidarovszky, "Continuous static games," in *Game Theory and Its Applications*, pp. 21–47, Springer, Tokyo, 2016.

[25] M. H. Zare, O. Y. Özaltın, and O. A. Prokopyev, "On a class of bilevel linear mixed-integer programs in adversarial settings," *Journal of Global Optimization*, vol. 71, no. 1, pp. 91–113, 2018.

[26] T. J. Webster, "Static games with continuous strategies," in *Introduction to Game Theory in Business and Economics*, pp. 167–184, Routledge, 2018.

[27] Y. A. Aboelnaga and M. F. Zidan, "Min-max solutions for parametric continuous static game under roughness (parameters in the cost function and feasible region is a rough set)," *Ural Mathematical Journal*, vol. 6, no. 2, pp. 3–14, 2020.

[28] M. S. Osman, A. Z. El-Banna, and M. M. Kamel, "On fuzzy continuous static games (FCSG)(Stackelberg leader with min-max followers)," *Journal of Fuzzy Mathematics*, vol. 7, pp. 259–266, 1999.

[29] M. S. Osman, A. Z. El-Banna, and A. H. Amer, "Study on large scale fuzzy Nash equilibrium solutions," *Journal of Fuzzy Mathematics*, vol. 7, pp. 267–276, 1999.

[30] H. A. Khalifa and R. A. Zeineldin, "An interactive approach for solving fuzzy cooperative continuous static games," *International Journal of Computer Applications*, vol. 113, no. 1, pp. 16–20, 2015.

[31] H. A. Khalifa, "Study on cooperative continuous static games under fuzzy environment," *International Journal of Computer Applications, Foundation of Computer Science*, vol. 13, pp. 20–29, 2019.

[32] Y. A. Elnaga, M. K. El-sayed, and A. S. Shehab, "A study on Nash min-max hybrid continuous static games under fuzzy environment," *Mathematical Sciences Letters*, vol. 10, no. 2, pp. 59–69, 2021.

[33] F. Kacher and M. Larbani, "Existence of equilibrium solution for a non-cooperative game with fuzzy goals and parameters," *Fuzzy Sets and Systems*, vol. 159, no. 2, pp. 164–176, 2008.

[34] S. Borkotokey and R. Mesiar, "The Shapley value of cooperative games under fuzzy settings: a survey," *International Journal of General Systems*, vol. 43, no. 1, pp. 75–95, 2014.

[35] T. Verma and A. Kumar, *Fuzzy Solution Concepts for Non-cooperative Games: Interval, Fuzzy and Intuitionistic Fuzzy Payoffs*, vol. 383, Springer, 2019.

[36] L. Silbermayr, "A review of non-cooperative newsvendor games with horizontal inventory interactions," *Omega*, vol. 92, article 102148, 2020.

[37] H. Galindo, J. M. Gallardo, and A. Jiménez-Losada, "A real Shapley value for cooperative games with fuzzy characteristic function," *Fuzzy Sets and Systems*, vol. 409, pp. 1–14, 2021.

[38] A. S. Shvedov, "On epsilon-cores of cooperative games with fuzzy payoffs," *Mathematical Notes*, vol. 110, no. 1-2, pp. 261–266, 2021.

[39] Z. Wang, J. Zhang, and Y. Li, "Development of cooperative game model between urban landscape design and urban brand image recognition," in *2021 5th international conference on trends in electronics and informatics (ICOEI)*, pp. 1015–1018, Tirunelveli, India, 2021, June.

[40] F. Dong, D. Jin, X. Zhao, J. Han, and W. Lu, "A non-cooperative game approach to the robust control design for a class of fuzzy dynamical systems," *ISA transactions*, vol. 125, pp. 119–133, 2022.

[41] H. A. Khalifa, S. A. Edalatpanah, and A. Alburaikan, "Toward the Nash equilibrium solutions for large-scale pentagonal fuzzy continuous static games," *Journal of Function Spaces*, vol. 2022, Article ID 3709186, 11 pages, 2022.

[42] H. A. Khalifa, D. Pamucar, A. Alburaikan, and W. A. Afifi, "On Stackelberg leader with min- max followers to solve fuzzy continuous static games," *Journal of Function Spaces (Special Issues: Fuzzy Sets and Their Applications in Mathematics)*, vol. 2022, article 4441340, 8 pages, 2022.

[43] H. Garg, S. A. Edalatpanah, S. El-Morsy, and H. A. El-Wahed Khalifa, "On stability of continuous cooperative static games with possibilistic parameters in the objective functions," *Computational Intelligence and Neuroscience (Special Issue: Artificial Intelligence and Machine Learning-Driven Decision-Making)*, vol. 2022, article 6979075, pp. 1–10, 2022.

[44] L. A. Zadeh, "Fuzzy sets," *Control*, vol. 8, no. 3, pp. 338–353, 1965.

[45] S. Jain, "Close interval approximation of piecewise quadratic fuzzy numbers for fuzzy fractional program," *Iranian journal of operations research*, vol. 2, no. 1, pp. 77–88, 2010.

[46] M. Sakawa and H. Yano, "Interactive decision making for multiobjective nonlinear programming problems with fuzzy parameters," *Fuzzy Sets and Systems*, vol. 29, no. 3, pp. 315–326, 1989.

[47] M. Sakawa and H. Yano, "An interactive fuzzy satisficing method for multiobjective nonlinear programming problems with fuzzy parameters," *Fuzzy Sets and Systems*, vol. 30, no. 3, pp. 221–238, 1989.

[48] R. Rockafellar, "Duality and stability in extremum problems involving convex functions," *Pacific Journal of Mathematics*, vol. 21, no. 1, pp. 167–187, 1967.

[49] H. Zaichenko, "Fuzzy Cooperative Games of Two Players under Uncertainty Conditions," in *IEEE 2nd International Conference on System Analysis & Intelligent Computing*, pp. 5–9, Kyiv, Ukraine, October 2020.

[50] K. Donahue, O. P. Hauser, M. A. Nowak, and C. Hilbe, "Evolving cooperation in multichannel games," *Nature Communications*, vol. 11, no. 1, article 3885, pp. 1–9, 2020.

[51] J. Zhou, A. Tur, O. Petrosian, and H. Gao, "Transferable utility cooperative differential games with continuous updating using Pontryagin maximum principle," *Mathematics*, vol. 9, no. 2, p. 163, 2021.